Journal of Polymer Science: Part C, Polymer Symposia, No. 2, 1963

PROCEEDINGS OF THE

Fourth Cellulose Conference

Held at Syracuse, New York, October 18-19, 1962

edited by *R. H. Marchessault*

State University College of Forestry at Syracuse University, Syracuse, New York

published by INTERSCIENCE PUBLISHERS a division of John Wiley & Sons, Inc.

No. 2 *1963*

Journal of Polymer Science, Part C, POLYMER SYMPOSIA

PROCEEDINGS OF THE

Fourth Cellulose Conference

edited by R. H. MARCHESSAULT

State University College of Forestry at Syracuse University,
Syracuse, New York

Held at Syracuse, New York, October 18–19, 1962

published by INTERSCIENCE PUBLISHERS,
a division of John Wiley & Sons, Inc.

JOURNAL OF POLYMER SCIENCE, PART C, *Polymer Symposia*

Editorial Board: R. M. Fuoss · J. J. Hermans · H. Mark
H. W. Melville · C. G. Overberger · G. Smets

Published at irregular intervals by Interscience Publishers, a Division of John Wiley & Sons, Inc. Publication Office at 20th and Northampton Streets, Easton, Pennsylvania. Executive, Editorial, and Circulation Offices at 605 Third Avenue, New York 16, New York. Subscription price, $154.00 per volume (including Part A: General Papers; and Part B: Polymer Letters). Foreign postage, $3.50 per volume (including Parts A and B)

Copyright © 1963, by John Wiley & Sons, Inc., Printed in U.S.A.

Editorial Comment

It is a great satisfaction for a conference chairman when he finally sees the proceedings brought to print. Besides marking the completion of his tasks, it means that the benefits of the conference will now be available to a much wider audience. Such a point of view might be taken as argument in favor of a much larger attendance at the conference in the first place. However, this is decidedly not the opinion of members of the Cellulose Research Institute, sponsors, and organizers of the Fourth Cellulose Conference. Our aim is to provide a "Gordon Conference" atmosphere where there is maximum contact between delegates under conditions to encourage scientific exchanges.

Attendance at the last conference, October 18 and 19, 1962 was 125. About two thirds of the delegates were from industrial laboratories and the remainder from academic and government institutions. Discussions both formal and informal were lively and frequently carried on by the younger members of the audience.

Aside from the usual contributions presented at these conferences, there was the novel feature this time of a half-day symposium entitled, "Molecular Architecture of Wood" organized by Dr. W. A. Côté. It is the opinion of many prominent workers in the field that the future of cellulose as a polymeric entity is locked in the molecular complexity of wood. The problem which faces the modern cellulose chemist is no longer one of making a new derivative or a higher alpha wood pulp, it is rather the total understanding of the molecular texture and microscopic morphology of wood. In scope and in challenge, the problem is very similar to that of the cell biologist as he sorts out the various components which make *life*, and probes each coil and crosslink of the complex protein molecules. In terms of separation and purification of nature's rich storehouse of chemicals within plants, it is often how the molecules are put together which is more important rather than what they are. There is still much to be learned about how the micellar "bricks," the hemicellulose "glue," and lignin "mortar" are combined and distributed in the woody cell.

While plans for the conference were still in their early stages, it was decided to dedicate the Proceedings of the Fourth Cellulose Conference to the founder of the older Institute for Cellulose Research in the Netherlands, P. H. Hermans. It was felt that the occasion of his 65th birthday and his retirement fro n the direction of the Institute were events that called for recognition of his contributions to the fundamental literature of cellulose. It was soon clear that many of "P. H.'s" friends and colleagues, who could not take part in the Cellulose Conference, wanted to join in this testi-

monial, hence a committee was formed consisting of the following members: Dr. G. Challa, Dr. J. J. Hermans, Dr. E. H. Immergut, Dr. E. C. Jahn, Dr. R. H. Marchessault, Dr. H. Mark, and Dr. D. Vermaas. Through the committee, contributions from friends and colleagues of P. H. Hermans were solicited. These have been included in this Proceedings issue *which is dedicated with friendship and appreciation as a tribute to the work of P. H. Hermans.*

At the same time as the Utrecht Cellulose Research Institute undergoes a change of leadership and we take this opportunity to congratulate Dr. G. Challa on his appointment as successor to P. H. Hermans, our own American C. R. I. is bidding a sad farewell to its first director, Dr. J. J. Hermans. In a few short years, he breathed such life into the organization that even the loss of all its senior staff and some of the supporters, still left breath for the resurgence which is now underway under the new director Dr. T. E. Timell.

The editorial profession is often put in the same category as the janitorial system of any institution, "very necessary, but not very important in itself." If this is true, then it is also true of the editorial assistants, secretaries, referees, printers, etc., yet without contributions from each of them, the task of bringing this issue to print would have been an impossible one. In particular, I wish to thank and acknowledge my indebtedness to the members of the committee listed above, the patience and understanding of the contributors, the promptness and dedication of the referees, and the assistance of Mr. Roger Truelsen and his staff at Interscience Publishers. Finally, a special thanks to our C. R. I. secretary, Miss Diana Casciano, who competently handled details of the conference and preparation of the manuscripts for publication.

R. H. Marchessault
General Chairman,
Fourth Cellulose Conference

Contents

H. Mark: P. H. Hermans. A Biography and Appreciation 1
Hardy L. Shirley: Welcoming Address to the Conference 5

GENERAL PAPERS

R. G. LeBel, D. A. I. Goring, and T. E. Timell: Solution Properties of Birch Xylan. I. Measurement of Molecular Weight 9
R. G. LeBel and D. A. I. Goring: Solution Properties of Birch Xylan. II. Fractionation and Configuration 29
R. H. Marchessault and T. E. Timell: Four Polymer-Homologous Series of Oligosaccharides from 4-*O*-Methylglucuronoxylan 49
J. K. N. Jones and P. E. Reid: Structural Studies on the Water-Soluble Arabinogalactans of Mountain and European Larch 63
Robert E. Semple: Investigation to the Efficacy of Water-Soluble Arabinogalactan as a Plasma Substitute 73
Conrad Schuerch: Ozonization of Cellulose and Wood 79
Alexander Meller: Some Considerations on the Kinetics of the Acid Hydrolysis of Poly- and Oligo-saccharides 97
T. E. Timmell: Effect of Deacetylation and Nitration on Normal Glycosidic Linkages in Cellulose 109
J. J. Hermans: Viscosity and Sedimentation in Dilute Solutions of Cellulosic Macromolecules 117
Jan Hermans, Jr.: Flow of Gels of Cellulose Microcrystals. I. Random and Liquid Crystalline Gels 129
M. R. Edelson and Jan Hermans, Jr.: Flow of Gels of Cellulose Microcrystals. II. Effect of Added Electrolyte 145
K. V. Ramalingam, G. N. Werezak, and J. W. Hodgins. Radiation-Induced Graft Polymerization of Styrene in Wood 153
R. Y.-M. Huang and W. H. Rapson. Grafting Polymers onto Cellulose by High-Energy Radiation. II. Effect of Swelling Agents on the Gamma-Ray Induced Direct Radiation Grafting by Styrene onto Cellulose 169
C. P. J. Glaudemans and E. Passaglia. Method for the Investigation of Carbohydrate Graft Copolymers 189

SYMPOSIUM ON MOLECULAR ARCHITECTURE OF WOOD

W. A. Côté. Introduction 201
Irving B. Sachs, Ira T. Clark, and John C. Pew. Investigation of Lignin Distribution in the Cell Wall of Certain Woods 203
Walter Liese. Tertiary Wall and Warty Layer in Wood Cells 213
Wilfred A. Côté, Jr.. Structural Factors Affecting the Permeability of Wood .. 231
Ellis B. Cowling and Alfred J. Stamm. An Approach to the Measurement of Solid-Solution Structures in Wood and Other Cellulosic Materials 243

J. D. Hale and L. P. Clermont: Influence of Prosenchyma Cell-Wall Morphology on Basic Physical and Chemical Characteristics of Wood 253
F. U. Klaehn: Chemical Nature of Genetic Material 263

PANEL DISCUSSION: FUTURE TRENDS IN CELLULOSE RESEARCH

Frank R. Charles: Future Trends in Cellulose Research 273
W. M. Hearon: Cellulose as a Chemical Raw Material 277
C. P. Donofrio: Paper and Nonwoven Fabrics 279
J. Wharton: Cellulose Textile and Science Technology 283

CONTRIBUTIONS FROM FRIENDS AND COLLEAGUES OF P. H. HERMANS

Hannes Sihtola, Leo Neimo, and Raimo Sumiala: Classification of Carbonyl Groups in Cellulose on the Basis of their Reaction Rates at Oximation 289
Olli Ant-Wuorinen and Asko Visapää: Verification of Trace Amounts of Acids in Cellulose 311
Ø. Ellefsen: Viscosity Measurements on Chemically Modified Cellulose 321
Robert F. Schwenker, Jr. and Louis R. Beck, Jr.: Study of the Pyrolytic Decomposition of Cellulose by Gas Chromotography 331
S. G. Hovenkamp: Sodium Dithiocarbonate as a By-Product in Xanthating Reactions. A Contribution to the Chemistry of Viscose 341
Erich Treiber and Henryk C. Nadziakiewicz: New Contributions to the State of Solutions of Viscose: Gel Particle Counting and Optical Rotatory Dispersion Studies on Viscose 357
Evelyn S. Putnam: Polymerization within Cellulose Matrices. Nature of the Strength Reinforcement 377
H. Yasuda, J. A. Wray, and V. Stannett: Preparation and Characterization of Some Cellulose Graft Copolymers. Part I 387
A. A. Katai, V. K. Kulshrestha, and R. H. Marchessault: Ceric Ion-Initiated Polymerization of Acrylonitrile in the Presence of Alcohols 403
H. Sobue, K. Matsuzaki, H. Komagata, and A. Ishida: Grafting of Styrene on Cellulose Acetate Films 415
T. Petitpas, M. Oberlin, et J. Mering: Confirmation d'une Hypothese de P. H. Hermans: Chaîne de la Cellulose II 423
W. Kast: Comparative X-Ray Orientation Measurements on Hermans Model Filaments 429
O. Kratky and G. Miholic: Small-Angle X-Ray Investigations with Absolute Intensity Measurements on Regenerated, Air-Swollen Cellulose 449
Lars Aggebrandt and Olof Samuelson: Penetration of Polymetaphosphate Solution into Regenerated Cellulose 477
P. Paulusma and D. Vermaas: Fractional Extraction of Regenerated Cellulose Fibers with Iron-Sodium Tartrate Solutions 487
J. K. Smith, W. J. Kitchen, and D. B. Mutton: Structural Study of Cellulosic Fibers 499
E. Klein and K. Bosarge: Optical Dispersion and Birefringence of High Tenacity Cellulose Fibers 515
H. Abe and W. Prins: Elasticity of Polyvinyl Alcohol Model Filaments in Swelling Equilibrium with Water 527

Author Index 547

Subject Index 548

JOURNAL OF POLYMER SCIENCE: PART C NO. 2, PP. 1–3 (1963)

P. H. Hermans

A Biography and Appreciation

It will be a pleasure for polymer chemists and physicists in all parts of the world to express feelings of their warm friendship and their kindest wishes to Dr. P. H. Hermans on the occasion of his 65th birthday and it is a great honor for the writer of these lines that he has been asked by benevolent friends to condense these feelings in a few sentences of appreciation, admiration, and felicitation.

Petrus Hendrik Hermans was born on March 21, 1898 in Djakarta, Indonesia. Soon afterwards his family returned to Europe. He studied chemistry at the Technical University in Delft, The Netherlands, and obtained his Ph.D. as a student of Professor Boeseken in March 1924. The title of his thesis was "Investigation of the Spatial Configuration of Some Glycols." A critical discussion of the significance of the boric acid and acetone compounds for stereochemistry." From 1925 to 1943 he worked for the Hollandse Kunstzije Industrie (HKI) in Breda, which merged later with Algemene Kunstzijde Unie (AKU); Hermans became Director of the Institute for Cellulose Research of AKU and Affiliated Companies in Utrecht in 1943.

In the course of his career P. H. Hermans contributed with great success to several fields which all had some connection with organic chemistry and polymer chemistry. He started in 1922 with the stereochemistry of organic

boric acid derivatives and continued until 1925. Then he became interested (1924–1927) in the kinetics of the decomposition of diacylperoxides, in particular dibenzoyl peroxide. One of the later publications, together with H. Gelissen, appeared in *J. Polymer Sci.*, **1**, 407 (1946). Around 1935 he started with H. L. Bredee the classical and well known study of the theory of filtration; it led to a quantitative relation for the progressive clogging of filters in the filtration of viscose. The "clogging constant" of Hermans and Bredee was rapidly accepted in the cellulose and rayon industries as a characteristic quantity of great value. Between 1937 and 1948 P. H. Hermans studied with a number of co-workers in a profound and systematic manner the deformation mechanism of regenerated cellulose. This work had its origin in the complicated problem of viscose spinning, where coagulation, neutralization, and orientation occur simultaneously. Hermans' approach to this problem consisted of an attempt to analyze each of these processes separately. He found a good object of study for this in his isotropic model filaments of swollen cellulose xanthate and swollen regenerated cellulose spun from viscose. The behavior observed on stretching these filaments: force-strain diagram, anisotropy of swelling, birefringence, and orientation of crystallites, was interpreted on the basis of network models, considering the crystallites as crosslinks.

This work on the deformation of model filaments led to several other developments mainly, during 1943–1946 to a study of the effect of water on the density and the refractive indices of both isotropic and oriented cellulose fibers. Since studies of the water absorption led, in a natural way, to estimates of the degree of crystallinity, it is understandable that Hermans soon decided to use x-rays as a tool for his investigations and from 1946 until now he carried out his well known, classical x-ray studies of regenerated and native cellulose fibers and of many full synthetic fibers. Most of this work was done in collaboration with the late Dr. Weidinger; it aimed at a quantitative description of the supermolecular structure of oriented systems of linear macromolecules.

While this work was still in full swing, Hermans realized the importance of synthetic polymers for fundamental and applied research and turned his experimental skill and theoretical resourcefulness to the study of the mechanism of polyamide and polyester formation with the aim to make a substantial contribution to the understanding of their fiber forming properties. Rapidly he entered the ranks of the older specialists in these fields and enriched our factual knowledge and our understanding of these important processes and products with great success. At the time of this writing this work is still going on and there is rarely an important scientific or technical meeting at which Hermans or one of his co-workers do not report on significant and interesting progress.

A few particularly interesting publications of P. H. Hermans are: *Contribution to the Physics of Cellulose Fibres*, Amsterdam, 1946. This is, essentially, a report on research done at the Cellulose Research Institute in Utrecht during the war years (1943–1945). Also, *Physics and Chemistry*

of Cellulose Fibres (with Particular Reference to Rayon), Amsterdam, 1949; Chapter on gels in *Colloid Science, II*, edited by H. R. Kruyt, Amsterdam, 1949; *Introduction to Theoretical Organic Chemistry*, Amsterdam, 1952; revised edition in 1954. This book illustrates clearly that although much of Hermans' work may be classified as physical chemistry, his early training as an organic chemist has made a lasting imprint on his scientific interest. It must be considered as quite remarkable that notwithstanding his many duties as director of the Cellulose Research Institute in Utrecht, Hermans found the time and the energy not only to make himself familiar with the modern developments in theoretical organic chemistry, but to contribute to the literature himself.

Thus P. H.—as he is affectionately called by all his friends to distinguish him from another eminent Dutch scientist (J. J.) of the same family name—has made significant and stimulating contributions in any field of science and technology which he decided to enter; he is renowned for his systematic and careful experimentation as well as for the critical and yet inspired way in which he interprets his results and molds them into platforms for new outlooks and new ventures. We, his friends and colleagues, greet him today as one of our best and wish him many more years of successful and rewarding activity to his own satisfaction and to the benefit of our science and of all of us.

H. Mark

Welcoming Address to the Conference

I am honored to open this Fourth Cellulose Conference and to welcome the members to our college. From the beginning these conferences have attracted international attention. Our college has been pleased to serve as host. Participants have been the "Who's Who of Cellulose and Polymer Chemistry" from academic circles, government, and industrial laboratories.

Future historians trying to determine the basic causes of the tremendously rapid development of the middle and late 20th Century are certain to recognize technology as the key element, but the thoughtful will seek to determine what it was that sparked technology to develop so rapidly. Some may point to the necessity created by war, others to the greatly increased population pressure, still others to the impetus arising from national independence, on the one hand, and international collaboration, on the other. All have had their influence. All will recognize that, whatever the cause, it was the research activities of government, industry, and universities that developed the new technology. I think that the key element that is characteristic of our time, however, is the collaboration among these three basic groups and the extent to which teamwork developed. Research men from government and industry hold seminars and participate in symposia at universities, and university professors consult with industries and government. These mutually stimulating contacts have certainly had a catalytic effect on our progress.

So, as we meet these two days in Syracuse to explore further nature's most abundant renewable polymer chemical, we are bringing together the driving forces and basic philosophies of national resource conservation, industrial technology, and the urge to understand natural processes. It is the interaction of the three that gives toughness and resilience to our technologic age and sparks scientific achievement.

HARDY L. SHIRLEY
Dean, State University
College of Forestry
Syracuse, New York

GENERAL PAPERS

JOURNAL OF POLYMER SCIENCE: PART C NO. 2, PP. 9–28 (1963)

Solution Properties of Birch Xylan. I. Measurement of Molecular Weight

R. G. LEBEL,* D. A. I. GORING, and T. E. TIMELL,† *Physical Chemistry Division, Pulp and Paper Research Institute of Canada, and Department of Chemistry, McGill University, Montreal, Canada*

INTRODUCTION

Much research on the hemicellulosic polysaccharides has been concerned with elucidation of structural details by the chemical identification of the various constituents present, i.e., hexosans, pentosans, and uronic acids. In contrast, there have been few systematic studies of solution properties of xylan or any other hemicellulose. The scope of the present investigation is the preparation of fractions of white birch xylan over as wide a range of molecular weight as possible and the characterization of these fractions in solution by physicochemical methods such as viscosity, sedimentation, and diffusion. The purpose of the work was to elucidate the size and configuration of the xylan molecule in solution and to compare its behavior with that of cellulose and cellulose derivatives. Glaudemans and Timell[1,2] have shown that the predominant hemicellulose in white birch is a 4-*O*-methylglucuronoxylan in which every tenth xylose unit, on an average, carries a 4-*O*-methyl-D-glucuronic acid residue as a terminal side chain. This material comprises up to 30% of the dry weight of the wood and can readily be isolated in high yield with little degradation by direct extraction of the wood with alkali in the absence of air. Because white birch is a typical North American hard wood and its xylan is so easily extracted, this species was chosen for the present study.

Central to the investigation was the reliable determination of the various molecular weight averages of the xylan and its fractions. A number of reports have been published from this laboratory on the weight-average molecular weights of hemicelluloses as measured by the light-scattering technique.[3–6] Recently there have been several indications that the light-scattering method gives unrepresentative results because of the extreme

* Holder of a National Research Council of Canada Studentship (1960–62); present address: Anglo Paper, Quebec City, Canada.

† Present address: Department of Forest Chemistry, State University College of Forestry at Syracuse University, Syracuse, N. Y.

difficulty of removing cellular debris from solutions of naturally occurring macromolecules.[7] Such errors would be expected to be most pronounced for low molecular weight material such as xylan, because only a small proportion of colloidal material would produce a relatively large effect on the scattering due to the molecules themselves. As a preliminary precaution it was decided to compare the results obtained with the light-scattering technique with weight-average molecular weights determined by other methods.

Ultracentrifugal techniques are among the most reliable methods of studying the solution properties of naturally occurring macromolecules. Yet ultracentrifuge determinations on xylan have not been reported. A linear polysaccharide of molecular weight between 10,000 and 30,000 would be expected to show a sedimentation velocity which, though small, was accurately measurable in the synthetic boundary cell. The sedimentation constant could then be combined with diffusion measurements to give molecular weights. The molecular weight range of 10,000–30,000 is ideal for measurement by the sedimentation equilibrium technique. The method has been well tested for mono-disperse globular molecules such as proteins[8,9] and lignins[10] and has been shown to be suitable for the determination of molecular weights of chain molecules in nonideal and polydisperse systems.[11,12] The equilibrium method gives a weight-average molecular weight and has the advantage that diffusion measurements are not necessary. Z-average molecular weights may also be evaluated and used for assessing the degree of heterogeneity of the macromolecule under study. A major disadvantage is the long time required to reach complete equilibrium. Recently, Van Holde and Baldwin[9] proposed the use of short columns of solution with distances of 1–3 mm. between the meniscus and the bottom of the cell. By this means, the time to reach equilibrium is reduced by as much as a hundredfold so that the technique can be used for the relatively rapid examination of a series of fractions. The precision of the method is indicated by the 3% agreement reported by Yphantis between the formula weight and the molecular weight of ribonuclease measured by the short-column technique.[8]

In the present study, sedimentation equilibrium was the main technique for the measurement of molecular weights. The method was used for unfractionated xylan and for a series of fractions. To test the reliability of the sedimentation equilibrium method, molecular weights by osmometry, sedimentation velocity, diffusion, and light scattering were measured on selected samples of unsubstituted xylan or on derivatives.

The acetate derivatives used in osmometry were dissolved in several organic solvents or solvent mixtures. For intrinsic viscosity, cupriethylenediamine (CED) was used as solvent as well as dimethyl sulfoxide (DMSO). However, the major solvent of the investigation was DMSO. This solvent has proved useful in the extraction[13,14] and fractionation[15] of xylan and also

in viscosity and light-scattering measurements.[3,15–17] Being colorless and having a density near to unity, it is particularly suitable for sedimentation measurements. Its chief disadvantage is that it is strongly hygroscopic, and a slight increase in its water content can affect its viscosity to a marked degree.[18,19] With reasonable care water uptake can be avoided.[19] It was therefore decided to use DMSO as solvent for both fractionation and physicochemical measurements.

The work is presented in three parts. The present paper is Part I, and deals with the molecular weight determinations. Fractionation and the characterization of the fraction by viscosity, diffusion, and molecular weight are described in Part II.[20] The third part which will be published later deals with the temperature dependence of the intrinsic viscosity.

Several of the experimental techniques used throughout the investigation are described in the present paper and results for some of the fractions of Part II are included in order to illustrate the type and quality of data obtained. Certain marked discrepancies were found in the light-scattering data, especially when compared with previously published work from this laboratory.[3] Therefore, in addition to measurements on a freshly prepared birch xylan, a number of experiments were repeated with the sample, the physicochemical characterization of which was described in an earlier publication.[3]

EXPERIMENTAL

Materials

White birch wood meal, extracted first with a benzene–alcohol mixture and then with water, was used as the starting material.

Care was taken to dry the DMSO as thoroughly as possible by distilling the solvent under vacuum over Drierite. A Perkin-Elmer Model 21 infrared spectrophotometer was used to estimate the residual water content in the distilled solvent.[19] Freshly distilled DMSO contained between 0.09 and 0.25% water. For uniformity a composition of 0.20% water was used throughout the present investigation.

Cuprietylenediamine for viscosity determinations was of 0.5*M* concentration. The solvents used in the precipitation and washing of the xylan were of technical grade and were purified by fractional distillation.

Preparation

White birch xylan was prepared after the method of Glaudemans and Timell[15] by directly extracting the wood meal with a solution of potassium hydroxide in an atmosphere of nitrogen. The hemicellulose was recovered by precipitation in a mixture of ethanol and acetic acid, washing with ethanol and petroleum ether, and drying in vacuum over calcium chloride

and potassium hydroxide. A batch of 500 g. of xylan was obtained from 1800 g. of wood meal. A paper chromatographic analysis[2] on the hydrolyzed crude xylan revealed that the sugars galactose, glucose, arabinose, and rhamnose made up, together, less than 1% of the hydrolyzate.

The xylan obtained by the above procedure was the potassium salt, i.e., the glucuronic acid groups were neutralized with potassium cations. For reasons discussed in a later section, it was desirable to work with the acidic form of the polysaccharide. This was prepared by acidifying potassium xylan with 0.1*N* hydrochloric acid. The material was then centrifugally washed free of chloride ions, rinsed with dry acetone and petroleum ether, and dried in vacuum over magnesium perchlorate. About 60 g. of acidic xylan was prepared in this manner, and most of the work was done with this bulk sample. Sulfated ash analyses confirmed by flame spectroscopy showed that the potassium content was reduced from 2.8% to 0.1% by the acidification process. The uronic acid content of the acidic xylan was found to be 11.4% by the method of Johansson, Lindberg, and Theander.[21]

Lignin was determined spectrophotometrically on xylans dissolved in DMSO. A suitable value for the extinction coefficient ϵ was found by measuring the absorbance of known amounts of alkali lignin (fraction D-6 in reference 22) dissolved in DMSO. A mean value of 14.5 l./cm.g. was obtained. The lignin content of the xylan was then computed from

$$\text{Lignin content, \%} = 0.69D/c \qquad (1)$$

in which D is the optical density measured in a 1 cm. cell and c the concentration of xylan in grams per deciliter.

The lignin content of the potassium xylan was 1.6%, which decreased to 1.1% for the acidic preparation. These figures may be compared with a lignin content of 0.3% found for a chlorite bleached xylan kindly supplied by Dr. D. W. Clayton.[23] Apparently the lignin cannot be completely eliminated by bleaching, and therefore a chlorite treatment was not given to the xylan in the present work.

Solubility

It was soon noticed that white birch xylan was only partially soluble in DMSO under certain conditions. Accordingly, the solubility of potassium and acidic xylan in the system DMSO–water was measured.

Solubility was estimated by shaking mixtures of xylan, DMSO, and water in a wrist action shaker for 24 hr. Various proportions of DMSO and water were used, but the xylan was always 1% by weight. All experiments were carried out at room temperature. After shaking, the solutions were centrifuged, decanted, and analyzed for dissolved xylan.

Results of the solubility investigation are shown in Figure 1. The solubility of potassium xylan was found to increase with an increase in water

content of the DMSO. Maximum solubility occurred at approximately 12% water. Upon further addition of water, the solubility decreased rapidly, and finally levelled off to a value of about 10% in pure water. In contrast, acidic xylan at a concentration of 1% was found to be completely soluble in DMSO–water mixtures containing between 0 and 12% water. Further addition of water markedly decreased the solubility.

The reason for the effect in Figure 1 is not definitely known. It is possible that the water solvates the ionizing potassium glucuronate sites while DMSO solvates the xylan chain itself. This twin-site solvation produces

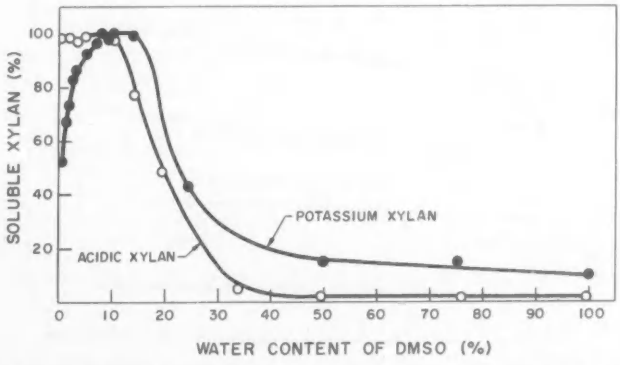

Fig. 1. Solubility of potassium and acidic white birch xylans in water–DMSO mixtures.

solubility with the potassium salt. In the acidic polysaccharide, ionization probably does not take place in DMSO; thus water is not necessary to produce solubility. Mixed solvent solubility is common in polymer systems, and preferential adsorption of solvent has been proposed as an explanation of the phenomenon.[24] In order to avoid the use of a mixed solvent in the present investigation and also to ensure complete solubility of the xylan, measurements in DMSO were restricted to the acidic polysaccharide in the anhydrous solvent.

Intrinsic Viscosity

Intrinsic viscosity determinations were made at 25 ± 0.01°C. with Ubbelohde-type viscometers as described by Craig and Henderson.[25] Viscosities were measured in DMSO and in 0.5*M* cupriethylenediamine (CED). The solutions and the solvent were clarified through a fine porosity Pyrex microfilter mounted on a hypodermic syringe in place of a needle. This attachment was easily replaced by the needle for delivery. The quantity of material introduced into the viscometer was determined by weighing the syringe before and after delivery.

Concentrations of xylan in DMSO were determined by quantitatively emptying the viscometer into five volum s of ethyl acetate, and the white precipitate was collected and washed in a weighed sintered glass filter. The residue was then dried with petroleum ether, desiccated over magnesium perchlorate in a vacuum oven at 98°C., and weighed. This method of concentration determination was checked by dissolving known amounts of xylan in DMSO and precipitating in ethyl acetate. The precipitate was collected and weighed. About 99% of the material was recovered.

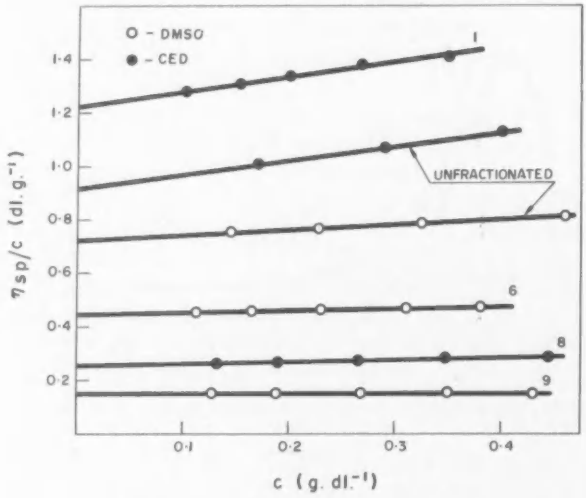

Fig. 2. η_{sp}/c vs. c for the unfractionated xylan and master fractions No. 1, 6, 8, and 9 in DMSO or CED. Preparation of the master fractions is described in Part II of the series.[20]

Great care was taken at all stages of the experiment to avoid the uptake of water from the atmosphere by the DMSO. All solutions were made up in glass-stoppered flasks which were placed in closed, wide-mouthed bottles containing a desiccant. Desiccating tubes were attached to the viscometer.

Examples of viscosity data plotted according to Huggins[26] are shown in Figure 2.

The effect of the water content of the solvent was assessed by measurement of $[\eta]$ in DMSO containing 0, 2, 4, 6, and 11% water. The intrinsic viscosity decreased to a minimum at 4% water. For the higher water contents, $[\eta]$ increased slightly but did not regain its value in dry DMSO. However, the effects were small, the maximum decrease in $[\eta]$ being only 8%. This indicated that any small variations in the moisture content of

the "dry" DMSO would have a negligible effect on the configuration of the polysaccharide in solution.

The stability of the acidic xylan in DMSO was demonstrated by measuring $[\eta]$ before and after the standing of a xylan solution for 3 weeks. No change in $[\eta]$ was observed.

Partial Specific Volume

Densities of solutions of xylan were measured with a 10 ml. density bottle at 25 ± 0.01°C. in the concentration range 0.6–1.5%. Measurements were made on five samples with uronic acid contents of 8.6–13.6% and intrinsic viscosities of 0.4–0.8 dl.g.$^{-1}$ The partial specific volume, $\bar{v}$, was calculated by Kramer's formula.[27] The average value for 16 determinations was 0.617 ± 0.006 ml./g. Values of $(1 - \bar{v}\rho)$, where ρ is the density of the solution, were also computed, and the average of 16 determinations was 0.321 ± 0.006. No trend with solution concentration, uronic acid content, or molecular weight was noted.

Sedimentation Equilibrium

A Spinco Model E ultracentrifuge equipped with a phase plate, schlieren optics, and with an RTIC temperature control was used to determine molecular weights by the short-column sedimentation equilibrium technique of Van Holde and Baldwin.[9] Standard double-sector cells were used with solvent in one channel and solution in the other. By means of suitable masks two cells were run simultaneously in the analytical rotor. In order to provide a liquid–liquid boundary at the bottom of the column, FC-43 (perfluorotributylamine) was added.[8] This fluorocarbon was found to be completely immiscible with DMSO. In one run, the same solution was evaluated with and without addition of FC-43, and identical molecular weights were found.

Column heights were between 0.8 and 1.0 mm. Centrifuge speeds were set at 20,410, 29,500, or 36,500 rpm. The duration of the runs ranged between 17 and 18 hr. This exceeded the time required to insure complete equilibrium as computed from the equation of Van Holde and Baldwin.[9]

The temperature was controlled at 25°C., and the phase-plate angle was 65°. Examples of schlieren diagrams are given in Figure 3. There was no indication of the formation of gel layer at the bottom of the cell in any of the runs. The schlieren patterns were enlarged 10 times and the height of the ordinate at the midpoint between the meniscus and the FC-43 boundary was measured. This ordinate was converted to the refractive index gradient, dn/dx, by means of a constant derived from the schlieren areas of synthetic boundaries for aqueous solutions of serum albumin and potassium chloride. Molecular weights were then computed from eq. (2):

$$\bar{M}_w = \left[\frac{RT}{(1 - \bar{v}\rho)\omega^2}\right]\left(\frac{1}{x_m c}\right)\frac{(dn/dx)}{(dn/dc)} \qquad (2)$$

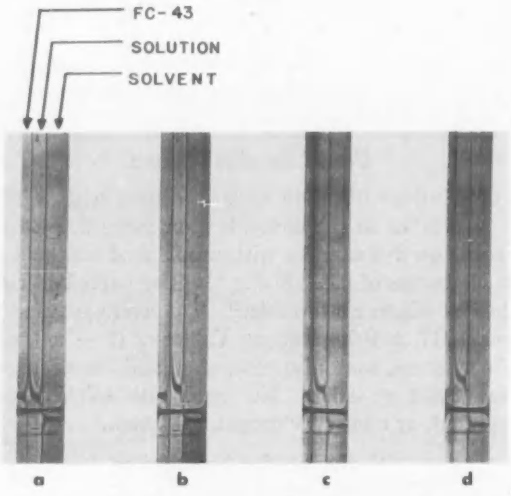

Fig. 3. Samples of the schlieren pattern for xylan. Centrifuge speed = 20410 rpm. Concentration increases from *a* to *d*.

in which x_m is the distance of the midpoint of the column from the center of the rotor and ω the angular velocity. The refractive index increment, dn/dc was found to be 0.062 ml./g. for xylan in DMSO.[20]

The method was tested by a determination of the molecular weight of crystalline bovine ribonuclease. The mean value for four concentrations was 13,540 which agrees well with the formula weight of 13,683.[8]

The sedimentation equilibrium molecular weight of the xylans was found to be markedly dependent upon the concentration, in contrast to the behavior of proteins[8,9] and lignins.[10] Schulz[28] and Wales and co-workers[29] have shown the dependence on concentration may be expressed as

$$1/\bar{M}_{w(\text{app})} = 1/\bar{M}_w + B_e c \tag{3}$$

where $\bar{M}_w$ is the true weight-average molecular weight at $c = 0$, $\bar{M}_{w(\text{app})}$ the apparent weight-average molecular weight calculated at finite concentration, and B_e a coefficient which equals the light-scattering virial coefficient and is twice the osmometric virial coefficient.

Examples of $1/\bar{M}_{w(\text{app})}$ versus c are shown in Figure 4 from which weight average molecular weights and virial coefficients were computed by means of eq. (3). The concentration range was 0.4–1.5 g./dl. Below 0.4 g./dl., the ordinate heights in the schlieren patterns were small and could not be measured accurately. The consistency of the data at different machine speeds in Figure 4 indicated that the variation in speed had no appreciable effect on the values of the molecular weight.

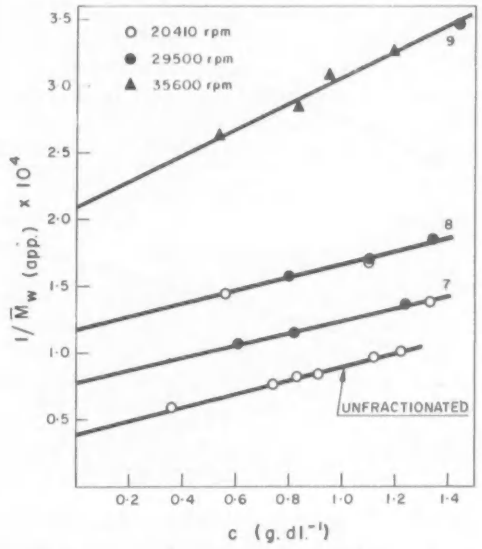

Fig. 4. Graph of $1/M_{w(app)}$ vs. c for unfractionated xylan and master fractions No. 7, 8, and 9 at various centrifuge speeds. The preparation of the master fractions is given in Part II.[20]

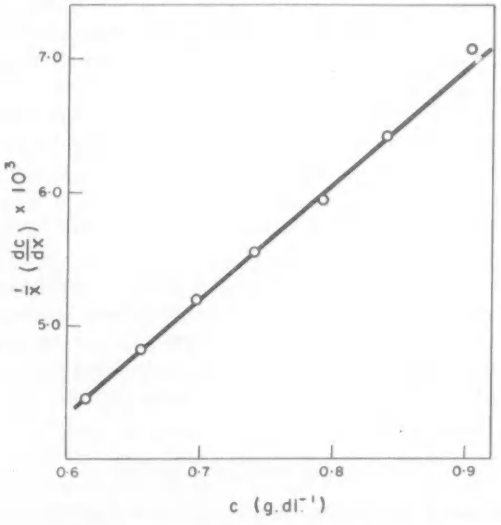

Fig. 5. Plot of $(1/x)(dc/dx)$ vs. c for xylan at $c = 0.74$ g./dl.

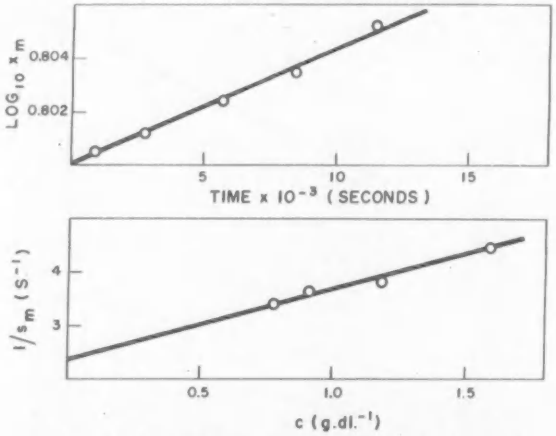

Fig. 6. Sedimentation velocity data for master fraction No. 2: (upper) log x_m vs time (c = 0.91 g./dl.; (lower) $1/s_m$ vs. c.

Z-average molecular weights were calculated from the schlieren patterns by the method of Van Holde and Baldwin.[9] From the slope of $(1/x)(dc/dx)$ versus c, $\bar{M}_z$ was determined from

$$\bar{M}_z = (1/x)(dc/dx)RT/(1 - \bar{v}\rho)\omega^2 c \qquad (4)$$

An example of a plot of $(1/x)(dc/dx)$ versus c is given in Figure 5. It is seen that there is a slight sinusoidal curvature in the graph which has been attributed to an optical effect due to diffraction at the ends of the column.[9,30] $\bar{M}_z$ was calculated from the slope of the best straight line through the central portion of the curve. A precision of no more than $\pm 20\%$ can be expected for $\bar{M}_z$ determined by this procedure.[8] Van Holde and Baldwin demonstrated that when $\bar{M}_z$ is concentration-dependent, the value given by eq. (4) corresponds to $(c_f + c_g)$, the sum of the concentration at the meniscus and at the base of the cell.[9] Plots of $1/\bar{M}_{z(\text{app})}$ versus $(c_f + c_g)$ were obtained for each master fraction, and $\bar{M}_z$ at $c = 0$ was computed by a least-squares extrapolation.

A test was also made to determine the effect of small changes in temperature on the molecular weight determined by the sedimentation equilibrium method. Runs on the unfractionated xylan were made at 20, 25, and 29°C. The three linear plots of $1/\bar{M}_{w(\text{app})}$ versus c were coincidental, indicating that temperature changes between 20 and 29°C. have a negligible effect on the value of $\bar{M}_w$ or B_c.

Sedimentation Velocity

One sample was characterized by the sedimentation velocity technique in order to provide a check on the molecular weight obtained by the sedimen-

tation equilibrium method. Velocity experiments were made at 59,780 rpm in a synthetic boundary-forming cell of the plunger type on master fraction No. 2. Single symmetrical peaks were observed. The maximum ordinate sedimentation coefficient, s_m was obtained in the usual manner[31] from the slope of the linear plots of log x_m versus t (Fig. 6), where x_m is the distance of the maximum ordinate from the center of the rotor. The value of $(s_m)_{c=0}$ was found by linear extrapolation of $1/s_m$ to zero concentration as shown in Figure 6.

Light Scattering

Light-scattering measurements were made with a Brice-Phoenix photometer by the techniques which have been described in several previous publications.[3,32,33] Cells adaptable to ultracentrifugation as described by Dandliker and Kraut[32] and modified by Goring and Timell[3] were used. The solutions were subjected to a preliminary ultracentrifugation at 140,000 g in a Spinco Model L ultracentrifuge. The concentration was determined after precentrifugation and no loss of material was detected.

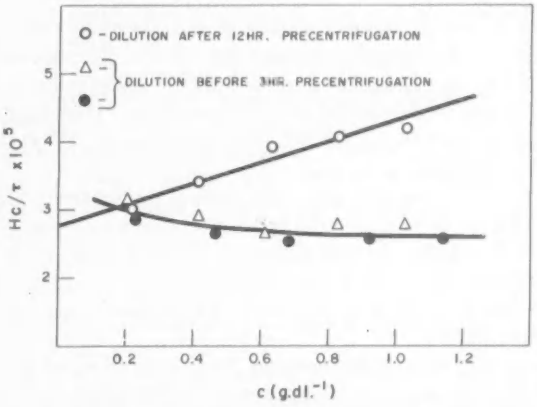

Fig. 7. Graphs of Hc/τ vs. c for xylan in DMSO. The duplicate data in the upwards curving plot were obtained by precentrifuging each dilution independently for 3 hr. The upper graph was the result of dilution after 12 hr. precentrifugation.

The-light scattering data were plotted as Hc/τ versus c and the molecular weight, M_{LS} and the light-scattering second virial coefficient, B_{LS} were calculated from the intercept and slope, respectively. Refractive index and dissymmetry corrections were applied to $(Hc/\tau)_{c=0}$ in computing M_{LS}.

Plots of Hc/τ versus c are shown in Figure 7. The concentration range was 0.2–1.0 g./dl. and was obtained by dilution of the original 1% solution. Two methods of dilution were used. Initially the solution was diluted

prior to precentrifugation and each concentration was precentrifuged independently before being placed in the light-scattering cell. This technique results in upward curving of the Hc/τ versus c plots shown in Figure 7 for two identical light-scattering runs. Subsequently the dilution was always made after precentrifugation. The conventional linear plot of Hc/τ versus c was then obtained as shown in Figure 7 for a xylan solution after 12 hr. precentrifugation. The origin of this effect is discussed later.

Osmometry

To obtain solutions suitable for osmotic pressure measurements, xylan was converted to an acetate derivative. A 2-g. batch was acetylated with acetic anhydride in the presence of dry pyridine with the polysaccharide swollen in freshly distilled formamide as recommended by Carson and Maclay.[34,35] The product was fully acetylated with an acetyl content of 39% as determined by the alcoholic-alkali method of Genung and Mallat.[36] However, the acetylated xylan was found to be insoluble in many organic solvents, including chloroform, pyridine, *m*-cresol, methylene chloride, and tetrachloroethane.

Extensive efforts to make a soluble mixed derivative of xylan failed. Acetylation with mixtures of 1:1 and 1:3 and 1:5 acetic–*n*-butyric anhydride and with mixtures of 1:1 and 1:5 acetic–isobutyric anhydride were tried, but the products obtained were all insoluble. Direct acylation with benzoyl chloride yielded a product soluble in chloroform, but it was found to be severely degraded.

A final attempt at esterification was undertaken by using DMSO as the swelling agent instead of formamide. The xylan was mixed with DMSO to give a thick paste. Acetylation then resulted in an ester which was partially degraded but completely soluble in a 9:1 chloroform–ethanol mixture. The acetate was also soluble in tetrachloroethane, *m*-cresol, and methylene chloride.

Osmotic pressure determinations on the sample of xylan and its soluble acetate derivative were made as previously described with the Stabin-Immergut[37] modification of the Zimm-Myerson osmometer.[38] A plot of osmotic height as a function of time indicated that with organic liquids as solvents, equilibrium was obtained after 9 hr. With DMSO it was necessary to extend this time to 12 hr. The osmotic height was determined at four or five different concentrations, and the data plotted according to

$$\pi/c = RT[(1/\bar{M}_n) + Bc] \tag{5}$$

where π is the osmotic pressure. The number-average molecular weight $\bar{M}_n$ and the osmotic second virial coefficient B were calculated from the intercept and slope of the π/c versus c graphs shown in Figure 8. The measurements in 9:1 chloroform-ethanol and in tetrachloroethane were

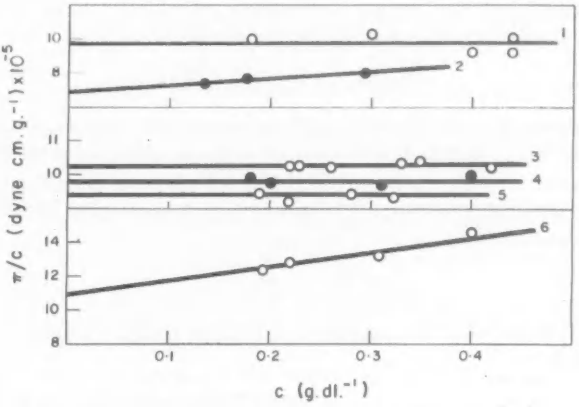

Fig. 8. π/c vs. c for xylan acetate in chloroform–ethanol and tetrachloroethane at various temperatures and for xylan in DMSO: (*1*) xylan acetate in 9:1 chloroform–ethanol at 40°C.; (*2*) xylan acetate in 9:1 chloroform–ethanol at 32°C.; Curves (*3*), (*4*), (*5*) xylan acetate in tetrachloroethane at 40, 32, and 25°C., respectively; (*6*) unfractionated xylan in DMSO at 25°C.

carried out at various temperatures to test for molecular association in the organic solvents.

In order to make the osmotic molecular weights of the acetate directly comparable with values from the other methods used in this investigation, it was necessary to determine the extent of degradation of the hemicellulose during the esterification. This was done viscometrically in DMSO and the $[\eta]$ values converted to $\overline{DP}_w$ by means of eq. (4) in Part II.[20] Two methods were employed. By one method, the acetate derivative was regenerated to the free acid by deacetylation with sodium methoxide.[39] The $\overline{DP}_w$ of the regenerated xylan was found to be 93 compared with 178 for the original sample. A control sodium methoxide treatment of the original non-acetylated xylan caused $\overline{DP}_w$ to decrease from 178 to 145. If an allowance is made for this effect, the acetylation is seen to produce a 36% reduction in $\overline{DP}_w$. Alternatively, xylan acetate was dissolved directly in CED and its intrinsic viscosity was measured. Under these conditions, complete saponification of the acetate groups takes place.[40] $\overline{DP}_w$ of the CED-regenerated xylan was 118 corresponding to a 34% reduction in $\overline{DP}_w$ during acetylation. This figure is in excellent agreement with the 36% degradation measured by the sodium methoxide deacetylation.

A correction of 35% was therefore applied to the observed molecular weights of the acetate to allow for degradation during acetylation. It is realized that this is a somewhat arbitrary procedure for such a large correction factor. But as shown later the anomalies found in osmometry were

quite pronounced, and even a substantial error in the correction for degradation would not alter the conclusions reached.

Degree of Polymerization

The degree of polymerization, $\overline{DP}$ represents the number of xylose residues in the linear backbone of the polysaccharide, exclusive of the glucuronic acid side chains. For some purposes, the $\overline{DP}$ is a more significant quantity than the molecular weight, $\bar{M}$ from which it is derived. The DP values were calculated from

$$\overline{DP} = \bar{M}/M_r \tag{6}$$

where M_r is the effective monomer molecular weight computed from the relationship

$$M_r = 132 + \frac{2508\ (\%\ \text{uronic acid})}{1940 - 19(\%\ \text{uronic acid})} \tag{7}$$

for the unsubstituted xylan and

$$M_r = 216 + \frac{3062\ (\%\ \text{uronic acid})}{1940 - 19(\%\ \text{uronic acid})} \tag{8}$$

for the fully-substituted acetate derivative. The $\overline{DP}_w$ and $\overline{DP}_n$ values in Tables I and II were computed by substituting the appropriate average for $\bar{M}$ in eq. (6).

TABLE I
Comparison of Molecular Properties of Xylan with Previously Prepared Sample

Property	Present xylan	Previous xylan
Uronic acid	11.4	10.9[a]
$[\eta]$ in DMSO	0.72	0.710
$[\eta]$ in CED	0.92	0.90
		0.89[a]
$\overline{DP}_w$ (sed. equil.)	178	184
$\overline{DP}_z$ "	242	—
B_e "	5.3×10^{-3}	5.5×10^{-3}
$\overline{DP}_n$ (osm. in DMSO)	151	131[b]
B "	3.0×10^{-3}	—
$\overline{DP}_n$ (osm. in $CHCl_3$–C_2H_5OH)	234	215[a]
$\overline{DP}_w$ (light scat.)	264	393
		500[a]
Dissymmetry (light scat.)	1.11	1.37
		1.5[a]
B_{LS} (light scat.)	1.22×10^{-3}	0.4×10^{-3}

[a] Previously reported by Goring and Timell.[3]
[b] Previously reported by Glaudemans and Timell.[15]

TABLE II
Osmotic Data for Xylan Acetate at Different Temperatures

Solvent	Temp., °C.	$\bar{M}_n$	$\overline{DP}_n$	$\overline{DP}_n$ (corr.)
9:1 Chloroform–ethanol	32	35900	152	234
"	40	26800	114	175
Tetrachloroethane	25	26900	114	175
	32	26100	111	171
	40	25500	108	166

RESULTS AND DISCUSSION

The crucial problems of molecular weight determination are perhaps best illustrated by the comparison in Table I between the results for unfractionated white birch xylan described earlier by Goring and Timell[3] and the sample prepared under similar conditions in the current study. Apart from the light-scattering results there is good correlation between the sets of data for the two samples. The uronic acid content, intrinsic viscosity, $\overline{DP}_w$ value, and virial coefficient from sedimentation equilibrium all agree within a few per cent. In contrast, $\overline{DP}_w$ from light scattering varies from 264 to 500, and there is a threefold discrepancy in the virial coefficients measured by the slope of the Hc/τ versus c plots. A major anomaly is the marked excess of the light-scattering molecular weight over the weight average found by sedimentation equilibrium.

The sedimentation equilibrium method was checked by sedimentation velocity and diffusion on master fraction No. 2.[20] The sedimentation constant from Fig. 6 was 0.425 S. As recorded in Part II of the series,[20] the diffusion constant of master fraction No. 2 was found to be 1.32×10^{-7} cm.^{2}/sec. Substitution into the Svedberg[27] equation gave a molecular weight of 24,900. For this fraction, $\bar{M}_w$ from sedimentation equilibrium was 25,000, and M_n from osmometry in DMSO was 22,500. For such low polydispersity, the molecular weight from the Svedberg equation would be very close to a weight average, particularly since the diffusion coefficient was determined by the area method.[10] Thus the excellent agreement between the molecular weights obtained by means of the two independent sedimentation techniques is strong confirmation of the validity of the ultracentrifugal methods.

The theoretical soundness of light scattering for the determination of molecular weights is often contrasted with the practical difficulties of applying the technique. Large discrepancies between molecular weights from light scattering and those computed from other methods have been reported. The anomalies have been ascribed to the presence of small amounts of colloidal material in the solution which are not effectively removed during the ultracentrifugation. Manley[41] observed that the light-

scattering molecular weights of ethyl hydroxyethyl cellulose were twice as great as those from sedimentation-diffusion and sedimentation equilibrium. Abe and Prins[42] also noted large discrepancies between the molecular weight measurements of polyanhydroglucose addition polymers by light scattering and by the Archibald technique. Similar results have been recently reported for carboxymethyl cellulose by Schurz[43] and by Sitaramaiah and Goring.[7]

An interesting observation can be made from Figure 7, where Hc/τ for the unfractionated xylan showed an upward curvature at the lower concentrations when the solutions were precentrifuged individually. The trend was reproducible for two runs. The negative slope is probably due to a more efficient removal of colloidal debris at the lower concentrations. Negative slopes to the Hc/τ versus c plots have also been reported by other workers.[44,45] A consequence of this effect is that even when positive slopes are obtained, the virial coefficient, B_{LS} is liable to be irregularly low. Significantly, there is a threefold discrepancy in B_{LS} for the two xylans in Table I, and the higher value which should equal B_e is only $^1/_4B_e$.

If the light-scattering molecular weights were too high because of contamination of the solution with colloidal debris, a more correct result would be expected for a xylan from which the high molecular weight material had been removed by fractionation. To test this, light-scattering measurements were made on the fifth fraction of an exploratory series, similar to the fractionations described in Part II.[20] The intrinsic viscosity of subfraction No. 5 in DMSO was 0.671 dl/g., which from eq. (4) in Part II corresponded to a sedimentation equilibrium $\overline{DP}_w$ of 155. The light-scattering molecular weight, corrected for a dissymmetry of 1.12, was 28,000. The uronic acid content was 10.2%. Thus from eqs. (6) and (7), $\overline{DP}_w = 191$. It is evident that the agreement between $\overline{DP}_w$ determined by sedimentation equilibrium and by light scattering is considerably better for subfraction No. 5 than for the unfractionated xylan in Table I. This result is an independent demonstration of the absence of any gross errors in the sedimentation equilibrium molecular weights.

Let us now consider the osmotic data. From Table I:

$$\frac{\overline{DP}_z \text{ (sed. equil.)}}{\overline{DP}_w \text{ (sed. equil.)}} = 1.36 \tag{9}$$

$$\frac{\overline{DP}_w \text{ (sed. equil.)}}{\overline{DP}_n \text{ (osm. in DMSO)}} = 1.18 \tag{10}$$

$$\frac{\overline{DP}_w \text{ (sed. equil.)}}{\overline{DP}_n \text{ (osm. in } CHCl_3\text{–}C_2H_5OH)} = 0.76 \tag{11}$$

If the imprecision of $\overline{DP}_z$ is taken into account, the results expressed in eqs. (9) and (10) are mutually consistent and support the correctness of the $\overline{DP}_n$ values from osmometry in DMSO. On the other hand, the result in

eq. (11) is untenable and suggests that the osmotic molecular weight in chloroform–ethanol is erroneously high.

Originally, 10% ethanol was added to the chloroform to eliminate association of the xylan in this solvent.[15] It was possible that some association remained giving high $\overline{DP}_n$ values even in the mixed solvent. In order to test this point, osmometry runs were made in chloroform–ethanol and in tetrachloroethane at higher temperatures. The results in Table II show a considerable decrease in $\overline{DP}_n$ with increase in temperature in chloroform–ethanol. A similar but smaller effect was found in tetrachloroethane. These results indicated that the association persisted at low temperatures and that an increase in temperature lowered the apparent molecular weight by thermal destruction of the aggregates.

The sedimentation equilibrium molecular weight in DMSO was constant for changes in temperature between 20 and 29°C. Apparently no molecular dissociation of xylan was taking place in DMSO in this temperature range. This indicated that the $\overline{DP}_n$ determined osmometrically in DMSO at 25°C. was representative of the unassociated xylan chain.

Further confirmation of the correctness of the results in DMSO is found in the ratio $B_e/B = 1.8$ (Table I) which theoretically should be 2.

The reasons for the discrepancies described in the above paragraphs may now be summarized as follows. (*a*) The light-scattering technique gives high and erratic molecular weights because of the presence of small proportions of colloidal debris in the solution. A representative weight-average molecular weight is given by the sedimentation equilibrium method. (*b*) Osmometry of xylan acetates in organic solvents tends to give high molecular weights because of molecular association. $\overline{DP}_n$ values for the unassociated chain are found by osmometry of the unsubstituted xylan in DMSO.

If the above assessment of the molecular weights by the various methods is correct, it means that much of the earlier work published by this and other laboratories on the molecular weight of hemicelluloses should be revised. This applies not only to the molecular weights themselves but also to conclusions drawn from the ratio of the degree of polymerization to the intrinsic viscosity. For example, it was pointed out in an earlier paper[3] that $[\eta]_{CED}/\overline{DP}_n$ was 4.7×10^{-3}, which was smaller than the value 8.1×10^{-3} quoted for cellulose in this molecular weight range by Immergut, Rånby, and Mark.[46] If the ratio is based on the $\overline{DP}_n$ of 151 for xylan in DMSO, a value of 6.1×10^{-3} is obtained, which is in better agreement with the figure of Immergut et al.[46] and in excellent agreement with a value of 6.2 from the data of Vink.[47] Similarly, the variation of $[\eta]_{CED}/\overline{DP}_n$ previously ascribed to uronic acid content may have been due to different degrees of association of the acetate in the chloroform–ethanol mixture used in osmometry.[3]

Revision of the estimate of the polydispersity of the xylan will also be

necessary, since the previous $\overline{DP}_w/\overline{DP}_n$ ratio of 2.4 was based on the erroneously high light-scattering molecular weights.[3] A low polydispersity for white birch xylan is indicated by the values of the ratios in eqs. (9) and (10). This supports the original proposal of Huesmann[48] and others[49,50] that xylan is extracted from wood in a relatively monodisperse state. It is also of interest that the $\overline{DP}_n$ of 151 is in good agreement with 150 found by Husemann[48] for beech xylan and 155 by Thompson and Wise[50] for aspen xylan. The light-scattering molecular weight of 175 for beech xylan determined by Horio et al.[44] is in excellent agreement with the sedimentation equilibrium value of 178 in Table I. This accord may be a fortuitous combination of degradation and light-scattering error, since the data of Horio et al. show some of the anomalies found in the present work, and their xylan was probably degraded.

A final word may be written concerning the insolubility of acetyl and other esters prepared by the method of Carson and Maclay.[34,35] This insolubility could possibly arise from the crosslinking of the polysaccharide chains during the esterification. Crosslinking may occur because of the presence of small quantities of crosslinking agents such as formaldehyde[51] as impurities. It also has been pointed out by Lindberg[52] that a portion of glucuronic acid in the xylan can be converted to a mixed glucuronic–acetic anhydride in the presence of acetic anhydride. The glucuronic–acetic anhydride formed can then in turn react with a neighboring xylan chain, and thus induce crosslinking. Whatever the cause of this effect, it is confusing that the method of Carson and Maclay yields a derivative which is sometimes completely soluble,[15] but often exhibits poor solubility as in this investigation. There can be no doubt that many of the anomalies in the molecular weight determinations would be resolved if more soluble derivatives were available. It is interesting to note that swelling of the polysaccharide in DMSO prior to acetylation gave a completely soluble derivative but with 35% degradation. The solubility may have been due to the elimination of the opportunity for crosslinking by the strong swelling effect of the DMSO. Further experiments may lead to a selection of conditions which would cause no degradation and yet yield a soluble derivative.

The authors are extremely grateful to Dr. R. F. Robertson for the use of his ultracentrifuge laboratory and to H. Sanderson for his assistance in running the ultracentrifuge.

References

1. Glaudemans, C. P. J., and T. E. Timell, *J. Am. Chem. Soc.*, **80,** 941 (1958).
2. Glaudemans, C. P. J., and T. E. Timell, *J. Am. Chem. Soc.*, **80,** 1209 (1958).
3. Goring, D. A. I., and T. E. Timell, *J. Phys. Chem.*, **64,** 1426 (1960).
4. Timell, T. E., *J. Am. Chem. Soc.*, **82,** 5211 (1960).
5. Banerjee, S. K., and T. E. Timell, *Tappi*, **43,** 849 (1960).
6. Jones, J. K. N., C. B. Purves, and T. E. Timell, *Can. J. Chem.*, **39,** 1059 (1961).
7. Sitaramaiah, G., and D. A. I. Goring, *J. Polymer Sci.*, **58,** 1107 (1962).
8. Yphantis, D. A., *Ann. N. Y. Acad. Sci.*, **88,** 586 (1960).
9. Van Holde, K. E., and R. L. Baldwin, *J. Phys. Chem.*, **62,** 734 (1958).
10. Rezanowich, A., W. Q. Yean, and D. A. I. Goring, *Svensk Papperstidn.*, in press.

11. Mosimann, H., *Helv. Chim. Acta*, **26**, 369 (1943).
12. Wales, M., *J. Phys. Colloid Chem.*, **55**, 282 (1951).
13. Hägglund, E., B. Lindberg, and J. McPherson, *Acta Chem. Scand.*, **10**, 1160 (1956).
14. Croon, I., and B. F. Enstrom, *Tappi*, **44**, 870 (1961).
15. Glaudemans, C. P. J., and T. E. Timell, *Svensk Papperstidn.*, **61**, 1 (1958).
16. Cowie, J. M. G., *Makromol. Chem.*, **42**, 230 (1961).
17. Cornell, R. H., and H. A. Swenson, *J. Appl. Polymer Sci.*, **5**, 641 (1961).
18. Cowie, J. M. G., and P. M. Toporowski, *Can. J. Chem.*, **39**, 2240 (1961).
19. LeBel, R. G., and D. A. I. Goring, *J. Chem. Eng. Data*, **7**, 100 (1962).
20. LeBel, R. G., and D. A. I. Goring, *J. Polymer Sci., Part C*, No. **2**, 29 (1963).
21. Johansson, A., B. Lindberg, and O. Theander, *Svensk Papperstidn.*, **57**, 41 (1954).
22. Gupta, P. R., and D. A. I. Goring, *Can. J. Chem.*, **38**, 248 (1960).
23. Clayton, D. W., *Svensk Papperstidn.*, in press.
24. Yoshino, T., and H. Tanzawa, *J. Chem. Phys.*, **36**, 2382 (1962).
25. Craig, A. W., and D. A. Henderson, *J. Polymer Sci.*, **19**, 215 (1956).
26. Huggins, M. L., *J. Am. Chem. Soc.*, **64**, 2716 (1942).
27. Svedberg, T., and K. O. Pedersen, *The Ultracentrifuge*, Oxford, 1940.
28. Schulz, G. V., *Z. Physik. Chem. (Leipzig)*, **A193**, 168 (1944).
29. Wales, M., M. Bender, J. W. Williams, and R. H. Ewart, *J. Chem. Phys.*, **14**, 353 (1946).
30. Ginsberg, A., P. Appel, and H. K. Schachman, *Arch. Biochem. Biophys.*, **65**, 545 (1956).
31. Schachman, H. K., *Ultracentrifugation in Biochemistry*, Academic Press, New York, 1959.
32. Huque, M. M., J. Jaworzyn, and D. A. I. Goring, *J. Polymer Sci.*, **39**, 9 (1959).
33. Goring, D. A. I., M. Senez, B. Melanson, and M. M. Huque, *J. Colloid Sci.*, **12**, 412 (1957).
34. Carson, J. F., and W. D. Maclay, *J. Am. Chem. Soc.*, **68**, 1015 (1946).
35. Carson, J. F., and W. D. Maclay, *J. Am. Chem. Soc.*, **70**, 293 (1948).
36. Genung, L. B., and R. C. Mallat, *Ind. Eng. Chem. Anal. Ed.*, **13**, 369 (1941).
37. Stabin, J. V., and E. H. Immergut, *J. Polymer Sci.*, **14**, 209 (1954).
38. Zimm, B. H., and I. Myerson, *J. Am. Chem. Soc.*, **68**, 911 (1946).
39. Whistler, R. L., and A. Jeanes, *Ind. Eng. Chem. Anal. Ed.*, **15**, 317 (1943).
40. Peterson, F. C., A. J. Barry, H. Unkauf, and L. E. Wise, *J. Am. Chem. Soc.*, **62**, 2361 (1940).
41. Manley, R. St. J., *Arkiv Kemi*, **9**, 519 (1956).
42. Abe, H., and W. Prins, *Makromol. Chem.*, **42**, 216 (1961).
43. Schurz, W. J., *Das Papier*, **14**, 518 (1960).
44. Horio, M., R. Imamura, and H. Inagaki, *Tappi*, **38**, 216 (1955).
45. Svenson, H. A., A. J. Morak, and S. Kurath, *J. Polymer Sci.*, **51**, 231 (1961).
46. Immergut, E. H., B. G. Rånby, and H. F. Mark, *Ind. Eng. Chem.*, **45**, 2483 (1953).
47. Vink, H., *Arkiv. Kemi*, **14**, 195 (1959).
48. Husemann, E., *J. Prakt. Chem.*, **155**, 13 (1940).
49. Millet, M. A., and A. J. Stamm, *J. Phys. Colloid Chem.*, **51**, 134 (1947).
50. Thompson, J. O., and L. E. Wise, *Tappi*, **35**, 331 (1952).
51. Hurwitz, M. D., and L. E. Colon, *Textile Res. J.*, **28**, 257 (1958).
52. Lindberg, B., private communication.

Synopsis

A 4-*O*-methyl-D-glucuronoxylan was prepared from white birch wood meal by direct extraction with alkali. The acidic form of the polysaccharide was found to be soluble in pure dimethyl sulfoxide (DMSO) but the potassium salt required addition of 12% by weight of water to induce complete solubility. The weight-average degree of polymerization $\overline{DP}_w$ of the acidic polysaccharide was 178 by the short-column sedimen-

tation equilibrium method. The molecular weight by sedimentation equilibrium was in very good agreement with the value determined by sedimentation velocity and diffusion measurements. Light-scattering molecular weights were erroneously high and virial coefficients erratically low because of the presence of a small proportion of diffcultly removed collodial debris in the solutions. Osmometry on the acetate derivative gave $\overline{DP}_n$ higher than $\overline{DP}_w$ by sedimentation equilibrium. A marked decrease in $\overline{DP}_n$ was found at higher temperatures. This indicated that at room temperature molecular association of the xylan acetate was taking place in the organic solvents used. Osmometry of xylan in DMSO gave $\overline{DP}_n = 151$ and $\overline{DP}_w/\overline{DP}_n = 1.18$, which demonstrated a low polydispersity of the polysaccharide when extracted from the wood.

Résumé

On a préparé le 4-*O*-méthyl-D-glucuronoxylane à partir de sciure de bois de bouleau blanc, par extraction directe avec un alcali. On a trouvé que le forme acide du polysaccharide était soluble dans le diméthylsulfoxyde pur (DMSO) mais que pour réaliser une solubilité complète du sel potassique, il était nécesssaire d'ajouter 12% en poids d'eau. Le degré de polymérisation moyen en poids $\overline{DP}_w$ du polysaccharide acide mesuré par la méthode de l'équilibre de sédimentation en colonne courte est de 178. Le poids moléculaire trouvé par équilibre de sédimentation est en excellent accord avec la valeur déterminée par des mesures de vitesse de sédimentation et de diffusion. Les poids moléculaires déterminés par diffusion lumineuse sont anormalement élevés et les coefficients du viriel trop bas par suite de la présence dans la solution de petites quantités de fragments colloïdaux difficles à éliminer. Les mesures d'osmose effectués sur l'acétate donnent un $\overline{DP}_n$ plus élevé que $\overline{DP}_w$ fourni par l'équilibre de sédimentation. On a observé une décroissance marquée de la valeur de $\overline{DP}_n$, aux plus hautes températures. Ceci indique qu'à température de chambre, l'association moléculaire de l'acétate du xylane se produit dans les solvants organiques utilisés. Les mesures d'osmose effectués sur le xylane dans le DMSO fournissent un $\overline{DP}_n$ de 151 et un rapport $\overline{DP}_w/\overline{DP}_n$ de 1.18 ce qui est l'indice d'une faible polydispersité du polysaccharide quand il a été extrait du bois.

Zusammenfassung

Ein 4-*O*-Methyl-D-glucuronoxylan wurde aus Weissbirken-Holzmehl durch direkte Extraktion mit Alkali dargestellt. Die saure Form des Polysaccharids war in reinem Dimethylsulfoxyd (DMSO) löslich, das Kaliumsalz erforderte hingegen zur vollständigen Löslichkeit einen Zusatz von 12 Gewichtsprozent Wasser. Nach der Methode des Sedimentationsgleichgewichts mit kurzer Säule betrug das Gewichtsmittel des Polymerisationsgrades $\overline{DP}_w$ des sauren Polysaccharides 178. Das aus dem Sedimentationsgleichgewicht erhaltene Molekulargewicht stimmte gut mit dem aus Sedimentationsgeschwindigkeit und Diffusion bestimmten Wert überein. Lichtstreuungs-Molekulargewichte waren wegen der Anwesenheit eines kleinen Anteils schwer zu entfernender kolloider Bruchstücke in der Lösung unverlässlich und zu hoch und die Virialkoeffizienten zu niedrig. Osmotische Messungen am Acetat lieferten ein $\overline{DP}_n$, das höher war als $\overline{DP}_w$ aus dem Sedimentationsgleichgewicht. Bei höherer Temperatur trat eine merkliche Abnahme von $\overline{DP}_n$ auf. Das spricht dafür, dass in den verwendeten organischen Lösungsmitteln bei Raumtemperatur eine Assoziation der Xylanacetatmoleküle auftritt. Osmotische Messungen an Xylan in DMSO lieferte $\overline{DP}_n = 151$ und $\overline{DP}_w/\overline{DP}_n = 1{,}18$, was eine geringe Polydispersität des aus dem Holz extrahierten Polysaccharids erkennen lässt.

JOURNAL OF POLYMER SCIENCE: PART C NO. 2, PP. 29–48 (1963)

Solution Properties of Birch Xylan. II. Fractionation and Configuration

R. G. LEBEL* and D. A. I. GORING, *Physical Chemistry Division, Pulp and Paper Research Institute of Canada, and Department of Chemistry, McGill University, Montreal, Canada*

INTRODUCTION

The first part of this investigation[1] presents a critical study of the methods for the determination of the molecular weight of white birch xylan. It was concluded that short-column sedimentation equilibrium with dimethyl sulfoxide as solvent yields correct values of the weight-average molecular weight. Henceforth in this paper, $\bar{M}_w$, $\overline{\mathrm{DP}}_w$, $\bar{M}_z$, and $\overline{\mathrm{DP}}_z$ will refer to molecular weights and degrees of polymerization determined by the sedimentation equilibrium technique.

The work to be described in the present section deals with the fractionation of white birch xylan and the physicochemical characterization of the fractions. Relatively few attempts have been made to fractionate a pure xylan according to molecular size. Husemann[2] fractionated a variety of xylans by adding methanol to a solution of the hemicellulose in 6% sodium hydroxide. Little resolution of intrinsic viscosity was obtained, and Husemann concluded that the xylan was uniform in molecular size. Glaudemans and Timell[3] fractionated solutions of white birch xylan in 5% potassium hydroxide using methanol and ethanol as precipitants. Methanol gave no fractionation with respect to chain length whereas a range of intrinsic viscosities was found in fractions precipitated with ethanol. Glaudemans and Timell[3] have also fractionated xylan in dimethyl sulfoxide by addition of ethanol. Fractionation occurred according to both intrinsic viscosity and uronic acid content. In the present investigation dimethyl sulfoxide has been used as an alternative to alkali as a solvent because of the possibility of degradation by alkali over the long times required to secure an efficient fractionation.

Many investigations have been published in which the variations of properties such as intrinsic viscosity or diffusion coefficient have been studied as a function of the molecular weight of a polymer. The various hydrodynamic theories of polymers[4–6] have been tested by their application to such data obtained over a series of well-defined fractions.[7–10] Con-

* Holder of a National Research Council of Canada Studentship (1960–62); present address: Anglo Paper, Quebec City, Canada.

versely, the molecular weight dependence of the intrinsic viscosity or diffusion coefficient can be used to elucidate the configuration of relatively unknown macromolecular systems derived from biological materials.[11-13] In the present work, the latter approach has been taken. The effect of the uronic acid side groups on the chain extension in the two solvents, dimethyl sulfoxide (DMSO) and cupriethylenediamine (CED) is considered and certain conclusions are drawn concerning the configuration of the molecule in comparison to cellulose under similar conditions of solvent and molecular weight.

The application of the hydrodynamic analysis as outlined above is based on the measurement of parameters such as the intrinsic viscosity and diffusion coefficient over a wide range of molecular weights. In Part I it was shown that the xylan as extracted from birch wood was relatively monodisperse.[1] This is confirmed in the present work by the narrow range of intrinsic viscosities found on fractionation. In order to extend the range of molecular weights an exploratory study was made of the acidic degradation of white birch xylan at 70°C. Low molecular weight fractions were then obtained by fractionation of a sample of xylan degraded under controlled conditions. In this manner the molecular weight range was extended satisfactorily.

EXPERIMENTAL RESULTS

The measurement of lignin content, uronic acid content, partial specific volume, and intrinsic viscosity were as described previously.[1]

Degraded Xylan

To extend the range in the low molecular weight region, xylan was degraded in an acidified DMSO medium, and the extent of chain breaking was measured viscometrically. To a 1% solution, concentrated HCl (12*N*) was added slowly until a pH value of 1 was indicated by measurement with a Beckman pH meter. The total time of acid addition was 30 ± 1 min. The temperature of the mixture was raised thereafter at 4°C./min. to 70 ± 1°C. and then maintained at this temperature. The solution was vigorously stirred during the entire course of the experiment.

After a predetermined period of hydrolysis, the solution was poured into five volumes of ethyl acetate containing 20% ethanol. The latter was found to prevent the formation of two liquid phases. Instantaneous precipitation occurred. The white, fluffy precipitate was centrifugally recovered and washed with 90% acetone until the supernatant became free of chloride ions. The precipitate was washed with dry acetone and petroleum ether, and then dried in vacuum over magnesium perchlorate.

By varying the time of hydrolysis, intrinsic viscosities between 0.7 and 0.06 dl./g. were obtained as shown in Figure 1. The time of acid addition (30 min.) plus the time of heating (10 min.) were converted into an approximately equivalent value of 5 min. at 70°C. by assuming that the rate of

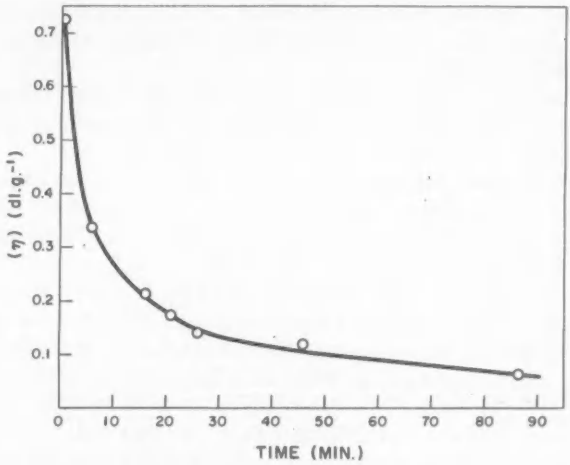

Fig. 1. The variation of $[\eta]$ with time of hydrolysis of acidic xylan.

hydrolysis was doubled by every 10° increase in the temperature. From these data, conditions were chosen under which a 12 g. batch of hydrolyzed xylan of intrinsic viscosity 0.36 dl./g. was prepared. On fractionation this was found to extend the viscosity range satisfactorily.

The potassium content of hydrolyzed xylan was found to be 0.1% which was the same as in the acidic form of the xylan prior to degradation.[1] The degraded xylan was found to contain 11.0% uronic acid, showing little change from the value of 11.4% for the undegraded sample.[1]

The results in Figure 1 show that there is an initial rapid chain breaking followed by a leveling-off of intrinsic viscosity at approximately 50 min. of hydrolysis. Meier[14] has shown that a rapid initial hydrolysis takes place in white birch xylan on acid cooking. Also the hydrolysis curve in Figure 1 is similar to the well-known pattern of acid degradation of cellulose.[15,16] Marchessault and Ranby[17] have pointed out that the inductive effect of glucuronic acid groups should produce weak links in the main chain which may give rise to an initial rapid reduction in the degree of polymerization. The present results though fragmentary are consistent with the proposal of weak links in the xylan chain.

Fractionation

Method. Xylan was fractionated by precipitation from DMSO with ethanol at 25°C. Ethanol was added dropwise until a very slight haze appeared. By visual inspection, it was not possible to tell when the correct amount of precipitant had been added. A Beckman DU spectrophotometer was used to evaluate the turbidity. By trial and error, it was found that a suitable fractionation occurred when enough ethanol was added until a transmittance of 85–90% was observed at a wave length

of 500 mμ. Extreme care was necessary in the precipitation of the first fraction, since a slight excess of ethanol would produce a large quantity of precipitated material.

After addition of the precipitant the system was allowed to stand for at least 20 hr. to establish equilibrium between the two phases. The turbidity of the solution was found to increase upon standing.

The precipitates were separated by centrifugation. The residues in the centrifuge cups, gellike in appearance, were transferred into a sintered glass filter and washed thoroughly with ethanol and petroleum ether. Final drying was over magnesium perchlorate *in vacuo*.

Details of a fractionation are given in Table I. Eight fractions were obtained over a total period of about 14 days. A ninth fraction was recovered by pouring the final clear supernatant into a large excess of ethyl acetate. Three batches (3 g. each) of xylan were fractionated after the manner shown in Table I. The average recovery was 93%. A range of intrinsic viscosity of only 0.88 to 0.45 dl./g. was obtained.

TABLE I
Fractionation of Xylan, 3 g. Batch No. 1

Fraction	EtOH, ml.	Transmission, %	Wt., g.	$[\eta]$, dl./g.
1	108	90	0.31	—
2	—[a]	86	0.21	0.82
3	9.7	87	0.30	0.78
4	9.5	89	0.34	0.76
5	30.7	90	0.36	0.67
6	15.2	89	0.28	0.62
7	32.4	89	0.33	0.57
8	60.9	86	0.23	0.55
9	150	—	0.10	0.45

[a] After separation of fraction No. 1, the turbidity of the solution continued to increase. Thus no further addition of ethanol was required for the precipitation of fraction No. 2.

In order to extend the range of viscosity, three batches (3 g. each) of the degraded xylan were fractionated, and intrinsic viscosities of between 0.14 and 0.46 dl./g. were realized. The samples obtained by fractionation of the undegraded xylan were all soluble in DMSO. Similarly, the degraded xylan itself gave clear solutions. However, the initial fraction of the degraded xylan after precipitation, isolation, and drying was largely insoluble. The subsequent fractions retained their solubility. The insoluble first fraction accounted for about 30% of the degraded material and had a uronic acid content of only 7.0%. The reason for this interesting phenomenon is dealt with in a later section.

Master Fractions. Each fraction was characterized by its intrinsic viscosity in DMSO. For the subsequent hydrodynamic studies, master fractions were made up by blending subfractions of nearly identical intrinsic viscosity. The selection of subfractions for master fractions is

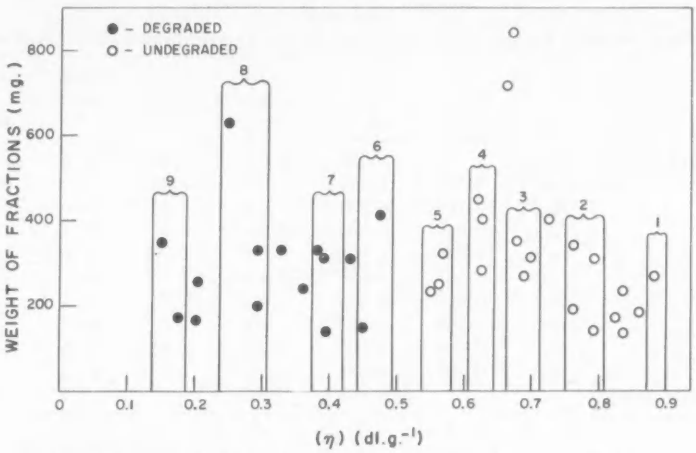

Fig. 2. Selection of subfractions for the composition of master fractions.

shown in Figure 2. Nine master fractions of sufficient weight representing as wide a range as possible of $[\eta]$ values were made up. Master fractions Nos. 1–5 were made up of subfractions from the undegraded xylan while master fractions Nos. 6–9 were comprised of degraded xylan subfractions. To eliminate insoluble xylan, lignin, and other unwanted foreign materials, the first and final subfractions of each series were not used. Bulky subfractions were also rejected because of their possible heterogeneity. The selected subfractions were dissolved in DMSO and homogeneously blended and the master fraction was recovered by precipitation in ethyl acetate, washing with ethanol and petroleum ether and drying over magnesium perchlorate.

Uronic acid contents of the master fractions are given in Table II. The trend shown by master fractions Nos. 1–5 and also Nos. 6–9 indicates that the uronic acid content increases as the fractionation proceeds. This was confirmed for three fractions of an exploratory fractionation for which the uronic acid content increased from 8.6 to 13.4% from the first to the final fraction.

Examples of η_{sp}/c versus c in DMSO and CED which were given in Part I of the series[1] illustrate the precision of the viscometric data for the master fractions. In neither solvent was there evidence of an increase of η_{sp}/c with decrease in c as would be expected for an ionizing polyelectrolyte in a solvent of low ionic strength.[18] The intrinsic viscosities obtained from the least square lines are given in Table II. For comparison, the weight-average intrinsic viscosity, $[\eta]_w$ for each master fraction in DMSO was computed from the weight and $[\eta]$ of the subfractions. The excellent agreement between $[\eta]$ and $[\eta]_w$ for the master fractions is a further illustration of the precision of the viscometric data and of the correctness of the procedure for preparing the master fractions.

TABLE II
Intrinsic Viscosity, Uronic Acid Content, and Weight-Average Degree of Polymerization

Sample	$[\eta]_w$, dl./g.	$[\eta]$, dl./g.	$[\eta]_{CED}$, dl./g.	$\frac{[\eta]_{CED}}{[\eta]}$	Uronic acid, %	$\overline{DP}_w$
Unfractionated xylan		0.720	0.917	1.28	11.4	178
Master fraction No. 1	0.877	0.877	1.222	1.40	8.2	194
No. 2	0.768	0.752	1.023	1.34	9.0	173
No. 3	0.682	0.663	0.866	1.31	10.4	155
No. 4	0.622	0.606	0.814	1.33	11.6	146
No. 5	0.557	0.580	0.742	1.28	13.7	133
No. 6	0.457	0.448	0.536	1.18	10.5	113
No. 7	0.369	0.383	0.402	1.04	12.3	85
No. 8	0.254	0.245	0.258	1.04	13.9	55
No. 9	0.151	0.153	0.147	0.96	14.2	31
Neutral xylan	—	0.654	—	—	2.2	163

The ratio of the intrinsic viscosity in CED, $[\eta]_{CED}$ to the value in DMSO, $[\eta]$ is also included in Table II. A definite trend in $[\eta]_{CED}/[\eta]$ can be observed, ranging from 1.40 to 0.96 from high to low molecular weights.

Some data are included in Table II for a neutral glucoxylan previously described by Bowering, Marchessault, and Timell.[19] The xylan was prepared by reduction of an esterified white birch glucuronoxylan and contained only a trace of acid groups.

Diffusion

Area diffusion coefficients were measured in the Zeiss diffusion interferometer as described previously for organosolv lignins.[20] For the more slowly diffusing xylan molecules it was necessary to mount the diffusion apparatus on a heavy steel table resting on a solid concrete floor so as to minimize vibrational disturbances. When these precautions were not observed, the interferograms were not reproducible and, in some cases, became visibly distorted. Care was taken to avoid water uptake by the

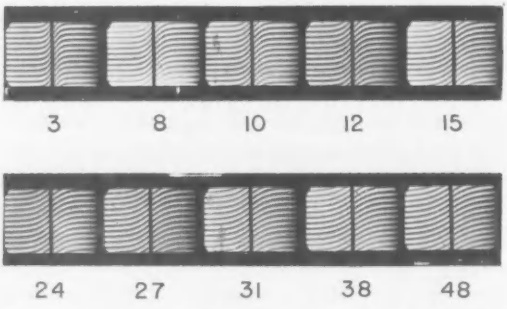

Fig. 3. Diffusion interferograms for master fraction No. 4 at $\bar{c}$ = 0.42 g./dl. The time in hours is shown under each of the pictures.

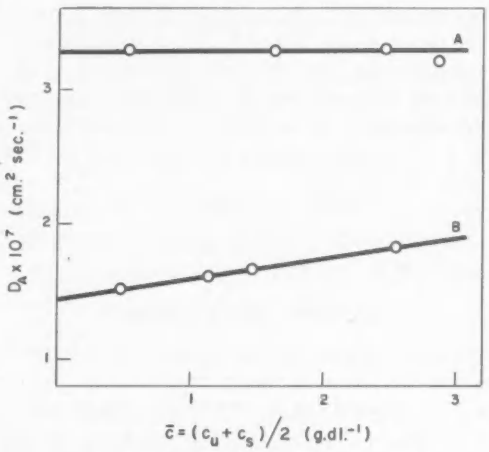

Fig. 4. Concentration dependence of D_A for a high and low molecular weight fraction: (*A*) $DP_w = 43$; (*B*) $\overline{DP}_w = 160$.

solvent because this produced marked distortion of the boundary. Photographs were taken at intervals of about 4 hr. over a period of 20–40 hr. depending on the rate of diffusion observed. The interferograms (Fig. 3) were enlarged and measured, and D_A computed at 25°C. as previously described.[20] The reproducibility of duplicate runs was 1%, and D_A measured for sucrose was 1.2% lower than the value of Gosting and Morris.[21]

To determine the concentration dependence of the diffusion coefficients, measurements were carried out on a high and low molecular weight subfraction at a series of concentrations ranging from 0.5 to 3 g./dl. A plot of the values of D_A against the average concentration, $\bar{c} = (c_u + c_s)/2$,

TABLE III
Sedimentation Equilibrium and Diffusion Data

Sample	$\bar{M}_w$	$\bar{M}_w$LK	$\bar{M}_z$	$\bar{M}_z/\bar{M}_w$	$B_e \times 10^3$, mole ml./g.^{2}	$D_A \times 10^7$, cm.^{2}/sec.
Unfractionated xylan	26500	25900	36000	1.36	5.30	—
Master fraction No. 1	27800	28000	30200	1.09	4.25	1.17
No. 2	25000	24600	35500	1.42	4.18	1.32
No. 3	22800	23500	27400	1.20	4.15	1.44
No. 4	21700	21700	27900	1.28	4.27	1.51
No. 5	20300	21100	28300	1.39	4.32	1.61
No. 6	16600	16900	22600	1.36	4.69	1.92
No. 7	12800	11400	15000	1.17	4.68	2.45
No. 8	8400	8000	16000	1.91	4.84	3.30
No. 9	4800	4600	—	—	8.65	4.97
Neutral xylan	24200	—	—	—	5.74	—

where c_u and c_s are respectively the concentration above and below the initial boundary, is shown in Figure 4. It is seen that for the low molecular weight xylan, the concentration dependence of D_A is negligible, whereas, for the high molecular weight material, D_A increases linearly with c. Diffusion measurements were made on each master fraction at a concentration of 1 g./dl. against solvent ($\bar{c}$ = 0.5 g./dl.). The values of D_A reported in Table III for master fractions Nos. 6, 7, 8, and 9 have been assumed independent of xylan concentration. A correction of -2% was applied to the higher molecular weight fractions to allow for the slight concentration dependence in Figure 4.

Refractive Index Increment

Values of dn/dc were calculated directly from the diffusion interferograms and the known concentration of xylan in the solution. An average of 0.062 $\pm$0.003 ml./g. was obtained for dn/dc from 27 determinations on different solutions and fractions of xylan. No trend with molecular weight or uronic acid content was observed. This value is comparable with 0.064 $\pm$0.006 ml./g. which was measured in a Brice-Phoenix differential refractometer as previously reported.[22]

Sedimentation Equilibrium

Weight-average and Z-average molecular weights of the master fractions were measured by means of the short-column sedimentation equilibrium technique of Van Holde and Baldwin[23] as described in Part I of the series.[1] The quality of the data is illustrated in Figure 4 of Part I.

Values of $\bar{M}_w$ and $\bar{M}_z$ are listed in Table III. Also included are the results for the second virial coefficient B_e determined from the concentration dependence of $\bar{M}_w$. The weight-average degree of polymerization, $\overline{\mathrm{DP}}_w$ was calculated from $\bar{M}_w$ as described previously[1] and is given in Table II.

Because of the distortion at the base and meniscus of the cell,[24] $\bar{M}_z$ was precise to no more than $\pm 20\%$. Therefore the ratio $\bar{M}_z/\bar{M}_w$ in Table III should be regarded as an indication of polydispersity rather than an exact measure. The erratic variations in $\bar{M}_z/\bar{M}_w$ are probably due to this inaccuracy in the determination of $\bar{M}_z$ rather than to abrupt changes in distribution from fraction to fraction.

The sedimentation equilibrium technique was tested by a calculation of the weight-average molecular weight $\bar{M}_{wx}$ at various depths of the cell. Appropriate experimental values of dn/dx and concentration (obtained graphically) were substituted into the sedimentation equilibrium equation [eq. (2), Part I]. The increase in $\bar{M}_{wx}$ from the meniscus to the base of the cell was usually less than 20%. A weight average throughout the cell was obtained from the equation of Lansing and Kraemer:[25]

$$\bar{M}_w(\mathrm{LK}) = \int \bar{M}_{wx}\, x\, c_x dx / \int x\, c_x\, dx \qquad (1)$$

The Lansing and Kraemer analysis was made for the master fractions at a series of concentrations. Values of $\bar{M}_w$(LK) at c = 0 were obtained

by linear extrapolation of $1/\bar{M}_w$(LK) versus c and are given in Table III. It is seen that the weight-average molecular weight computed by the Lansing and Kraemer integration was in good agreement with $\bar{M}_w$ obtained by the hinge point method of Van Holde and Baldwin.[23]

DISCUSSION

Molecular Heterogeneity

The fractionation results showed clearly that the xylan was being fractionated with respect to uronic acid as well as molecular weight. Xylan low in uronic acid is precipitated first during the fractionation process. This selection is superimposed on the initial precipitation of high molecular weight fractions. Therefore a trend of increasing uronic acid with decrease in molecular weight is realized. This result supports conclusively the earlier findings of Glaudemans and Timell.[3] Xylans of varying uronic acid content have been reported by Bjorkqvist and Jörgensen,[26] who found that the hemicellulose fractions obtained from the sequential extraction of a birch holocellulose preswollen in liquid ammonia showed a uronic acid content ranging from 4.9 to 17.9%. Similarly Croon and Enström[27] showed that during a fractional extraction of a birch holocellulose with alkali, the most easily extracted xylan contained more uronic acid.

Clayton[28] has shown that the glycosidic bond between the 4-*O*-methylglucuronosyl groups and the main chain is not as unstable to alkali as expected.[29,30] The extraction with 24% aqueous KOH at room temperature employed in the present work was not likely to remove any uronic acid side chains from the xylan. Also cleavage of the main chain was probably minimal. Thus the xylan in white birch must be deposited in the cell with individual molecules having varying proportions of uronic acid on the polyanhydroxylose backbone.

It is interesting to note in Table II that the trend in uronic acid content for master fractions Nos. 1–5 is repeated in master fractions Nos. 6–9 from the degraded xylan. Significantly, the insoluble first fraction which accounted for 30% of the degraded xylan had only 7.0% uronic acid. Several reasons, other than its low uronic acid content for the insolubility of the first fraction of the degraded xylan were considered and tested. The formation of disulfide or sulfhydryl bridges between the xylan chains might have occurred, the presence of sulfur being attributed to the possible decomposition of DMSO. Sulfur analyses were made on a number of fractions in a Leco apparatus. The presence of sulfur could not be detected. This proved not only the absence of chemically combined sulfur but also that the fractions had been properly washed free of DMSO. Cationic crosslinking by divalent ions could also have produced the insolubility of the first fraction. A suspension of the insoluble xylan was shaken in DMSO in the presence of a small amount of Dowex 50 cation exchange resin. After two weeks of shaking, no noticeable increase in solubility was observed. The possibility of producing an insoluble product by the reaction

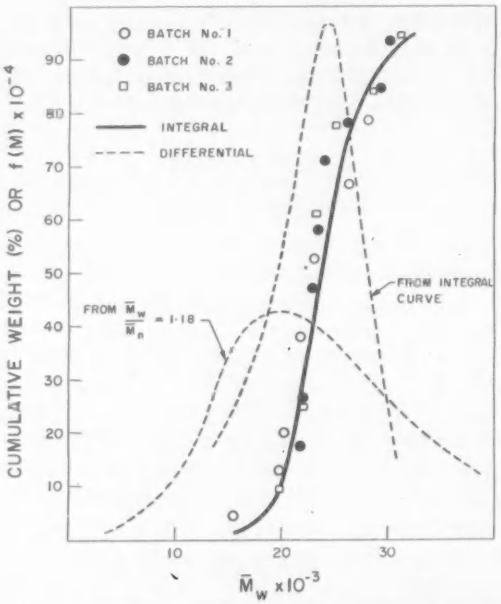

Fig. 5. A cumulative weight distribution for the fractionation of the undegraded xylan: (——) mean for the three fractionations; (- -) differential distributions from (*a*) the integral curve and (*b*) the log exponential distribution for $\bar{M}_w/\bar{M}_n = 1.18$.

of DMSO with HCl was considered. A control hydrolysis was performed in the absence of xylan. No precipitation or turbidity was found to take place when the reaction mixture was poured into ethyl acetate.

The consistently negative result of the above tests suggested that the insolubility of the first fraction from the degraded xylan was due to the low uronic acid content of the molecule.[27,29] Low uronic acid content will make possible closer alignment of the chain molecules and promote intermolecular hydrogen bonding. Alignment would produce a more orderly arrangement of the hemicellulosic chains, which in turn would probably be detectable by means of an x-ray diffraction analysis. Samples of an initially precipitated fraction and a soluble fraction were analyzed by the x-ray technique described by Ruck, Kouris, and Manley.[31,32] A broad diffused ring indicating an amorphous structure was obtained for the soluble fraction. A discernably sharper ring was obtained for the insoluble material, which corresponds to the 4.98 A. spacing found by Marchessault and Timell[33] for crystalline xylan. This result therefore supports the proposal that the insolubility of part of the degraded xylan was due to its tendency to form aggregated structures of ordered chains held together by hydrogen bonds. It is important to distinguish between this effect and the solubility of a synthetic polymer which depends on the solute–solvent interaction along the entire polymer chain. For glucuronoxylan in DMSO,

solubility is more likely to be governed by the ability of the irregularly spaced uronic acid groups to prevent formation of ordered structures by interchain association. Therefore, the uronic acid content would not necessarily be expected to influence the configuration of the molecule in the same way that flexible polymer molecules swell or shrink in good or bad solvents.[34]

We may now consider by how much the variation in uronic acid content suppressed the fractionation with respect to molecular weight. In Figure 5 an integral distribution curve of molecular weight is drawn for the three fractionations of the undegraded xylan; $\bar{M}_w$ was computed for each subfraction from $[\eta]$ by means of an equation analogous to eq. (4). The reproducibility was good if the well-known variability of fractionation data is taken into account. The range in $\bar{M}_w$ was extremely narrow. The ratio of $\bar{M}_w/\bar{M}_n$ computed statistically from $\bar{M}_w$ and the weight of each fraction was only 1.03. As shown in the preceding paper of the series,[1] $\overline{\mathrm{DP}}_w/\overline{\mathrm{DP}}_n$ from osmometry and sedimentation equilibrium of the xylan in DMSO was 1.18. In Figure 5, a logarithmic exponential distribution[25] corresponding to $\bar{M}_w/\bar{M}_n = 1.18$ is compared with the mean experimental differential distribution for the three parallel fractionations. It is clear that the experimental distribution curve is considerably sharper than the theoretical distribution based on $\bar{M}_w/\bar{M}_n = 1.18$. Thus the somewhat low efficiency of the fractionation with respect to molecular weight is demonstrated.

A $\overline{\mathrm{DP}}_w/\overline{\mathrm{DP}}_n$ ratio of 1.18 is small compared with the value of 2 for the "normal" distribution found in synthetic palymers.[34] Thus the true polydispersity of the hemicellulose was not great even though it was obscured by the suppression of fractionation due to the variation in uronic acid content. Previous work on xylan has indicated an arrow distribution of molecular sizes.[2,35,36] Perhaps the widest range of intrinsic viscosities was reported by Glaudemans and Timell[3] for fractionation from aqueous KOH with ethanol as precipitant. Their data yielded a $\overline{\mathrm{DP}}_w/\overline{\mathrm{DP}}_n$ ratio of 1.22 which agrees favorably with the present value of 1.18 from number-average and weight-average molecular weights of the unfractionated xylan. One of the few manifestations of a wide polydispersity in hardwood xylans has been the average of 2.4 reported by Goring and Timell[22] for $\overline{\mathrm{DP}}_w/\overline{\mathrm{DP}}_n$ from light scattering and osmometry. In Part I of the series[1] it was demonstrated that the molecular weight determined by the light-scattering technique were erroneously high. Therefore the ratio of 2.4 for $\overline{\mathrm{DP}}_w/\overline{\mathrm{DP}}_n$ must be regarded as being too high also.

Because of the low polydispersity of the undegraded xylan, fractions from this material would be expected to be relatively monodisperse. Three independent methods of obtaining molecular weight averages were applied to master fraction No. 2, namely $\bar{M}_n$ from osmotic pressure[1] $\bar{M}_{sD}$ from sedimentation velocity-diffusion,[1] and $\bar{M}_w$ from sedimentation equilibrium. The results gave

$$\bar{M}_w:\bar{M}_{sD}:\bar{M}_n = 1.11:1.10:1 \qquad (2)$$

which confirmed small polydispersity. If the unusually high value for master fraction No. 8 is omitted, the mean $\bar{M}_z/\bar{M}_w$ ratio in Table III is 1.27. No marked increase is noted for master fractions Nos. 6 and 7 from the degraded xylan. Thus, comparison of $\bar{M}_w$ with $\bar{M}_z$ in spite of the imprecision of the latter, supports a rather low polydispersity of molecular weight for the master fractions.

Configuration

It is of interest now to discuss to what extent the uronic acid side chains influenced the configuration of the molecule in solution. The trend of uronic acid content with $\overline{DP}_w$ is shown in Figure 6. It is seen that a prominent "step" in uronic acid content occurred between master fractions Nos. 5 and 6 corresponding to the division between fractions from the undegraded and degraded xylan. There was no parallel step in the graph of $[\eta]$ versus $\overline{DP}_w$ in either DMSO or CED as solvent. Similarly there was no trace of a uronic acid induced step in the variation of D_A with $\overline{DP}_w$ shown in Figure 6. The point for the neutral xylan[19] in Figure 7 was found

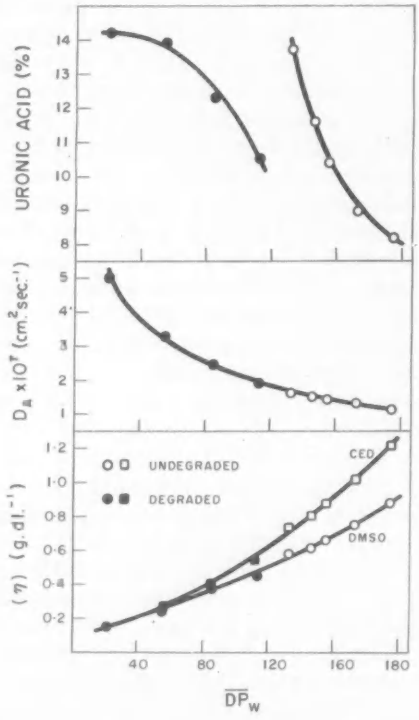

Fig. 6. Variation of intrinsic viscosity, diffusion constant, and uronic acid with degree of polymerization of the master fractions.

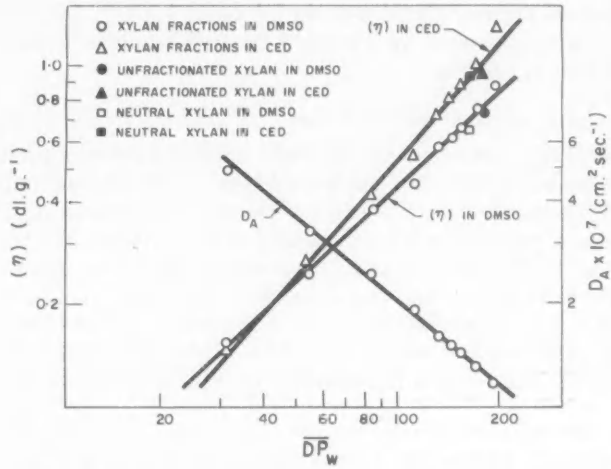

Fig. 7. Double logarithmic plots of $[\eta]$ and D_A vs. $\overline{DP}_w$ for various samples of white birch xylan. The $[\eta]$ value for the point for neutral xylan in CED was taken from the data of Bowering et al.[19]

to lie within experimental error of the log $[\eta]$ versus log $\overline{DP}_w$ lines for the acidic xylans in DMSO or CED. This confirms the result of Bowering, Marchessault, and Timell[19] and proves incorrect the previous suggestion that the viscosity in CED was sensitive to the uronic acid content because of polyelectrolyte expansion of the xylan chain.[22]

The intrinsic viscosity is a measure of the effective hydrodynamic volume of a macromolecule in solution. The diffusion constant varies inversely as the radius of the equivalent hydrodynamic sphere. Therefore D_A and more particularly $[\eta]$ would be sensitive to changes in the configuration. The independence of $[\eta]$ and D_A to uronic acid content shows that the side chains have little effect on the extension of the xylan molecule in solution. This is in contrast to the behavior of substituted cellulose derivatives. The intrinsic viscosities of highly substituted cellulose nitrates are markedly dependent on the degree of substitution, DS.[37] Cornell and Swenson[38] have shown that the constant K in eq. (3) is almost doubled when DS for diethylacetamide cellulose xanthate increases from 0.4 to 1.2. If the uronic acid side chain is considered a substituent on the xylose, the DS for the fractions in Table II ranged from 0.07 to 0.12. This corresponds to contour separations on the main chain of 40–70 A., to be compared with 5 A. for a monosubstituted cellulose. It is therefore not surprising in view of their wide physical separation that the uronic acid groups have little effect on the configuration of the xylan chain.

Let us now consider the variation of $[\eta]$ with $\overline{DP}_w$ in terms of the familiar Mark-Houwink equation

$$[\eta] = K\overline{DP}_w{}^a \tag{3}$$

As shown in Figure 7 the plot of log $[\eta]$ versus log $\overline{DP}_w$ for DMSO as solvent is well represented by a straight line with relatively little scatter. From the least square line

$$[\eta] = 5.9 \times 10^{-3} \overline{DP}_w^{0.94} \tag{4}$$

The value of the exponent a provides information on the configuration of the molecule in solution, its magnitude depending on the model approximated by the randomly coiled polymer chain. An exponent of 0.5 corresponds to a compact, solvent-immobilizing coil, whereas the exponent of unity is the highest obtainable for a random coil[4] and indicates the asymptotic limit of complete free draining. From the a value of 0.94 in eq. (4) the conclusion may be drawn that over the range of molecular weights studied, acidic xylan in DMSO has a form which lies between a solvent-immobilizing and a free-draining configuration but close to the latter.

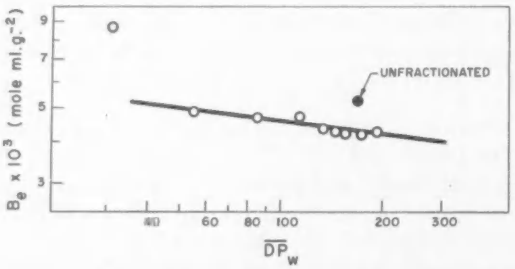

Fig. 8. Log–log plot of sedimentation equilibrium virial coefficient vs. $\overline{DP}_w$ for xylan fractions in DMSO.

Expressions analogous to eq. (3) relate the degree of polymerization with the diffusion coefficients. Figure 7 shows the logarithmic plot of D_A against $\overline{DP}_w$. The straight line corresponds to the relationship

$$D_A = 7.3 \times 10^{-6} \, DP_w^{-0.79} \tag{5}$$

The exponent in eq. (5) also has a characteristic value depending on the shape of the molecule. For a compact, solvent-immobilizing coil it is -0.5, while a free-draining configuration yields a value of -1.0. The exponent of -0.79 in eq. (5) again suggests that the molecule of xylan has a form between that of a free-draining and solvent-immobilizing coil.

Some confirmation of the numerical value of a in eq. (4) may be obtained from the increase of B_e with decrease in $\overline{DP}_w$ shown in Figure 8. A similar trend has been obtained by a number of other investigators.[11,39,40] Flory[34] has shown that the second virial coefficient can be represented over limited ranges of molecular weight in the form $K_I M^{\epsilon}$, where K_I is a proportionality factor and ϵ a negative exponent varying from -0.10 to -0.30. Neglect-

ing the points for the unfractionated material and master fraction No. 9 the least-square line in Figure 8 is

$$B_\epsilon = 8.2 \times 10^{-3}\ \overline{DP}_w^{-0.13} \tag{6}$$

Kobayashi[40] has shown that the exponent ϵ can be expressed as $\epsilon = (1 - a)$ for randomly coiled linear polymers. The value of a computed from the above is 0.87 which is in fair agreement with 0.94 in eq. (4).

A plot of log $[\eta]$ versus log $\overline{DP}_w$ for xylan in CED is also shown in Figure 7, from which

$$[\eta]_{CED} = 2.6 \times 10^{-3}\ \overline{DP}_w^{1.15} \tag{7}$$

The exponent of 1.15 is higher than the asymptotic limit of unity for a completely free-draining coil. This indicates that in the solvent CED the molecule is no longer spherically symmetrical but acquires a rodlike character. For reasons previously mentioned, it is unlikely that this effect is due to the uronic acid side chains. It may arise from an increase in chain stiffness due to the complexing of the CED with the xylose units as postulated for cellulose.[41] At the low $\overline{DP}_w$ range of 31–194, inflexibility of the polysaccharide chain would produce a tendency of the molecule to be rodlike,[42] which would cause the exponent in eq. (7) to be greater than unity.

Unfortunately it is difficult to compare directly the hydrodynamic behavior of the xylan chain with that of cellulose because data for cellulose in the $\overline{DP}_w$ range 30–200 is sparse. For example it would be interesting to establish the Mark-Houwink equation for low $\overline{DP}_w$ cellulose in CED in order to find out whether the value of a would exceed unity as it does with xylan. An approximate comparison between the two polysaccharides may be made in terms of the ratio $[\eta]/\overline{DP}_w$ shown in Table IV. For the celluloses, $[\eta]/\overline{DP}_w$ was obtained by extrapolation of the log $[\eta]$ versus $\overline{DP}_w$ lines to a $\overline{DP}_w$ of 150. The $[\eta]/\overline{DP}_w$ value of 5.6×10^{-3} for xylan in CED is in

TABLE IV

Value of $[\eta]/DP_w$ at $DP_w = 150$ for Cellulose, Cellulose Derivatives, and Xylan

Solute	Solvent	$\frac{[\eta]}{\overline{DP}_w} \times 10^3$	Reference
Cellulose	CED	5.9	43
Cellulose	CED	5.9	44
Cellulose	Cuoxam	4.1	44
Cellulose	Cuoxam	3.9	45
Cellulose	Cuoxam	4.4	43
Cellulose	EWNN	6.9	46
Cellulose	Cadoxen	7.1	47
Ethylhydroxyethyl cellulose	Water	10.0	7
Hydroxyethyl cellulose	Water	10.5	48
Carboxymethyl cellulose	0.1*M* NaCl	14.1	10
Xylan	DMSO	4.3	Present work
Xylan	CED	5.6	Present work

good agreement with 5.9×10^{-3} from the results both of Newman, Loeb, and Conrad[43] and of Marx[44] for cellulose in CED. In cuoxam, the $[\eta]/\overline{DP}_w$ values are somewhat smaller and in EWNN and Cadoxen, they are higher. The $[\eta]/\overline{DP}_w$ ratios for the cellulose derivatives in water are considerably higher than those for cellulose. The derivatives all carry polar groups which would be capable of electrostatic interaction in an aqueous solvent of low or zero ionic strength. This would cause expansion of the molecule to give the high $[\eta]/\overline{DP}_w$ values. The agreement between the $[\eta]/\overline{DP}_w$ ratios for cellulose and xylan in CED suggests but does not prove the configurational similarity of the two macromolecules. More data with other xylans and low molecular weight celluloses are required for an answer to the question.

Hydrodynamic Theories

If the xylan chain is coiled in DMSO, then it should be possible to test the various hydrodynamic theories of polymer solutions with the present data. Computations have been carried out in which the theories of Kirkwood and Riseman,[4] Kurata and Yamakawa,[6] and Mandelkern and Flory[49] have been tested. Because of the varying content of pendant side groups, the present series of xylan fractions are somewhat less than ideal for this purpose. Therefore the results are now reported in summary only.

The Kirkwood-Riseman effective bond length was found to be 23 A., which may be compared with 23.2 A. for cellulose in Cadoxen,[47] 23.3 A. for hydroxyethyl cellulose in water,[48] and 21 A. for cellulose in EWNN.[46] When the bond length and the intrinsic viscosity was substituted into the appropriate equations, the calculated monomer frictional constant was found to be about $^1/_8$ the value of 15.9×10^{-9} g./sec. determined by diffusion experiments on xylose in DMSO. However, the molecular frictional constant, F_0 computed by substitution of the experimental monomer frictional constant in the Kirkwood-Riseman equations agreed well with experimental values of F_0 calculated from

$$D_A = RT/F_0 \tag{8}$$

An absolute test of the Kurata-Yamakawa[6] theory was not possible because molecular dimensions and θ temperatures were not measured. Instead, the ability to the theory to correlate the intrinsic viscosity and the diffusion coefficient was examined. The draining and excluded volume parameters were calculated by use of the viscosity data. These parameters were then used to compute F_0. Comparison with the experimentally determined F_0 showed good agreement, in contrast to the results of a similar analysis based on the Kirkwood-Riseman theory.[4]

The only way in which the results differed markedly from those expected for the cellulose chain was in the value of the Flory constant, $\Phi^1/_3\, P^{-1}$. From high to low molecular weight this parameter increased from 1.7×10^6 to 2.2×10^6 in a curve which smoothly extrapolated to the value of

2.54×10^6 for xylose at $\overline{DP}_w = 1$. For cellulose or its derivatives[7,10] $\Phi^{1/3} P^{-1} \simeq 3 \times 10^6$.

The quantity $\Phi^{1/3} P^{-1}$ may be considered to represent, except for a proportionality factor, a ratio of the effective hydrodynamic radii for the viscosity and the frictional processes. For a hard, incompressible sphere, a combination of the Einstein viscosity equation and Stoke's law gives $\Phi^{1/3} P^{-1} = 2.1 \times 10^6$. In contrast, a prolate ellipsoid[50] with axial ratio of 300 has $\Phi^{1/3} P^{-1} = 3.6 \times 10^6$. If the parameter is calculated from the viscosity and diffusion data of Polson[51] for small molecules, such as glucose and pentaerythritol, it is found to vary between 2.3×10^6 and 2.6×10^6. It is interesting to note that the value for xylose falls into this range. For a variety of flexible chain polymers $\Phi^{1/3} P^{-1}$ has been found to be a constant independent of the nature of the polymer, solvent or temperature and equal to 2.6×10^6.[34] It was therefore an unexpected result to find the parameter to be low in the case of xylan. No explanation of this effect is offered at present, but further investigation with low molecular weight modal systems may elucidate the anomaly.

The authors wish to thank Dr. Manley for providing the x-ray diffraction data and Dr. Timell without whose assistance and advice this work would not have been possible.

References

1. LeBel, R. G., D. A. I. Goring, and T. E. Timell, *J. Polymer Sci., Part C*, No. 2, 9 (1963).
2. Husemann, E., *J. prakt. Chem.*, **155**, 13 (1940).
3. Glaudemans, C. P. J., and T. E. Timell, *Svensk Papperstidn.*, **61**, 1 (1958).
4. Kirkwood, J. G., and J. J. Riseman, *J. Chem. Phys.*, **16**, 565 (1948).
5. Debye, P., and A. M. Bueche, *J. Chem. Phys.*, **16**, 573 (1948).
6. Kurata, M., and H. Yamakawa, *J. Chem. Phys.*, **29**, 311 (1958).
7. Manley, R. St. J., *Arkiv. Kemi*, **9**, 519 (1956).
8. Fox, T. G, J. B. Kinsinger, H. F. Mason, and E. M. Schuele, *Polymer*, **3**, 71 (1962).
9. Marrinan, H. J., and J. J. Hermans, *J. Phys. Chem.*, **65**, 385 (1961).
10. Sitaramaiah, G., and D. A. I. Goring, *J. Polymer Sci.*, **58**, 1107 (1962).
11. Cowie, J. M. G., *Makromol. Chem.*, **42**, 230 (1961).
12. Krigbaum, W. R., and L. H. Sperling, *J. Phys. Chem.*, **64**, 99 (1960).
13. Gupta, P. R., and D. A. I. Goring, *Can. J. Chem.*, **38**, 270 (1960).
14. Meier, H., *Svensk Papperstidn.*, **65**, 299 (1962).
15. Battista, O. A., *Ind. Eng. Chem.*, **42**, 502 (1950).
16. Immergut, E. H., and B. G. Rånby, *Ind. Eng. Chem.*, **48**, 1183 (1956).
17. Marchessault, R. H., and B. G. Rånby, *Svensk Papperstidn.*, **62**, 230 (1959).
18. Goring, D. A. I., and A. Rezanowich, *J. Colloid Sci.*, **15**, 472 (1960).
19. Bowering, W. D. S., R. H. Marchessault, and T. E. Timell, *Svensk Papperstidn.* **64**, 191 (1961).
20. Rezanowich, A., W. Q. Yean, and D. A. I. Goring, *Svensk Papperstidn.*, in press.
21. Gosting, L. J., and M. S. Morris, *J. Am. Chem. Soc.*, **71**, 1998 (1949).
22. Goring, D. A. I., and T. E. Timell, *J. Phys. Chem.*, **64**, 1426 (1960).
23. Van Holde, K. E., and R. L. Baldwin, *J. Phys. Chem.*, **62**, 734 (1958).
24. Yphantis, D. A., *Ann. N. Y. Acad. Sci.*, **88**, 586 (1960).
25. Lansing, W. D., and E. O. Kraemer, *J. Am. Chem. Soc.*, **57**, 1369 (1935).
26. Bjorkqvist, K. J., and L. Jörgensen, *Acta Chem. Scand.*, **5**, 978 (1951).
27. Croon, I., and B. F. Enström, *Tappi*, **44**, 870 (1961).
28. Clayton, D. W., *Svensk Papperstidn.*, in press.

29. Hamilton, J. K., and N. S. Thompson, *Pulp Paper Mag. Can.*, **61**, T263 (1960).
30. Hamilton, J. K., E. V. Partlow, and N. S. Thompson, *Tappi*, **41**, 803 (1958).
31. Ruck, H., M. Kouris, and R. St. J. Manley, *J. Ultrastructure Res.*, **3**, 46 (1959).
32. Kouris, M., H. Ruck, and S. G. Mason, *Can. J. Chem.*, **36**, 931 (1958).
33. Marchessault, R. H., and T. E. Timell, *J. Phys. Chem.*, **64**, 704 (1960).
34. Flory, P. J., *Principles of Polymer Chemistry*, Cornell Univ. Press, Ithaca, N. Y., 1953.
35. Millet, M. A., and A. J. Stamm, *J. Phys. Colloid Chem.*, **51**, 134 (1947).
36. Thompson, J. O., and L. E. Wise, *Tappi*, **35**, 331 (1952).
37. Lindsley, C. H., and M. B. Frank, *Ind. Eng. Chem.*, **45**, 2491 (1953).
38. Cornell, R. H., and H. A. Swenson, *J. Appl. Polymer Sci.*, **5**, 641 (1961).
39. Cohn-Ginsberg, E., T. G Fox, and H. F. Mason, *Polymer*, **3**, 97 (1962).
40. Kobayashi, H., *J. Polymer Sci.*, **39**, 369 (1959).
41. Nicoll, W. D., N. L. Cox, and R. F. Conway, in *Cellulose*, E. Ott and H. M. Spurlin, Eds., Interscience, New York, 1954.
42. Huque, M. M., D. A. I. Goring, and S. G. Mason, *Can. J. Chem.*, **36**, 952 (1958).
43. Newman, S., L. Loeb, and C. M. Conrad, *J. Polymer Sci.*, **10**, 463 (1953).
44. Marx, M., *Makromol. Chem.*, **16**, 157 (1955).
45. Kraemer, E. O., *Ind. Eng. Chem.*, **30**, 1200 (1938).
46. Claesson, S., W. Bergmann, and G. Jayme, *Svensk Papperstidn.*, **62**, 141 (1959).
47. Henley, D., *Arkiv Kemi*, **18**, 327 (1961).
48. Brown, W., *Arkiv Kemi*, **18**, 227 (1961).
49. Mandelkern, L., and P. J. Flory, *J. Chem. Phys.*, **20**, 212 (1952).
50. Scheraga, H. A., and L. Mandelkern, *J. Am. Chem. Soc.*, **75**, 179 (1953).
51. Polson, A., *J. Phys. Colloid Chem.*, **54**, 649 (1950).

Synopsis

A 4-*O*-methyl-D-glucuronoxylan from white birch was fractionated by precipitation from dimethyl sulfoxide (DMSO) with ethanol. Intrinsic viscosities of 0.88–0.45 dl./g. were obtained. This narrow range confirmed the low polydispersity previously indicated by the $\overline{DP}_w/\overline{DP}_n$ ratio of 1.18 for the unfractionated xylan. In order to extend the range of molecular weights the xylan was degraded. On fractionation of the degraded material, $[\eta]$ values of 0.46–0.14 dl./g. were obtained. Nine masters fractions were made up by blending subfractions of nearly identical $[\eta]$ values. The intrinsic viscosities of the master fractions ranged from 0.88 to 0.15 dl./g. in DMSO and from 1.22 to 0.15 dl./g. in cupriethylenediamine (CED). Area diffusion constants, D_A were from 5.0×10^{-7} to 1.2×10^{-7} cm.^{2}/sec., corresponding to sedimentation equilibrium weight average degrees of polymerization of 31–194. The uronic acid content varied between 8.2 and 14.2%. There was no correlation between the trends in $[\eta]$ or D_A and the uronic acid content. It was concluded that the influence of the side chains on the configuration of the molecule was negligible. The exponent determined from the logarithmic dependence of $[\eta]$ on log $\overline{DP}_w$ was 0.94 in DMSO. This result suggested that the configuration of acidic xylan in DMSO has a form which lies between a solvent-immobilizing and a free-draining coil, but close to the latter. This was corroborated by the corresponding exponent of −0.79 for the molecular weight dependence of D_A. The exponent of 1.15 determined from log $\overline{DP}_w$ vs. log $[\eta]$ in CED indicated an asymmetric configuration in the complexing solvent. The ratios of $[\eta]/DP_w$ in DMSO and CED were 4.3×10^{-3} and 5.6×10^{-3}, respectively. The latter was in good agreement with the published values for cellulose in CED at $\overline{DP}_w = 150$. This indicated but did not prove the configurational similarity of cellulose and xylan in CED.

Résumé

On fractionne un 4-*O*-méthyl-D-glucuronoxylane provenant d'un bouleau blanc par le diméthylsulfoxyde (DMSO) contenant de l'éthanol. On obtient une viscosité in trinsèque de 0.86 → 0.45 dl. g.$^{-1}$. Cet étroit domaine confirme la faible polydispersit

indiquée précédemment par le rapport $\overline{DP}_w/\overline{DP}_n = 1.18$ pour le xylane non fractionné. Dans le but d'augmenter ce domaine de poids moléculaire, le xylane est dégradé. Après fractionnement du matériel dégradé, on obtient des valeurs de (η) égales à 0.46 → 0.14 dl.g.$^{-1}$. On a préparé 9 fractions importantes en mélangeant des fractions secondaires ayant des valeurs équivalentes de η. La viscosité intrinsèque des fractions principales s'étend de 0.88 à 0.15 dl g^{-1} dans le DMSO et de 1.22 à 0.15 dl g^{-1} dans la cuprié thylènediamine (CED). Les constantes de diffusion de surface D_A s'étendent de 5.0×10^{-7} à 1.2×10^{7} cm^{2}sec^{-1} correspondant à l'équilibre de sédimentation du degré de polymérisation moyen en poids de 31 à 194. La teneur en acide uronique varie entre 8.2 et 14.2%. Il n'y a pas de corrélation entre les variations de (η) ou D_A avec la teneur en acide uronique. On conclut que l'influence de la chaîne latérale sur la configuration de la molécule est négligeable. L'exposant déterminé au départ de la dépendance logarithmique de (η) en fonction du log $\overline{DP}_w$ est égale à 0.94 dans le DMSO. Ces résultats suggèrent que la configuration du xylane acide dans le DMSO a une forme qui se situe entre une immobilisation par le solvant et un écoulement libre, mais enfermée dans un réseau. Ceci est confirmé par l'exposant égal à −0.79 pour la dépendance du poids moléculaire en fonction de D_A. L'exposant 1.15 déterminé au départ du log $\overline{DP}_w$ en fonction du log (η) dans le CED indique une configuration asymétrique dans un solvant complexant. Les rapports $[\eta]/\overline{DP}_n$ dans DMSO et dans le CED sont respectivement de $4.3\ 10^{-3}$ et $5.6\ 10^{-3}$. Ce dernier est en bon accord avec les valeurs publiées pour la cellulose dans le CED à $\overline{DP}_w = 150$. Ceci indique mais ne prouve pas la similitude de configuration entre la cellulose et le xylane dans le CED.

Zusammenfassung

Ein 4-*O*-Methyl-D-glucuronoxylan aus weisser Birke wurde durch Fällung mit Äthanol aus Dimethylsulfoxyd (DMSO) fraktioniert. Es wurden Viskositätszahlen von 0,88 bis 0,45 dl.g^{-1} erhalten. Dieser enge Bereich bestätigt die dem früher am unfraktionierten Xylan bestimmten Verhältnis $\overline{DP}_w/\overline{DP}_n$ von 1,18 entsprechende niedrige Polydispersität. Um den Molekulargewichtsbereich zu erweitern wurde das Xylan abgebaut. Bei der Fraktionierung des abgebauten Materials wurden $[\eta]$-Werte von 0,46 bis 0,14 dl.g^{-1} erhalten. Durch Vereinigung von Subfraktionen mit nahezu identischen $[\eta]$-Werten wurden neun Hauptfraktionen hergestellt. Die Viskositätszahlen der Hauptfraktionen erstreckten sich von 0,88 bis 0,15 dl.g^{-1} in DMSO und von 1,22 bis 0,15 dl.g^{-1} in Cupriäthylendiamin (CED). Areadiffusionskonstanten, D_A, betrugen $5{,}0 \times 10^{-7}$ bis $1{,}2 \times 10^{-4}$ cm.^{2}sec^{-1}. entsprechend Sedimentationsgleichgewichts-Gewichtsmittelwerten des Polymerisationsgrades von 31 bis 194. Der Uronsäuregehalt variierte von 8,2 bis 14,2%. Es bestand kein Zusammenhang zwischen dem Trend der $[\eta]$- oder D_A-Werte und dem Uronsäuregehalt. Der Einfluss der Seitenketten auf die Molekülkonfiguration scheint vernachlässigbar klein zu sein. Der aus der logarithmischen Abhängigkeit von $[\eta]$ von log $\overline{DP}_w$ bestimmte Exponent betrug in DMSO 0,94. Das läss erkennen, dass die Konfiguration von saurem Xylan in DMSO eine Form zwischen der eines undurchspülten und der eines durchspülten Knäuels, aber letzterer näherliegend, hat. Das wurde durch den entsprechenden Exponenten von −0,79 in der Molekulargewichtsabhängigkeit von D_A bestätigt. Der Exponent 1,15 aus dem log $\overline{DP}_w$ − log $[\eta]$-Diagramm in CED spricht für eine asymmetrische Konfiguration im komplexbildenden Lösungsmittel. Das Verhältnis $[\eta]/\overline{DP}_w$ betrug in DMSO bzw. CED $4{,}3 \times 10^{-3}$ bzw. $5{,}6 \times 10^{-3}$. Letzteres stand mit dem Literaturwert für Cellulose in CED bei $\overline{DP}_w = 150$ in guter Übereinstimmung. Das gibt einen Hinweis, wenn schon keinen Beweis, auf die Ähnlichkeit der Konfiguration von Cellulose und Xylan in CED.

Discussion

R. H. Marchessault (*State University College of Forestry, Syracuse University, Syracuse, New York*): Would the speaker comment on the hazards or drawbacks of applying the polymer hydrodynamic theories to such low molecular weight polymers?

D. A. I. Goring: Polymer hydrodynamic theories have come from elaboration of the theories for simple models, e.g., the sphere, the rod, the ellipsoid, etc. As the molecular weight is reduced, the polymer molecule begins to lose its random nature. Chain flexibility becomes increasingly important and the effective configuration which the polymer presents to the solvent tends to change. This low molecular weight transition region has been neglected. It should prove a fruitful area for hydrodynamic studies. Hazards and drawbacks would arise if attempts were made to interpret results exclusively in terms of the theories for randomly coiling high polymers. A more general approach is necessary in which the viscometric and frictional properties are compared with the behavior expected for models such as those listed above.

G. N. Richards (*British Rayon Research Association, Manchester, England*): Will Dr. Goring tell us more about experimental conditions and conclusions in the hydrolysis experiments which show a limiting viscosity value? Do these results provide unambiguous evidence for the presence of hydrolysis sensitive linkages in the hemicellulose molecule and if so, is there any evidence available on their distribution?

D. A. I. Goring: Hydrolysis was carried out in 300 ml. of DMSO to which 35 ml. of 12*N* aqueous HCl was added to give pH = 1. Thus the reaction mixture contained a substantial concentration of HCl, but the activity of the acid as measured by pH corresponds to *N*/10 in water. As evidence for an acid-sensitive link, the degradation curve is certainly unambiguous. Interestingly, the leveling-off value of $[\eta]$ corresponds to the $\overline{DP}_w$ of 10 which is close to the average separation of the uronic acid side chains. However, the conversion of $[\eta]$ to $\overline{DP}_w$ in this low range is not very precise.

JOURNAL OF POLYMER SCIENCE: PART C NO. 2, PP. 49–61 (1963)

Four Polymer-Homologous Series of Oligosaccharides from a 4-*O*-Methylglucuronoxylan

R. H. MARCHESSAULT, *Research and Development Division, American Viscose Corporation, Marcus Hook, Pennsylvania,** and T. E. TIMELL, *Pulp and Paper Research Institute of Canada and Department of Chemistry, McGill University, Montreal, Quebec, Canada**

When a 4-*O*-methylglucuronoxylan from the wood of white birch (*Betula papyrifera*) was subjected to the action of a commercial enzyme (pectinase), there were obtained two series of polymer-homologous oligosaccharides.[1] The structure of these sugars and a possible action pattern of the enzyme preparation were discussed in an earlier communication.[2] The present paper is concerned with some properties of the oligosaccharides not dealt with previously.

RESULTS AND DISCUSSION

One of the homologous series consisted of five neutral oligosaccharides, ranging from xylobiose up to and including xylohexaose. Their melting points and specific rotations are presented in Table I. The same oligosaccharides have previously been obtained by Whistler and Tu[3] and by

TABLE I
Melting Point and Specific Rotation of Xylose Oligosaccharides

Compound	Melting point, °C.	$[\alpha]_D^{25}$
Xylobiose	184.5–185.0	−25.6°
Xylotriose	215–216	−48.1°
Xylotetraose	224–226	−61.9°
Xylopentaose	240–242	−72.9°
Xylohexaose	237–242	−78.5°

Bishop.[4] The second series was composed of five acid oligosaccharides, from an aldotetra- to an aldooctaouronic acid. Application of the methylation and/or periodate oxidation techniques showed that all five acids had the same general structure, indicated in Figure 1, with the 4-*O*-methylglucuronic acid group located at the nonreducing end of the xylooligosaccharides.

* Present address: Department of Forest Chemistry, State University College of Forestry, Syracuse 10, N. Y.

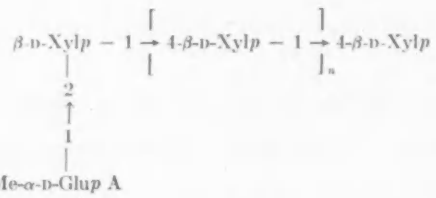

Fig. 1. Structure of the aldotetra- (n = 1), aldopenta-(n = 2), aldohexa- (n = 3), aldohepta- (n = 4), and aldoheptaouronic (n = 5) acids; β-D-Xyl$p$ = β-D-xylopyranose, 4-O-Me-α-D-GlupA = 4-O-Methyl-α-D-glucopyranosyluronic acid.

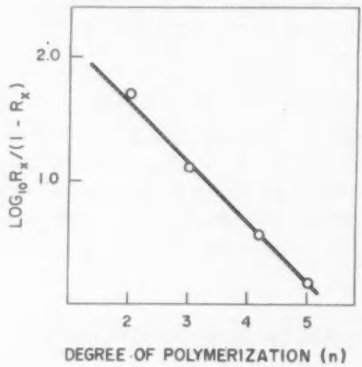

Fig. 2. Relation between R_x value and degree of polymerization of xylitol oligosaccharides.

Rotatory Studies

The neutral oligosaccharides were reduced with sodium borohydride to the corresponding alditols, which were obtained in quantitative yield. These new polyols could not be induced to crystallize. When the chromatographic mobility of the four alditols was plotted against their degree of polymerization in a manner similar to that suggested by French and Wild,[5] a linear relationship was obtained, thus confirming the homologous nature of the sugars (Fig. 2). Chromatographic mobilities and specific rotations are given in Table II.

TABLE II
R_x Value and Specific Rotation of Xylitol Oligosaccharides[a]

Compound	R_x	$[\alpha]_D^{25}$
Xylobiitol	0.83	−36.4°
Xylotriitol	0.56	−53.9°
Xylotetraitol	0.32	−64.2°
Xylopentaitol	0.13	−67.4°

[a] R_x = rate of movement on the paper chromatogram relative to D-xylose.

Since xylitol is optically inactive,[6,7] the alcohol endgroup of the alditol oligosaccharides could be expected to make only a minor contribution to their rotation. Xylose has a specific rotation of +19° in water and will thus probably render the rotation of the corresponding reducing oligosaccharides less negative, especially for the lower members of the series, where the reducing endgroup makes the main rotatory contribution. Inspection of the values in Tables I and II reveals that the first three alditols have a more negative rotation than the xylobiose, xylotriose, and xylotetraose. The xylopentaitol, however, has a slightly less negative rotation than the xylopentaose, and observation which cannot be explained at the present stage unless it is attributed to experimental error.

According to Freudenberg and co-workers,[8] a polymer-homologous series of sugars will exhibit a linear relationship between $[M]_n/n$ and $(n-1)/n$, where $[M]_n$ is the molecular rotation and n is the degree of polymerization of the oligosaccharide (starting at $n = 2$). Extrapolation to $n = \infty$ $[(n-1)/n = 1]$ would give a value for the molecular (and hence also specific) rotation of a polysaccharide of infinite length, containing only the type of glycosidic linkages present in the oligosaccharides. Using this extrapolation procedure, Wolfrom and his co-workers have determined the specific rotation to be expected for cellulose[9-11] and for cellulose triacetate.[12,13]

The specific rotations of the present acid oligosaccharides are given in Table III. The 30 to 40 values reported in the literature for the first member of the series, the ubiquitous 2-*O*-(4-*O*-methyl-α-D-glucosyluronic acid)-D-xylopyranose, cover a range as wide as +70 to +110°. Five chromatographically pure specimens of this amorphous compound, available from previous studies, had the rotations given in Table IV. Evidently, the specific rotation of the aldobiouronic acid is probably very close to

TABLE III
Specific Rotation of Acid Oligosaccharides

Compound	$[\alpha]_D^{25}$
Aldotetraouronic acid	+23.4°
Aldopentaouronic acid	+0.6°
Aldohexaouronic acid	−11.8°
Aldoheptaouronic acid	−20.8°
Aldooctaouronic acid	−25.7°

TABLE IV
Specific Rotation of Aldobiouronic Acids Isolated from Various Sources

Source	$[\alpha]_D^{25}$
Ginkgo wood	+104.0°
Yellow birch wood	+107.9°
Aspen wood	+109.1°
White birch bark	+109.3°
White birch wood	+110.0°

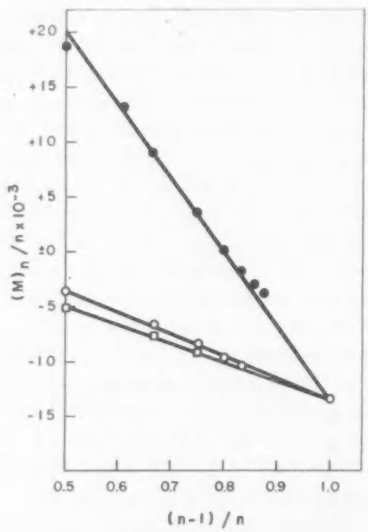

Fig. 3. Relation between molecular rotation per monomer residue and degree of polymerization for three series of oligosaccharides: (●) acid oligosaccharides; (○) neutral oligosaccharides; (□) alditol oligosaccharides.

+110° in water. The aldotriouronic acid has been obtained from some ten different sources, usually in the form of its crystalline trihydrate. The values reported for its specific rotation vary less than those of the biouronic acid, a value for $[\alpha]_D$ of +59° representing an average.[14–16]

In Figure 3 molecular rotations per monomer residue have been plotted against degrees of polymerization according to Freudenberg[8] for the acid, neutral, and reduced oligosaccharides. On extrapolation to $n = \infty$, the three linear plots meet in one point. This is what would be expected, since with increasing degree of polymerization the rotatory contribution of the α-linked side chains and the endgroups would gradually disappear, the inner, β-linked xylopyranose residues finally becoming completely dominating. The value for $[M]_n/n$ for $n =$ W is −13,500. The molecular weight of the anhydroxylose unit is 132, and the specific rotation in water of an infinitely long, linear, and β-(1 → 4)-linked xylan should accordingly be −102°.

It should be noted at this point that the plot in Figure 3 is not strictly valid for the acid oligosaccharides since it tacitly assumes that the xylose moiety of the aldobiouronic acid makes the same contribution as the nonreducing xylose moiety in the neutral chain. A more correct plot would be one with $(n - 2)/n$ on the abscissa, thus treating the aldobiouronic acid unit at the nonreducing end as a single rotatory entity. However, the fact that the present plot with $(n - 1)/n$ exhibits satisfactory linearity, in essence confirms the assumption.

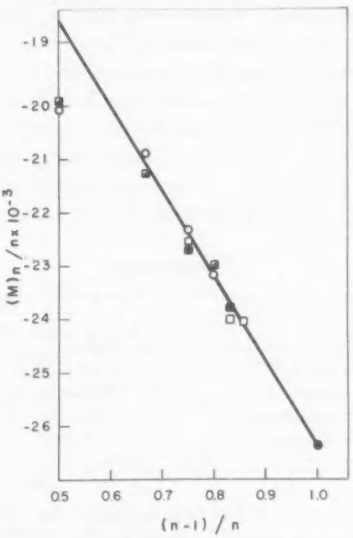

Fig. 4. Relation between molecular rotation per monomer residue and degree of polymerization for the β-acetates of the xylooligosaccharides: (○) present study; (■) Whistler and Tu;[19] (□) Bishop.[4]

One of the few true xylans existing in nature occurs (together with an arabinoxylan and a glucan) in esparto grass. This β-(1 → 4)-linked polysaccharide contains on the average one branching point per molecule and has been reported to have a specific rotation of −92° in aqueous alkali.[17] An esparto xylan, previously isolated by Croon and Timell[18] was subjected to autohydrolysis for removal of residual traces of uronic acid. The purified product had a number-average degree of polymerization of 35 and a specific rotation of −99° in 10% aqueous sodium hydroxide. If xylobiose is assumed to have $[\alpha]_D$ of −26° and an infinitely long xylan has $[\alpha]_D$ of −102°, a calculation according to Freudenberg[8] gives a theoretical value of −97.4° for the specific rotation in water of a xylan containing 35 xylose residues. Unfortunately, esparto xylan is not soluble in water. When the specific rotations of several water-soluble arabino-glucuronoxylans were determined in both water and 10% aqueous sodium hydroxide, identical results were obtained with the two solvents. The esparto grass xylan therefore probably had a specific rotation of −99° also in water, in good agreement with the calculated value of −97.4°. The rotatory contribution of the branching occurring in the esparto xylan is not known.

Acetylation of the neutral oligosaccharides with acetic anhydride in the presence of sodium acetate gave the corresponding fully substituted β-acetates. Their melting point and specific rotation in chloroform are presented in Table V. Molecular rotations are plotted in Figure 4 against

degrees of polymerization. Values reported by Whistler and Tu[19] and by Bishop[4] for the same sugar acetates have also been included. The molecular rotations of the disaccharides cannot be fitted to the line through the other points. Since all investigators found very nearly the same specific rotation for this compound, the deviation can hardly be ascribed to experimental errors. A similar, albeit lesser, discrepancy has been noted by Wolfrom and Fields[12] for a trisaccharide belonging to two polymer-homologous series of α- and β-acetates from cellulose.

TABLE V
Melting Point and Specific Rotation of Acetylated Xylose Oligosaccharides

Compound	Melting point, °C.	$[\alpha]_D^{25}$
β-Xylobiose hexaacetate	155.5–156.5	−75.1°
β-Xylotriose octaacetate	108.0–109.5	−83.0°
β-Xylotetraose decaacetate	200–201	−92.4°
β-Xylopentaose dodecaacetate	249–250	−98.0°

Extrapolation to $n = \infty$ of the plot in Figure 4 gives a molecular rotation of −26,300 and hence a specific rotation of −122° for an infinitely long, fully acetylated xylan. Attempts to prepare a fully soluble acetate from the esparto xylan all failed, and the calculated value therefore remains unverified.

Recent developments[20–22] have shown that an empirical correlation exists between the ability of a polypeptide molecule to assume an ordered conformation in solution and its optical rotatory dispersion. In general, when contiguous monomers in a polypeptide assume a helical conformation relative to the preceding unit, the rotatory dispersion behavior of such a polymer is complex, that is, a nonlinear relationship is obtained when the data are plotted according to the modified Drude equation:

$$[\alpha]_\lambda \lambda^2 = k + [\alpha]_\lambda \lambda_c^2$$

where $[\alpha]_\lambda$ is the specific rotation at a given wavelength and k and λ_c are constants. Polymers which exhibit a linear relationship between $[\alpha]_\lambda \lambda^2$ and $[\alpha]_\lambda$ are said to show simple optical rotatory behavior.

Only a few rotatory dispersion studies have so far been reported for polysaccharides, such as a corn amylose[23] and a partly methylated cellulose.[24] No similar study appears to have been made so far with a series of oligosaccharides. An oligopeptide series has been found to possess a transition point at which further increase in chain length caused an abrupt change from simple to complex dispersion.[25]

The four neutral xylooligosaccharides were subjected to a rotatory dispersion study within the range of 350–750 mμ, using a Rudolph polarimeter in conjunction with a Beckman monochromator. The results are presented in Figure 5. The linearity observed throughout clearly classes the rotatory dispersion behavior of the oligosaccharides as simple. In

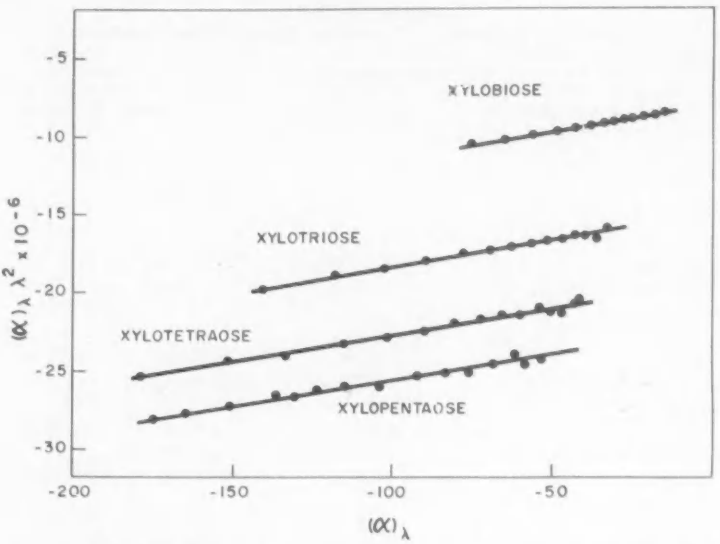

Fig. 5. Modified Drude plots for aqueous solutions of xylooligosaccharides; $[\alpha]_\lambda$ in degrees; λ in mμ.

terms of the empirical correlation between rotatory dispersion and molecular conformation which has been used for polypeptides one would conclude that contiguous xylose residues are rotationally independent. This fact is also the basis for the interpretation of the linear relationship between molecular rotation and degree of polymerization of the xylooligosaccharides (Fig. 3). It should be noted that if contiguous residues made equal contributions both due to their asymmetric carbon atoms and a helical conformation, the optical superposition principal would still apply. It is also possible to observe simple dispersion and yet have a helical conformation in solution if the intrinsic contribution of the helix to the total rotation is small. Thus, until some estimate of the latter is available for polysaccharides as it is for polypeptides[26] one cannot conclude unequivocally as to the solution conformation of polysaccharides from rotatory dispersion data.

It is interesting to note in this connection that a series of five β-(1 → 2)-linked glucooligosaccharides studied by Gorin, Spencer, and Westlake[27] showed molecular rotations which were independent of the degree of polymerization and thus did not obey the Freudenberg equation. The derived alditols exhibited an even more irregular behavior. The rotatory contribution of the endgroups is very low in the polyol series,[11] and the phenomenon is therefore probably attributable to the inner sugar residues. The authors suggest tentatively that the phenomenon could be caused by an arrangement of the glucose units such that it would contribute to the overall rotation of the oligosaccharides.[27]

TABLE VI
CuKα X-Ray Reflections of Crystalline Xylose Oligosaccharides

d Spacings, A.[a]				
Xylobiose	Xylotriose	Xylotetraose	Xylopentaose	Xylohexaose
	13.3 vw			
		12.0 vvw		
			11.5 vvw	
10.1 w				
9.2 m				
8.2 vw	8.2 vw	8.1 w		
7.4 vw		7.44 w	7.7 vw	
6.75 m	6.5 vw			
	6.1 vw			
5.73 vs	5.41 m		5.40 m	5.37 w
5.32 m	5.13 s	5.385 vw	5.09 mm	
5.10				
4.86 vw	4.86 s	4.92 vs	4.90 s	4.90 vs
4.52 s	4.61 s	4.66 m	4.39 vvw	
4.32 s	4.39 vw	4.14 s	4.06 s	4.12 vs
4.10 s	4.04 m			
3.96 vw	3.79 m	3.84 vw	3.96 s	3.96 w
3.82 m	3.64 m	3.19 w	3.81 vw	
3.66 m	3.42 vw	3.03 mm	3.61 vw	3.46 w
3.53 vw	3.37 m		3.18 vw	
3.365 m	3.26 vw		3.03 m	3.01 w
3.02 s	3.18 vw			
	3.07 m			
2.865 s	2.91 w	2.95 vw	2.86 vw	2.86 w
2.80 s	2.79 vw	2.838 m	2.77 vw	
2.705 s	2.71 vw	2.665	2.66 vw	

(*continued*)

Constants for the Drude equation can be derived from plots as shown in Figure 5. The dispersion constant λ_c was essentially the same for all samples, namely 187 mμ.

The same dispersion constant was observed for the completely acetylated xylotriose and xylopentaose while the constant k had the values 23×10^6 and 31×10^6, respectively.

X-Ray Studies

X-ray powder diffraction data for the xylooligosaccharides are summarized in Table VI. The relative intensities were estimated visually. Comparison with data reported for an esparto xylan[28] reveals that from the xylotetraose the principal lines are the same as in the polysaccharide. Cellotetraose, similarly, has been found[9] to be the first glucoöligosaccharide to give the x-ray diffraction pattern typical of cellulose II.

It should be noted that xylans and xylooligosaccharides can form crystalline hydrates.[3,28] The highest degree of hydration was reported for xylan samples crystallized in the presence of water only.[28] The oligo-

TABLE VI (*continued*)

Xylobiose	Xylotriose	Xylotetraose	Xylopentaose	Xylohexaose
2.57 m	2.62 m	2.50 vw	2.52 vw	
2.495 m	2.52 vw	2.34 m	2.42 vw	2.40 w
2.40 m	2.46 vw		2.34 w	
2.33 vw	2.38 vw		2.28 vw	
2.28 m	2.33 w		2.16 vw	
2.235 m	2.22 w		2.03 vw	
2.20 vw	2.14 w			
2.143 vw	2.09 vw			
2.097 m	2.04 vw			
2.055 vw	2.01 vw			
2.018 w				
1.988 w	1.96 vw	1.96 vw	1.92 vw	
1.915 m	1.93 vw	1.89 vw	1.84 vw	
1.782 m	1.87 vw	1.76 vw	1.76 vw	
1.683 m	1.85 vw		1.66 vw	
1.652 w	1.79 vw			
1.628 vw	1.70 vw			
1.564 vw	1.71 vw			
1.54 vw	1.68 vw			
1.508 vw	1.65 vw			
1.48 vw	1.62 vw			
1.45 vw	1.57 vw			
1.40 vw	1.54 vw			
1.31 w	1.46 vw			
1.175 vw	1.44 vw			
1.15 vw	1.39 vw			
1.12 vw	1.29 vw			
	1.255 vw			
	1.255 vw			

[a] v = very; w = weak; m = moderate; s = strong.

saccharides, which are usually crystallized from alcohol–water mixtures, do not show the same high preference for water and in the present case the strongest reflection for the xylotetraose and xylopentaose are in good agreement with those found for the unhydrated, crystalline xylan.

The diffraction data for the acetylated oligosaccharides are contained in Table VII. The diffractogram from β-xylopentaose dodecaacetate was indistinguishable from that of an annealed acetylated xylan.

EXPERIMENTAL

Isolation of Oligosaccharides

Neutral and acid oligosaccharides were obtained by enzymic hydrolysis of a 4-*O*-methylglucuronoxylan from the wood of white birch as described previously.[2] The neutral sugars were identified through their melting point, specific rotation, equivalent weight, and degree of polymerization. The aldotetra-,[29] aldopenta-,[30] and aldohexaouronic[31] acids were identified by methylation and periodate oxidation techniques. The first five neutral

TABLE VII
CuKα X-Ray Reflections of Crystalline Acetylated Xylose Oligosaccharides

d spacings, A.			
β-Xylobiose hexaacetate	β-Xylotriose octaacetate	β-Xylotetraose decaacetate	β-Xylopentaose dodecaacetate
15.0 m	14.03 w	12.0 w	15.6 w
10.5 s	10.48 s		9.72 w
8.5 w	9.03 s		
7.5 s	7.38 w	7.1 m	7.25 vs
6.4 m	6.53 vs	6.4 m	6.24 s
6.2 m	6.09 w		
5.5 m	5.72 m		
5.1 w	5.37 w		5.06 s
4.9 w	5.07 s	4.9 m	
4.5 m	4.72 w		4.44 s
4.35 m	4.31 w		
4.15 s			
4.0 w			4.00 w
3.9 w			
3.6 w	3.69 w		3.62 w
3.5 s	3.43 vw		
3.3 w	3.28 vw		
3.2 w			3.22 w
3.05 w	2.98 w		3.02 w
2.9 w		2.95 m	
2.7 vw		2.80 m	
2.2 vw			

oligosaccharides were converted to their fully substituted β-acetates which were characterized through their melting point and specific rotation.[2]

Preparation of Xylitol Oligosaccharides

In a typical experiment, xylobiose (1.0 g.) was dissolved in water (100 ml.) and sodium borohydride (2.0 g.) was added. After 24 hr. at 30°C. the solution was treated with excess Amberlite IR-120 exchange resin (acid form), filtered, and evaporated to dryness. Boric acid was removed by repeated evaporations from methanol and the residue was dried *in vacuo*. Yield of a white, semisolid product was 1.0 g. Xylotriose, xylotetraose, and xylopentaose in the same way gave the corresponding alditols as white, crisp solids, all in quantitative yield. On paper chromatography in ethyl acetate: acetic acid: water (18:7:8) no color was developed with the *o*-aminodiphenyl spray reagent.[32] The sugars were detected on the paper chromatogram with the permanganate–periodate reagent.[33] R_x values are given in Table II.

Determination of Specific Rotations

Rotatory dispersion measurements were carried out at 19°C. with a Rudolph Model 80 polarimeter with a 1-dm. tube. Samples were allowed

to equilibrate for at least 6 hr. before readings were taken by the photoelectric detection method. A xenon light source was used in conjunction with a Beckman monochromator to cover the region 350–750 mμ. All other rotations were measured in water or in chloroform with a Zeiss photoelectric polarimeter at 25°C. with a 1-dm. tube. With the use of a mercury lamp, measurements were carried out at 546 and 578 mμ and were extrapolated to 589 mμ (sodium D-line) with the aid of the Drude equation. The specific rotation of the aldobiouronic acid was determined from measurements with five authentic and pure samples, previously isolated in this laboratory from various sources (Table IV). The solvent was water and the concentrations were 2–3 g./100 ml.

X-Ray Diffraction Measurements

X-ray diffraction powder diagrams were obtained with a General Electric universal camera and CuK_α radiation. Spacings were read directly from the film, a calibrated scale being used to allow for film shrinkage during processing. Intensities were estimated visually. The results are presented in Tables VI and VII.

References

1. Timell, T. E., *Chem. Ind. (London)*, **1959**, 999.
2. Timell, T. E., *Svensk Papperstidn.*, **65**, 454 (1962).
3. Whistler, R. L., and C.-C. Tu, *J. Am. Chem. Soc.*, **74**, 3609 (1952).
4. Bishop, C. T., *Can. J. Chem.*, **33**, 1073 (1955).
5. French, D., and G. M. Wild, *J. Am. Chem. Soc.*, **75**, 2612 (1953).
6. Hockett, R. C., and C. S. Hudson, *J. Am. Chem. Soc.*, **57**, 1753 (1935).
7. Wolfrom, M. L., and E. J. Kohn, *J. Am. Chem. Soc.*, **64**, 1739 (1942).
8. Freudenberg, K., and C. Blomqvist, *Ber.*, **68**, 2070 (1935).
9. Wolfrom, M. L., and J. C. Dacons, *J. Am. Chem. Soc.*, **74**, 5331 (1952).
10. Wolfrom, M. L., J. C. Dacons, and D. L. Fields, *Tappi*, **39**, 803 (1956).
11. Wolfrom, M. L., and D. L. Field, *Tappi*, **41**, 204 (1958).
12. Dickey, E. E., and M. L. Wolfrom, *J. Am. Chem. Soc.*, **71**, 825 (1949).
13. Wolfrom, M. L., and D. L. Fields, *Tappi*, **40**, 335 (1957).
14. Hamilton, J. K., and N. S. Thompson, *J. Am. Chem. Soc.*, **79**, 6464 (1957).
15. Srivastava, H. C., and G. A. Adams, *J. Am. Chem. Soc.*, **81**, 2409 (1959).
16. Adams, G. A., *Can. J. Chem.*, **37**, 29 (1959).
17. Chanda, S. K., E. L. Hirst, J. K. N. Jones, and E. G. V. Percival, *J. Chem. Soc.*, **1950**, 1289.
18. Croon, I., and T. E. Timell, *J. Am. Chem. Soc.*, **82**, 3416 (1960).
19. Whistler, R. L., and C.-C. Tu, *J. Am. Chem. Soc.*, **73**, 1389 (1951); *ibid.* **74**, 4334 (1952).
20. Yang, J. T., and P. M. Doty, *J. Am. Chem. Soc.*, **79**, 761 (1957).
21. Djerassi, C., *Optical Rotatory Dispersion*, McGraw-Hill, New York, 1960.
22. Schellman, J. A., and C. G. Schellman, *J. Polymer Sci.*, **49**, 129 (1961).
23. Wolff, I. A., P. R. Watson, and E. Rist, *J. Am. Chem. Soc.*, **74**, 3064 (1952).
24. Neely, W. B., *J. Am. Chem. Soc.*, **82**, 4354 (1960).
25. Goodman, M., E. E. Schmitt, and D. Yphantis, *J. Am. Chem. Soc.*, **82**, 3483 (1960).
26. Moffitt, W., *J. Chem. Phys.*, **25**, 467 (1956).

27. Gorin, P. A. J., J. F. T. Spencer, and D. W. S. Westlake, *Can. J. Chem.*, **39**, 1067 (1961).
28. Marchessault, R. H., and T. E. Timell, *J. Phys. Chem.*, **64**, 704 (1960).
29. Timell, T. E., *Can. J. Chem.*, **40**, 22 (1962).
30. Timell, T. E., *Acta Chem. Scand.*, **16**, 1027 (1962).
31. Timell, T. E., *J. Org. Chem.*, **27**, 1804 (1962).
32. Timell, T. E., C. P. J. Glaudemans, and A. L. Currie, *Anal. Chem.*, **28**, 1916 (1956).
33. Lemieux, R. U., and H. F. Bauer, *Anal. Chem.*, **26**, 920 (1954).

Synopsis

Two series of oligosaccharides, one neutral and the other acidic, have been isolated by partial enzymic hydrolysis of a 4-*O*-methylglucuronoxylan from birch wood. The neutral xylooligosaccharides were converted to the β-acetates and were also reduced to the corresponding alditols. When the molecular rotations of the acid, neutral, and alditol oligomers were plotted against their degree of polymerization according to Freudenberg, straight lines were obtained which could be extrapolated to one point. The specific rotation of an infinitely long xylan thus obtained was −102°. The calculated and found values for the rotation of an esparto xylan agreed well. The molecular rotation of the acetylated xylobiose did not conform to the Freudenberg relationship. A rotatory dispersion study showed that the xylooligosaccharides exhibited "simple" rotatory behavior. Detailed x-ray powder diffraction data were reported for four of the neutral oligosaccharides and their acetate derivatives. Their crystallinity decreased with increasing degree of polymerization. The principal lines of the xylotetraose and xylopentaose were the same as in the xylan.

Résumé

Deux séries d'oligosaccharides, les uns neutres, les autres acides, ont été isolés par hydrolyse enzymatique partielle du 4-*O*-méthylglucuronoxylane provenant du bois de bouleau. Les xylo-oligosaccharides neutres ont été transformés en acétates et ont également été réduits en alditols correspondants. Si l'on porte les rotations moléculaires des oligomères acides, neutres et sans forme d'alditols en fonction de leur degré de polymérisation conformément à la relation de Freudenberg, on obtient des lignes droites qui peuvent être extrapolées en un point unique. La rotation spécifique d'un xylane de longueur infinie ainsi obtenue était de −102°. Les rotations calculées et trouvées expérimentalement d'un xylane esparto concordent parfaitement. La rotation moléculaire du xylobiose acétylé ne suit pas la relation de Freudenberg. Une étude de dispersion rotatoire montre que les xylo-oligosaccharides manifestent un comportement rotatoire "simple". Des résultats détaillés de la diffraction des rayons-X au moyen de la méthode des poudres ont été rapportés pour les quatre oligosaccharides neutres et leurs dérivés sous forme d'acétate. Leur cristallinité décroît avec l'augmentation du degré de polymérisation. Les principales propriétés du xylotétraose et du xylopentaose sont les mêmes que celles du xylane.

Zusammenfassung

Zwei Oligosaccharidreihen, eine neutrale und eine saure, wurden durch partielle, enzymatische Hydrolyse eines 4-*O*-Methylglukuronxylans aus Birkenholz isoliert. Die neutralen Xylo-Oligosaccharide wurden zu den β-Acetaten umgesetzt und auch zu den entsprechenden Alditolen reduziert. Beim Auftragen der molaren Drehung der sauren, neutralen und Alditol-Oligomeren gegen den Polymerisationsgrad nach Freudenberg wurden Gerade erhalten, die sich zu einem gemeinsamen Schnittpunkt extrapolieren liessen. Die so erhaltene spezifische Drehung eines unendlich langen Xylans betrug −102°. Der für die Drehung eines Espartograsxylans berechnete Wert stimmte mit

dem gefundenen gut überein. Die molare Drehung der acetylierten Xylobiose gehorchte der Beziehung von Freudenberg nicht. Eine Rotationsdispersionsuntersuchung zeigte, dass die Xylo-Oligosaccharide "einfaches" Rotationsverhalten aufweisen. Genaue Daten für Röntgen-Pulverdiagramme von vier der neutralen Oligosaccharide und ihren Acetatderivaten wurden mitgeteilt. Ihre Kristallinität nahm mit steigendem Polymerisationsgrad ab. Die Hauptlinien der Xylotetraose und Xylopentaose stimmten mit denen des Xylans überein.

JOURNAL OF POLYMER SCIENCE: PART C NO. 2, PP. 63-71 (1963)

Structural Studies on the Water-Soluble Arabinogalactans of Mountain and European Larch*

J. K. N. JONES and P. E. REID, *Department of Chemistry, Queen's University, Kingston, Ontario, Canada*

Water-soluble polysaccharides have been isolated from a number of species of larch,[1] but intensive structural studies have only been carried out on those from eastern,[2,3] European,[4-8] and western larches.[9-18] We were interested in comparing the structures of these water soluble polysaccharides with the structure of that isolated from mountain larch to ascertain if there were any differences which might be a result of the elevated altitude which is the natural habitat of mountain larch.

Mountain larch heartwood shavings were extracted with benzene and ethanol and then with cold water. From this cold water extract a crude polysaccharide was obtained which represented 9.1% of the dry weight of the wood. Wood shavings (ca. 0.001 in. thick) offer the advantage over sawdust in that they are easier to handle in large quantities.

The crude polysaccharide contained galactose, arabinose and uronic acid and traces of other sugars.

Moving boundary electrophoresis in 0.5*M* borate buffer indicated the presence of three components, one of which failed to migrate. The crude polysaccharide was fractionated by the addition of Cetavlon hydroxide to a boric acid solution of the polysaccharide, and fractions with similar physical constants were pooled. A purified fraction migrated as a single peak on moving boundary electrophoresis and contained galactose 78.6%, arabinose 14.6%, and glucuronic acid 6.8%. Fractionation of the polysaccharide methyl ether with chloroform-light petroleum yielded a main fraction representing 90% by weight. Thus the polysaccharide is probably homogeneous. Bouveng examined the water-soluble polysaccharide of mountain larch[16] but found only two components, neither of which contained uronic acid.

The sugars isolated after a partial hydrolysis of the polysaccharide are shown in Table I. Galactose, arabinose, 3-*O*-β-L-arabinopyranosyl-L-arabinose, 3-*O*-β-D-galactopyranosyl-D-galactose, and 6-*O*-β-D-galactopyranosyl-D-galactose were definitely identified. The trisaccharide fraction was a mixture of at least three components and preliminary partial hydrolysis experiments suggested that one of these was *O*-D-galactopyranosyl-

*Abstracted from the Ph.D. Thesis of P. E. Reid, Queen's University, Kingston, Ontario, Canada, 1963.

TABLE I
Products of Partial Hydrolysis of Mountain Larch Polysaccharide

Neutral sugars	Acidic sugars
Monosaccharides	
Galactose	
Arabinose	
Disaccharides	
3-*O*-β-L-Arabinopyranosyl-L-arabinose	6-*O*-β-D-Glucopyranosyl-galactose
3-*O*-β-D-Galactopyranosyl-D-galactose	
6-*O*-β-D-Galactopyranosyl-D-galactose	
Trisaccharides	
O-D-Galactopyranosyl-(1 → 6)-*O*-D-galactopyranosyl-(1 → 6)-D-galactose	
Unknown components	
Higher oligosaccharides	
Unresolved mixture	

(1 → 6)-*O*-D-galactopyranosyl (1 → 6)-D-galactose. The aldobiouronic acid was identified on the basis of paper and gas phase chromatography of the hydrolyzate of its methyl ether.

Table II lists shows the sugars isolated on hydrolysis of the methylated polysaccharide. 2-*O*-Methyl-D-galactose, 2,4-di-*O*-methyl-D-galactose, 2,3,4-tri-*O*-methyl-D-galactose and 2,3,4,6-tetra-*O*-methyl-D-galactose were definitely identified. The identification of 2,5-di-*O*-methyl-L-arabinose, 2,3,4-tri-*O*-methyl-L-arabinose, 2,3,5-tri-*O*-methyl-L-arabinose and 2,3,4-tri-*O*-methyl glucuronic acid rests upon extensive paper chromatography of the compounds and gas phase chromatographic examination of the compounds and some derivatives.

TABLE II
Components Isolated from Hydrolyzate of Polysaccharide Methyl Ether

2-*O*-Methyl-D-galactose
2,4-Di-*O*-methyl-D-galactose
2,3,4-Tri-*O*-methyl-D-galactose
2,3,4,6-Tetra-*O*-methyl-D-galactose
2,5-Di-*O*-methyl-L-arabinose
2,3,4-Tri-*O*-methyl-L-arabinose
2,3,5-Tri-*O*-methyl-L-arabinose
2,3,4-Tri-*O*-methylglucuronic acid

Smith degradation[19] yielded an alcohol-soluble fraction and a degraded polysaccharide (cf. Fig. 1). The former was resolved into four components by paper chromatography. The detection of an arabinosyl-glycerol in Fraction I, if correct, is of structural significance. The identification is based upon the fact that this fraction before hydrolysis showed, in addition to arabinose and glycerol, a component moving behind arabinose which gave a color with silver nitrate but not with *p*-anisidine, whereas after hydrolysis only arabinose and glycerol could be detected.

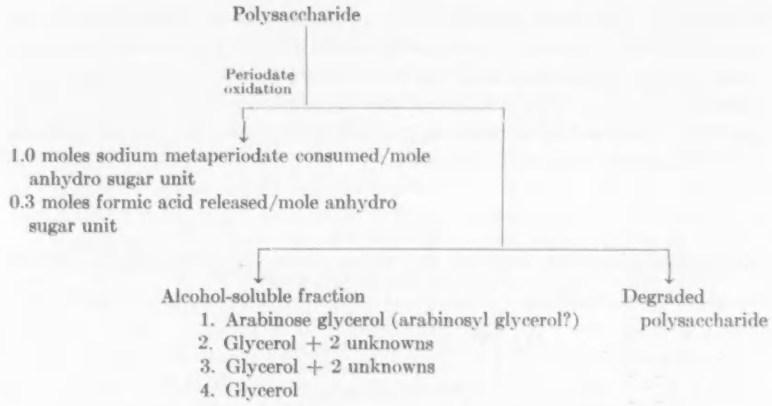
Polysaccharide
Periodate oxidation
1.0 moles sodium metaperiodate consumed/mole anhydro sugar unit
0.3 moles formic acid released/mole anhydro sugar unit
Alcohol-soluble fraction
1. Arabinose glycerol (arabinosyl glycerol?)
2. Glycerol + 2 unknowns
3. Glycerol + 2 unknowns
4. Glycerol
Degraded polysaccharide

Fig. 1. Periodate oxidation of mountain larch polysaccharide.

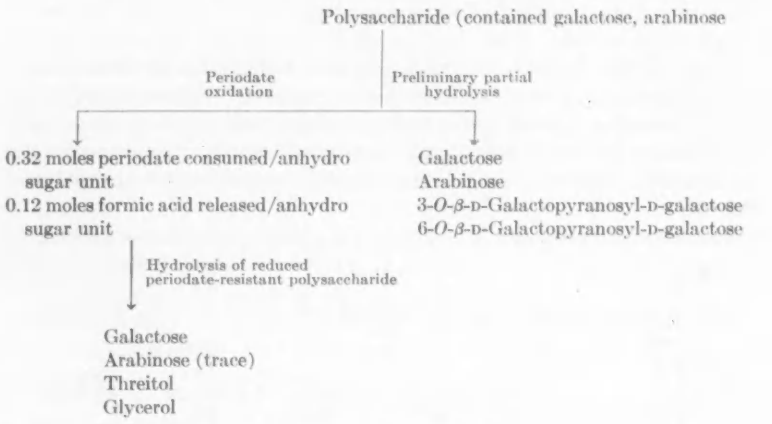

Fig. 2. Examination of degraded polysaccharide.

Figure 2 shows some of the properties of the degraded polysaccharide. It contained only galactose and arabinose, and a preliminary partial hydrolysis indicated the presence of 3-*O*-β-D-galactopyranosyl-D-galactose and smaller quantities of 6-*O*-β-D-galactopyranosyl-D-galactose. On periodate oxidation the consumption of sodium metaperiodate and release of formic acid were small. The reduced, periodate-resistant portion of the polysaccharide on hydrolysis gave galactose, a trace of arabinose, threitol, and glycerol. The degraded polysaccharide proved very difficult to methylate, and a fully methylated product could not be obtained.

Table III lists the sugars identified by gas phase chromatography from the hydrolyzate of the partially methylated and periodate-degraded poly-

saccharide. Structural significance is attributed to the detection of the arabinose, and tetramethyl galactose and also to the trimethyl hexose which could only be an artifact as a result of failure to methylate nonreducing terminal residues. The 2,4,6-tri-*O*-methyl galactose was present in large quantities relative to the other sugars and only small amounts of 2,3,4-tri-*O*-methyl-D-galactose were detected.

TABLE III

Components Indicated by Gas-Phase Chromatography in the Hydrolyzate of Degraded Polysaccharide Methyl Ether

2,4-Di-*O*-methyl-D-galactose
2,3,4-Tri-*O*-methyl-D-galactose
2,4,6-Tri-*O*-methyl-D-galactose
2,3,4,6-Tetra-*O*-methyl-D-galactose
2,3,5-Tri-*O*-methyl-L-arabinose
2,3,4-Tri-*O*-methyl-L-arabinose
At least four unknown components

These results indicate that the degraded polysaccharide is composed predominantly of 1 → 3 linked galactose residues. However, no unique structure can be proposed for the undergraded polysaccharide on the basis of the evidence presented here but the general features of the structure can be outlined. Figure 3 shows some possible structures for the polysaccharide.

The structure proposed is a skeleton of galactose residues consisting in the main of a backbone 1 → 3-linked galactose residues, each of which is

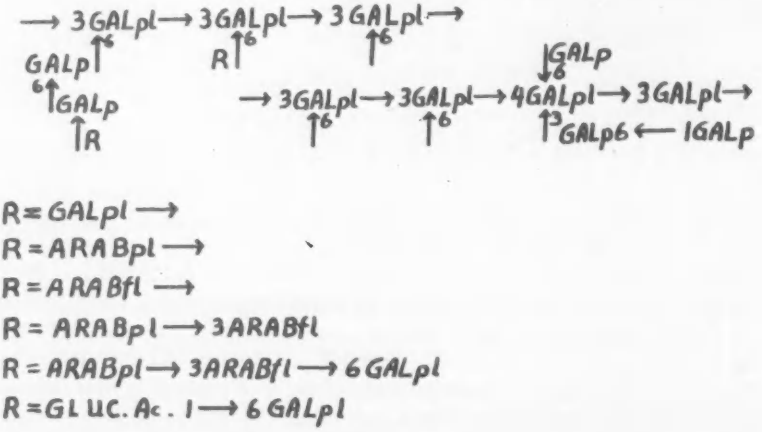

Fig. 3. Possible structures for mountain larch water-soluble polysaccharides. Here GAL_P = galactopyranose; $ARAB_P$ = arabinopyranose; ARABf = arabinofuranose GLUC. Ac. = glucuronic acid.

substituted at position 6 by a chain of 1 → 6-linked galactose residues or by terminal residues. Linkages of the 1 → 6 type may also be present in the backbone. This skeleton accounts for the isolation of 2,4-di-*O*-methyl-D-galactose and 2,3,4-tri-*O*-methyl-D-galactose from the methylated polysaccharide and for the galactose oligosaccharide isolated after partial hydrolysis. Periodate oxidation by the Smith method[19] would be expected to remove the galactose side chains leaving a backbone which on methylation should yield large quantities of 2,4,6-tri-*O*-methyl-D-galactose as in fact was found. Terminal nonreducing residues are shown in Figure 3 as R.

That galactose, arabinopyranose, and arabinofuranose are terminal nonreducing residues follows from the methylation data on the original polysaccharide. As 2,3,4-tri-*O*-methyl glucuronic acid was the only methylated uronic acid detected all of it must be present as nonreducing terminal residues and therefore the polysaccharide cannot be a mixture of a polyuronide and an arabinogalactan. The aldobiouronic acid isolated after partial hydrolysis indicates that some at least of the glucuronic acid is linked to position 6 of a galactose residue.

Some of the arabinose residues are present as 3-*O*-*β*-L-arabinopyranosyl-L-arabinofuranose end groups. This is indicated by the isolation of 3-*O*-*β*-L-arabinopyranosyl-L-arabinose on partial hydrolysis and by the fact that 2,5-di-*O*-methyl-L-arabinose was the only dimethyl arabinose present. The mode of attachment of the 3-*O*-*β*-L-arabinopyranosyl-L-arabinofuranose residue to the galactose skeleton is uncertain. The presence of nonreducing terminal arabinose residues in the degraded polysaccharide indicates that a portion of the grouping is attached to a nonoxidizable galactose residue, and accordingly it has been placed on position 6 of a galactose residue in the backbone.

The isolation of an arabinosyl glycerol from the alcohol-soluble fraction obtained on Smith degradation of the original polysaccharide indicates that some of the 3-*O*-*β*-L-arabinopyranosyl-L-arabinofuranose residues must be attached to an oxidizable galactose residue. The most likely position of attachment is therefore position 6 of a galactose residue in a side chain, since other positions of attachment would require the isolation of methyl ethers which were not in fact found.

The isolation of 2-*O*-methyl-D-galactose from the methylated polysaccharide indicates the presence of some 1 → 4 linkages. One possible arrangement accounting for the detection of this sugar is shown in Figure 3. After periodate oxidation, reduction, and hydrolysis, the galactose residues attached to position 3 and 6 would be removed, and further oxidation followed by reduction and hydrolysis would yield threitol. Such a structure would require the presence of 2,3,6-tri-*O*-methyl-D-galactose in the hydrolyzate of the methylated degraded polysaccharide. Whether this was present is as yet unknown.

It is not claimed that the structure presented here is the actual structure or the only possible structure on the basis of the evidence but only that it represents the gross structural features of the polysaccharide. Indeed, it

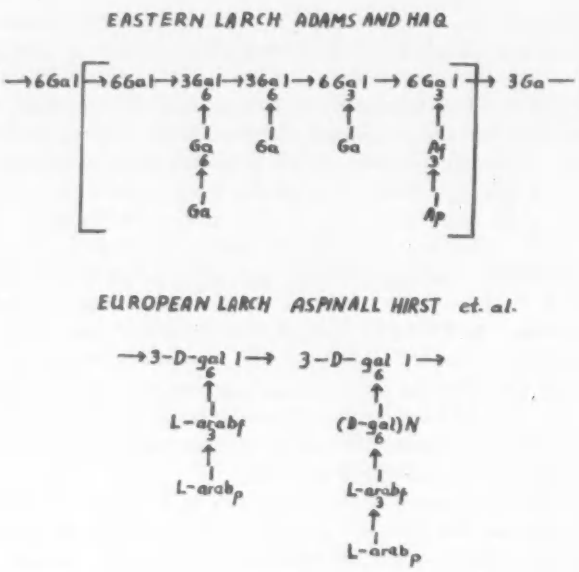

Figure 4.

does not account for the detection of 2,3,4-tri-*O*-methyl-L-arabinose in the methylated degraded polysaccharide.

The structures which have been proposed for the water soluble polysaccharides of eastern and European larches are shown in Figure 4.

There is one striking difference between the polysaccharide from mountain larch and those from eastern and European larches and indeed from all water-soluble larch polysaccharides so far examined, namely, the presence of glucuronic acid in the present polysaccharide. Aside from this and the fact that mountain larch polysaccharide has terminal nonreducing arabinose residues the structure is similar to that proposed for European larch but shows differences to that proposed for eastern larch particularly in the nature of the backbone. The water-soluble polysaccharide of western larch has been extensively studied. Bouveng[16–18] and Bouveng and Lindberg[14,15] have shown that the structure proposed by White[9–12] is incomplete in several respects. It is clear from their results, however, that while in their gross features the polysaccharides of western larch are similar to those of European, eastern and mountain larch, they differ in the fine details of structure.

It was mentioned above that the polysaccharide obtained on Smith degradation of European larch water-soluble polysaccharide was difficult to methylate. Hirst, Jones, et al.[4–6] have studied the structure of this material, and in a recent publication of Aspinall[7] and Nicolson[8] the structure shown in Figure 4 is proposed for this polysaccharide.

The polysaccharide thus obtained contained galactose and arabinose and consumed 0.22 moles of sodium metaperiodate and released 0.07 moles of formic acid/anhydro sugar unit. The periodate-resistant material contained only galactose. Gas-phase chromatographic examination of the hydrolyzate of the partially methylated polysaccharide indicated a composition qualitatively similar to that obtained from the degraded polysaccharide of mountain larch (Table III) with the possibility that very small quantities of 2,5-di-*O*-methyl-arabinose were also present. The quantity of 2,4,6-tri-*O*-methyl-D-galactose was once again very large and 2,3,4-tri-*O*-methyl-D-galactose very small. As with mountain larch, structural significance is attributed to the tetramethyl- and trimethylhexoses and to the trimethylpentoses.

It can been seen therefore that the evidence obtained fits well with the structure proposed by Aspinall et al.[7,8] (Fig. 4).

Thus the Smith periodate oxidation of the polysaccharide would be expected to remove all the galactose side chains and also some of arabinose residues leaving a polysaccharide which on methylation should yield essentially the methylated sugars found. The periodate consumption and formic acid released for this polysaccharide should be low and all the remaining arabinose should disappear again as was the case. The only unexplained observation is the detection of 2,3,4-tri-*O*-methyl-L-arabinose in the product of hydrolysis of methylated degraded polysaccharides.

Experimental details for this work will be published elsewhere.[20]

References

1. Whistler, R. L., and C. L. Smart, *Polysaccharide Chemistry*, Academic Press, New York, 1953.
2. Adams, G. A., *Can. J. Chem.*, **38**, 280 (1960).
3. Adams, G. A., and P. Haq, *Can. J. Chem.*, **39**, 1563 (1961).
4. Campbell, W. G., E. L. Hirst, and J. K. N. Jones, *Nature*, **147**, 25 (1941).
5. Campbell, W. G., E. L. Hirst, and J. K. N. Jones, *J. Chem. Soc.*, **1948**, 774.
6. Jones, J. K. N., *J. Chem. Soc.*, **1953**, 1672.
7. Aspinall, G. O., E. L. Hirst, and E. Ramstead, *J. Chem. Soc.*, **1958**, 2503.
8. Aspinall, G. O., and A. Nicolson, *J. Chem. Soc.*, **1960**, 2503.
9. White, E. V., *J. Am. Chem. Soc.*, **63**, 2871 (1941).
10. White, E. V., *J. Am. Chem. Soc.*, **64**, 302 (1942).
11. White, E. V., *J. Am. Chem. Soc.*, **64**, 1507 (1942).
12. White, E. V., *J. Am. Chem. Soc.*, **64**, 2833 (1942).
13. White, E. V., and W. Low, *J. Am. Chem. Soc.*, **65**, 2430 (1943).
14. Bouveng, H. G., and B. Lindberg, *Acta Chem. Scand.*, **10**, 1515 (1956).
15. Bouveng, H. G., and B. Lindberg, *Acta Chem. Scand.*, **12**, 1977 (1958).
16. Bouveng, H. G., *Acta Chem. Scand.*, **13**, 1869 (1959).
17. Bouveng, H. G., *Acta Chem. Scand.*, **13**, 1877 (1959).
18. Bouveng, H. G., *Acta Chem. Scand.*, **15**, 78 (1961).
19. Goldstein, J., G. W. Hay, B. A. Lewis, and F. Smith, paper presented at 135th National Meeting, American Chemical Society, Boston, April 1959.
20. Reid, P. E., Ph.D. thesis, Queen's University, Kingston, Ontario, Canada, 1963.

Synopsis

The water-soluble extract of mountain larch (*Larix Lylalli Parl*) heartwood has been shown to be a mixture of at least three components. Fractionation of an aqueous boric acid solution of the mixture with Cetavlon hydroxide yielded a polysaccharide which moved as a single component on moving boundary electrophoresis. A purified fraction contained 78.6% galactose, 14.6% arabinose, and 6.8% uronic acid. A partial hydrolysis of the polysaccharide yielded D-galactose, L-arabinose, 3-*O*-β-L-arabinopyranosyl-L-arabinose, 3-*O*-β-D-galactopyranosyl-D-galactose, 6-*O*-β-D-galactopyranosyl-D-galactose and 6-*O*-β-D-glucopyruronosyl-D-galactose. In addition, preliminary experiments indicated the presence of *O*-D-galactopyranosyl-(1 → 6)-*O*-galactopyranosyl-(1 → 6)-D-galactose. From these data along with the results of a Smith degradation and analysis of the product, a structure is proposed for the arabinogalactan of mountain larch. This structure differs only in the fine details from those proposed for the water-soluble polysaccharides of western, eastern, and European larch. The most unique structural feature of the mountain larch polysaccharide is the presence of glucuronic acid as nonreducing terminal residues.

Résumé

L'extrait soluble dans l'eau, du bois de coeur du mélèze de montagne est un mélange d'au moins trois constituants. Le fractionnement d'une solution aqueuse d'acide borique de ce mélange avec l'hydroxyde de cetavlon donne un polysaccharide, qui se déplace comme un seul constituant dans l'électrophorèse à front variable et qui contient 78.6% de galactose, 14.6% d'arabinose et 6.8% d'acide uronique. Une hydrolyse partielle du polysaccharide donne du D-galactose, L-arabinose, 3-*O*-β-L-arabinopyranosyle-L-arabinose, 3-*O*-β-D-galactopyranosyle-D-galactose, 6-*O*-β-D-galactopyranosyle-D-galactose et 6-*O*-β-D-glucopyranosyle-D-galactose. Des expériences préliminaires indiquaient en outre la présence de *O*-D-galactopyranosyle-(1 → 6)-*O*-galactopyranosyl-(1 → 6)-D-galactose. À partir des résultats cités, des résultats d'une dégradation suivant Smith et de l'analyse des produits, on propose une structure pour l'arabinogalactose du melèze des montagnes. Cette structure varie seulement dans les détails fins de la structure proposée pour le polysaccharide, soluble dans l'eau, du mélèze occidental, oriental et européen. Le caractère structural le plus exceptionnel du mélèze de montagne est la présence de l'acide glucuronique comme groupe terminal non-réducteur.

Zusammenfassung

Der wasserlösliche Extrakt aus Berglärchen-(*Larix Lylalli Parl*)-kernholz besteht aus einer Mischung von zumindest drei Komponenten. Fraktionierung einer Lösung der Mischung in wässriger Borsäure mit Cetavlonhydroxyd lieferte ein Polysaccharid, das sich bei der Elektrophorese mit bewegter Grenzfläche also einkomponentig erwies und 78,6% Galactose, 14,6% Arabinose und 7,2% Uronsäure enthielt. Die partielle Hydrolyse des Polysaccharids ergab D-Galactose, L-Arabinose, 3-*O*-β-L-Arabinopyranosyl-L-arabinose, 3-*O*-β-D-Galactopyranosyl-D-galactose, 6-*O*-β-D-Galactopyranosyl-D-galactose und 6-*O*-β-D-Glucopyranosyl-D-galactose. Ausserdem sprachen vorläufige Versuche für die Anwesenheit von *O*-D-Galactopyranosyl(1 → 6)-*O*-galactopyranosyl-(1 → 6)-D-galactose. Auf Grund dieser Daten sowie eines Abbaus nach Smith und einer Analyse des Produkts wird eine Struktur für das Arabinogalactan aus Berglärche vorgeschlagen. Diese Struktur unterscheidet sich nur in einzelnen Feinheiten von der für die wasserlöslichen Polysaccharide von westlicher, östlicher und europäischer Lärche vorgeschlagenen. Die auffallendste Struktureigentümlichkeit des Berglärchen-Polysaccharids bildet die Anwesenheit von Glucuronsäure als nicht-reduzierende Endgruppe.

Discussion

R. H. Marchessault (*College of Forestry, Syracuse, New York*): Do you have any idea why it is that the water-soluble arabinogalactans are directly extractable from wood with water, but the water-soluble acetyl xylans are not?

P. Reid: I am afraid I do not know the answer, but presumably it could be a question of the availability of the compound to the extractive agent, e.g., we found that the yield of water-soluble polysaccharide extractable from Loblolly pine sawdust apparently depended on the mesh size of the sample used.

T. E. Timell (*Department of Chemistry, McGill University, Montreal, Canada*): You have stressed the structural differences between your arabinogalactan from mountain larch and the arabinogalactan from eastern larch (tamarack) studied recently by Adams and Haq. These workers isolated by partial hydrolysis of the polymer no less than nine oligosaccharides, several or which were tri- and tetrasaccharides. There is no doubt that in this way the structure of a polysaccharide can be nailed down far more accurately than by any other method, for example the methylation technique. I feel that quite possibly all arabinogalactans in the various species of *Larix* might be very similar and that the different structures assigned to them in the literature have resulted from the fact that often different methods were used by different investigators.

P. Reid: I agree that it is very satisfactory to obtain a large number of oligosaccharides. I should emphasise that we are not claiming that the structure we proposed for mountain larch arabinoga'actan is the only possible structure, but only that it seems to fit quite well with the evidence we have obtained so far. It may well be, as Dr. Timell suggests, that all larch arabinogalactans are very similar, but I feel that more work will be required to elucidate this point.

JOURNAL OF POLYMER SCIENCE: PART C NO. 2, PP. 73–78 (1963)

Investigation into the Efficacy of Water-Soluble Arabinogalactan as a Plasma Substitute

ROBERT E. SEMPLE, *Department of Physiology, Queen's University, Kingston, Ontario, Canada*

To qualify as a useful plasma substitute or plasma volume expander (to use a ridiculous term that is nevertheless in some favor today), a substance must satisfy a number of requirements. Thus, it must not be toxic, it must not be stored in any part of the body, it must not act as a specific drug (diuretic, etc.); on the positive side it must have the necessary physical and chemical properties to ensure that it will survive in the circulation long enough to be useful. In this latter connection most colloids with molecular weights much less than that of mammalian albumin (ca. 70,000) are not efficient plasma substitutes.

Several high molecular weight carbohydrates have been tried as plasma substitutes in the past. Bayliss[1] used acacia (gum arabic) in saline during the 1914–18 war and often obtained good results. Various pectins have also been used.[2] Both these materials suffer from the fact that it is extremely difficult to manufacture them so that their properties are predictable. Furthermore, there was considerable evidence that, in the case of acacia at least, the macromolecules were stored by the liver.[3] The investigations of Grönwall and Ingelman[4] led to the development of dextran solutions that proved to be useful plasma substitutes. Today dextran is probably the most widely used and probably the most efficacious material available.

The interest shown by Professor J. K. N. Jones and his group in the Department of Chemistry at Queen's University in the arabinogalactan of larch led us to extract, purify, and test this substance with a view to determining whether or not it possessed properties that would make it a useful plasma substitute. The original water-soluble material was a yellowish powder which, when made up in aqueous solution, produced a faint yellow solution when the pH was adjusted below 5.8, and a dark brown solution in more alkaline solutions. A purer product was obtained when a 2% solution was passed down, in turn, two ion exchange columns (Dowex IR 120 and Duolite A-4). The resulting material, when dried, was a white powder and when dissolved in water produced a faint straw-colored solution which did not change color with changes in hydrogen ion concentration.

This product was examined by Tiselius electrophoresis for homogeneity,

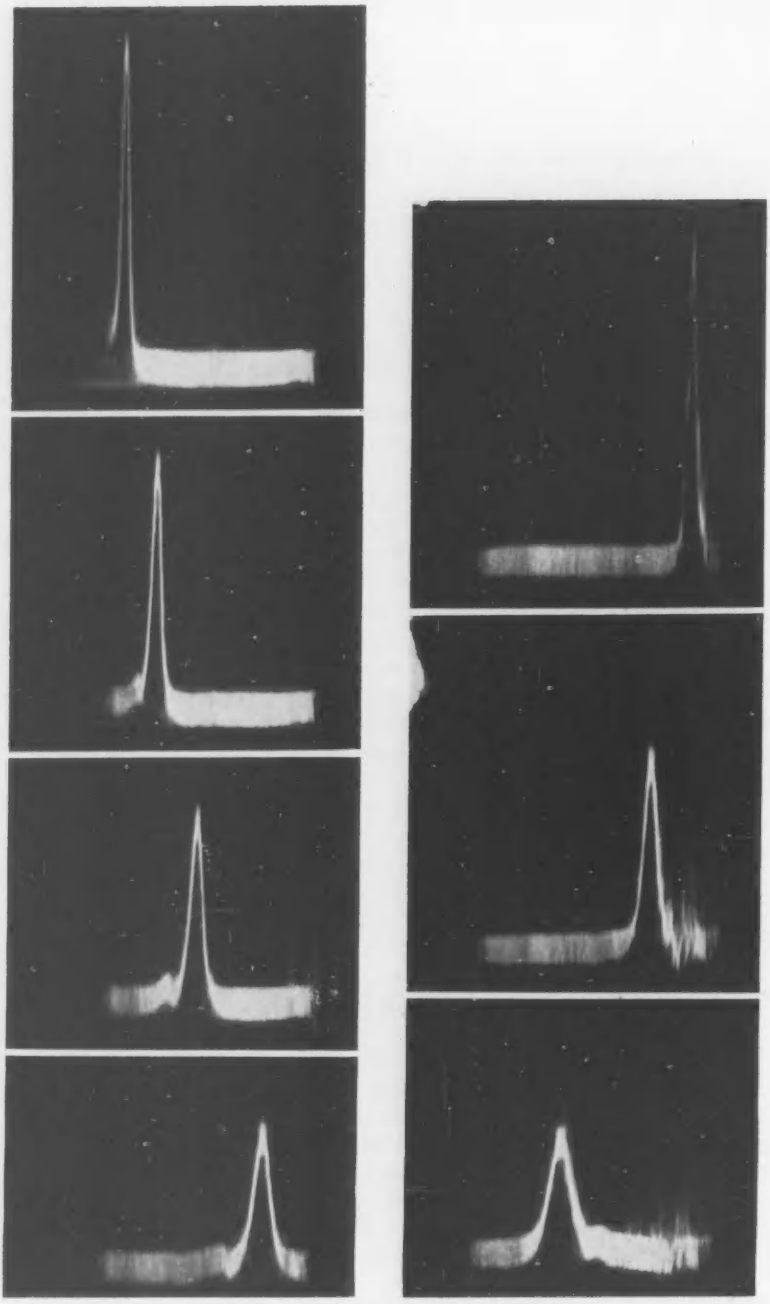

Fig. 1. Tiselius electrophoretic patterns on the larch arabinogalactan used in the physiological experiments described in the text. Note the presence of a small amount of a secondary component.

and both relative and inherent viscosities, as defined by Cragg,[5] were measured with the use of Ostwald viscosity pipets. The electrophoretic patterns obtained indicated that the arabinogalactan produced was not homogenous, but that there was only a very small amount of a secondary component present (Figure 1). Viscosity measurements showed that aqueous solutions of this material exhibited low relative viscosities (Table I), particularly when compared with dextran. A similar result was obtained when inherent viscosities were calculated. Thus, the average inherent viscosity of an aqueous arabinogalactan solution (0.20 g./100 ml.) was 0.074 (range: 0.070–0.081). This is low when the comparable viscosity for clinically useful dextrans is considered (ca. 0.324). These results indicated that the larch arabinogalactan either had a low average molecular weight or was very highly branched, or both.

TABLE I
Relative Viscosities of Dog Plasma, Dextran, and Arabinogalactan Solutions

	Relative viscosity[a]	
	Range	Mean
Dog plasma	1.32–1.38	1.35
Dextran[b]	4.45–4.52	4.29
Arabinogalactan[b]	1.28–1.32	1.30

[a] Ten measurements were made with each of the fluids listed.
[b] 5.5 g./100 ml. solution.

The preliminary physiological tests were somewhat encouraging. Thus, *in vitro* mixtures of rabbit, dog, or human blood with aqueous arabinogalactan solutions resulted in no observable clumping of erythrocytes or in any other cell abnormalities. Similarly, repeated injections of the solutions of arabinogalactan gave no anaphylactoid or pyrogenic reactions.

These preliminary tests led to experiments which had as their objective the evaluation of this material as a therapeutic agent in haemorrhagic shock. Eight dogs were bled by the method described by Walcott,[6,7] and the volume of blood lost was replaced by an equal volume of an aqueous solution of arabinogalactan (5.5 g./100 ml.). The following measurements were made during a control period as well as after bleeding and after infusions: blood pressure and heart rate; respiratory rate; plasma and blood volumes; rectal, muscle, and skin temperatures. Samples of plasma, secured at appropriate times following infusion, were analyzed for arabinogalactan.

Animals bled in this way and then infused with an isotonic solution of NaCl do not survive much longer than do controls. On the other hand, if the animals are given infusions of clinical dextran solutions, they survive indefinitely.[8] In Figure 2 typical blood pressure changes are shown for animals treated with isotonic NaCl, dextran and arabinogalactan solutions. Note that with the arabinogalactan solution blood pressure was restored

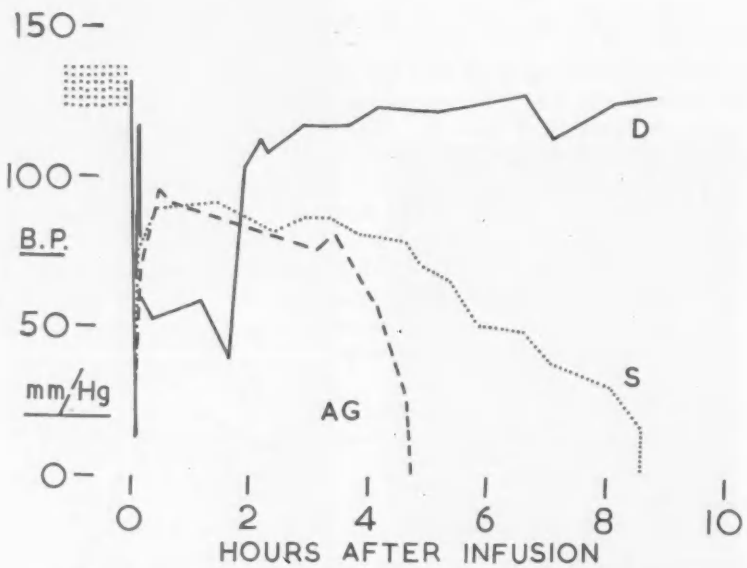

Fig. 2. Sample blood pressure changes after a Walcott haemorrhage (at zero time) followed immediately by an infusion of: (*D*) clinical dextran solution; (*S*) isotonic NaCl; (*AG*) 5.5 g./100 ml. aqueous solution of larch arabinogalactan. These records are atypical, in that the average survival time of animals receiving arabinogalactan was not significantly different from that of animals that received saline (see text).

for only a brief period of time and declined thereafter. Of the eight dogs that received the arabinogalactan solution, four died within 6 hr., two survived for 6–7 hr. and two survived for more than 15 hr. The blood pressure changes as well as the survival times noted above strongly indicated that the carbohydrate was leaving the circulation very rapidly, thus failing to maintain colloid osmotic pressure or circulating plasma volume. The results of the plasma volume measurements supported these conclusions; chemical analyses of plasma samples also showed a rapid disappearance of this colloid from the circulation. In the bled dogs, as in the control animals, the arabinogalactan did not seem to be toxic in any way, nor were there any detectable pyrogenic or other reactions.

In conclusion, one can say that although the arabinogalactan appears to qualify as a plasma substitute on the basis of desirable negative properties (it is not toxic, does not cause anaphylactoid or pyrogenic reactions in the test animals, and does not act as a specific drug) it does not have the vital positive property of remaining for a useful period of time in the circulation. The mean molecular weight of the material used was undoubtedly much too low. Thus this form of arabinogalactan cannot be considered as a plasma substitute. If available, a higher molecular weight fraction of the material would be worth investigating. Alternatively, if the

present material could be synthetically polymerized in some way, making the effective colloidal moiety much larger, further investigations could be worthwhile.

References

1. Bayliss, W. M., *Proc. Roy. Soc.*, **B89,** 381 (1916).
2. Jacobson, S. D., and C. J. Smyth, *Proc. Soc. Exptl. Biol., N. Y.*, **50,** 218 (1942).
3. Falkenstein, D. F., and R. L. Jackson, *J. Pediat., St. Louis,* **16,** 701 (1940).
4. Grönwall, A., and B. Ingelman, *Acta Physiol. Scand.*, **7,** 97 (1944).
5. Cragg, L. H., *J. Colloid Sci.*, **1,** 261 (1946).
6. Walcott, W. W., *Am. J. Physiol.*, **143,** 254 (1945).
7. Wang, I. C., and W. W. Walcott, *Am. J. Physiol.*, **170,** 143 (1952).
8. Semple, R. E., *Can. J. Biochem. Physiol.*, **32,** 670 (1954).

Synopsis

An arabinogalactan was extracted from shavings of Eastern larch and was purified by repeated alcohol precipitation and by ion exchange resins. The product dissolved readily in water to give a clear solution which exhibited low relative and inherent viscosities when compared with dextran solutions which have proved useful as plasma substitutes. Arabinogalactan solutions, when mixed with rabbit, dog or human blood, had no detectable effect on the erythrocytes nor did repeated injections cause any undesirable reactions in rabbits. These solutions did not restore, for any appreciable length of time, the blood pressure or circulating plasma volume of dogs made hypotensive by haemorrhage nor did they improve, significantly, the survival rate of such animals. Analysis of blood samples showed that the arabinogalactan disappeared from the circulation at a rapid rate. It was concluded that the mean molecular weight of this arabinogalactan preparation was too small to be physiologically useful; if another fraction, with an appreciably higher mean molecular weight, were available a further study of this material as a possible plasma substitute would be worthwhile.

Résumé

Un arabinogalactane a été extrait de copeaux de mélèzes d'Orient et a été purifié par précipitation répétée dans l'alcool et au moyen de résines échangeuses d'ions. Le produit qui est dissous rapidement dans l'eau afin de donner une solution limpide montre une viscosité inhérente relativement faible comparée à des solutions de dextrane qui manifestent une utilisation comme substituts du plasma. Des solutions d'arabinogalactane quand elles sont mélangées au sang de lapin, de chien ou du sang humain, n'ont pas d'influence détectable sur les érythrocytes et des injections répétées ne provoquent pas de réactions indésirables chez les lapins. Ces solutions ne rétablissent pas, pour une durée de temps appréciable, la pression sanguine ou le volume du plasma en circulation chez des chiens rendus hypotensifs par hémorragie et n'éprouvent pas non plus de manière significative la durée de survie de tels animaux. L'analyse d'échantillons de sang montre que l'arabinogalactane disparaît de la circulation avec une grande vitesse. Il a été conclu que le poids moléculaire moyen de cet échantillon d'arabinogalactane était trop bas pour être physiologiquement utile; si une autre fraction de poids moléculaire moyen plus élevé s'avérait utile, une étude ultérieure de ce produit comme substitut possible du plasma pourrait valoir la peine.

Zusammenfassung

Aus Spänen von östlicher Lärche wurde ein Arabinogalactan extrahiert und durch wiederholte Fällung mit Alkohol und über Ionenaustauscher gereinigt. Das Produk löste sich leicht in Wasser unter Bildung einer klaren Lösung, die im Vergleich zu dem

als Plasmaersatzmittel verwendeten Dextranlösungen eine nur geringe Viskositätserhöhung zeigte. Arabinogalactanlösungen hatten beim Vermischen mit Kaninchen-, Hunde- oder Menschenblut weder einen nachweisbaren Einfluss auf die Erythrocyten, noch verursachten wiederholte Injektionen beim Kaninchen irgendwelche unerwünschten Reaktionen. Solche Lösungen ergaben bei Hunden, die hämorrhagisch hypotensive gemacht worden waren, keine zeitlich in Betracht kommende Wiedererhöhung des Blutdrukes oder des circulierenden Plasmavolumens, und lieferten auch keine signifikant Verbesserung der Überlebensrate solcher Tiere. Offenbar war das mittlere Molekulargewicht dieses Arabinogalactanpräparates zu klein, um physiologisch brauchbar zu sein; falls eine weitere Fraktion mit beträchtlich höherem mittleren Molekulargewicht zugänglich wäre, würde eine Untersuchung dieses Materials als möglicher Plasmaerstazstoff der Mühe wert sein.

Discussion

Melvin A. Lipson (*Forest Chemistry Dept., College of Forestry, Syracuse, N. Y.*): Eliminating physiological and toxicological requirements for a plasma substitute, can we infer from your work that a prime criterion for an effective plasma substitute is its proximity in relative viscosity to that of natural plasma?

If not, why is dextran so effective as compared to the polysaccharide which you described?

R. E. Semple: (*1*) No. The prime criterion is in fact the ability of a macromolecule to stay in the circulation for a useful period of time. Viscosity measurements are very useful in estimating molecular weight. Of course, if the relative viscosity of the material is very high with respect to the viscosity of plasma, one would hesitate to consider the material as a potential plasma substitute.

(*2*) Principally because the mean molecular weight of effective dextrans is considerably higher than that of arabinogalactan described today.

JOURNAL OF POLYMER SCIENCE: PART C NO. 2, PP. 79–95 (1963)

Ozonization of Cellulose and Wood*

CONRAD SCHUERCH, *Department of Chemistry, State University College of Forestry at Syracuse University, Syracuse, New York*

The problem of carrying out successful chemical reactions on solid polymers is frequently one of transporting reagent into well-distributed sites and producing homogeneous reaction. Spurlin has discussed the solubility, swelling, and reactivity of cellulose and has given most valuable guidelines for carrying out liquid-phase reactions on cellulose.[1] An additional complication may be introduced, however, when the reagent is a gas which can be applied directly to a polymer-rich phase rather than necessarily having to be first dissolved in a liquid. Xanthation, nitration, hydrolysis[2] of cellulose, and its oxidation[3] with nitrogen dioxide are such reactions. The reactions of cellulose and wood with ozone also have a number of features of interest that have not been explained adequately in the published literature and these are the subject of this report.

Ozone has been investigated as a bleaching agent,[4–6] and has been shown to delignify beechwood,[7] acting as a pulping chemical. It is known also to degrade cellulose[8–12] and to attack carbohydrate material[13] as well as lignin.[14] We have studied its relative rates of reaction with wood polysaccharides and lignin, and as part of a continuing interest in the effect of solvents on reactions of lignin[15] have done so in a few different solvent systems.

We have found it helpful to define our results[16,17] on the ozonization of wood and of unbleached kraft pulp in terms of a simplified model which is applicable to chemical reactions on any solid polymer (Fig. 1). In general a molecule of reagent (x) will be separated from reaction site (y) by a distance which can be subdivided in three. Across the first section of free-flowing liquid or gas (d_1), the reagent is transported rapidly by convection. The second section (d_2) is immobilized solvent or fluid of some type and the reagent travels here by diffusion. The third (d_3) is the solid phase proper through which the reagent must also pass by diffusion.

In addition it should be remembered that the reagent crosses interfaces between gas and liquid, liquid and solid, or gas and solid. In nearly any reaction on cellulose or wood, the process will be diffusion-controlled, and the primary problem for successful, rapid and homogeneous reaction is to minimize distances d_2 and d_3 and/or maximize the corresponding rates of

* This article summarizes the conclusions drawn from studies by Z. Osawa, W. A. Erby, E. Carpenter, and R. Aksentijevich. Some of the initial studies were with the assistance of K. V. Sarkanen. The author gratefully acknowledges the support of the Herman Frasch Foundation for a portion of this work.

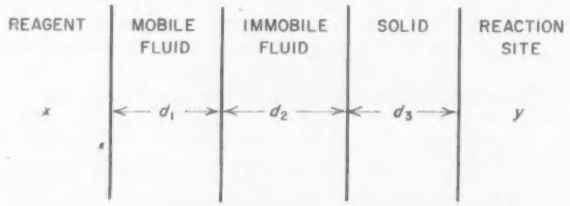

Fig. 1. Transport of reagent in reactions on cellulosic systems.

diffusion. Sufficient plasticizer in the form of solvent or reagent must be present to permit a reasonable rate of diffusion through the polymer matrix but excessive amounts of a good solvent will cause swelling and increase distance d_3 unnecessarily. (Compare the action of ozone on rubber.[18]) In addition, it is clear from our results and from comparisons with earlier work by Doreé that the gas–solid interface can represent a substantial transport barrier.

The possible advantage of a gas phase reaction on wood or cellulose is that the rate of diffusion in the immobile gas phase will be substantially higher and the distance d_2 may be substantially decreased as well. The distance d_2 will often in liquids be of very substantial size and can represent a serious barrier to chemical reaction. In a single fiber some solvent can be effectively immobilized in flaws, fissures, pits, and in the lumen. In clumps of fibers, solvent is often sufficiently immobilized to prevent reaction until long after reaction on accessible individual fibers is complete. In wood particles, immobilized solvent is effectively of the same dimensions as the particle and any reagent which cannot be introduced into the particle in the initial impregnation must diffuse over distances which are extremely large on a molecular scale. This undoubtedly sets the lower limit on useable temperatures for liquid phase pulping reactions. In contrast, the low viscosity and negligible association of gases permits ready permeation of fiber sheets or clumps by rapid convection (d_2 therefore, approaches zero), and to the extent that any particular wood sample approaches in structure an open celled foam, a reasonably even reaction from cell to cell can be expected by the simple expedient of pressure fluctuation.

OZONIZATION OF PULP

When the ozonization of pulp or cellulose is carried out under different conditions, the results obtained vary markedly and these differences can be correlated with changes in the transport system defined above. In our case unbleached kraft pulp was used, cellulose degradation was measured by decrease in cuprammonium viscosity, and lignin degradation was measured by increase in brightness. Increase in brightness is, of course, not a quantitative measure of lignin degradation, but is of interest in its own right. Usually viscosities and brightness were also measured after reduction of the pulp with sodium borohydride.

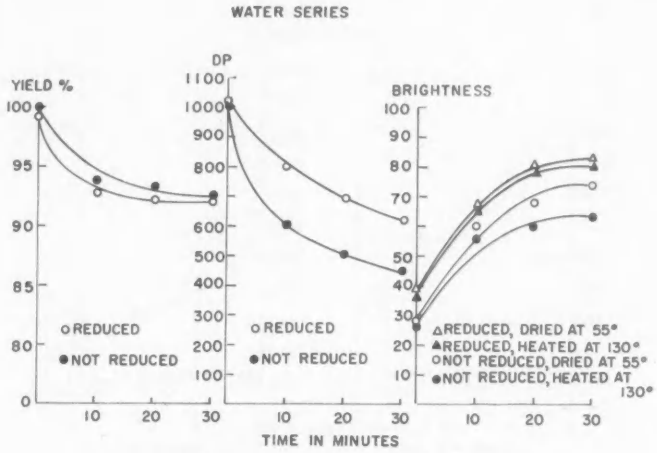

Fig. 2. Gas-phase ozonization of kraft pulp.

Previous investigators of the ozonization of cellulose have emphasized the sensitivity of the reaction to moisture content of the cellulose. (In this study: % moisture = $(w_{H_2O}/w_{\text{dry solid}}) \times 100$.) Dorée[10,11] investigated cellulose degradation by ozone over a period of years and came to a basically sound explanation of this phenomenon. At very low moisture contents, cellulose was effectively impervious to ozone attack except for superficial surface oxidation. At very high water contents the rate of cellulose degradation is decreased by the slow rate of diffusion of the ozone through a liquid layer. At a narrow range of moisture content, Dorée found a substantially higher rate of reaction than at either lower or higher moisture contents. This was at 50% moisture content on cotton fiber.[10,11]

A patent issued to Brabender and co-workers[4] reports a similar phenomenon on the bleaching of cellulosic pulp pads. They observed that both ozone consumption and brightness increase were greatest at an intermediate moisture content. (Actually this is a rate effect.) However, Dorée observed his maximum at 50% moisture content and Brabender observed his at 30 to 45% consistency or 230–120% moisture content. Although our moisture control was less precise, we set our experimental conditions so that our pulps contained approximately 100% moisture content. Under these conditions the rate of reaction as measured by brightness increase and cellulose degradation was indeed very rapid. In $^1/_2$ hr. brightness increased from about 30 to 73 and cellulose degree of polymerization decreased from 1000 to 450 (Fig. 2).

When unbleached kraft pulp was well dispersed in water at one percent concentration and treated with a large excess of ozone, even with vigorous stirring the rate of reaction is substantially less than that obtained on pulp pads with 100% moisture content. The reason becomes apparent if the pulp susyension is diluted tenfold. At a concentration of 0.1%, the indi-

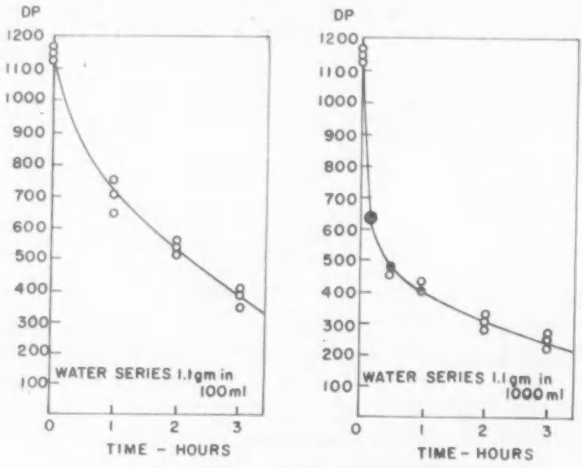

Fig. 3. Liquid-phase organization of kraft pulp.

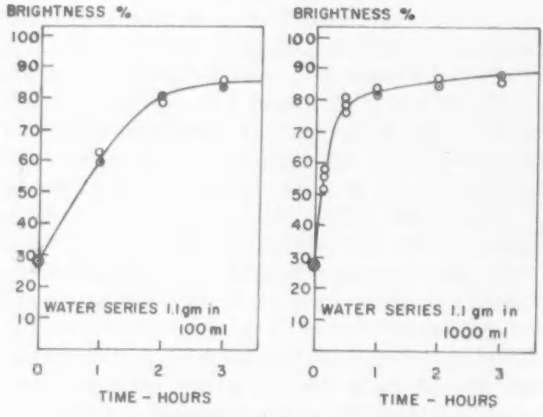

Fig. 4. Liquid-phase ozonization of kraft pulp.

vidual fibers can be completely separated and the rate of reaction is at least that obtained on moist pulp pads (Figs. 3–5).

It seems possible to explain these results in terms of the model previously presented. In bone dry cellulose the rate of diffusion of ozone in the solid phase (d_3) is so slow that reaction is limited to a superficial attack on the polymer surface. The rate of diffusion in d_3 increases with increase in moisture content up to the fiber saturation point (about 25%). With further increases in moisture content no change in the cellulose phase can be postulated. Instead one must postulate that an immobilized gas phase (in d_2) is replaced by an immobilized liquid phase containing a lower concentra-

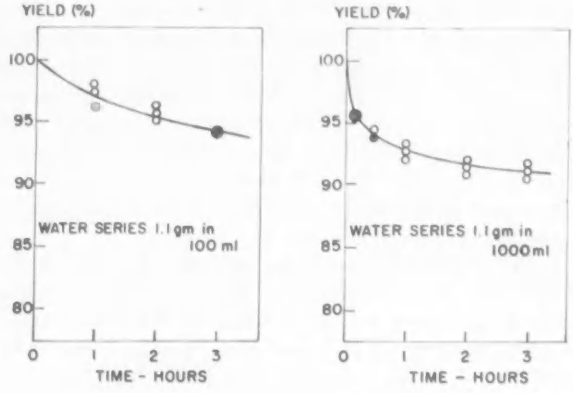

Fig. 5. Liquid-phase ozonization of kraft pulp.

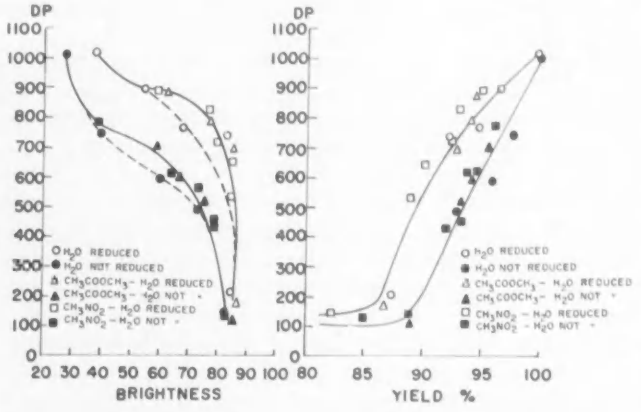

Fig. 6. Relation between DP and (left) brightness and (right) yield.

tion of ozone and less available surface area. The less surface area, lower ozone concentration, and lower rate of diffusion all would tend to lower the rate of ozonization, but the rate increases. The only change in the system that can be assumed to enhance the overall rate is the exchange of a gas–solid interface by a gas-liquid interface. Capture of ozone must be much more efficient by a liquid layer than by solid cellulose. In cotton, approximately 50% moisture content will furnish such a layer while wood fibers with their much larger lumens require substantially more, up to 120–230%.

If the immobilized water layer (d_2) becomes greater than this, the rate of diffusion in the liquid layer is rate-determining, and this situation obtains even in pulp suspensions as dilute as 1% concentration. Only when the fibers are completely separated and freely accessible to flowing solvent saturated with ozone does the overall rate of reaction reach s maximum.

In addition to a fast rate of ozonization we were interested also in specificity of attack on the lignin and colored materials. Our approach to this problem was based on the premise that plant cell wall materials should be considered to have a hydrophilic cellulosic structure interpenetrated by an organophilic lignin matrix, and that to some degree we might expect more specific attack on the lignin by the use of organic solvents that wet it more effectively than does water. In bleaching of cellulose with ozone, the ideal system would be one which permitted permeation of the lignin with minimum accessibility of the cellulose.

Our choice of solvents, nitromethane and methylacetate, was suggested by our experience with lignin solubility behavior and lignin accessibility to chemical attack in various solvent systems.[1] Neither nitromethane nor methyl acetate is more than a mediocre solvent for lignin, but their cohesive energy densities and small molecular volumes at least allow these compounds to permeate lignin effectively, for model experiments indicate that lignin reactions proceed rather rapidly in wood particles suspended in them.[15a] Better solvents for lignin have more hydrogen-bonding character and would be expected to interact strongly with cellulose also.

Four solvent systems: water, nitromethane, water–nitromethane, and water–methyl acetate, were tested for 1% pulp suspensions, and the results from this very limited sample were somewhat different from expected. It was not possible to obtain high brightnesses in pure nitromethane. The reason was clearly apparent from the physical state of the pulp which associated into clumps. The rate of diffusion of ozone into these clumps was sufficiently slow that attack occurred preferentially on individual separate fibers and homogeneous reaction was completely prevented. By the time reasonable brightness had been achieved, very serious degradation had occurred. In contrast in water and aqueous systems, the pulp at 1% concentration was dispersed, and reaction appeared homogeneous. The results in water and in water with 10% nitromethane or 24.2% methyl acetate were, therefore, substantially better than in the pure organic solvent alone. However, if one plots the degree of polymerization against brightness of the various pulp samples it is rather difficult to see any marked specificity in any aqueous solvent system (Fig. 6). The reagent is quite indiscriminate and the degree of brightness achieved at a given degree of polymerization (or at a given yield) is about the same in different aqueous mixtures. This result was not expected, for it was hoped that the addition of nitromethane or methyl acetate would make the lignin more accessible and increase the rate of attack on the lignin. If this effect exists, it is only a minor one. Nevertheless, the use of organic solvents in water increased the rate of attack very substantially, whether this was measured by changes in yield of pulp, brightness or degree of polymerization. Unbleached pulp suspended in water was raised from a brightness of less than 30 to a brightness of about 70 in 3 hr. (Fig. 7). The same change occurred in water–nitromethane, 91:9 in 1 hr. Changes in degree of polymerization and yield followed the same trend. Water–methyl acetate solutions gave similar but

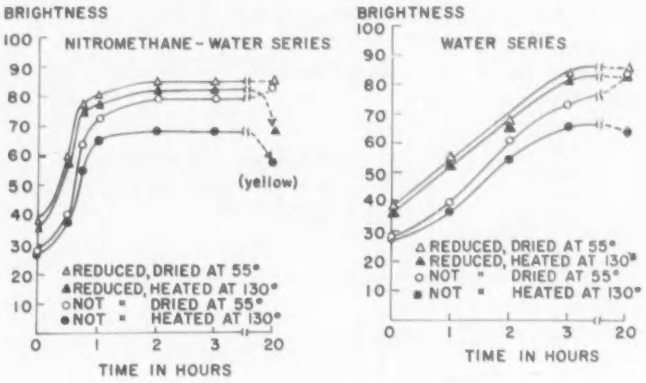

Fig. 7. Liquid-phase ozonization of kraft pulp.

smaller changes and were investigated in less detail. The reason for this effect is not clear. It does not appear to be due to increased concentration of ozone because it occurred in solutions containing as little as 1% nitromethane. There is also little influence on the viscosity of the water. In any case the rate of reaction in no case was as high as that observed in pulp pads or in extreme dilution. In the latter case, brightness values on kraft pulp rose from a value of 28 to 78 points in ½ hr., and the degree of polymerization dropped to 470.

The reduction of ozonized pulps with sodium borohydride has as expected a very favorable effect (Figs. 6 and 7). The reduced pulps had a higher cuprammonium viscosity, higher brightness, and higher heat stability than the unreduced pulps. These results are characteristic of a cellulose containing carbonyl groups which are stabilized by reduction. There also is, of course, some loss in yield from the mildly basic borohydride reduction. The pulps before reduction, however, appear qualitatively to bond very firmly to each other and to form a tougher more coherent sheet of paper than the reduced fibers. This behavior has previously been observed for other mildly oxidized pulps.

OZONIZATION OF WOOD

The same transport problems are evident in the ozonization of wood[17] as in the ozonization of pulp.[16] Our first exploratory series of experiments was an investigation of the attack of ozone on suspensions of Norway spruce wood meal suspended in water and in nitromethane at 0°C. Under these conditions attack on the wood is relatively slow and indiscriminate. After 48 hr. in water or nitromethane, over 80% of the wood remained as a solid residue and appeared to sight to be little changed. (Even a sample of basswood meal required 20 hr. similar treatment for complete whitening.) Of the spruce wood, 40–50% remained analyzable as holocellulose and about

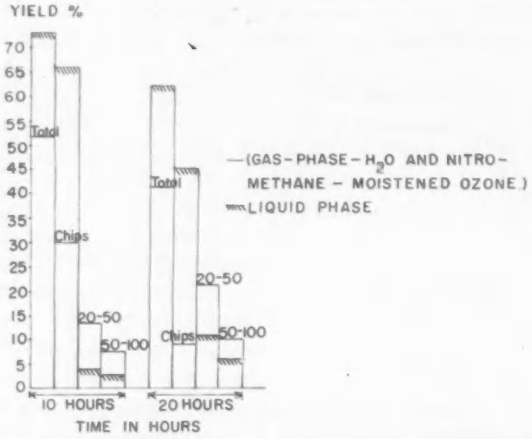

Fig. 8. Washed yields from 10 and 20 hr. ozonolyses of basswood.

one-fourth to one-third of the lignin remained as Klason lignin. The difference between the sum of these two values and the weight of the solid residue was a measure of degraded material that remained behind in the woody tissue and increased in quantity as reaction proceeded, until at 48 hr. it amounted to about 25% of the weight of the original wood. There was some difference in selectivity due to the different solvent characteristics of nitromethane and water but in general the reaction was topochemically heterogeneous and limited largely to the surface.

More extensive series of experiments were carried out on larger particle size wood: small chips of Norway spruce, veneer strips of gum wood and Douglas fir, shavings of basswood, wheat straw, and small pieces of Douglas fir bark. The wood samples were conditioned in desiccators over water or water–nitromethane before reaction in the gas phase and were evacuated and then treated with solvent before reacting in the liquid phase. The products obtained were subjected to mechanical action after ozonization to separate into fibers, fiber bundles, and under-reacted wood. These were separated by screening in water and the water-solubles were lost in the process. The products were characterized by yield to fibers, fiber bundles, and under-reacted wood, and viscosities and brightness values were obtained on certain of the most interesting fiber samples. The wood ozonized in gas was strongly acid and smelled strongly of acetic acid. The bulk of the data was obtained on Norway spruce chips and therefore does not represent the most advantageous example that could be chosen.

Some generalizations can be made from this series. First, with all samples reaction in the gas phase is faster than in the liquid phase and occurs more deeply in the structure. As a result, there is less superficial burning of the wood and lower yields of water-soluble material; more of the wood appears as solid material, i.e., fiber and fiber bundles.

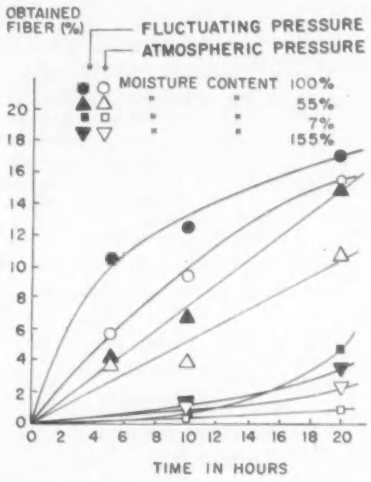

Fig. 9. Rate of ozonization of Norway sprucewood chips.

The greatly enhanced rate of reaction and more homogeneous attack in the gas phase is clearly shown on the bar graphs of Figure 8 that report results on the ozonolysis of basswood shavings.

Secondly, these results are definitely further improved by the use of a fluctuating pressure which permits the ozone to be transported into the structure by convection rather than diffusion. Reaction is made much more rapid, and attack is more homogeneous. Our techniques of pressure fluctuation at this time were rather primitive and changed the pressure from 1 atm. to 1.4 atm. about four times per minute. This does not allow for very much exchange by convection but the improvement is nevertheless very clear on comparison of the rate curves of Figure 9. These data were obtained on Norway spruce chips.

The reaction in the gas phase is markedly influenced by the moisture content of the wood sample as has been noted before. The optimum moisture content is clearly near 100% in Norway spruce (Figs. 10 and 11), and we interpret this to mean that ozone capture by a layer of free water is much more effective than by cellulose fully plasticized with water at the fiber saturation point.

A fourth factor which influences the course of the reaction is the wood species, and the reason is, of course, the different permeability of the various species to gas. Thus, the spruces are more difficult to affect extensively than an open structured wood such as basswood. Wheat straw, interestingly enough, is extremely impervious to gas-phase attack, and ozonization results in a superficial burning to water-soluble material with little fiber formation. At the opposite extreme, $^3/_4$-in. cubes of aspen and yellow poplar wood were ozonized extensively under fluctuating pressure and crumbled to fibers when washed with water.

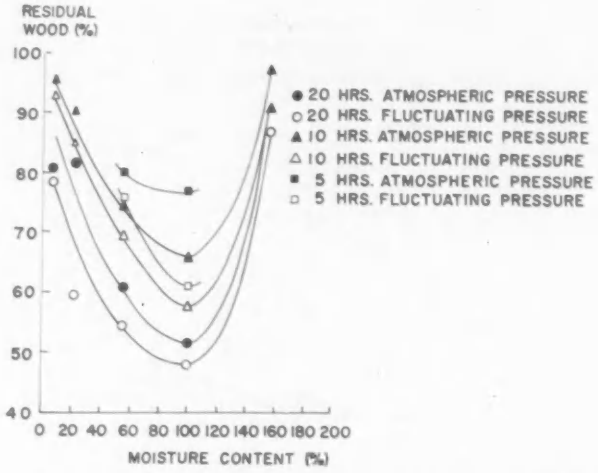

Fig. 10. Residual wood from gas-phase ozonization of Norway sprucewood chips as a function of moisture content.

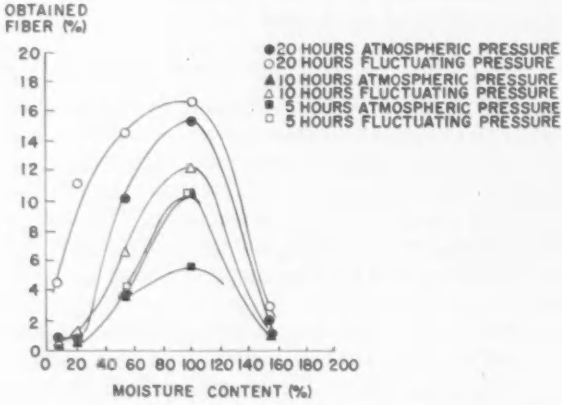

Fig. 11. Fiber production from gas-phase ozonization of Norway sprucewood chips as a function of moisture content.

A fifth factor which influences the course of the reaction by affecting gas permeability is the particular plant structure involved. Thus the open structured springwoods with large lumens and comparatively small cell walls react much more rapidly than summerwood. This observation was made on spruce, basswood, and gum. When basswood was ozonized further, the summerwood also reacted with ozone and eventually was defibered. Douglas fir bark, when ozonized at atmospheric pressure appeared completely impervious to gas transport and did not react at all. It is interesting that gas impermeability is important physiologically to this structure as

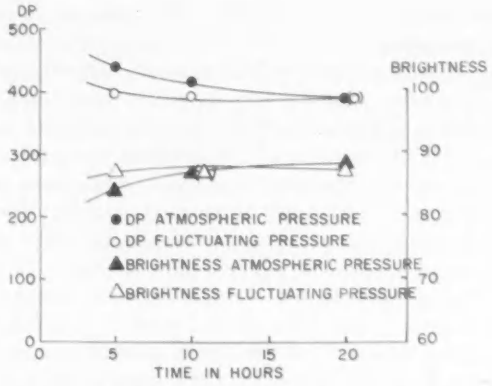

Fig. 12. Brightness and degrees of polymerization of Norway spruce fibers from gas-phase ozonization of Figs. 8 and 9.

it must be to wheat straw, another resistant tissue. The results reported in Figure 9 on Norway spruce demonstrate that after an initial period, the influence of a fluctuating pressure becomes less important. This reflects the fact that initially attack is on the open celled springwood of the species and homogeneous attack is enhanced by gas convection. Afterwards, however, the summerwood remains and does not act as to open a structure; reaction remains relatively heterogeneous.

Ozone is an exceptionally useful chemical for investigating the native supermolecular structure of cellulose in wood, since it attacks preferntially the amorphous regions of the cellulose, and can be used before prior pulping of the wood by chemicals which will affect the amorphous-crystalline ratio. We have, therefore, isolated fibers from basswood after ozonization for 5, 10, and 20 hr. and the degrees of polymerization of these products were 407, 380, and 300, respectively. Obviously even after only 5 hr. of ozonization, the readily accessible regions of the cellulose have been oxidized, and the residual cellulose is being degraded at a greatly reduced rate. If one extrapolates these values back to zero time, one reaches the conclusion that there must be in native basswood ordered regions corresponding in length to units of 450 glucose units. An even more clearly defined levelling-off effect was found in Norway spruce (Fig. 12). At various degrees of delignification fibers were separated and had degrees of polymerization close to 400. This again is a striking difference from that found on ozonization[12] or hydrolysis of chemically treated celluloses.

The high brightness obtainable on pulps obtained directly from wood without bleaching of any sort is also clearly indicated on the same figure.

To summarize our results thus far: ozone acts as a rather indiscriminate reagent degrading any of the wood substituents with which it comes in contact. Because of its great reactivity, the results obtained depend very greatly on the permeability and rate of transfer of the ozone. Its selectivity

between physical structures is, therefore, as notable as its chemical reactivity. It is quite possible that yields of cellulose of 40–50% based on wood substance may be obtained from certain woods at degrees of polymerization around 400. For some purposes this should be an interesting material. The water-soluble products undoubtedly contain methanol and acetic and oxalic acids. What other water-soluble products are present will require further investigation, but mold growth is rapid on the wash waters. Ozonization is not suggested as a feasible commercial process at this stage but the possibilities of pulping wood under such radically different conditions from those currently employed, should be explored to the full.

In addition, this research should be considered as an interpretation of the way in which gaseous reagents in general react with cellulosic materials. Ozone is a good indicator of the difficulties of gaseous permeation and penetration. It should not be difficult to list dozens of chemical reagents of reasonable vapor pressure that react with alcoholic or other functional groups found in wood and that might impart useful properties to the material. Many of the problems of their application may be suggested by the results obtained with ozone, and the technique of fluctuating pressure should be generally useful in any case in which the entire quantity of chemical needed cannot be introduced in the initial impregnation, or where liquid viscosities and entrapped air limit penetration.

EXPERIMENTAL

Ozonization of Kraft Pulp

Unbleached, air-dried kraft pulp of known moisture content equivalent to 1.1 g. and 0.4 g. of bone-dry fiber were used for the liquid- and gas-phase bleaching experiments, respectively.

Ozone was prepared at a concentration of about 2.1 wt.-% by passing moisture-free oxygen through a conventional laboratory high voltage ozone generator at a rate of 280–315 ml./min. The 120 v. line voltage was converted to 12,000 v. and 30 ma. by an Acme Electric Company transformer, Serial No. 160.

The reaction vessel consisted of a glass cylinder, 25 cm. tall and 2.9 mm. wide, in the bottom of which was a gas exit or entry tube and a coarse sintered glass plate. At the top was a 24/40 ground glass female joint and a gas entry or exit tube at one side near the top. (This vessel was made by suitable modification of a sintered glass crucible.)

For gas-phase ozonizations, the top was closed with a glass stopper, ozone at 20°C. was passed in from the top gas entry tube and was forced through an 0.4 g. pad of pulp previously formed on the sintered glass from aqueous suspension by suction. The pulp on test experiments was found to contain ca. 100% moisture initially and was still moist after 30 min. ozonization.

For liquid-phase ozonizations, a sample of 1.1 g. of pulp dispersed in 100 ml. of solvent was placed in the reaction vessel and stirred by means of a

glass shaft with six paddles that was driven by an electric motor and passed through a one-holed glass stopper. The ozone stream was passed in from the bottom of the vessel and dispersed by the sintered glass plate and rapid stirring. Solvents used were pure distilled water, redistilled reagent grade nitromethane, water containing 10% nitromethane, and water containing 24.2% methyl acetate. After ozonization, solvent was drained off through a coarse grade sintered glass crucible, the ozonized pulp washed thoroughly with distilled water, the water displaced with acetone, and the samples dried at 55°C. in a vacuum oven. The data given in Figures 3, 4, and 5 were later results than those of Figures 2, 6, and 7 and differ slightly in experimental conditions.

Sodium Borohydride Reduction

After having been washed with water, ozonized pulp samples were suspended in 100 ml. of aqueous 1% sodium borohydride overnight, washed, and dried as above.

Analytical Methods

All yields were calculated on a bone-dry basis, and drying was carried out in a vacuum oven at 55°C.

The degree of polymerization was determined by a conventional viscosity method which was a slightly modified Tappi[19] standard method T-230-Sm-50, cupriethylenediamine being used as solvent.

The brightness of small air-dried pressed sheets was measured by a brightness meter (Photo Volt Corporation, Model No. 610) or on an Elrepho G-50-660e instrument against brightness standards of 85.5 or 81.2.

In determining heat stability, sheets on which brightness had been measured were heated at a temperature of 130°C. for 3 hr. under vacuum. After heat treatment, brightness was measured on the same meter.

The ozone concentration in the flowing gas was determined by passing a known volume of gas through a neutral aqueous solution of potassium iodide (10 g./100 ml.), acidifying, and titrating with standard 0.1*N* sodium thiosulfate.[20] Ozone concentration was 2.1 wt.-% at 315 ml./min. flow rate. Absorption in acidified potassium iodide, a method recommended by Linstead et al.[21] but now discredited, gave a value of 3.4% at 283 ml./min.

Klason lignin was by the Tappi Standard method.[19]

Holocellulose was determined by the acid chlorite method.[22]

Preparation of Wood Samples

Norway spruce wood meal (40–80 mesh; benzene: ethanol 2:1 extracted) from a freshly felled log was used. Norway spruce wood chips (approximately 30 × 100 × 100–200 mm.) were equilibrated to 20% moisture content at 100% R. H. Other samples were soaked overnight in water and drained dry by suction for 155% moisture content, or soaked and centrifuged for 100% moisture content, or soaked and dried first by suction then by heating in a vacuum oven at 50°C. to obtain 55% moisture content.

Basswood shavings were prepared on a commercial planer from a seasoned basswood plank and were approximately 0.2–0.4 mm. thick, 10–15 mm. wide, and 5–10 mm. long, with considerable variation. No attempt was made to separate fractions by particle size or to extract with solvents. Eastern spruce shavings were prepared similarly.

Air-dried gum veneer slices approximately 1 × 2 × 0.1 cm. in size, pieces of Douglas fir bark about 0.3 cm. in thickness, and cubes of aspen and yellow poplar wood about 2 cm. on a side were subjected to ozonization in preliminary studies.

Ozonization of Wood

The exploratory ozonizations were carried out by suspending 1-g. samples of Norway spruce woodmeal in 10 ml. of solvent, (water or nitromethane) and passing ozonized oxygen through the suspension at 75 ml./min. Ozone concentration was found to be 10.9% on absorption in acidified potassium iodide. Five small cells containing substrate were placed in series and no consumption of ozone was determinable analytically. The wood meal was filtered, washed with reaction solvent, ethanol, water, ethanol and ether, dried *in vacuo* at 55°C., and analyzed for lignin and holocellulose. The wash liquors were concentrated and the residue dried in the same manner.

Samples of basswood shavings were evacuated in a desiccator and water containing 10% nitromethane was run over the shavings. The suspension of shavings (about 10 g.) was treated in a glass cylinder with ozone passing through a sintered glass plate at the bottom of the cylinder and bubbling through the mixture. The rate of flow was 283 ml./min. and the measured ozone concentration 3.4% ozone by the acid method. The same reaction conditions were maintained for the ozonization of wheat straw and basswood shavings in the gas phase except that the ozonized oxygen was presaturated with the solvent mixture and the substrates were conditioned for several days over the solvent in a desiccator. These data are reported in the bar graphs of Figure 8.

For all other experiments two ozonizers as described above were used, in series, a rate of oxygen flow equal to 1250 ml./min. and a measured ozone concentration of 1.0%. Pressure fluctuations of 1–1.4 atm. were developed by means of a magnetic solenoid valve which was opened by a timer four times per minute. The high rate of flow was maintained to produce a significant pressure fluctuation in some experiments and comparable conditions in others. The gas stream was passed through water before entering the reactor to prevent drying of the wood chips. After the chips were ozonized, the fiber and residual chips were separated by a high speed disintegrator. Fibers were collected by running a large amount of water over the sample on a 30 mesh screen and fibers were collected on a 100-mesh screen. The fibers and chips were collected individually, water was drained off by suction, and the solids were washed with acetone and dried at 55°C. *in vacuo*. In the experiments reported on Figure 8 20, 50, and 100 mesh screens were used.

References

1. Spurlin, H. M., in *Cellulose and Cellulose Derivatives*, E. Ott, H. M. Spurlin, and M. W. Grafflin, Eds., Interscience, New York, 1954, pp. 673–712.

2. Restricted report of the Noguchi Institute, Tokyo to the F. A. O. Technical Panel on Wood Chemistry, October 1960.

3. Yackel, E. C., and W. O. Kenyon, *J. Am. Chem. Soc.*, **64,** 121 (1942); C. C. Unruh and W. O. Kenyon, *J. Am. Chem. Soc.*, **64,** 127 (1942).

4. Brabender, G. J., J. W. Bard, and J. M. Daily, U. S. Pat. 2,466,633 (April 5, 1949).

5. Whitner, T. C., U. S. Pat. 2,438,100 (Mar. 16, 1948).

6. Howlett, E., *Textile Mfr.*, **72,** 412 (1946).

7. Dorée, C., and M. Cunningham, *J. Chem. Soc.*, **103,** 677 (1913).

8. Bogarty, H., K. S. Campbell, and W. D. Appel, *Textile Res. J.*, **22,** 81 (1952).

9. Dorée, C., and A. C. Healey, *J. Textile Inst.*, **29,** T29 (1938).

10. Cunningham, M., and C. Dorée, *J. Chem. Soc.*, **101,** 497 (1912).

11. Dorée, C., and A. C. Healey, *J. Textile Inst.*, **29,** 27T (1938).

12. Samuelson, O., G. Grangard, K. Jonsson, and K. Schramm, *Svensk Papperstidn.*, **56,** 779 (1953).

13. Mester, L., in *Ozone Chemistry and Technology*, Advances in Chemistry Series, Am. Chem. Soc., Washington, D. C., 1959.

14. Brauns, F. E., *The Chemistry of Lignin*, Academic Press, New York, 1952.

15. See, for example (a) J. Nakano and C. Schuerch, *J. Am. Chem. Soc.*, **82,** 1677 (1960); (b) C. Schuerch, *J. Am. Chem. Soc.*, **74,** 5061 (1952); (c) H. G. Arlt, Jr., K. Sarkanen, and C. Schuerch, *J. Am. Chem. Soc.*, **78,** 1904 (1956); (d) C. Schuerch, *J. Am. Chem. Soc.*, **73,** 2385 (1951); (e) W. A. Erby and C. Schuerch, *Tappi*, **45,** 409 (1962).

16. Osawa, Z., and C. Schuerch, *Tappi*, **46,** 79 (1963).

17. Osawa, Z., W. A. Erby, K. V. Sarkanen, E. Carpenter, and C. Schuerch, *Tappi*, **46,** 84 (1963).

18. Buckley, D. J., and S. B. Robison, *J. Polymer Sci.*, **19,** 145 (1956); E. H. Andrews and M. Braden, *J. Polymer Sci.*, **55,** 787 (1961).

19. Testing Methods, Recommended Practices and Specifications, Technical Association of the Pulp and Paper Industry, New York.

20. *Basic Manual of Laboratory Ozonization Techniques*, First Revision, The Welsbach Corporation, Philadelphia, Pa.

21. Linstead, R. P., J. A. Elvidge, and M. Whalley, *A Course in Modern Techniques of Organic Chemistry*, Butterworth, London, 1955, p. 121.

22. Wise, L. E., *Ind. Eng. Chem., Anal. Ed.*, **17,** 63 (1945).

Synopsis

Ozonization of kraft pulp and various woods has been carried out under a variety of conditions: in suspension in water, in solvents that preferentially wet lignin, in mixtures of the two and in the gas phase at various moisture contents using both constant and fluctuating gas pressures. Both cellulose and lignin are degraded simultaneously and the specificity of attack in aqueous solvents is little affected by the addition of lignin solvents. The rate and homogeneity of the reaction are completely dominated by the problem of transporting ozone simultaneously to all reaction sites. A simplified model of a reaction is presented to assist in rationalizing what transport process is rate-determining under specific conditions. Under our optimum conditions kraft pulp was bleached to brightnesses about 78 in about $^1/_2$ hr., but cellulose was degraded to a degree of polymerization of 474 in the same time. Reduction of oxidized pulps by sodium borohydride increased heat stability, brightness and cuprammonium viscosity values. Wood meal, shavings, chips, and blocks were pulped at room temperature with ozone to give fibers with a level-off degree of polymerization of 400–450. The reaction is most rapid and homogeneous if carried out using a fluctuating gas pressure and wood containing 100%

moisture. The limiting factor of the reaction is then the gas permeability of the particular wood species and tissues employed.

Résumé

On a effectué, dans différentes conditions, l'ozonisation de la pulpe "kraft" et de divers bois: en suspension dans l'eau, dans des solvants qui mouillent préférentiellement la lignine, dans un mélange des deux et en phase gazeuse à divers taux d'humidité en utilisant des pressions de gaz constantes et variables. La cellulose et la lignine sont dégradées simultanément et la spécificité d'attaque en solution aqueuse est peu affectée par addition de solvants de la lignine. Le problème de l'arrivée simultanée d'ozone, à tous les sites de réaction, est le facteur déterminant de la vitesse et de l'homogénéité de la réaction. On propose un modèle simplifié d'une réaction admettant de façon rationnelle que le processus de transfert est déterminant de vitesse dans des conditions spécifiques. Dans les conditions optima, le pulpe "kraft" est décolorée à une brillance d'environ 78 en une demi-heure environ, mais la cellulose est dégradée à un degré de polymérisation de 474 dans le même temps. La réduction des pulpes oxydées par le borohydrure de sodium augmente la stabilité calorifique, la brillance et les valeurs de viscosité cupriam-moniacale. Des moulures, des tournures, des copeaux et des blocs de bois ont été transformés en pulpe à température de chambre avec de l'ozone pour donner des fibres d'un degré de polymérisation de 400–450. La réaction est plus rapide et homogène si elle est effectuée à pression variable de gaz et avec du bois contenant 100% d'humidité. Le facteur limitatif de la réaction est dès lors la perméabilité au gaz des espèces particulières de bois et de tissus employés.

Zusammenfassung

Die Ozonisierung von Kraftpulp und verschiedenen Hölzern wurde unter einer Reihe von Versuchsbedingungen durchgeführt: suspendiert in Wasser, in Lösungsmitteln, die bevorzugt Lignin benetzen, in Mischungen aus beiden und in Gasphase bei verschiedenem Feuchtigkeitsgehalt sowohl bei konstantem als auch fluktuierendem Gasdruck. Cellulose and Lignin werden gleichzeitig abgebaut und die Angriffsspezifität in wässrigen Lösungsmitteln wird durch den Zusatz von Ligninlösungsmitteln nur wenig beeinfluss. Geschwindigkeit und Homogenität der Reaktion hängen völlig vom Problem des gleichzeitigen Ozontransportes an alle Reaktionsstellen ab. Ein vereinfachtes Reaktionsmodell wird als Hilfsmittel bei der Klärung der Frage nach dem unter bestimmten Bedingungen geschwindigkeitsbestimmenden Transportprozess angegeben. Unter den optimalen verwendeten Bedingungen wurde Kraftpulp in etwa einer halben Stunde zu einer Helligkeit von etwa 78 gebleicht, gleichzeitig jedoch Cellulose zu einen Polymerisationsgrad von 474 abgebaut. Reduktion des oxydierten Pulps mit Natriumborhydrid erhöhte Hitzebeständigkeit, Helligkeit und Viskositätswerte in Cuprammonium. Holzmehl, -späne, -schnitzel und -blöcke wurden bei Raumtemperatur mit Ozon unter Bildung von Fasern mit einem Ausgleichspolymerisationsgrad von 400–450 verpulpt. Die Reaktion verläuft mit einem fluktuierenden Gasdruck und mit Holz mit 100% Feuchtigkeitsgehalt am raschesten und mit höchsten Homogenitätsgrad. Der kritische Faktor für die Reaktion ist unter diesen Bedingungen die Gaspermeabilität der speziellen Holzart und der verwendeten Gewebe.

Discussion

J. K. N. Jones (*Queen's University, Kingston, Ontario, Canada*): What happens to the hemicelluloses during the ozonization of wood?

C. Schuerch: We have not carried out any study of the products yet by classical organic techniques. Presumbly they are degraded and rendered water-soluble. In any case, extensive ozonization followed by chromatographic studies of the resistant residue

should give some insight into the distribution of hemicelluloses in the crystalline portion of the native cell wall.

H. P. Panzer (*American Machine & Foundry Co., Springdale, Connecticut*): My question relates to a technical detail of the work. I would like to ask in which range the ozone pressure was fluctuated and what was the frequency of the pressure change?

C. Schuerch: With our equipment we varied the pressure from 1.0 to 1.4 atm. A variation from 0.5 to 1.5 atm. could, of course, remove up to two thirds of the residual gas per cycle and would be much more advantageous.

R. H. Marchessault (*State University College of Forestry, Syracuse, New York*): "Level-off DP" is a relative term and the actual value depends on the method of hydrolysis as well as the sample history. What exactly are the conditions which you used?

C. Schuerch: The wood was ozonized for 5, 10, and 20 hr. The portion which was completely delignified and in fibrous form was dissolved and viscosity measured. It was clear that a very rapid drop in D.P. had occurred, and that the D.P. changed very little after 5 hr. of ozonization. This D.P. is roughly twice that obtained by ozonization of chemical pulps under similar conditions (or limit hydrolysis).

JOURNAL OF POLYMER SCIENCE: PART C NO. 2, PP. 97–107 (1963)

Some Considerations on the Kinetics of the Acid Hydrolysis of Poly- and Oligo-saccharides

ALEXANDER MELLER, *Research Laboratory, Australian Paper Manufacturers Limited, Melbourne, Australia*

INTRODUCTION

Despite the comparatively large amount of work devoted to the kinetics of the acid catalyzed hydrolysis of polysaccharides, in particular of cellulose, the problems involved cannot be considered to have been fully clarified. Recently some aspects of the kinetics of both the homogeneous and heterogeneous acid hydrolysis of cellulose have been critically surveyed and discussed.[1,2]

With the increasing interest in the effect of chemical modification of cellulose on the stability of the glucosidic bonds[3,4] and, in general, of the chemical constitution of wood and other polysaccharides on their resistance to acid solutions,[5–9] it is probably imperative to have a full understanding of the kinetics of the acid hydrolysis of those oligo- and polysaccharides which represent condensed chains of the same sugar unit (e.g., cellotriose, amylose, cellulose).

The kinetics of the homogeneous acid hydrolysis of cellulose were extensively studied by Freudenberg and collaborators.[10–13] The interpretation of the experimental rate data was based on the theoretical (statistical) considerations of Kuhn.[14] This theory was supported by the evaluation of rate measurements on the hydrolysis of cellotriose (and cellotetraose).[10–13]

The Theory of Kuhn and the Kinetics of Hydrolysis of Cellobiose

According to the theory of Kuhn,[14] the glucosidic bonds in cellotriose are hydrolyzed more slowly than in cellobiose, which is formed in the hydrolysis of cellotriose by random splitting of either of the glucosidic bonds. The rate equation for interpreting the kinetics of the hydrolysis of cellotriose used by Freudenberg and collaborators[13] was

$$1 - \alpha = \frac{k_2 - k_1}{k_2 - 2k_1} e^{-2kt} - \frac{k_1}{k_2 - 2k_1} e^{-kt} \qquad (1)$$

in which α is the degree of splitting, k_1 is the hydrolysis rate constant for cellotriose and k_2 is that for cellobiose. The value of k_2 was obtained from the experimental rate data on the hydrolysis of cellobiose; approximate

values of k_1 were obtained by extrapolating the first order rate plot (ln $(1 - \alpha)$ versus t) to small values of time on the basis of the rate data for the hydrolysis of cellotriose. It was claimed[10–13] that the values for 1-α calculated by means of eq. (1) and found experimentally were in good agreement.

Using these rate data and the values for k_1 and k_2 of Freudenberg and collaborators the validity or applicability of eq. (1) was tested by plotting $\ln \{[(1 - \alpha)/e^{-k_2 t} + [k_1/(k_2 - 2k_1)]\}$ against t. These plots should be straight lines with the gradient of $(k_2 - 2k_1)$ and the intercept with the ordinate $\ln [(k_2 - k_1)/(k_2 - 2k_1)]$. However, as shown in Figures 1 and 2 the plots depart from linearity which cannot be easily reconciled with the validity of eq. (1) for the interpretation of the kinetics of acid hydrolysis of cellotriose.

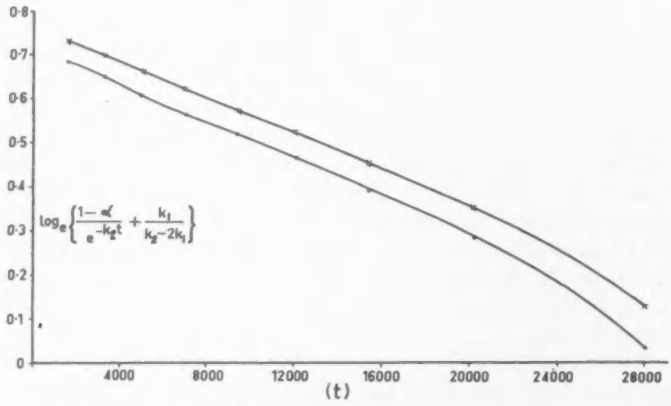

Fig. 1. Cellotriose hydrolysis rate plots according to the rate equation of Kuhn for hydrolysis at 18°C.: (×) $k_1 = 0.636 \times 10^{-4}$, $k_2 = 1.07 \times 10^{-4}$; (●) $k_1 = 0.64 \times 10^{-4}$ $k_2 = 1.07 \times 10^{-4}$. All values of $(1 - \alpha)$ from data of Freudenberg et al.[10–13]

In seeking the cause of the departures from linearity of the plots in accordance with eq. (1), i.e. the validity or applicability of this equation, let us assume that the underlying theoretical considerations are (*a*) correct but the equation is not applicable under the experimental conditions used, or (*b*) not correct. As to (*a*), it is possible that (*1*) the analytical method used for measuring the rate of formation of the reducing end groups is not entirely reliable, (*2*) the hydrolysis reaction is accompanied by other reactions, and (*3*) a corrollary of (*2*), namely, that under the reaction conditions the measured rate is not entirely that of the hydrolysis of cellotriose.

The analytical method used was that of Romjin-Willstätter-Schudel as modified by Goebel[15] which may have some uncertainties, but it has been widely used with slight modifications for the purpose in question.

Regarding the possibility of the hydrolysis of cellotriose being accompanied by other reactions it should be mentioned that Freudenberg and

collaborators[10–13] themselves realized this and checked this point to some extent. On allowing glucose to stand in 51% sulfuric acid at 18°C. for eight weeks and at 30°C. for two weeks almost the same iodine numbers were obtained and the optical rotation remained constant. On leaving cellobiose in 51% sulfuric acid for five weeks at both temperatures the final titration value was found to be the same as for glucose. Recent investigations by Noto La Diega, however, have shown[16] that on subjecting cellobiose to sulfuric acid solutions (51%, 60%, and 72% at 18° and 30°C.) the hydrolysis is accompanied by destruction of the monomer formed,

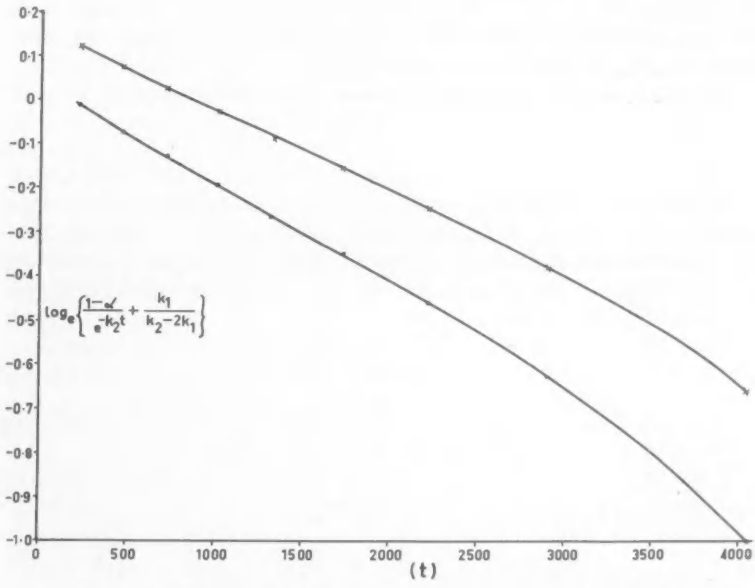

Fig. 2. Cellotriose hydrolysis rate plots according to the rate equation of Kuhn for hydrolysis at 30°C.: (×) $k_1 = 4.5 \times 10^{-4}$, $k_2 = 6.94 \times 10^{-4}$; (●) $k_1 = 4.6 \times 10^{-4}$, $k_2 = 6.94 \times 10^{-4}$. All values of $(1 - \alpha)$ from data of Freudenberg et al.[10–13]

condensation of the monomer to a dimer of gentiobiose, and condensation of the cellobiose to a tetramer. The rate constants of the hydrolysis of cellobiose with 51% sulfuric acid at both temperatures derived from rate measurements corrected for the side reactions,[16] do not differ very markedly from those of Freudenberg and collaborators, but the side reactions with 60% and 71% sulfuric acid are so marked that they cannot be disregarded when the hydrolysis rate constants are computed.

The possibility that under the experimental conditions (i.e., strong sulfuric acid solution) the measured rate is not entirely that of the hydrolysis of cellotriose will be discussed below.

The Considerations of Klages and the Kinetics of Hydrolysis of Oligosaccharides

As to (*b*), i.e., the possibility that the theory of Kuhn[14] is not correct, it may be mentioned that the correctness or validity of the theory was supported by the agreement between calculated and experimental values of the degree of splitting the glucosidic bonds, but there are other equations which fulfil this requirement to the same degree as does eq. (1). It may, thus, be justified to consider a second theory[17,18] according to which the reducing terminal glucose unit in cellotriose is hydrolyzed at the same rate as cellobiose but faster than the nonreducing glucose unit. This theory was strongly advocated by Klages[17,18] and was supported by the results of the rate measurements on the hydrolysis of pentamethylglucose, octamethylcellobiose, and hendekamethylcellotriose.[18]

The rate equation used for evaluating the kinetic results was:[18]

$$1 - \alpha = [(n\text{-}1)\, e^{-k_1 t} + e^{-k_2 t}]/n \tag{2}$$

where α is the degree of splitting of both the interunit and methylglucosidic bonds, n the number of glucosidic interunit bonds, k_1 the rate constant for the hydrolysis of glucosidic interunit bonds and k_2 that of the methyl glucosidic bond. For oligosaccharides with $n = 2$ (octamethylcellobiose and cellotriose) we have

$$1 - \alpha = 0.5\, e^{-k_1 t} + 0.5\, e^{-k_2 t} \tag{3}$$

Thus a plot of $\ln \{[1-\alpha/e^{-k_2 t}] - 0.5\}$ against t should give a straight line with a slope of $k_2 - k_1$ and an intercept with the ordinate of ln 0.5.

Using the value of k_2 obtained from the hydrolysis rate measurements on pentamethylglucose and the rate data of the hydrolysis of octamethylcellobiose,[18] the plot required by eq. (3) is a straight line with the intercept of ln 0.5. From the gradient of the line the value of k_1 can be computed. It should also be mentioned that for $n = 3$, eq. (2) becomes

$$\ln \{[(1\text{-}\alpha)/e^{-k_1 t}] - 0.333\} = \ln 0.667 + (k_2 - k_1)\, t \tag{4}$$

Using the results of rate measurements on hendekamethylcellotriose[18] and the value of k_2, the plot of $\ln \{[(1-\alpha)/e^{-k_2 t}] - 0.333\}$ against t gives a straight line with an intercept of ln 0.6667 and the evaluation of the slope leads to the same k_1 value as that obtained from the evaluation of the results on octamethylcellobiose. The validity of the considerations of Klages for these cases is thus confirmed.

Using the rate on cellotriose and cellotetraose, and the rate constants for the hydrolysis of cellobiose at 18 and 30°C. (51% sulfuric acid), but applying the equation of Klages, the plots of $\ln \{[(1 - \alpha)/e^{-k_2 t}] - (1/n)\}$ against t are not straight lines. The intercepts approximate the value of ln 0.5 for cellotriose at 30°C.

The "Anomalous" Behaviour of Strong Sulfuric Acid Solutions in the Hydrolysis of Cellobiose

It appears that the rate equation of Kuhn when applied to the rate data on cellotriose and cellotetraose is not satisfactory insofar as the plots required by this equation are not straight lines. The rate equation of Klages when applied to the data on octamethylcellobiose and hendecamethylcellotriose is entirely satisfactory, but it satisfies some of the rate data only for the very early part of the hydrolysis of cellotriose and cellotetraose.

Rate measurements of the hydrolysis of octamethylcellobiose and hendecamethylcellotriose were conducted at 98°C. with 0.1*N* HCl, whereas those of cellotriose and cellotetraose were performed at 18 and 30°C. with 51% H_2SO_4. Thus it is possible that the shortcoming of eq. (2) and also of eq. (1) is related to the particular action of strong sulfuric acid solutions. In order to support this hypothesis rate data would be needed on the hydrolysis of both cellotriose and cellotetraose with dilute acids at high temperatures and of the glucosides with strong sulfuric acids at low temperatures. Regrettably the literature does not contain such data. However sufficient rate data are available from the literature on the hydrolysis of cellobiose with strong sulfuric acid at low temperatures as well as with dilute hydrochloric and sulfuric acids at high temperatures. These data are listed in Table I, along with the Arrhenius activation energy E and frequency factor A.

Novikova and Konkin[1] found that in accordance with Hammett's acidity function the plot of log k was a linear function of H_0, for the hydrolysis of cellobiose with hydrochloric acid solutions giving a slope of unity. Although the plot of log k against H_0 was approximately linear for the hydrolysis of cellobiose with strong sulfuric acid solutions, the slope was only 0.55–0.65. Noto La Diega[16] found the same, using the data on the hydrolysis of cellobiose with strong sulfuric acid solutions, i.e., the Hammett plot, was approximately linear, but with a slope of only 0.5–0.6. It thus appears that strong sulfuric acid solutions at low temperatures (18–30°C.) are somewhat "anomalous" in their action on cellobiose (and also on cellulose[16]). In order to resolve this anomaly two possibilities may be considered, viz., (*1*) the reaction mechanism (the rate-determining step) in the hydrolysis with strong sulfuric acid solutions at low temperatures is not the same as that with weak and strong hydrochloric acid solutions at both low and high temperatures (40–90°C.), and (*2*) sulfuric acid does not fit into the Hammett acidity scale. As to the latter, there are some instances known where sulfuric acid does not obey the Hammett acidity function.[22] As to the former, it can be seen in Figure 3 that taking the rate constants of the hydrolysis of cellobiose with 1*N* HCl for different temperatures the plot of log k values against $1/T$ on extrapolation to 40°C. gives a value for log $k = 0.26 \times 10^{-5}$ which is very close to the log $k = 0.22 \times 10^{-5}$ value obtained by extrapolation of the plot of log k for 40°C. against $-H_0$ values to that corresponding to 1*N* HCl.

TABLE I

Acid	Temp., °C.	k, min.$^{-1}$	E, kcal/mole	A, min.$^{-1}$	Reference[a]
1N HCl	80	44.94 $\times 10^{-4}$	30.7	4.6 $\times 10^{-6}$	19*
"	[70	12.36 $\times 10^{-4}$]			
"	60	3.216 $\times 10^{-4}$			
"	[40	0.18 $\times 10^{-4}$]			
22.4% HCl	40	12.25 $\times 10^{-4}$			1
16.2 "	"	3.12 $\times 10^{-4}$			
7.04 "	"	0.5 $\times 10^{-4}$			
1N HCl	["	0.19 $\times 10^{-4}$]			
0.5N H_2SO_4	70	3.4 $\times 10^{-4}$			10–13
1N H_2SO_4	80	20.82 $\times 10^{-4}$	31.2	4.66 $\times 10^{16}$	20
"	75	11.0 $\times 10^{-4}$			
"	[70	5.7 $\times 10^{-4}$]			
"	[40	7.08 $\times 10^{-6}$]			
1N H_2SO_4	90	61.0 $\times 10^{-4}$	29.6	4.1 $\times 10^{16}$	21*
"	80	19.0 $\times 10^{-4}$			
"	[70	5.6 $\times 10^{-4}$]			
"	[40	8.6 $\times 10^{-6}$]			
1N H_2SO_4	80	18.3 $\times 10^{-4}$			18
8% H_2SO_4	75	17.17 $\times 10^{-4}$	29.6	1.6 $\times 10^{16}$	18
"	[70	9.20 $\times 10^{-4}$]			
"	65	4.83 $\times 10^{-4}$			
"	55	1.38 $\times 10^{-4}$			
"	[40	1.43 $\times 10^{-5}$]			
15.77% H_2SO_4	40	0.33 $\times 10^{-4}$			1
35.55 "	"	3.38 $\times 10^{-4}$			
50.98 "	"	20.9 $\times 10^{-4}$			
8% H_2SO_4	[40	2.88 $\times 10^{-5}$]			
1N "	["	20.9 $\times 10^{-6}$]			
51% H_2SO_4	18	1.07 $\times 10^{-4}$	27.3	3.4 $\times 10^{16}$	10–13*
"	30	6.94 $\times 10^{-4}$			
"	[40	29.20 $\times 10^{-4}$]			
51.17% H_2SO_4	18	1.02 $\times 10^{-4}$	27.72	6.5 $\times 10^{16}$	16*
"	30	6.8 $\times 10^{-4}$			
"	[40	28.52 $\times 10^{-4}$]			
64.37% H_2SO_4	18	6.9 $\times 10^{-4}$	26.682	41.5 $\times 10^{16}$	
"	30	45.88 $\times 10^{-4}$			
"	[40	19.42 $\times 10^{-3}$]			
71.0% H_2SO_4	18	19.59 $\times 10^{-4}$	27.675	116.4 $\times 10^{16}$	
"	30	130.02 $\times 10^{-4}$			
"	[40	5.493 $\times 10^{-2}$]			

[a] The asterisk (*) indicates that the literature reference contains the full experimental data; some references do not contain the results of rate measurements but give the rate constants derived by the relevant author(s); some of the values were obtained by the writer by inter- or extrapolation of the available data, shown by brackets.

It appears therefore that both the activation energy and frequency factor of the hydrolysis of cellobiose with hydrochloric acid solutions are practically independent of temperature. The rate controlling step in the hydrolysis is first order and is in agreement with Hammett's acidity function, i.e.,

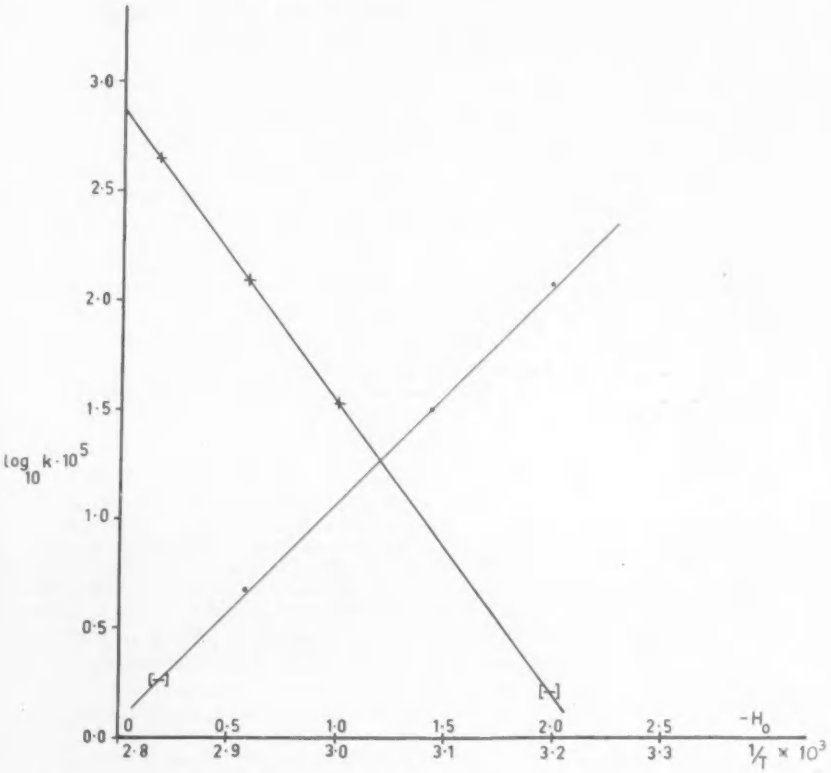

Fig. 3. Relationship between log k and $1/T$ and H_0 for cellobiose in hydrochloric acid solutions: (×) log $k \times 10^5$ vs. $1/T$, 1N HCl, data of Moelwyn-Hughes;[19] (●) log $k \times 10^5$ vs. $-H_0$, 40°C., data of Novikova and Konkin.[1] Points in brackets are extrapolated values.

the mechanism involves a protonation either of the ring oxygen or of the glycosidic oxygen (fast) and either a subsequent hydrolysis to form a carbonium ion or a ring opening and formation of an ion (slow).[22–26]

On the basis of the rate constants of the hydrolysis of cellobiose with 1N and 8% H_2SO_4, the plots of log k against $1/T$ are reasonably straight lines, but the log k values obtained by extrapolation to 40°C. (the points in brackets in Fig. 4) are considerably lower than the log k values obtained by extrapolation of the plots of log k for 40°C. against $-H_0$ to the $-H_0$ values of 8% and 1N H_2SO_4, as shown in Figure 4. The k values computed and listed in Table I above differ by a factor of two for 8% H_2SO_4 and of three for 1N H_2SO_4. The results of this analysis, therefore, support the assumption that the step which controls the rate of hydrolysis with hydrochloric acid is not entirely rate controlling in the hydrolysis with strong cold sulfuric acid solutions.

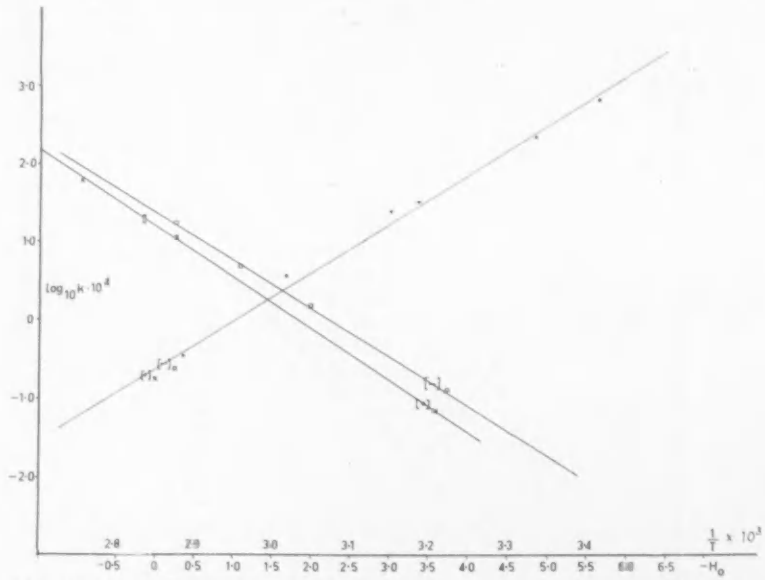

Fig. 4. Relationship between log k and $1/T$ and H_0 for cellobiose in sulfuric acid solutions: (□) $k \times 10^4$ vs. $1/T$, 8% H_2SO_4, data of Srivastava et al.[9]; (×) log $k \times 10^4$ vs. $1/T$, 1N H_2SO_4, data of Sharples[20] and Senju and Shimizu;[21] (●) log $k \times 10^4$ vs. $-H_0$, 40°C., data of Sharples[20] and Senju and Shimizu.[21] Points in brackets are extrapolated values.

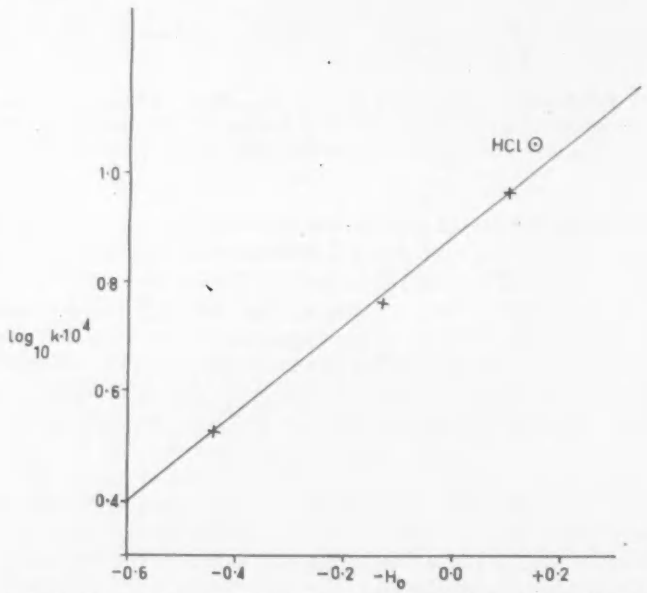

Fig. 5. Relationship between log k and H_0 for cellobiose in weak sulfuric acid solutions at 70°C.

The Similarity Between the Hydrolysing Action of Hydrochloric and Dilute Sulfuric Acid Solutions at High Temperatures

Weak sulfuric acid solutions at high temperatures seem to be similar to hydrochloric acid in their action on cellobiose; for k values for 70°C. at different sulfuric acid concentrations, the Hammett plot, as shown in Figure 5, is a reasonably straight line with an approximate slope of 0.8. In fact, the value of k for 40°C. derived by extrapolation to the $-H_0$ value of 1*N* HCl does not differ greatly from the experimental k value for 70°C. with 1*N* HCl.

In conclusion it is believed that a clarification of the problems involved in the hydrolysis of cellobiose with strong cold sulfuric acid solutions may help to formulate the theoretical basis for the interpretation of the kinetics of hydrolysis of cellotriose, cellotetraose and, most likely, of cellulose with these hydrolyzing solutions.

References

1. Novikova, L. I., and A. A. Konkin, *Zh. Prikl. Khim.*, **32**, 1105 (1959).
2. Nelson, Mary L., *J. Polymer Sci.*, **43**, 351 (1960).
3. Kuznetsova, Z. I., and V. I. Ivanov, *Izv. Akad. Nauk, SSSR, Otd. Khim. Nauk*, **1959**, 1678.
4. Virkola, N. E., *Paperi ja Puu*, **49**, 367 (1958).
5. Marchessault, R. H., and B. G. Rånby, *Svensk Papperstidn.*, **62**, 230 (1959).
6. Hamilton, J. K., and Norman S. Thompson, *J. Am. Chem. Soc.*, **79**, 6464 (1957).
7. Whistler, R. L., and G. N. Richards, *J. Am. Chem. Soc.*, **80**, 4888 (1958).
8. Lindberg, B., and L. Selleby, *Acta Chem. Scand.*, **14**, 1051 (1960).
9. Srivastava, H. C., C. T. Bishop, and G. A. Adams, *J. Org. Chem.*, **26**, 3958 (1961).
10. Freudenberg, K., *Ber.*, **54**, 767 (1921).
11. Freudenberg, K., and E. Braun, *Ann.*, **460**, 288 (1928).
12. Freudenberg, K., W. Kuhn, W. Dürr, F. Bolz, and G. Steinbrunn, *Ber.*, **63**, 1510 (1930).
13. Freudenberg, K., and G. Blomqvist, *Ber.*, **68**, 2070 (1935).
14. Kuhn, W., *Ber.*, **63**, 1503 (1930).
15. Goebel, W. F., *J. Biol. Chem.*, **72**, 801 (1927).
16. Noto La Diega, G., *Chim. Ind. (Milan)*, **41**, 408, 414, 539, 598 (1959).
17. Klages, F., *Z. Physik. Chem.*, **A159**, 357 (1932).
18. Klages, F., *Ann.*, **520**, 71 (1935).
19. Moelwyn-Hughes, E. A., *Trans. Faraday Soc.*, **24**, 309 (1928); *ibid.*, **25**, 81, 503 (1929).
20. Sharples, A., *Trans. Faraday Soc.*, **53**, 1003 (1957).
21. Senju, R., and M. Shimizu, *J. Agr. Chem. Soc. (Japan)*, **25**, 231 (1951).
22. Rogovin, Z. A., A. A. Konkin, and Rymashevskaya, *Chem. Abstr.*, **48**, 4449 (1954).
23. Paul, M. A., and F. A. Long, *Chem. Revs.*, **57**, 1 (1957).
24. McIntyre, D., and F. A. Long, *J. Am. Chem. Soc.*, **76**, 3240 (1954).
25. Bunton, C. A., T. A. Lewis, D. R. Llewellyn, and C. A. Vernon, *J. Chem. Soc.*, **1955**, 4419.
26. Shafizadeh, F., and A. Thompson, *J. Org. Chem.*, **21**, 1059 (1956).

Synopsis

The rate data of Freudenberg and collaborators on the acid-catalyzed hydrolysis of cellotriose have been used to test the validity of the rate equation of Kuhn by plotting $\ln -[(1 - \alpha)/e^{-kst} - (k_1k_2 - 2k_1)]$ against t (where α is the degree of hydrolysis,

t is the time of hydrolysis; and k_1 and k_2 are the hydrolysis rate constants for cellotriose and cellobiose, respectively). A departure from linearity of the plots has been found which cannot be reconciled with the validity of the rate equation of Kuhn for the interpretation of the kinetics of acid hydrolysis of cellotriose. It is possible that the hydrolysis is accompanied by other reactions (destruction of the monomer formed, condensation of the monomer to a dimer and of the dimer to a tetramer) or that under the experimental conditions (i.e., strong sulfuric acid) the measured rate is not entirely that of the hydrolysis of cellotriose. In support of the latter hypothesis rate constants for the hydrolysis of cellobiose with strong sulfuric acid solutions at low temperatures and with dilute hydrochloric and sulfuric acid solutions at high temperatures have been collected from the literature. On plotting log k against $1/T$ (where k is the hydrolysis rate constant of cellobiose and T is the absolute temperature) for $1N$ HCl at high temperatures extrapolation to 40°C. gives a value for log k very close to that obtained by extrapolation of the plot of log k against $-H_0$ values (Hammett's acidity functions) at 40°C. The plots of log k against $1/T$ for sulfuric acid solutions when extrapolated to 40°C. give values for log k which are considerably lower than those obtained by extrapolation of the plots of log k against $-H_0$ at 40°C.

Résumé

On a vérifié la validité de l'équation de vitesse de Kuhn (11) en mettant en graphique $\log_e\left(\frac{1-\alpha}{e^{-k_2 t}} - \frac{k_1}{k_2 - 2k_1}\right)$ en fonction de t, à partir des données cinétiques de l'hyerolyse acide du cellotriose, obtenues par Freudenberg et ses collaborateurs (10) (a = le degré d'hydrolyse, t = le temps d'hydrolyse, k_2 = la constante de vitesse d'hydrolyse du cellubiose). On a observé dans les diagrammes un écart à la linéarité, qui n'est pas conciliable avec la validité de l'équation cinétique de Kuhn lors de l'interprétation des cinétiques d'hydrolyse acide du cellotriose. Il est possible que l'hydrolyse soit accompagnée d'autres réactions (destruction du monomère formé, condensation du monomère en dimère et du dimère en tétramère (13)) ou que dans les conditions expérimentales (entre autres, le milieu acide sulfurique fort) la vitesse que l'on mesure n'est pas entièrement celle de l'hydrolyse du cellotriose. En raison de cette dernière hypothèse on a recherché dans la littérature les constantes de vitesse de l'hydrolyse du cellobiose en milieu acide sulfurique concentré à basse température et en solution chlorhydrique et sulfurique diluée à haute température. En mettant en graphique $\log_{10} k$ en fonction de $1/T$ (k = constante de vitesse d'hydrolyse du cellobiose, T = température absolue) pour une solution HCl $1N$ à de hautes températures, l'extrapolation à 40°C donne une valeur de $\log_{10} k$ qui se rapproche fortement de celle obtenue par extrapolation dans le programme $\log_{10} k$ en fonction de $-H_0$ à 40°C (H_0 est la fonction d'acidité de Hammett). Les diagrammes $\log_{10} k$ en fonction de $1/T$ dans le cas de solutions d'acide sulfurique, donnent par extrapolation à 40°C des valeurs de $\log_{10} k$ qui sont de loin inférieures à celles obtenues par extrapolation dans les diagrammes $\log_{10} k$ en fonction de $-H_0$ à 40°C.

Zusammenfassung

Unter Benützung der Geschwindigkeitsdaten von Freudenberg und Mitarbeitern (10) für die säurekatalysierte Hydrolyse von Cellotriose wurde die Gültigkeit der Geschwindigkeitsgleichung von Kuhn (11) durch Auftragen von $\log_e\left(\frac{1-\alpha}{e^{-k_2 t}} - \frac{k_1}{k_2 - 2k_1}\right)$ gegen t (α = Hydrolysengrad; t = Hydrolysendauer; k_2 = Geschwindigkeitskonstante der Hydrolyse der Cellobiose) geprüft. Es wurde eine Abweichung von der linearen Abhängigkeit festgestellt, die sich mit der Gültigkeit der Kuhnschen Geschwindigkeitsgleichung für die Interpretierung der Kinetik der sauren Hydrolyse von Cellotriose nicht vereinen lässt. Es ist möglich, dass die Hydrolyse von anderen Reaktionen begleitet wird (Zerstörung des gebildeten Monomeren, Kondensation des Monomeren zu einem

Dimeren und des Dimeren zu einem Tetrameren (13)) oder dass unter den Versuchsbedingungen (nämlich starke Schwefelsäure) die gemessene Geschwindigkeit nicht bloss die der Hydrolyse von Cellotriose ist. Zur Stütze dieser letzteren Hypothese wurden Geschwindigkeitskonstanten für die Hydrolyse von Cellobiose mit starken Schwefelsäurelösungen bei niedriger Temperatur und mit verdünnten Chlorwasserstoff- und Schwefelsäurelösungen bei höherer Temperatur aus der Literatur zusammengetragen. Beim Auftragen von $\log_{10}k$ gegen $1/T$ (k = Geschwindigkeitskonstante für die Hydrolyse von Cellobiose; T = absolute Temperatur) für 1N bei hoher Temperatur liefert die Extrapolation auf 40°C einen Wert für $\log_{10}k$, der sehr nahe bei dem durch Extrapolation im $\log_{10}k$ gegen H_0-(Hammetts Säurefunktion)-Diagramm bei 40°C erhaltenen Wert liegt. Das $\log_{10}k - 1/T$-Diagramm für Schwefelsäurelösungen liefert bei Extrapolation auf 40°C Werte für $\log_{10}k$, die beträchtlich niedriger als die durch Extrapolation im $\log_{10}k$-$-H_0$-Diagramm bei 40°C erhaltenen sind.

JOURNAL OF POLYMER SCIENCE: PART C NO. 2, PP. 109-116 (1963)

Effect of Deacetylation and Nitration on Normal Glycosidic Linkages in Cellulose

T. E. TIMELL, *Pulp and Paper Research Institute of Canada, and Department of Chemistry, McGill University, Montreal, Quebec, Canada*

INTRODUCTION

Berl and Rueff,[1] thirty years ago, seem to have been the first to observe that if cellulose is treated with a mixture of nitric acid and phosphoric acid containing phosphorus pentoxide, the resulting nitrates form extremely viscous solutions. They concluded that the esterification conditions were probably mild enough to leave the cellulose molecules largely intact. The procedure was later modified by Staudinger and Mohr,[2] by Davidson,[3] and by Alexander and Mitchell.[4] These nitration techniques have often been used for converting cellulose with a minimum of degradation into an organo-soluble derivative, suitable for determination of both molecular weights[5-7] and molecular-weight distributions.[8-10] An added advantage is the fact that the swelling action of the acid mixture is such that cellulose nitrates can be obtained in quantitative yields from most plant products.[8,10-12]

While it has been generally assumed in the past that the nitric acid–phosphoric acid–phosphorus pentoxide mixture causes little or no depolymerization of cellulose, no direct proof for the correctness of this assumption has so far been produced. Both Gralén[13] and Golowa and Iwanow[14] have claimed that a certain number of the glucosidic bonds in cellulose are actually broken during the nitration. Cellulose is rapidly degraded by nitric acid alone and is quite unstable in solutions of phosphoric acid. Its presumed stability towards the nitration mixture is therefore hardly what would be expected *a priori*, even if allowance is made for the fact that water is absent and that the nitration is almost instantaneous.

It was the aim of the present study to produce direct experimental evidence as to the effect of the nitration mixture on a cellulose containing only (1 → 4)-linked β-D-glucopyranose residues. A cellulose triacetate from cotton was deacetylated under mild conditions and the resulting cellulose was converted to a nitrate with the above mixture. As a comparison, nitration was also carried out with acetyl nitrate,[15] a reagent which has also been claimed to cause little or no degradation of cellulose.[16,17] The number-average molecular weights of the acetate, the cellulose, and the nitrates were determined by osmometry. In addition, the weight-average

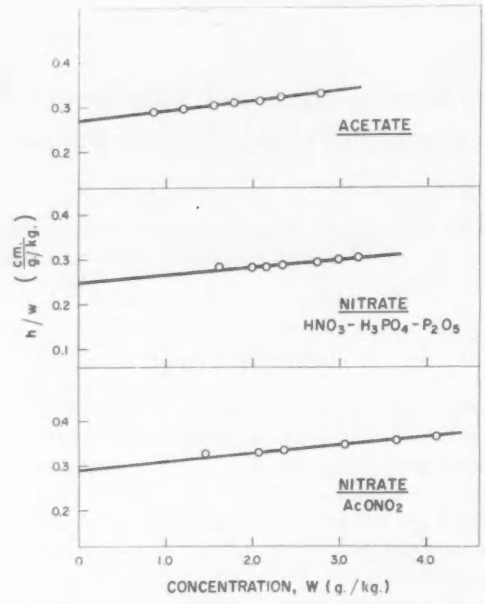

Fig. 1. Osmometry data for cellulose acetate and two cellulose nitrates.

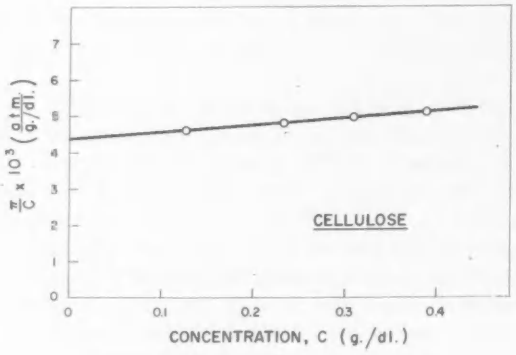

Fig. 2. Osmometry data for cellulose.

molecular weights of the acetate and the first nitrate were estimated by light scattering.

RESULTS

Cotton, previously activated with aqueous alkali, was treated with an acetic acid–acetic anhydride mixture containing perchloric acid as a catalyst. The triacetate was recovered in the form of a fine, continuous fila-

ment. A portion of the product was deacetylated with sodium methoxide–methanol. Both the acetate and the cellulose were completely amorphous as indicated by their x-ray diagrams. The cellulose filament was nitrated under standard conditions with the mixture of Alexander and Mitchell[4] to give a nitrate in a yield of 93%. Attempts to achieve a quantitative recovery of the nitrated cellulose by varying the experimental conditions failed. Nitration with an acetic acid solution of acetyl nitrate was carried out as described previously.[17]

The molecular weights of the acetate and the nitrates were determined with Zimm-Myerson osmometers[18] as modified by Stabin and Immergut.[19] The experimental results are given in Figure 1. Osmotic pressure measurements with the cellulose were carried out in diluted cadoxen[20,21] solutions in a Vink[22] osmometer as modified by Palm.[23] The results are presented in Figure 2. Degree of substitution (D.S.), molecular weight of the repeating unit (M_R), reduced osmotic pressure [$(h/w)_{w=0}$ or $(\pi/C)_{C=0}$], number-average molecular weight ($\bar{M}_n$), and degree of polymerization ($\bar{P}_n$) of the four specimens are presented in Table I.

TABLE I
Osmometry Data

Polymer	D.S.	M_R	$(h/w)_{w=0}$	$\bar{M}_n$	$\bar{P}_n$
Acetate	2.68	274.5	0.268	96,000	350
Cellulose	—	162	4.35[a]	58,160	359
Nitrate (HNO_3–H_3PO_4–P_2O_5)	2.76	286.3	0.250	102,800	360
Nitrate ($AcONO_2$)	2.45	273.0	0.290	88,600	325

[a] $(\pi/C)_{C=0}$.

Light-scattering measurements were made with a modified Brice-Phoenix photometer, essentially as described previously.[7,24] Solutions were clarified by ultracentrifugations. Measurements with the cellulose acetate were carried out in methylene chloride solutions. The data were plotted according to Zimm,[25] giving a value for Kc/R_θ of 5.3×10^{-6}, corresponding to a weight-average molecular weight of 189,000 and a degree of polymerization of 690. The solvent for the nitrate was acetone. In this case the data were plotted according to Debye[26] with correction applied for dissymmetry. The molecular weight was 198,000, giving a degree of polymerization of 691.

DISCUSSION

It is evident from the data in Table I that the deacetylation caused no rupture of glycosidic bonds in the cellulose. This is what could be expected since treatment of acetylated oligosaccharides with sodium methoxide in methanol has long been used for producing the unsubstituted oligomers. The data of Vink[22] are also in agreement with this conclusion.

The number-average degree of polymerization of the cellulose remained

unchanged after nitration with the acid mixture. It is well known that if only a few bonds are broken in a polymer, its weight-average molecular weight will be much more affected than the number-average value. The weight-average degree of polymerization of the cellulose also remained unchanged on nitration. The reagent accordingly left the β-(1 $\rightarrow$ 4)-glucosidic bonds in the cellulose entirely intact.

Staudinger and Mohr[2] in their earlier investigation, arrived at the same conclusion, using celluloses of various chain lengths. It should be noted, however, that their evidence was only indirect, as molecular weights were estimated by viscometry and the values for the original cellulose were based on measurements with the corresponding acetyl derivative. The possible occurrence of "abnormal" linkages in native celluloses has received much attention, particularly in recent years.[27] The effect of the nitrating agent on such linkages is unknown. It is interesting to note, however, that a cellulose from unopened cotton bolls, when nitrated by the present procedure, had a weight-average degree of polymerization as high as 15,000.[7] If "abnormal" linkages are present in cotton cellulose, they must either be extremely few or completely stable towards the nitrating reagent.

Nitration with acetyl nitrate apparently caused a slight but noticeable degradation of the cellulose. Earlier evidence[16,17] indicated that this reagent effected no more depolymerization than the acid mixture, the two methods giving identical results, at least when used with very pure celluloses.[17] The present degree of nitration was much lower than the level of trisubstitution usually attained with acetyl nitrate, and this might possibly account for the discrepancy.

The results show that cellulose can be converted without depolymerization into an organo-soluble derivative by nitration with an acid mixture of the type used here. The possibility of transforming cellulose into a polymer-homologous acetate does not appear to have been realized so far. Actually, such a derivative would be even more useful since acetates are more stable in solutions than nitrates and, unlike the latter, can easily be de-esterified to yield a cellulose with the same degree of polymerization.

EXPERIMENTAL

Preparation of Cellulose Acetate

Raw Coastland cotton (220 g.), previously extracted with ethanol–benzene, was immersed in 17% aqueous sodium hydroxide for activation, after which most of the alkali was removed by washing with water. The product was washed with dilute acetic acid by filtration, and the water was displaced with glacial acetic acid. The wet material was placed in a mixture consisting of glacial acetic acid (5 liters), acetic anhydride (2.5 liters), and perchloric acid (50 ml.). After shaking at room temperature for 20 min., no cellulose remained undissolved. After a total reaction time of 45 min. the solution was poured into cold water (40 liters). The precipitated cellulose acetate was washed with water until neutral and then dried in the

air. The product was dissolved in a mixture of methylene chloride and ethanol (4:1, v/v, 5 liters). The resulting solution was subjected to centrifugation at 18,000 rpm, filtered through glass wool, and added slowly in a fine stream and with stirring to petroleum ether (5 liters for each 2 liters of solution). The continuous filament produced was collected and dried, giving 360 g. of acetate, corresponding to a yield of 96%. The acetyl content of the product was 43.0%.[28]

Deacetylation

A portion of the cellulose acetate (100 g.) was shaken with 0.1*N* methanolic sodium methoxide (3 liters) at room temperature for 2 hr. The fibrous material was washed successively with anhydrous methanol, methanol containing 5% acetic acid, and methanol. The yield was 59 g. (quantitative); acetyl content, nil.

Nitrations

Cellulose (10 g.) was treated at +17°C. for 1 hr. with a mixture (700 ml.) of nitric acid, phosphoric acid, and phosphorus pentoxide (64:26:10, w/w), prepared from colorless, fuming nitric acid and phosphorus pentoxide.[4] The reaction mixture was poured into 10 liters of 25% aqueous sodium chloride, cooled to −25°C. The nitrate was recovered by filtration, washed with ice-water until neutral, and dried from methanol. The yield was 16.5 g., corresponding to 93%. Nitration with acetyl nitrate in glacial acetic acid was carried out as described elsewhere;[17] the yield was 95%. Nitrogen determinations were carried out by a modified Kjeldahl method.[29]

Osmotic Pressure Measurements

The solvent for the acetate was a 9:1 (v/v) mixture of chloroform and ethanol, and for the nitrates *n*-butyl acetate. The membranes were made from untreated cellophane films and the temperature was 30°C. The osmometers were of the Stabin-Immergut type,[19] allowing equilibrium to be attained in 5–7 hr. Number-average molecular weights were calculated from the simplified relationship

$$\bar{M}_n = 25{,}700/(h/w)_{w=0}$$

where h was the osmotic height in centimeter solution and w was the concentration in grams per kilogram solution.

For the cellulose, the solvent was cadoxen, prepared according to Donetzhuber.[30] Before measurements, the solutions were carefully diluted with an equal volume of water. The osmometer was of the type developed by Vink[22] and later modified by Palm,[23] recently used by Henley.[31] The membrane was cellophane. The molecular weight was obtained from the relationship

$$\bar{M}_n = RT/(\pi/C)_{C=0}$$

where π was the osmotic pressure in atmospheres and C was the concentration in grams per deciliter.

Light-Scattering Measurements

A 0.2% solution of cellulose acetate in methylene chloride was clarified by centrifugation at 30,000 rpm for 7 hr. Five solutions were prepared, ranging in concentration from 0.07 to 0.15%, and were centrifuged directly[32] in the light-scattering cells[24] at 25,000 rpm for 1 hr. The instrument, a Brice-Phoenix photometer, was modified as described elsewhere.[33] Measurements and calculations were carried out as reported earlier.[7,24] Light-scattering measurements were carried out with the cellulose nitrate in the same way except that the solvent was acetone. Refractive index increments were determined with a Brice-Phoenix differential refractometer.

The author wishes to express his gratitude to Dr. Olov E. Öhrn, Billerud A. B., Säffle, Sweden, for determination of the number-average molecular weight of the cellulose and for helpful criticism of the manuscript. His thanks are also due to Dr. D. A. I. Goring for valuable advice and to Mr. F. S. Spencer for technical assistance.

References

1. Berl, E., and G. Rueff, *Ber.*, **63,** 3212 (1930); *Cellulosechem.*, **12,** 53 (1931); *ibid.*, **14,** 115 (1933).
2. Staudinger, H., and R. Mohr, *Ber.*, **70,** 2296 (1937).
3. Davidson, G. F., *J. Textile Inst.*, **29,** T195 (1938).
4. Alexander, W. J., and R. L. Mitchell, *Anal. Chem.*, **21,** 1497 (1949).
5. Jullander, I., *Arkiv Kemi, Mineral., Geol.*, **A21,** No. 8 (1945).
6. Schulz, G. V., and M. Marx, *Makromol. Chem.*, **14,** 52 (1954).
7. Goring, D. A. I., and T. E. Timell, *Svensk Papperstidn.*, **63,** 524 (1960); *Tappi*, **45,** 454 (1962).
8. Heuser, E., and L. Jörgensen, *Tappi*, **34,** 57 (1951).
9. Mitchell, R. L., *Ind. Eng. Chem.*, **45,** 2526 (1953).
10. Timell, T. E., *Tappi*, **40,** 25, 30 (1957).
11. Bryde, Ö., *Svensk Papperstidn.*, **52,** 389 (1949).
12. Timell, T. E., *Svensk Papperstidn.*, **60,** 836 (1957).
13. Gralén, N., *Sedimentation and Diffusion Measurements on Cellulose and Cellulose Derivatives*, Uppsala, 1944.
14. Golowa, O. P., and W. I. Iwanow, *Über das Molekulargewicht der Zellulose*, Akademie Verlag, Berlin, 1953.
15. Bouchonnet, A., F. Trombe, and G. Petitpas, *Bull. Soc. Chim. France*, **4,** 560, 894, 1085 (1937).
16. Harland, W. G., *J. Textile Inst.*, **45,** T678 (1954).
17. Bennett, C. F., and T. E. Timell, *Svensk Papperstidn.*, **58,** 281 (1955).
18. Zimm, B. H., and I. Myerson, *J. Am. Chem. Soc.*, **68,** 911 (1946).
19. Stabin, J. V., and E. H. Immergut, *J. Polymer Sci.*, **14,** 209 (1954).
20. Jayme, G., and K. Neuschäffer, *Naturwissenschaften*, **44,** 62 (1957); *Makromol. Chem.*, **23,** 71 (1957).
21. Henley, D., *Svensk Papperstidn.*, **63,** 143 (1960).
22. Vink, H., *Arkiv Kemi*, **13,** 193 (1958).
23. Palm, G., Institute of Physical Chemistry, Uppsala, to be published.
24. Goring, D. A. I., and T. E. Timell, *J. Phys. Chem.*, **64,** 1426 (1960).
25. Zimm, B. H., *J. Chem. Phys.*, **16,** 1093, 1099 (1948).

26. Debye, P., *J. Appl. Phys.*, **15**, 338 (1944); *J. Chem. Phys.*, **14**, 636 (1946); *J. Phys. Colloid Chem.*, **51**, 18 (1947).
27. Marchessault, R. H., and B. G. Rånby, *Svensk Papperstidn.*, **62**, 230 (1959); *J. Polymer Sci.*, **36**, 651 (1959).
28. Gennung, L. B., and R. C. Mallat, *Ind. Eng. Chem. Anal. Ed.*, **15**, 319 (1943).
29. Timell, T. E., and C. B. Purves, *Svensk Papperstidn.*, **54**, 303 (1951).
30. Donetzhuber, A., *Svensk Papperstidn.*, **63**, 447 (1960).
31. Henley, D., *Arkiv Kemi*, **18**, 327 (1961).
32. Dandliker, W. B., and J. Kraut, *J. Am. Chem. Soc.*, **78**, 2380 (1956).
33. Huque, M. M., J. Jaworzyn, and D. A. I. Goring, *J. Polymer Sci.*, **39**, 9 (1959).

Synopsis

A cellulose triacetate, prepared from cotton, has been deacetylated under mild conditions to yield a cellulose which was converted into the nitrate derivative with a nitric acid–phosphoric acid–phosphorus pentoxide mixture. The number-average degrees of polymerization of the three products were 350, 359, and 360, respectively, as determined by osmometry. The corresponding weight-average values for the acetate and the nitrate were 690 and 691, as estimated from light-scattering measurements. It is concluded that neither the deacetylation nor the nitration caused any noticeable rupture of normal glycosidic bonds in cellulose. Nitration with acetyl nitrate gave a product with a degree of polymerization of 325, indicating some depolymerization.

Résumé

Un triacétate de cellulose, préparé à partir de coton, a été désacétylé dans des conditions douces, pour obtenir une cellulose qu'on a convertie en nitrate au moyen d'un mélange d'acide nitrique, d'acide phosphorique et de pentoxyde de phosphore. Les degrés de polymérisation moyen en nombre des trois produits déterminés par osmose sont respectivement 350, 359 et 360. Les valeurs moyennes en poids correspondants, déterminées par diffusion lumineuse, pour l'acétate et le nitrate sont 690 et 691. On en conclut que ni la désacétylation ni la nitration ne provoquent de rupture importante des liens glycosidiques normaux dans la cellulose. La nitration par le nitrate d'acétyle donne un produit ayant un degré de polymérisation de 325, signe d'une certaine dépolymérisation.

Zusammenfassung

Ein aus Baumwolle hergestelltes Cellulosetriacetat wurde unter milden Bedingungen zu einer Cellulose deacetyliert, die mit einem Salpetersäure-Phosphorsäure-Phosphorpentoxyd-Gemisch ins Nitrat umgewandelt wurde. Das osmometrisch bestimmte Zahlenmittel des Polymerisationsgrades der drei Produkte betrug 350 bzw. 359 bzw. 360. Die entsprechenden, durch Lichtstreuung bestimmten Gewichtsmittelwerte betrugen für das Acetat 690 und für das Nitrat 691. Man kommt zu dem Schluss, dass weder die Deacetylierung noch die Nitrierung eine merkliche Spaltung der normalen Glykosidbindungen der Cellulose verursacht. Nitrierung mit Acetylnitrat lieferte ein Produkt mit dem Polymerisationsgrad 325, was für eine gewisse Depolymerisation spricht.

Discussion

J. J. Hermans (*Chemstrand Research Center, Durham, N. C.*): Without being too optimistic about the stability of cellulose nitrate in solution, is it not true that this polymer is much more stable in butyl acetate than in acetone, and that even in acetone the exclusion of water improves the situation considerably?

T. E. Timell: Yes, it is true that cellulose nitrate is much more stable in ester solvents than in acetone and that water enhances its instability in acetone. However, even in solvents such as ethyl or butyl acetate, it is not absolutely stable. Depolymerization is

quite noticeable when fractionations are carried out in acetone over a prolonged period of time. Being a poor solvent, acetone is also often preferred for osmotic pressure or light scattering measurements.

R. H. Marchessault (*College of Forestry, Syracuse, New York*): What do you mean by abnormal linkages? Why not carry your study to cellulose oligosaccharides?

T. E. Timell: Using the term "abnormal linkages" I was thinking primarily of linkages modified by neighboring groups, such as carboxyl or carbonyl groups. Accidental incorporation of, for example, a xylose residue into cellulose would also create "abnormal" linkages.

If you want to prove that a particular reagent does not modify a low-molecular weight compound in any way, the proof will require *quantitative recovery* after the reaction. Quantitative yields are not easy to achieve in carbohydrate chemistry. Even with a yield of 99%, you would still have to allow for the possible occurrence of one "abnormal" linkage out of a total number of 100 bonds. Under these circumstances it is better to use a polysaccharide. Although a quantitative yield after the reaction is of course highly desirable also in this case, a slight loss of material can always be tolerated.

JOURNAL OF POLYMER SCIENCE: PART C NO. 2, PP. 117–128 (1963)

Viscosity and Sedimentation in Dilute Solutions of Cellulosic Macromolecules

J. J. HERMANS, *Chemstrand Research Center, Inc., Research Triangle Park, Durham, North Carolina*

Introduction

A complete treatment of the hydrodynamics of polymer solutions should include such diversified topics as sedimentation, viscosity, birefringence of flow, viscoelastic behavior, non-Newtonian flow, the behavior observed in dynamic measurements, the effect of shear-rate on light scattering. The present discussion is restricted to viscosity of and sedimentation in very dilute solutions of cellulosic polymers, in an attempt to compare existing theories with experimental data. Non-Newtonian effects will not be considered, in other words the viscosity is meant to be the viscosity at the limit of zero shear rate. Moreover, the term "dilute" solution is supposed to apply to the range of concentrations in which the reduced specific viscosity varies (approximately) linearly with the concentration of the polymer. In practice this is usually from about 1 wt.-% down to about 0.02 wt.-%. Significant deviations from this linear behavior at very low concentrations have been reported by many authors and have been attributed sometimes to the existence of a "critical concentration" where the solute molecules begin to overlap[1] and sometimes to effects caused by adsorption of the polymer on the capillary wall of the viscometer.[2] The data are conflicting, and their significance is still in debate. For this reason, the very low concentrations at which these phenomena have been observed will not be considered in this review, and it will be assumed that the linear extrapolation leads to the correct value of the intrinsic viscosity.

It is noted also that no attempt is made to cover the existing literature concerning cellulosic polymers. The data that will be considered are chosen merely for the purpose of illustration.

Even within the strict limitations indicated there is room for considerable guesswork and controversy. The reason for this is that there does not exist a detailed theory of viscosity or sedimentation that is independent of a model. A theory must therefore (1) postulate a model, and (2) develop a theory for this model. For simple models such as impenetrable spheres, ellipsoids or rods, the theory is straightforward, but for other models approximations must be introduced, and different authors have used different approaches.

The Model of Rods or Ellipsoids

The oldest model used to explain viscosity and sedimentation of cellulosic molecules is that of a rigid rod or ellipsoid. This was done, for example, in the work of Mosimann, Signer and others. By way of example, Table I shows the axial ratio α/β of cellulose nitrate molecules calculated by Mosimann[3] from intrinsic viscosity and rate of sedimentation. This calculation contains a certain element of arbitrariness because it assumes that the molecular volume of the solute is known. The simplest and probably the best approach is to use the partial specific volume,[4] but admittedly this ignores the possible effect of solvation. For the same reason, the estimate of the "theoretical" axis ratio $(\alpha/\beta)_{\text{the}}$ must be based on somewhat arbitrary assumptions concerning the thickness of the molecule. Consequently, the important aspect of the figures in Table I is not so much their absolute value, but rather the general trend: as the molecular weight is increased, the ratio between $(\alpha/\beta)_{\text{exp}}$ and $(\alpha/\beta)_{\text{the}}$ decreases steadily. This has been interpreted as meaning that the molecules of low molecular weight are extended but that there is increased tendency to coil when the molecular weight is increased.

TABLE I

Axial Ratio α/β of Cellulose Nitrate Molecules Calculated from Sedimentation and Viscosity by Mosimann[3] and Compared with the "Theoretical" Value

M	α/β (theoretical)	α/β (sedimentation)	α/β (viscosity)
600,000	1,000	300	560
200,000	350	200	300
80,000	140	140	160
30,000	53	60	95
6,000	12	15	18

Similar conclusions have been drawn from studies of electrically charged cellulose derivatives. Tait, Vetter, Swanson, and Debye[4] applied Simha's formula for ellipsoids to the intrinsic viscosity of cellulose xanthate in dilute aqueous alkali and found that the long axis of the ellipsoid calculated from the data gets closer to the fully extended length of the molecule as the concentration of alkali is decreased. Table II shows an additional example from the work of Pals,[5] who investigated carboxymethyl cellulose and pectinate in dilute salt solutions. These data could be explained on the basis of a random coil expanded by electrostatic forces. In fact, the agreement with the predicted effect of the ionic strength was almost quantitative, even at quite low ionic strengths. Pals observed also, however, that the intrinsic viscosities extrapolated to zero ionic strength could be described equally well by assuming an ellipsoidal molecule, the long axis of which turned out to be very close to the fully extended length L (see Table II).

Notwithstanding the success of the rod model, there are good reasons to consider other models as well. In the first place, even if the rigid ellipsoid

TABLE II
Intrinsic Viscosity [η] Extrapolated to Zero Ionic Strength and Molecular Dimensions Derived from Simha's Formula for Ellipsoids. Carboxymethyl Cellulose and Pectinate[4]

	$10^{-4}M$	[η], ml./g.	β, A.	α, A.	L, A.
CMC-73	15.0	8000	7.4	4400	3630
CMC-72	6.4	2900	6.8	2300	1630
Pectinate	4.6	1300	7.0	1540	1370

is considered a satisfactory model for low molecular weights, it fails at high molecular weights. In the second place, it remains to be seen whether properties other than viscosity and sedimentation can be explained by this model. In this connection it should be mentioned that according to Tait, Vetter, Swanson, and Debye the light scattering by solutions of cellulose xanthate could not be explained by the rod model.

Earlier Theories of Random Coils

Attempts to apply the model of random coils to cellulosics have frequently been made. The problem is complicated by the variety of aspects involved: (1) choice between ellipsoidal and spherical shape, (2) excluded volume effect, (3) hydrodynamic interaction of the chain segments, (4) effect of polydispersity. To facilitate the discussion, a very brief summary of the earlier theories is given. Recent modifications will be mentioned in a later section.

The relation between intrinsic viscosity [η] and molecular weight M is often written in the form of Mark's equation:

$$[\eta] = KM^{\epsilon} \tag{1}$$

where K and ϵ are constants. Now if all hydrodynamic interaction between the chain segments is neglected (free-drained model), the theory predicts[6] that [η] is proportional to the square of the radius of gyration. For a chain obeying Gaussian statistics this means proportionality with M. Although, in a limited range of molecular weights, many cellulosics have been found for which the exponent ϵ in eq. (1) is close to 1, the model of a free-drained Gaussian coil cannot be considered as adequate. One of the reasons for this is that it would require that the sedimentation rate is independent of M.

Next consider the other extreme, where the hydrodynamic interaction of the chain segments is so pronounced that the molecule behaves essentially as impermeable to the flow of liquid around it. This model is often referred to as "equivalent particle,"[7] i.e., the molecule is assumed to behave as thought it were a rigid sphere or ellipsoid. For a sphere the intrinsic viscosity becomes proportional to R^3/M and the sedimentation rate S becomes proportional to M/R, where R is the effective radius of the molecule.

It is observed at this point that the molecular dimension which is accessible to experiment by means of light scattering is the z-average square of the radius of gyration ρ. It will be assumed that R and ρ are proportional to each other, so that the equations for the equivalent sphere may be written

$$\begin{aligned} [\eta] &= K\rho^3/M \\ S &= BM/\rho \end{aligned} \tag{2}$$

where K and B are constants. When the statistics are Gaussian this means that both $[\eta]$ and S will be proportional to $M^{1/2}$. To explain deviations from this simple relationship with M, Sadron[7] suggested that at low values of M the sphere had to be replaced by an ellipsoid. Flory,[8] on the other hand, attributed deviations from this $[\eta]$–M or S–M relation to the effect of excluded volume. He writes

$$\rho = \rho_0\alpha \tag{3}$$

where ρ_0 is the radius of gyration in the absence of a volume effect (i.e., in a theta solvent) and is proportional to $M^{1/2}$, while α is an expansion factor due to excluded volume. This factor is related to M as follows,

$$\alpha^5 - \alpha^3 = CM^{1/2} \tag{4}$$

where C is related to the second virial coefficient.[8]

Kirkwood and Riseman,[9] Debye and Bueche,[10] and Brinkman[11] developed theories for "partial free draining." The Kirkwood-Riseman calculation made use of Gaussian statistics, which led to results in terms of molecular weight. On the other hand, Brinkman, and likewise Debye and Bueche, introduced an effective molecular radius R, and expressed the final result in terms of M and R. As shown by Debye and Bueche,[10] this result becomes very similar to that of Kirkwood and Riseman if Gaussian statistics are assumed,[12] even though the mathematical relationships are quite different. A simple, but quite good approximation is[13]

$$\begin{aligned} [\eta] &= A\rho^2(1 + aM/\rho)^{-1} \\ S &= B(1 + cM/\rho) \end{aligned} \tag{5}$$

where A, B, a, and c are constants that depend on the following two parameters: the effective bond length and the frictional coefficient per monomer unit. When gaussian statistics apply, eq. (5) becomes

$$\begin{aligned} [\eta] &= A'M(1 + a'M^{1/2})^{-1} \\ S &= B(1 + c'M^{1/2}) \end{aligned} \tag{6}$$

The result for S given in eq. (6) was derived from an approximate theory of the hydrodynamic interaction by Hermans.[14] That for $[\eta]$ was found by Peterlin.[15] The advantage of eq. (5) over eq. (6) lies in the fact that it is not dependent on Gaussian statistics. We will revert to this later.

Comparison with Experimental Data

When these earlier theories are compared with experimental data, particularly those pertaining to cellulosic macromolecules, the following results emerge.

1. The eq. (6) for the sedimentation rate S is obeyed by cellulose over a very wide range of molecular weights.[16] This is not true, however, of Eq. 6 for $[\eta]$. According to this equation, a plot of $M/[\eta]$ versus $M^{1/2}$ should

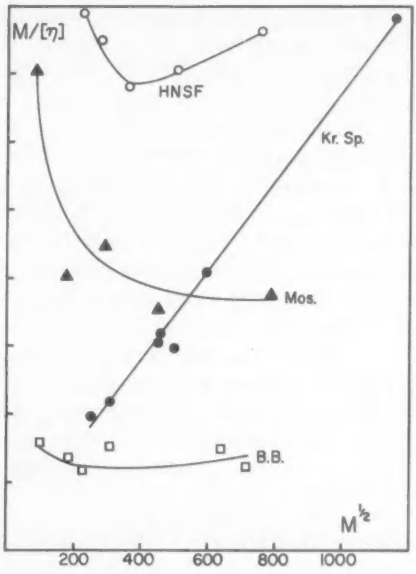

Fig. 1. $M/[\eta]$ vs. $M^{1/2}$ for: [○(HNSF)] cellulose nitrate in ethyl acetate (Hunt, Newman, Scheraga and Flory[18]); [▲(Mos.)] cellulose nitrate in acetone (Mosimann[3]); [●(Kr.Sp.)] cellulose tricaproate in dioxane (Krigbaum and Sperling)[19]; [□(B.B.)] Cellulose nitrate in acetone (Badger and Blaker)[32].

give a straight line. By way of example, Figure 1 shows four sets of data, and only one of them is in agreement with the prediction (Kr.Sp. in Fig. 1). It is somewhat doubtful whether the data of Badger and Blaker (B.B. in Fig. 1) must be considered as lying on a curve or on a horizontal line. The curve was drawn because Badger and Blaker themselves[32] pointed out that a plot of $[\eta]/M$ versus M appeared to show a maximum, and they quoted other data for cellulosics from the literature to substantiate this statement.

2. The frictional coefficient per monomer unit calculated from the constants appearing in the Kirkwood-Riseman or Debye-Bueche equations always turns out to be about an order of magnitude below that which one would expect from Stokes' law. This is true not only for cellulosics, but for almost all polymers studied. One could argue that Stokes' law is not

necessarily applicable to particles of molecular dimensions, but the success of this law in the estimation of diffusion coefficients and ionic mobilities of low molecular weight compounds suggests strongly that the discrepancy should not exceed a factor of 2 or 3. There appears to be a way out of this difficulty, as will be shown in the section on polydispersity.

3. Flory's equation (2) for $[\eta]$, in combination with eqs. (3) and (4), has been very successful in describing experimental data for many noncellulosic polymers. Its strength lies particularly in its ability to predict the effect of solvent and temperature through the relation between $[\eta]$ and second virial coefficient. It has been observed, however, that when the expansion factor α is calculated from $[\eta]$, the ratio $(\alpha^5 - \alpha^3)/M^{1/2}$ is not quite independent of M but goes through a maximum.[17,18] (See in this connection the next section.)

Much greater are the discrepancies observed when the equations are applied to cellulose derivatives, where the "constant" K of eq. (2) increases very markedly with increasing molecular weight. Hunt, Newman, Scheraga, and Flory[18] found a twofold change in K for cellulose nitrate in ethylacetate when the molecular weight changed from 35,000 to 260,000. Krigbaum and Sperling,[19] in their studies of cellulose tricaproate in 1-chloronaphthalene found that the K value for a molecular weight of about 1 million was about 5 times larger than that for M about 60,000. A similar trend was observed by Brown[20] in his work on hydroxyethyl cellulose. Finally, mention is made of Cowie's data[21] concerning amylose in dimethylsulfoxide, where K showed an almost 10-fold change when the molecular weight was varied from 200,000 to 3 million. As pointed out by Kurata and Yamakawa,[22] this is indicative of partial free drainage.

Recent Modifications of the Theories

The flat maximum observed with several noncellulosic polymers when $(\alpha^5 - \alpha^3)/M^{1/2}$ is plotted against M was explained by Krigbaum,[23] who introduced several refinements in Flory's excluded volume theory. More recently, however, Stockmayer[24,25] has pointed out that two problems are involved: the excluded volume theory on the one hand and the relation between α and $[\eta]$ on the other hand.

Kurata, Yamakawa, and Utiyama[26] have reconsidered the theory of Kirkwood and Riseman for chains which show non-Gaussian behavior as a result of volume exclusion. This changes the relation between $[\eta]$ and α. In particular, at the limit of almost complete impenetrability, it is found that $[\eta]$ is proportional to $\alpha^{2.73}$ rather than to α^3. Kurata, Stockmayer, and Roig[25] have pointed out that if this new relation is used to calculate α from $[\eta]$, the value of $(\alpha^5 - \alpha^3)/M^{1/2}$ does no longer pass through a maximum but becomes a monotonically increasing function of M. This result is in agreement with computer data of Wall and Erpenbeck[27] for a diamond lattice chain and also with the theory of Kurata, Stockmayer, and Roig

who developed a modification of the excluded volume theory and came to the conclusion that Flory's equation (4) is to be replaced by

$$\alpha^3 - \alpha = C'(1 + 3/\alpha^2)^{-3/2}M^{1/2} \tag{7}$$

Stockmayer[28] has mentioned that this functional relationship may be approximated by the following very simple one:

$$\alpha^3 = 1 + C''M^{1/2} \tag{8}$$

If this is done, it follows from the result of Kurata, Yamakawa, and Utiyama that near the limit of impenetrable particles:

$$(M^{-1/2}[\eta])^{1.24} = A'' + B''M^{1/2} \tag{9}$$

where A'' and B'' are constants. This relation is tested in Figures 2 and 3 for the four examples that were considered also in Figure 1. It is seen that the plots of eq. (9) show a considerable improvement over those of eq. (6). Nevertheless, two serious objections must be raised. In the first place, three of the four lines in Figures 2 and 3 have a negative intercept with the $(M^{-1/2}[\eta])^{1.24}$ axis, whereas A'' in eq. (9) is positive. In the second place, the theory of the excluded volume is of doubtful value for cellulose derivatives. This is apparent from the fact that the effect of temperature and of solvent on the molecular dimensions of cellulosic polymers is uncommonly small.[18,19] It is shown perhaps even more clearly by the fact that for some cellulose derivatives the ratio ρ^2/M decreases rather than increases with increasing M. This is true for cellulose tricaproate (Kr.Sp. in Figs. 1 and 3). The same phenomenon was observed by Brown[20] in his work on hydroxyethyl cellulose in water.

Effect of Polydispersity

At the limit of free draining, the intrinsic viscosity of a polymer-homologous mixture is proportional to the weight average of ρ^2,

$$[\eta] = A\langle\rho^2\rangle_w \tag{10}$$

At the other extreme, the "equivalent sphere," the determinative quantities in a polydisperse sample are the number averages, and eq. (2) must be replaced by

$$[\eta] = K\langle\rho^3\rangle_n/\langle M\rangle_n \tag{11}$$

Kurata, Yamakawa, and Utiyama,[26] in their theory of the viscosity of chains with excluded volume, have paid considerable attention to the manner in which polydispersity is to be accounted for. The matter is rather complicated and their considerations will not be repeated here, for two reasons. In the first place, as has already been said at the end of the previous section, there are reasons to believe that the theory of the excluded volume effect may lose much of its usefulness in cellulosic macromolecules. In the second place, it is believed that the very simple method suggested by Marrinan and Hermans[13] is quite adequate to account for polydispersity.

As explained in a previous section, eq. (5) should be approximately valid for a monodisperse sample, irrespective of whether gaussian statistics apply or not. This equation must now be given a form that applies to a polymer-

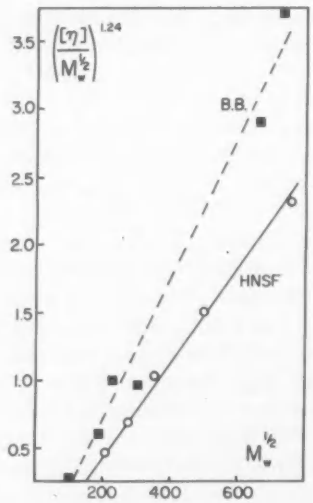

Fig. 2. $(M^{-1/2}[\eta])^{1.24}$ vs. $M^{1/2}$ for [O(HNSF)] cellulose nitrate in ethyl acetate (Hunt, Newman, Scheraga and Flory[18]); [■(B.B.)] Cellulose nitrate in acetone (Badger and Blaker[32]).

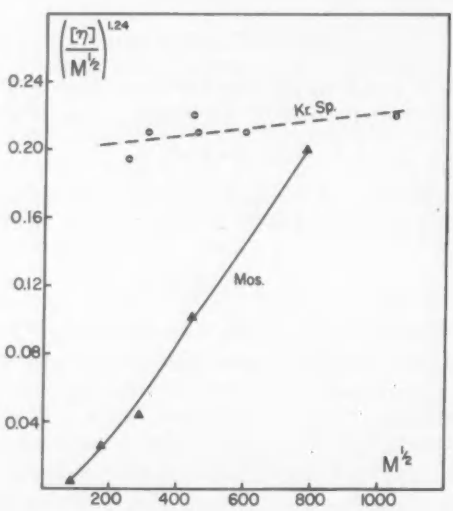

Fig. 3. $(M^{-1/2}[\eta])^{1.24}$ vs. $M^{1/2}$ for [O(Kr. Sp.)] cellulose tricaproate in dioxane (Krigbaum and Sperling[19]); [▲(Mos.)] cellulose nitrate in acetone (Mosimann[3]).

homologous mixture. To account for the fact that eq. (10) must result at the limit of negligible hydrodynamic interaction and that eq. (11) must follow at the "equivalent particle" limit, Marrinan and Hermans suggested the equation

$$[\eta] = A\langle\rho^2\rangle_w[1 + a\langle M\rangle_n\langle\rho^2\rangle_w/\langle\rho^3\rangle_n]^{-1} \quad (12)$$

Thus, plotting $\langle\rho^2\rangle_w/[\eta]$ versus $\langle M\rangle_n\langle\rho^2\rangle_w/\langle\rho^3\rangle_n$ one should obtain a straight line, from which the constants A and a can be derived. Applying this to the data of Hunt, Newman, Scheraga, and Flory[18] and those of Huque, Goring, and Mason[29] for cellulose nitrate in ethyl acetate, it was found[13] that the data did indeed lie on a straight line within experimental error over the very large molecular weight range of about 50,000 to about 3 million. Similar reasoning has been developed[13] for the sedimentation rate S, but the result depends on the technique used to measure S, and the argument will not be repeated here.

Gratifyingly, the frictional coefficient per monomer unit derived from the data in the manner described turned out to have a very reasonable value. Application of Stokes' law led to a monomer radius of about 3 A, irrespective of whether viscosity or sedimentation was used. It would appear, therefore, that the unrealistic values found in earlier work may well have been due to the fact that polydispersity was not properly accounted for.

It is significant that the theoretical relations are obeyed down to the lowest molecular weight investigated. In other words, there is no indication that particular attention must be paid to ellipsoidal rather than spherical coil shape at low values of M. This does not prove, however, that ellipsoidal shapes do not occur. It must be borne in mind that eq. (10) which applies at the limit of free draining is independent of the shape. To what extent explicit consideration of ellipsoidal shape will affect the form of eq. (12) is as yet unknown. It is conceivable that the formula is not very sensitive to the overall shape of the molecule.

Conclusions

Tentatively it is concluded that cellulosic macromolecules in dilute solution behave like partially free-drained random coils. It is believed that these coils assume rather extended forms when the molecular weight is low, but if this is true, eq. (12) does not appear to be overly sensitive to shape. For this reason, no attention has been paid to the statistics of wormlike chains[30] which has been discussed in connection with cellulosics by several authors.[18,31] It is, of course, possible that specific attention to the extended shape must be paid when the molecular weight is below about 50,000.

To apply Eq. 12, the radius of gyration must be known. Also, since the quantity measured is $\langle\rho^2\rangle_z$, some knowledge of the molecular weight distribution is required to compute $\langle\rho^2\rangle_w$ and $\langle\rho^3\rangle_n$. The only data for which this information is available with sufficient accuracy are those of Hunt,

Newman, Scheraga and Flory and Huque, Goring and Mason. Similar data for cellulose derivatives have been reported by other authors, but it was found that in all of them the range of molecular weights studied was too narrow or the scatter shown by the graphs too great to allow of any definite conclusion.

Note: After the completion of this review, W. H. Stockmayer (Hanover, N. H.) kindly drew the author's attention to recent work by Stockmayer and Fixman,[33] who have reconsidered the relation between the intrinsic viscosity $[\eta]$ and the expansion factor α, and suggest the following relation between $[\eta]$ and M:

$$[\eta] = KM^{1/2} + DM,$$

where D is related to the second virial coefficient. Thus $M^{-1/2}[\eta]$ rather than $(M^{-1/2}[\eta])^{1.24}$ should be a linear function of $M^{1/2}$. When this is applied to the data of Badger and Blaker (B.B. in Fig. 2), Krigbaum and Sperling (Kr. Sp. in Fig. 3) and Mosimann (Mos. in Fig. 3), it is found that the amount of scatter in the experimental curves allows one to indeed draw a straight line. The results of Hunt, Newman, Scheraga, and Flory (HNSF in Fig. 2), however, give distinct curvature. Also, the intercept with the $M^{-1/2}[\eta]$ axis is again negative in all cases except Kr. Sp.

The conclusion that there is some draining in cellulosic molecules, at least in cellulose nitrate, was drawn also by Kurata and Stockmayer.[34]

References

1. Streeter, D. J., and R. F. Boyer, *Ind. Eng. Chem.*, **43**, 1791 (1951); *J. Polymer Sci.*, **14**, 5 (1954); T. Kawai and K. Saito, *J. Polymer Sci.*, **26**, 213 (1957); N. Hirai, *Kobunshi Kagaku*, **14**, 252 (1957); W. R. Krigbaum, *J. Polymer Sci.*, **26**, 222 (1957).

2. Öhrn, O. E., *J. Polymer Sci.*, **17**, 137 (1959); *ibid.*, **19**, 199 (1956); M. Takeda and R. Endo, *J. Phys. Chem.*, **60**, 1202 (1956).

3. Mosimann, H., *Helv. Chim. Acta*, **26**, 61 (1943).

4. Tait, C. W., R. J. Vetter, J. M. Swanson, and P. Debye, *J. Polymer Sci.*, **7**, 261 (1951).

5. Pals, D. T. F., and J. J. Hermans, *Rec. Trav. Chim.*, **71**, 433 (1952).

6. Debye, P., *J. Chem. Phys.*, **14**, 636 (1946).

7. Sadron, Ch., *J. Chim. Phys.*, **44**, 22 (1947); *J. Polymer Sci.*, **3**, 812 (1948).

8. Flory, P. J., *Principles of Polymer Chemistry*, Cornell Univ. Press, Ithaca, N. Y., 1953, p. 595 and following; P. J. Flory and T. G Fox, *J. Polymer Sci.*, **5**, 745 (1950); *J. Am. Chem. Soc.*, **73**, 1904, 1915 (1951); L. Mandelkern and P. J. Flory, *J. Chem. Phys.*, **20**, 212 (1952).

9. Kirkwood, J. G., and J. Riseman, *J. Chem. Phys.*, **16**, 565 (1948).

10. Debye, P., and A. M. Bueche, *J. Chem. Phys.*, **16**, 573 (1948).

11. Brinkman, H. C., *Koninkl. Ned. Akad. Wetenschap. Proc.*, **50**, 618 (1947); *Physica*, **13**, 447 (1947).

12. Hermans, J. J., *Flow Properties of Disperse Systems*, North Holland, Amsterdam, 1953, p. 235.

13. Marriman, H. J., and J. J. Hermans, *J. Phys. Chem.*, **65**, 385 (1961).

14. Hermans, J. J., *Rec. Trav. Chim.*, **63**, 219 (1944).

15. Peterlin, A., *Proc. Akad. Ljubljana, Math. Phys. Sect.*, **12**, 59 (1950); *J. Polymer Sci.*, **5**, 473 (1950).

16. Hermans, J. J., *J. Polymer Sci.*, **1**, 233 (1946).

17. Krigbaum, W. R., and P. J. Flory, *J. Polymer Sci.*, **11**, 37 (1953); N. T. Notley and P. Debye, *J. Polymer Sci.*, **24**, 275 (1957).

18. Hunt, M. L., S. Newman, H. A. Scheraga, and P. J. Flory, *J. Phys. Chem.*, **60** 1278 (1956).

19. Krigbaum, W. R., and L. H. Sperling, *J. Phys. Chem.*, **64**, 99 (1960).
20. Brown, W., *Arkiv Kemi*, **18**, 227 (1961).
21. Cowie, J. M. G., *Makromol. Chem.*, **42**, 230 (1961).
22. Kurata, M., and H. Yamakawa, *J. Chem. Phys.*, **29**, 311 (1958).
23. Krigbaum, W. R., *J. Chem. Phys.*, **23**, 2113 (1955).
24. Stockmayer, W. H., *Makromol. Chem.*, **35**, 54 (1960); M. Kurata and W. H. Stockmayer, *Repts. Progr. Polymer Phys. Japan*, **5**, 23 (1962).
25. Kurata, M., W. H. Stockmayer, and A. Roig, *J. Chem. Phys.*, **33**, 151 (1960).
26. Kurata, M., H. Yamakawa, and H. Utiyama, *Makromol. Chem.*, **34**, 139 (1959); M. Kurata and H. Yamakawa, *J. Chem. Phys.*, **29**, 311 (1958).
27. Wall, F. T., and J. J. Erpenbeck, *J. Chem. Phys.*, **30**, 634 (1959).
28. Stockmayer, W. H., communication at the American Chemical Society Polymer Symposium at Lansing, Mich., June 1962.
29. Huque, M. M., D. A. I. Goring, and S. G. Mason, *Can. J. Chem.*, **36**, 952 (1958).
30. Kratky, O., and G. Porod, *Rec. Trav. Chim.*, **68**, 1106 (1949); J. J. Hermans and R. Ullman, *Physica*, **18**, 951 (1952); A. Peterlin, *J. Chim. Phys.*, **47**, 669 (1950); *J. Polymer Sci.*, **8**, 173 (1952).
31. Holtzer, A. M., H. Benoit, and P. M. Doty, *J. Phys. Chem.*, **58**, 624 (1954).
32. Badger, R. M., and R. H. Blaker, *J. Phys. Colloid Chem.*, **53**, 1056 (1949).
33. Stockmayer, W. H., and M. Fixman, to be published.
34. Kurata, M., and W. H. Stockmayer, *Advan. Polymer Sci.*, to be published.

Synopsis

In this review some experimental data are compared with existing theories. After briefly discussing the application of the rigid rod model, a comparison is made with the theories of Flory, Kirkwood-Riseman (KR) and Brinkman-Debye-Bueche (BDB). For cellulose derivatives the "constant" in Flory's expression for the intrinsic viscosity $[\eta]$ varies strongly with the molecular weight. The KR and BDB expression for the sedimentation rate of Gaussian chains is obeyed very well by cellulose, but the frictional coefficient per monomer unit is too low and the corresponding expression for $[\eta]$ does not apply. The application of recent modifications of the viscosity theory by Kurata and co-workers and of the excluded volume theory by Stockmayer and co-workers suggests that at the limit of nearly complete impermeability, the quantity $Y = (M^{-1/2}[\eta])^{1.24}$ is a linear function of $M^{1/2}$. Cellulose derivatives appear to obey this relation, but the intercept with the Y-axis sometimes has the wrong sign. The procedure of Marrinan and Hermans, who used a modified KR expression for polydisperse systems in a form which is independent of the chain statistics appears to represent the data best of all.

Résumé

Dans cet article on compare certains résultats expérimentaux avec les théories existantes. Après une brève discussion sur l'application du modèle du bâtonnet rigide, on fait la comparaison entre les théories de Flory, Kirkwood-Riseman (KR) et Brinkman-Debye-Bueche (BDB). Pour les dérivés cellulosiques la "constante" dans l'expression de Flory pour la viscosité intrinsèque (η) varie fortement avec le poids moléculaire. L'expression de KR et BDB pour la vitesse de sédimentation de chaînes gaussiennes est très bien respectée par la cellulose, mais le coefficient frictionnel par unité monomérique est trop faible et l'expression correspondante pour (η) ne s'applique pas. L'application de modifications récentes à la théorie de la viscosité par Kurata et collaborateurs et à la théorie du volume exclu par Stockmayer et collaborateurs suggère qu' à la limite de l'imperméabilité presque complète la quantité $Y = (M^{-1/2}(\eta))^{1.24}$ est une fonction linéaire de $M^{1/2}$. Les dérivés cellulosiques semblent obéir a cette relation, mais l'intersection avec l'axe Y a parfois un signe contraire. Le procédé de Marrinan et Hermans, qui utilise une expression de KR modifiée pour des systèmes polydispersés, sous une

forme qui est indépendante des statistiques de la chaîne, semble représenter les résultats de la meilleure façon.

Zusammenfassung

Im vorliegenden Bericht werden einige Versuchsergebnisse mit den bekannten Theorien verglichen. Nach einer kurzen Diskussion der Anwendung des Starren-Stäbchen-Modells wird ein Vergleich mit der Theorie von Flory, Kirkwood-Riseman (KR) und Brinkman-Debye-Bueche (BDB) durchgeführt. Bei Cellulosederivaten hängt die "Konstante" in der Beziehung von Flory für die Viskositätszahl $[\eta]$ stark vom Molekulargewicht ab. Cellulose gehorcht der KR- und BDB-Beziehung für die Sedimentationsgeschwindigkeit Gauss-scher Ketten sehr gut, der Reibungskoeffizient pro Monomereinheit ist jedoch zu niedrig und der entsprechende Ausdruck für $[\eta]$ hat keine Gültigkeit. Die Anwendung der neureren Modifikation der Viskositätstheorie von Kurata und Mitarbeitern und der Theorie des ausgeschlossenen Volumens von Stockmayer und Mitarbeitern zeigt, dass in der Grenze nahezu völliger Impermeabilität die Grösse $Y = (M^{-1/2}[\eta])^{0.24}$ eine lineare Funktion von $M^{1/2}$ ist. Cellulose derivate scheinen dieser Beziehung zu gehorchen, der Abschnitt auf der Y-Achse hat jedoch manchmal das verkehrte Vorzeichen. Am besten scheint das Verfahren von Marrinan und Hermans, die einen modifizierten KR-Ausdruck für Polymersysteme in einer von der Kettenstatistik unabhängigen Form benützten, auf die Ergebnisse anwendbar zu sein.

JOURNAL OF POLYMER SCIENCE: PART C NO. 2, PP. 129–144 (1963)

Flow of Gels of Cellulose Microcrystals. I. Random and Liquid Crystalline Gels

JAN HERMANS, JR., *American Viscose Corporation, Research and Development Division, Marcus Hook, Pennsylvania*

INTRODUCTION

Recently it was reported from this laboratory that gels can be formed by the action of very large shear stresses on aqueous suspensions of level-off DP cellulose.[1] The latter material, which is obtained by hydrolyzing pure α-cellulose under suitable conditions of pH and temperature for prolonged periods of time, is characterized by an average degree of polymerization (DP) of the individual cellulose molecule which is not decreased any further by continued hydrolysis under the same conditions. It is obtained in yields of about 90% of the starting material and possesses a very high degree of crystallinity as determined by x-ray methods. It is believed that level-off DP cellulose consists of the crystalline regions of the original α-cellulose which are much more slowly attacked by acid than the more randomly coiled chain segments connecting them.[1,2]

As was stated, attrition of level-off DP cellulose in aqueous suspension by a large shear stress produces a gel. This is explained by assuming that the crystalline regions are in large numbers sheared off the weakened cellulose fibers and dispersed in the solvent.[1] These microcrystals, as made visible by the electron microscope,[3] are elongated particles with lengths of the order of 0.4 μ and thicknesses of the order of 0.04 μ. Their dimensions vary with the source of the α-cellulose, and, perhaps, with the methods used for hydrolysis and subsequent attrition. The work of Mukherjee and Woods[4] and of Marchessault et al.[5] has shown that ramie crystallites can be prepared of dimensions approximately 1 $\mu \times 60$ A. $\times$ 100 A., and that these particles represent the individual crystalline regions of the cellulose fiber. Given the dimensions of the microcrystals in the preparations studied here, these particles apparently contain several of these crystalline regions side by side, as can also be seen by careful inspection of their texture as revealed by electron micrographs (e.g., Figures 3 and 4 of this paper).

While considerable work has been done on the properties of dilute suspensions of the microcrystals, the properties of concentrated, gellike solutions have received almost no attention. We have determined the flow behavior of a number of these cellulose gels, and the results of these experi-

ments, and the conclusions that can be drawn from them are reported below.

EXPERIMENTAL

Materials

The level-off DP cellulose studied in this investigation was a sample of the commercial product Avicel of the American Viscose Corporation. The material is prepared from high alpha purified wood cellulose by a procedure which has been described.[1] A gel made from a sample of cotton linter, prepared in the same manner has also been studied.

Attrition

There are various ways of attriting the weakened fibers of the level-off DP cellulose so that sufficient microcrystals are sheared off to produce a gel. Figure 1 shows schematic diagrams of the parts active in attrition of a Hobart mixer, Waring Blendor, homogenizer, and roll mill. In the two former and the latter of these instruments local high shear rates are produced by the rapid motion of certain parts. In the third instrument, the high shear rates occur in the orifice through which the suspension is forced

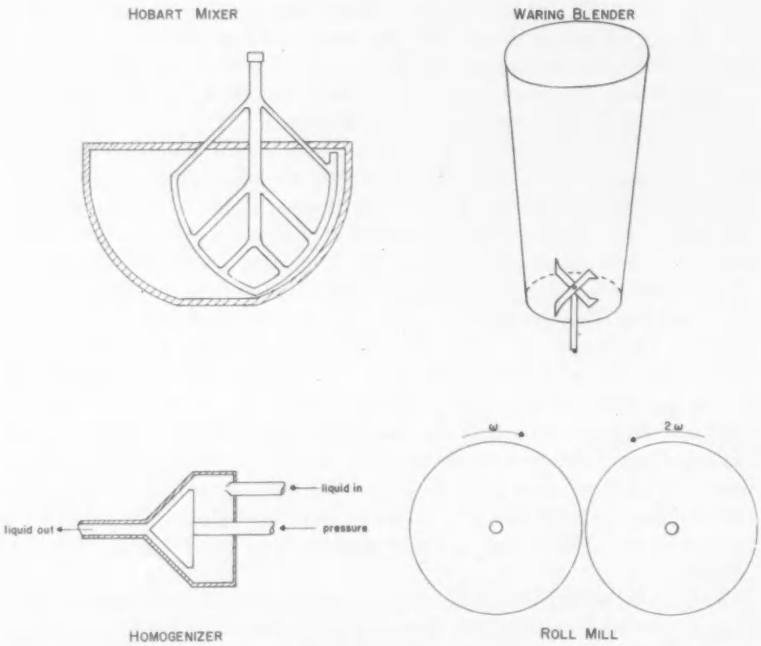

Fig. 1. Schematic diagrams of equipment used to attrite level-off DP cellulose in suspension.

by a large pressure. The choice of the attriting equipment turns out not to alter the properties of the gel qualitatively. However, the instruments shown are not equally effective in shearing off the microcrystals and thus producing gels of high stiffness and viscosity. In general, a lengthier attrition will produce a stiffer and more viscous gel and gels of different stiffness are obtained by attriting at various concentrations and subsequently diluting to the same concentration.

Three gels were studied in this investigation. One was a gel made from wood level-off DP cellulose by rather gentle attrition in a Hobart mixer. We estimate that about 15% of the total amount of cellulose was present in the gel in the form of microcrystals. Secondly, a gel containing only the microcrystals of the gel just described was prepared (see below). In the third place, a gel was prepared from cotton linter level-off DP cellulose using a roll mill. It turns out that the cotton microcrystals are much more easily sheared off, so that the cotton cellulose gel contained almost no unattrited fibers.

Measurement

A Rao flow birefringence viscometer[6] was used as a viscometer to determine the flow curves of the gels investigated. The instrument, which is of the Couette type, is illustrated in Figure 2. Dimensions are: inner cylinder, length 10.0 cm., diameter 3.6 cm., outer cylinder diameter 4.00 cm. The outer cylinder rotates at a speed which can be varied from 1/30 to 10^3 rpm. The torque on the inner cylinder produced by the resistance to flow of the liquid between the two cylinders, is measured by a strain gage which may be attached to one arm of the inner cylinder assembly at a distance of 5.08 cm. from the center of rotation. The values of the angular velocity of the outer cylinder and of the measured force are proportional to values of the shear rate or (velocity) gradient q and shear stress τ of the liquid between the cylinders. Using the known dimensions of the instrument we arrived at the following relations: $q = 1.00$ sec.$^{-1}$/rpm, $\tau = 22$ dyne cm.$^{-2}$/g. Data of one of these variables as a function of the other constitute the flow curve of the sample. A calibration was performed using N.B.S. standard viscosity oils. The shear stress was found to be proportional to the shear rate, and the ratio τ/q was equal within 5% to the value of the viscosity indicated for the various oils.

An additional measurement may be necessary to determine the property that is most characteristic of the gel, the yield stress, i.e., the value of the shear stress needed to get a shear rate greater than zero.[7] The measurement is performed by attaching a string weighted via a pulley to one arm of the inner cylinder assembly and determining the absence or occurrence of a continuous shearing motion with the displacement indicator gage attached to the other arm, while the outer cylinder is stationary. For the determination of the yield stress the weight attached to the string is increased in steps of 1 g. Making the increases smaller does not improve the accuracy

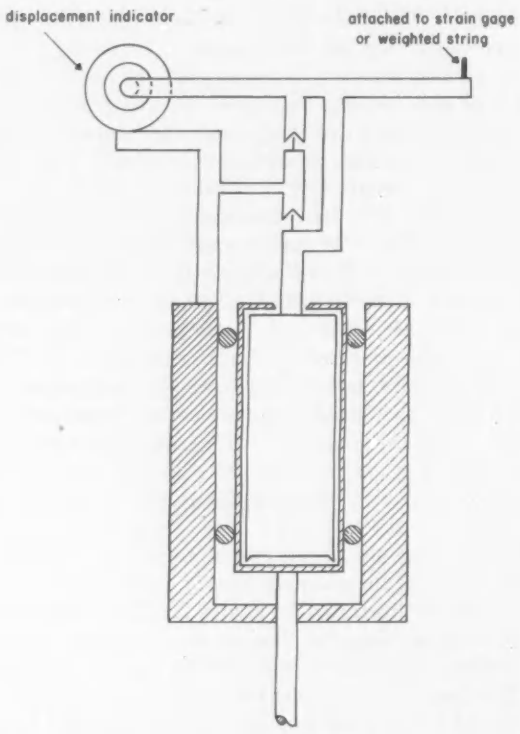

Fig. 2. Diagram of the Rao flow birefringence viscometer used.

of the experiment, since the measurement is not reproducible within a more narrow limit.

In all our measurements the temperature of the gels was 25°C. The experiments described were performed with the assistance of Mr. A. G. Lankitus.

RESULTS

Fractionation

The wood cellulose gel studied contains sheared off microcrystals and the much larger incompletely attrited fibers. Thus, the particle size distribution is extremely broad.[1] This is illustrated by Figure 3, an electron micrograph of Hobart-attrited wood level-off DP cellulose (gel 1). It was of interest to determine the relative effect of the presence of particles of the different sizes on the mechanical properties of the gel. Accordingly, a fractionation using a Serval Model Sla centrifuge was developed which we proceed to describe.

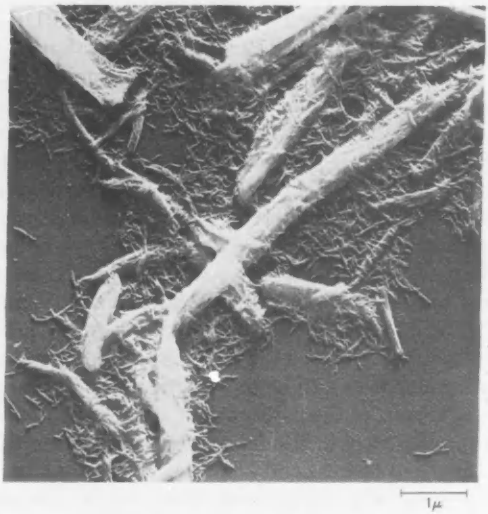

Fig. 3. Electron micrograph made by drying a diluted gel of Hobart-attrited wood level-off DP cellulose on collodion and shadow casting with Pd. 10,000×.

Fig. 4. Electron micrograph prepared in the same way as that in Figure 3 from a gel containing only microcrystals. 10,000×.

Since the smallest microcrystals in the cellulose gels have molecular weights of several tens of millions, and since the particles are compact and considerably denser than water (partial specific volume $\bar{v}$ = 0.669 ml./g.[5]) relatively gentle centrifugation (1 hr at 20,000*g*) suffices to separate a dilute

suspension (concentration below 1%) of attrited level-off DP cellulose into water and a concentrated gel. At lower speeds and shorter times of centrifugation such dilute suspensions will yield a precipitate containing unattrited fibers, while the smaller fiber fragments and the microcrystals remain in solution. By repeating this procedure a suspension of only microcrystals can be prepared. If one then collects the supernatant and centrifuges it at 20,000g for 1 hr., a gel containing only microcrystals collects at the bottom of the tube.[8] An electron micrograph of the particles in the microcrystal gel is shown in Figure 4. It is seen that particles consisting of bundles of more than a few microcrystals which are still in the same relative position as they were in the cellulose fiber now constitute a small fraction by weight of the total. The microcrystals apparently have dimensions falling in an appreciable range. We shall choose an elongated particle of length 0.4 μ and width 0.04 μ to be representative of this range. The molecular weight of a brick of these dimensions is about 580×10^6.

The fiber fragments vary in size from a few times larger than the microcrystals to as large as 10 μ long and 1 μ wide. Electron micrographs of the fiber fraction demonstrate the presence of some microcrystals, which are only removed by repeated washing with water. It is remarkable that as the fiber fraction is washed free of microcrystals, it looses its gel properties and turns into a fibrous precipitate. Therefore, measurements of the properties of only the microcrystal gel are reported below.

Flow Curves

Curves of the shear stress τ versus the shear rate (or gradient) q of a series of dilutions of a Hobart-attrited wood cellulose gel (gel 1) are shown in Figure 5. Measurements were also made at shear rates above 70 sec.$^{-1}$, but these data are not shown, since it was found that the shear stress is almost constant in the shear rate range from 70 to 1000 sec.$^{-1}$. The value of the yield stress, i.e., τ ($q = 0$), is finite. This quantity is, of course, an important characteristic of the gel.

It should be noted that in experiments with homogeneous gels, constant τ values are measured almost at once after application of the desired shear rates and that these are independent of the shear rates experienced by the gels in the viscometer before this measurement. As a minor exception to this rule it was noted that, if the gel has been standing in the viscometer for many hours without agitation, slightly higher τ's are measured initially.

The flow curves of gels containing microcrystals which were extracted from the material in gel 1 were measured at a series of concentrations and these results are shown in Figure 6. Again, τ ($q = 1000$) is not much higher than τ ($q = 70$). A comparison of Figures 5 and 6 shows that much lower concentrations of the microcrystals suffice to give shear stresses as high as those of the unfractionated gel. This is in accordance with the view that the microcrystals alone are responsible for the gel properties and leads one to expect that the flow curves of Figure 5 show the largest viscosities (i.e., shear stress to shear rate ratios) and the largest yield stresses

attainable for gels of given concentrations of cellulose in water in the absence of additives.

It will be noted that all but one of the yield stresses in Figure 5 are higher than the τ values at 2 sec.$^{-1}$ of the same gels. The shear-rate region be-

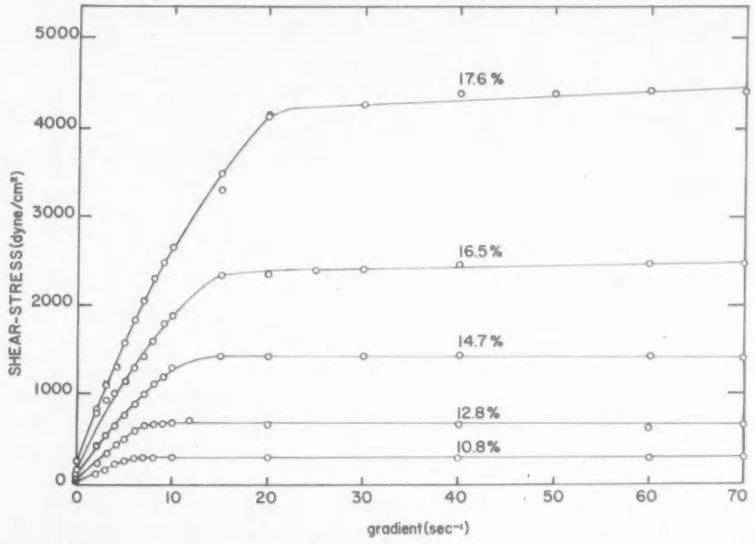

Fig. 5. Flow curves (i.e., plots of shear stress vs. shear rate or velocity gradient) of a series of dilutions of a Hobart-attrited wood cellulose gel.

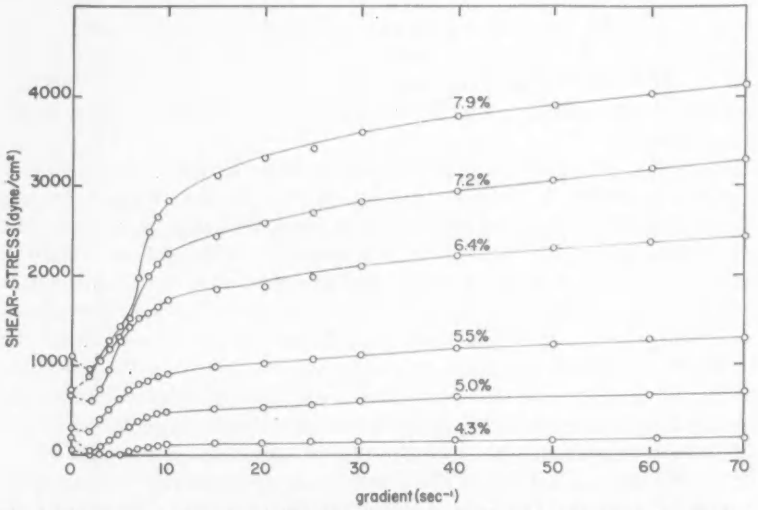

Fig. 6. Flow curves of a series of dilutions of a gel containing only microcrystals, prepared from the wood level-off DP cellulose gel of Figure 5.

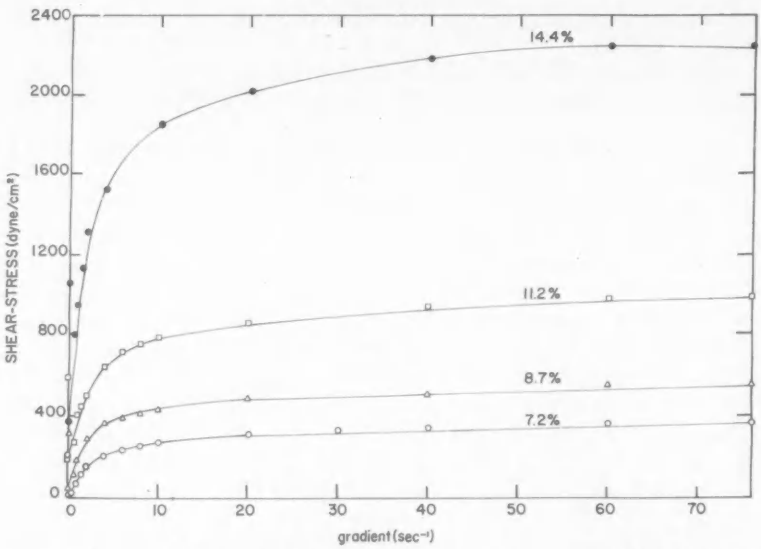

Fig. 7. Flow curves of a series of dilutions of a roll mill-attrited cotton level-off DP cellulose gel.

tween 0 and 2 sec.$^{-1}$ was not investigated at the time these experiments were performed. Later, it became possible to make measurements in the range 1/20 to 2 sec.$^{-1}$, and a series of experiments was performed on dilutions of a roll mill-attrited sample of cotton linter level-off DP cellulose which showed abnormally high yield stresses, similar to those of the microcrystal gel. The results are presented in Figures 7 and 8. Again, shear stresses measured at shear rates between 80 and 1000 sec.$^{-1}$ are about constant. The data of Figure 7 do not differ much from those of Figures 5 and 6 except that the shear rate at which the τ vs. q curves flatten out is somewhat lower.

Inspection of Figure 8 reveals the presence of an irregularity in each flow curve at a gradient between 0.5 and 1.0 sec.$^{-1}$. Such an irregularity was also found in the experiments on the microcrystal gel (Fig. 5) in the higher shear rate range of 5–7 sec.$^{-1}$, but was absent with the gels of Figure 3. It is also found that if the gel was sheared at a shear rate on one side of that at which the irregularity occurs and a measurement is made afterwards on the same side, the measured shear stress does not change with time. If, however, the second measurement is done at a shear rate on the other side of the irregularity (0.5 sec.$^{-1}$), a short time elapses before the measured shear stress is constant, its initial value being higher than the final one at shear rate below 0.5 sec.$^{-1}$ and lower than the final value at shear rates above 0.5 sec.$^{-1}$. Linked to this behavior is the observation of two different yield stresses, both obtainable experimentally using the method described. A yield stress lying at the extrapolation to $q = 0$ of the lower part

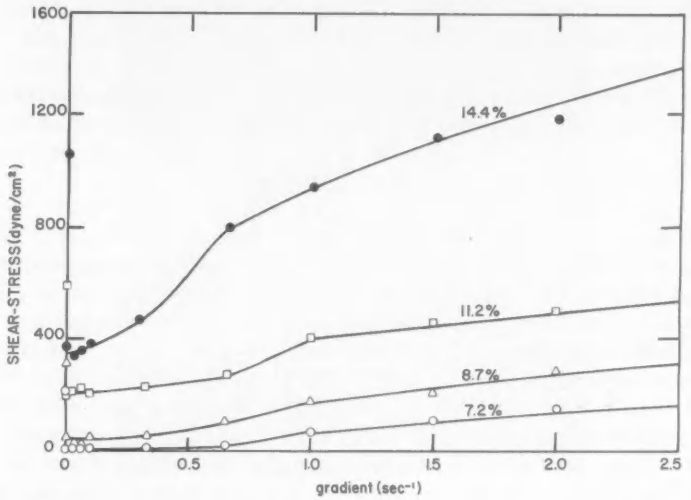

Fig. 8. The data of Figure 7 plotted on a different scale. Note the measurement of two different values of the yield stress (i.e., shear stress at zero gradient) for each gel.

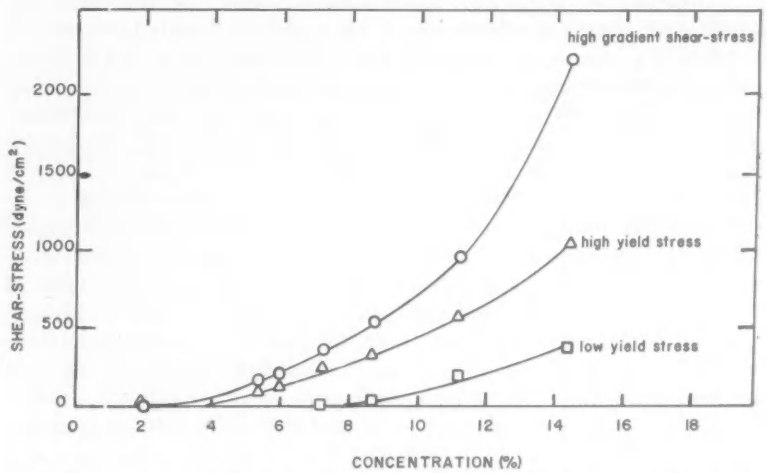

Fig. 9. Shear stresses at a gradient of 80 sec.$^{-1}$ and the two yield stresses of the gels of Figures 7 and 8 plotted vs. concentration.

of the flow curve is obtained if the gel is sheared at a low shear rate (<0.5 sec.$^{-1}$) just before the measurement. A higher value is obtained, if the gel is sheared at a high shear rate (in our experiments 75 sec.$^{-1}$) just before the measurement of the yield stress. The excess stiffness of the gel induced by the fast shearing is removed by subsequent shearing at gradients below 0.5 sec.$^{-1}$

The yield stresses of the gels of Figures 7 and 8 and some further dilutions and the shear stresses at 80 sec.$^{-1}$ of the same gels have been collected in Figure 9. Note that below some fairly well defined finite concentration each of these parameters becomes extremely small, and that this occurs at a higher concentration for the low yield stress than for the high yield stress.

DISCUSSION

At an early stage the formation of a gel by mechanical attrition of a suspension of level-off DP cellulose has been attributed to the appearance of many microcrystals,[1] i.e., the elongated particles observed earlier in dilute suspensions of ultrasonically attrited hydrocellulose by Rånby[3] and by Mukherjee and Woods.[4] The experiments presented here completely bear this out, in that gels containing only microcrystals could be prepared which had much greater stiffness and viscosity than the gels of attrited level-off DP cellulose of the same concentrations from which they were prepared.

The flow properties of the gels investigated are reminiscent of those of certain clays reported in the literature.[9,10] The properties of these clay suspensions have been attributed to the presence of elongated rigid particles To explain their behavior it is assumed that each elongated particle is in partial contact with a few others and that the contact is made durable by the presence of a noncovalent crosslink. This model can explain the necessity of applying a shear stress greater than some finite value, the yield stress, to produce a shear rate different from zero, since the resting network has properties of a solid. When a shear stress larger than the yield stress is applied, the particle network is destroyed, but aggregates persist, so that the viscosity (= shear stress/shear rate) is high. As the shear stress is increased, the aggregates become smaller, and the viscosity decreases considerably. It would appear to us that the same model applies to the cellulose gels under discussion. When the data of Figures 5–9 are converted to values of the specific viscosity and these values compared with data on concentrated solutions of rigid particles of approximately the same dimensions in which interparticle interaction was shown to be minimal (poly-γ-benzyl-L-glutamate in *m*-cresol),[11] it is found that the values for the gels are several orders of magnitude higher than those for the polypeptide solutions at the same concentration. This indicates the existence of strong particle interactions in the gels.

Unfortunately, the acceptance of the model of a particle network does not allow us to analyze any of our data quantitatively, since the necessary theory has not been developed.[7] Nevertheless, the model will be useful as a reference in the discussion which follows.

It has been noted in the results section that the gels do not show thixotropic behavior to an appreciable extent. If we apply our model, this indicates that the time needed for the formation of the network from the separate small aggregates existing in the flowing solution is very small. While this information is of no further use at the moment, it will have to be

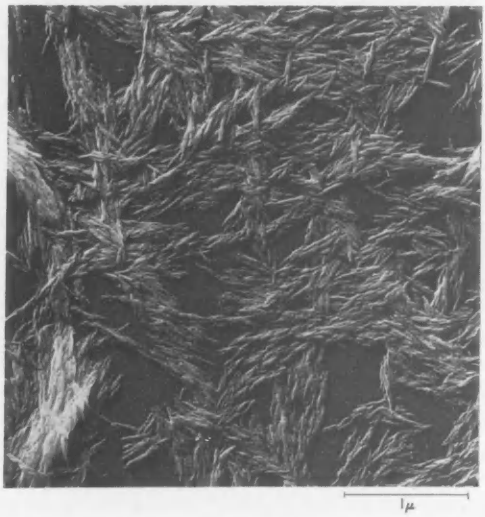

Fig. 10. Electron micrograph prepared from the gel of cotton linter level-off DP cellulose. 19,000×.

taken into account whenever the nature of the crosslinks is under discussion.

One property of the gels which we have not yet discussed in terms of the particle network model is the increase of the rigidity by previous shearing and the irregularity in the flow curves occurring at low shear stresses. These two properties are linked by the observation that gradients larger than those at which the irregularity occurs will produce the excess rigidity, while shearing at smaller gradients will destroy any excess rigidity present in a matter of a few minutes. It is interesting to note here that the 7% solution of cotton cellulose of Figures 7–9 is not a gel (yield stress = 0) when first sheared below 1 sec.$^{-1}$, but is a gel when first sheared at 75 sec.$^{-1}$. Inspection of Figure 8 reveals that this is true of solutions in the concentration range of about 4–8%. Below this range the systems are not gels under any conditions, while above this range they are gels independently of the flow history, although the yield stress is still dependent on the previous flow. We have found no reports of a similar behavior of other systems in the literature; apparently the cellulose gels have aspects which distinguish them considerably from the other systems we have mentioned. A suggested explanation of the anomalous behavior follows.

Cellulose microcrystals have been shown to possess a tendency to aggregate side by side in dilute solution.[12] To illustrate this, we have included an electron micrograph made from the cotton cellulose gel studies here (Fig. 10). We would like to suggest that the tendency to lateral aggregation shown by the crystallites is also responsible for the anomalous behavior discussed above. It has been reported by Marchessault et al.[8] that

gels of cellulose microcrystals are birefringent after application of a shearing motion. These authors noted that birefringent units could be observed in the microscope and they likened these to liquid crystals. Apparently, when the liquid crystal, formed by the shearing motion, is no longer sheared, it forms a gel as it is, i.e. before the individual microcrystals can diffuse to random orientations. Thus, in order to explain the measurement of two different yield stresses it is sufficient to assume that this oriented gel has a larger yield stress to obtain shear in the direction of the orientation (i.e., the same direction in which shear was previously applied to the gel). This opinion is also supported by the observation that the two yield stresses differ by the largest amount for the cotton cellulose gel in which the microcrystals have the greatest tendency to side by side alignment.

The irregularity which occurs in the flow curves showing two yield stresses at gradients about half those at which the flow curves flatten out, can also be explained. Obviously, the liquid crystal structure is not formed spontaneously, but is brought into being by the mechanical alignment of the microcrystals caused by the shearing motion. This suggests that the formation of the liquid crystal from the randomly oriented system is a cooperative phenomenon and that its formation perhaps takes place at a single critical gradient.

Similarly, the observation of the loss of the excess rigidity in a short time by shearing at gradients below this critical gradient is easily explained by realizing that the microcrystals are held tightly in position only when the gel is not sheared, but can diffuse to random orientation in a fairly short time (of the order of the rotatory diffusion constant) when the crosslinks are continuously being broken and reformed by a shearing motion. As a result, if we start with an oriented gel, the observed shear stresses will decrease with time and the particle orientation will gradually become random at these low gradients.

In completion of our discussion of the effect of liquid crystal formation at high shear rates, it is interesting to note that only one yield stress is measured for each of the gels of Figure 5, which contain a large concentration of unattrited fibers besides microcrystals. Apparently the presence of these fibers prevents the formation of the liquid crystal phase, probably because of the irregular shape of the fibers.

In conclusion, we would like to point out that the formation of liquid crystalline or anisotropic phases in solutions of elongated rodlike particles has been the subject of considerable theoretical and experimental work. Onsager's theory[13] treats solutions of particles with strong electrostatic repulsions, which may give birefringent solutions at very low concentration. Flory's statistical treatment[14] shows that anisotropic solutions will result in systems without strong particle–particle interaction because of problems of packing asymmetrical particles in any way but with their long axes nearly parallel. In particular, Flory's theory derives values of the largest volume fraction, φ^*, below which these systems are isotropic, and of the volume fraction $\varphi^{*\prime}$ above which they are homogeneously anisotropic

(if the overall volume fraction, φ $\varphi^* < \varphi < \varphi^{*\prime}$, the system contains two phases). Experiments on solution of polypeptides in apolar solvents gave data of φ^* and φ^* in fair agreement with the theory.[11,15] For rodlike particles of an axial ratio of 10 (our "typical" microcrystal introduced above), Flory's theory gives a value of $\varphi^* = 0.64$, clearly much above the volume fractions of the gels studied here. Since electrostatic forces of the kind introduced in Onsager's theory appear to be insignificant in the present case (as follows from the data on the effect of salt on the gels reported in the following paper[16]), it appears that the action of shearing the gel is indeed critical in producing a system of particles with a sufficient degree of parallel alignment and that the subsequent coming into play of the strong cross linking forces responsible for the gel properties allows the liquid crystalline phase to be maintained. What is, then, the physical nature of these cross links is, of course, a problem which is hereby raised, but to which the results presented in this paper give no answer.

The author is indebted to many people of the Corporate Applied Research Department of the American Viscose Corporation for unpublished information and practical knowledge regarding the materials studied in this paper. He would like, in particular, to mention the aid received from Dr. O. A. Battista and Mr. E. Fleck. The author is especially grateful to Dr. W. A. Sisson for stimulating his enthusiasm in the early stages of this work, for providing the gels studied and the electron micrograph shown in Figure 10, and his willingness to discuss the results at all times in a critical manner.

The electron micrographs shown in Figures 3, 4, and 10 were prepared by Mr. Morehead of this laboratory.

References

1. Battista, O. A., and P. A. Smith, *Ind. Eng. Chem.*, **54**, 20 (1962); U.S. Pat. 2,978,446 (April 4, 1961); O. A. Battista, U.S. Pat. 3,023,104 (Feb. 27, 1962).

2. Battista, O. A., and S. Coppick, *Textile Res. J.*, **17**, 419 (1947); O. A. Battista, *Ind. Eng. Chem.*, **42**, 502 (1950).

3. Rånby, B. G., *Discussions Faraday Soc.*, **No. 11**, 158 (1951); *Arkiv Kemi*, **4**, 249 (1952).

4. Mukherjee, S. M., and H. J. Woods, *Biochim. Biophys. Acta*, **10**, 499 (1953).

5. Marchessault, R. H., F. F. Morehead, and M. J. Koch, *J. Colloid Sci.*, **16**, 327 (1961).

6. Edsall, J. T., A. Rich, and M. Goldstein, *Rev. Sci. Instr.*, **23**, 695 (1956).

7. Roscoe, R., in *Flow Properties of Disperse Systems*, J. J. Hermans, Ed., North Holland, Amsterdam, 1953, p. 1; J. J. Hermans, *ibid.*, p. 61; A. G. Ward and P. R. Saunders in *Rheology*, Vol. II, F. R. Eirich, Ed., Academic Press, New York, 1958, p. 313; J. D. Ferry, *Adv. Protein Chem.*, **4**, 1 (1948).

8. Marchessault, R. H., F. F. Morehead, and N. M. Walters, *Nature*, **184**, 632 (1959).

9. Williamson, R. V., and W. W. Heckert, *Ind. Eng. Chem.*, **23**, 667 (1931).

10. Gabrysh, A. F., T. Ree, H. Eyring, N. McKee, and I. Cutler, *Trans. Soc. Rheology*, **5**, 67 (1961).

11. Hermans, J., Jr., *J. Colloid Sci.*, **17**, 638 (1962).

12. Marchessault, R. H., M. J. Koch, and J. T. Yang, *J. Colloid Sci.*, **16**, 345 (1961).

13. Onsager, L., *Ann. N.Y. Acad. Sci.*, **56**, 627 (1949).

14. Flory, P. J., *Proc. Roy. Soc. (London)*, **A234**, 73 (1956).

15. Robinson, C., J. C. Ward, and R. B. Beevers, *Discussions Faraday Soc.*, **25**, 29 (1958); P. J. Flory, *J. Polymer Sci.*, **49**, 104 (1961).

16. Edelson, M. R., and J. Hermans, Jr., *J. Polymer Sci., Part C*, No. **2**, 145 (1963).

Synopsis

The flow properties of gels of microcrystalline cellulose have been investigated by measurements of the shear stress τ as a function of the shear rate q in a Couette viscometer. Flow curves (i.e., plots of τ versus q) of a gel of attrited wood level-off DP cellulose are characterized by a finite value of τ at $q = 0$, the yield stress, values of τ which increase with q between $q = 0$ and ca. 20 sec.$^{-1}$ and an almost constant value of τ in the range $20 < q < 1000$ sec.$^{-1}$. The values of τ at any q increase with the concentration but do not depend significantly on the flow history of the gel. The flow curves of a gel containing only the microcrystals and not the unattrited fiber fragments of the first gel are qualitatively similar, but given values of τ (q) are measured at much lower concentrations of the microcrystals than of the mixture of microcrystals and fibers of the attrited wood cellulose. With the microcrystal gel and with a gel prepared from cotton cellulose, which contains only microcrystals, it is also observed that the yield stress depends on the shear rate applied to the gel prior to the measurement. A low value of the yield stress, lying at the extrapolation of the flow curve to zero shear rate, is measured when a low shear rate was applied before the measurement of the yield stress, and a higher value is measured when the shear rate applied before the measurement is greater than a "critical" shear rate. This critical shear rate has a value of about 5 sec.$^{-1}$ for the wood microcrystal gel and of about 0.5 sec.$^{-1}$ for the cotton cellulose gel. At these shear rates the flow curves have an unusually steep portion. It is also noted that in a given range of concentrations (4–8% for the cotton cellulose gel) the solution is not a gel (yield stress equal to zero) unless a shear rate larger than the critical shear rate was first applied to it. The properties of the cellulose gels are discussed in terms of a particle network model, the microcrystals having an axial ratio of about ten. Qualitatively, this can explain the observation of a yield stress and the decrease of the ratio τ/q (the viscosity) with the shear rate. The measurement of two values of the yield stress, depending on the previous shear rate, is explained by assuming that the elongated particles are by the shearing motion oriented with their long axes almost parallel and that a liquid crystalline phase is formed in this way. This is made plausible by referring to the observation of birefringence in these gels by Marchessault et al. It must be assumed that the liquid crystalline phase forms a gel as it is, and that this gel has a greater resistance to shear, at least in the same direction in which it was first sheared to produce it. Finally, it is pointed out that a theory based on the particle network model, with which we might analyze our data quantitatively, has not been developed.

Résumé

On a étudié les propriétés d'écoulement de gels de cellulose microcristalline en mesurant la dépendance de la tension de cisaillement (τ) vis-à-vis de la vistesse de cisaillement (q) dans un viscosimètre de Couette. Les courbes d'écoulement (τ porté en fonction de q) d'un gel de cellulose de bois sont caractérisées par une valeur finie de τ, pour $q = 0$, qui est la tension de rendement, valeurs de τ qui augmentent avec q entre $q = 0$ et $q =$ environ 20 sec^{-1} et enfin par une valeur presque constante de τ dans le domaine où q est compris entre 20 et 1000 sec^{-1}. Les valeurs de τ, pour une certaine valeur de q, augmentent avec la concentration mais ne dépendent pas de façon significative de l'historique de l'écoulement du gel. Les courbes d'écoulement d'un gel contenant seulement des microcristaux et pas de fragments de fibre du premier/gel sont qualitativement semblables mais on obtient certains valeurs de τ pour les microcristaux à des concentrations beaucoup plus faibles que pour les mélanges de microcristaux et de fibres de cellulose de bois. Avec un gel microcristallin et avec un gel préparé à partir de cellulose de coton et qui contient seulement des microcristaux, on observe aussi que la tension de rendement dépend de la vitesse de cisaillement appliquée au gel avant la mesure. Une faible valeur de la tension de rendement située au point d'extrapolation de la courbe d'écoulement pour une vitesse de cisaillement nulle, est mesurée lorsqu'on a appliqué une faible vitesse de cisaillement

avant de mesurer la tension de rendement tandis qu'une valeur élevée est mesurée quand la vitesse de cisaillement appliquée avant les mesures est supérieure à une vitesse de cisaillement "critique." Cette valeur critique est d'environ 5 sec^{-1} pour un gel microcristallin de bois et de 0.5 sec^{-1} pour un gel de cellulose de coton. Pour de telles vitesses de cisaillement, les courbes d'écoulement présentent une pente particulièrement forte. On remarque également que dans un domaine déterminé de concentration (4 à 8% pour un gel de cellulose de coton), la solution n'est pas un gel (tension de rendement égale à zéro) à moins qu'on ne lui ait appliqué au préalable une tension de cisaillement supérieure à la valeur critique. Les propriétés des gels de cellulose sont interprêtées sur la base d'un modèle réticulaire des particules, les microcristaux possèdent un rapport axial d'à peu près dix. Qualitativement cela peut expliquer le fait qu'on a observé une tension de rendement ainsi qu'une décroissance du rapport τ/q (la viscosité) avec la vitesse de cisaillement. Le fait, qu'on mesure deux valeurs pour la tension de rendement suivant la vitesse de cisaillement appliqué au préalable, s'explique en supposant que les particules allongées sont orientées par le mouvement du au cisaillement, leurs axes de longueurs devenant presque parallèles et que de cette façon il se forme une phase liquide cristalline. Cela semble plausible si on se réfère aux observations sur la biréfringence de ces gels faits par Marchessault et al. Il faut supposer que la phase cristalline liquide forme un gel et que ce gel possède une résistance plus grande au cisaillement, du moins dans la direction où le premier cisaillement s'est exercé. Pour finir, on signale qu'une théorie, basée sur un modéle réticulaire des particules, qui permettrait une analyse quantitative de nos résultats, n'a pas été développée.

Zusammenfassung

Das Fliessverhalten von Gelen aus mikrokristalliner Cellulose wurde durch Messung der Schubspannung (τ) in Abhängigkeit von der Schergeschwindigkeit (q) in einem Couette-Viskosimeter untersucht. Fliesskurven (d.h. $\tau - q -$ Diagramme) einer zerriebenen Holzzellulose mit ausgeglichenem DP werden durch einen endlichen τ-Wert bei $q = 0$, die Deformationsspannung, durch steigende τ-Werte bei Zunahme von q zwischen $q = 0$ und ca. 20 sec^{-1} und einen fast konstanten τ-Wert im Bereich $20 < q < 1000$ sec^{-1} charakterisiert. Die τ-Werte nehmen bei beliebigem q mit der Konzentration zu, zeigen aber keine ausgeprägte Abhängigkeit von der Fliess-Vorgeschichte des Gels. Die Fliesskurven eines Gels mit blossen Mikrokristallen ohne unzerriebene Faserbruchstücke des ersten Gels sind qualitativ ähnlich, ein gegebener Wert von τ (q) wird aber bei viel geringerer Mikrokristallkonzentration gemessen als bei dem Mikrokristall-Fasergemisch der zerriebenen Holzzellulose. An dem Mikrokristallgel wurde, ebenso wie en einem aus Baumwollzellulose hergestellten und nur Mikrokristalle enthaltenden Gel beobachtet, dass die Deformationsspannung von der am Gel vor der Messung angewendeten Schergeschwindigkeit abhängt. Ein niedriger Wert der durch Extrapolation der Fliesskurve auf Schergeschwindigkeit Null erhaltenen Deformationsspannung wird bei Anwendung einer neidrigen Schergeschwindigkeit vor der Messung der Deformationsspannung und ein höherer Wert bei Anwendung einer Schergeschwindigkeit, grösser als eine "kritische" Schergeschwindigkeit vor der Messung erhalten. Diese "kritische" Schergeschwindigkeit beträgt für das Holz-Mikrokristallgel etwa 5 sec^{-1} und für das Baumwollcellulosegel etwa 0,5 sec^{-1}. Bei diesen Schergeschwindigkeiten besitzen die Fliesskurven einen ungewöhnlich steilen Teil. Weiters wird festgestellt, dass in einem gegebenen Konzentrationsbereich (4 bis 8% beim Baumwollcellulosegel) die Lösung sich nicht als Gel verhält (Deformationsspannung gleich Null), wenn sie nicht zuerst unter einier grösseren als der kritischen Schergeschwindigkeit stand. Die Eigenschaften der Cellulosegele werden anhand eines Partikelnetzwerk-Modells mit Mikrokristallen mit einem Achsenverhältnis von etwa zehn diskutiert. Das Auftreten einer Deformationsspannung und die Abnahme des Quotienten τ/q (der Viskosität) mit der Schergeschwindigkeit kann so qualitativ erklärt werden. Die Messung von zwei Werten der Deformationsspannung in Abhängigkeit von der vorhergehenden Schergeschwindigkeit wird durch die Annahme erklärt, dass die

länglichen Teilchen durch die Scherbewegung mit ihren langen Achsen fast parallel orientiert werden und dass auf diese Weise eine flüssig-kristalline Phase gebildet wird. Das wird durch die Beobachtung einer Doppelbrechung in diesen Gelen durch Marchessault et al. plausibel gemacht. Man muss annehmen, dass die flüssig-kristalline Phase ein Gel bildet und dass dieses Gel, zumindest in der Richtung, die der Scherrichtung bei seiner Erzeugung entspricht, einen grosseren Scherungswiderstand besitzt. Eine Theorie, die zur quantitativen Analyse der Ergebnisse ausreicht, wurde auf Grundlage des Partikelnetzwerk-Modells noch nicht entwickelt.

JOURNAL OF POLYMER SCIENCE: PART C NO. 2, PP. 145–152 (1963)

Flow of Gels of Cellulose Microcrystals. II. Effect of Added Electrolyte

M. R. EDELSON and JAN HERMANS, JR., *American Viscose Corporation, Research and Development Division, Marcus Hook, Pennsylvania*

INTRODUCTION

In the preceding communication[1] a characterization was presented of the flow properties of gels of cellulose microcrystals. These properties were qualitatively explained in terms of the model of a particle network which is generally used to account for the properties of gels. It was also pointed out that a quantitative theory based on this model is lacking, so that we were unable to go beyond the qualitative analysis presented.[2] This is unfortunate, since it is highly desirable to obtain information on the nature of the particle network and on the nature of the noncovalent crosslinks which hold it together. We have, therefore, resorted to a study of the flow properties of gels to which materials other than cellulose and solvent (water) were added, in the hope that the effect of these additions on the flow curves would reveal something about the nature of the crosslinks.

Out first choice fell on a study of the effect of the addition of salts, since the presence of salts is known to influence the flow properties of many colloidal solutions and gels by changing the electrostatic forces between charged particles.[3] One might first ask what basis there is for assuming that the microcrystals are charged particles, since cellulose is not an ionizing substance. In relation to this question, it may be noted that it has been shown that ramie microcrystals aggregate in dilute suspension in the presence of low concentrations of added salts and precipitate at higher salt concentrations.[4,5] The microcrystals present in the gels of wood cellulose studied here can also be suspended in water at low concentrations, and these dilute suspensions are stable for very long times. However, upon the addition of a drop of 1*N* KCl solution to a few milliliters of these suspensions, a precipitate removable by very mild centrifugation and containing all the suspended cellulose forms in a very short time. Therefore, it would appear likely that the cellulose microcrystals are charged particles. This is also indicated by the fact that in a dilute suspension the larger fiber fragments can with a microscope be seen to move towards the cathode in an electric field.[4]

To gain information on the nature and magnitude of the charge carried by the microcrystals, titrations with acid and base were performed on level-off DP cellulose to determine the amounts of groups ionizable in the pH range between 2 and 11 in the material. Further, the flow curves of gels before and after addition of small amounts of electrolyte stock solution were determined in order to establish the influence of the charge on the crosslinks whose existence was assumed to explain the formation of the gel.

EXPERIMENTAL

For methods not described below we refer to the foregoing article.[1]

Titrations

Unattrited level-off DP cellulose was repeatedly washed with boiled water c.q. 0.1*N* KCl, by suspension and centrifugation. Suspensions of the washed material were then brought to low pH with 1*N* HCl and titrated at 25°C. with stepwise increasing amounts of CO_2-free 1*N* KOH while a stream of CO_2-free nitrogen was led over the surface of the solution. The pH was measured after the addition of each aliquot of base with a Beckman Model G pH-meter standardized at pH 4.00, pH 6.85, and pH 9.18 with standard buffers. The experiments were accompanied by a reference titration of the amount of water present in the sample. Because of the large amounts of cellulose which had to be present to get measurable changes in the titration curve, this volume was considerably less than the total volume of the sample (30 ml.). The upper limit to the concentration of level-off DP cellulose in the suspension titrated was about 5 g. in each titration. Above this concentration the suspensions can not be stirred adequately. Concentrations were obtained by dry weight determinations on the sample after the titration. The titrations reported were performed by Mr. A. G. Lankitus.

Materials

The problem of repeatedly producing the same gel for experimental purposes was solved by making use of a roll mill-attrited level-off DP cellulose containing 60% water. Gels with viscosities varying less than 5% can be prepared by adding water to this material in a Hobart mixer. The only precaution necessary is that the water be added slowly enough that lumps of gel in water (rather than: drops of water in the gel) do not form. After dilution to concentrations below 20%, one half hour's action of the Hobart mixer at medium speed does not lead to noticeable further attrition, while by this procedure the gel becomes almost although not quite homogeneous (see below).

RESULTS

Titration Curves

The titration curves of a suspension of 4.6 g. cellulose in 25.4 ml. of water and of the corresponding blank are shown in Figure 1. Titration in 0.1*N*

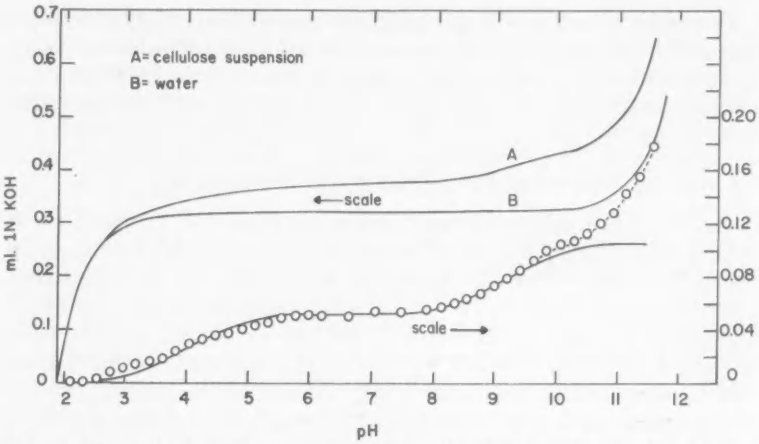

Fig. 1. Plots of (A) titration curve of a suspension of 4.6 g. wood level-off DP cellulose in 25.4 ml. of water, (B) titration curve of 25.4 ml. water, and (O) difference between curves A and B. Left-hand ordinate for curves A and B, right-hand ordinate for difference curve. Curves A and B were so adjusted that the difference is zero at low pH. The continuous curve drawn to fit the difference data is the sum of two titration steps with pK's of 4.0 and 9.2. The dashed curve was drawn to fit the experimental data.

KCl gave essentially the same results. The ordinates have been adjusted so that there is no discrepancy between the two curves at very low pH. The difference between the two curves has been plotted in the same figure. One notes ionizations in two distinct pH ranges. In fact, the data can be fitted by the sum of two curves of x versus pH of the form

$$\log [x/(a - x)] = \text{pH} - \text{p}K \qquad (1)$$

where x is the volume of base added, with pK's 4.0 and 9.2 and with identical values of $a = 0.052$ ml. The value of a indicates that one mole of each ionizing group is present per unit of molecular weight 88,500. Identification of the ionizing groups is made possible by the observation that the titration curve of level-off DP cellulose which has been washed with 0.1N KCl contains the step with a pK of 4 in the same amount while the step with a pK of 9 is absent. Since the starting material was obtained by acid hydrolysis, followed by neutralization with ammonia and a final washing with distilled water, it follows that the material with a pK of 9 is ammonia, present at neutral pH as ammonium ions which serve as counterions to negatively charged groups with a pK of 4 present on the cellulose. It is highly probable that the latter are carboxyl groups, since a titration of nitrogen oxide-oxidized cellulose (degree of oxidation: 0.06) gave a value of 4.1 for the pK of C_6 carboxyl groups.

We may therefore conclude that a microcrystal of dimensions 0.4 × 0.04 × 0.04 μ^3 and approximate molecular weight 580 × 10^6 carries 6600 negatively charged carboxylate ions at neutrality.

The titration curves of Figure 1 indicate that cellulose releases hydrogen ions or binds hydroxyl ions in measurable quantity at pH values above 11. This observation may have some bearing on the fact that many chemical reactions of cellulose are facilitated by "swelling" the cellulose with strong base.

Effect of Electrolytes on the Flow Curves

To 12% gels of roll mill-attrited level-off DP cellulose, prepared as described, small amounts of 0.8–2*M* solutions of salt were added while the gel was stirred well. The flow curves of these gels were then measured. Since it was found that the flow curves are not altered qualitatively by the addition of the salt, we can characterize them conveniently by the value of the shear stress at 80 sec.$^{-1}$, which is roughly the value measured in the entire range from 20 to 1000 sec.$^{-1}$ and by the two values of the yield stress.[1] Table I shows these data for a gel to which no salt solution has been added and for a gel containing 0.08*M* sodium chloride. While the differences between the values in the first and second line of Table I are quite large, it turned out that in a measurement at 1000 sec.$^{-1}$ the shear stress decreases, to become constant after about $^1/_2$ hr. Subsequent measurement of the shear stress at 80 sec.$^{-1}$ and the two yield stresses gave considerably lower values (see Table I). The difference between the values in the third and fourth line is small (although significant).

TABLE I
Values of the Two Yield Stresses and the Shear Stress at a Shear Rate of 80 sec.$^{-1}$ for 12% Gels in the Presence and Absence of Salt

	Yield stress, dyne/cm.^{2}		
	Low value	High value, after shearing at 80 sec.$^{-1}$	Shear stress at 80 sec.$^{-1}$
No salt	120	120	1400
0.08*M* NaCl	160	440	2200
After 1 hr. at 1000 sec.$^{-1}$, no salt	120	120	1000
After 1 hr. at 1000 sec.$^{-1}$, 0.08*M* NaCl	160	220	1400

Neglecting the quite small expected decrease in all shear-stresses due to dilution by the addition of the salt solution, we arrive at the conclusion that the flow properties of the gels are not much different in the presence of salt. The initial increase of all shear-stresses upon the addition of salt must be due to insufficient mixing of gel and salt solution.* This effect is discussed further below.

* A distinct inhomogeneity ("graininess") can, in fact, be noted with the naked eye in gels containing salt before the shearing at 1000 sec.$^{-1}$ but not after this treatment.

Essentially the same data as those of Table I are obtained if solutions of NaCl, $CaCl_2$, and $NaNO_2$ are added to produce final concentrations ranging from 0.004 to 0.08*M*. In another experiment 1% by volume of 1*N* HCl was added to 12% gels. A similar increase in all values of the shear stress as observed upon the addition of salt solution was observed if mixing of gel and acid had been insufficient, but the increase was abolished by shearing 1 hr. at 1000 sec.$^{-1}$. Only upon addition of 1% by volume of 1*N* KOH did we measure a change in the flow curve which persisted after the additional mixing in the viscometer. All values of the shear stress at shear rates below 80 sec.$^{-1}$ were in this case higher, by amounts varying from 50 to 100%.

Finally, it is interesting to mention that a second addition of salt solution to a gel which was made thoroughly homogeneous by shearing at 1000 sec.$^{-1}$ does not produce the increase in shear stress observed upon the first addition.

DISCUSSION

The questions which we raised in the introduction are, from the results presented, seen to be answered as follows. It is shown that the microcrystals are charged particles, a typical microcrystal of length 0.4 μ and width 0.04 μ carrying 6600 negatively charged carboxylate ions at neutral pH, provided these are distributed homogeneously throughout the material. On the other hand, the presence of this charge affects the interaction between the particles in either a resting or a flowing 12% gel to a minor extent only. This is probably so because the magnitude of the charge is insufficient and the repulsive forces between the negatively charged microcrystals small compared with the other interactions playing a role. This result is not only of importance to the understanding of the nature of these interactions, but is also significant in that it excludes the possibility that the liquid crystalline phase observed at high shear rates (see our previous paper[1]) is of the type occurring with highly charged elongated particles analyzed theoretically by Onsager.[6]

We propose to conclude this article with an analysis of the reasons for the increase in the viscosity of the gels when small amounts of salt solutions are insufficiently mixed with them. This analysis shall be made using the model of a particle network introduced in our previous paper. If small amounts of liquid are added to a gel and are distributed through the bulk of the gel as drops, but not used to dilute the gel, i.e., to expand the particle network, the resulting system will practically behave in our rheological experiment as if these drops of very fluid liquid were not present. In order to disperse the added liquid rapidly through the particle network it will be necessary to temporarily break the crosslinks, and the most expedient way of doing this is by shearing the system. We have seen from our experiments that with 12% gels shearing for 1 hr. at 1000 sec.$^{-1}$ is amply sufficient to make the system homogeneous.

When a small fraction of salt solution, rather than water, is added and not sufficiently mixed in, we observe an increase in the stiffness of the gel. In the light of what has been mentioned in the preceding paragraph, it is clear that this can be explained by assuming that the particle network occupies less volume than it did in the original gel, since the small amounts of salt solution present here and there do not contribute to the rheological behavior. The reason for the contraction of the particle network is, presumably, that if the added liquid has a composition different from that of the solvent (water), not only is there a tendency for (or gain in entropy through) expansion of the particle network throughout the available liquid, but also is there a tendency for a mixing of the two solvents. The latter can of course be partly realized most rapidly by a contraction of the particle network, which releases solvent which can then quickly mix with the added liquid. While this argument shows that one condition (a negative free energy change) necessary for a contraction is fulfilled, it is by no means certain that this condition is a sufficient one. It may, for instance, be necessary that the added liquid is a precipitant for the microcrystals, as is here the case, since this would make the diffusion of the microcrystals from the gel into the added liquid a very slow process. The analysis as given does, however, provide an explanation for the observation that addition of salt solution to a gel which contains some salt which is well distributed inside the particle network, does not cause an increase in the stiffness. In this case the gain in entropy to be had by mixing solvent and added liquid is very much smaller and insufficient to compensate for the loss of entropy caused by a contraction of the particle network.

References

1. Hermans, J., Jr., *J. Polymer Sci., Part C*, No. **2**, 129 (1963).
2. Hermans, J. J., *Flow Properties of Disperse Systems*, North Holland, Amsterdam, 1953, p. 61.
3. Verwey, E. J. W., and J. Th. G. Overbeek, *Theory of the Stability of Lyophobic Colloids*, Elsevier, Amsterdam, 1948.
4. Rånby, B. G., *Discussions Faraday Soc.*, **No. 11**, 158 (1951).
5. Marchessault, R. H., M. J. Koch, and J. T. Yang, *J. Colloid Sci.*, **16**, 345 (1961).
6. Onsager, L., *Ann. N. Y. Acad. Sci.*, **56**, 627 (1949).

Synopsis

The behavior as polyelectrolytes of the microcrystals which are responsible for the formation of gels of microcrystalline cellulose has been investigated in two ways. In the first place, it has been determined by potentiometric titration with strong acid and base that a measurable amount of carboxyl groups are present in the material, the preparation of wood level-off DP cellulose studied having one carboxyl group per unit of molecular weight 88,500. This means that a "typical" microcrystal of molecular weight 580×10^6 carries 6,600 negatively charged carboxylate ions at neutral pH. In the second place, the influence of added electrolyte on the flow properties of the gels has been measured. Provided the gel and the added salt solution are properly mixed, only a small increase in the shear stress at any shear rate is measured. This is also true when 1 vol.-% of 1*N* HCl is added to a gel to neutralize the carboxyl groups. It is therefore concluded that the charges on the microcrystals do not contribute much to the inter-

particle forces responsible for the gel properties. It is also noted that if gel and salt solution are improperly mixed, the measured shear stresses are up to twice as large as they are after thorough mixing. This observation is explained by assuming that the salt solution initially draws water out of the gel, which, itself, becomes concentrated and hence more rigid and viscous. The fact that the salt solution is a precipitant for the microcrystals prevents the latter from diffusing into it and is, therefore, probably a necessary condition for finding the initial increase in stiffness observed here.

Résumé

On a étudié de deux façons différentes le comportement, en tant que polyélectrolytes, des microcristaux responsables de la formation des gels de cellulose microcristalline. En premier lieu on a trouvé par titration potentiomètrique en présence d'un acide ou d'une base forte qu'une quantité mesurable de groupes carboxyles étaient présents dans le matériau; la préparation de cellulose de bois étudiée entraîne la présence d'un groupe carboxylique par unité de P.M. 88.500. Ceci veut dire qu'un microcristal typique de poids moléculaire apparent de 580 million porte 6.600 ions carboxylates chargés négativement au pH neutre. En second lieu, on a mesuré l'influence de l'addition d'un électrolyte sur les propriétés d'écoulement du gel. A condition que le gel fourni et la solution saline soit bein mélangés, on ne mesure qu'une faible augmentation de tension-élongation quelque soit la vitesse d'élongation. Ceci est également vrai lordqu'on ajoute au gel un pourcent par volume de HCl 1*N* afin de neutraliser les groupes carboxyliques. On peut donc conclure que les charges sur les microcristaux ne contribuent pas beaucoup aux forces entre particules responsables des propriétés du gel. On note aussi que, si le gel et la solution saline sont mal mélangés, les valeurs des tensions-élongations vont jusqu'à devenir deux fois plus élevées que ce qu'elles sont après mélange complet. Cette observation s'explique bien si l'on suppose que la solution saline enlève d'abord l'eau du gel, qui devient ainsi plus concentré et ainsi plus rigide et visqueux. Le fait que la solution saline est un précipitant pour les microcristaux, empêche ces derniers de diffuser dans cette solution et est, dès lors, sans doute une condition nécessaire pour avoir l'augmentation initiale observée ici.

Zusammenfassung

Das Verhalten der für die Gelbildung mikrokristalliner Cellulose verantwortlichen Mikrokristalle als Polyelektrolyte wurde in zweifacher Weise untersucht. Zuerst wurde durch potentiometrische Titration mit starker Säure und Base festgestellt, dass ein Messbarer Betrag an Carboxylgruppen vorhanden ist; das untersuchte Holzcellulosepräparat mit ausgeglichenem DP besitzt eine Carboxylgruppe auf eine Molekulargewichtseinheit von 88,500. Das bedeutet dass ein "typischer" Mikrokristall vom Molekulargewicht 580 Millionen bei neutralem pH 6,600 negativ geladene Carboxylationen trägt. Zweitens wurde der Einfluss eines zugesetzten Elektrolyten auf das Fliessverhalten des Gels untersucht. Bei ausreichender Mischung des Gels und der zugesetzten Salzlösung wird nur eine kleine Zunahme der Schubspannung bei beliebiger Schergeschwindigkeit gemessen. Das gilt auch bei Zusatz von 1*N* HCl zum Gel zur Entladung der Carboxylgruppen. Man kommt daher zu dem Schluss, dass die Ladungen am Mikrokristall keinen grossen Beitrag zu den für die Geleigenschaften massbegenden Kräften zwischen den Partikeln liefern. Bei ungenügender Mischung von Gel und Salzlosung sind die gemessenen Schubspannungen bis zu doppelt so gross als nach gründlicher Mischung. Diese Beobachtung wird durch die Annahme erklärt, dass die Salzlösung dem Gel anfänglich Wasser entzieht und das Gel dadurch starrer und viskoser wird. Der Umstand, dass die Salzlösung ein Fällungsmittel für die Mikrokristalle ist, vehindert diese an einer Diffusion in die Salzlösung und ist daher wahrscheinlich eine notwendige Voraussetzung für das Auftreten der hier beobachteten Steifigkeitszunahme.

Discussion

D. A. I. Goring (*Pulp and Paper Research Institute of Canada, Montreal, Canada*): It seems possible that the marked increase in yield point after high shear could be related to the orientation of the crystallites in the shear field. Have you observed such an orientation? What direction in the plane of shear would it be expected to take—along or perpendicular to the streamlines?

J. Hermans, Jr.: I think that the particles are oriented with their long axes parallel to the streamlines. The results of Marchessault, Morehead, and Walter, showing birefringence in gels of cellulose microcrystals would appear to have some bearing on this point.

R. H. Marchessault (*College of Forestry, Syracuse, N.Y.*): If your reference gel were diluted to the 1% level what would be the axial ratio of the "flow unit"?

J. Hermans, Jr.: This axial ratio varies considerably from particle to particle, but a figure of ten would appear fairly characteristic.

G. N. Richards (*AMF British Res. Lab., Reading, England*): Is there any possibility of breakage of covalent bonds under your high shear conditions? Could this type of effect (particularly in the noncrystalline component) lead to crosslinking via free radical formation and so provide a partial explanation of increased yield points?

J. Hermans, Jr.: Because of the ready reversibility of the observed phenomena and the ease with which very low shear rates destroy the increase in gel strength in a few seconds, I do not feel that covalent crosslinks formed by the shearing motion contribute to this increase.

J. K. Craver (*Advanced Organic Research, Monsanto Chemical Co., St. Louis, Mo.*): Would Dr. Hermans comment on the theory advanced by Dr. Battista that the microcrystallites are aligned at right angles to the cellulose fiber direction?

J. Hermans, Jr. (after consultation with Dr. Battista in Marcus Hook): The viewpoint that the cellulose microcrystals are aligned at right angles to the fiber axis was never held by Dr. Battista, who feels that it is highly unfortunate that this seems to be so on account of the artist's schematic drawing in his recent article (O. A. Battista and P. A. Smith, *Ind. Eng. Chem.*, **54**, 20 (1962). In the figure on page 23 the bundles of microcrystals should be oriented in the same direction as the arrow).

D. B. Mutton (*Industrial Cellulose Research Ltd., Hawkesbury, Ontario, Canada*): You referred to the presence of carboxyl groups on the surface of the microcrystals. Have you any opinion concerning the origin of these carboxyl groups? Do you think they are present in the original cellulose or are they formed by oxidation during preparation of the microcrystals or gel?

J. Hermans, Jr.: The origin of the carboxyl groups has not been investigated by us. It would be interesting to see if they are already present in the α-cellulose used as a starting material for the preparation of our level-off DP cellulose.

Yun Jen (*General Electric Co., Coshocton, Ohio*): What salt did you use? Do you expect polyvalent salts may change the gel characteristics in a different manner?

J. Hermans, Jr.: The salts used were NaCl, $CaCl_2$, and $NaNO_3$, which all have a very similar effect. Apparently, the divalent cation does not produce an appreciable number of crosslinks between carboxylate ions on different microcrystals.

N. C. Eastman (*Union Carbide, South Charleston, W. Va.*): Is a portion of the DP cellulose resistant to shear in the Hobart-Waring Blendors. In other words, are all crystalline regions in the undegraded fibers more or less uniform?

J. Hermans, Jr.: Work performed by our development section would indicate that in the particular wood cellulose used, the resistance to mechanical attrition varies very much from fiber to fiber.

JOURNAL OF POLYMER SCIENCE: PART C NO. 2, PP. 153–167 (1963

Radiation-Induced Graft Polymerization of Styrene in Wood

K. V. RAMALINGAM,* G. N. WEREZAK, and J. W. HODGINS
McMaster University, Hamilton, Ontario, Canada

I. INTRODUCTION

Construction is well advanced on Canada's first commercial nuclear power reactor, located at Douglas Point, on Lake Huron near Kinkardine, Ontario. To a considerable extent, the experience with this facility will establish the trend of Canada's nuclear power development in the future, for it will be the first sizeable heavy water power reactor. As the start-up day approaches, so does the availability of a cheap source of gamma radiation in the form of discharged fuel elements, and this prospect justifies some speculation as to ancillary chemical industries which might be developed to exploit this radiation source.

There has been a good deal of thought devoted to the employment of gamma radiation in the chemical process industries, and it has become apparent that economic feasibility is achieved only if the reaction product has high unit value, if high gamma efficiency results from a chain reaction or if the gamma source is very cheap.

The present study has as its genesis an interest in this latter criterion. I emphasize this point because there are other ionizing radiations–notably electron beams–which will be equally effective in initiating graft polymerization, and which are more convenient radiation sources for experimental work in this field. But there is available on our campus a one-megawatt swimming pool reactor as a radiation facility, and this study therefore fits in well with a research emphasis in the broad field of radiation engineering, which includes as well experiments in the far ultraviolet and in radiative heat transfer.

This particular study was directed at the investigation of the alteration of the properties of wood in which graft copolymerization had been initiated by gamma radiation of wood impregnated with a suitable monomer. Red pine sapwood was chosen as the substrate because of its permeability and relative uniformity, and the current discussion is limited to the grafting reaction with polystyrene.

A good deal of work has been reported on the employment of gamma radiation as a polymerization initiator, both for crosslinking and for grafting

* Present address: Department of Chemistry, McGill University, Montreal, Quebec.

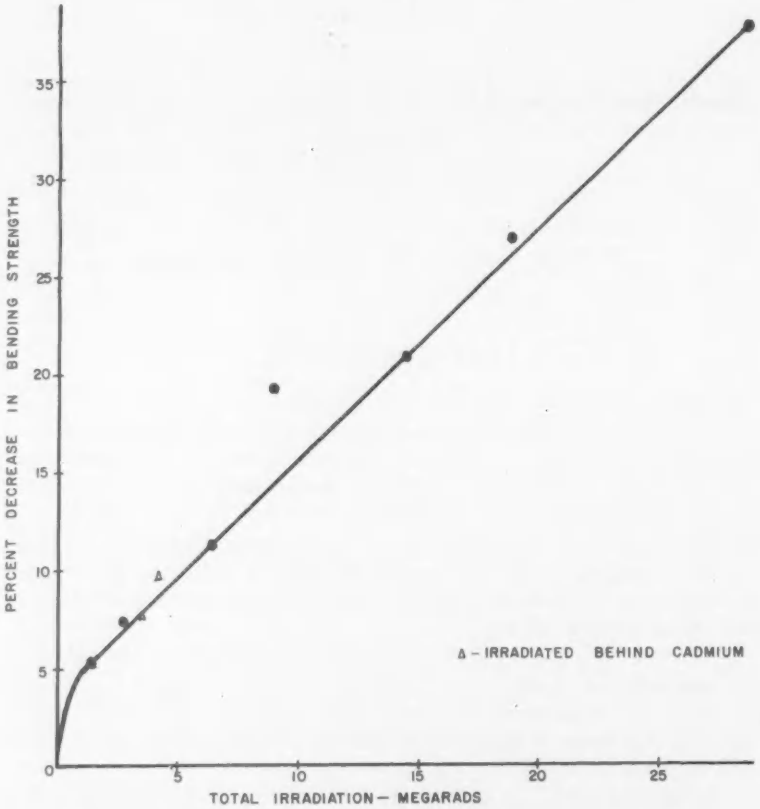

Fig. 1. Decrease in bending strength of wood as a function of γ dosage.

reactions. For example, the improvement of polyethylene by gamma-initiated crosslinking appears to have commercial feasibility.[1] Among the graft copolymers which have been studied are those of pure cellulose with styrene, methyl methacrylate, acrylonitrile, and other monomers.[2–5] Relatively little information is available on the properties of this type of material compared with the graft copolymers prepared from synthetic chain compounds where grafting almost invariably produces improvement of the mechanical properties of the main chain polymer.[6] One reason for this disparity may well be the fact that exposure to ionizing radiation produces significant degradation of the cellulose chain itself.[7–9] For this reason a close control of the radiation is necessary, for depolymerization of the cellulose must be minimized while the grafting is being initiated by the gamma flux.

Grafting reactions in wood have been reported by Karpov and co-workers in Russia,[10] by the group at the University of West Virginia

directed by Kent and Harmison,[5] and by Kenaga, Fennessey, and Stannett.[11] Because of its heterogeneity, the effect of radiation upon the properties of wood is quite different from that on pure cellulose. This is probably due to the effect of the lignin, which is itself quite resistant to radiation damage and therefore reduces the scission of the cellulose chains.[12] It is therefore possible to modify the cellulose in wood by radiation grafting, with a resultant enhancement of the physical and mechanical properties. The effect of gamma radiation on the bending strength of wood is illustrated in Figure 1. The bending strength of wood is an important criterion of its acceptability as a structural material, and also as an indicator of cellulose chain degradation

II. EXPERIMENTAL PROCEDURES

Physical Properties

The red pine sapwood used as the substrate for these experiments was especially selected and obtained in planks 54 in. long, 1 in. in thickness.

Fig. 2. Inner tube of impregnation apparatus.

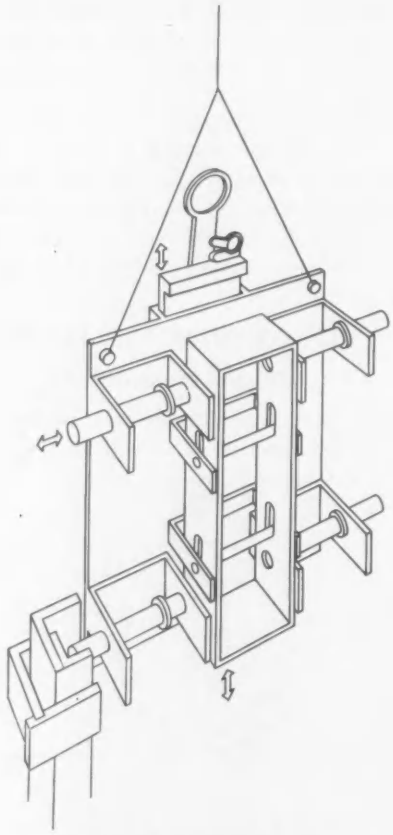

Fig. 3. Rear view of irradiation truck.

Samples were processed in groups of three, cut end to end from the planks. One piece in each group was retained as a control, one was irradiated without impregnation, and the third piece was both impregnated and irradiated The sample size (16 × 3/4 × 3/4 in.) was chosen so that a standard A.S.T.M. test procedure could be carried out.[13]

The styrene was reagent chemical grade, shaken with 10 wt.-% sodium hydroxide solution, washed with water, and dried over anhydrous calcium sulfate. This procedure removed the stabilizer (*p*-tert-butyl pyrocatechol).

Impregnation was carried out in a glass chamber illustrated in Figure 2. Wood samples were placed in the tube suspended below the cover, and the pressure reduced to less than 1μ for periods up to 12 hr. The impregnant was added without admitting air, until the samples were totally immersed, and the pressure then raised by means of nitrogen to 35 psi. Samples were left in the impregnator for periods up to 36 hr., depending upon the quantity

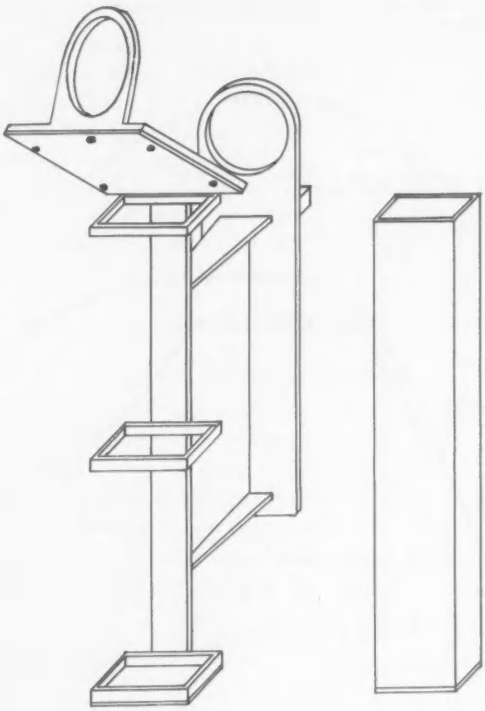

Fig. 4. Cadmium irradiation casket.

of impregnant desired. The wood was then encased in aluminum foil to prevent loss of styrene, and sealed into polyethylene bags to prevent ingress of water during irradiation. Three samples at a time were fastened in a vertical position to the holder on the truck (Fig. 3) which then traveled down the face of the instrument bridge in the McMaster nuclear reactor. (American Machine and Foundry swimming pool reactor, operating at 1 Mw. power level.) In the wood used, there was a sufficiently high content of manganese that considerable radioactivity resulted from exposure to the radiation of the reactor core. Thus many of the experiments were performed with the samples encased in a cadmium casket (thickness = 0.030 in.), which served to attenuate the thermal neutron flux sufficiently to permit handling of the sample immediately after irradiation (Fig. 4).

The gamma dosage was measured by the change in color of cobalt glass disks, calibrated with reference to the Fricke Ferrous sulfate dosimetric procedure. Careful flux records have been kept throughout, and the samples were irradiated at a distance of 21 in. in front of the reactor core, 10 in. above the grid plate. Over the experimental period, the flux profile lay

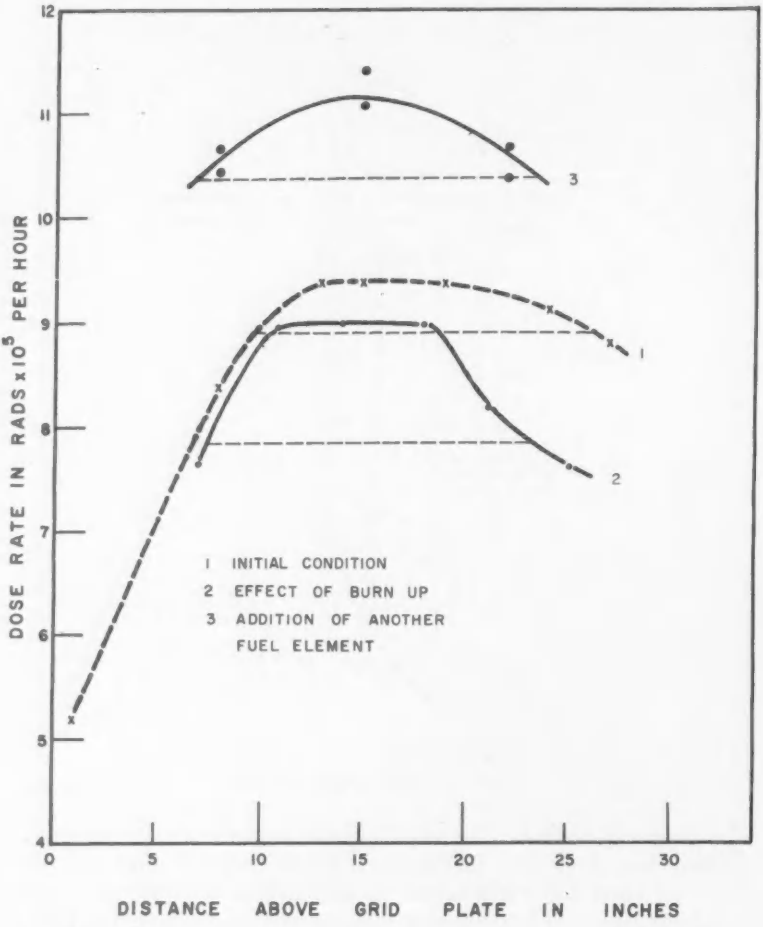

Fig. 5. Flux profiles in the swimming pool reactor. Distance between wood and front face of No. 10 fuel element is 21 in.

between the limits shown in Figure 5. In this position the dose rate is about 1 Mrad/hr.

After irradiation, the wood was enclosed in an aluminum pressure canister, and the temperature elevated to about 85-105°C. for periods of up to 24 hr. to complete the polymerization.

In order that the physical tests were comparable, the treated specimens were equilibrated with an atmosphere of 75% R.H. and 25°C. before testing. Load-deformation tests were carried out on a Tinius-Olsen Universal testing machine, following standard A.S.T.M. procedure.

The percentage of grafting was determined by grinding samples of the

wood to 60 mesh and extracting the samples in Soxhlet equipment to constant weight with hot benzene, in which the homopolymer is soluble, but not the graft copolymer. This procedure results in a very rough indication of the actual extent of grafting, as Stannett and his co-workers point out,[14] but did indicate quite clearly the difference in character between homopolymer and graft copolymer.

Moisture absorption was determined on dried samples ($4 \times {}^3/_4 \times {}^3/_4$ in.) stored to constant weight in an atmosphere of 75% R.H. at 25°C.

Liquid water absorption was determined on dried samples immersed in distilled water at 25°C. and 1 atm. pressure.

III. RESULTS

Alteration in Physical Properties

Early experiments with pure styrene made it evident that virtually no combination with cellulose was being achieved, since nearly all of the homopolymer could be recovered by benzene extraction. It was concluded that suitable contact between cellulose and styrene was not being achieved, due to lack of penetration of the impregnant.

In order to produce swelling within the wood structure and also to provide methyl groups in the vicinity of the cellulose, methanol and water

TABLE I
Typical Results of Polymerization in Wood; Benzene Extraction of Polymer

Series	Impregnant	Irradiation dose, Mrad	Thermal treatment	Weight increase, %	Wt. polymer extracted g.[a]
a	Pure styrene	Nil	105°C., 24 hr.	100	94.0
b	Pure styrene	4.5	105°C., 24 hr.	100	90.5
c	Pure styrene	9.0	105°C., 24 hr.	100	85.4
d	Pure styrene	14.4	105°C., 24 hr.	100	72.6
e	Pure styrene	18.9	105°C., 24 hr.	110	52.0
f	30% Styrene + 61% methanol + 9% water	4.5	105°C., 24 hr.	38	4.8
g	30% Styrene + 61% methanol + 9% water	9.0	105°C., 24 hr.	40	5.7
h	52% Styrene + 43.5% methanol + 4.5% water	4.5	105°C., 24 hr.	70	19.0
i	52% Styrene + 43.5% methanol + 4.5% water	9.0	105°C., 24 hr.	70	21.4
j	76% Styrene + 1.5% water + 22.5% methanol	4.5	105°C., 24 hr.	90	19.1
k	76% Styrene + 1.5% water + 22.5% methanol	9.0	105°C., 24 hr.	95	20.1
l	76% Styrene + 1.5% water + 22.3% methanol + 0.2% benzoyl peroxide	Nil	105°C., 24 hr.	74	81.8

[a] Weight of polymer extracted per 100 g. of polystyrene formed, per 100 g. of dry wood.

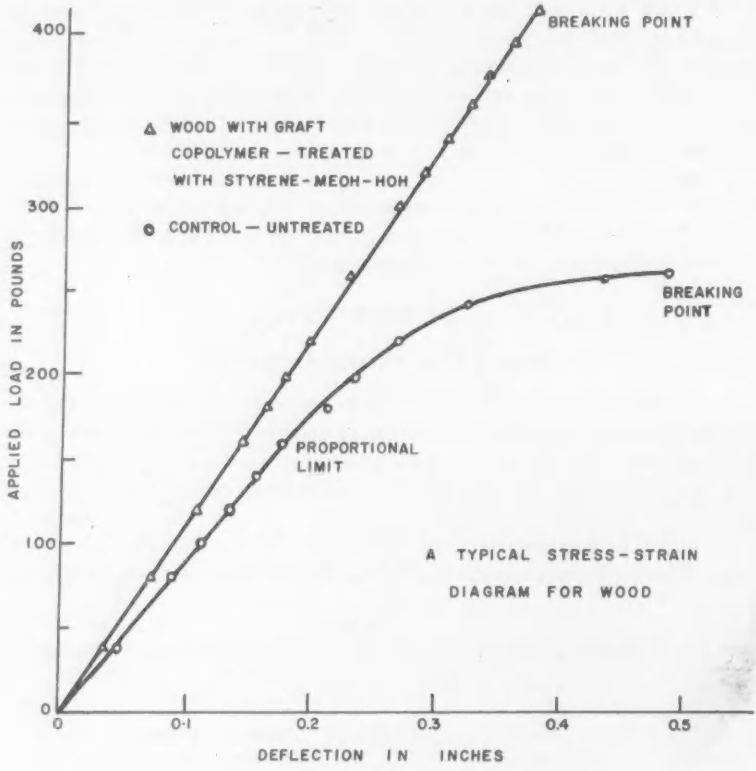

Fig. 6. Load-deflection characteristics of wood samples.

were added to the styrene. Preliminary results are shown in Table I. These results illustrate the effect of the gamma radiation on the nature of the polymer (as determined by the extraction) and the effect of using a ternary solution instead of pure styrene.

At this point in the experimental procedure, the typical changes in properties shown in Table II were observed, under the conditions noted.

TABLE II
Changes in Physical Properties of Treated Wood[a]

Sample	Bending strength increase, %	Shrinkage, based on conditioned vol., %	Swelling, based on swollen sample, %	Vol. increase due to treatment, %
Untreated		5.0	15.0	
Treated	45	0.9	1.1	8–9

[a] Treatment: impregnant 76 wt.-% styrene + 22.5 wt.-% methanol + 1.5 wt.-% water; gamma dosage: 4.5 Mrad; heating treatment: 105°C. for 24 hr.

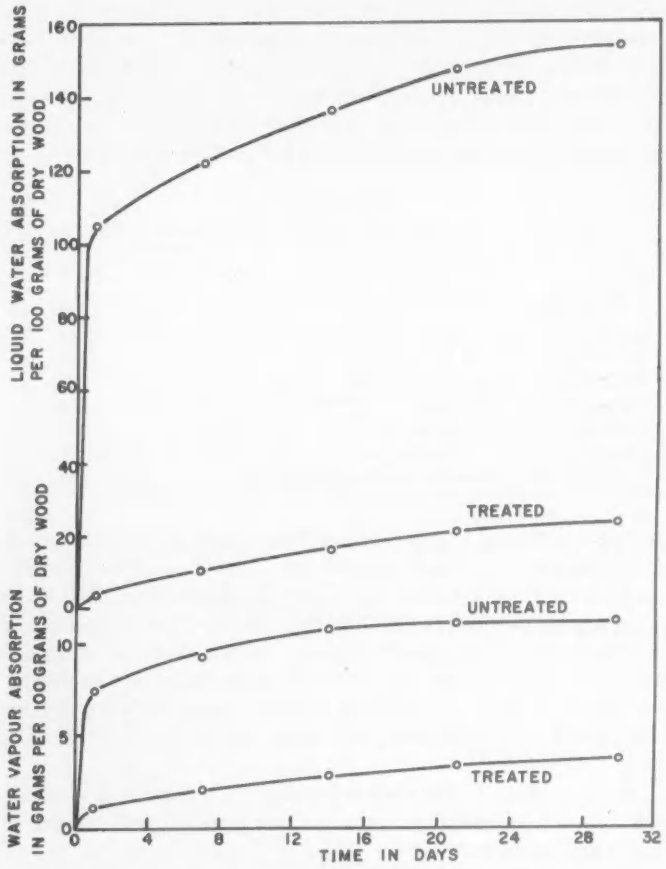

Fig. 7. Water absorption characteristics of wood. Samples immersed in distilled water at room temperature and under atmospheric pressure. Exposed to 76% R. H. at 25°C.

In Figure 6 is illustrated a typical pair of load–deflection curves. In addition to a significantly higher bending strength, the mechanical nature of the material has been altered, and the load–deflection curves of this material are invariably linear right up to the point of failure.

The rate of water vapor and liquid absorption are illustrated in Figure 7.

Because of the fairly wide variability of the material and the interdependence of the experimental conditions and the polymerization reaction, it was at this point deemed advisable to embark on a study of the optimal conditions, based upon a statistical experimental design. Using the bending strength as an indicator, a two-fractorial experimental design was set up, with the following six variables: time of evacuation, composition of impregnant, uptake of impregnant, total gamma dosage, duration

of heating treatment, and temperature of heating treatment. Because of the very large number of experiments involved in a complete factorial design, a fractional replicate ($^1/_8$) was employed, accepting the attendant wider confidence limits. A gradient search of the results did establish definite trends, and the optimal conditions indicated by two fractional replicate designs involving 96 experiments are listed in Table III.

TABLE III
Optimal Conditions for Gamma-Initiated Grafting of Polystyrene in Red Pine Sapwood

Evacuation period (25°C., 1 μ), hr.	11.5
Impregnant composition	
Styrene; wt.-%	53
Methanol, wt.-%	43
Water, wt.-%	4
Impregnant uptake (approx.), %	125
Irradiation dosage, Mrad	4
Heating treatment temperature, °C.	75
Heating treatment duration, hr.	9
Average enhancement of bending strength, %	55

Two other physical characteristics have been examined: resistance to microbiological attack and flammability. Samples of the treated wood and controls were furnished to the Forest Products Research Laboratory of the Department of Forestry of Canada. Dr. T. S. McKnight inoculated the samples with a culture of Lenzites Trabea, and the samples were incubated for three months, buried in soil with one corner exposed. The weight loss by decay of the treated samples (based on oven-dry weight) averaged about 14%, compared to a mean loss of 71% by the untreated controls.

The flammability of this material would be a serious deterrent to its use in structures. For this reason experiments are currently being carried out with halogenated styrenes.

Free Radical Investigation by Electron Spin Resonance Spectrometry

The radiation grafting on cellulose can proceed either by a free-radical mechanism directly, or by means of free radicals formed by thermal decomposition of organic peroxides. The radicals formed on the cellulose chains by either or both of these means can combine with a reactive monomer present at the radical site to form a graft copolymer. Free radicals in irradiated pure cellulose have been detected by Abraham and Whiffen,[15] using electron spin resonance spectrometry, and it is probable that the radicals are located along the cellulose chains in amorphous and crystalline regions.

As an attempt at mechanism elucidation, a study was made of the electron spin resonance spectra of wood, cellulose, and lignin, at a frequency of 9×10^9 cycles/sec. with the use of an automatic recording spectrometer which yields the first derivative of the true resonance curve.

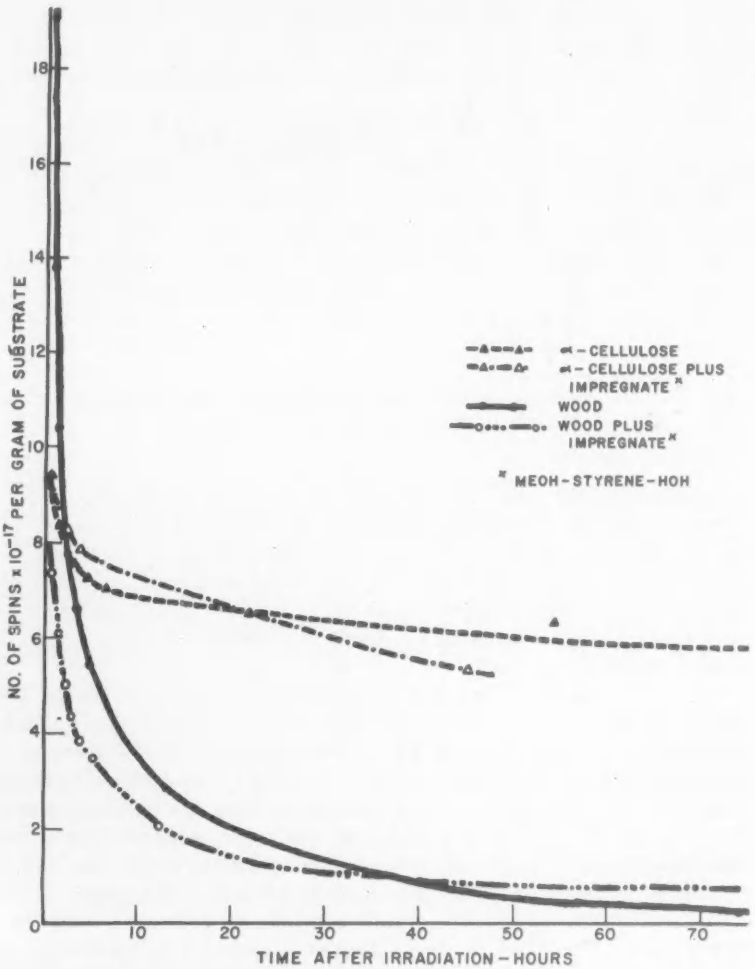
NO. OF SPINS x 10^{-17} PER GRAM OF SUBSTRATE
TIME AFTER IRRADIATION – HOURS
α – CELLULOSE
α – CELLULOSE PLUS IMPREGNATE*
WOOD
WOOD PLUS IMPREGNATE*
* MEOH – STYRENE – HOH

Fig. 8. Free radical concentrations in irradiated samples. Decay at 25°C. Radiation dosage ca. 10 Mrads.

Since it was desired to measure the change of free radical concentration with time, it was necessary to start the ESR measurements as soon as possible after irradiation. To avoid neutron activation of the manganese in the wood, the samples were all irradiated in a cadmium cylinder fitted to the front face of the irradiation truck, which acted as a neutron filter. The samples were irradiated in special polyethylene capsules, and were transferred directly into the spectrometer cavity after a dosage of about 10 Mrad, administered in about 30 min. Residual radioactivity was less than 10 mC.

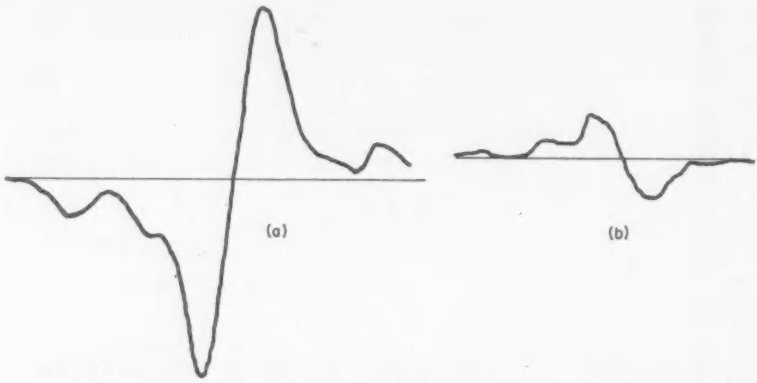

Fig. 9. Effect of heating on free radical concentration. (*a*) ESR spectrum immediately after irradiation, (b) ESR spectrum after heating the same sample for 2 hr. at 105°C.

For quantitative estimation of radical concentration diphenyl picryl hydrazyl was used as a primary standard. It was found that 0.01 mg. of the standard (corresponding to 1.5×10^{16} spins) resulted in a satisfactory signal in the desired sensitivity range. True resonance curves were obtained by graphical integration of the derivative curves, and radical concentrations were calculated by comparison with the spectra obtained with the standard.

For samples of wood and cellulose irradiated in the presence of air, there was invariably observed an initial decay of free radicals which proceeded at a rapid rate for 4–5 hr., followed by a very slow decay at a rate dependent upon the nature of the substrate. The radicals detected originated from the wood, cellulose, and lignin, but not the impregnant. Many spectra have been analyzed, and the resulting decay curves are illustrated in Figure 8. In all of the samples irradiated in air, the characteristic sharp decay occurred, from a concentration in the neighborhood of $1–2 \times 10^{18}$ spins/pg. to less than half of this concentration within the first 4–5 hr. The effect of the heating step is shown in Figure 9. As expected, the radical concentration drops sharply after heating, due presumably to formation of graft polymer. For wood samples irradiated *in vacuo*, however, this initial sharp decay did not result, and the initial radical concentration showed only very slight decrease over several days.

Careful examination was made of the ESR spectra of irradiated wood, periodate lignin, dioxane lignin, Braun's native lignin (western cedar), and pure α-cellulose in order to determine whether the hyperfine structure was distinctive enough to identify the radicals in irradiated wood as cellulose radicals. Lignin yields a free radical spectrum on irradiation and such a specific identification has up to this time proved impossible.

The rapid decay observed on admitting air to a sample of wood irradiated *in vacuo* is indicative that oxygen acts as a radical scavenger. Samples

which were evacuated and impregnated before irradiation would, of course, contain little free oxygen, and the decay in radical concentration can reasonably be attributed to the grafting reaction.

IV. DISCUSSION OF RESULTS

It is probable that the initial radiolytic attack is concentrated on the hemicelluloses, which offer only minor contribution to the strength of wood.[16] The alteration in the nature of the load-deflection curves suggests that the chains of α-cellulose have been modified by grafting of polystyrene. In untreated wood, the force necessary to move the cellulose chains with respect to one another as in bending, is that required to overcome relatively weak van der Waal's forces between adjacent chains. However, in the modified wood, there are also primary valence forces introduced by the polystyrene side chains, which increases the bending strength.

Electron spin measurements gave a persistent maximum radical concentration of about 2×10^{18} radicals/g. If the number of cellulose units per chain is taken as 1500–3000, this number of spins corresponds to only one or two free radicals per cellulose molecular unit, which does suggest that the unpaired electron location is at the end of the molecule. If this be true, it also explains why a maximum enhancement is reached when graft polymerization on wood is initiated by ionizing radiation. A further check on this point is currently in progress, in which irradiation of wood will be carried out *in vacuo* in a gamma cell at an elevated temperature.

V. CONCLUSIONS

Gamma irradiation can be employed effectively in the initiation of graft copolymerization of styrene with the cellulose in wood. The dosage necessary (less than 5 Mrad) is sufficiently low that the degradation of the cellulose is not significant with respect to the enhancement of physical properties. Bending strength is increased by about one-half. Penetration of water vapor and liquid are drastically reduced, dimensional changes associated with water absorption are correspondingly reduced. Resistance to microbiological attack is increased.

It should be pointed out that the improvement in bending strength for wood containing graft copolymer is of the same order as that observed for wood containing homopolymerized styrene. The differences are in the physical appearance (the copolymerized material has a much more uniform surface sheen) and in the insolubility of the grafted polystyrene in aromatic solvents.

The transient species associated with the graft copolymerization have been identified by electron spin resonance spectrometry as free radicals. The radicals arise from the wood, not the impregnant, and the concentration suggests only one or two unpaired electrons per molecular unit, probably therefore on the terminal units. Radical concentrations are significant for a long time after irradiation. No differentiation has yet been made

between long-lived radicals and persistence of unstable radical precursors, it may well be that the radicals detected a long time after irradiation arise from thermal decomposition of organic peroxides. These concentrations are too low for titrimetric determination.

The authors are pleased to have the opportunity to acknowledge their indebtedness to the National Research Council of Canada and the Defence Research Board of Canada, who provided the funds for this research. Our gratitude is expressed, too, to Dr. C. Purves, of McGill University for the periodate lignin, to Dr. J. M. Pepper of University of Saskatchewan for the dioxane lignin, and to Dr. I. A. Pearl, of the Institute of Paper Chemistry for the native lignin. Dr. T. S. McKnight, of the Forest Products Laboratories of Canada kindly performed the microbiological tests for us.

The opportunity to use the electron spin resonance spectrometer was provided through the courtesy of Dr. H. E. Petch and Mr. J. G. Chambers made possible the electron spin measurements by his valuable advice and guidance.

References

1. Charlesby, A., *Proc. Roy. Soc.* (*London*), **A215,** 187 (1952).
2. Arthur, J. C., Jr., and R. J. Demint, *Textile Res. J.*, **30,** 505 (1960).
3. Kobayaski, Y., *J. Polymer Sci.*, **51,** 359 (1961).
4. Chapiro, A., and V. Stannett, *Intern. J. Appl. Radiation Isotopes*, **8,** 164 (1960).
5. Harmison, L. T., and J. A. Kent, *Nucleonics*, **20,** 94 (1962).
6. Charlesby, A., *Atomic Radiation and Polymers*, Pergamon Press, London, 1960.
7. Pan, H.-P., B. C. Procton, S. A. Goldblith, H. M. Morgan, and R. Z. Naar, *Textile Res. J.*, **29,** 415 (1959).
8. Porter, B. P., V. W. Tripp, I. V. deGray, and M. C. Rollins, *Textile Res. J.*, **30,** 510 (1960).
9. Glegg, R. E., and Z. O. Kertesz, *J. Polymer Sci.*, **26,** 289 (1957).
10. Karpov, V. L., Yu. M. Malinskiĭ, V. I. Serenkov, R. S. Klimanova, and A. S. Freiden, *Nucleonics*, **18,** 88 (March 1960).
11. Kenaga, D. R., J. P. Fennessey, and V. T. Stannett, *Forest Prod. J.*, **12,** 161 (1962).
12. Lawton, E. J., W. D. Bellamy, R. E. Hungate, M. P. Bryant, and E. Hall, *Science*, **113,** 380 (1951).
13. *ASTM Standards on Wood, Wood Preservatives and Related Materials*, by American Society for Testing Materials, Philadelphia, 1959.
14. Stannett, V., et al., *Chem. Eng. News*, p. 57 (June 18, 1962).
15. Abraham, R. J., and D. H. Whiffen, *Trans. Faraday Soc.*, **54,** 1291 (1958).
16. Tezzler, O., and H. A. Rutherford, *Nuclear Sci. Abstr.*, **12,** No. 11351 (1958).

Synopsis

Grafting of polystyrene to the cellulose in red pine sapwood has been accomplished by gamma irradiation of the ternary solution of styrene, methanol, and water. The resulting material possesses substantially enhanced bending strength and dimensional stability. Optimum conditions have been determined by a factorial experimental design. Electron spin resonance studies have revealed two distinct types of long-lived free radicals, one of which is the specific precursor for the grafting reaction.

Résumé

On a greffé du polystyrène sur la cellulose d'aubier de pin rouge par irradiation gamma du mélange ternaire styrène-méthanol-eau. Le matériel obtenu a une plus grande résistance à la flexion, et une plus grande stabilité structurelle. On a déterminé les meilleures conditions opératoires par l'étude expérimentale des différents facteurs. Les études

de résonance de spin électronique ont prouvé l'existence de deux types de radicaux libres de longue durée de vie. L'un des deux est le précurseur spécifique de la réaction de greffage.

Zusammenfassung

Aufpfropfung von Polystyrol auf die Cellulose im Rotföhrensplintholz wurde durch γ-Bestrahlung der ternären Mischung von Styrol, Methanol und Wasser erreicht. Das erhaltene Material besitzt eine wesentlich verbesserte Biegefestigkeit und Massbeständigkeit. Die optimalen Bedingungen wurden durch Faktorenversuche ermittelt. Elektronspinresonanz-Messungen liessen das Vorhandensein von zwei Typen langlebiger, freier Radikale erkennen, von denen einer für die Aufpfropfreaktion verantwortlich ist.

Discussion

R. Schmut (*West Virginia Pulp & Paper Co., Mechanicsville, N. Y.*): (1) In view of statement 3 of introduction, what are the costs? (2) Wettability of surface?

J. W. Hodgins: (1) For the mechanical advantages gained, the cost is prohibitive, not because of the cost of irradiation, but because of the cost of the styrene which is used in large amounts. (2) The surface wettability of the treated material is considerably decreased, although we have not measured the contact angles.

J. K. Craver (*Monsanto Chemical Co., St. Louis, Mo.*): Since monomeric styrene is a bulky and hydrophobic molecule and the homopolymer is not a structurally strong plastic, why was it chosen in preference to, say, acrylonitrile or vinyl acetate?

J. W. Hodgins: Styrene was chosen as the first monomer in this system because so much data were already at hand on the gamma-initiated polymerization. The G values had been well established and were so much lower than those for cellulose that it seemed wise to exploit this difference.

Current work is centered upon acrylonitrile and the earliest experiments do, in fact, show its superiority as far as the increase in bending strength is concerned. The exploratory experiments produced a product with an enhancement of more than 80% in bending strength.

JOURNAL OF POLYMER SCIENCE: PART C NO. 2, PP. 169–188 (1963)

Grafting Polymers onto Cellulose by High-Energy Radiation. II. Effect of Swelling Agents on the Gamma-Ray Induced Direct Radiation Grafting of Styrene onto Cellulose

R. Y.-M. HUANG* and W. H. RAPSON, *Department of Chemical Engineering and Applied Chemistry, University of Toronto, Toronto, Ontario, Canada*

INTRODUCTION

High energy radiation-induced grafting of vinyl monomers onto cellulose has attracted considerable attention during the past few years. Various methods by which radiation grafting onto cellulose can be achieved have been described recently in the published and patent literature and have been the subject of several reviews.

Relatively few detailed studies have been published, however, on the direct radiation grafting of styrene onto cellulose. Okamura, et al.[1] first reported the radiation grafting of styrene onto cellulose by irradiating a suspension of preswollen cellulose in a styrene–methanol solution. Sakurada and co-workers[2–6] have shown that the addition of small amounts of water to the system greatly enhances direct radiation grafting of vinyl monomers onto polyvinyl alcohols and cellulose. Similar effects were also reported by Chapiro and Stannett[7] in the direct radiation grafting of styrene onto hydrophilic polymers such as polyvinyl alcohol and cellulose. A pre-irradiation technique for grafting styrene and other vinyl monomers onto cellulose has been described by Shinohara,[8] and Kobayashi[9] has reported the radiation grafting of styrene onto rayon by pre-irradiation of the rayon in a solution of hydrogen peroxide. Since completion of the present work, a patent has been issued which described the effect of water and other aqueous swelling agents in the direct radiation grafting of vinyl monomers onto cellulose.[10]

The radiation grafting methods described above all involve the use of various techniques to swell the cellulose in order to aid the diffusion of monomer into the hydrogen-bonded cellulose structure. It has been previously shown that in the absence of swelling very little radiation grafting of styrene onto cellulose occurs, even at high radiation doses.[11]

* Present address: Industrial Cellulose Research Ltd., Hawkesbury, Ontario, Canada.

In the first paper of this series,[11] the use of solvent-exchange techniques for the direct radiation grafting of styrene onto cotton cellulose was reported. The present paper is concerned with the effect of aqueous and nonaqueous swelling agents in the grafting of styrene onto cotton and rayon by direct irradiation with gamma-rays. The Co^{60} source used in this study had a dose rate of 1.4 Mrads/hr., which is higher than most dose rates reported in the literature for radiation grafting using gamma rays.

EXPERIMENTAL

Cellulosic Materials

Cotton Linters. Pure cotton linters were obtained from the Buckeye Cellulose Corporation, Memphis, Tennessee. The α-cellulose content was 99.7%, and the viscosity-average degree of polymerization was 2170.

Cotton Yarn. 20/1 bleached cotton yarn, manufactured by the York Knitting Mills, Toronto, Ontario, was obtained through the courtesy of the Textile Department, Ontario Research Foundation, Toronto, Ontario.

Rayon. High strength tire yarn, 1669 denier, with a degree of polymerization of 327, was kindly provided by Industrial Cellulose Research Limited, Hawkesbury, Ontario.

All cellulose samples were used as obtained without further purification.

Styrene Monomer

Styrene monomer was purified in the usual manner by shaking with 10% sodium hydroxide solution to remove inhibitor and washing with distilled water. It was dried overnight over anhydrous calcium chloride and then distilled under vacuum.

Swelling Agents

Distilled water was used without any further purification.

Formamide of 99% purity was obtained from the Matheson Company, Inc.

Dimethyl sulfoxide, pure grade, was obtained from the Matheson, Coleman and Bell Division of Matheson Company, Inc.

Formic acid (97%) obtained from Eastman Organic Chemicals was dried over an excess of anhydrous copper sulfate and then distilled under vacuum.

Acetic acid, CP reagent grade, 99.8% purity, was obtained from Canadian Industries, Limited.

Solvent Additives

Absolute ethyl alcohol was purified to remove traces of water by the magnesium ethoxide method.[12]

Methyl alcohol, Fisher ACS reagent grade, was purified by treatment with magnesium activated by iodine.[12]

High purity acetone was dried over anhydrous potassium carbonate.[12]

Irradiation

The irradiations were carried out in a Gamma-Cell 220, an 18,000 curie Co^{60} irradiation facility, located at the Department of Chemical Engineering and Applied Chemistry, University of Toronto. The source had a central field intensity of 1.44×10^6 rads/hr. in June 1961, as calibrated by ferrous chemical dosimetry by the Commercial Products Division of Atomic Energy of Canada, Limited. All experiments described in this paper were carried out at dose rates ranging from 1.27 to 1.44 Mrads/hr. Details of a similar irradiation facility are described elsewhere.[13] During the irradiations, the sample exposure cavity was cooled by a stream of compressed air, and the temperature was measured by means of a thermistor thermometer. The total irradiation dose of a sample was regulated by controlling the total exposure time. All experiments were conducted in air.

Extraction

After irradiation, the grafted samples were soaked in benzene overnight to remove the loosely bound polystyrene homopolymer. They were then extracted with benzene in a Soxhlet apparatus for 72 hr. The extracted samples were dried in an oven at 100–105°C. for 2 hr. and weighed to determine the extent of grafting. The weight increase after extraction was taken to be the weight of polystyrene grafted to the cellulose.

The per cent grafting was calculated as follows:

$$\% \text{ grafting} = \frac{\text{bone dry weight of grafted product—bone dry weight of original cellulose}}{\text{bone dry weight of cellulose}} \times 100$$

Grafting efficiency is a measure of the efficiency of monomer use, and is defined as follows:

$$\text{grafting efficiency } \% = \frac{\text{weight of grafted polymer} \times 100}{\text{weight of grafted polymer} + \text{weight of homopolymer}} \times 100$$

Radiation Homopolymerization of Styrene in Bulk and in Solution

Radiation homopolymerization of styrene in bulk was carried out by irradiating 10 ml. of styrene at different dose levels. For radiation homopolymerization in solution, various amounts of solvent additives were added volumetrically to the styrene. The amount of polystyrene formed was determined gravimetrically.[14]

Strength Properties

Properties of the grafted yarn were kindly determined by Industrial Cellulose Research, Limited, Hawkesbury, Ont. by standard methods.

Infrared Spectra

The infrared spectra were measured by using the KBr pellet technique on a Perkin-Elmer Model 21 spectrophotometer.

Photomicrographs

The photomicrographs were kindly prepared by the Industrial Cellulose Research Ltd., Hawkesbury, Ont. on sections 2–3μ thick and enlarged to a magnification of 800×. The cross sections in the control yarn were approximately 15μ in diameter.

Preparation of Samples

Approximately 0.5 g. of rayon or cotton yarn were wound off a spool, weighed, and placed in 57 × 28 mm. (15 ml. capacity) or 108 × 28 mm. (40 ml. capacity) specimen bottles fitted with screw caps. In the case of cotton linters, the sample was simply weighed and placed in the bottles. The samples were conditioned by the addition of known amounts swelling agents by means of a micrometer syringe. The bottles were then quickly stoppered and then samples allowed to equilibrate for 24 hr. In some cases, the water content of the fiber was approached from the wet side, the fibers being first soaked in water and then gradually dried to the desired water content. After conditioning of the fibers, 10 ml. of styrene or a styrene–solvent mixture containing 10 ml. of styrene was added. The mixture was allowed to stand 2 hr. before irradiation. In cases where the fibers were not preswollen, the swelling agent was added directly to the styrene or styrene–solvent mixture.

RESULTS

Homopolymerization of Styrene in Bulk and in Solution at High Dose Rates

The radiation homopolymerization of styrene in bulk has been extensively investigated and the available data have recently been summarized by Chapiro.[15] Most of the data, however, have been obtained at low and medium dose rates. No data were available in the literature from a high dose-rate gamma-ray source. Figure 1 shows the radiation homopolymerization of styrene in bulk in air at a dose rate of 1.42 Mrads/hr. The per cent polymerization of styrene increases linearly with radiation dose in the range 0–8 Mrads. The polymerization rate increases slightly from then on, until a sharp rise is observed after a radiation dose of 30 Mrads corresponding to 37.5% polymerization. The increase in polymerization rate at high degrees of conversion can be attributed to the gel effect.[16] Similar increases in the radiation polymerization rate of styrene at high conversions have been observed by Ballantine et al.[17] The homopolymerization rate obtained in the present work at a dose rate of 1.42

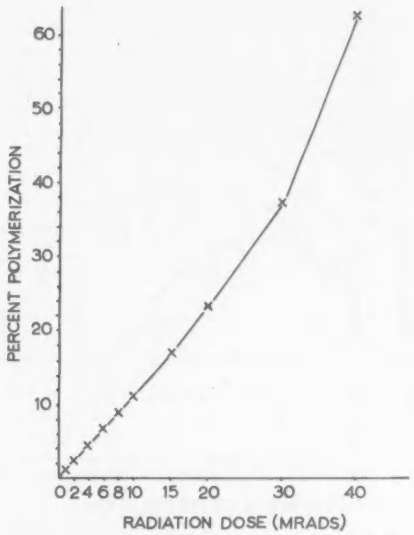

Fig. 1. Gamma-ray-induced radiation polymerization of styrene in bulk. Dose rate 1.42 Mrads/hr.; temperature 37°C.

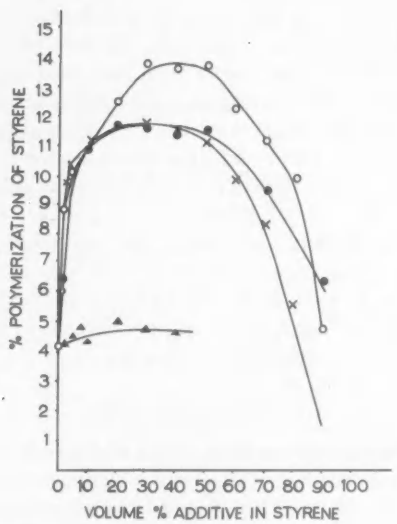

Fig. 2. Gamma-ray-induced radiation polymerization of styrene in solution: (×) methanol–styrene; (○) ethanol–styrene; (●) 95% ethanol–styrene; (▲) water–styrene. Total dose 4 Mrads; dose rate 1.36–1.40 Mrads/hr.; temperature 37°C.

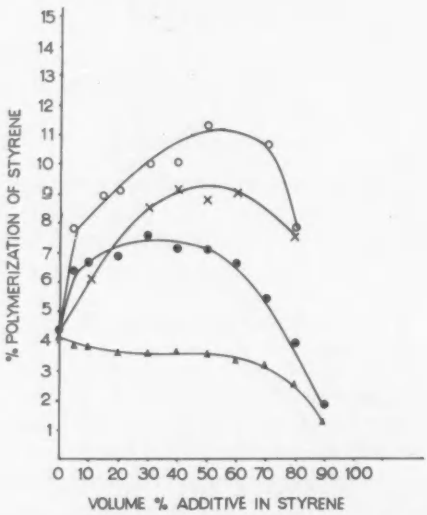

Fig. 3. Gamma-ray-induced radiation polymerization of styrene in solution: (○) acetic acid–styrene; (●) acetone–styrene; (▲) benzene–styrene; (×) dioxane–styrene. Total dose 4 Mrads; dose rate 1.36–1.40 Mrads/hr.; temperature 37°C.

Mrads/hr. (395 rads/sec.) and 37°C. was 362×10^{-7} moles/l. sec. or 1.07%/Mrad in the dose range 0–8 Mrads.

The effect of additives on the radiation polymerization of styrene at a high dose rate of 1.4 Mrads/hr. is shown in Figures 2 and 3. The addition of ethanol, methanol, acetone, acetic acid, and dioxane result in a sensitization of the styrene polymerization. The radiation polymerization of styrene in solution at low dose rates has been recently reviewed by Chapiro.[18] The addition of water had little effect on the radiation polymerization of styrene. This appears to result from the limited solubility of water in styrene. Water and styrene are immiscible, and each phase is radiolyzed without affecting the other. The radiation polymerization of styrene in aqueous emulsion and suspension has been shown[19,20] to be sensitized by radicals formed from the radiolysis of water. The present results indicate that no sensitization of polymerization is observed in the absence of emulsifying or suspension techniques.

Grafting onto Rayon

Radiation Grafting in Styrene Bulk. The addition of water to a styrene–solvent system to enhance grafting onto polyvinyl alcohol and cellulose has been previously reported by Sakurada et al.[2–6] and by Chapiro and Stannett.[7] The amount of water added, however, has previously been expressed on a per cent weight basis of the styrene–solvent solution. No reports are available on the effect of water in grafting onto cellulose with-

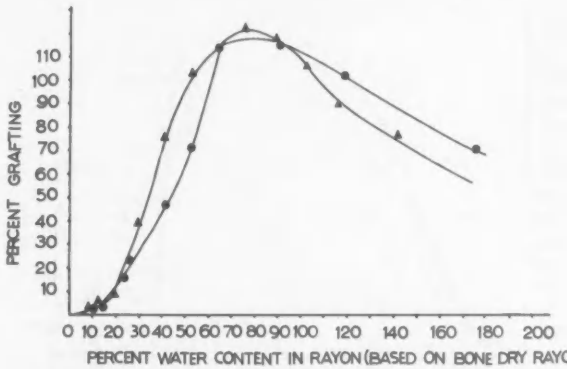

Fig. 4. Direct radiation grafting of styrene onto rayon; effect of preswelling rayon with water: (▲) rayon pre-swollen with water; (●) water added directly to styrene. Total dose 4 Mrads; temperature 37°C.

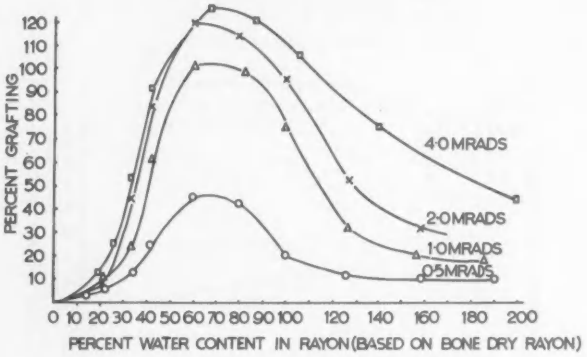

Fig. 5. Effect of water preswelling and radiation dose on the direct radiation grafting of styrene onto rayon. Temperature 37°C.

out any solvent additives. Figure 4 shows the effect of preswelling the rayon with water as a function of the water content of rayon in the direct radiation grafting of styrene onto rayon. Grafting starts to occur at approximately 20–30% water content in the rayon, rises to a maximum at 70–80%, and then falls off with excess water content. A similar grafting curve is obtained whether the rayon is preswollen first or water is added directly to the system. The solubility of water in styrene is very low (0.1% at 40°C.);[21] thus the water content of the rayon appears to be the controlling factor in direct radiation grafting in bulk styrene. It is interesting to note that similar trends are obtained at different levels of radiation dose, as shown in Figure 5. The effect of various nonaqueous swelling agents on the direct radiation grafting onto cellulose is shown in Figure 6. Figure 7 shows the effect of increasing radiation dose on grafting onto rayon swol-

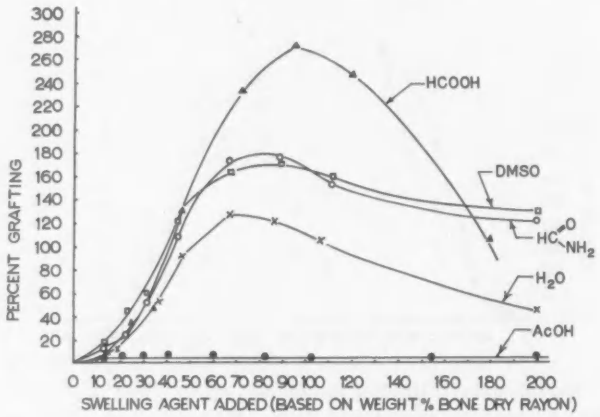

Fig. 6. Effect of nonaqueous swelling agents on the direct radiation grafting of styrene onto rayon. Total dose 4 Mrads; temperature 37°C.

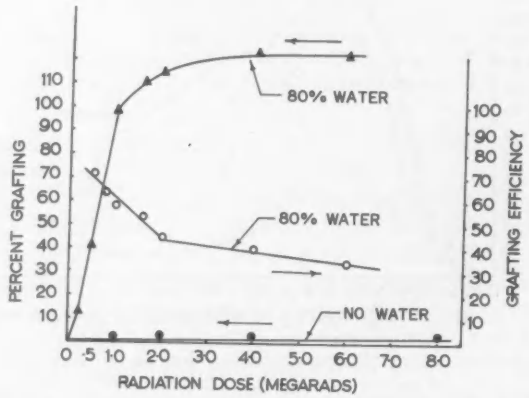

Fig. 7. Effect of radiation dose on grafting and grafting efficiency in the direct radiation grafting of styrene to rayon: (▲) grafting of rayon swollen with 80% water; (●) grafting of rayon without preswelling with water; (○) grafting efficiency of rayon swollen with 80% water.

len with 80% water. Grafting increases linearly with radiation dose till approximatey 100% grafting and then levels off. This can be attributed to the fact that at higher levels of grafting, the reaction becomes diffusion controlled. The efficiency of grafting is shown in the same figure and is seen to decrease with increasing radiation dose. Despite the use of excess monomer, fairly high efficiency of grafting can be obtained with direct radiation grafting in air.

Radiation Grafting in Styrene Solution. Radiation grafting in styrene–solvent solutions is shown in Figure 8. Practically no grafting occurs when

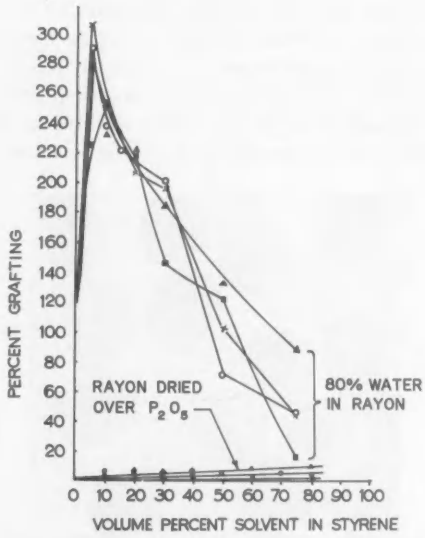

Fig. 8. Direct radiation grafting of styrene onto rayon in styrene–solvent solution; effect of solvent additives and fiber preswelling with water: (×) acetic acid; (○) ethanol; (▲) methanol; (■) acetone.

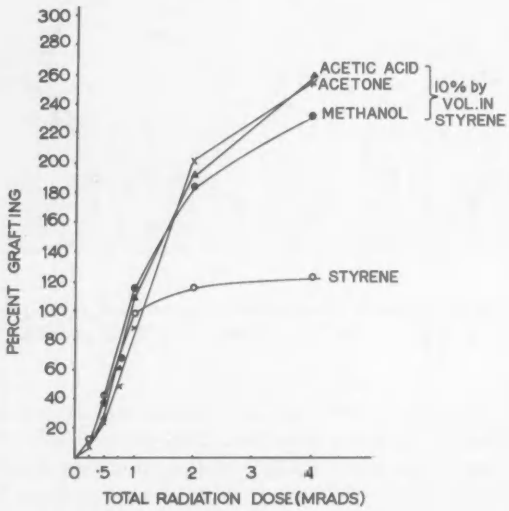

Fig. 9. Effect of total radiation dose on grafting in styrene–solvent solution. Rayon preswollen to 80% water content. Temperature 37°C.

rayon which has been dried over P_2O_5 is irradiated in styrene–solvent mixtures. The presence of small amounts of water is sufficient, however, to cause substantial grafting to occur. When rayon has been swollen with water and then irradiated in styrene–solvent solution, grafting occurs very readily. Water can also be added directly to the styrene–solvent solution. The effect of water in radiation grafting in solution has been previously

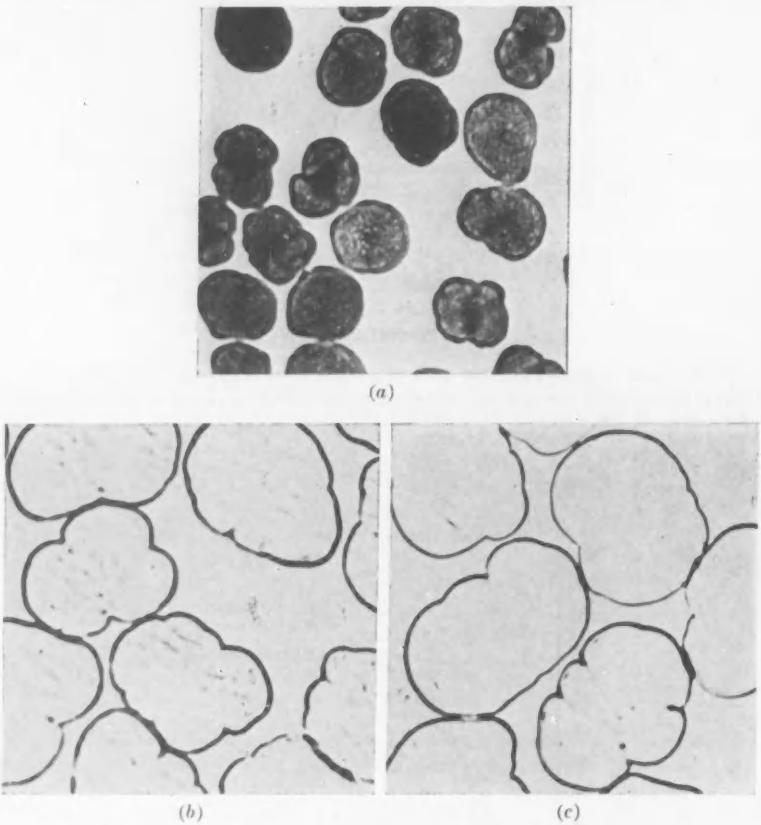

(*a*) (*b*) (*c*)

Fig. 10. Photomicrographs of cross sections of control and rayon–polystyrene graft copolymers: (*a*) control; (*b*) 156.7% grafting; (*c*) 176.4% grafting. Magnification 800×.

reported by Sakurada et al.[2–6] and by Chapiro and Stannett.[7] Figure 9 shows the effect of radiation dose in a 10% styrene/solvent system on grafting in solution. It is seen that the grafting proceeds smoothly over the range 0–4 Mrads and the per cent grafting increases almost linearly with radiation dose. No leveling off of the grafting curve is observed as in the case of bulk grafting. It is of interest to note that up to a radiation dose of

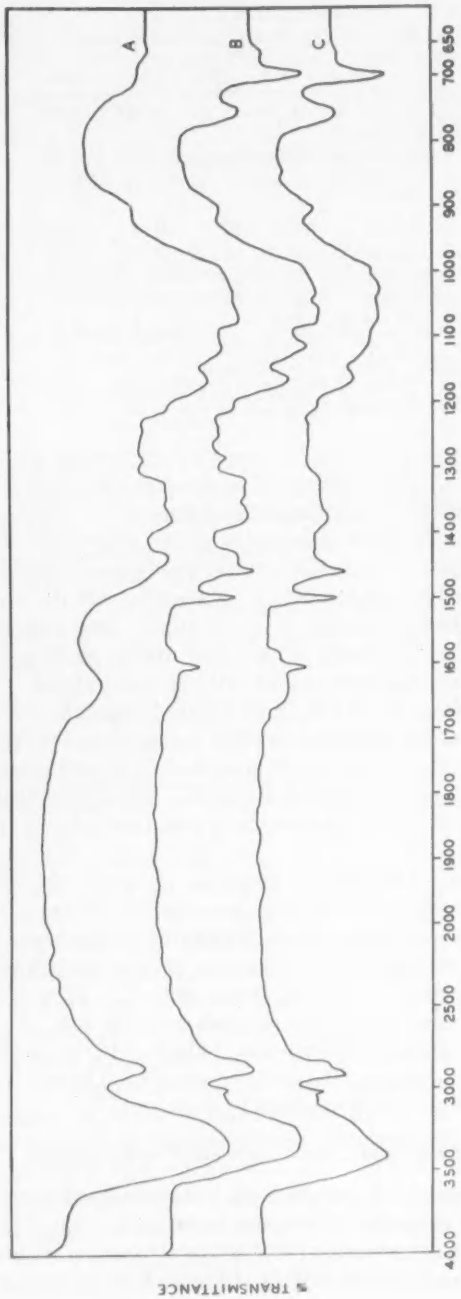

Fig. 11. Infrared spectra of cellulose–polystyrene graft copolymers: (*A*) cotton cellulose; (*B*) cotton–polystyrene graft; (*C*) rayon–polystyrene graft.

TABLE I
Strength Properties of Rayon–Polystyrene Graft Copolymers (Single Fiber Tests)

Grafting, %	0	15.8	24.2	65	105	156.7	278.7
Denier	1.57	1.59	1.77	2.69	3.97	5.00	5.93
Tenacity, g./den.							
Conditioned	4.96	4.64	4.23	2.49	1.83	1.68	1.49
Wet	3.84	2.89	2.85	1.70	1.16	1.22	0.87
Elongation at break, %							
Conditioned	18.9	18.4	17.6	41.2	53.9	38.7	38.4
Wet	29.1	26.8	27.9	58.8	76.4	39.8	34.7
Modulus, g./den.							
Conditioned, initial	93.6	96.2	82.0	36.9	35.5	35.0	34.1
Wet, initial, at 5% strain	5.5	6.9	6.8	3.3	4.6	5.8	10.6
Secondary swelling, %	59.3	42.5	38.9	—	—	10.1	5.4
Moisture regain, %	12.2	10.6	9.9	—	—	6.3	4.4

1 Mrad, grafting onto water swollen rayon in bulk styrene and in styrene–solvent systems yields approximately the same per cent grafting.

Strength Properties. The strength properties of the rayon–polystyrene graft copolymers at various amounts of grafting are shown in Table I. Fiber denier increases with the percentage of polystyrene grafted, tenacity decreases considerably due to increase in diameter but the breaking load or tenacity × denier remained substantially unchanged. Breaking elongation increased markedly at 65 and 105% grafting. Secondary swelling and moisture regain decreased with per cent grafting.

Photomicrographs. Figure 10 shows photomicrographs of cross sections of control and grafted filaments enlarged to a magnification of 800×. It is seen that the diameter of the filaments increase with grafting but the general shape of the cross section is retained. The control filaments were dyed with Congo red but the grafted yarns were hydrophobic and resistant to dyeing.

Infrared Spectra. The infrared spectrum of cotton cellulose obtained by using the potassium bromide pellet technique is shown in Figure 11*A*. The infrared spectrum of a cotton–polystyrene graft copolymer (75% grafting) is shown in Figure 11*B*. There are several bands which are characteristic of polystyrene. Among these, the —C—H out-of-plane deformation at 694 cm.$^{-1}$ has been suggested by Faraone, et al.[22] for the quantitative estimation of polystyrene. Figure 11*C* shows the infrared spectrum of a rayon–polystyrene graft copolymer. The spectra in general are similar to those previously reported by Kobayashi.[9]

Grafting onto Cotton Yarn and Cotton Linters

Radiation Grafting in Styrene in Bulk. Radiation grafting onto cotton yarn and linters preswollen with water is shown in Figure 12. Grafting starts to occur at approximately 10% water content on cellulose, rises to a maximum at approximately 20%, and levels off without decreasing as in

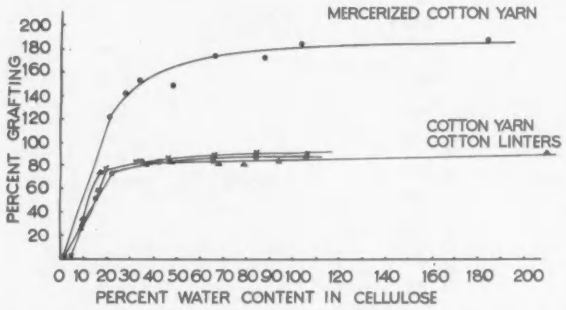

Fig. 12. Direct radiation grafting of styrene onto cotton cellulose, effect of preswelling with water: (●) mercerized cotton yarn, preswollen with water; (▲) cotton yarn, preswollen with water; (×) cotton linters, preswollen with water; (○) cotton yarn, water added directly to styrene. Total dose 4 Mrads; temperature 37°C.

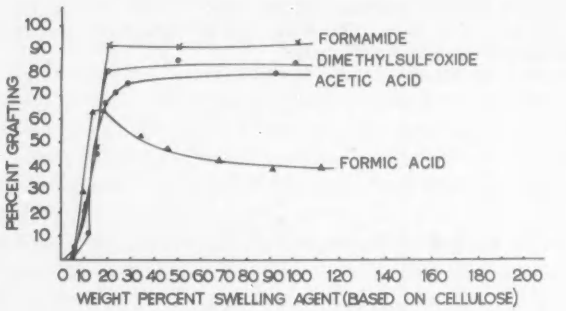

Fig. 13. Effect of nonaqueous swelling agents on the direct radiation grafting of styrene to cotton yarn. Total dose 4 Mrads; temperature 37°C.

the case of rayon. No grafting was obtained for nonswollen yarn. Mercerization of the cotton yarn led to a substantial increase in the amount of grafting, which can be attributed to the increased accessibility of the mercerized cellulose. The effect of nonaqueous swelling agents on the direct radiation grafting of styrene is shown in Figure 13. Figure 14 shows the effect of increasing radiation dose on radiation grafting onto preconditioned cotton yarn, mercerized yarn, and rayon. Grafting onto rayon occurs more readily than for cotton cellulose at comparable radiation doses, which can be attributed to the higher accessibility of rayon. Similar results have been previously reported by Okamura, et al.[1]

Radiation Grafting in Styrene–Solvent Solution. Figure 15 shows the effect of the radiation grafting of cotton yarn in styrene solutions containing methanol, ethanol, and acetic acid. Grafting has been found to proceed readily in these styrene–solvent systems without the presence of water, unlike the case for rayon. Preconditioning of the cotton yarn with water and then irradiating in monomer solution, did not result in any enhance-

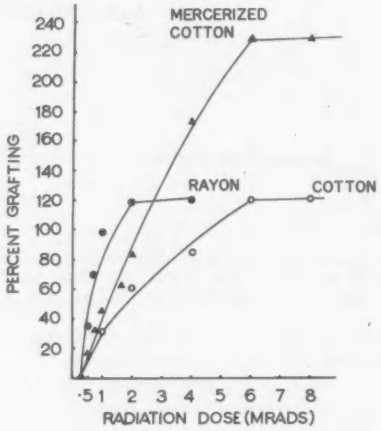

Fig. 14. Direct radiation grafting of styrene onto cellulose, effect of increasing radiation dose and type of cellulose. The cotton and mercerized cotton were swollen with 40% water and the rayon with 80% water.

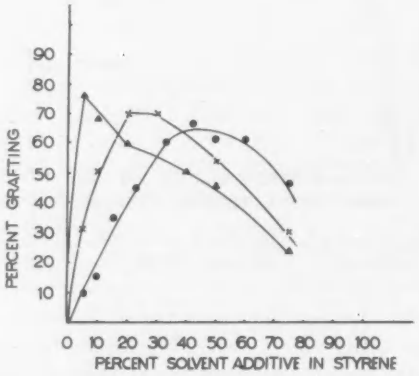

Fig. 15. Direct radiation grafting onto cotton cellulose in styrene–solvent solution: (▲) methanol–styrene; (×) ethanol–styrene; (●) acetic acid–styrene. Total dose 4 Mrads; temperature 37°C.; no water added.

ment of grafting and even resulted in a decrease of grafting, as shown in Figure 16. No logical reason can be given for this behavior, one possible explanation being that the cotton is swollen to a maximum by the water and the addition of solvents tended to decrease rather than increase the swelling.

DISCUSSION

Direct radiation grafting onto cellulose is believed to take place through free radicals which are formed on the cellulose backbone. The presence of

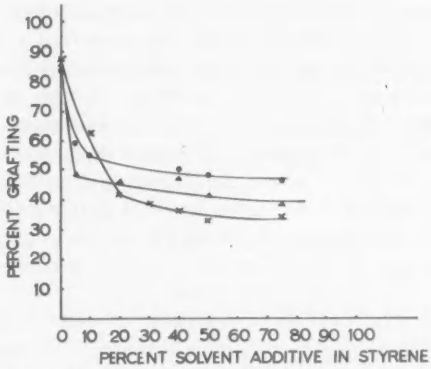

Fig. 16. Direct radiation grafting onto cotton cellulose in styrene–solvent solution: (▲) Methanol–styrene; (×) ethanol–styrene; (●) acetic acid–styrene. Total dose 4 Mrads; temperature 37°C.; cotton yarn preswollen with 40% water.

free radicals in irradiated cellulose has been reported by several investigators.[23,24] It has also been postulated that radicals are formed on the cellulose backbone by the secondary action of radicals produced during the radiolysis of water; however, the fact that polar swelling agents other than water can also promote radiation grafting suggests that the secondary abstraction mechanism is a relatively unimportant process in the grafting systems employed in the present work.

The direct radiation grafting of styrene onto cellulose is a heterogeneous fibrous reaction in which penetration of styrene into the fiber is necessary for grafting to occur. In the dry state cellulose is very strongly hydrogen bonded and virtually impermeable to nonpolar substances. In a previous paper,[11] a solvent-exchange technique was used to gradually introduce or "include" styrene into cotton cellulose prior to radiation grafting. Long and Thompson[25] have observed that the diffusion of organic vapor into plasticized hydrophilic film is faster than into unplasticized film. This effect is believed to be caused by the breaking of hydrogen bonds with water or other swelling agents, thus providing greater segmental mobility of the polymer molecules and facilitating the diffusion of organic vapor.

The effect of water in enhancing the grafting of vinyl monomers onto hydrophilic polymers has been previously reported by Sakurada. et al.[2–6] and by Chapiro and Stannett,[7] who employed styrene solvent solutions to which water was added. Sakurada. et al.[2–6] attributed this to the enhanced diffusion of monomer into the polymer and also postulated the increased formation of polymer radicals by secondary abstraction by ·H and ·OH radicals produced in the radioloysis of water. As pointed out above, our results suggest that the latter mechanism is unimportant. Chapiro and Stannett[7] have explained this phenomena on the basis of a swelling effect which enhances diffusion into the polymer film.

Although previous published work has been concerned only with miscible

systems, the present results indicate that enhancement of diffusion by swelling occurs even in systems where the penetrant molecules are not miscible with the swelling agent. Thus cellulose fibers swollen with water are penetrated by the hydrophobic monomer styrene, and a substantial degree of grafting can be obtained. Nonaqueous polar swelling agents may be equally effective in promoting diffusion of styrene into the cellulose fibers. In fact, as shown in Figure 6, strong swelling agents such as formamide may produce even higher levels of grafting than are obtained with water. The effectiveness of these polar liquids in promoting diffusion and grafting appears to depend mainly on their swelling power for cellulose.

The intercrystalline swelling of cellulose by water and by other polar swelling agents occurs predominantly in the accessible amorphous regions of cellulose. The diffusion and therefore the grafting of styrene is probably restricted to these regions. Sakurada, et al.[6] have shown that no change in the x-ray diffraction pattern was observed in polyvinyl alcohol grafted with large amounts of methyl methacrylate and reported that grafting probably occurred only in the amorphous regions. In the present work, under comparable conditions of swelling, less grafting was obtained with cotton than with rayon, presumably because of cotton's higher crystallinity.

The differences observed in the behavior of rayon and cotton are probably related to differences in the fine structure of the two types of fiber. Maximum grafting in bulk styrene at a given radiation dose is obtained at 60–80% moisture content for rayon and only 15–20% water for cotton. This difference is likely due to the fact that rayon is more accessible than cotton and will swell more. The minimum amount of swelling agent required for any grafting to occur in bulk styrene is also much higher for rayon than for cotton.

In bulk grafting to rayon, the grafting curve passes through a maximum at 60–80% water content and then falls off. In this case, maximum grafting appears to occur at the point of maximum swelling of rayon in water; beyond this, additional water probably forms a diffusion barrier and inhibits the diffusion of styrene. On the other hand, in the case of cotton, the degree of grafting does not decrease after the maximum is reached at a water content of about 20%. Perhaps the pores available for diffusion in the accessible regions of cotton are so large that, at least within the range studied, additional swelling agent beyond that required for maximum swelling has no significant effect on diffusion. No independent data are available in the literature on the diffusion of styrene or other monomers into swollen cellulose.

Differences between rayon and cotton are also observed for grafting in styrene/solvent mixtures. Methanol, ethanol, and acetic acid have no appreciable swelling action on rayon, and grafting in mixtures of styrene and these solvents occur only when water is present. On the other hand, these nonaqueous solvents have sufficient swelling action on cotton that

grafting occurs quite readily in styrene–solvent mixtures in the absence of water. For styrene–solvent systems, as well as for bulk styrene, the lower accessibility of cotton resulted in less grafting than in the case of rayon under comparable conditions.

The presence of air has an inhibiting effect at low radiation doses, but above a certain minimum dose grafting proceeds readily. Most of the previous work on radiation grafting onto cellulose has been carried out in vacuum. The present work shows that the radiation grafting reaction can be conveniently carried out in air under proper reaction conditions.

We wish to thank the National Research Council of Canada for a major research grant which enabled the purchase of the Gamma-cell 220, 18,000 Co^{60} curie irradiation facility. One of us (R. Y.-M. Huang) wishes to acknowledge generous financial assistance in the form of a Canadian Industries Limited Research Fellowship 1960–1961 and summer maintenance grants from the School of Engineering Research, University of Toronto. We are also indebted to Dr. D. B. Mutton, Industrial Cellulose Research Ltd., Hawkesbury, Ont. for kindly arranging the physical test and for helpful discussions.

References

1. Okamura, S., T. Iwasaki, Y. Kobayashi, and K. Hayashi, paper presented at the International Atomic Energy Conference on the Application of Large Radiation Sources in Industry and Especially to Chemical Processes, Warsaw, Poland, September 1959.
2. Sakurada, I., T. Okada, and Y. Akiyama, *Doitai To Hoshasen*, **3**, 35 (1960).
3. Sakurada, I., T. Okada, and E. Kugo, *Doitai To Hoshasen*, **2**, 297 (1959).
4. Sakurada, I., T. Okada, and E. Kugo, *Doitai To Hoshasen*, **2**, 306 (1959).
5. Sakurada, I., T. Okada, and E. Kugo, *Doitai To Hoshasen*, **2**, 316 (1959).
6. Sakurada, I., T. Okada, M. Uchida, and E. Kugo, *Doitai To Hoshasen*, **2**, 581 (1959).
7. Chapiro, A., and V. Stannett, *Intern. J. Appl. Radiation Isotopes*, **8**, 4 (1960).
8. Shinohara, Y., *Kobunshi Kagaku*, **17**, 197 (1960).
9. Kobayashi, Y., *J. Polymer Sci.*, **51**, 359 (1961).
10. Hendricks, R. W., Can. Pat. 644,643, July 10, 1962.
11. Rapson, W. H., R. Y.-M. Huang, B. Immergut, and E. H. Immergut, paper presented at 138th Meeting, American Chemical Society, New York, N. Y., September 11–16, 1960; R. Y.-M. Huang, B. Immergut, and W. H. Rapson, paper presented at 138th Meeting, American Chemical Society, New York, N. Y., September 11–16, 1960; R. Y.-M. Huang, B. Immergut, and W. H. Rapson, *J. Polymer Sci.*, **A1**, 1257 (1963).
12. Vogel, A. I., *A Textbook of Practical Organic Chemistry*, Longman, Green, New York, 1951, pp. 165–170.
13. Rice, F. G., and W. D. Smythe, *Ind. Eng. Chem.*, **52**, No. 5, 47A (1960).
14. Boundy, R. H., and R. F. Boyer, *Styrene, Its Polymers, Copolymers and Derivatives*, Reinhold, New York, 1952, p. 157.
15. Chapiro, A., *Radiation Chemistry of Polymeric Systems*, Interscience, New York, 1962, p. 164.
16. Trommsdorf, E., E. Kohle, and P. Lagally, *Makromol. Chem.*, **1**, 169 (1948).
17. Ballantine, D. S., P. Colombo, A. Glines, and B. Manowitz, *Chem. Eng. Progr. Symp. Series*, **50**, No. 11, 267 (1954).
18. Chapiro, A., *Radiation Chemistry of Polymeric Systems*, Interscience, New York, 1962, Chap. 7.
19. Vanderhoff, J. W., E. B. Bradford, H. L. Tarkowski, and B. W. Wilkinson, *J. Polymer Sci.*, **50**, 265 (1961).
20. Chapiro, A., and N. Maeda, *J. Chim. Phys.*, **56**, 230 (1959).

21. Boundy, R. H., and R. F. Boyer, *Styrene, Its Polymers, Copolymers and Derivatives*, Reinhold, New York, 1952, p. 53.
22. Faraone, G., G. Parasacco, and C. Cogrossi, *J. Appl. Polymer Sci.*, **5**, 16 (1961).
23. Abraham, R. J., and D. H. Whiffen, *Trans. Faraday Soc.*, **54**, 1291 (1958).
24. Florin, R. E., paper presented at 138th Meeting, American Chemical Society, New York, N. Y., September 11–16, 1960; private communication.
25. Long, F. A., and L. J. Thompson, *J. Polymer Sci.*, **14**, 321 (1954).

Synopsis

The direct radiation graft copolymerization of styrene onto cotton cellulose and rayon by gamma-ray irradiation from a Co^{60} source at a high dose rate of 1.4 Mrads/hr. was investigated. The grafting was carried out in air at radiation doses in the range of 0–8 Mrads. Varying amounts of grafting of up to several hundred per cent were obtained by controlling reaction variables of cellulose preswelling, total radiation dose, and styrene–solvent composition. Direct radiation graft copolymerization onto cellulose is a heterogeneous fibrous reaction in which the diffusion of styrene monomer onto the cellulose plays a key role. No grafting was obtained when unconditioned cellulose was irradiated in bulk styrene. Grafting occurred readily, however, when the cellulose was first preswollen with a polar swelling agent such as water, formamide, formic acid, or dimethyl sulfoxide, then placed in bulk styrene or styrene–solvent solution and irradiated. The effect of water in the radiation grafting was investigated. In bulk styrene, for a given radiation dose, grafting was found to depend on the water content of the preswollen cellulose. For rayon, grafting increased sharply after 30% water content in rayon, passed through a maximum at 60–80%, and then decreased again. For cotton cellulose, grafting occurred after 10% water content, increased up to approximately 20%, and then remained constant. Efficiency of grafting was found to decrease with increasing per cent grafting and radiation dose. The effect of solvent additives such as methanol, ethanol and acetic acid on the grafting was studied. Addition of small quantities of water to the styrene–solvent system was found to be necessary in grafting onto rayon but not onto cotton cellulose. The enhanced grafting obtained by preswelling the cellulose or by carrying out the grafting in solutions containing swelling agents is interpreted in terms of a "plasticizing effect." The swelling agent is assumed to promote the diffusion of styrene monomer by breaking some of the hydrogen bonds and loosening the cellulose chains. Mercerization of cotton cellulose resulted in a twofold increase in the amount of grafting. Grafting occurred more readily onto rayon than onto cotton cellulose under comparable conditions. It is postulated to take place only in the amorphous (accessible) regions of cellulose. Strength properties, microphotographs of grafting cross sections, and the infrared spectra of rayon–polystyrene graft copolymers are presented.

Résumé

On a étudié la copolymérisation greffée du styrène par radiation directe de la cellulose de croton et rayonne par irradiation de rayons-gamma d'une source de Co^{60} à une vitesse de dose élevée de 1.4 Mrads/heure. On a effectué le greffage à l'air, à des doses de radiation dans un domaine de 0 à 8 Mrads. On a obtenu des quantités différentes de greffage jusqu'à plusieurs centaines de pourcent en controlant les variables de la réaction de la cellulose préalablement mélangée, la dose de radiation totale et la composition styrène/solvant. La copolymérisation greffée par radiation directe sur cellulose est une réaction hétérogène sur fibre dans laquelle la diffusion du monomère styrène dans la cellulose joue un rôle clef. Aucun greffage n'a été obtenu quand la cellulose non-conditionnée est irradiée dans le styrène en bloc. Le greffage s'effectue rapidement seulement quand la cellulose est d'abord mélangée avec un agent de mélange polaire tel que l'eau, le formamide, l'acide formique, le diméthylsulfoxyde etc., puis en présence du styrène en bloc ou de la solution styrène/solvant et irradié. On a étudié l'effet et l'eau

sur le greffage par radiation. Dans le styrène en bloc, pour une dose donnée d'irradiation, le greffage dépend de la teneur en eau de la cellulose pré-mélangée. Pour la rayonne, le greffage augmente fortement après une teneur de 20% en eau dans la rayonne, passe par un maximum à 60–80% et diminue à nouveau. Pour la cellulose de coton, le greffage s'effectue au-delà d'une teneur de 10% en eau, augmente jusqu'approximativement 20% et reste alors constant. L'efficacité de greffage diminue avec l'augmentation du pourcent de greffage et la dose de radiation. On a étudié l'effet des solvants additifs tels que le méthanol, l'éthanol, l'acide acétique sur le greffage. L'addition de faibles quantités d'eau au système styrène/solvant est nécessaire dans le greffage sur rayonne mais pas dans le greffage sur la cellulose de coton. On interprète l'augmentation de greffage obtenu par pré-mélange de cellulose ou en effectuant le greffage dans des solutions contenant des agents de mélange en termes d'un effet de plastification. On admet que l'agent gonflant facilite la diffusion du monomère styrène par rupture des liens hydrogène et relâchement des chaînes cellulosiques. La mercérisation de la cellulose de coton conduit à une augmentation double de la quantité de greffage. Le greffage s'effectue plus rapidement sur la rayonne que sur la cellulose de coton dans des conditions comparables. On suppose que participent seules les régions amorphes (accessibles) de la cellulose. On décrit les propriétés de résistance, des micro-photographies de sections de greffage et des spectres infra-rouges de copolymères greffés rayonne-polystyrène.

Zusammenfassung

Die direkte Strahlungspfropfcopolymerisation von Styrol auf Baumwollcellulose und Rayon durch γ-Strahlung einer Co-60-quelle bei einer hohen Dosisleistung von 1,4 Mrad/h wurde untersucht. Die Aufpfropfung wurde unter Luft bei Strahlungsdosen im Bereich von 0–8 Mrad ausgeführt. In Abhängigkeit von den Reaktionsbedingungen wie Cellulosevorquellung, Gesamtbestrahlungsdosis und Styrol–Lösungsmittelverhältnis wurde Aufpfropfung bis zu einigen hundert Prozent erhalten. Die direkte Strahlungspfropfcopolymerisation auf Cellulose ist eine heterogene Faserreaktion, bei welcher die Diffusion des monomeren Styrols in die Cellulose eine Schlüsselrolle spielt. Bei der Bestrahlung von unkonditionierter Cellulose in reinem Styrol wurde keine Aufpfropfung erhalten. Aufpfropfung trat jedoch leicht ein, wenn die Cellulose in einem polaren Quellungsmittel wie Wasser, Formamid, Ameisensäure, Dimethylsulfoxyd etc. vorgequollen wurde und dann in reines Styrol oder ein Styrol–Lösungsmittelgemisch gebracht und bestrahlt wurde. Der Einfluss von Wasser auf die Strahlungsaufpfropfung wurde untersucht. Bei reinem Styrol war bei einer gegebenen Strahlungsdosis die Aufpfropfung vom Wassergehalt der vorgequollenen Cellulose abhängig. Bei Rayon nahm die Aufpfropfung bei einem Gehalt von 30% Wasser in Rayon scharf zu, ging bei 60–80% durch ein Maximum und nahm dann wieder ab. Bei Baumwollcellulose trat Aufpfropfung bei einem Wassergehalt von 10% ein, nahm bis zu etwa 20% zu und blieb dann konstant. Die Pfropfungsausbeute nahm mit steigendem Gehalt an Aufgepfropftem und steigender Strahlungsdosis ab. Der Einfluss von Lösungsmittelzusätzen wie Methanol, Äthanol und Essigsäure auf die Aufpfropfung wurde untersucht. Ein Zusatz kleiner Wassermengen zum Styrol–Lösungsmittelsystem erwies sich für die Aufpfropfung auf Rayon, aber nicht für die auf Baumwollcellulose, als notwendig. Die erhöhte, durch Vorquellung der Cellulose oder durch Ausführung der Aufpfropfung in Quellungsmittel enthaltenden Lösungen erhaltene Aufpfropfung wird als "Weichmachungseffekt" gedeutet. Es wird angenommen, dass das Quellungsmittel die Diffusion des Styrols durch Zerstörung einiger Wasserstoffbindungen und Auflockerung der Celluloseketten erleichtert. Mercerisierung von Baumwollcellulose führt zu einer zweifachen Zunahme der aufgepfropften Menge. Die Aufpfropfung auf Rayon trat unter vergleichbaren Bedingungen leichter ein als auf Baumwollcellulose. Es wird angenommen, dass sie nur in den amorphen (zugänglichen) Cellulosebereichen stattfindet. Festigkeitseigenschaften, Mikroaufnahmen von Pfropfquerschnitten und Infrarotspektren von Rayon-Polystyrolpfropfcopolymeren werden mitgeteilt.

Discussion

R. H. Marchessault (*Cellulose Research Institute, College of Forestry, Syracuse, N. Y.*): I wonder if we should not stop using the word "graft copolymer" in referring to fiber occlude polymers. There is no evidence that the change in fiber properties observed require a true chemical bond between the cellulose and the polymer. I think *"in situ"* polymerized polymer is preferable terminology.

R. Y.-M. Huang: The term graft copolymer in the present paper follows the commonly used terminology in radiation induced or chemical grafting. The question of whether to use words such as *"in situ"* polymerization instead of graft copolymerization is one which should be considered from the viewpoint of the entire field of grafting rather than for fibers or cellulose alone. Dr. Marchessault's point is well taken, but we prefer to use the term "graft copolymer" keeping in mind the limitations of this terminology, instead of *"in situ"* polymerization. The change in fiber properties is certainly no direct evidence of a true chemical bond between the cellulose and the polymer, but many unique properties can be observed.

S. Hossain (*Central Research Division, ABITIBI Power and Paper Co., Sault St. Marie, Ontario, Canada*): As we are back again to the topic of "grafting" or "polymerization *in situ*," I should like to have a point settled. This morning I got the distinct impression, in spite of a certain degree of ambiguity in the method of calculation, that "grafting" confers a high degree of hydrophobicity on cellulose. Since the hydroxyl groups are not involved in "grafting" how is this possible? Is this effect a genuine one?

W. H. Rapson: A high degree of water repellancy is created by grafting polystyrene onto cellulose in substantial quantity, but on soaking in water a significant amount is absorbed. Based on the grafted polymer, the water absorption is very low, but based only on the cellulose portion, the water absorption is about half that of the original cellulose. The moisture regain on the other hand is very close to that of the original cellulose when calculated on the weight of the cellulose part of the grafted copolymer. This indicates that the hydroxyl groups are still available for hydrogen bonding with water. Presumably the hydrophobicity is caused by the long hydrophobic polystyrene chains bound to the cellulose hindering, but not entirely preventing access of water to the cellulose.

Dr. Rudolph Schmut (*West Virginia Pulp & Paper Co., Mechanicsville, N. Y.*): Are data available on low level grafting (1–5%) in industrial ranges?

W. H. Rapson: Not in our work. Since we have 1–3% experimental error, we have not considered products with such low level of add-on to be significant.

W. H. Rapson: For most purposes there is no need to extract any homopolymer from a grafted material. We do so in our laboratory work merely to determine "add-on." It is the effect of the vinyl polymer on the cellulosic material which is important, and not the academic question of whether or not it is really grafted.

JOURNAL OF POLYMER SCIENCE: PART C NO. 2, PP. 189–197 (1963)

Method for the Investigation of Carbohydrate Graft Copolymers

C. P. J. GLAUDEMANS* and E. PASSAGLIA,† *Research and Development Division, American Viscose Corporation, Marcus Hook, Pennsylvania*

INTRODUCTION

Conclusive proof or disproof for the existence of true cellulose graft copolymers has never been published. The solubility characteristics of the reaction products have frequently been used as criteria of grafting. However, it is not clear that solubility alone is a sufficient criterion to demonstrate the existence of a true bond between the cellulose substrate and the hypothetically grafted side branch.

In this paper we suggest a method based on molecular weight determination which, under proper circumstances, could yield an unequivocal answer on the question of the existence of true grafting. The method has been used to investigate the nature of the graft copolymers obtained by the use of a ferrous salt–hydrogen peroxide redox system,[1] as well as a ceric (IV) salt[2] system, both in conjunction with a carbohydrate polymer. The preliminary results are that no grafting occurred when ferrous ammonium sulfate and hydrogen peroxide were used as initiating system for cellulose-polystyrene grafting. With the use of ceric (IV) salt initiation for the preparation of an amylose–polymethyl methacrylate graft, the molecular weight of the polymethyl methacrylate was so high that no definite conclusions could be drawn, and efforts to lower the molecular weight[3] while maintaining a high level of grafting were unsuccessful.

METHOD

The method is based on knowing the molecular weight of the substrate, the polymerized side chain (called the polymer hereafter), and the mixture (or true graft copolymer) of substrate and polymer.

Consider a polymer substrate s which has been graft copolymerized with a polymer p. We will call the resulting mixture of substrate, graft copolymer, and ungrafted, *in situ*-polymerized polymer, the "mixture." Let the number-average molecular weights of the substrate, polymer and

* Present address: Laboratory of Chemistry, NIAMD, National Institutes of Health, Bethesda, Maryland.

† Present address: Division of Organic and Fibrous Materials, National Bureau of Standards, Washington, D.C.

mixture be M_s, M_p, and M_m, respectively. Consider that we start with a chains of substrate and polymerize in their presence b chains of polymer. We define fraction add-on, g, as:

$$g = bM_p/aM_s \tag{1}$$

Let f be the fraction of polymer chains which are attached to the substrate and $(1 - f)$ be the fraction unattached; then

$$M_m = \frac{aM_s + bM_p}{a + b(1 - f)} \tag{2}$$

Substituting for b from eq. (1) gives

$$M_m = \frac{M_s(1 + g)}{1 + (1 - f)gM_s/M_p} \tag{3}$$

and solving for f we obtain

$$f = \frac{M_m(g + M_p/M_s) - M_p(1 + g)}{gM_m} \tag{4}$$

By measuring M_m, M_s, and M_p, f can be calculated, and the extent of grafting determined. The limiting cases for M_m are:

For $f = 0$ (no grafting):

$$M_{m(f=0)} = \frac{M_s(1 + g)}{1 + gM_s/M_p} \tag{5}$$

For $f = 1$ (complete grafting):

$$M_{m(f=1)} = M_s(1 + g) \tag{6}$$

M_m is intermediate between these values when $0 < f < 1$. It can be seen that if $M_p \gg M_s$, eq. (6) becomes identical to eq. (5) (unless g is very large) and the method becomes useless.

DISCUSSION AND RESULTS

The mechanism for the initiation of graft copolymerization with ferrous salts and hydrogen peroxide has been discussed by Richards,[4] and he has made it very plausible that of the two possible radicals formed, namely the polyvinyl radical, and the hydroxyl radical, it is the latter which may interact with the cellulose:

$$Fe^{2+} + H_2O_2 \rightarrow Fe^{3+} + OH^- + OH.$$

$$.OH + \text{Cellulose—}\underset{|}{C}HOH \rightarrow H_2O + \text{Cellulose—}\underset{|}{C}OH$$

$$\text{Cellulose—}\underset{|}{C}OH + \text{Monomer} \rightarrow \text{Cellulose—}\underset{|}{\overset{|}{C}}OH$$

$$\text{polymer}$$

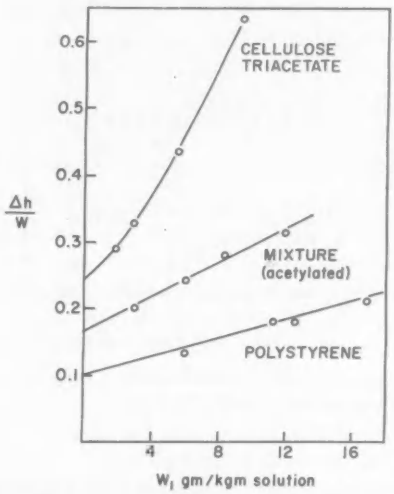

Fig. 1. Reduced osmotic height vs. concentration for the polymers derived from graft copolymer IA.

The preparation of the graft followed the procedure of Landells and Whewell[1] and Richards.[4] Rayon was treated with ferrous ammonium sulfate in aqueous acetic acid, and reacted at the boiling point with styrene in water containing hydrogen peroxide. The resultant product was extracted with acetone in a soxhlet to constant weight, after which it showed a weight increase over the original rayon of 380%. This product was then acetylated to completion, yielding a material which was soluble in acetone–benzene mixtures. Osmometric measurements yielded the number-average molecular weight M_m = 154,000 (Fig. 1). Acid degradation of the cellulose component in the acetylated graft yielded polystyrene, the molecular weight of which was measured osometrically in acetone–benzene, giving a result for M_p of 253,000. A sample of rayon substrate was acetylated in a fashion identical to that for the grafted sample. Its number-average molecular weight, M_s, was 103,000.

The weight increase by polymerization in the cellulose was 380%. In conjunction with the molecular weight of the unacetylated cellulose (58,000) and of the polystyrene (253,000) it is seen that the mole ratio of polystyrene to cellulose in the "graft" is 0.87:1. On the basis of the acetylated cellulose, g becomes 2.13 for the acetylated graft. By using eq. (5), which gives the lowest possible value of M_m, it can be seen that the number-average molecular weight of a true mixture of the acetylated cellulose and the polystyrene should be 172,000. This is higher than the measured value (154,000). Thus, substitution of the values into eq. (4) leads to a value for $f = -0.26$. Considering the fact that the error in f due to the error in M is ± 0.20 for $\Delta M/M = 0.07$ this essentially means that $f = 0$. Also,

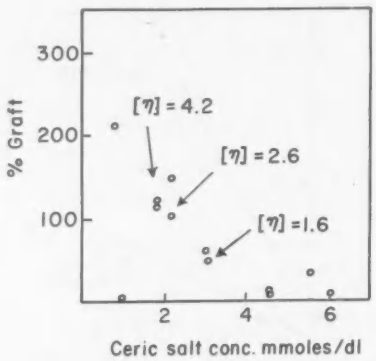

Fig. 2. Variation of per cent add-on with ceric salt concentration. The intrinsic viscosities indicated are those of the polymethyl methacrylate (in benzene) after hydrolysis of the graft copolymer.

with little or no grafting, f could be negative if the cellulose degraded during the reaction.

There is a possibility that a covalent link between the cellulose and the polystyrene was ruptured during the acetylation of the graft. This possibility is remote, since it is most likely an ether linkage or a carbon–carbon linkage, and was not investigated.

When fractionated amylose,[5] having a $\bar{M}_v/\bar{M}_n$ ratio of 1.3, was reacted with methyl methacrylate in the presence of ceric (IV) ammonium nitrate and nitric acid, a product was obtained, the composition of which was 68.5% polymethyl methacrylate and 31.5% amylose (after extraction with acetone and aqueous sodium hydroxide to constant weight). The molecular weight, M_s, of the amylose substrate as measured by osmometry on the acetate derivative was 91,000, corrected for the acetate. The molecular weight of the acetylated graft copolymer, M_m, was 301,000. Swelling and dissolution of the grafted material in dimethyl sulfoxide, followed by dialysis against water, and subsequent hydrolysis in aqueous sulfuric acid, yielded polymethyl methacrylate, the number-average molecular weight of which was $M_p = 1.4 \times 10^6$. This value should be considered inaccurate ($\pm 50\%$), since it falls outside the scope of osmometry. However, the order of magnitude should be correct.

In conjunction with eqs. (4), (5), and (6), it can be seen that no justifiable conclusion can be drawn in this case with regard to f. Because M_p is so much larger than M_s, the molecular weight of the amylose molecule, attached to the enormous grafted chain will be an insignificant fraction of the total molecular weight, and removal of this carbohydrate fraction will go undetected when the molecular weight of the polymethylmethacrylate is measured. It was thought that increase of the ceric (IV) ion concentration during the polymerization would decrease the molecular weight of the vinyl polymer,[3] and thus render a study of this system possible. How-

ever, although molecular weights of the polymethyl methacrylate did indeed decrease (Fig. 2), so did g, so that at sufficiently low M_p, g was too small to allow any conclusion to be drawn.

EXPERIMENTAL

I. Ferrous Salt–Hydrogen Peroxide Initiation

A. Preparation of the Graft Copolymer. Cellulose fiber (0.3 den., 0.5 in. length), 5.5 g. was soaked in ferrous ammonium sulfate (0.1%), dissolved in aqueous 0.1*N* acetic acid, for 20 min. It was collected by filtration and dried overnight. This was added to boiling water, containing 0.03% hydrogen peroxide and 40 ml. styrene (distilled). The system had previously been saturated with nitrogen. The reaction was kept at a boil under the passage of nitrogen for 2 hr., with stirring. The material was collected on the filter, extracted three times with boiling acetone, and left overnight in benzene. It was then extracted with benzene in the Soxhlet for 3 days. The weight was 26.275 g. Reextraction of this material (IA) in the Soxhlet (benzene) for one day failed to lower this (26.48 g.).

B. Preparation of a Soluble Derivative. The above material (IA, 5.0 g.) was swollen in benzene and solvent-exchanged to anhydrous pyridine (100 ml.). Acetic anhydride (70 ml.) was added, and the mixure was heated under reflux for 2 hr. to yield a dark brown solution. It was isolated by pouring it on ice, and the resulting stringy precipitate was washed with water and methanol. The yield was 5.1 g. This material (IB) was nearly instantly soluble in benzene–acetone (50:50, v/v). Its infrared spectrum failed to show hydroxyl absorption. The triacetate derivative of the cellulose substrate was prepared identically.

C. Hydrolysis of the Acetylated Graft Copolymer. The acetylated polymer IB (1.884 g.) was dissolved in benzene–acetone (50:50, v/v). Methanol (20 ml.) mixed with concentrated aqueous hydrochloric acid (5 ml.) was added and the solution was heated on the steam bath for 48 hr. to yield a gummy precipitate. Methanol (6 volumes) was added, and the total precipitate collected on the centrifuge. After drying in air it was stirred in benzene overnight, a small amount of haze centrifuged off, and poured into methanol. Drying yielded 1.313 g. of polymer. Calculated weight loss for this polymer (based on a polystyrene: cellulose acetate weight ratio of 3.8:1.78) 0.595 g. Found: 0.571 g. The material was poorly soluble in benzene (hazy solution). Since it was believed that even a small amount of carbohydrate material could inhibit good dissolution, the polymer was acetylated with acetic anhydride and anhydrous pyridine. The product was smoothly soluble in benzene–acetone (50:50 v/v). The infrared spectrum showed polystyrene and a very small carbonyl peak.

D. Osmotic Pressure Measurements. The static method was used. Equilibria were attained from above as well as below and were observed over at least 24 hr. Cells were rinsed overnight with the solution to be measured. The density of the benzene–acetone was found to be 0.825. The

concentration was expressed as grams solute/kilogram solution, and the molecular weights were derived from the equation:[6]

$$\bar{M} = 25{,}300/(\Delta h/w)_0$$

The cellulose triacetate was measured in chloroform/ethanol (95/5 v/v), the density of which was 1.454.

II. Ceric Salt Initiation

A. Preparation of the Graft. Amylose (5.4 g.) was autoclaved in 200 ml. of water (118°C., 2.5 hr.) and methyl methacrylate (20 ml.) was added together with an emulsifying agent at a temperature below 40°C. While stirring under N_2, a solution (15 ml.) of ceric ammonium nitrate (0.1M) in 1*N* HNO_3 was added. Stirring was continued for 2.25 hr. Ferrous ammonium sulfate was added to stop the reaction, and the mixture was poured into acetone (2 liters), and left overnight. The precipitate was collected, dispersed in dilute sulfuric acid, filtered and washed thoroughly with ice water; the weight was 17.99 g. The material was extracted with acetone on the Soxhlet for 10 days; the weight was 17.66 g. It was then extracted for 1.5 hr. with 500 ml. 1% sodium hydroxide in water (under nitrogen), washed with dilute acetic acid, water, and acetone, and air dried; the weight of this material (IIA) was 17.22 g. Number-average molecular weight studies were done on the above sample.

For a viscosity study on the molecular weights of the grafted vinyl polymers, the samples were prepared anologously. However, while the ceric ion content was varied, the nitric acid concentration was not kept constant either. The results in Figure 2 should therefore not be taken as a study of the ceric salt variable, but only as a rough indication of the possible variation in $\bar{M}_p$ with $[Ce^{4+}]$.

Reaction conditions for the preparations of the latter graft copolymers in as far as they differed from the above procedure are given in Table I.

TABLE I

Graft, %	Amylose, g./100 ml. water	MMA, ml./100 ml. water	Ce^{4+}/100 ml. water
120	1	5	2 ml. 1*M* ceric salt in 1.5*N* HNO_3
120–150	1	5	2.2 ml. 1*M* ceric salt in 1.5*N* HNO_3
50	1	5	3 ml. 1*M* ceric salt in 1.5*N* HNO_3
0	1	5	1 ml. 0.1*M* ceric salt in 1.5*N* HNO_3
0	1	5	5 ml. 0.1*M* ceric salt in 1.5*N* HNO_3

B. Acetylation of Material IIA. The material (1 g.) was acetylated at room temperature with pyridine (25 ml.) and acetic anhydride (25 ml.). After isolation as for the acetate of IA, it was dissolved in chloroform, centrifuged to remove a haze, and collected by pouring into heptane (IIB).

C. Hydrolysis of Material IIA. The copolymer IIA (2 g.) was dispersed in dimethyl sulfoxide (50 ml.). The swollen mass (partly in solution) was transferred to a cellophane dialysis bag, and dialyzed versus distilled water for one week. It was quantitatively transferred to a flask with 500 ml. 0.7*N* sulfuric acid, refluxed for 6 hr., and the residue washed with aqueous sodium bicarbonate followed by water. The dried product (1.37 g. polymethyl methacrylate) was soluble in chloroform.

TABLE II
Osmotic Pressure Data for Acetylated Copolymer IIB

C, g./100 ml.	$\Delta h/c$ (Δh in cm.)
0.355	1.000
0.530	1.300
0.886	1.735
0	0.580

TABLE III
Osmotic Pressure Data for Hydrolyzed Copolymer IIC

W, g./kg. solution	$\Delta h/w$ (Δh in cm.)
1.38	0.050
2.07	0.053
3.45	0.095
5.16	0.137
7.45	0.211
0	0.020

D. Osmometric Pressure Measurements. Measurements were made in chloroform at 30°C. for the acetylated copolymer IIB, and in chloroform–ethanol (95:5 v/v) for the hydrolyzed copolymer IIC. Equilibria were observed up to 72 hr., and were approached from above as well as below for polymer IIB. For polymer IIC equilibria were approached only from above. The data are given in Tables II and III, respectively.

The authors are grateful for the untiring help of Mr. G. F. Goodley, who assisted in a good deal of the experimental work.

References

1. Landells, G., and C. S. Whewell, *J. Soc. Dyers Colourists* **67**, 338 (1951); *ibid.*, **71**, 171 (1955).
2. Mino, G., and S. Kaizerman, *J. Polymer Sci.*, **31**, 242 (1958).
3. Mino, G., S. Kaizerman, and E. Rasmussen, *J. Polymer Sci.*, **38**, 393 (1959).
4. Richards, G. N., *J. Appl. Polymer Sci.*, **5**, 539 (1961).
5. Corn Amylose NRRL 14 SSP, Northern Utilization Research and Development Division, Peoria, Ill. U. S. Dept. of Agriculture.
6. Ott, E., H. M. Spurlin, and M. W. Grafflin, *Cellulose and Cellulose Derivatives*, Interscience, New York, 1955, p. 1149.

Synopsis

A method has been developed to characterize carbohydrate graft copolymers. When the procedure was applied to a graft copolymer obtained by reacting cellulose with styrene through catalysis by the ferrous ammonium sulfate–hydrogen peroxide redox system, no covalent link was found between the cellulose and the polystyrene.

Résumé

On a développé une méthode d'identification des copolymères greffés d'hydrates de carbone. Quand on applique le mode opératoire à un copolymère greffé obtenu par réaction de cellulose et de styrène, catalysée par le système rédox sulfate ferreux et ammonium—eau oxygénée, on ne trouve pas de liaison covalente entre la cellulose et le polystyrène.

Zusammenfassung

Es wird eine Methode fur die Charakterisierung von Propfpolymeren auf Kohlenhydraten beschrieben. Anwendung dieser Methode auf ein Propfpolymer aus Cellulose und Styrol (mit Eisen -(II)- ammoniumsulfat und Wasserstoffperoxyd als Starter) ergab das Fehlen einer Kovalenten Bindung zwischen Cellulose und Polystyrol.

Discussion

G. N. Richards (*AMF British Research Lab., Reading, England*): (*1*) Regarding the question concerning the possibility of degradation of cellulose during acetylation in pyridine, it was shown at the Shirley Institute that this method causes negligible degradation.

(*2*) Dr. Glaudeman's method of detecting grafting is elegantly simple in its conception, but there appears to be an error in its execution.

The value of m_s used is that of the original cellulose, whereas it is very probable that under the conditions of grafting by the Landells method, extensive degradation occurs. This is shown qualitatively, e. g., by the tendering of treated fibers, and the occurrence of such degradation would invalidate the conclusion that grafting has not occurred.

C. P. J. Glaudemans: First, it must be pointed out, that even if degradation took place during the acetylation, this would be of little concern to us, as both the substrate, as well as the "graft" copolymer, were acetylated under identical conditions.

Concerning Dr. Richards' second remark, it is true that cellulose will degrade to some extent when treated with the peroxide system described by Landells. However, it is impossible to say to what extent this degradation will occur in the presence of a polymerizable monomer. In all probability, it will then be less. It was for this reason that we decided to take for M_s the value obtained from the untreated substrate. Some degradation may explain the negative value we found for f. The objection raised is not an invalid one, therefore. For example, if we assume that the number-average molecular weight of the substrate has decreased by one-third in the polymerization reaction, f is calculated to be between 0.3 and 0.4, e.g., grafting did take place to some extent, but the mixture contained largely occluded polymer.

J. J. Hermans (*Chemstrand Research Center, Durham, North Carolina*): It may be worthwhile to draw attention to a simple and quick method to prove grafting and to get a fairly good idea of the extent of grafting. This is the method of density gradient centrifugation. If a mixture of two solvents is subjected to centrifugation, a density gradient is established. When the system is chosen properly, a polymer that is dissolved in this mixture collects in a band around the point where the density of the mixture is equal to the effective density of the polymer. The homopolymer, the substrate and the graft will, therefore, collect in separate bands. Very little material is needed to do this experiment.

Andrew A. Katai (*Department of Forest Chemistry, College of Forestry, Syracuse, New York*): In connection with ceric ion initiated grafting it was noted recently that the amount of polymer retained by the cellulose after extraction follows the same order as the swelling ability of the solvent used during the grafting process. It was suggested that little or no grafting occurs, rather homopolymer is trapped in the intermicellar spaces of the cellulose. Our results seem to confirm this hypothesis. Would you care to comment on this?

C. P. J. Glaudemans: The fact that the amount of grafting is proportional to the swelling power of the solvent used, does not, in my opinion, in itself indicate that occlusion rather than grafting takes place. Clearly, the better the solvent can penetrate the substrate the better the chances for extensive grafting.

W. H. Rapson (*Department of Chemical Engineering, University of Toronto, Toronto, Canada*): Was the graft fractionated in any way?

C. P. J. Glaudemans: No.

W. H. Rapson: Our work and that of others has shown that very few cellulose molecules have any grafted vinyl polymer molecules on them (only about 1 in 20 for 100% add-on). Since the experimental error involved in the type of experimental measurements reported in this paper is probably at least 5%, it would not be expected that unfractionated material would provide data indicating grafting by the mathematical method used. While a positive result would prove grafting, a negative result (like the one given) is indeterminate if only a few cellulose molecules have vinyl polymers grafted onto them.

SYMPOSIUM ON MOLECULAR ARCHITECTURE OF WOOD

JOURNAL OF POLYMER SCIENCE: PART C NO. 2, P. 201 (1963)

Symposium on Molecular Architecture of Wood

For the first time in this series of cellulose conferences, a symposium on topics related to the organization of the major wood components in the cell was incorporated into the program. The papers selected for presentation in this session were varied, the subject matter of some being somewhat foreign to cellulose chemists while others were on topics more familiar to them. The reaction to this symposium was, as might be supposed, a mixed one, depending on the interests of the individual. In general, the idea was well received, it being accepted that better utilization of wood can only come from a better understanding of its fundamental morphology.

A sad note was injected into the program by the illness of one of the speakers scheduled for the Symposium. Dr. Friedrich Klaehn was unable to present his paper on: "The Chemical Nature of the Genetic Material in Plants." Two days after the cellulose conference, the field of tree improvement lost one of its most vigorous leaders. Dr. Klaehn was a native of Germany where he was trained as a forester. He held two degrees from the University of Gottingen: Diplom-Forstwirt and Doctor of Philosophy. Dr. Klaehn died at the age of 46. He had been on the faculty of the State University College of Forestry since 1955 and was developing an outstanding program in research and teaching of tree improvement. His paper, presented in these Proceedings, was virtually in final form before he was stricken. The details of preparation for publication were completed by his colleagues: Mr. Clyde Hunt and Dr. F. A. Valentine.

W. A. Côté

JOURNAL OF POLYMER SCIENCE: PART C NO. 2, PP. 203–212 (1963)

Investigation of Lignin Distribution in the Cell Wall of Certain Woods

IRVING B. SACHS, IRA T. CLARK, and JOHN C. PEW, *Forest Products Laboratory, Forest Service, U. S. Department of Agriculture, Madison, Wisconsin**

Introduction

Knowledge of submicroscopic structure and organization of the wood cell has been aided greatly by the use of modern equipment and techniques. Evidence of the distribution of lignin in the cell wall has been provided by Bailey,[1] Ritter,[2] Jayme and Wettstein,[3] Lange,[4] and others. More recently, the electron microscope has made it possible to examine this complex polymer of plant tissue.

Hodge and Wardrop[5] were able to demonstrate the presence of lignin between the microfibrils of *Pseudotsuga* before delignification. Mühlethaler[6] obtained electron micrographs of lignin isolated from sections of *Nothofagus cunninghamii*.

The present investigation uses chemical means and enzymes to isolate lignin for electron microscope studies, utilizing sections of wood tissue prepared according to the micrurgical techniques developed for electron microscopy of biological materials. A staining technique is introduced that permits detection of lignin in cell walls by means of electron microscopy.

Materials and Methods

Sound, green loblolly pine (*Pinus taeda*), white spruce (*Picea glauca*), and sugar maple (*Acer saccharum*) were treated with aqueous hydrofluoric acid in order to limit swelling and distortion. The concentration of the hydrofluoric acid was gradually increased in increments of about 5% from 20 to 80%, and specimens held in 80% acid for $^1/_2$–160 hr. The acid concentration was then diminished stepwise in 10% increments and the specimens finally washed free of acid. They were then boiled gently in 2% hydrochloric acid to remove last traces of carbohydrate and again washed acid free. In addition, sound green spruce was treated with periodate as in the Purves[7] method for preparing lignin. Both the HF- and periodate-treated sections were then embedded in methacrylate resin, either after treatment with 1% OsO_4 or without heavy metal treatment, sectioned at $^1/_{40}$ μ and examined with an RCA EMU3D electron micro-

* Maintained in cooperation with the University of Wisconsin.

scope. The glass knives used in the microtomy of material were prepared by heat tempering processes used by Sachs.[8]

Results and Discussion

With a micromanipulator, Bailey[1] removed a portion of the compound middle lamella in virtually a pure state; Lange[4] approached the problem with a microspectrographic method. Despite the difference in methods, both Bailey and Lange showed that an average of 74% lignin exists in the compound middle lamella and approximately 15–16% in the other layers of the cell wall. For the broad-leaved woods, the values of lignin concentration in the secondary wall were lower. Meier[9] arrived at the same conclusion in an electron microscopic study of wood samples which have undergone degradation by different fungi. Asunmaa[10] contributed information as a result of electron microscopy that well-ordered crystalline structure is not present in the compound middle lamella. These studies and previous conventional staining reactions have shown that the compound middle lamella is heavily lignified and that the highest density of lignin in the wood cell is in the compound middle lamella.

In the loblolly pine studied at the Forest Products Laboratory (Figs. 1 and 2) the lignin appears somewhat spongy and forms a continuous network after carbohydrate removal. The very dense black dots (Figs. 2 and 3) may be random deposits of metallic osmium, since this specimen had been treated with 1% OsO_4. Lignin distribution appears to be in accord with the findings of the other researchers mentioned in that the lignin is

Fig. 1. Loblolly pine wood before treatment. 20,500×.

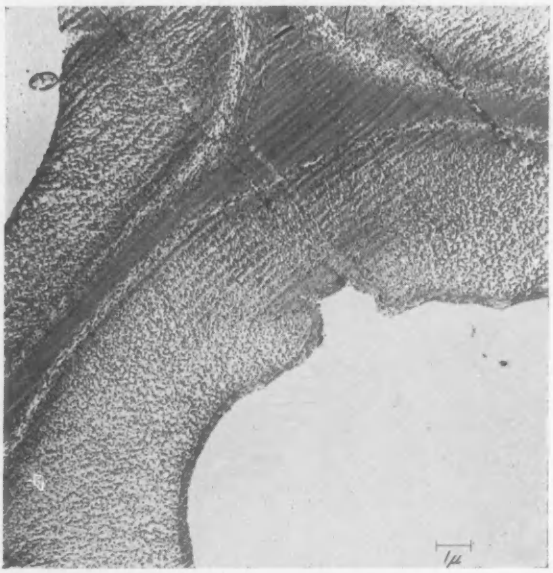

Fig. 2. Lignin obtained by treatment of loblolly pine with HF. 12,000×.

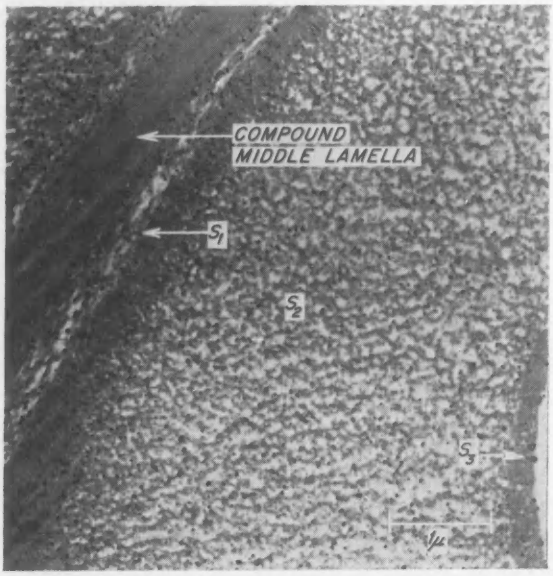

Fig. 3. HF acid lignin from loblolly pine. High magnification of Fig. 2. 32,000×.

Fig. 4. HF acid lignin from loblolly pine with subsequent treatment by calcium chlorite. 8,500×.

highly concentrated in the compound middle lamella and then decreases in the secondary layer. However, an increase in density near the lumen is evident that suggests a high concentration of lignin in the S_3 layer.

The lignin in the compound middle lamella appears dense and without structure. On either side of the compound middle lamella it appears to be laterally oriented. This may mark the position of the S_1 layer. Lignin in the secondary wall is dispersed in a random network. The S_3 lignin appears nearly as dense as the lignin of the compound middle lamella (Fig. 3).

Hydrofluoric acid lignin that had not been stained with OsO_4 was treated with aqueous calcium chlorite (55 g./l.) for 90 min., embedded, and sectioned. Bodies 200–600 A. in diameter were visible throughout the compound middle lamella (Fig. 4). These may represent areas of densified or more highly polymerized lignin in the compound middle lamella.

Lignin that is obtained by treatment of spruce with periodate or HF has a spongelike appearance similar to that obtained from loblolly pine by treatment with HF. Figure 5 shows HF spruce lignin, and Figure 6 shows lignin isolated from spruce by periodate treatment. Figure 7 shows lignin that was obtained from spruce by swelling with 8% aqueous NaOH and digested with enzyme (*trichoderma viride*). These again show

lignin concentrated in the compound middle lamella, lateral orientation at the S_1 position, uniform distribution throughout the secondary wall, and the presence of a S_3 layer.

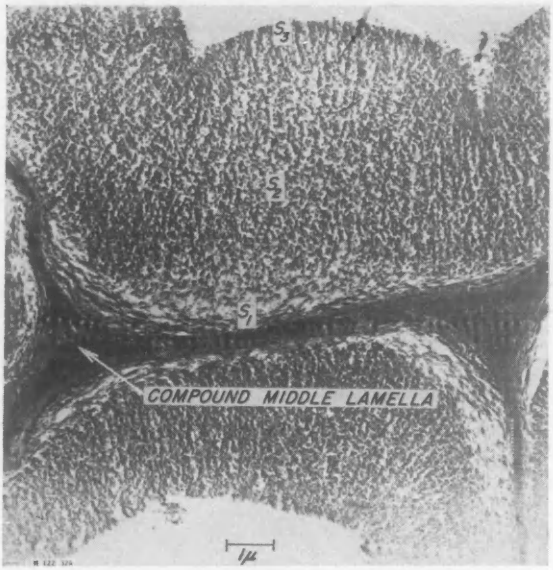

Fig. 5. HF acid spruce lignin. 16,000×.

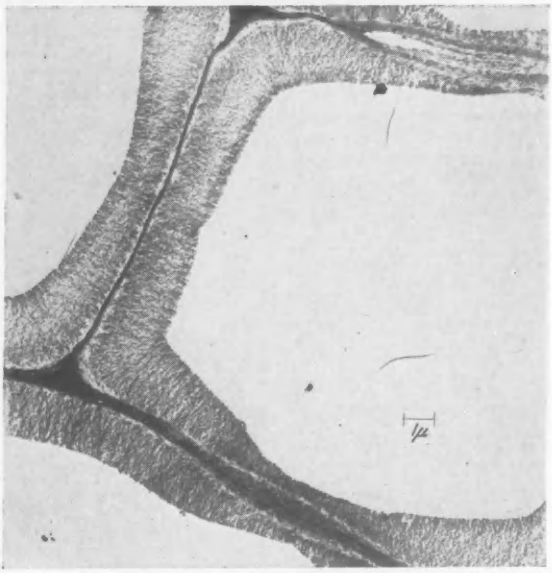

Fig. 6. Spruce periodate lignin. 10,000×.

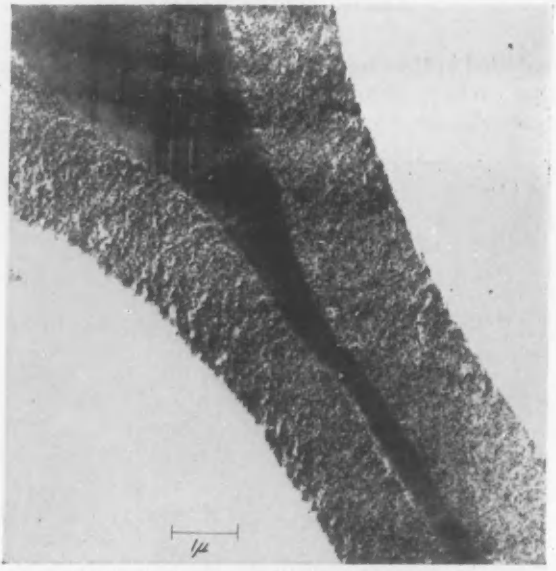

Fig. 7. Spruce lignin obtained by swelling with NaOH and treatment with *trichoderma viride*. 20,500×.

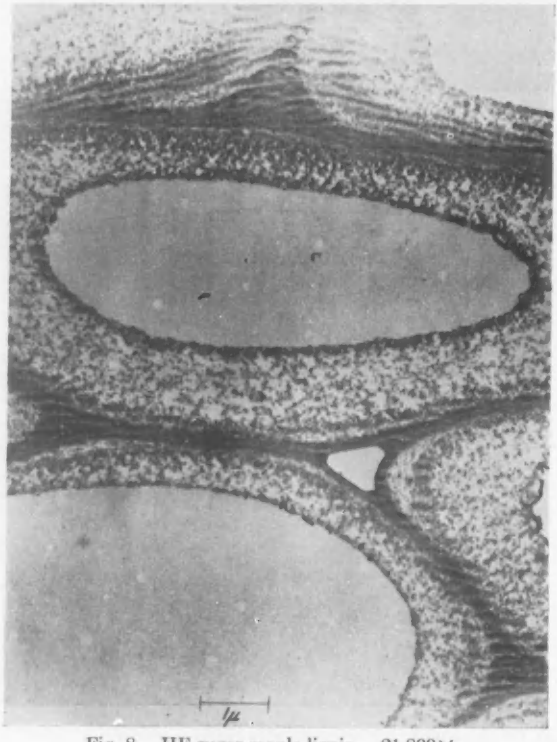

Fig. 8. HF sugar maple lignin. 21,800×.

Fig. 9. Rapidly swollen HF maple lignin. 7,000×.

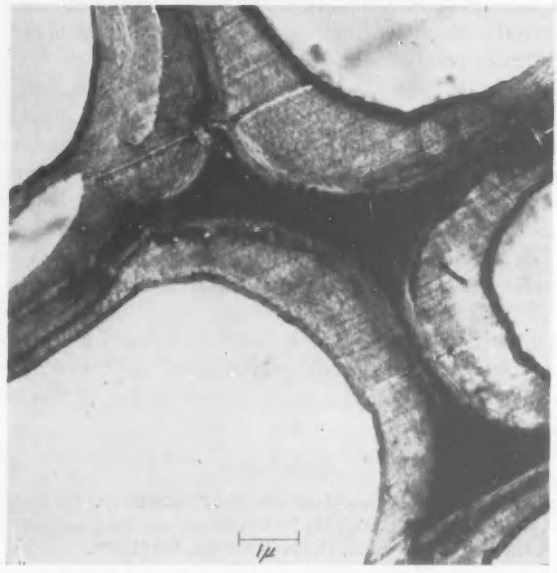

Fig. 10. Spruce wood treated with *p*-(acetoxymercuri)aniline. 18,500×.

In the wood of broad-leaved trees lignin is also distributed throughout the cellular structure, but a greater proportion of it is concentrated in the compound middle lamella, and the network in the secondary wall is less dense than in softwoods. This is shown in Figure 8, which is sugar maple lignin that was obtained by treatment of the wood with HF for 160 hr., and was completely free of carbohydrate. Maple lignin obtained by a rapid 2-hr. treatment, which resulted in excessive swelling and some distortion, shows a similar distribution (Fig. 9).

Chemical analysis that were run on parallel samples indicate the HF lignin to be substantially carbohydrate-free. Carbon-hydrogen analysis and methoxyl content correspond to those of lignin obtained by other treatments such as by H_2SO_4. The lignin isolated from loblolly pine was 26.4% of the wood and contained 0.2% reducing substance. That from spruce was 26.32% of the wood and contained 0.3% reducing substance. The periodate lignin contained 3.6% reducing substance. The enzyme lignin contained about 50% reducing substance. The maple lignin specimen treated in HF for 160 hr. was completely free of carbohydrate. That from the 2-hr. treatment contained 18.5% nonlignin materials.

It is possible that the lignin has been structurally or chemically modified (swelling, coagulation, or polymerization) as a result of chemical treatments, or there may be differences in the structural pattern when in association with the cellulose microfibrils.

To avoid these effects and to obtain contrast for the electron microscope, sections of spruce were treated with *p*-(acetoxymercuri)aniline which reacts with coniferyl aldehyde groups in lignin. Specimens treated in this manner show the same distribution pattern of lignin as observed in the specimens described earlier (Fig. 10).

The present study presents evidence that in wood the greatest density of lignin appears in the middle lamella, the primary wall, and the S_3 layer. In the secondary wall it exists as a branched, three-dimensional network interspersed around the crystalline cell wall structures. Layering of the cell wall lignin is evident in area of the compound middle lamella in lignin specimens isolated by all treatments used and represents the location of primary walls and S_1 layers. Separations at these locations may be the result of swelling or microtomy and point to structural weaknesses in these areas.

Clearly, additional information is needed on the fine structure of the cell wall, and correlation of chemical methods and modern microscopy techniques should bring about greater understanding of the organization at the intracellular level.

References

1. Bailey, A. J., *Ind. Eng. Chem. Anal. Ed.*, **8**, 52 (1936).
2. Ritter, G. J., *Ind. Eng. Chem.*, **17**, 1194 (1925).
3. Jayme, G., and R. Wettstein, *Papier-Fabr.*, **36**, 519 (1938).
4. Lange, P. W., *Svensk Papperstidn.*, **57**, 525 (1954).
5. Hodge, A. J., and A. B. Wardrop, *Australian Sci. Res.*, **3B**, 265 (1950).
6. Mühlethaler, K., *Biochim. Biophys. Acta*, **3**, 15 (1949).

7. Ritchie, P. F., and C. B. Purves, *Pulp Paper Mag. Canada*, **48**, Pt. 2, 74 (1947).
8. Sachs, I. B., *Forest Prod. J.*, **13**, 80 (1963).
9. Meier, H., *Holz Roh. Werkstoff*, **13**, 323 (1955).
10. Asunmaa, S., *Svensk Papperstidn.*, **58**, 308 (1955).

Synopsis

Sound, green loblolly pine, white spruce, and sugar maple were treated chemically to remove the cellulose and hemicellulose framework of wood cells in order to study, with the electron microscope, the distribution of lignin throughout the compound middle lamella and secondary cell walls. To limit swelling and distortion, sections of wood 30 μ to 2 mm. thick were treated with aqueous hydrofluoric acid in gradually increasing concentrations. Other sections were treated with periodic acid or *tricoderma viride* enzyme. The material was then embedded in acrylic resin, sectioned at $^1/_{40}$ μ, and observed with an electron microscope. In the species of woods studied, much of the lignin appears in the middle lamella. Considerable lignin uniformly distributed is present in the secondary wall with a definite increase in the secondary wall adjacent to the cell lumen. After carbohydrate removal, the secondary wall lignin appears somewhat spongy and forms a continuous network. The lignin of the S_1 is fairly compact, diminishing in density adjacent to the S_2 layer. That in the S_2 is dispersed in a random network and the lignin in the S_3 is as dense and compact as the lignin of the compound middle lamella. Sections of spruce treated with *p*-(acetoxymercuri)aniline showed the same distribution pattern of lignin as observed in the chemically treated specimens. In addition, effects of possible differential swelling across the cell wall layer were noted that may represent structural weaknesses in these areas. Loblolly pine lignin, which was isolated by hydrofluoric acid treatment and followed by a secondary treatment with calcium chlorite, revealed a pattern of small bodies 200–600 A. in diameter in the middle lamella.

Résumé

On a traité chimiquement le bois du pin vert, du sapin blanc et de l'érable à sucre, afin d'éliminer la charpente de cellulose et de hémicellulose des cellules de bois, et d'étudier, à l'aide du microscope électronique, la distribution de lignine dans les lamelles composées médianes et dans les parois cellulaires secondaires. Des sections de bois d'une épaisseur de 30 μ à 2 mm ont été traitées avec des solutions de plus en plus concentrées d'acide fluorhydrique, jusqu'au moment où le gonflement et la distorsion atteignent le maximum. D'autres sections ont été traitées avec l'acide periodique ou avec l'enzyme *tricoderma viride*. Ensuite les produits étaient incrustés dans la résine acrylique, sectionnés à $^1/_{40}$ μ et observés à l'aide du microscope électronique. Dans les espèces de bois étudiées la plus grande partie de la lignine se trouve dans les lamelles médianes. Dans les parois secondaires se trouve une quantité considérable et uniformément distribuée de lignine, avec une augmentation bien définie dans la paroi secondaire adjacente au lumen cellulaire. Après l'élimination des hydrocarbures la paroi secondaire semble un peu spongieuse et forme un réseau continu. La lignine de la S_1 est relativement compacte, et la densité diminue au voisinage de la couche S_2. Celle de la S_2 est dispersée selon un réseau statistique, et la lignine de la S_3 est aussi dense et aussi compacte que celle des lamelles médianes. Les sections de sapin traitées avec la *p*-(acétoxymercuri)aniline montraient la même distribution de la lignine que celle des sections qui étaient traitées chimiquement. De plus, on a noté des effets d'un gonflement différentiel possible de l'autre côté de la paroi cellulaire, qui peuvent indiquer des faiblesses structurelles dans ces zones. La lignine du pin isolée par un traitement avec l'acide fluorhydrique, suivi d'un traitement secondaire avec le chlorite de calcium, montrait un réseau de petites particules (diamètre 200 à 600 A.) dans les lamelles médianes.

Zusammenfassung

Gesunde grüne Weihrauchkiefer, Weissfichte und Zuckerahorn wurden zur Entfernung des Cellulose- und Hemicellulosegerüstes der Holzzellen chemisch behandelt, um elektronenmikroskopisch die Verteilung von Lignin innerhalb der zusammengesetzten Mittellamelle und der sekundären Zellwände untersuchen zu können. Um Quellung und Verformung hintanzuhalten wurden 30 μ bis 2 mm dicke Holzschnitte mit wässriger Fluorwasserstoffsäure in schrittweise zunehmender Konzentration behandelt. Andere Schnitte wurden mit Perjodsäure oder dem Enzym *Tricoderma viride* behandelt. Das Material wurde dann in Acrylharz eingebettet, $^1/_{40}$ μ-Schnitte angefertigt und mit dem Elektronenmikroskop untersucht. In den untersuchten Holzarten erscheint ein grosser Teil des Lignins in der Mittellamelle. Eine beträchtliche Ligninmenge ist einheitlich verteilt in der Sekundärwand vorhanden, wobei eine eindeutige Zunahme in der dem Zell-Lumen benachbarten Sekundärwand auftritt. Nach der Entfernung der Kohlehydrate erscheint das Lignin der Sekundärwand etwas schwammartig und bildet ein kontinuierliches Netzwerk. Das Lignin von S_1 ist ziemlich kompakt und nimmt in der Nähe der S_2-Schichte an Dichte ab. Dasjenige in S_2 ist in ein statistisches Netzwerk verteilt und das Lignin in S_3 ist ebenso dicht und kompakt wie das Lignin der zusammengesetzten Mittellamelle. Fichtenschnitte zeigten bei Behandlung mit *p*-(Acetoxy mercuri)-anilin den gleichen Verteilungszustand von Lignin, wie er bei den chemisch behandelten Proben beobachtet wurde. Ausserdem wurden Effekte einer möglicherweise differentiellen Quellung in der Zellwandschichte beobachtet, die Anzeichen für Strukturunregelmässigkeiten in diesen Bereichen bilden können. Weihrauchkieferlignin, das durch Fluorwasserstoffsäure-Behandlung isoliert und dann einer sekundären Behandlung mit Kalziumchlorit unterzogen worden war, zeigte eine Anordnung von kleinen Körpern, 200–600 A. im Durchmesser, in der Mittellamelle.

Discussion

D. A. I. Goring (*Pulp and Paper Research Institute of Canada, Montreal, Canada*): We have observed a granular structure of small spherical bodies, 30–60 A. in diameter by high resolution electron microscopy of lignin sulphonate macromolecules. Have you any indication of a structure of this size range in the lignin of the middle lamella or the cell wall?

I. Clark: The smallest lignin structures detected in the present work were granular particles as small as 200 A. that appeared in the compound middle lamella of HF spruce lignin that was treated with calcium chlorite.

C. Schuerch (*Forest Chemistry Dept., College of Forestry, Syracuse, N. Y.*): Might it be possible to separate by physical methods, density differences, etc. lignins from the middle lamella, secondary wall, etc. in order to search for chemical differences in structure?

I. Clark: Lignin isolated by means of hydrofluoric acid retains the approximate dimensions of the original wood while still wet. It has sufficient tensile strength to retain its structure, but is soft and pliable. In this condition, it might be possible to remove fractions by means of a micromanipulator. When dried it shrinks, is quite fragile, and would be difficult to handle. In either instance, it is a typical acid lignin and might not contribute any new information on chemical differences of lignin.

E. B. Cowling (*Yale University, School of Forestry, New Haven, Conn.*): Do you believe that the pores shown in the S_2 layer of coniferous woods between fragments of lignin existed in the wood before removal of the carbohydrates or were they formed or enlarged by the swelling action of the reagents during the removal of the carbohydrate material.

I. Clark: It is quite likely that the pores visible in the S_2 layer of lignin that was isolated by HF were enlarged by the swelling action of the HF or by loss of fine lignin structure. However, periodate lignin which was not subjected to excessive swelling during isolation also shows a porous structure.

JOURNAL OF POLYMER SCIENCE: PART C NO. 2, PP. 213–219 (1963)

Tertiary Wall and Warty Layer in Wood Cells

WALTER LIESE, *Forstbotanisches Institut und Institut für Holzforschung und Holztechnik, Universität München, Munich, Germany*

I. TERTIARY WALL

The lignified cell wall of tracheids, fibers, and vessels of softwoods and hardwoods is separated from the cell lumen by a distinct layer. The presence of such a lining was first established in 1843 by Hartig,[16] and later confirmed by several other workers. Different names have been applied to this part of the cell wall: ptychode,[16] tertiary wall,[9,37] inner layer of the secondary wall,[19] and S_3.[42] The question of terminology has been discussed in detail by Bucher.[4] Since this layer is in many ways different from the outer and central part of the secondary wall, we prefer, in agreement with other workers,[4,30,33] the term "tertiary wall," recognizing the objections towards a change of the established terminology.[2,34] The term is being used without any ontogenetic significance. Whereas much effort has been directed in the past to explore the general structure of the lignified cell wall, not so much attention has been paid to the tertiary wall. This layer, however, seems to be not only interesting for the differentiation of the cell wall, but also has some influence on technically important cell wall and wood properties.

Light Microscope Studies

When transverse sections are investigated with the light microscope between crossed nicols, the tertiary wall appears as a birefringent layer in contrast to the dark secondary wall. This reveals a flat orientation of the elementary fibrils in relation to the cell axis. Certain species, like *Picea abies* and *Betula verrucosa* sometimes do not present such evidence for the existence of the tertiary wall. The lack of a birefringent inner layer does not mean that the tertiary wall is absent, since its recognition in cross sections by using the polarizing microscope depends on a flat, helical microfibrillar orientation. As will be discussed later, the orientation of the microfibrils within the tertiary wall varies considerably.

Further knowledge about the tertiary wall and its properties has been obtained by using swelling and staining reactions. Bucher,[4] in particular, investigated the structure of the tertiary wall in tracheids of several conifers and established its morphological individuality. The presence of the tertiary wall was confirmed also for fibers of hardwood species by a similar technique.[10] Our investigations showed that the different forms of the

tertiary wall in conifer tracheids are related to some extent to preparation artifacts. By applying such a chemical treatment it is essential to distinguish the tertiary wall clearly from the additional warty layer. Since both lamellae differ from the secondary wall and show a similar behavior, procedural misinterpretations are possible. These difficulties in recognizing and investigating the tertiary wall contributed to the lack of information about this layer until electron microscopy enabled its direct observation. The work of recent years, therefore, broadened our knowledge about the fine structure of the tertiary wall to a considerable degree.

Electron Microscopic Studies

1. Thickness. The tertiary wall, as a thin layer, lines the entire cell lumen. Sections show that its thickness is quite even within one cell. Differences may occur between different cells, between species and especially between softwoods and hardwoods. In softwood species, such as *Pinus silvestris* and *Picea abies*, the thickness of the tertiary wall is generally about 700–800 A.; however, it is sometimes considerably thinner. Compared to softwood species the hardwood species mostly have a thinner lining. Differences exist among the species: the tertiary wall appears to be thicker in *Robinia*, *Castanea*, and *Fagus* than in *Betula*, *Fraxinus*, and *Tilia*. Further studies are necessary, to obtain more information about its thickness in different species.

2. Texture. The texture of the tertiary wall can be investigated ideally on species which do not have an additional warty layer, since the warts may veil its structure. The tertiary wall is composed of microfibrils and amorphous material as a matrix (Fig. 1). The thickness of the microfibrils varies on shadowed replicas between 120 and 180 A. Whereas the microfibrils

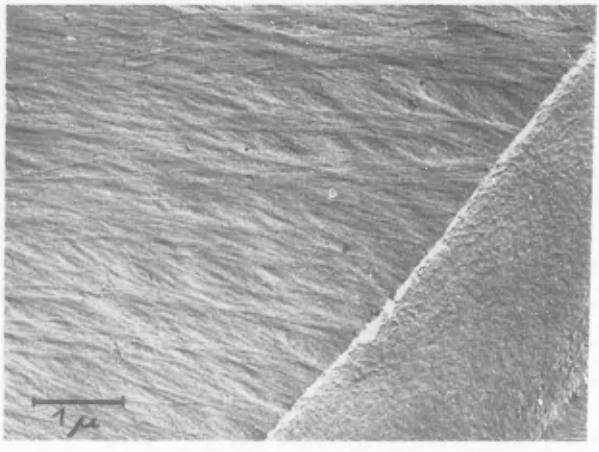

Fig. 1. Tertiary wall of a tracheid with a slightly woven texture of microfibrils; *Picea abies;* in the right corner hypha of blue stain fungus.

in the secondary wall lie in a preferred parallel arrangement, the texture of the tertiary wall is remarkably different. The microfibrils are often joined into small bundles and criss-cross each other at an angle of preferably 20–30° (Fig. 2). Consequently, a slightly woven texture originates which is the typical feature of the tertiary wall. Because of these bundles of microfibrils, the tertiary wall often displays an uneven surface in cross sections of cells. During our electron microscopical studies of several hundreds of softwoods and hardwoods, we at no time found species with strictly parallel-oriented microfibrils in the tertiary wall. The appearance of this woven texture in the tertiary wall can vary in different ways. The meshwork can be loose or tight, and the cross angle may amount to approxi-

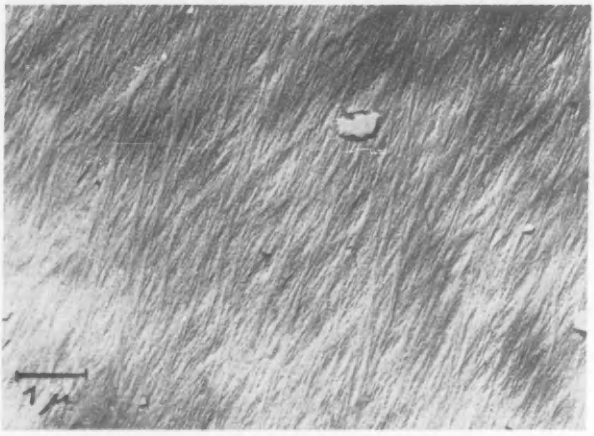

Fig. 2. Tertiary wall of a fiber; *Fagus silvatica*.

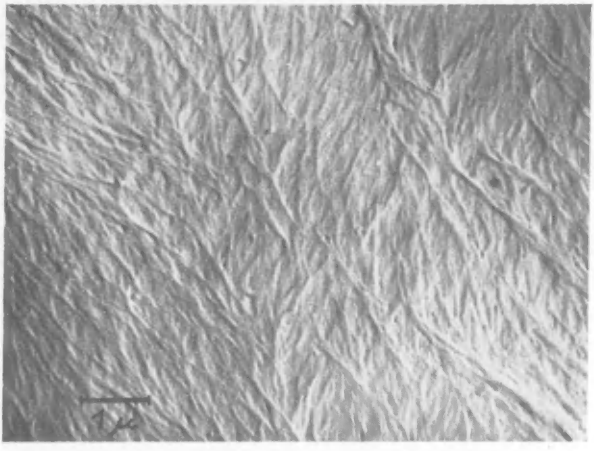

Fig. 3. Tertiary wall of a tracheid with intensively woven texture; *Picea abies*.

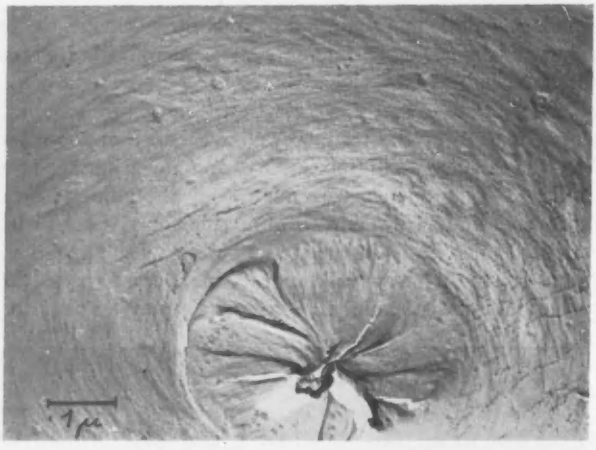

Fig. 4. Tertiary wall of a pit chamber with a woven texture; *Picea abies*.

mately 50° (Fig. 3). The tertiary wall of one cell may show different forms. In some cases its appearance resembles the texture of the primary wall.

The tertiary wall covers not only the inside of tracheids, fibers, and vessels, but also the chamber of bordered pits and the channels of simple pits (Fig. 4). Here it possesses the same woven texture, as has been described for it in the cell wall. It should also be mentioned, however, that the lamellates of the secondary wall do not always show a strictly parallel arrangement.

3. Orientation of Microfibrils. The tertiary wall exhibits a wide variation regarding its microfibrillar orientation. The microfibrils are wound within the cell either in righthand (Z) or lefthand (S) direction. This tendency seems to be almost equal for *Pinus silvestris*, whereas for *Picea abies*, *Larix decidua*, and *Sequoia gigantea* a preferable lefthand orientation could be observed.

Due to the criss-cross texture of the tertiary wall, it is difficult to obtain

TABLE I

Orientation of Microfibrils in the Tertiary Wall in Relation to the Cell Axis

Angular deviation	Number of observations		
	Pinus silvestris	*Picea abies*	*Pseudotsuga taxifolia*
20–30°	1	2	2
30–40°	3	2	2
40–50°	2	5	1
50–60°	3	6	1
60–70°	2	3	1
70–80°	9	6	6
80–89°	46	5	4

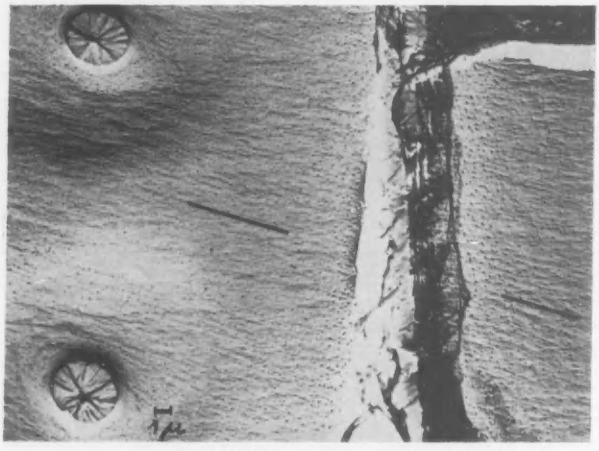

Fig. 5. Tertiary wall with a flat helical orientation of microfibrils; *Pinus silvestris.*

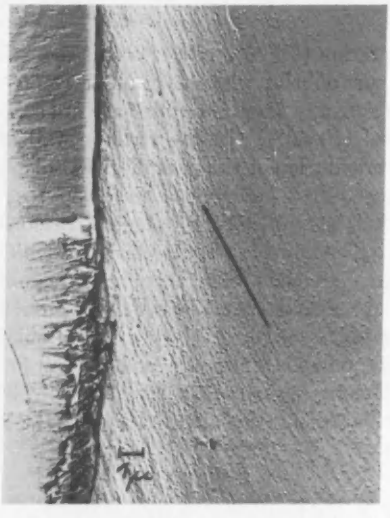

Fig. 6. Tertiary wall with a steep helical orientation of microfibrils; *Pinus silvestris.*

exact results of the slope of orientation in relation to the cell axis. However, by combining the varying orientations an approximate measure can be obtained.[24] Consequently the data given in Table I, are combined by groups.

As it can be seen from these results, the orientation of the microfibrils differs considerably. The tracheids of *Pinus silvestris* show preferentially a flat helical orientation, with an angle of 80–89° to the cell axis (Fig. 5). There are often other tracheids, however, lying alongside, which exhibit

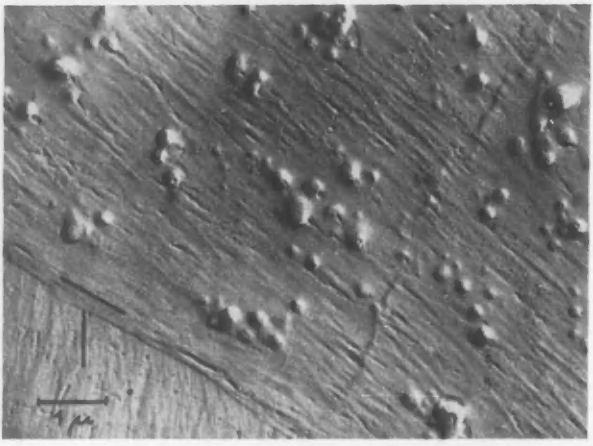

Fig. 7. Different orientation of microfibrils in the tertiary wall and the upper lamella of the secondary wall; *Pinus silvestris*.

a rather steep orientation (Fig. 6). *Picea abies* has a wide variation in the orientation of the microfibrils, whereas in other conifers like *Pseudotsuga taxifolia*, *Larix decidua*, and *Taxus baccata*, they are arranged mostly in the form of a flat spiral (70–89°). In the tertiary wall of hardwood fibers, a moderate helical orientation of the microfibrils is displayed preferentially for *Betula verrucosa* 60–80°, for *Fagus silvatica* 50–70°, for *Populus nigra* 70–80°, and for *Salix alba* 50–60°, although here considerable variation could be observed. The flow of the microfibrils is modified by the openings of the pits, which are entwined around them in a streamlike pattern.

The orientation in the tertiary wall is rather different from the secondary wall lamella, lying just beneath (Fig. 7). Measurements of these differences could be made on cells where the tertiary wall has been partially removed.[24] Table II contains such data for *Pinus silvestris* and *Picea abies*. Since the microfibrillar orientation of both lamellae, the tertiary wall and the

TABLE II

Differences in the Orientation of Microfibrils between the Tertiary Wall and the Upper Lamella of the Secondary Wall

Angular deviation	Number of observations	
	Pinus silvestris	*Picea abies*
1–10°	3	1
10–20°	4	2
20–30°	3	4
30–40°	5	3
40–50°	4	
50–60°	1	1
60–70°		

S_2 lamella, can change within one cell, the angle of divergence can consequently vary.

4. Chemical Nature. Because the tertiary wall is composed of only a thin lamella, it is difficult to isolate it from the adjoining secondary wall. Therefore, not much has been known until now about its chemical nature. Several observations indicate that the chemical composition differs from that of the secondary wall. It is well known, especially from the work of Bucher,[4,5] who also summarized the observations of other authors, that the tertiary wall has a certain resistance to acids and alkalis, which lead to specific swelling and staining properties. While the whole secondary wall expands, the tertiary wall still remains more or less unchanged. It appears largely destroyed in sulfite pulp and seems to be well preserved in sulfate pulp.[32] Furthermore, the tertiary wall has a remarkable resistance against the ectoenzymes of certain wood-destroying fungi.[3,28,29] The hyphae of the so-called soft rot fungi grow preferably within the secondary wall, which will be completely destroyed by their action, whereas the tertiary wall remains apparently unattacked until the last stages. The tertiary wall also demonstrates a high resistance against attacks of brown rot fungi, since the ectoenzymes seem to diffuse through the tertiary wall into the secondary wall, where the hydrolysis occurs. In contrast, the ectoenzymes of white rot fungi destroy all parts of the cell wall quite equally. This resistance of the tertiary wall might be attributed to a greater lignification, which has been found in conifer tracheids.[36] Investigations by Meier and Yllner[32] revealed a considerable amount of xylan and mannan in the tertiary wall. Wardrop and Dadswell[43] concluded that it is composed partly of cellulose. By analyzing fractions from microsections Meier[31] found that the cellulose content decreases in the innermost part of the summerwood tracheids of *Pinus silvestris*, whereas the glucuronoarabinoxylan content is high. There are indications that the same applies also for the summerwood tracheids of *Picea abies*.

5. Development. According to the apposition theory the tertiary wall is deposited as the last part of the cell wall. Observations with the polarizing microscope on differentiating tracheids, however, show that partially developed cells already have a thin refractive layer near the protoplast. The microfibrils of this layer therefore, must have a similar orientation as those of the tertiary wall. This fact was presented by Strasburger[41] and Dippel.[9] Assuming that the refractive lamella in developing tracheids corresponds to the later tertiary wall, one could consider this birefringent layer to participate in the formation of the lamellae of the secondary wall, an idea which is supported by Frey-Wyssling.[11] Further electron microscopic studies will clarify the origin and development of the tertiary wall.

In the gelatinous fibers of tension wood, a lamella of greater density and apparently more compact organization exists either between the S_2 and the G layer or as the inner boundary of the G layer. It seems to be equivalent to the tertiary wall.[6,43] In the tracheids of compression wood of conifers the tertiary wall appears to be absent, as was already observed by Hartig[17]

and has been confirmed by electron microscopical studies. The suberin layer of the cell wall in bottle cork (*Quercus suber*) is covered against the lumen by a distinct tertiary wall, which seems to be incrusted with osmiophilic substances.[39]

As the above survey shows, formation and chemical composition of the tertiary wall are not yet fully understood and further work is regarded as necessary. Special attention must be tendered also to clarify its importance for certain properties of lignified cells, such as absorption and diffusion of liquids, swelling properties, as well as behavior during chemical dissolution.

II. WARTY LAYER

For a long time it was thought that the tertiary wall forms the innermost lining in wood cells. Electron microscopical studies, however, revealed, that in most species an additional layer against the cell lumen exists, the so-called warty layer.[14,15,20,23,26] This peculiar structure covers the tertiary wall in tracheids, fibers and vessels, and consequently also in the chambers of bordered pits and the channels of simple pits. It is present in wood cells throughout the tree, in springwood and summerwood, in sapwood and heartwood, in branches and in roots of the stem. The warty layer consists of more or less spherical particles, the warts, which are often covered by an additional layer (Figs. 8–10). It has to be distinguished from protoplasmic material, which occurs with the replica technic in parenchyma cells and from extraneous material derived from heartwood formation.

Appearance of the Warty Layer

The appearance of the warty layer can be quite varied. This is due to the number and size of the warts and the presence or absence of the addi-

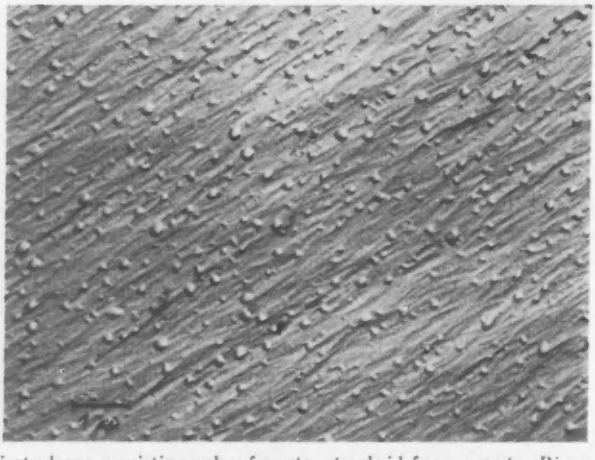

Fig. 8. Warty layer consisting only of warts; tracheid from a root; *Pinus silvestris*.

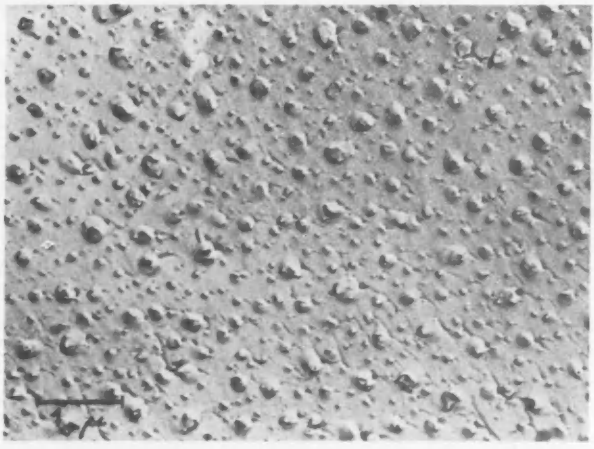

Fig. 9. Warty layer consisting of warts and amorphous layer; *Cedrus atlantica*.

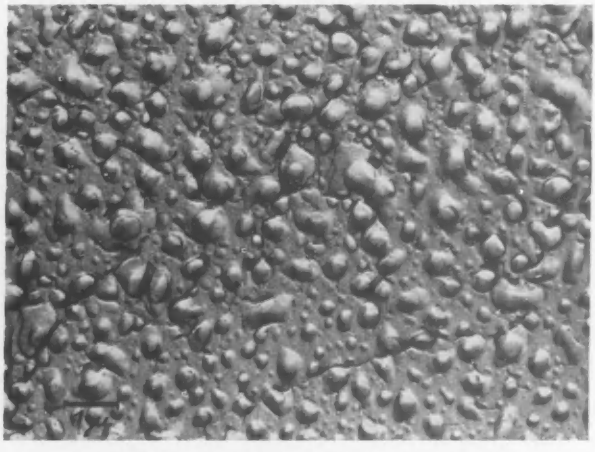

Fig. 10. Warty layer lining a vessel; *Fagus silvatica*.

tional layer. The frequency of the warts can range from a very dense arrangement, where one is lying beside the other, to such a sparsity that the cell wall seems to be almost without warts. Their distribution is mostly quite regular. Within species the frequency varies to some extent. In general, however, a distinction is possible between species and even genera such as *Picea*, with very few warts, others like *Larix* with frequent warts, and finally species with very dense warts, as present in *Callitris*. Conifers with resin canals often have a less pronounced warty layer, with the distinct exception of *Pinus*. Within most of the genera, all the species investigated until now, possess a similar pattern of the warty layer. The

genus *Pinus*, however, shows a remarkable split between the Haploxylon species and the Diploxylon species.[12,21] While the former rarely display a distinct warty layer, it is well developed in the latter. The dimensions of the warts vary considerably. Extensive measurements were made on their size and distribution within a cell, tree and species, resulting in a range from $<0.01\mu$ to $>1\mu$ (Fig. 11). The average diameter lies in the range 0.1–0.2 μ. Only a few species such as *Widdringtonia dracomontana* have warts larger than 0.5 μ[22] (Fig. 12). Since the optical resolution of the light microscope is about 0.2 μ, the presence of a warty layer can be seen in most of the species with the light microscope, as has been verified by an investigation[25] of several hundreds of softwood and hardwood species (Fig. 13). Until electron microscopical studies gave evidence of this structure, only a few observations were obtained regarding a "granular appearance" of the cell wall.[1,13,18]

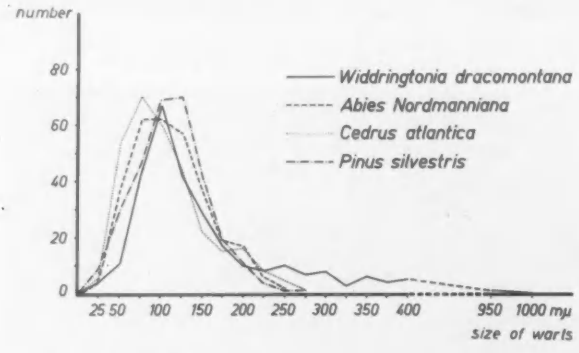

Fig. 11. Size distribution of 300 warts on cell wall tracheids.

The discernibility of the warts in the electron microscope is different in different species. In some species the warts are clearly recognized; they appear to lie directly on top of the tertiary wall so that its microfibrils are distinctly visible between the warts (Fig. 8). In other species they are covered by an additional layer, which forms pouches into the cell lumen in which the warts are cased (Figs. 9, 10, and 12). This layer seems to be amorphous in most cases, yet sometimes it contains a fibrillar structure (Fig. 14). In these cases the tertiary wall is not detectable and also the warts appear obscure. The presence or absence of such a layer is quite coincident within species and genera, but there are exceptions.

Furthermore the pit chambers are covered with warts. Their size is smaller and not so variable as in the tracheids. In half bordered pit pairs, only the side from the tracheary element displays a warty layer.

The existence of the warty layer is not restricted to normal differentiated, lignified cells of softwoods and hardwoods. It is present in compression and tension wood, in the tracheids of vascular bundles from needles (Fig. 15),

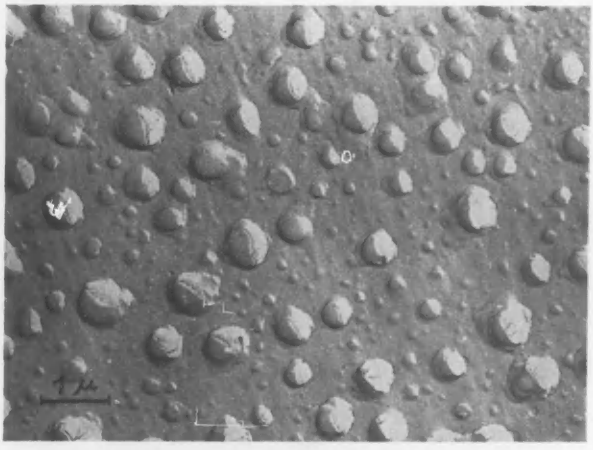

Fig. 12. Warty layer; *Widdringtonia dracomontana*.

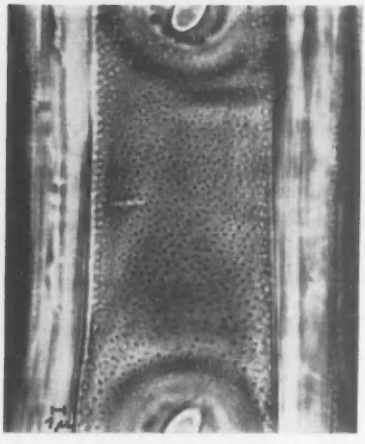

Fig. 13. Warty layer in the light microscope; *Cedrus deodara*.

in unlignified cells, like cotton hairs, and also in vascular cells of herbacous plants.[27]

On the basis of detailed investigations about the appearance of the warty layer its taxonomic significance can be judged. The variability regarding frequency and size of the warts reduce its value for identification purposes. On the other hand, some characters, like the absence of the warty layer in certain species and genera, as well as the big warts of several species, could be used to some advantage together with other anatomical features. So are the macroscopically similar European conifers, *Picea abies* and *Abies alba*, usually distinguished by the different structure of the rays and the absence of resin canals in *Abies*. In addition the latter clearly shows warts

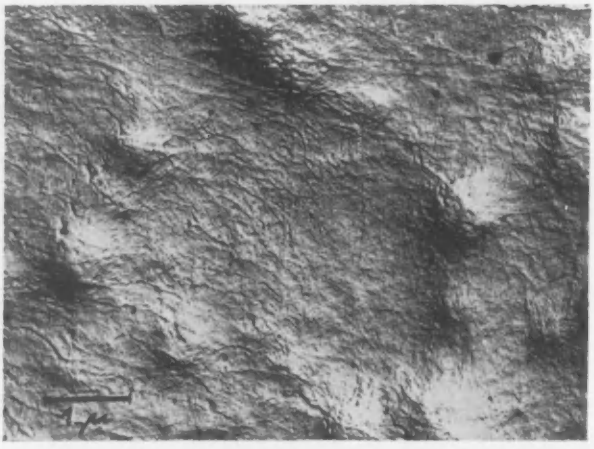

Fig. 14. Warty layer with fibrillar membrane (tonoplast); *Dalbergia sissoo.*

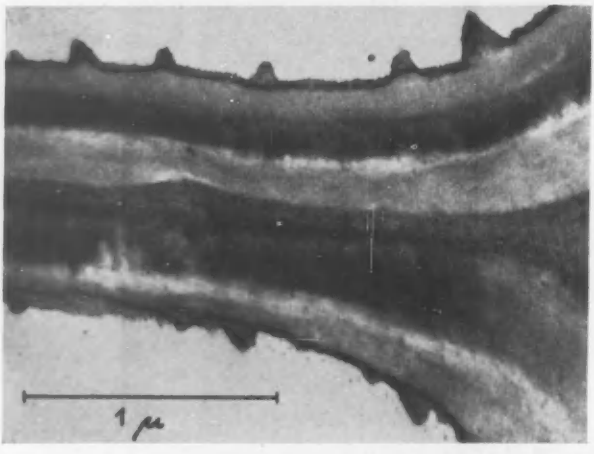

Fig. 15. Warty layer in the tracheids of a vascular bundle from a needle; *Pinus silvestris;* in cooperation with Dr. Ledbetter, Harvard University.

in the light microscope, which are not visible in *Picea*. The warty layer also has some value for the systematic classification of genera and species. As was already mentioned for *Pinus*, the two subgenera and even some of the sections differ remarkably in the frequency and size of the warts. An attempt has been made to compare the appearance of the warty layer within the different species with their classification by Pilger.[21] In certain families, all species investigated thus far exhibit with the aid of the light microscope, a pronounced warty layer like that of the Cycadaceae, Cupressaceae, Dipterocarpaceae, Magnoliaceae, Lauraceae, Leguminosae, Myr-

taceae and Wintereaceae. Anatomical descriptions of wood species, therefore, should also include observations of the warty layer, if possible.

Chemical Nature

The chemical composition of the warty layer is not fully known. Ultraviolet examinations on isolated material have shown that its two components, the warts and the membrane are chemically different, for only the former are ultraviolet absorbing.[46] In addition they are extremely dense to electrons. The warty layer seems to be isotropic in polarized light between crossed nicols. Its refractive index has been calculated as n = 1,52. This figure corresponds to those of embedding materials, such as

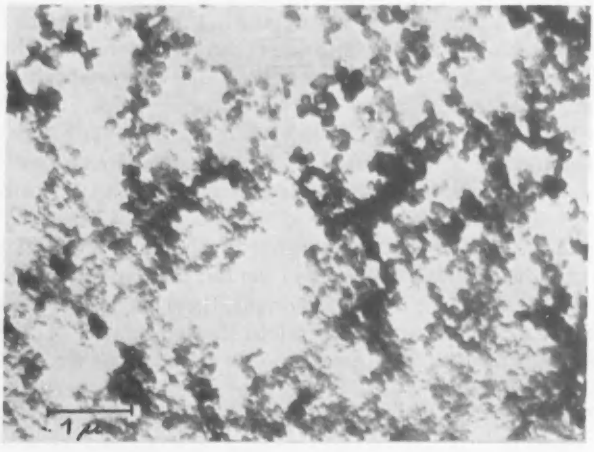

Fig. 16. Warts as remnants after cell wall dissolution.

Canada balsam. Consequently, the warty layer is to some extent suppressed in permanent slides, whereas it can be seen much more easily in sections mounted only in water. It contains osmiophilic substances and with appropriate staining it exhibits protein and lignin.

The warty layer is remarkably resistant to chemical dissolution. Studies concerning its solubility showed a resistance to 98% sulfuric acid, 17.5% sodium hydroxide, hydrogen peroxide, sodium hypochlorite, but a solubility after acetylation or treatment with sodium hydroxide and chlorine water, and hydrogen peroxide and acetic acid.[8,46] This resistance of the warty layer made its isolation possible by using the method of Pew,[35] which consists of soaking sections in formaldehyde and then triturating with 72% and concentrated sulfuric acid (Fig. 16). A microchemical analysis of such remains from several conifer species resulted in a carbon content of 47–60%, a hydrogen content of 5.5–6%, an oxygen content of 32–40%, and a methoxyl content of 3.6–7.1%; the nitrogen content of this material was low (0.6–2.1%).[8]

This remarkable resistance of the warty layer against chemical dissolution might explain difficulties regarding the filterability of solutions in the production of cellulose acetate and viscoses.[40] The filters are often blocked by material which has not been dissolved. This haze or "gel" consists of a nearly monodisperse fraction of spherical or potato shaped particles, as well as membrane fragments. Since similar remnants can be obtained from the warty layer (Fig. 16), it is probable that the above material also belongs to this layer.

Development

The warty layer develops during the last stages of cell differentiation. Light microscopical studies on the conifer *Actinostrobus*, where the warts are clearly visible, proved that they appear in the tracheids some cell rows behind the cambium, when lignification occurred (Phloroglucin-HCl staining) and the protoplasm disappeared.[46] Origin and composition of the warty layer could be clarified with the electron microscope.[27,45] In the last stages of the differentiation of vascular cells the protoplast lines the wall only in the form of a small tube. It is surrounded by two membranes, against the cell wall the plasma membrane (ectoplast, plasmalemma) and against the vacuole the tonoplast. Between them exists the remaining cytoplasm. With progressive aging of the cell, spherical particles occur within the cytoplasm. When in the last stage of differentiation the tonoplast collapses on the plasmamembrane, these particles are covered by the former and pouches are built up into the cell lumen. Their content corresponds with the warts, whereas the tonoplast forms the layer, which covers the warts. The warty layer, therefore, is the remainder of the dying protoplast. The reasons for its variable appearance in different

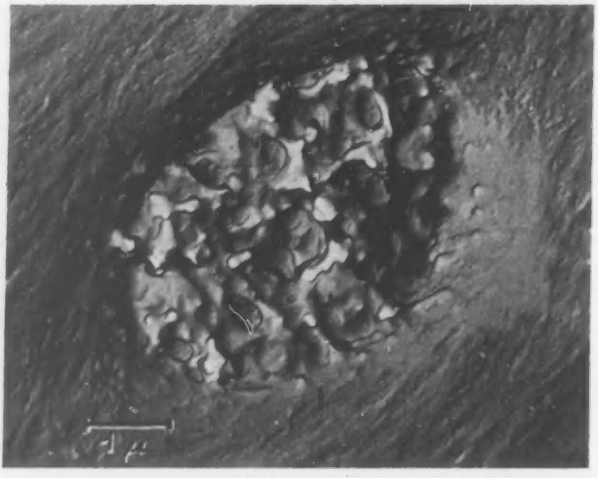

Fig. 17. Vestured pit opening; *Dipterocarpus griffithii*.

species will be discussed elsewhere. On the basis of these results, it can be excluded, that residual components of the cytoplasm are involved to a greater extent in the formation of the tertiary wall. Whereas the tertiary wall is a part of the cell wall, the warty layer is an individual structure arising from the dying protoplasm. Further studies, however, are necessary to clarify the individuality or identity of tertiary wall and plasmamembrane. Wardrop and Davies[45] conclude, from their studies on *Actinostrobus*, that the warty layer consists also of localized cell wall thickenings. Consequently, they regard the warty layer as a feature of the cell wall rather than one of the adjacent cytoplasmatic membrane.

The warty layer sometimes resembles the so-called vestures, which are excrescenses from the pits into the cell lumen (Fig. 17). They are also formed by the cytoplasm during the last stages of cell differentiation,[1] and the analogy of both structures has been discussed by Côté and Day,[7] and Schmid and Machado.[38] A pronounced similarity exists between the warty layer and the sculpturing of the pollenexine. These structures arise from the degenerating protoplast of the tapetal cell in a similar way as the warty layer. Differences, however, exist between both of them regarding their solubility with certain procedures.[8]

Tertiary wall and warty layer are two distinct layers inside wood cells. Their properties are in many ways different from the main part of the cell wall, the secondary wall. Since all liquids, which have to diffuse from the cell lumen into the cell wall or vice versa must move through both layers, there is little doubt that they will influence certain cell wall and wood properties such as adhesion, diffusion and solubility.[44] Further work concerning these structures, especially their chemical nature, is necessary. Since their appearance can vary between species, the different behavior of wood species under certain chemical procedures might find further explanation.

References

1. Bailey, I. W., *J. Arn. Arb.*, **14**, 259 (1933).
2. Bailey, I. W., *Phytomorphology*, **7**, 136 (1957).
3. Bailey, I. W., and M. R. Vestal, *J. Arn. Arb.*, **18**, 196 (1937).
4. Bucher, H., Die Tertiärlamelle von Holzfasern und ihre Erscheinungsformen bei Coniferen *Attisholz* (1953).
5. Bucher, H., *Chimia*, **13**, 397 (1959).
6. Côté, W. A., and A. C. Day, *Forest Prod. J.*, **12**, 333 (1962).
7. Côté, W. A., and A. C. Day, *Tappi*, **45**, 906 (1962).
8. Cronshaw, J., G. W. Davies, and A. B. Wardrop, *Holzforsch.*, **15**, 75 (1960).
9. Dippel, L., *Mikroskop*, 1867–1869, 1898.
10. Ficker, K. H., Inaugural Dissertation Universität Freiburg i. Br., 1959.
11. Frey-Wyssling, A., *Die pflanzliche Zellwand*, Springer-Verlag, Berlin, 1959.
12. Frey-Wyssling, A., K. Mühlethaler, und H. H. Bosshard, *Holz Roh- Werkstoff*, **13**, 245 (1955); *ibid.*, **14**, 161 (1956).
13. Greguss, P., *Xylotomische Bestimmung der heute lebenden Gymnospermen*, Budapest, 1955.
14. Harada, H., *Nippon Ringaku Kaishi*, **35**, 393 (1953).
15. Harada, H., Y. Miyazaki, and T. Wakashima, *Ringyo Shikensho Kenkyu Hokoku*, **60**, (1958).

16. Hartig, Th., *Beiträge zur Entwicklungsgeschichte der Pflanzen*, Berlin, 1843.
17. Hartig, R., *Holzuntersuchungen. Altes und Neues*, Berlin, 1901.
18. Huber, B., und Ch. Rouschal: *Mikrophotographischer Atlas mediterraner Hölzer*, Berlin, 1954.
19. Kerr, Th., and I. W. Bailey, *J. Arn. Arb.*, **15**, 327 (1934).
20. Liese, W., *Proceedings of the Stockholm Electron Microscopy Conference*, 276 (1956).
21. Liese, W., Holz als Roh- und Werkstoff **14**, 417 (1956).
22. Liese, W., *Ber. Dtsch. Bot. Ges.*, **70**, 21 (1957).
23. Liese, W., *Naturwiss.*, **44**, 240 (1957).
24. Liese, W., *Holz Roh- Werkstoff*, **18**, 296 (1960).
25. Liese, W., unpublished results.
26. Liese, W., and I. Johann, *Planta*, **44**, 269 (1954).
27. Liese, W., and M. C. Ledbetter, *Nature*, **197**, 201 (1963).
28. Liese, W., and R. Schmid, *Angew. Botanik*, **36**, 291 (1962).
29. Meier, H., *Holz Roh- Werkstoff*, **13**, 323 (1955).
30. Meier, H., *Holzforschung*, **11**, 41 (1957).
31. Meier, H., *J. Polymer Sci.*, **51**, 11 (1961).
32. Meier, H., and S. Yllner, *Svensk Papperstidn.*, **59**, 395 (1956).
33. Mühlethaler, K., in *The Cell: Biochemistry, Physiology, Morphology*, J. Brachet and A. E. Mirsky, Eds., Vol. IV, New York–London, 1961.
34. Nečešany, V., *Svensk Papperstidn.*, **60**, 10 (1957).
35. Pew, J. C., *J. Forestry*, **47**, 196 (1949).
36. Sachs, J., J. Clark, and J. Pew, *J. Polymer Sci., Part C*, No. **2**, 203 (1963).
37. Sanio, C., *Botan. Ztg.*, **18**, 201, 209 (1860).
38. Schmid, R., and R. D. Machado, *Holz Roh- Werkstoff*, **21**, 41 (1963).
39. Sitte, P., *Protoplasma*, **54**, 555 (1962).
40. Sperling, C. H., and U. Easterwood, *J. Appl. Polymer Sci.*, **4**, 25 (1960).
41. Strasburger, E., *Über den Bau und das Wachstum der Zellhäute*, Jena, 1882.
42. Wardrop, A. B., *Holzforsch.*, **8**, 12 (1954).
43. Wardrop, A. B., and H. E. Dadswell, *Holzforsch.*, **11**, 33 (1957).
44. Wardrop, A. B., and G. W. Davies, *Australian J. Botany*, **6**, 96 (1958).
45. Wardrop, A. B., and G. W. Davies, *Nature*, **194**, 497 (1962).
46. Wardrop, A. B., W. Liese, and G. W. Davies, *Holzforsch.*, **13**, 115 (1959).

Synopsis

The tertiary wall is the innermost layer of the cell wall in wood cells of softwoods and hardwoods. It is also designated as the inner layer of the secondary wall or S_3 layer. The appearance and properties, however, of this layer are in many respects different from the other parts of the cell wall. In most of the wood species, the tertiary wall is covered by a so-called warty membrane. It consists of small excrescences upon the tertiary wall and often of an additional layer of amorphous material. The warty membrane is formed in the concluding stages of cell differentiation, where lignification is complete or nearly so. It consists mainly of dehybrids of the protoplasm. Though the intensity of the wart structure is fairly uniform within genera, its taxonomic significance is limited. The warty membrane is highly resistant against chemicals. There is some evidence that the so-called "gels," consisting of membrane fragments and spherical particles which cause trouble during pulping, are related to the warty membrane. Liquids for pulping and preservation, which have to diffuse from the cell lumen into the cell wall, have to move through the tertiary wall and the warty membrane. Their structure may contribute to the different behavior of wood species in pulping and preservation.

Résumé

La paroi tertiaire est la couche la plus interne de la paroi cellulaire des bois mous et des bois durs. Elle est aussi considérée comme la couche interne de la couche secon-

daire: la couche S_3. Cependant l'aspect et les propriétés de cette couche sont, à beaucoup de points de vue, différentes des autres parties de la paroi cellulaire. Dans la plupart des sortes de bois, la couche tertiaire est recouverte par une membrane. Celle-ci est constituée de petites excroissances sur la couche tertiaire et souvent d'une couche supplémentaire de matériaux amorphes. La paroi cellulaire elle-même présente parfois des différences d'épaisseur locale, qui ressemble à une verrue. La membrane épaissie est formée au cours de l'étape finale de la différentiation des cellules, où la lignification est complète ou à peu près. Celle-ci est constituée principalement de débris du protoplasme. Quoique l'intensité de la structure verruqueuse est presque uniforme, sa signification taxonomique est limitée. La membrane verruqueuse est fortement résistante aux agents chimiques. Il est probable que ces'gels'ainsi appelés qui sont constitués de fragments de membrane et de particules sphériques qui provoque des troubles pendant la formation de la pulpe, sont fonctions de la même membrane. Des liquides nécessaires à la formation de la pulpe et la préservation, qui doivent diffuser du lumen de la cellule vers la paroi cellulaire doivent traverser la paroi tertiaire et la membrane verruqueuse. Leurs structures peuvent contribuer aux différents comportements des espèces de bois lors de la formation de la pulpe et de la préservation.

Zusammenfassung

Die Tertiärwand ist die innerste Schichte der Zellwand in Holzzellen von Weich- und Harthölzern. Sie wird auch als innere Schichte der Sekundärwand, S_3-Schichte, bezeichnet. Das Aussehen und die Eigenschaften dieser Schichte weichen jedoch in vieler Hinsicht von denen der anderen Teile der Zellwand ab. Bei den meisten Holzarten wird die Tertiärwand von einer sogenannten Warzenmembrane bedeckt. Diese besteht aus kleinen Auswüchsen auf der Tertiärwand und oft auch aus einer zusätzlichen Schichte amorphen Materials. Auch die Zellwand selbst zeigt manchmal lokale Verdickungen, die den Warzen ähneln. Die Warzenmembrane wird während des Schlussstadiums der Zelldifferenzierung gebildet, wenn die Ligninbildung schon vollständig oder fast vollständig ist. Sie besteht hauptsächlich aus Protoplasma-Dehybriden. Obgleich die Intensität der Warzenstruktur innerhalb der Genera ziemlich einheitlich ist, ist doch ihre taxonomische Signifikanz beschränkt. Die Warzenmembrane ist gegen Chemikalien sehr widerstandsfähig. Es bestehen gewisse Hinweise, dass die sogenannten "Gele," die aus Membranbruchstücken und kugelförmigen Teilchen bestehen und bei der Pulpbildung Störungen verursachen, zur Warzenmembrane in Beziehung stehen. Flüssigkeiten zur Pulpbildung und zur Konservierung, die vom Zell-Lumen in die Zellwand diffundieren sollen, müssen sich durch die Tertiärwand und die Warzenmembrane durchbewegen. Ihre Struktur kann zu dem unterschiedlichen Verhalten der Holzarten bei der Pulpbildung und Konservierung beitragen.

JOURNAL OF POLYMER SCIENCE: PART C NO. 2, PP. 231–242 (1963)

Structural Factors Affecting the Permeability of Wood

WILFRED A. CÔTÉ, JR., *Electron Microscopy Laboratory, Wood Products Engineering Department, State University College of Forestry at Syracuse University, Syracuse, New York*

INTRODUCTION

Permeability to liquids and gases is a property of wood that greatly influences its processing by pulping, its impregnation with preservative chemicals, or its seasoning and conditioning for use as lumber. The permeability of wood affects processing time and product quality, both of which are invariably related to cost factors.

The effect of gross anatomical structure on permeability is recognized, and studies on the theoretical and the practical aspects of this property have been reported.[1–20] The simpler-structured softwoods are perhaps better known than the hardwoods at the gross and microscopic level, but both groups have been studied intensively at the submicroscopic level in recent years.[21–33] Seasoning methods are known to influence permeability[34,35] and probably affect anatomical structure in some way. The superior resolving power of the electron microscope permits the investigation of ultrastructures in the woody cell wall to help determine the effect of variation in fine structure on the properties of wood.[21,36,37]

The movement of liquids through wood is primarily along the grain, through the tubular elements found in conifers as well as hardwoods. The structure of the bordered pit pair is a key factor influencing flow from cell to cell. Half-bordered and simple pits are also involved when the effect of rays on total permeability is considered. The influence of heartwood formation on the reduction of intercell flow is now somewhat better understood. Heartwood formation affects degree of incrustation, pit aspiration in conifers, tylosis development in hardwoods, and extractives content, in most instances rendering this portion of the wood less permeable than the sapwood zone.[38–48]

GROSS STRUCTURAL FACTORS

Coniferous Woods

Because of the relatively simple and homogeneous anatomical structure of coniferous wood, the paths of flow from cell to cell are limited. Movement along the grain must be primarily through the imperforate tracheids which are the predominant cell type. The arrangement of longitudinal

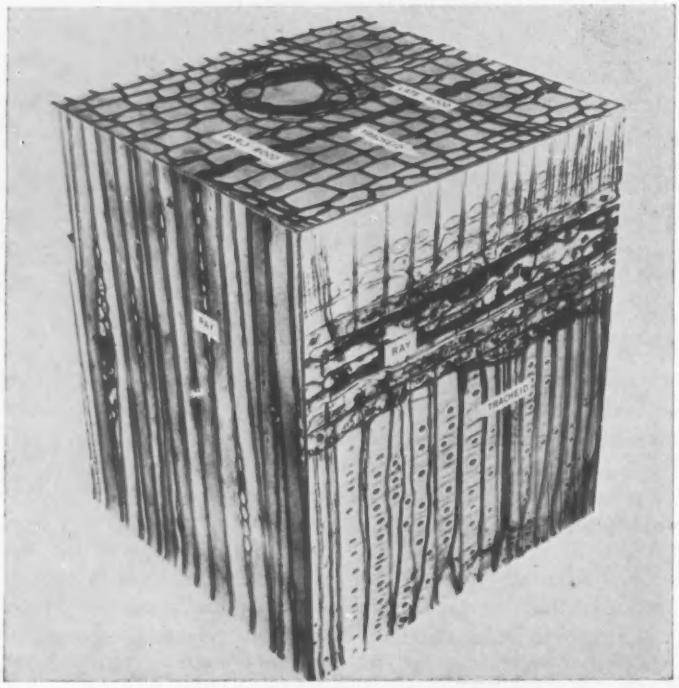

Fig. 1. Photomicrographic representation of a cube of eastern white pine showing longitudinal tracheids, resin canal, rays, bordered pits on the radial surface of the tracheids, and half-bordered pit pairs at the ray–tracheid contact areas.

tracheids provides for stepwise, lateral movement in the tangential direction through the bordered pit pairs (Fig. 1).

The only other longitudinally-oriented structures in softwood are the resin canals and the longitudinal parenchyma. The influence of these elements on permeability is variable and may often be negligible. Canals are not present in all softwoods, and when present, they are often plugged with resin or tylosoids.[4] The longitudinal parenchyma cells are usually filled with stored materials which should hinder movement through the lumens. Furthermore, they are distributed rather sporadically in most species, and are proportionally much less significant than tracheids.

The rays in softwood are of demonstrated significance in radial movement, at least in certain species. Assuming that good communication exists between longitudinal tracheids and ray parenchyma cells via half-bordered pit pairs, rays should contribute substantially to lateral movement in the radial direction. Every tracheid makes contact with at least one ray and most of them have several ray contact areas. Species whose rays are composed of tracheids as well as parenchyma would be expected to provide less occluded pathways for liquid movement since these prosenchy-

matous cells have no contents as the parenchyma cells do. However, Sargent[12] reports that in species where the rays are made up solely of parenchyma, the rays nevertheless contribute greatly to the overall permeability of the wood. Wardrop and Davies[20] state that, in *Pinus radiata*, ray parenchyma cells are penetrated to a greater extent than the ray tracheids. Sargent's study[12] with creosote shows that rays in latewood are less permeable than the earlywood portion. This is surprising since the latewood tracheids are known to be more permeable than the earlywood elements. He also indicates that creosote penetration is less in the heartwood portion of a ray than in the sapwood zone. Fusiform rays (those containing horizontal resin canals), also contribute to increased permeability according to his investigations.

Hardwoods

Longitudinal liquid movement in hardwoods is primarily through the perforated elements, the vessels, and laterally through bordered and half-bordered pit pairs into surrounding elements[20] (Fig. 2). The role of the other types of cells in the conduction of liquids and gases is not readily determined because of their complex assortment and arrangement in the tissue of hardwoods. Capillarity experiments using stains indicate that thick-walled, narrow-lumened elements such as libriform fibers play but a minor role. Wider-lumened cells such as fiber tracheids, on the other hand, are structurally better adapted for conduction. These elements, and others such as vasicentric tracheids, are often heavily pitted, permitting better

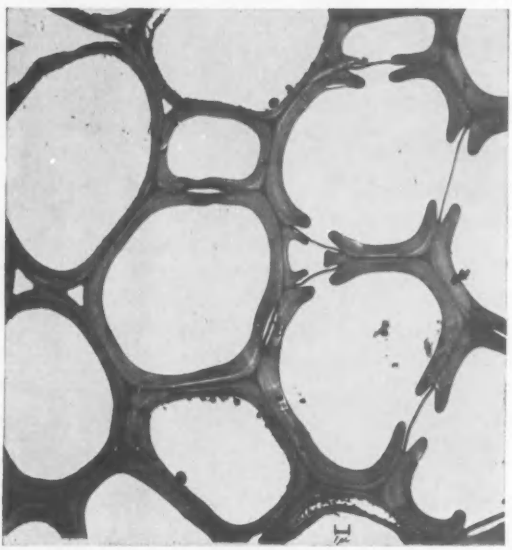

Fig. 2. Electron micrograph of a cross section of red oak wood. The relative thickness of the membranes in bordered pit pairs can be seen. 2000×.

communication with adjoining cells. Longitudinal parenchyma cells are apparently more permeable than the fibers.[20] As in softwood, the capillary staining of hardwood blocks shows a clear demarcation at the sapwood–heartwood boundary, the sapwood exhibiting a much deeper stain than the heartwood.

The effect of rays in promoting conduction is evidently more variable in hardwoods than in softwoods. At least in some species, lateral movement of liquids is aided greatly by ray penetration.[20] The uniseriate rays in oak appear to be more permeable than most of the other elements except the vessels. The broad rays of oak are definitely less permeable than the uniseriate rays, but both types show lower permeability in heartwood than in sapwood.

The wood of sycamore is a good example of the great variability of hardwood with respect to this property. The broad rays of this species exhibit no staining whatsoever, even though the neighboring vessels and other longitudinal tissue are deeply stained. The explanation for this situation can be found by examining individual vessel elements with the microscope. Ray contact areas are absent or very rare, so there are no pits communicating between vessels and rays. Similar structural anomalies may be the cause of permeability differences in other species.

PIT STRUCTURE

Bordered Pits

A bordered pit is an opening in the secondary wall of a wood cell in which the pit membrane is overarched by the cell wall. A bordered pit pair consists of two such pits located opposite each other, as between two contiguous coniferous tracheids. Bordered pits occur in both hardwoods and softwoods, and their structure is similar in both instances when viewed with the light microscope. However, electron microscopy reveals that the pit membranes are different.

Coniferous Bordered Pit Membranes. In conifers the bordered pit membrane is composed of cellulosic strands radiating from a central torus or thickening to the margin of the pit cavity (Fig. 3). In some species the openings between microfibrils in the membrane are large enough to permit the passage of particles 0.2μ in diameter, or larger. The central thickening is well developed in some woods, but in others the torus may be lacking.[26, 44]

Liquid flow through the bordered pit membrane is unobstructed when the torus is in the normal, medial position. When it is displaced to one pit border or the other and sealed in the aspirated condition, the bordered pit is closed very effectively against liquid flow (Fig. 4).[16, 20, 42, 46] Movement through an aspirated pit is then limited to diffusion through the torus. The presence of warts on the pit border can prevent a perfect seal and thus permit seepage through the pit (Fig. 5).[44]

Incrustation of the pit membrane during heartwood formation also restricts the movement of liquid through the bordered pit pair. The micro-

Fig. 3. Electron micrograph of a bordered pit membrane from the sapwood of Douglas fir. Note the microfibrillar strands radiating from the central thickening and the relatively large openings between strands. The depression in the torus illustrates the flexibility of this structure as it is pressed into the pit opening behind, thereby aspirating the pit. 3500×.

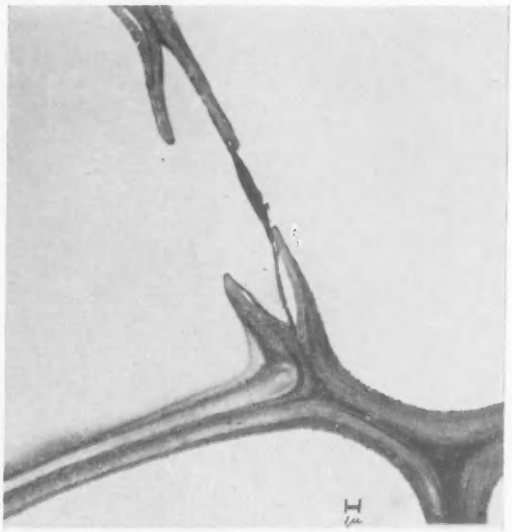

Fig. 4. Electron micrograph of a section through an aspirated pit in redwood. Compare with Fig. 3. Note that the membrane can move from the central position to either border. 2000×.

Fig. 5. Warts can be seen on the lower border of this pit in the electron micrograph. They are also present on the inner surface under the membrane. These warts could presumably prevent a perfect seal of the torus across the pit opening. 9300×.

Fig. 6. Portions of the incrusted pit membrane from heartwood of western red cedar. The nodular thickenings on the microfibrillar strands reduce the openings in the membrane to a very small size. Sapwood membranes are not incrusted. 6800×.

Fig. 7. Surface of the pit membrane in basswood. The microfibrillar structure of this membrane is also typical of the primary walls of wood cells. Note the lack of openings in the membrane, compared with softwood membranes, as in Fig. 3. 20,000×.

fibrillar strands become coated with materials until the openings between strands are very small.[21,33] In some species, such as western red cedar, the heartwood pit membranes appear virtually impermeable when viewed with the electron microscope (Fig. 6).[45]

Hardwood Bordered Pit Membranes. The membrane of hardwood bordered pit pairs is actually the primary wall which is continuous across the openings of the secondary wall. The microfibrils are more or less randomly arranged. The strands do not radiate from a central point and there is no torus present. The most significant departure from softwood membrane structure is the lack of openings (Fig. 7).[22,30] Movement across this membrane must be by diffusion, but even so, the volume of liquid transferred from vessel to adjoining cells must be considerable in a living tree.

The above condition changes with the transformation of sapwood into heartwood. The surface of the membrane becomes incrusted so that the microfibrils are not as readily discernible when heartwood specimens are observed with the electron microscope.[22]

Simple Pits

A simple pit differs from a bordered pit only in the nature of the secondary wall that surrounds the opening. There is no border overarching the membrane and the cavity is either of constant width from cell lumen to membrane, or it many gradually narrow towards the membrane. Simple pit pairs occur between parenchyma cells.

The membranes of simple pits in hardwoods and softwoods are the same as in hardwood bordered pits. There are no openings visible with the aid of the electron microscope and they are also subject to incrustation during heartwood formation.

Half-Bordered Pit Pairs

A half-bordered pit pair is the intercellular pairing of a bordered pit and a simple pit. The most common occurrence of this combination is between a ray parenchyma cell (simple pit) and a tracheid, vessel, or other prosenchymatous element (bordered pit). The membrane in half-bordered pit pairs is invariably nonporous and lacks a torus. Movement across this membrane is by diffusion (Fig. 8).

In coniferous sapwood the membrane between ray cells and tracheids is evidently quite permeable to creosote, or it is perhaps easily ruptured.[12,37] In hardwoods, the diameter of the membrane in half-bordered pit pairs is a critical dimension. Chattaway[38] reports that when the diameter is greater than 10μ, the increased activity of ray parenchyma cells during heartwood formation is sufficient to balloon the membrane out into the adjoining vessel, forming a tylosis. When the pit diameter is less than 10μ, the membrane can resist the increased pressure and there is no extrusion of the membrane, but gummy exudations are forced through the membrane into the neighboring cell. This phenomenon was confirmed by the electron microscopic investigations of white birch by Côté and Marton.[25]

Fig. 8. Electron micrograph showing portions of two half-bordered pit membranes of the windowlike type found in eastern white pine. Note the microfibrils in the less incrusted portions of the surface. 5600×.

In either case, this activity affects the permeability of the heartwood by occluding the vessels to varying degrees. The presence of tyloses in the vessels is generally more effective in restricting flow because there are a large number of membranes forced into a single vessel and each one can extend across the cell lumen. The tyloses are often squeezed together so that a foam-like matrix packs the vessel lumen. The gum secretions rarely fill the cell lumen, but they nevertheless restrict flow and have other deleterious effects on wood processing.[25]

SAPWOOD–HEARTWOOD TRANSFORMATION

A number of changes, some of them structural, are generally associated with the transformation of sapwood into heartwood. Among these are: (*1*) general darkening of the wood, sometimes accompanied by distinct coloration; (*2*) infiltration with extractive materials; (*3*) change in moisture–air ratio; (*4*) depletion of stored starch; (*5*) death of longitudinal and ray parenchyma cells; (*6*) formation of tyloses in hardwood vessels; (*7*) increase in natural durability; (*8*) decrease in permeability; (*9*) pit aspiration. Not all of these characteristics are necessarily found in all wood species. Some species exhibit no distinct color change. Of course, tyloses do not occur in softwoods, but tylosoids can be found in the resin canals of some coniferous species. In most cases several of these indicators can be recognized.

According to Chattaway,[39] true heartwood can be identified by the absence of living ray parenchyma cells. Frey-Wyssling and Bosshard[27] use a

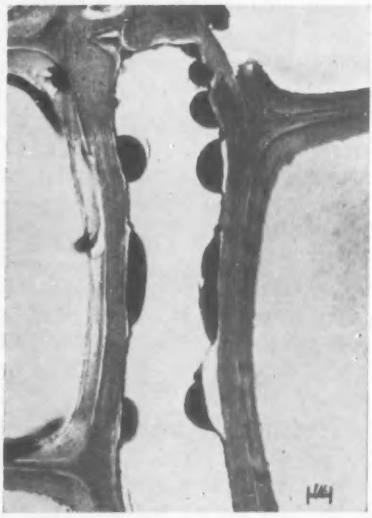

Fig. 9. Part of a ray parenchyma cell from the heartwood of eastern hemlock. The cell contents have been reduced to the electron-dense layer lining the lumen. Since this material also covers the pit opening in the upper right, it would be expected to reduce the permeability. 3600×.

similar cytological method to distinguish sapwood from heartwood. Krahmer and Côté[45] find that air permeability is a sensitive indicator of heartwood formation in coniferous wood. A number of investigators, including Phillips,[46] find that pits in green sapwood are unaspirated, while in heartwood and in air-dried sapwood they are aspirated.

Structural alterations account for much of the reduction in heartwood permeability. Three pit closure factors can be distinguished in softwoods, and more than one may be involved in reducing permeability in a given species.[44] Pit aspiration is apparently related to heartwood formation, but limitations of technique make it difficult to state this unequivocally. The occlusion of pit membranes with extractives, as in incense-cedar, is clearly related to heartwood formation.[48] Extraction of such heartwood with hot water and organic solvents generally improves its permeability, and in some species the improvement is very significant.[45,48]

The third factor, incrustation of the pit membranes with an amorphous, lignin-like substance, accompanies the formation of heartwood in some species.[44,45] This type of incrustation is not removable by organic solvents. Treatment with sodium chlorite in dilute acetic acid removes the incrustation and ozonization also attacks this very resistant material. Though these methods definitely improve the permeability of heartwood, and the incrustations have been removed when the membranes are studied with the electron microscope, an accurate evaluation of the permeability data is precluded since cell wall components may also be degraded.

In sapwood the ray cells are filled with protoplasmic material. The cell contents are gradually reduced until in the dead cell, in the heartwood, only a layer of electron-dense material coats the lumen wall (Fig. 9). Preusser et al.[47] report that these dense materials, which they found in intercellular spaces of European beech rays, are phenolic substances changed by condensation reactions into relatively insoluble compounds. They confirm Frey-Wyssling's suggestion that lignification and heartwood formation are similar processes. The coating of ligno-complex substances on half-bordered pit pair membranes would be expected to affect permeability and is probably an important factor in rendering heartwood less permeable than sapwood.

Transient cell wall capillaries have been suspected of contributing to the overall permeability of wood. However, proof of this possibility is still lacking. The removal of extractives from the cell walls of heartwood may improve its permeability, but the greater permeability of the pits masks this effect.

Wardrop and Davies[19] do not agree that the main path of impregnating liquid is through the cell wall capillaries. The ultimate staining or impregnation of the secondary wall can be explained by the diffusion of material from the lumen into the cell wall, but the pits provide the main flow path between cells.

Some of the information on ultra structure of wood reported here was developed in a study supported by the National Science Foundation. Contributions made by Dr. R. L. Krahmer, Mr. Arnold C. Day, and Mr. Zoltan Koran are gratefully acknowledged.

References

1. Bailey, I. W., *Forestry Quart.*, **11**, 12 (1913).
2. Buro, A., and E.-A. Buro, *Holz Roh- Werkstoff*, **17**, 462 (1959).
3. Davies, G. W., *CSIRO Forest Prod. Newsletter*, No. 248 (1958).
4. Hunt, G. M., and G. A. Garratt, *Wood Preservation*, 2nd Ed., McGraw-Hill, New York, 1953.
5. Johnston, H. W., *Pulp Paper Mag. Canada*, **27**, 342 (1929).
6. Johnston, H. W., and O. Maass, *Can. J. Res.*, **3**, 140 (1930).
7. Krahmer, R. L., *Forest Prod. J.*, **11**, 439 (1961).
8. Liese, W., *Halz Pok-Wenkstoff*, **9**, 374 (1951).
9. Liese, W., and W. A. Côté, Jr., The influence of the structure of wood on its preservative treatment. Proceedings, FAO ad hoc Meeting on wood preservation, Rome, Dec. 1–4, 1959.
10. Miller, D. J., *Forest Prod. J.*, **11**, 14 (1961).
11. Noe, R. W., E. S. P. R. I. Rept. No. 28, Oct. 21, 1960, State Univ. College of Forestry at Syracuse University, Syracuse, N. Y.
12. Sargent, J. W., unpublished thesis, M. S. degree, State University College of Forestry at Syracuse University, Syracuse, N. Y., June 1959.
13. Smith, D. N., *Timber Technol.*, Sept. 1958.
14. Smith, D. N., and E. Lee, Dept. Sci. Ind. Res., Forest Prod. Res. Special Report No. 13, 1958.
15. Stamm, A. J., *USDA Tech. Bull.*, No. 929, 1946.
16. Stone, C. D., unpublished master's thesis, University of Washington, Seattle, Wash., 1931.
17. Stone, J. E., *Pulp Paper Mag. Can.*, **57**, 139 (1956).
18. Tamblyn, N., *Proc. Fifth World Forestry Congr., Seattle, Wash., Sept. 1960*, 1510–1516.
19. Wardrop, A. B., and G. W. Davies, *Australian J. Bot.*, **6**, 96 (1958).
20. Wardrop, A. B., and G. W. Davies, *Holzforschung*, **15**, 129 (1961).
21. Côté, W. A., Jr., Doctorate thesis, State University College of Forestry at Syracuse University, Syracuse, N. Y., June 1958.
22. Côté, W. A., Jr., *Forest Prod. J.*, **8**, 296 (1958).
23. Côté, W. A., Jr., and A. C. Day, *Tappi*, **45**, 906 (1962).
24. Côté, W. A., Jr., and R. L. Krahmer, *Tappi*, **45**, 119 (1962).
25. Côté, W. A., Jr., and R. Marton, *Tappi*, **45**, 46 (1962).
26. Eicke, R., *Ber. Deut. bot. Ges.*, **71**, 231 (1958).
27. Frey-Wyssling, A., and H. H. Bosshard, *Holzforschung*, **13**, 129 (1959).
28. Harada, H., *Trans. 65th Meet. Japan Forestry Soc.*, **31**, 1 (1956).
29. Jayme, G., and D. Fengel, *Holz. Roh- Werkstoff*, **17**, 226 (1959).
30. Liese, W., *Holz Roh- Werkstoff*, **15**, 449 (1957).
31. Liese, W., and W. A. Côté, Jr., *Proc. Fifth World Forestry Congr., Seattle, September 1960.*
32. Liese, W., and M. Fahnenbrock-Hartmann, *Biochim. Biophys. Acta*, **11**, 190 (1953).
33. Stemsrud, F., *Holzforschung*, **10**, 69 (1956).
34. Ellwood, E. L., and B. A. Ecklund, paper presented at Annual Meeting of West Coast Kiln Clubs, Medford, Oregon, 1961.
35. Erickson, H. D., and R. J. Crawford, *Proc. Am. Wood-Preservers' Assoc.*, **55**, 210 (1959).
36. Côté, W. A., Jr., and R. L. Krahmer, *Proc. Fifth Intern. Congr. Electron Microscopy, August 1962.*
37. Liese, W., *Holzindustrie*, **8**, 1 (1956).
38. Chattaway, M. M., *Australian J. Sci. Res. Ser. B*, **2**, 227 (1949).
39. Chattaway, M. M., *Australian Forestry*, **16**, 25 (1952).
40. Frey-Wyssling, A., H. H. Bosshard, and K. Mühlethaler, *Planta*, **47**, 115 (1956).
41. Gardner, J. A. F., and G. M. Barton, *Forest Prod. J.*, **8**, 189 (1958).

42. Griffin, G., Further note on the position of the tori in bordered pits in relation to penetration of preservatives. *J. Forestry*, **22**, 82 (1924).

43. Harris, J. M., *Nature*, **172**, 552 (1954).

44. Krahmer, R. L., Unpublished doctoral dissertation, State University College of Forestry at Syracuse University, Syracuse, N. Y., June 1962.

45. Krahmer, R. L., and W. A. Côté, Jr., *Tappi*, **46** (1), 42 (1963).

46. Phillips, E. W. J., *Forestry*, **7**, 109 (1933).

47. Preusser, H. J., H. H. Dietrichs, and H. Gottwald, *Holzforschung*, **15**, 65 (1961).

48. Skaar, C., Laboratory Project 9.10. Progress Report No. 2, September 1959, University of California, Forest Prod. Lab., unpublished.

Synopsis

The obvious differences between sapwood and heartwood such as color, decay resistance, stored starch, extractives content and dry weight have long been recognized. The greater permeability of sapwood to liquids is also known. Though these characteristic properties can, in some cases, be attributed to chemical components, others are apparently related to physical and structural factors. Some of these factors have been investigated in these electron microscope studies. Permeability to liquids and gases is a property of importance to industrial wood users. In softwoods the mechanism of pit closure is basic to this question due to the imperforate nature of tracheids. In addition, bordered pit membranes appear to undergo the greatest modification as sapwood is converted into heartwood. Three factors were found to influence pit permeability: pit aspiration, pit occlusion with extractives, and pit incrustation with ligno-complex substances.

Résumé

On a longuement reconnu les différences manifestes entre le bois d'écorce et le bois interne, telles la couleur, la résistance à la destruction, la quantité d'amidon, le contenu des extraits et le poids sec. Le plus grande perméabilité du bois interne aux liquides est également connue. Bien que ces propriétés caractéristiques peuvent, dans certains cas, être attribuées aux composants chimiques, d'autres sont apparemment reliées à des facteurs physiques et à des facteurs de structure. Certains de ces facteurs ont été étudiés dans cette étude au microscope électronique. La perméabilité des liquides et des gaz est une propriété importante pour les usages industriels du bois. Dans des bois mous le mécanisme de fermeture des cavités est fondamental pour cette question due à la nature imperméable des trachéides. De plus les membranes entourant la cavité semblent subir la modification la plus forte lorsque le bois externe est converti en bois interne. On a trouvé que trois facteurs influencent la perméabilité des cavités: l'aspiration de la cavité, l'occlusion de la cavité avec des substances extractives et l'incrustation de la cavité avec des substances complexes de lignine.

Zusammenfassung

Die augenscheinlichen Unterschiede zwischen Splintholz und Kernholz, wie Farbe, Dauerhaftigkeit, Stärkespeicherung, Gehalt an Extrahierbarem und Trockengewicht sind schon lange bekannt. Ebenso ist die höhere Permeabilität von Splintholz für Flüssigkeiten bekannt. Obgleich diese charakteristischen Eigenschaften in einigen Fällen bestimmten chemischen Komponenten zukommen, stehen andere doch in Beziehung zu physikalischen und strukturellen Faktoren. Einige dieser Faktoren wurden in der vorliegenden Arbeit elektronenmikroskopisch untersucht. Flüssigkeits- und Gaspermeabilität ist eine für die Verbraucher in der Industrie wichtige Eigenschaft. Bei Weichhölzern ist wegen des nichtperforierten Charakters der Tracheiden der Mechanismus des Lochverschlusses für diese Frage von entscheidender Bedeutung. Ausserdem scheinen die Membranen an den Löchern bei der Umwandlung von Splintholz in Kernholz die grosste Modifizierung zu erfahren. Drei Faktoren haben auf die Lochpermeabilität Einfluss: Lochaspiration, Lochverschluss mit Extrahierbarem und Lochinkrustierung mit Ligno-Komplexsubstanzen.

JOURNAL OF POLYMER SCIENCE: PART C NO. 2, PP. 243–252 (1963)

An Approach to the Measurement of Solid-Solution Structures in Wood and Other Cellulosic Materials*

ELLIS B. COWLING, *Yale University School of Forestry, New Haven, Connecticut,* and ALFRED J. STAMM, *North Carolina State College, Raleigh, North Carolina*

Introduction

Whenever wood or cotton is treated with reagents such as pulping chemicals, saccharifying acids, mercerizing or dimensional stabilizing agents, or even the extracellular enzymes of invading decay fungi, the reagents first penetrate the microscopically visible (gross) capillary structure of the fibers—the cell lumens, pit apertures, and pit membrane pores. They then penetrate the spaces between microfibrils within the various layers of the fiber wall. Finally, if moisture or other swelling liquids are present, the walls of the fibers expand and a solid solution is created by the swelling liquid in the amorphous regions within the microfibrils. During this process of expansion, the swelling liquid and any dissolved solute molecules present diffuse into and expand the solid structure and thus gain access to a large molecular surface that exists between the various constituents of the fiber wall. These expanded solid-solution structures in the past have been referred to as transient cell-wall capillaries.

Derived cellulosic materials, such as rayon and cellophane, contain no cellular or microfibrillar structure. Thus the only pathways available for movement of fluids through these materials result from forming solid solutions.

The total surface area of the various structures within cellulosic materials is very large. For spruce wood with a specific gravity of 0.4, for example, the total surface area of the gross capillaries is approximately 2×10^3 cm.^{2}/g. or 15 ft.^{2}/in.^{3} of wood. Although this area seems very large, it is several orders of magnitude smaller than the molecular surface area formed by contact between the solid and the swelling liquid within the solid solution, which is approximately 3×10^6 cm.^{2}/g. or 0.5 acres/in.^{3} of wood.[1] (The term "contact area" might be more accurate than "surface area" since the latter implies a pre-existing, rather than a transient, surface area.) Cotton, cellophane, and other cellulosic materials have internal contact areas of this same order of magnitude. Thus, in the presence of

* This research is being supported by a grant to the Yale School of Forestry from the Pioneering Research Program of the Institute of Paper Chemistry at Appleton, Wisconsin.

moisture and other swelling solvents, the accessibility of cellulosic materials is determined primarily by the molecular surface exposed in the solid-solution structures of the materials.

The mechanism of the swelling by which the solid solutions are formed may be visualized most simply as spreading apart of the cellulose and other constituent molecules as a consequence of penetration by the solvent molecules. The volume increase that takes place is approximately equal to the volume of the swelling liquid that enters the solid structure. Different solvents have characteristic capacities to swell cellulosic materials. Thus the dimensions of the solid solutions and the magnitude of the molecular surface accessible to dissolved reagents are related to the swelling capacity of the liquid. Various liquids are listed in Table I in order of decreasing swelling capacity.

TABLE I

Swelling Capacity of Various Organic Solvents Liquids for Wood to that of Water[a]

Swelling medium	Relative swelling
n-Butylamine	139
Formamide	123
Formic acid	120
Pyridine	118
Water	100
Methyl alcohol	95
Ethylene glycol monoethyl ether	87
Ethyl alcohol	83
Methyl acetate	80
Acetic acid	75
Propionic acid	67
Acetone	63
Dioxane	62
Propyl alcohol	45
n-Butyl alcohol	13.5
Amyl alcohol	4.9
Chloroform	3.2
Ethyl ether	3.0
Carbon tetrachloride	1.7
Benzene	0.0

[a] Data of Stamm.[1]

The variable extent of formation of solid solutions has a pronounced influence on accessibility, as is well illustrated by the data of Schuerch.[2] When no moisture was present in wood treated with ozone in the gas phase, ozonation was very slight and confined to the gross capillary surfaces of the fibers. But when moisture was present and the wood was fully swollen (at or above the fiber saturation point)* the extent of ozonation was many

* The fiber saturation point of wood is that moisture content at which the fiber lumens are devoid of moisture but at which the walls are fully saturated with water; this is 24–32% of the oven-dry weight of the wood, depending on the species.

orders of magnitude larger than that of the oven-dried material. This clearly indicates that the cellulose and other constituents of wood are packed together so tightly that, in the absence of a swelling solvent, only a very small proportion of the potential molecular surface is accessible even to very small molecules in the gas phase.

In view of the foregoing, the accessibility, and to a large extent the susceptibility, of cellulosic materials to chemical reagents may be defined as a function of the dimensions and surface properties of the reagent molecules in relation to the dimensions and surface properties within the solid-solution structures of the material when swollen by a given liquid. This internal structure provides almost all of the sites of moisture sorption in all cellulosic materials. They are the sites of action of pulping, hydrolizing, and dimensional stabilizing agents in wood. It is within these solid solutions in cotton and rayon that many dyes are deposited and mercerizing agents must act. Thus these tiny molecular spaces are of considerable practical significance in industrial applications of cellulose as well as of fundamental interest to the fiber anatomist. For these reasons it is of major importance to determine the size and shape of these created spaces and to learn more about their surface properties. The purpose of this paper is to indicate one approach to this task with the use of wood as the material of test.

Theory of the Method

As discussed above, the accessibility of cellulosic materials to reagents may be defined as a function of the dimensions and surface properties of the reagent molecules in relation to the dimensions and surface properties of the extended solid. From this it follows that a reliable measure of accessibility should make it possible to use reagent molecules of essentially similar surface properties but different molecular size as a series of "go-no-go gauges" to estimate the dimensions of the openings in the extended solid structure of wood. Such a reliable measure of accessibility is provided by changes in shrinkage properties of wood wafers after impregnation with a series of solutions of polymer molecules of increasing molecular weight. Molecules smaller than the openings in the extended solid structure will readily diffuse into these fine spaces and, by bulking, restrain the normal tendency of the wafers to shrink when dried below their fiber saturation point. Dissolved polymer molecules of progressively increasing molecular size will enter the cell walls less readily and should show progressively decreasing antishrink efficiency. Polymer molecules larger than the openings in the extended solid structure will be unable to enter and thus should show only negligible antishrink efficiency. These theoretical relationships are illustrated by the upper graph in Figure 1. The distribution of dimensions of the openings in the extended solid structure can be calculated from the relationship between antishrink efficiency and the molecular size of the impregnated molecules by graphical differentiation of the upper curve. The result is a frequency distribution of opening

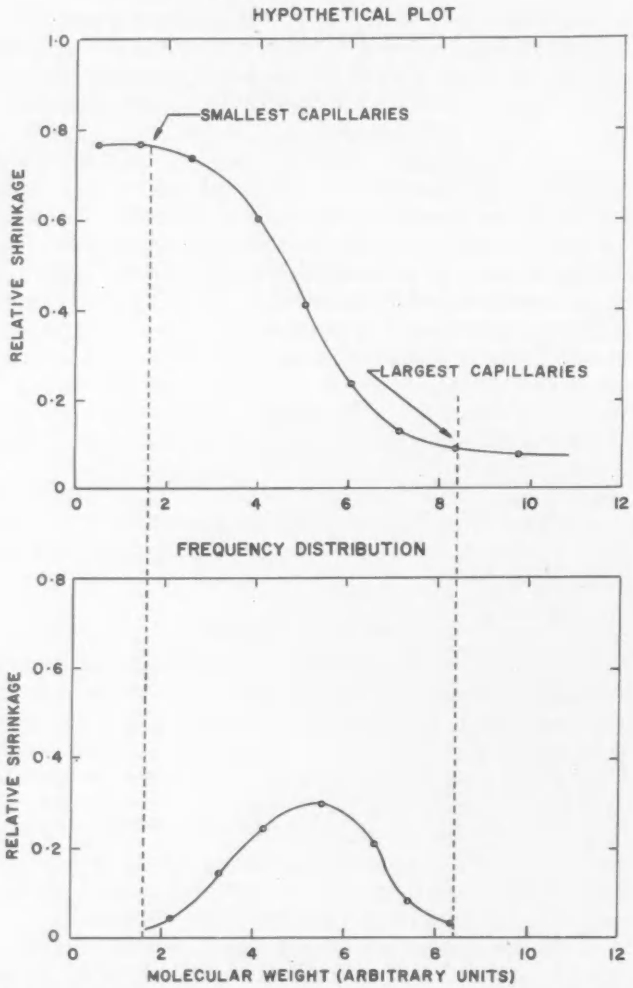

Fig. 1. Hypothetical plot showing relative shrinkage for a series of polymer fractions of increasing molecular weight and a derived frequency distribution of the dimensions of the openings in the solid-solution structures (capillaries) in molecular weight units.

dimensions of the type shown by the lower curve in Figure 1. By using the effective molecular radius in solution of each polymer fraction the molecular weight units of the abscissa may be converted to Ångstrom units.

Materials and Methods

In order to apply this theoretical approach to the determination of size of openings in the solid solutions within the various wood species, cross-

sectional wafers should be cut from defect-free specimens of that wood species. The wafers should be thinner in the direction of the grain than the average length of the wood fibers so that at least one end of each fiber will be open to penetration by the polymer solution. The wafers should be so cut that two opposite edges are as nearly parallel to the annual rings as possible so that the specimens will remain rectangular upon swelling and shrinking. The radial and tangential dimensions of the wafers should be measured with a micrometer gauge to the nearest 0.001 in. We have found $1 \times 1 \times {}^1/_8$ in. softwood wafers very convenient for this purpose. The wafers should be carefully machined to give smooth radial and tangential edges for contact with the bearing points of the micrometer gauge. To insure that repeated measurements are made at the same point on the specimens, a jig that will hold the specimens truly parallel with the direction of measurement is useful.

After machining, the wafers should be dried slowly enough to insure that they will dry in a stress-free condition. Drying can be accomplished very conveniently at room or slightly elevated temperatures by using a vacuum desiccator containing phosphorus pentoxide or magnesium perchlorate. The radial and tangential dimensions of the dry wafers, D_d, should then be measured to the nearest 0.001 in. as quickly as possible after removal from the desiccating atmosphere.

After measurement dry, the wafers should be vacuum impregnated to refusal with distilled water and again measured to the nearest 0.001 in. to obtain their water-swollen dimensions, D_s, after swelling equilibrium is attained. Impregnation can be accomplished by drawing a vacuum of 5 mm. Hg or less on the test specimens for a period of at least 30 min. Then without breaking the vacuum, water should be run into the container to submerge the wafers. The vacuum then should be released slowly, and the submerged specimens left standing in water at atmospheric pressure overnight to attain swelling equilibrium.

After measurement wet, the wafers should be randomly organized in replicate groups of three or more. Each group should be submerged in aqueous solutions of a graded series of polymer fractions of increasing molecular weight until they attain diffusion equilibrium (usually in less than ten days). The amount of solution used should be sufficiently greater for each group than the volume of the wood samples to insure that the water in the lumen of the wood cells will not significantly dilute the polymer solution concentration. The concentration of treating solution (w/v), C_p, necessary to insure complete replacement of water with polymer within the cell walls after drying can be calculated according to eq. (1):

$$C_p = 1.25F_{sp}S_pS_w/1 - (S_w/S_{ws}) \quad (1)$$

where 1.25 is a safety factor of 25 %, F_{sp} is the fiber saturation point of the wood species used expressed as a decimal fraction of the moisture-free weight of the test specimen, S_p is the specific gravity of the polymer, S_w is the specific gravity of the wood based on its moisture-free weight and

water-swollen volume, S_{ws} is the specific gravity of dry wood substance (1.53), determined in water.

After the ten-day equilibration period the concentration of polymer in the solvent within and without the wafer should be equal. The wafers should then be removed from the treating solution, slowly dried to constant weight, and again measured to the nearest 0.001 in. to obtain their radial and tangential dry dimensions after treatment, D_t. Very slow drying of the treated wafers is essential to insure quantitative replacement of the solvent within the cell walls with polymer and to avoid stresses in the material due to shrinkage.

When polymers that are susceptible to microbial degradation are used, 0.01% merthiolate or other preservative should be added to the treating solutions. The temperature of the diffusion treatment should be selected to insure that the polymer and solvent are miscible in all proportions.

The antishrink efficiency of each treating solution in both the tangential and radial directions should be calculated as relative shrinkage, S_r, according to eq. (2):

$$S_r = (D_t - D_d) - (D_s - D_d) \tag{2}$$

where D_s is the water-saturated dimension of the wafer and D_t and D_d are dry dimensions of the wafer after inward diffusion of the polymer and before inward diffusion of the polymer, respectively. The average relative shrinkage values obtained for each group of test wafers treated with each fraction in the polymer series should be plotted against molecular weight to give a graph of the type shown in Figure 1.

Some wood species (redwood is a noteworthy example) contain appreciable amounts of soluble extractives that normally are deposited within the cell walls where they decrease the effective amount of bulking that can subsequently occur. With such wood species, it is essential either to: (1) extract these materials and determine the extractive-free dimensions of the solid-solution structures; or (2) attempt to measure the remaining available bulking structure without extraction while recognizing that to whatever extent the extractives are removed during subsequent diffusion treatments the structural dimensions will be enlarged beyond what they were in the presence of all extractable materials characteristic of that wood.

Selection of Polymeric Materials

The following five attributes are essential in polymeric materials suitable for determination of the dimensions of the solid-solution spaces in cellulosic materials.

1. Molecular Weight Range. In order to determine the entire frequency distribution of capillary dimensions in a given cellulosic material, the polymer must be available in a series of molecular weight fractions whose effective molecular dimensions in solution extend from somewhat above to somewhat below the range of internal dimensions that are to be measured. Where only more restricted information is desired, however, a less com-

plete range could be used, for example, to determine whether molecules of a given polysaccharide or protein molecule could penetrate the cell wall structure. The range of molecular weights needed for use with any given cellulosic material will have to be determined by trial and error. On the basis of previous work with cotton and wood, however, molecules with radii of gyration between 2 and 50 Ångstrom units will be most useful.

2. Monodispersity. The individual polymer fractions in a given series must be relatively monodisperse. This will insure that whatever antishrink efficiency is observed is pertinent to the average rather than just to the smaller molecules in the fraction. If a given fraction contains molecules of a very wide range of molecular weights, it is possible that only the smaller molecules would enter the cell wall structure, thus giving quite misleading results.

3. Miscibility. Each fraction of the polymer series must be miscible with the swelling solvent in all proportions. Impregnation of the polymer into the fine structure is accomplished by diffusion from the wood cell lumen. After the swollen test wafers are immersed in the polymer solution an equilibrium is established whereby the concentration of the polymer in the solvent outside the wafers, within the gross capillaries, and within the cell wall structure of the wafers are all equal. After this equilibrium is established the solvent is gradually evaporated during drying. This evaporation occurs primarily from the wood cell lumen so that the concentration of the polymer in the solvent in the lumen constantly increases. This establishes a very high gradient of polymer concentration from the lumen into the fine structure of the cell wall. Eventually a thin film of essentially pure polymer is established on the surfaces of the cell lumens. Assuming miscibility of solvent and polymer in all proportions, diffusion under these high gradient conditions permits quantitative replacement of the solvent within the cell wall structure with the pure polymer unless the polymer molecules are so large that they are unable to penetrate the cell walls. If the polymer is not miscible with the solvent in all proportions, precipitation of the polymer will occur in the lumen and diffusion will cease leading to very low apparent antishrink efficiencies.

Although it is most convenient to use polymers that are soluble in water, polymers soluble in other solvents can be used if the water is replaced by other suitable solvents by solvent exchange. For example, water could be replaced with ethanol and ethanol with benzene in order to use benzene soluble polymeric materials. This exchange of solvents must be accomplished without altering dimensions of the cell wall structure if data on their dimensions is to be pertinent in general to water-swollen wood rather than to solvent-exchanged material specifically.

4. Molecular Size and Shape. In order to transform to Ångstrom units the molecular weight scale on an experimentally determined frequency distribution such as that shown in Figure 1, the effective molecular radius of each polymer fraction must be determined. If the polymer molecules are rigid spheres, antishrink efficiency data will define the minimum radius

of the structural openings. If, on the other hand, the polymer molecules exist in solution as random coils that are capable of a certain amount of conformational adjustment during diffusion into the fine structure, the data will be more difficult to interpret in terms of specific capillary dimensions. In such cases determinations of density, axial ratio, radius of gyration, and other form factors will be essential.

5. Nonselective Adsorption. Each polymer fraction must be free to diffuse within the cell wall structure and thus must not be selectively adsorbed on the surfaces. Otherwise, adsorption will occur in the structure nearest the gross capillary surface, resulting in diminution of the effective diameter and consequently retarding diffusion into the less readily accessible portions of the structure.

Application to Other Cellulosic Materials

The theoretical approach suggested in this paper for determining transient capillary dimensions can be applied to any cellulosic or other high polymeric material whose changes in dimension during swelling can be measured reliably. Very accurate thickness gauges, for example, could be used for antishrink efficiency measurements in paper or cellophane film. In both of these cases it would be necessary to start with swelling relaxed material. With suitable adaptation it could be applied to various types of rubber and other high polymeric materials.

Summary

When liquids, vapors, or dissolved materials such as pulping chemicals interact with wood or wood fibers they first enter the gross capillary structure of the wood: the lumen, the pit apertures, and the pit membrane pores. They then penetrate the spaces between microfibrils within the various layers of the secondary wall and the compound middle lamella. Finally, if moisture or other swelling liquids are present, the walls of the wood cells expand, and a fine solid-solution structure is created in the amorphous regions within the microfibrils. Fluids then enter these fine structures as they are formed and gain access to the internal surface of the high molecular weight constituents of the wood fiber.

Thus, the accessibility of cell-wall constituents to reagents such as pulping chemicals, saccharifying acids, mercerizing agents, dimensional stabilizing agents, and even the extra-cellular enzymes of decay fungi is determined by the dimensions and surface properties of these structures in relation to the dimensions and surface properties of the reagents in question. Thus the importance and need for further study of solid-solution structures and particularly for determination of their dimensions is obvious.

One approach to determining the dimensions of the solid-solution spaces occupied by swelling solvents is to measure the shrinkage properties of the material before and after diffusion of a series of polymeric solutes of increasing molecular weight into the cell walls. Molecules smaller than the solid-solution spaces will enter the structure and by bulking, restrain

the normal tendency of the fibers to shrink when they are dried below the fiber saturation point. Dissolved molecules of progressively increasing molecular size will enter the structure less readily and show progressively decreasing antishrink efficiency. Polymer molecules larger than the structural spaces will have negligible antishrink efficiency. The distribution of dimensions of these spaces in samples of various cellulosic materials can then be calculated from the relationship between the effective molecular radius of the polymer in water solution and their antishrink efficiency.

This same technique of using gross swelling measurements and a graded series of polymer fractions of known molecular size offers the possibility of determining the effective size of the fine cell-wall openings of wood and other cellulosic materials as well as those in other three-dimensional high polymer systems.

References

1. Stamm, A. J., in *Wood Chemistry*, L. E. Wise and E. C. Jahn, Eds., Vol. 2, Reinhold, New York, pp. 691–814.
2. Schuerch, C., *J. Polymer Sci., Part C*, No. **2**, 79 (1963).

Synopsis

A technique is described for determining the size distribution of solid-solution structures in wood and other cellulosic materials. The method involves the measurement of the relative shrinkage of the material before and after diffusion of a series of polymeric solutes of increasing molecular weight into the cell walls. Molecules smaller than the solid-solution spaces will enter the structure and by bulking, restrain the normal tendency of the fibers to shrink when they are dried below the fiber saturation point. Dissolved molecules of progressively increasing molecular size will enter the structure less readily and show progressively decreasing antishrink efficiency. Polymer molecules larger than the structural spaces will have negligible antishrink efficiency. The distribution of dimensions of these spaces in samples of various cellulosic materials can then be calculated from the relationship between the effective molecular radius of the polymer in water solution and their antishrink efficiency.

Résumé

On décrit une technique pour déterminer la distribution des grandeurs des capillaires des parois cellulaires de passage du bois et des autres structures cellulosiques. La méthode consiste à mesurer la contraction relative du matériau avant et après la diffusion d'une série de solutions polymériques de poids moléculaires croissants, à travers les parois cellulaires. Les molécules qui sont plus petites que les capillaires entreront dans la structure et inhibent ainsi la tendance normale des fibres à se contracter quand on les sèche en-dessous de leur point de saturation. Quand le poids moléculaire des molécules en solution augmente, ils entrent plus difficilement dans les structures et ils montrent une efficacité d'anti-contraction progressivement décroissante. L'effet des molécules dont la grandeur dépasse celle des espaces structurels est négligeable. On sait calculer la distribution par grandeur de ces capillaires dans des échantillons de plusieurs matériaux cellulosiques en partant de la relation entre le rayon moléculaire effectif du polymère en solution aqueuse et l'efficacité d'anti-contraction.

Zusammenfassung

Ein Verfahren zur Bestimmung der Grössenverteilung von Zellwandkapillaren in Holz und anderen Cellulosestrukturen wird beschrieben. Die Methode bedient sich der

Messung der relativen Schrumpfung des Materials vor und nach der Diffusion einer Reihe von gelösten Polymeren steigenden Molekulargewichts in die Zellwände. Kleinere Moleküle als die Hohlräume der festen Lösung werden in die Struktur eindringen und durch ihren Raumbedarf die normale Schrumpfungstendenz der Faser bei der Trocknung unterhalb des Faser-Sättigungspunktes herabsetzen. Gelöste Moleküle werden mit steigender Molekülgrösse immer weniger leicht in die Struktur eindringen und eine ständig abnehmende Anti-Schrumpfwirkung zeigen. Grössere Moleküle als die Strukturhohlräume werden eine vernachlässigbar kleine Anti-Schrumpfwirkung bestitzen. Die Verteilung der Hohlraumdimensionen in Proben aus verschiedenen Cellulosematerialien kann dann aus der Beziehung zwischen dem effektiven Molekülradius des Polymeren in wässriger Lösung und seiner Anti-Schrumpfwirkung berechnet werden.

JOURNAL OF POLYMER SCIENCE: PART C NO. 2, PP. 253–261 (1963)

Influence of Prosenchyma Cell-Wall Morphology on Basic Physical and Chemical Characteristics of Wood*

J. D. HALE and L. P. CLERMONT, *Ottawa Laboratory, Department of Forestry of Canada, Forest Products Research Branch, Ottawa, Ontario, Canada*

Wood of a large tree is likely to exhibit a wide range of variation in such visible anatomical characteristics as width of annual layers and relative proportions of latewood and earlywood. Such variations are typically associated with corresponding variation in technological properties of wood. The visible anatomical features that typically distinguish such variant types of wood are in turn related to variations in cell-wall morphology. This brief report indicates how the variation in cell-wall morphology that is responsible for extreme variation in physical (or mechanical) properties of wood in different parts of the same stem must also be responsible for significant variation in basic chemical composition of wood.

Annual Ring Structure Related to Cell-Wall Morphology and to Technological Properties of Wood

Current conception of the structure of the walls of the principal cellular components of wood which rests originally on the contributions of Bailey and Kerr[1] envisages the secondary wall of prosenchyma cells as a triple-layered structure. In this triple structure the middle layer is relatively thick compared with the thin, skinlike nature of the outer and innermost layers.

Prosenchyma is a collective term for the elongated cells with tapering ends which are commonly known as tracheids or fibers. Prosenchyma cells are, therefore, the principal cellular components of wood. Packed closely together with their long axes preponderantly parallel to the axis of the stem or root whose wood they compose, the prosenchyma cells, by their combined properties, largely determine the properties of wood.[2] The preponderant direction of the prosenchyma cells is the direction of the grain.

Annual rings are distinguishable in wood because the process of tree growth provides seasonal variations in prosenchyma cell structure that form visible unconformities between neighboring annual layers. In most woods with conspicuous annual layers the unconformity in structure is a significant difference between earlywood, composed of thin-walled prosen-

* Department of Forestry of Canada, Forest Products Research Branch Contribution Number P-9.

chyma, and latewood, composed of prosenchyma with thick walls. Latewood prosenchyma is also characterized by smaller cell cavities than that of earlywood. Prominent latewood may, therefore, have specific gravity much higher than that of the earlywood.

It is useful here to cite elementary information regarding the anatomical basis of wood technology by reference to the fact that woods composed principally of thick-walled prosenchyma are thereby relatively heavy with consequent high strength and high capacity for dimensional change in response to changes in moisture content.[2] Moreover, wood of species normally characterized by extreme contrast in thickness of prosenchyma cell-walls in prominent bands of latewood and earlywood, may, thereby, be subject to a considerable range of variation in density and related properties within the same stem if the annual layers vary significantly in width. Normal variation in physical or mechanical properties may typically be related to variation in width of annual rings when variation in width of rings entails significant variation in relative proportions of earlywood and latewood.[3,5]

Cell-Wall Morphology

It is convenient to refer here to a diagrammatic representation of the triple-layered prosenchyma cell-wall currently conceived by anatomists. Reference to Figure 1 represents the cell wall dissected to show the three layers distinguished by Bailey and Kerr[1] as S1, S2, and S3, respectively, each characterized by distinctive alignment of its fibrillar components. The diagram purports to illustrate the general condition typical of thin-walled and thick-walled cells. Within the same specimen of wood the difference in thickness of the triple wall exhibited by the two types of cell is mainly in the thickness of the middle S2 layer, since the outer and inner layers of the cell wall are skinlike and contribute about the same total thickness whether the whole triple wall is thick or thin.

It is believed that the α-cellulose is contained principally in the S2 layer, whereas the lignin is principally intercellular in the middle lamella and primary wall, although some also occurs in all three layers of the secondary wall.[6] Localized intercellular distribution, therefore, provides a fairly constant source for most of the lignin in wood regardless of the thickness of prosenchyma cell walls, whereas the principal source of α-cellulose, the S2 layer of the secondary wall, exhibits extreme variation from a minimum in thin-walled earlywood prosenchyma to a maximum in the thick-walled prosenchyma of latewood. It is, therefore, natural that latewood should be a richer source of α-cellulose than earlywood. Moreover, in species where trends of variation in prosenchyma cell-wall thickness may be traceable, as in certain species of pine where the mean thickness of prosenchyma cell walls may decrease toward upper levels of the tree, it may be expected that the α-cellulose content will also vary as a function of the thickness of the prosenchyma cell wall.

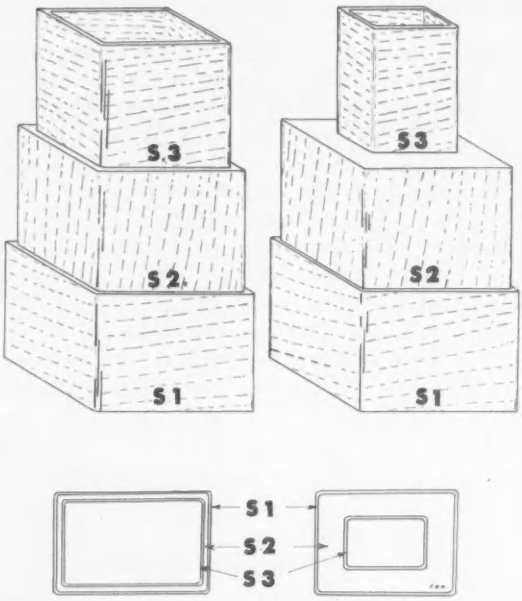

Fig. 1. Conventional diagram highly magnified to indicate structure of secondary walls of normal thin-walled prosenchyma cell (left) and thick-walled prosenchyma cell (right). Dissected to show three differentiated layers in transverse (lower) and side view (upper). Dotted lines indicate direction of alignment of submicroscopic fibrils which, in S1 and S3, is nearly perpendicular to that of the thick midlayer, S2.

Effects of Cell-Wall Morphology on Strength

It is noteworthy that recent investigations of the tensile strength of single prosenchyma cells undertaken by Jayne[4] and by Leopold and McIntosh[7] have shown significantly greater strength per unit of cross sections of cell-wall substance in latewood cells than in cells of earlywood. Since most of the parallel chain molecules composing the α-cellulose crystallites are contained in the midlayer of the prosenchyma cell wall, it seems logical to conclude that the extremely great tensile strength of latewood prosenchyma is related to its thick S2 layer of parallel fibrils composed of crystallites. The low tensile strength of earlywood prosenchyma, which has only a thin S2 layer, may be largely influenced by the skinlike helical layers, S1 and S3. The fact that tensile stress parallel to the cell axis is nearly perpendicular to the helical fibrils of the S1 and S3 layers may contribute to the relatively lower tensile strength reported for earlywood. Since these helical layers form a much greater proportion of the cell wall in early wood than in latewood, relative tensile weakness of these layers could significantly reduce the strength per unit of cell-wall area.

Effects of Cell-Wall Morphology on Chemical Properties

It is important to note here that Ritter and Fleck[8] long ago found higher lignin content in earlywood than in latewood and in some eight species, including both hardwoods and softwoods, have reported significantly higher cellulose content in the latewood. The work of Bailey and Kerr[1] on cell-wall morphology by which Ritter and Fleck might have explained their results was, of course, not available to these earlier authors.

In order to obtain additional evidence based on current methods of analysis that variation in structure related to the thickness of prosenchyma cell-walls must also affect the α-cellulose content, chemical analyses of selected samples of wood were undertaken. Specimens of wood of red pine and Douglas fir selected for conspicuous latewood content were analyzed by standard TAPPI procedure to determine the relative amounts of α-cellulose in earlywood and latewood. In both species, higher α-cellulose

TABLE I

Chemical Analyses of Latewood and Earlywood of Douglas Fir and Red Pine[a,b]

	Alcohol–benzene solubility, %	Lignin, %	Holocellulose, %	α-Cellulose based on	
				% of wood	% of holocellulose
Douglas Fir					
Earlywood	4.09	31.2	70.9	47.8	67.4
Latewood	2.85	28.1	75.3	56.2	74.6
Red Pine					
Earlywood	5.67	27.9	73.2	45.3	61.9
Latewood	4.66	24.7	74.8	53.0	70.9

[a] Specimens for analysis were about 4 to 5 in. outside the pith from the 27th to 40th annual layers in both species.

[b] The holocellulose determination was made by the procedure of Wise, Murphy, and d'Addieco.[9] All other analyses were made by current TAPPI standard procedures. Lignin, holocellulose, and α-cellulose are expressed in percentage of extractive-free, moisture-free wood. Extractives are expressed as per cent of original moisture-free wood.

TABLE II

Analyses of Douglas Fir Specimens from a Log of 23-In. Diameter Showing 430 Annual Rings

Position of sample in number of rings distant from pith	Alcohol–benzene solubility, %	Lignin, %	Holocellulose, %	α-Cellulose based on	
				% of wood	% of holocellulose
27–32	2.83	30.3	68.5	46.3	67.6
41–47	2.99	29.8	68.6	49.0	71.5
75–85	3.77	29.5	67.7	48.2	71.2
219–230	5.33	29.5	67.3	49.4	73.3
322–400	5.04	32.4	66.2	43.6	65.9

was found in latewood than in earlywood, thus supporting the hypothesis indicated by the difference in cell-wall morphology of these two regions of the annual layer (see Table I). It is significant that these results show,

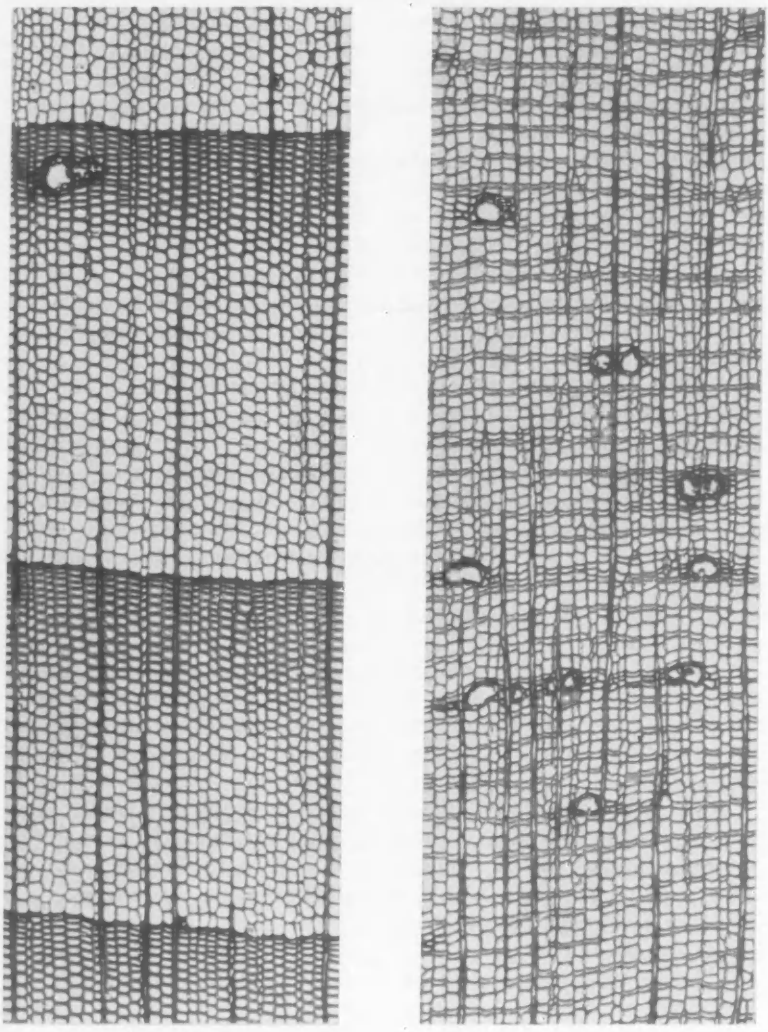

a *b*

Fig. 2. Douglas fir transverse sections of wood ×50. Each section represents a rectangular surface of wood about 1 mm. wide. (*a*) Wood of the 50th and 51st annual layers. Specific gravity of this wood is close to that of average Douglas fir. (*b*) Overmature wood. It was formed after the stem was about 400 years old. Composed of thin-walled prosenchyma, this wood is abnormally light in weight for Douglas fir.

not merely higher α-cellulose content in the latewood, but also that the α-cellulose comprises a significantly larger proportion of the total carbohydrates in latewood than in earlywood.

Some additional analyses were undertaken on wood sampled at various distances from the pith in a short section of veneer log of Douglas fir of about 2-ft. diameter which showed over 400 annual rings. Results of these analyses are tabulated in Table II.

The low α-cellulose of the innermost sample centering at about the 30th annual layer is attributed to the wide annual rings with relatively small proportion of latewood. The low α-cellulose of the outermost sample is attributed to the generally thin-walled prosenchyma typically associated with the extreme slow growth of wood characteristic of overmature trees (Fig. 2). A decline in width of annual rings from the region of the pith toward the bark is a familiar pattern of growth exhibited by forest-grown trees, so that the occurrence of wood formed of relatively wide annual rings in early growth of a tree represents a normal condition well known to foresters and technologists.

Particular attention is directed to the relatively high lignin and low α-cellulose recorded for the outermost specimen which occupied a position about 11 in. from the pith. It was composed of the outer annual layers formed after the portion of stem tested was more than 300 years old. Such wood represents a condition of overmaturity that is likely to occur in the outer wood of large old trees. Trees that have reached this condition grow very slowly as is shown by the extremely narrow annual layers of overmature wood. This wood is characteristically low in density for its species because of the abnormally thin walls and relatively large cell cavities of its prosenchyma.

This type of overmature wood is characteristic of many different species, but the age at which trees may attain this stage of overmaturity is subject to wide variation. While 400 years may seem a ripe old age, many trees of Douglas fir become much older than this before showing the symptoms of overmaturity implied by the formation of this typically lightweight wood. It seems probable that environmental influence as well as inherited characteristics may be involved in determining the age at which overmaturity becomes evident. This particular wood was selected because it embodied the type of overmature wood with thin-walled prosenchyma which, it was assumed, would test the hypothesis that abnormally thin-walled prosenchyma is characteristically low in α-cellulose. The fact that this overmature wood is significantly low in α-cellulose serves to confirm our hypothesis.

Observations are being pursued with other species that typically develop overmature wood.

Anatomy of Specimens Tested

Attention is directed to the illustrations of structure of the wood of Douglas fir shown in Figure 2. Figure 2*a* illustrates wood formed when the stem was relatively young (about 50 years old) growing at a rate of some

20 rings per radial inch and producing a normal width of latewood. The wood in this part of the stem was about normal in specific gravity (about 0.45 based on saturated volume and oven-dry weight) and having reasonable complement of latewood with characteristic thick-walled cells. Its cellulose and lignin contents seem characteristic of mature wood. Figure 2*b* illustrates the type of overmature wood of Douglas fir formed after this stem was over 300 years old. This is the type of wood with thin-walled cells, insignificant proportions of visible latewood and extremely low specific gravity for Douglas fir (about 0.35). The fact that such wood with abnormally thin-walled prosenchyma for its species is relatively low in α-cellulose is to be expected on the basis of the morphology of its thin cell walls as predicted.

Summary and Conclusions

Relationship between cell-wall morphology and both physical and chemical properties of normal wood (free from reaction wood) has been indicated. The information presented warrants the following conclusions.

1. Normal patterns of variation in morphology of the secondary cell-wall effect corresponding variations in physical or mechanical properties of prosenchyma cells which in turn may cause wide variation in these properties of the wood of variable species.

2. Evident variation in thickness of prosenchyma cell walls may be so associated with variation in relative proportions of the lignin and α-cellulose constituents of the cell walls as to effect significant variation in chemical properties of wood of variable species.

3. The variation in cell-wall morphology capable of effecting variations in physical, mechanical, and chemical properties of wood is illustrated in the basic difference between thin-walled and thick-walled prosenchyma.

4. Within the same species, thin-walled prosenchyma cells are relatively high in lignin and low in α-cellulose, whereas normally thick-walled prosenchyma is lower in lignin and higher in α-cellulose.

5. Significant differences in content of lignin and α-cellulose are shown in analyses of earlywood and latewood of the same annual layers.

6. Overmature wood of relatively old trees has characteristically thin-walled prosenchyma with higher lignin and lower α-cellulose content than wood formed during earlier stages of growth.

7. In view of the variation in physical and chemical properties of wood that may occur within the same log, there is obvious need for anatomical control over selection and appraisal of wood material used for any critical program of testing or research.

References

1. Bailey, I. W., and T. Kerr, *J. Arnold Arboretum*, **18,** 185 (1937).
2. Hale, J. D., *Forest Prod. J.*, **7,** 140 (1957).
3. Hale, J. D., *Tappi*, **45,** 538 (1962).
4. Jayne, B. A., *Tappi*, **42,** 461 (1959).

5. Keith, C. T., *Forest Prod. J.*, **11**, 122 (1961).
6. Lange, P., *Tappi*, **42**, 786 (1959).
7. Leopold, B., and D. C. McIntosh, *Tappi*, **44**, 235 (1961).
8. Ritter, G. V., and L. C. Fleck, *Ind. Eng. Chem.*, **18**, 608 (1926).
9. Wise, L. E., N. Murphy, and A. A. d'Addieco, *Paper Trade J.*, **122**, 2 (1946).

Synopsis

Physical variation in thickness of the prosenchyma cell-walls that is so evidently associated with variation in density and in related physical and mechanical properties of wood is also linked with variation in relative proportions of the lignin and α-cellulose constituents of the prosenchyma cell walls and, thereby, may cause significant variation in chemical properties of variable species. Examples cited in two coniferous species illustrate how wood composed of prosenchyma cells with thin walls is relatively high in lignin and low in α-cellulose, whereas that composed of normally thick-walled prosenchyma is lower in lignin and higher in α-cellulose content. Thus earlywood tends to have higher lignin and lower α-cellulose than latewood of the same annual ring. Local variation in the proportion of earlywood and latewood may, therefore, induce corresponding fluctuation in α-cellulose content within the same tree. The fact that overmature wood of relatively old trees has characteristically thin-walled prosenchyma with higher lignin and lower α-cellulose content than is characteristic of wood formed during earlier stages of the tree's growth introduces another recognizable cause of physical and chemical variation in large trees. In view of the anatomical basis of variation in physical, mechanical and chemical properties of wood that may occur in the same log, there is obvious need for anatomical control of selection and appraisal of wood material used for any critical program of testing or research.

Résumé

La variation physique de l'épaisseur des parois cellulaires du prosenchyme qui est associée de façon si évidente avec les variations de la densité et des propriétés physiques et mécaniques correspondantes du bois est aussi reliée à la variation des proportions relatives de la lignine et des constituents alpha-cellulosiques des parois cellulaires du prosenchyme et dès lors peut causer une variation appréciable des propriétés chimiques de différentes espèces. Des exemples tirés de deux espèces de conifères illustrent comment du bois composé de cellules de prosenchyme à parois minces contient relativement beaucoup de lignine et peu d'alpha-cellulose, alors que le bois composé de prosenchyme à parois d'épaisseur normale contient moins de lignine et plus d'alpha-cellulose. Ainsi du bois de printemps tend à avoir plus de lignine et moins d'alpha-cellulose que le bois d'automne du même anneau annuel. Une variation locale de la proportion de bois de printemps et de bois d'automne peut dès lors induire une fluctuation correspondante de la teneur en alpha-cellulose dans le même arbre. Le fait que du bois trop mur d'arbres relativement vieux présente un prosenchyme à parois minces caractéristique avec un contenu en lignine plus élevé et en alpha-cellulose plus bas que celui qui caractérise le bois formé durant les premiers stades de la croissance de l'arbre, introduit une autre cause reconnaissable de variation physique et chimique dans les grands arbres. Étant donné la base anatomique des variations des propriétés physiques, mécaniques et chimiques du bois qui peut se trouver dans le même rondin, il y a un besoin manifeste de contrôle anatomique de la sélection et de l'appréciation de bois utilisé pour n'importe quel programme critique.

Zusammenfassung

Die physikalische Änderung der Dicke von Prosenchym-Zellwänden, die so augenscheinlich mit einer Änderung der Dichte und verwandter physikalischer und mechanischer Eigenschaften des Holzes verknüpft ist, hängt auch mit einer Änderung der

relativen Anteile der Lignin- und α-Cellulosebausteine der Prosenchym-Zellwände zusammen und kann dadurch eine charakteristische Änderung der chemischen Eigenschaften verursachen. Beispiele aus zwei Coniferenarten zeigen, dass Holz mit Prosenchymzellen mit dünnen Wänden verhältnismässig hohen Lignin- und niedrigen α-Cellulosegehalt aufweist, während solches mit normal dickwandigem Prosenchym niedrigeren Lignin- und höheren α-Cellulosegehalt besitzt. Es zeigt daher das Frühlungsholz eine Tendenz zu höherem Lignin- und niedrigerem α-Cellulosegehalt als das Spätholz des gleichen Jahresringes. Lokale Variationen im Verhältnis zwischen Frühholz und Spätholz können daher zu einer entsprechenden Schwankung im α-Cellulosegehalt innerhalb desselben Baumes führen. Die Tatsache, dass überreifes Holz verhältnismässig alter Bäume charakteristisch dünnwandiges Prosenchym mit höherem Lignin- und niedrigerem α-Cellulosegehalt, als für Holz aus früheren Wachstumsstadien des Baumes charakteristisch ist, besitzt, lässt eine weitere Ursache für physikalische und chemische Veränderungen bei grossen Bäumen erkennen. In Hinblick auf die anatomische Grundlage für die Veränderungen der physikalischen, mechanischen und chemischen Eigenschaften von Holz, die im gleichen Block auftreten können, besteht offenbar ein Bedürfnis für eine anatomische Kontrolle der Auswahl und Beurteilung von Holz für jedes kritische Test- und Forschungsprogramm.

JOURNAL OF POLYMER SCIENCE: PART C NO. 2, PP. 263–270 (1963)

Chemical Nature of Genetic Material

F. U. KLAEHN,* *College of Forestry, State University of New York, Syracuse, New York*

Recent advances in genetics have been accelerated by the use of fungi, bacteria, and viruses. One of the primary advantages of these organisms for this type of research is their ability to multiply at a tremendous rate. They can be investigated in detail by modern methods which have resulted in important new information. There is also an increasing tendency for geneticists and biochemists to think in common terms when considering biological problems and to use each other's techniques. Most stimulating, however, for new approaches in the field of genetics have been the results obtained from chemical investigations of the cell nucleus, which is the center of inheritance of all living organisms.

Since the rediscovery of Mendel's work in 1900 and for forty years thereafter, geneticists worked almost exclusively with animals and higher plants. Important knowledge of classical genetics was derived primarily from studies of the garden pea, maize, fruit fly, mouse, and man. The "factor" or Johannsen's "gene" is the unit of inheritance. Thomas Hunt Morgan and others showed in the second decade of this century that the genes are located in the chromosomes and are arranged in linear form. The numerous genes carried in a single chromosome are linked (i.e., they tend to be transmitted to the offspring as a group). During the process of meiosis, linked genes may recombine through crossing over between homologous chromosomes. The frequency of recombination for any two linked genes is a function of the distance between them. This provides the basis for the development of linear genetic maps of gene loci. Gene maps of *Drosophila* were largely developed by Morgan and his school.

Until recently it was thought that the process of crossing over does not alter individual genes, i.e., crossing over occurs between genes not within them. This led to the assumption that the gene is the primary biological unit which occupies a definite position in the chromosome—a locus—and which is transmitted as such from one generation to another. In recent years, however, experimental results have accumulated that, according to Beadle,[1] can be interpreted to mean that the gene is divisible by intragenic crossing over. Much of this evidence was derived from microbial genetics.

When the chromosome set of salmon sperm is investigated chemically only two substances are found, deoxyribonucleic acid (DNA) and a rela-

* Deceased, October 21, 1962.

tively inert type of protein. The protein belongs to a class called protamines which consists of about 90% arginine. This protein is formed late in the maturation of the sperms, replacing a more complex protein, histone. The protamine, in turn, seems to be replaced by histone soon after fertilization. This leaves only the DNA as the material transmitted from generation to generation by male salmon.

It should be mentioned here that nucleic acid was well known in the last century. Its relative uniformity in composition (or what was thought to be its uniformity), however, made it appear unlikely to be the component in which genetic information could be stored and transmitted from generation to generation. It was thought that the proteins, highly variable in structure and configuration, were responsible for inheritance.

In 1944 Avery, MacLeod, and McCarty showed that highly purified preparations of DNA obtained from a certain strain of bacteria, when added to cultures of a related strain, resulted in a permanent genetic change of that related strain. This as well as other experimental results indicated that DNA and not the proteins had to be considered as the carrier of genetic information. This has been supported recently through studies with viruses, organisms which are composed exclusively of protein and nucleic acid, DNA or RNA (ribonucleic acid). Reproduction of certain viruses has been brought about by transmission of only the nucleic acid component to the host cell.

The role of DNA as the genetic material in inheritance is also supported by correlations found between the properties of genetic material and the amount of DNA analyzed. DNA is found exclusively in the cell nuclei and is relatively constant per cell nucleus whereas the amount of protein may change drastically, depending upon the physiological condition of the cell. There is also a correlation between chromosome number and amount of DNA. Haploid cells have only half the amount of DNA in diploid cells.

Many experiments indicate that DNA, once formed, is metabolically inert and does not participate in cellular metabolism to the same extent as do other cellular materials. Some geneticists believe that this metabolic inertness is further evidence for the genetic role of DNA since only material which is highly stable can serve the purpose of storing and transmitting genetic information unchanged over long periods of time.

If DNA is the carrier of genetic information there must be something about its structure which enables it to fulfill all the properties of a gene. This means it must be able to reproduce itself unchanged from one cell generation to another, but has the capacity to change occasionally (i.e., to mutate) and to direct the cells in their functions.

DNA can be isolated from cells of nearly all living organisms. Independent of the source, all DNA has many of the same chemical and physical properties. It is a macromolecule of variable molecular weight. In general, it is composed of four repeating units, the nucleotides which contain phosphoric acid, a 5-carbon sugar (deoxyribose), and a purine or pyrimidine base. The difference between the nucleotides lies in the bases. Four bases

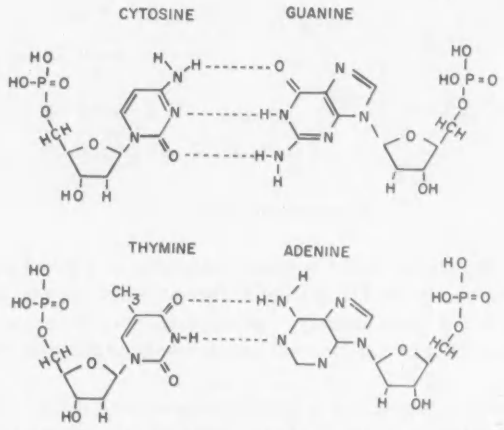

Fig. 1. Chemical structure of the four nucleotides of DNA: cytosine–guanine and thymine–adenine.

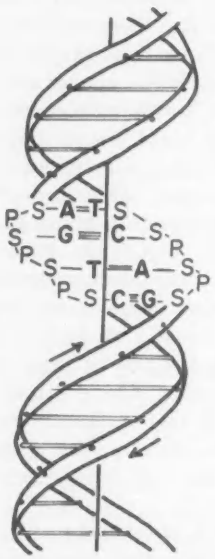

Fig. 2. Diagrammatic representation of the Watson-Crick DNA structure: (P) phosphate; (S) sugar; (A) adenine; (T) thymine; (G) guanine; (C) cytosine. Horizontal parallel lines symbolize hydrogen bonding between complementary bases.

are most frequently found in DNA, two purines (adenine and guanine) and two pyrimidines (cytosine and thymine). The chemical structures of these bases are presented in Figure 1.

Chargaff and his co-workers extracted DNA from many different sources and measured the relative proportions of the four nucleotides in the

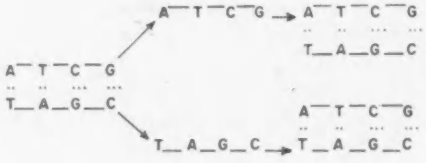

Fig. 3. Replications of DNA.

polymer. They found that the relative amount of a given nucleotide, for instance adenine, in the DNA from higher animals, insects, higher plants, fungi, etc., varied tremendously. When, however, the amounts of purine nucleotides and the pyrimidine nucleotides were added, the two sums were equal.

In 1953 Watson and Crick suggested a model for DNA. This structure is based upon the construction of molecular models arranged in such a way as to conform to the physical characteristics of the DNA molecule. On the basis of evidence derived from conventional chemical methods of analysis and x-ray diffraction techniques these workers suggested that DNA occurs in the form of very long, double right-handed helices as shown in Figure 2. In each helix two polynucleotide chains are joined together around a common axis by hydrogen bonds between paired pyrimidine and purine bases. The phosphate and sugar groups form the outside strands of the helix, and the bases are inside. The unique feature of the structure lies in the arrangement of the bases. These are arranged perpendicular to the fiber axis in specific complementary pairs, adenine with thymine (A–T) and guanine with cytosine (G–C). In Figure 2 the horizontal parallel lines symbolize the hydrogen bonding between complementary bases. These base sequences are arranged in linear form.

The diameter of the Watson-Crick double helix is 20 A. and its pitch is 34 A. The distance along the axis between base pairs is 3.4 A., with 10 base pairs per turn of the helix. The length of the DNA molecule is about 3×10^4 nucleotides or 15,000 nucleotide pairs. An almost unlimited variability is possible in DNA, a basic requirement for any molecule carrying genetic information. At least hundreds of base pairs probably correspond to a gene.

Unlike some DNA models developed by other workers, the Watson and Crick structure is most satisfactory from the biological point of view because it provides a reasonable basis for the replication of DNA. According to Watson and Crick, the replication process takes place in such a way that the complementary nucleotide chains separate by breakage of the weak hydrogen bonds. The single chains then acquire partners by incorporating at each base level the complementary building material from the cell environment. This process is shown in Figure 3. In this figure molecule of DNA consists of four pairs of nucleotides. (The hydrogen bonds between the various pairs are represented by dots, and the sugar-

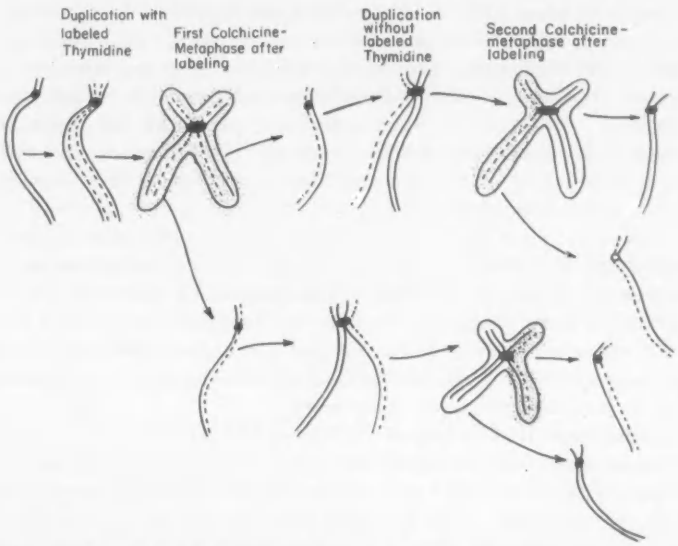
Duplication with labeled Thymidine
First Colchicine-Metaphase after labeling
Duplication without labeled Thymidine
Second Colchicine-metaphase after labeling

Fig. 4. Results and interpretation of Taylor's results.[2] Solid lines represent nonlabeled chromosomes; dashed lines represent labeled material.

phosphate backbones are indicated by dashes.) After replication, the two strands separate. Strand I, above, directs the synthesis of a new strand II, and the original strand II directs the formation of a new strand I. This method of replication permits the preservation of identity from generation to generation, because a strand once formed will remain intact and will dictate the structure of the new complementary strand. In addition, if the base sequence serves as the code of heredity, there is a way to preserve and transmit the code indefinitely, if no mutation occurs.

Experiments with microorganisms and higher plants have been conducted to test the validity of the Watson and Crick hypothesis and to obtain information on the replication of DNA. Techniques used in these studies involve the incorporation of radioisotopes into DNA molecules during replication. The distribution of the label among the daughter chromosomes or DNA molecule following subsequent replications provide information on the mechanism involved. Taylor's experiment with *Vicia faba*, the broad-bean, illustrates this technique.[2] Seedlings of this plant were grown for one cell division in solutions of tritium-labeled thymidine. Tritium, a radioactive isotope of hydrogen, emits a very low energy β radiation when it decays. The plants were then removed from the labeled solution and placed in nutrient solutions lacking the isotope but containing colchicine, a mitotic poison whose presence results in the doubling of the chromosome number in the cell. At intervals the distribution of the label in the chromosomes was investigated by autoradiography. The mitotic divisions were

studied in all cases. The results are shown in Figure 4. It was found that after removal from the isotope solution, but before the subsequent mitotic division, all chromosomes are equally labeled. After one division in the absence of isotopes, one-half of the chromosomes were labeled and one-half nonlabeled. After two divisions about one-quarter of the chromosomes were labeled. This indicates that the isotope distribution is semiconservative, a requirement of the Watson-Crick hypothesis. Other experiments have shown similar results.

It is not yet clear how the two chains of the double helix of the DNA molecule separate when duplication occurs. Theoretically this can come about by untwisting or by systematic breakage and reunion. The problem, however, is not a simple one because the molecular weight of DNA indicates that the helices must have a length of at least 1000 or more turns. This means that the length of the DNA per chromosome of a higher plant could be measured almost in meter units.

Another important feature of the Watson-Crick model is that it provides mechanisms by which mutations can occur. In the normal process of DNA replication an adenine base pairs with a thymine base and a cytosine base bonds with guanine. This has been shown in Figure 3. As a very rare exception, however, an adenine base may select a cytosine base, and this cytosine base will in the next replication pair with guanine. The C–G (cytosine–guanine) pair would then have replaced the original adenine–thymine pair. Other substitutions might occur by the same mechanism. Mutational changes might also result from the loss of base pairs, inversion of pair sequences or duplications. Due to the stability of the DNA molecule, errors in selecting the right base or, as some people have put it, errors in the sequence of the "Morse code" occur very seldom. If they occur more frequently, they are undetectable.

The problem of gene function and DNA has created special interest. It was found, for instance, that in bacterial viruses, DNA injected into the host cell causes the cell to synthesize the protein material that is to constitute the coats of the daughter viruses. The question is whether or not DNA serves directly as a template (pattern or model) for protein synthesis and whether or not the chromosomes are the actual sites of protein formation. Experimental results have revealed that protein synthesis occurs mainly in the cytoplasm and is associated with specific elements called microsomes. Therefore we must conclude that an intermediate substance operates between the gene and the microsome. Recent evidence indicates this intermediate is RNA (ribonucleic acid). RNA differs from DNA in its base composition and its pentose sugar component. The three bases, adenine, guanine, and cytosine, are present as in DNA. The fourth base, uracil, is found in the place of thymine. RNA is largely, but not exclusively, found in the cytoplasm of the cell. RNA is also involved in the synthesis of proteins, and recent experimental results on the synthesis of protein *in vitro*, suggest that a number of different RNA's are required for this synthesis. A model of the RNA molecule has not been proposed yet.

Concluding this short review on the chemical nature of the genetic material a few generally accepted assumptions may be made.

1. The primary genetic material in all cellular forms of life and in some viruses appears to be deoxyribonucleic acid (DNA), but in some plant and animal viruses it is ribonucleic acid (RNA).

2. The genetic information consists of specific sequences of the bases in the DNA or RNA molecule.

3. In bacterial viruses, the DNA or genetic material seems to consist of one continuous double helix.

4. It is assumed that the double helix of DNA replicates by the separation of the two complementary polynucleotide chains. Each strand then serves as a template for the synthesis of a new partner. The actual mechanism by which this occurs is still unknown. Mutations may be the result of a substitution of certain base pairs, rearrangement, duplication or deletion of base pairs.

A gene, the elementary biological unit, may now be defined from the chemical point of view as a unit of nucleic acid or a DNA segment with a specific cellular function.

Literature references to particular work mentioned or cited in this review are available in the bibliographies of the papers and books listed at the end of the paper.[3–5]

References

1. Beadle, G. W., *Gene Structure and Function*, University of Missouri, College of Agriculture, Agri. Exptl. Sta. Res. Bull. No. 588, Columbia, Mo., 1957.

2. Taylor, J. H., *Am. Naturalist*, **91**, 209 (1957).

3. Beadle, G. W., in *Chemical Basis of Heredity*, McElroy and Glass, Eds., Johns Hopkins Press, Baltimore, Md., 1957.

4. Bonner, D. M., *Heredity*, Prentice-Hall, Engelwood Cliffs, N. J., 1961.

5. Strauss, B. D., *An Outline of Chemical Genetics*, Saunders, Philadelphia, Pa., 1960.

Synopsis

A review is given of the generally accepted assumptions concerning the chemical nature of the genetic material. The primary genetic material in all cellular forms of life and in some viruses appears to be deoxyribonucleic acid (DNA), but in some plant and animal viruses, it is ribonucleic acid (RNA). The genetic information consists of specific sequences of the bases in the DNA or RNA molecule. In bacterial viruses, the DNA or genetic material seems to consist of one continuous double helix. It is assumed that the double helix of DNA replicates by the separation of the two complementary polynucleotide chains. Each strand then serves as a template for the synthesis of a new partner. The actual mechanism by which this occurs is still unknown. Mutations may be the result of a substitution of certain base pairs, rearrangement, duplication, or deletion of base pairs. A gene, the elementary biological unit, may now be defined from the chemical point of view as a unit of nucleic acid or a DNA segment with a specific cellular function.

Résumé

Un compte rendu est donné au sujet des conceptions généralement acceptées concernant la nature chimique de la substance génétique. La substance génétique de base dans toutes les formes cellulaires de la vie et dans plusieurs virus, semble être l'acide

déoxyribonucléique (DNA) mais chez plusieurs virus de plantes et d'animaux c'est l'acide ribonucléique (RNA). Les connaissances génétiques sont en accord avec des suites spécifiqes de bases dans la molécule de DNA or RNA. Dans les virus bactériels la DNA ou substance génétique semble être constituée d'une hélice double continue. On admet que la double hélice du DNA se scinde en deux chaînes polynucléotides complémentaires. Chaque tronçon sert alors de base pour la synthèse d'un nouveau partenaire. Le mécanisme par lequel ceci a lieu n'est pas encore connu. Les mutations peuvent être le résultant d'une substituation de certains couples de base, d'un réarrangement, d'une duplication de séparation de couples de base. Un gène, l'unité élémentaire en biologie, peut maintenant être défini du point de vue chimique comme une unité d'acide nucléique ou d'un segment DNA avec une fonction cellulaire spécifique.

Zusammenfassung

Es wird ein Überblick über die allgemein angenommenen Ansichten bezüglich der chemischen Natur des genetischen Materials gegeben. Das primäre genetische Material scheint in allen zellulären Lebensformen und in einigen Viren Desoxyribonucleinsäure (DNA) zu sein, bei einigen Pflanzen- und Tierviren ist es aber Ribonucleinsäure (RNA). Die genetische Information besteht aus spezifischen Basensequenzen im DNA- oder RNA-Molekül. In Bakterienviren scheint DNA oder genetisches Material aus einer kontinuierlichen Doppelhelix zu bestehen. Es wird angenommen, dass sich die DNA-Doppelhelix durch Trennung der beiden komplementären Polynucleotidketten reproduziert. Jede Kette dient dann als Matrix für die Syntheses eines neuen Partners. Der tatsächliche Mechanismus für diesen Vorgang ist noch unbekannt. Mutationen können das Ergebnis einer Substitution gewisser Basenpaare, einer Umlagerung, Duplizierung oder Vernichtung von Basenpaaren sein. Ein Gen, die biologische Grundeinheit, kann jetzt vom chemischen Gesichtspunkt aus als Nucleinsäureeinheit oder DNA-Segment mit spezifischer Zellfunktion definiert werden.

PANEL DISCUSSION: FUTURE TRENDS IN CELLULOSE RESEARCH

JOURNAL OF POLYMER SCIENCE: PART C NO. 2, PP. 273–276 (1963)

Future Trends in Cellulose Research*

FRANK R. CHARLES, *Industrial Cellulose Research, Ltd., Hawkesbury Ontario, Canada*

Future trends in cellulose research is, beyond all doubt, a most important topic for discussion. Powerful forces are at work today to rob cellulose of its heritage, and we must all work to ensure that research takes the right direction and is done on a scale comparable to that of our synthetic polymer competitors.

Cellulose Needs to Develop as a Chemical Industry

The cellulose industry, after a century of phenomenal expansion, almost unchallenged until the last decade, must guard against being on the defensive with respect to the plastics industry. This giant new chemical industry, growing exponentially, is taking cheap and abundant raw materials into its factories and is producing, to order, chain molecules of every conceivable length, strength, flexibility, durability, reactivity, or inertness. These turn up in containers, bags, films, industrial fibers, textiles and a host of other products.

Where does this leave cellulose?

Cellulose is abundant in nature and holds the potential of a full competitive stature if research and development are carried out intelligently and aggressively. Cellulose must manifest that it, too, is a chemical industry and must develop its full potential as a chemical industry.

Basic research into the fundamentals of cellulose offers a challenging and a definite path to success and must be expanded to meet this new and aggressive competitive situation.

Cellulose products can and must be developed in chemically altered forms, chemically altered to eliminate existing deficiencies, to anticipate intensified competition from synthetic polymers, to create exciting new fields of use, and to take over existing fields from other raw materials. Directions this chemical alteration may take are derivative formation, crosslinking, graft polymerization, and inspired new transformations to be conceived in the unbridled imagination of basic research scientists working in this field and unshackled by current problems.

Concurrently with chemical alteration, metamorphosis of cellulose by synthetic polymer protection must be exhaustively studied in all its infinite varieties and aspects—single fiber coatings, web coatings, film and

* Discussion for this paper appears on pp. 258 and 286 of this issue.

fabric coatings, anchor coatings, overlays, mechanical blends, coprecipitation, etc.

Ways should also be sought to develop cellulose as a raw material for the manufacture of organic chemicals.

Cellulose has unique and unparalleled natural advantages. Supremely hydrophilic, it gives us comfortable apparel and absorbent cloths and papers. Cellulose alone of all polymers has the ability to fibrillate, which gives us the miracle of paper and board.

However, it is just these properties that we have to temper by research in order that cellulose may manifest, where the end-use so requires, still greater strength and toughness, water resistance, chemical resistance, reduced swelling, reduced flammability.

Even without chemical alteration, cellulose, one of nature's stereospecific chain molecules, has all that it takes to acquire properties far superior to those attainable today.

A newly recognized fundamental principle in the science of materials is that a two-phase system, composed of a high-strength, high-modulus material and another material of comparatively low modulus, may possess greater strength and toughness than the high-strength component alone. This is due to the isolation of flaws in the high-strength elements by the surrounding low-modulus substance, preventing crack propagation. This type of composite structure enables the high-strength substance to perform closer to its theoretical limit. The extraordinary strength and elasticity of the glass fiber-reinforced fishing rod point this out.

We have this type of situation on a supermolecular level in regenerated cellulose. It is a two-phase material wherein the high-strength, high-modulus component is the crystalline cellulose, and the less ordered or amorphous material is the low-modulus component.

In glass fiber-reinforced plastics, the finer the denier of the glass fibers and the better their dispersion, the higher is the composite strength. Thus in regenerated cellulose, if means can be found to disperse the crystalline cellulose to near unit-cell strings, a much larger percentage of the theoretical 60 g./den. of the C-O-C bond should be attained, while retaining a good part of the extensibility of the amorphous cellulose component. This essentially physical change may not of course be accomplished without intermediate chemical transformations. Also, dissolving pulps of improved purity and controlled chain length distribution may be necessary.

To develop our full potential as a chemical industry, we will have to relate the behavior of cellulose, far more than now, to its fundamental chemical and physical properties. This will require systematically planned attacks on the fine structure by means of computer, NMR spectroscopy, electron microscopy, x-ray diffraction, radioactive tracers, infrared spectroscopy, mass spectrometry, and instruments and techniques yet to come, to lay bare the fine chemical-structural differences of different cellulose forms. How do the atoms lie in the molecule, the molecules in the unit cell, the unit cells in the crystallite, the crystallites in the microfibril and the micro-

fibrils in the fiber? Where and how is the amorphous cellulose located with respect to all these different sized units? What are the differences of these arrangements in cotton, wood cellulose, high yield pulps, beaten fibers, cellophane, super-4-tire yarn, polynosics, cellulose derivatives, crosslinked cellulose, grafted cellulose? Where and how are the hemicelluloses or lignin located? Where and how are the crosslinks or grafts located? How long are they?

Some excellent work of this type has already been done, but the surface has only been scratched, and the extent of the promise of achievement invites a really intensive program of research.

Nonfibrous Uses

Again in the modification of physical form, but going in the opposite direction we have the microcrystalline cellulose commercially called Avicel. Cellulose is acid-hydrolyzed to levelling-off degree of polymerization and then mechanically sheared in water to break up remaining intercrystallite chains and thus separate the crystalline particles and remove their broom-like ends. It is reported that these crystals have potential in hard-compacted structural materials, resistant to the penetration of an ordinary nail and even to an oxyacetylene torch, and as raw material for the production of cellulose derivatives in a new colloidal form.

Better Yield from Wood is Needed

One of the important future trends in cellulose research for paper end-use is to retain as much as possible of the hemicellulose and lignin in the cellulose fiber. This is desirable for obvious economic reasons and also for improved properties and new fields of use. Great strides are already being made in this direction, and good brightnesses are being obtained from high yield pulps. On the other hand, there are many problems to be solved, one of which is the increased susceptibility to degradation due to the noncellulose impurities. We still specify cotton rag cellulose for legal documents and currency to last a hundred years. It is said that the ordinary books produced today will be yellow and crumbled in 25 years. Studies to understand and inhibit this degradation is one obvious direction for cellulose research.

Hemicelluloses

The field of hemicellulose is rightfully a part of cellulose research. Some woods have very high hemicellulose proportions and yield pentosans and hexosans or their derivatives of quite a good degree of polymerization. These have a great potential for films and gums. If applications can be successfully developed for these hemicelluloses, it will also help to clear up a waste disposal problem. We must not forget either the use of hemicelluloses as a chemical raw material for the manufacture of industrial organic chemicals.

Personnel

A most important consideration is the attraction of the best qualified scientific personnel into cellulose research; the more cellulose proves it is a chemical industry the easier this will be.

The organization of our scientific manpower is of paramount importance. We have already stressed that emphasis on instrumental methods is obligatory—instruments dictate the pace of research. This means relying more on the younger personnel. One of the largest chemical organizations in the world has found that most of the valuable new ideas in their research organizations are coming from chemists 5 years out of university. This means we should get our young, up-to-date, active chemists and physicists quickly at grips with important problems and avoid using them for routine work. In cellulose research, as in all other research, brains are our best raw material.

JOURNAL OF POLYMER SCIENCE: PART C NO. 2, PP. 277–278 (1963)

Cellulose as a Chemical Raw Material*

W. M. HEARON, *Crown Zellerbach Corporation, San Francisco, California*

Cellulose is not commonly thought of as a chemical raw material in the same sense as benzene, alcohol, ethylene, formaldehyde, etc. However, it has been a raw material for derivatives such as cellulose nitrate, cellulose acetate, methyl cellulose, carboxymethyl cellulose, and hydroxyethyl cellulose. What I would like to discuss is cellulose as a chemical raw material for producing products where the glucoside chain no longer exists or at least is not the predominant factor affecting properties. Part of this discussion will be fact; part speculation.

At first glance cellulose might not appear to be an attractive chemical raw material, since it is a polymer and often not in a highly purified form. Against these defects, however, there are several outstanding advantages. First, as we all know, it is nature's most abundant organic raw material. Second, it is being forever replenished. A fact not well known, for example, is that we are today growing 1.34 trees in the United States for every tree that is cut down or lost by fire or biological attrition. Lastly, it is an inexpensive raw material. Cotton linters cost 6–8¢/lb. and you can today buy 90 G.E. kraft from Europe for $122 per ton; domestically you can buy semibleached kraft for $100 per ton. When you compare cellulose at 5–6¢/lb. with such high volume chemical raw materials as ethylene at 4.5¢/lb., benzene at 3.4¢/lb., or ethanol at 7.8¢/lb., you find that it is in the same price range.

The most obvious chemical product to be made from cellulose is glucose. While the hydrolysis of cellulose to glucose is not being done commercially in the United States there are European plants in operation and advanced development programs on new processes both in Europe and Japan. The dilute sulfuric acid process developed at the Forest Products Laboratory in Madison, Wisconsin, was used in the Springfield, Oregon, wood hydrolysis plant. While this plant never ran successfully, its failure was due more to poor engineering and other wartime factors than to basic defects in the process.

There is reason to suspect that the greater difficulty hydrolyzing cellulose as compared with starch may be attributable more to the physical structure of cellulose than to the type of glucoside linkage. Many new techniques are now available for changing the physical forms of materials, and one of these may render cellulose much more susceptible to hydrolysis. If this is true, cellulose may be the preferred raw material for the manufacture of glucose.

In passing, I wonder how easily the microcrystalline cellulose recently

* Discussion for this paper appears on pp. 285 and 286 of this issue.

reported by O. A. Battista and P. A. Smith is hydrolyzed. With its freedom from debris and colloidal size it might break down readily to high purity glucose.

Instead of producing glucose by hydrolyzing cellulose, methyl glucoside can be made if methanolic hydrogen chloride is reacted with cellulose acetate. This is a beautiful reaction, giving essentially 100% yield of the equilibrium mixture of α and β isomers and little coloration. Methyl glucoside is presently being manufactured from starch and is being used to make polyethers for urethane foams. Perhaps cellulose would find a place as a raw material for serving this market.

While the partial hydrolysis of cellulose to short-chain fragments has not been very successful, such products if they could be obtained in good yield might find use as starting points for plasticizers, detergents, surface-active agents, and crosslinking agents.

The microbiological degradation of cellulose has given some interesting products. Different cellulolytic microorganisms have given acetic acid, n-butanol, butyric acid, ethanol, methane, and lactic acid. While none of these degradations is economically feasible, the action of microorganisms on cellulose would appear to be an attractive area for further research, particularly when coupled with various mechanical pretreatments of the cellulose.

The action of strong mineral acids on cellulose will produce very satisfactory yields of levulinic acid through the intermediate formation of glucose and this reaction is the basis for a commercial plant now under construction in the Northwest. In the laboratory it is possible to stop the sequence of reactions short of full conversion to levulinic acid and 5-hydroxymethyl-2-furfural can be isolated.

Another interesting degradation of cellulose which might prove commercially attractive with further development is the production of *meso*-tartaric acid. When cellulose is oxidized with nitrogen tetroxide to oxycellulose and hydrolyzed with hydrochloric acid, a 28% yield of *meso*-tartaric acid is obtained. This oxidative hydrolysis of cellulose presents a potential area for fruitful research.

Perhaps one of the most interesting products which can be made from cellulose is levoglucosan. Cellulose when heated in a vacuum to relatively high temperatures produces respectable quantities of this 1,6-anhydroglucose. It, in turn, can be polymerized. Its trimethyl ether when treated with sodium in liquid ammonia produces phenol in over 50% yields. While these reactions do not presently represent an attractive commercial route to phenol, they do show the possibilities which exist for converting cellulose to useful organic chemicals—chemicals which at first glance seem impossible as products from cellulose.

Because of the ready and continued availability of large quantities of cellulose and its relatively low cost, it is potentially an attractive raw material for producing other chemicals. With the establishment of a few commercial processes utilizing cellulose to make chemicals, it would appear that extensive research is justified which would be directed toward finding new degradative reactions of cellulose. Successful results of such research could have a profound impact on both the wood and chemical industries.

JOURNAL OF POLYMER SCIENCE: PART C NO. 2, PP. 279–282 (1963)

Paper and Nonwoven Fabrics*

C. P. DONOFRIO, *Champion Papers Inc., Hamilton, Ohio*

An analysis of the life cycles in world industries as we now know them indicates by the Gompertz technique that the critical year for the paper board industry will occur at about 2219—it will be outlived by one other business only—insurance. The life cycle of its closest ally, silvichemicals, may be even longer if we identify its birth as the time when Moses tossed a log into the brackish water and sweetened it (Exodus 22:27).

As with most forecasts, we can view this with complacency, alarm, or apathy depending on our feelings and interpretation. We can speculate on the future characteristics of the paper industry, its products, and even on the role of cellulose itself; only one certainty will evolve—thin sheets of materials, irrespective of composition, will continue to serve mankind in many and varied ways whether felted, extruded, woven, or assembled by means not yet conceived. The single outstanding characteristic of the paper industry has been its ability to generate an enormous amount of useful surface per unit mass of fibrous cellulose at a low cost. Yet, except for a relatively narrow class of applications, cellulose is not the best suited nor the most desirable base material for the end-use in mind. In the industry itself, "coated" surfaces are growing faster than the "uncoated." In this instance, as in many other products, cellulose serves as the carrier or filler which in combination with something else does the job better. Functioning as a carrier does not necessarily demote the status of cellulose in the polymer kingdom. Mylar and polyolefin films as well are also used as carriers, as exemplified in new abrasive papers, carbon paper, proofing paper, and duplicating masters for office reproduction.

It can be said that the major trend in cellulose applications and research is a continued one toward more and improved combinations of cellulose with other materials which achieve the best balance of performance and economy at a given time. The same can also be said for many other fields that are responding to the needs of the marketplace. It is the need of the end user that ultimately determines the best choice of materials, and it is the attempt to satisfy that need that stimulates research toward new and improved materials.

Wherever thin substrates are desired for a new development first consideration is usually given to paper because of its cost and availability. As science and technology advance to serve us in new and more convenient

* Discussion for this paper appears on pp. 285 and 286 of this issue.

ways, more and more is demanded of materials including paper. I want to review some of these new developments to illustrate what is demanded of paper or cellulose, particularly where these materials are being subjected to "new" physical and chemical stimuli.

In the publication field there is the perpetual trend toward lightweighting with concomitant maintenance of opacity. We are moving closer and closer to the limitations of the shape and geometry of cellulosic fibers. This, coupled with the adverse density and cost factors of mineral constituents, will likely encourage more work in the physical disassembly of cellulose with the aim of developing an expanded or foamed system wherein air rather than mineral pigment will contribute opacity. Obviously, this will also call for new approaches for bonding the entities together. Similar approaches will probably be taken with coatings as well. We have heard of cellulose microcrystals (Avicel) that are smooth, opaque, and free-flowing; a material of this kind may find a place alone or with dyes for controlling opacity. It may find a place also in new forming techniques which provide for laying down multilayers of materials (not the same as cylinders) and thereby facilitate the formation of more uniform and improved architecture possessing both more planar surface and improved light scattering properties. New paper-forming developments in England may be potentially suitable for putting together such multilayer sheets. This same system may also provide a means of improving dimensional stability of paper by incorporating noncellulosic fibers in the intermediate layers.

There is another form of "disassembled" cellulose developed by du Pont which works in a different way. These are highly swollen fine cellulose particles which can be used to impart greater strength to conventional self-bonding fibrous substrates. This is the cellulose analog of the polyester and polyamide fibrids which serve as the binder in the du Pont "textryl" system.

Presently there is much work going on in the blending of cellulose with man-made fibers. One company alone reports to have worked with some 40 or more "exotic" fibers. Glass, aluminum, Dacron, nylon, and self-bonding acrylic and rayon fibers are among those that have been investigated in both consumer and industrial products, such as moldable automotive parts, filtering media, wearing apparel, and special papers.

Cellulose assists in the forming of thin layers of glass fiber subsequently used in forming polyester panels and forms. There is perhaps more interest than activity in nonwovens formed on the paper machine—almost every paper mill has an old paper machine which it would like to relegate to large-volume nonwoven business. However, most nonwovens are formed by dry processing in very small volumes compared to paper and mostly from synthetic fibers.

Sweden is reported to have experimented with paper bed-sheets, and there has been much said about disposable wearing apparel. It is no secret that as soon as the garment industry or another develops a technology for jointing garment pieces together inexpensively and at high speed dis-

posable garments will open the way for the large volume manufacture of nonwovens on as grand a scale as paper. This will come, but we are not sure when, and it will enhance a not-too-new trend toward softer, stronger, and comfort-giving cellulose.

Paper and other forms of cellulosic films provide a lot of useful surface cheaply where much surface is needed for certain industrial processes—in particular, separation processes which are receiving more and more attention in response to the needs for water treatment, waste disposal, and industrial processes. Apart from the conventional applications in filtration, cellulose is a good potential candidate for an excellent and effective absorptive or ion-exchange surface for the removal of refractory materials from water. There is also, as most of us already know, growing activity and interest in dialysis and electrodialysis as separation processes for water treatment and industrial processes. We also know that parchment and cellophane, the old standbys for dialysis, are being replaced by improved membranes. We are also aware of the present limitations of cellulose in these processes; however, it might prove quite fruitful if we were to orient some phases of work on the modification of cellulose in response to these exciting challenges.

In packaging, paper and paperboard materials will show a sustained growth rate but not of the magnitude of that to be exhibited by composite substrates and structures combining plastics, paper, metal, and other materials.

Cellulose not only makes the use of foils and some plastics possible for many packages but also contributes strength, protection, and other attributes for the satisfactory containment of products. There is a long list of polyolefins, vinyls, urethanes, and other synthetic materials bonded onto cellulose in film or foams. This activity, the "marriage of convenience" for plastics, foils, and paper, will continue with great vigor to overcome the present day limitations of certain monolithic materials and to meet the challenges of future needs. We can look forward to superior composite gas barriers for containing carbonated liquids and aerosols to contain dehydrated foods prepared by freeze drying and other techniques, to withstand temperatures of cooking in vending machines, to transmit radiation for heating, or to insulate in other instances; these are a few of the avenues being pursued which subjects cellulose to new environments.

A paper-forming process of Finnish origin prescribes a system wherein dry and separated cellulose fibers are deposited by means of 20,000 volts or more electric field onto a grounded forming surface carrying a thin layer of adhesive. This also allows for accomplishing some preferred orientation of the fibers. Further developments are underway in the electrostatic coating of paper.

Of perhaps greatest interest and challenge are the increasing number of new printing developments which subject cellulosic substrates to electric fields, radiant energy, and magnetism.

The electrostatic printing principle is being exploited in at least four proc-

esses, all of which require cellulosic substrates of special electrophysical characteristics. The process developed by RCA (Electrofax) combines a photoconductive coating with a paper substrate and Videograph utilizes a chargeable dielectric film coating on paper. Under these conditions the resistance-capacitance effects of cellulose particularly as affected by absorption of water become of enormous importance. We usually think of cellulose as an insulator and we also recognize that under many conditions it is highly susceptible to static electrification. Resins with which cellulose is often combined are also susceptible to the same electrophysical effects which can be beneficial or harmful, depending on the application.

There are an increasing number of applications in computer readout, office printing, and facsimile transmission where conductive substrates are required, and these are presently being made by various means depending on the level of conductivity prescribed by a particular system. Several groups are actively engaged in the elimination of static electrification of paper. There is also evidence that at least an equivalent amount of effort is being expended toward the development of semi- or permanently charged substrates which may be useful for a number of applications including atmolysis.

While some segments of printing are undergoing rapid and interesting changes, certain printing techniques are being used in developing solid-state devices on film surfaces and for developing opaque images in clear cellulosic films. These changes and developments in printing and communications are placing greater performance demands on cellulose over that which it can provide in its role as a carrier. So, if we formulate or speculate on new ways of changing cellulose we must keep foremost in our minds the major technological changes which dictate the development of new or modified thin sheets of material. The foregoing has been an attempt to identify some of these changes—we can be sure that these represent only a few. We also realize that we have dwelled mostly on applications and hardly at all on the basic research aspects which they involve. We can be sure, however, the changes and developments noted here will have great impact on the future course of basic cellulose research.

JOURNAL OF POLYMER SCIENCE: PART C NO. 2, PP. 283–286 (1963)

Cellulose Textile Science and Technology

J. WHARTON, *Courtaulds (North America) Inc., Mobile, Alabama*

Active research in the viscose rayon production field has led to major advances not only in economy of production but also in making available types of man-made cellulosic fibers which have great potential for the future.

It must be remembered that cellulose and cellulosic fibers are essentially hydrophilic. It is doubtful whether research time and effort based on an attempt to convert cellulose to a hydrophobic material will offer any economy or practical commercial rewards in the foreseeable future, since the vast majority of fiber-forming synthetic polymers already tend to be hydrophobic in character and fibers spun from these polymers are adequate to meet present and short-term future needs. The fact, however, that cellulose is hydrophilic does result in very beneficial effects for cellulose fibers used in apparel, towels, many nonwovens, etc.

Excluding cellulose acetate, the greatest research gains have been achieved not by trying to convert cellulose to another compound prior to fabric production but rather by getting the most out of cellulose by proper arrangement of the cellulose chains and control of the hydrogen bonding conditions which occur between the chains. Three examples of such development in the cellulose man-made fiber production field are tire yarn fibers, crimped fibers, and high wet modulus fibers.

Continuous improvements have been made in the properties of cellulosic tire yarn fibers, mainly through efforts to achieve a more and more homogeneous structure within the fiber itself. The cellulosic tire yarn fibers of today are a tremendous advance over those made ten to fifteen years ago and there is no doubt that the intensive research efforts of today to produce improved viscose tire yarn fibers in terms of strength, flex life, etc., will result in even better commercial products over the next few years. (The properties of matter being what they are, it is difficult to use presently available 100% nylon in a tire without the "setting" effects that lead to "morning thump.") The absence of this effect in tires which use rayon or Tyrex has enabled man-made cellulosic tire yarn fibers to hold the new car tire market.

The properties of crimped viscose staple fiber depend on the formation of natural crimp through having uneven fiber skin and core formation. This is a case distinct from the general trend to improve fibers by greater structural regularity, since the very lack of homogeneity in the fiber here confers a major benefit. In thermoplastic fibers, crimp is put in by mechanical distortion when the fiber is heated enough to accept deformation, but in

crimped rayon fibers the crimp is not mechanical but is due to strain effects within the fiber, essentially the same as those found in such natural fibers as wool or curly hair. If crimp is removed from crimped viscouse rayon fibers by putting them under tension, crimp can always be reasserted by wetting out the fiber provided the tension is released during the wetting out process. For this reason, heavy denier viscose crimped staples are admirably suited for such end uses as carpets, scatter rugs, and pile cut bedspreads. Recent research has resulted in the production of a finer and more intense crimp together with a higher fiber extensibility leading to a higher work of rupture and, therefore, improved wear life. It is interesting to note that the present total volume of viscose crimp staple sold in the U.S.A. alone totals some 120 million pounds per year.

High wet modulus viscose fibers represent one of the more important fiber innovations of recent years. Prior to 1953 it was not fully recognized that cotton fibers showed less shrinkage, when converted into fabrics, than rayon, because of their much lower extensibility when wet, therefore giving high resistance to tension in the wet state. Work on crosslinked fibers, which had a lower extension than normal rayon, indicated that these fibers produced more stable fabrics, and from then on much research was done towards the production of high tenacity, lower extensibility types of rayon through reorganization of the cellulose structure within the fiber itself.

Tachikawa of Japan was perhaps the first experimentalist to produce high wet modulus viscose fibers, but he does not seem to have fully appreciated, for many years, the profound effect which he got in the Toramomen fibers which he produced, so far as resistance to shrinkage potential was concerned. He appeared to have been more concerned with producing a cellulosic fiber based on minimum degradation from high D. P. cellulose raw material.

At the present time there appear to be two main types of high wet modulus viscose staple fiber and perhaps more are yet to come. One type has quite high tenacity, a somewhat reduced extension compared with normal rayon, rather poor resistance to caustic soda solutions, and quite high abrasion resistance; the other type can have very high tenacity, quite low extension, great stability to caustic soda, and a firmer, less rayonlike, hand in fabric, but rather lower abrasion resistance than the first type. There seems to be room for both these types according to the end use concerned. It is the desire of the rayon industry to compete with cotton by producing fibers superior to cotton, although in the past cotton has had some advantage apart from those based on the fact that it is a subsidized vegetable of export importance. There is no doubt that very interesting developments from man-made cellulose fibers having a high wet modulus will be seen over the next few years. Quite extraordinary cellulose fibers have been produced on an experimental basis, some of which have a tenacity of 12 g./den.

While much can be done in the production of cellulose man-made fibers to give new types, scheduled for a variety of end uses, it has been necessary for the cellulosic fiber producers to do much research and development work

concerned with the after-finishing or treatment of fabrics which contain a high percentage of cellulose man-made fiber. The textile and finishing industry itself had not done all that it might have done, through lack of research, to after-treat such fabrics so as to achieve the best consumer results. However, it is now possible to produce admirable wash–wear fabrics from 100% man-made cellulosic fibers. Certain of the man-made high wet modulus cellulosic fibers have properties superior to those of cotton in their ability to accept wash–wear finishes without very marked loss in tensile or tear properties.

I was interested in the discussions during this Conference concerning the possibility of graft polymerization, homopolymerization, or *in situ* polymerization within cellulose structures so far as the use of noncellulosic polymer-forming materials are concerned. An important case of what may be graft polymerization within cellulosic fibers is represented by the Belfast process in which the use of epichlorohydrin and caustic soda on a cellulosic fabric in the wet state results in the fibers within the yarns, and the yarns within the fabric, having a "memory" for the wet spatial conditions under which graft polymerization took place. This memory leads to recovery from wrinkles in the wet state. Combinations of graft polymerization, homopolymerization, and crosslinking within cellulosic fibers have been the subject of much research work within the rayon fiber producing industry over the past ten years. Cross-linked viscose fibers have been produced in large commercial quantities, and the resilience and other characteristics of such fibers have resulted in advantage for certain end-use products. It is, however, interesting to note that the major advantages associated with graft polymerization and homopolymerization within cellulosic fibers have been those associated with fabric treatment enabling fabrics made from cellulose to compete adequately in wash–wear properties with those made from certain thermoplastic fibers in which the memory is induced through mechanical deformation while the fabric is in a heat-sensitive state.

The future of man-made cellulosic fibers appears to be firmly established—the present demand for these fibers both in the United States and throughout the world is at a very high level. The research of the past ten years and the research now in progress leading to new developments promise an excellent future in terms of volume. Efficiency and improved know-how in production can increase demand through giving high consumer value at minimum cost.

Discussion

G. N. Richards (*AMF British Research Lab., Reading, England*): I should like to add to the possibilities considered by Dr. Hearon, the reminder that low molecular weight acids such as formic and oxalic acids can be prepared in high yield by interaction of sodium hydroxide and cellulose (e.g., in sawdust).

The specific oxidation of cellulose to cause scission between C_2 and C_3 yielding the dialdehyde, can, of course, be effected by periodate. This does not, however, solve the problem, because the hydrolysis of the product to C_2 and C_4 fragments cannot be carried out without degradation of these fragments.

Reduction of the dialdehyde cellulose solves some of this problem, of course, and makes possible a convenient synthesis of glycol aldehyde and erythritol bysub sequent hydrolysis.

N. C. Eastman (*Charleston, West Virginia*): Gas, oil, and coal won't be available forever as sources of raw materials for chemical production. What is the possibility of reducing cellulose (or wood) to six-carbon fragments or hexane compounds or derivatives. Will such compounds take over when coal, etc., give out?

R. H. Marchessault (*College of Forestry, Syracuse, New York*): Although starch is better for hydrolysis than cellulose could not the hemicellulose be just as attractive?

J. K. Craver (*Monsanto Chemical Co., St. Louis, Missouri*): I must urge you to consider the problems of competing with the chemical business. This is a tough game. We already have many processes for producing phenol and the profits here are minimal, but the cellulose-producing industry has one almost unique product now—paper. Paper is the target of the plastic film and metal foil industries now, but if paper—cellulosic paper, that is—can be improved in properties, it can hold its present markets and compete more successfully in new markets. The improvement of paper pulps by chemical additives seems a more worthy target than the search for chemical commodities from cellulose.

C. Schuerch (*Forest Chemistry Dept., College of Forestry, Syracuse, New York*): Levoglucosan can be produced in yields probably as high as 60% from cellulose under ideal conditions. Methylation gives a trimethyl ether which can be polymerized to products of DP 20–40 at least. This is a start to another linear polymer, in contrast to branched levoglucosan polymers produced from the unsubstituted monomer.

L. R. Thiesmeyer (*Pulp & Paper Research Institute of Canada, Montreal, Canada*): Research in our industry must follow a two-pronged attack. We are faced with competitive materials which offer not only better properties, but also lower costs. Therefore, while the cellulose chemists seek new and improved products, other researchers must seek major reductions in costs. These will not come from minor modifications to existing plants and processes, but from revolutionary new technology. Our industry has been too content with the rising costs it has experienced. There are complaints about this, of course, but not much active additional support to do something about it.

C. P. J. Glaudemans (*National Institutes of Health, Bethesda, Maryland*): What are the applications of all the efforts in the field of cellulose graft copolymerization?

D. B. Mutton (*Industrial Cellulose Research, Ltd., Hawkesbury, Ontario, Canada*): I would like to comment further on Dr. Glaudemans' remarks on grafting. I have no better idea than he has whether any commercial application will ever be made of this process. I think, however, we should not forget that our state of knowledge about grafting is still very elementary. This is emphasized by the fact that we do not yet know whether what we call grafting involves chemical bonding or simply *in situ* polymerization. I feel that commercial application of grafting and a complete evaluation of its possibilities may well depend on a better understanding of the nature and properties of graft copolymers. We may well have to control the location of the graft within the fiber, the frequency of grafting along the cellulose chain, and the chain length of the synthetic polymer side chain. At present we know very little about any of these subjects.

CONTRIBUTIONS FROM FRIENDS AND COLLEAGUES OF P. H. HERMANS

JOURNAL OF POLYMER SCIENCE: PART C NO. 2, PP. 289–310 (1963)

Classification of Carbonyl Groups in Cellulose on the Basis of their Reaction Rates at Oximation

HANNES SIHTOLA, LEO NEIMO, and RAIMO SUMIALA, *The Finnish Pulp and Paper Research Institute, Helsinki, Finland*

INTRODUCTION

Since the beginning of this century, copper number determinations taken as a measure of the reducing capacity of cellulose have played an important role in cellulose analysis, both in scientific research and in routine testing. However, during the last two decades it has become increasingly evident that the copper number accounts neither for the state of oxidation of cellulose nor for the amount of carbonyl groups of the material. Lately, oxidized cellulose has to an increased extent been characterized by determination of the aldehyde or carbonyl group content, and these procedures are tending to oust the use of copper number methods.

The methods adapted for the determination of carbonyl groups may be divided into two main groups: (*1*) those based upon the condensation of various compounds with the carbonyl groups, and (*2*) those based upon oxidation or reduction reactions, in which the carbonyl groups are oxidized to carboxyls or reduced to hydroxyls.

A thorough review by Stübchen-Kirchner, published in 1960,[1] gives a reasonably detailed picture of the scope of the most important methods employed for the determination of carbonyl groups. Mention should also be made of works by Cyrot[2] and Rochas et al.[3] concerning the oximation of cellulose, and by Albertsson and Samuelson,[4] who investigated the use of hydrazine in the determination of carbonyl groups. An improved modification of the method of Geiger and Wissler has also been described recently.[5,6] A common feature of all these methods is that the reaction between the reagent and the carbonyl groups is allowed to attain a state of equilibrium, following which there is determined by some suitable means either the consumption of the reagent or the amount of reaction product. As a consequence, the sum is obtained of all the carbonyl groups which are capable of reacting with the reagent concerned, regardless of the sensitivity of the different carbonyl groups to this reagent. Accordingly, and dependent on the nature of the carbonyl groups, the different methods may give consistent results for one pulp, whereas the values for another pulp may differ considerably. Recent results obtained at the Finnish Pulp and Paper Research Institute[7–9] have clearly established this.

It is evident, from both a scientific and a technical point of view, that

the principal interest should be attached to the reactivity rather than to the total amount of carbonyl groups. The behavior of cellulose in different processes is determined by groups with the greatest reactivity, and therefore a characterization of cellulose by the amounts of these groups is of major importance. This paper presents a report on attempts to develop a method for the classification and quantitative determination of carbonyl groups on the basis of their reactivity.

DEVELOPMENT OF THE METHOD

When a study was made of the oximation of carbonyl groups according to the method of Cyrot[2] and Rochas,[3] it was observed that the stability in acid medium of oximes of model compounds prepared from cellulose varied considerably,[7,8,10] and it was also found that the hydrolysis of these oximes is a second-order reaction. For this reason it was presumed that the inclination of different carbonyl groups to form oximes should also depend on the type of the carbonyl group. This conception is supported by the theory of Lee and Kolthoff[11] and by the analysis of mixtures of low-molecular carbonyl compounds based on this theory.[12–14] However, the procedures employed in these investigations cannot be adapted to the analysis of the carbonyl groups of cellulose, as only two-component systems have been considered. Obviously, several kinds of carbonyl groups of differing reactivity are to be found in cellulose, and thus the theory must be extended to fit a multicomponent system.

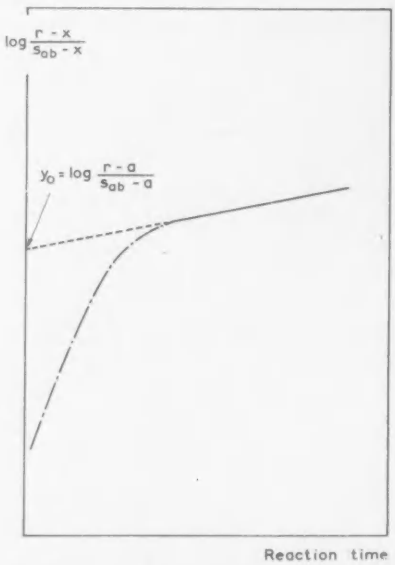

Fig. 1. Reaction rate plot of two simultaneous second-order reactions.

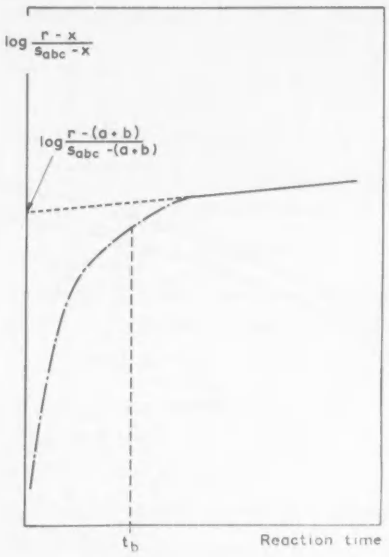

Fig. 2. Reaction rate plot of three simultaneous second-order reactions.

The method is based on keeping the pH of the oximation reaction mixture constant by employing an automatic titrator by means of which the hydrochloric acid liberated during the reaction is continuously neutralized with sodium hydroxide. The consumption of sodium hydroxide is recorded as a function of time. If the base consumption at time t is x, the initial concentration of hydroxylamine hydrochloride is r, and the total amount of carbonyl groups is s (r, s, and x expressed in the same units), then log $[(r - x)/(s - x)]$ plotted against t is a straight line, with a slope which is proportional to the rate constant of the reaction, provided the reaction is of second order. If the system contains two or more components reacting at differing rates, the plot is a straight line only for that portion in which the faster reacting components have already been consumed, and the slowest reaction is still proceeding. The amount of the slowest reacting component can be calculated from the intersection of this line with the y axis ($t = 0$). In order to arrive at the amounts and the reaction rates of the faster reacting components, the share of the slowest reacting component must be taken into account. At each instant, relevant values are subtracted from r and x, and a new plot of log $[(r - x)/(s - x)]$ against t is drawn. Here, s is the sum of the faster reacting components, obtained from the above-mentioned intersection with the y axis. The amount and the reaction rate of the component next to the slowest one can be computed from the straight-line portion of the new plot. The same procedure is repeated until all the components have been separated out. A detailed presentation of the theory is given below.

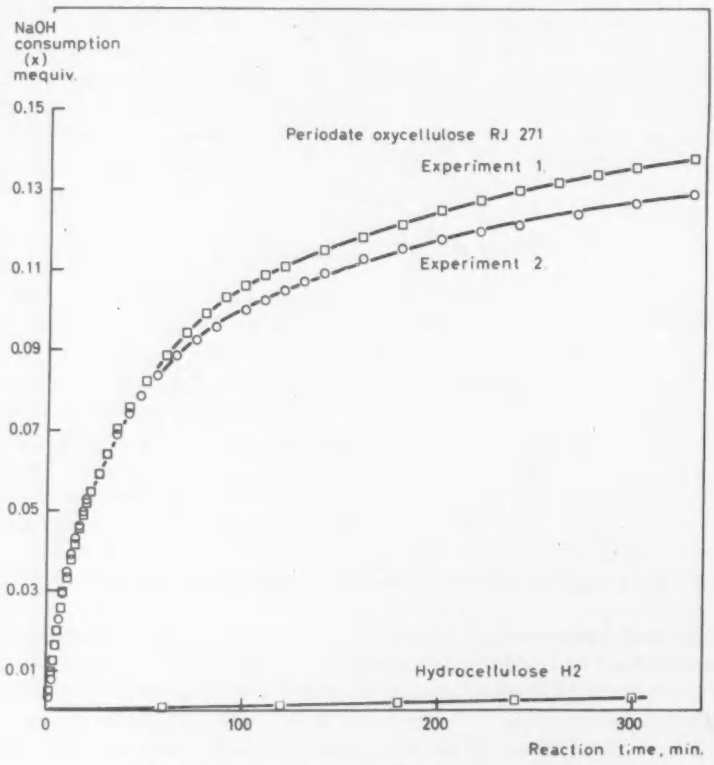

Fig. 3. Sodium hydroxide consumption during oximation.

Siggia and Hanna developed a method for the analysis of low molecular weight carbonyl compounds.[14] Attempts were made to employ this method for the differentiation of the carbonyl groups of cellulose, but when methanol was used as liquid medium there resulted highly irregular titration curves and poor reproducibility. The sodium hydroxide consumption of a blank was found to be several times the total carbonyl content of the cellulose sample. This was found to be caused by rapid self-decomposition of hydroxylamine hydrochloride in methanol, both in the absence of cellulose and in the presence of carbonyl-free cellulose. The self-decomposition depended on the temperature and on other prevailing experimental conditions. The reaction was also carried out in parallel with a blank test, in order to eliminate the influence of the self-decomposition. However, this resulted in no improvement, for the obvious reason that the small amount of hydroxylamine consumed by the cellulose was obtained as the difference between two substantial and essentially inaccurate figures.

A higher degree of accuracy was attained when water replaced methanol as the liquid medium. The self-decomposition of hydroxylamine hydro-

chloride was then decisively decreased. At the moment the experiment is always carried out concurrently with a blank, the sodium hydroxide consumption of the reaction mixture being corrected by the corresponding alkali consumption value of the blank.

THEORY

If two reactant molecules A and R are concerned in a chemical reaction, then the simplest second-order reaction is represented by

$$A + R \rightarrow \text{products}$$

If the initial concentrations of A and R are a and r, respectively, and x is the decrease in each after time t, then the rate of the reaction is given by

$$dx/dt = k(a - x)(r - x) \tag{1}$$

On integration, and taking into consideration that $x = 0$ when $t = 0$, and $x = x$ when $t = t$, it is seen that

$$k = 2.303/t(r - a) \log [a(r - x)/r(a - x)] \tag{2}$$

where k is the second-order reaction constant. Equation (2) may be rearranged to take the form

$$y = \log [(r - x)/(a - x)] = \log r/a + kt(r - a)/2.303 \tag{3}$$

The plot of $\log [(r - x)/(a - x)]$ against t should thus be a straight line which intersects the y axis at the point $y_0 = \log r/a$. The slope n of this line is equal to

$$m = k(r - a)/2.303 \tag{4}$$

If R is involved in two simultaneous reactions, e.g.

$$R + A \rightarrow \text{products}$$
$$R + B \rightarrow \text{products}$$

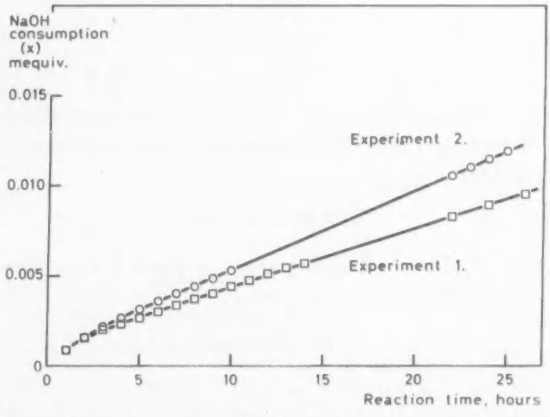

Fig. 4. Sodium hydroxide consumption during the oxination of hydrocellulose.

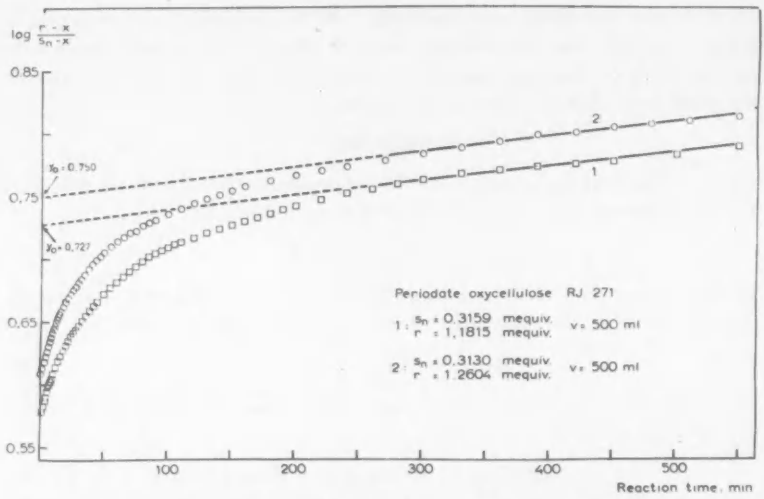

Fig. 5. Reaction rate curves at the oxidation of periodate oxycellulose. First stage of the calculation. (Separation of the slowest reacting component)

a, b, and r are the initial concentrations of A, B, and R, respectively, and $r - (x_a + x_b)$, $a - x_a$, and $b - x_b$ are the corresponding concentrations after time t, then the rates of reaction are given by

$$dx_a/dt = k_a[r - (x_a + x_b)](a - x_a)$$

and

$$dx_b/dt = k_b[r - (x_a + x_b)](b - x_b)$$

or

$$dx/dt = dx_a/dt + dx_b/dt = [k_a(a - x_a) + k_b(b - x_b)][r - (x_a + x_b)] \quad (5)$$

The exact solution of eq. (5) is possible only in special cases. If it is assumed that $k_b \ll k_a$ and t is long, i.e., that at the time of observation the reaction of R with A is practically completed, then there remains the two-component system

$$R + B \rightarrow \text{products}$$

The apparent initial concentrations are $r - a$ and b, respectively, and at time t the respective concentrations are $r - a - x_b$ and $b - x_b$. Writing

$$a + b = s_{ab}$$

or

$$b = s_{ab} - a \quad (6)$$

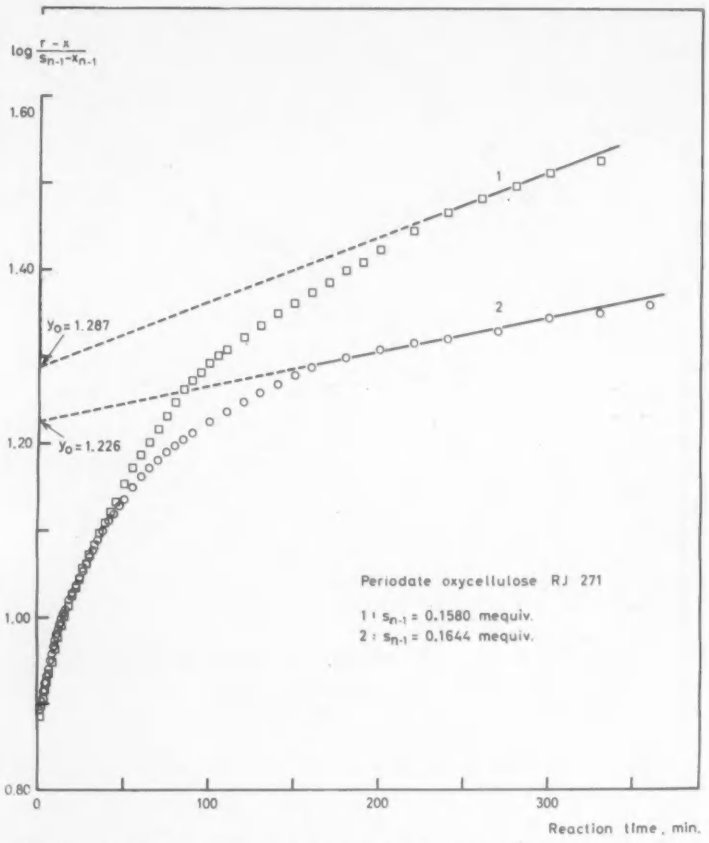

Fig. 6. Reaction rate curves at the oxidation of periodate oxycellulose. Second stage of the calculation.

and substituting in eq. (2), it follows that

$$k = 2.303/(r - s_{ab})t \log (s_{ab} - a)[r - (a + x_b)]/(r - a)[s_{ab} - (a + x_b)] \quad (7)$$

Since it was assumed that the reaction of R with A was completed, a is equal to x_a. On the other hand $x_a + x_b = x$. Accordingly, eq. (7) may be written

$$k = 2.303/(r - s_{ab})t \log [(s_{ab} - a)(r - x)/(r - a)(s_{ab} - x)] \quad (8)$$

Equation (8) is of the same general form as eq. (2), and may be rearranged to give a result comparable with eq. (3), or

$$<y = \log [(r - x)/(s_{ab} - x)] = \log [(r - a)/(s_{ab} - a)] + kt(r - s_{ab})/2.303 \quad (9)$$

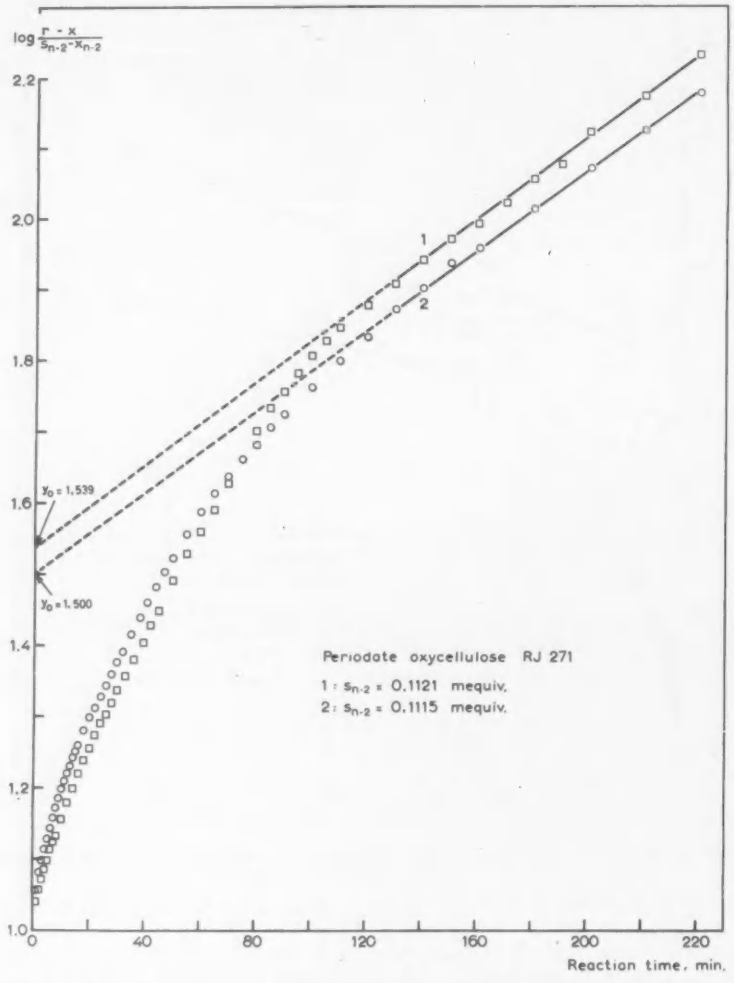

Fig. 7. Reaction rate curves at the oxidation of periodate oxycellulose. Third stage of the calculation.

The plot of log $[(r - x)/(s_{ab} - x)]$ against t thus results in a straight line, the slope being proportional to the rate of the slowest reaction. The intersection with the y axis is given by $y_0 = \log [(r - a)/(s_{ab} - a)]$ (Fig. 1). As the above derivation was based on the assumption that the faster reaction had been almost brought to an end, no attention should be paid to that part of the reaction period where this reaction is still in marked progress.

Writing l for the antilogarithm of the intercept with the y axis (Fig. 1),

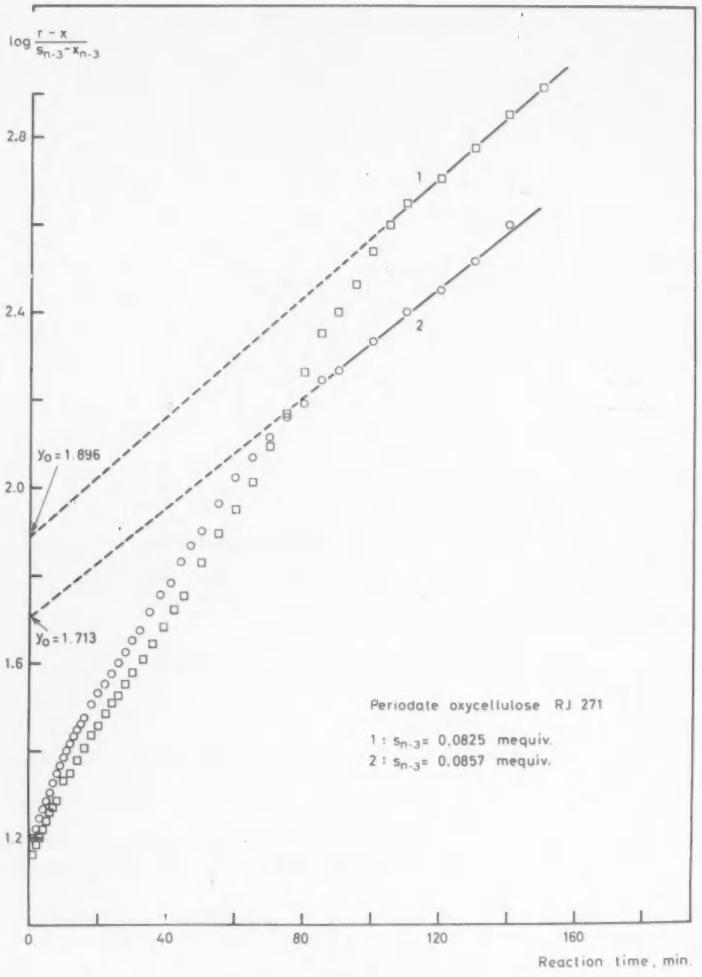

Fig. 8. Reaction rate curves at the oximation of periodate oxycellulose. Fourth stage of the calculation.

$$(r - a)/(s_{ab} - a) = l$$

there follows

$$a = (ls_{ab} - r)/(l - 1) \tag{10}$$

The initial concentration (a) of the faster reacting component (A) is thus arrived at through the slower reaction. As there are only two components,

$$b = s_{ab} - a \tag{11}$$

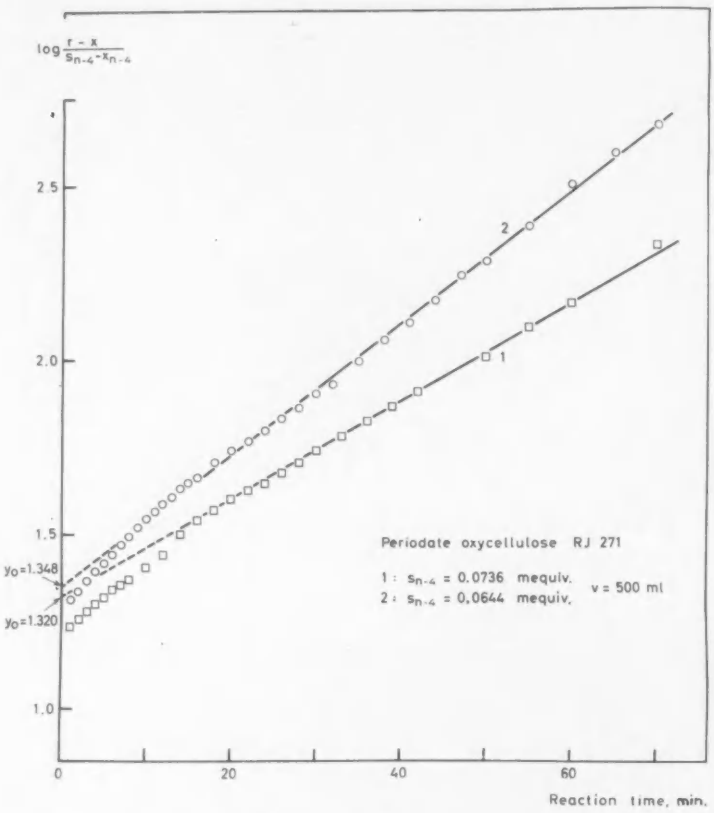

Fig. 9. Reaction rate curves at the oximation of periodate oxycellulose. Fifth stage of the calculation.

If we consider the reaction of R with three components, e.g.,

$$\begin{aligned} R + A &\rightarrow \text{products} \quad \text{(reaction 1)} \\ R + B &\rightarrow \text{products} \quad \text{(reaction 2)} \\ R + C &\rightarrow \text{products} \quad \text{(reaction 3)} \end{aligned}$$

and assume the first two reactions to be almost completed, only the third reaction is in progress after a sufficient period of time. For the components,

$$a + b + c = s_{abc}$$

or

$$c = s_{abc} - (a + b) \tag{12}$$

At the apparent beginning of the third reaction, the concentrations of R and C are $r - (a + b)$ and $s_{abc} - (a + b)$, respectively. At time t, the

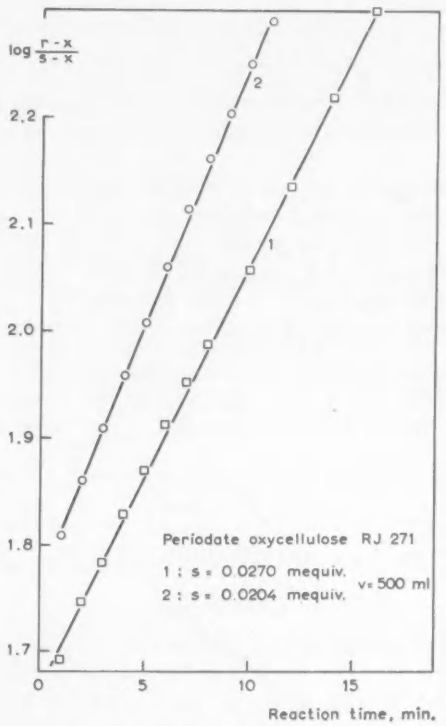

Fig. 10. Last stage of the calculation. Reaction rate plot for the most reactive component.

corresponding concentrations are $r - (a + b + x_c)$ and $s_{abc} - (a + b + x_c)$. By utilizing the same procedure as above,

$$k = 2.303/(r - s_{abc})t \log [s_{abc} - (a + b)][r - (a + b + x_c)]/[r - (a + b)][s_{abc} - (a + b + x_c)] \quad (13)$$

By taking into consideration that $a + b + x_c = x$ and rearranging, there is finally obtained

$$y = \log [(r - x)/(s_{abc} - x)] = \log [r - (a + b)]/[s_{abc} - (a + b)] + kt(r - s_{abc})/2.303 \quad (14)$$

In Figure 2, the straight-line portion represents eq. (14). As before, the faster reactions are to be disregarded. From the intersection with the y axis,

$$l = [r - (a + b)][s_{abc} - (a + b)]$$

or

$$(a + b) = (ls_{abc} - r)/(l - 1) \tag{15}$$

On the basis of the slowest reaction there is thus obtained the sum of the faster reacting components, provided the initial sum of all components (s_{abc}) is known.

If the three-component system is examined at the instant t_b, then in view of its slowness, reaction 3 cannot be perceived in practice, and thus the system can be treated as a two-component system, the sum of reacting components being $s_{ab} = a + b$. Equation (9) can be applied, s_{ab} being the sum $a + b$ obtained from eq. (15). A new plot must accordingly be drawn, computed by means of values a, b, and s_{ab} only, and employing corrected

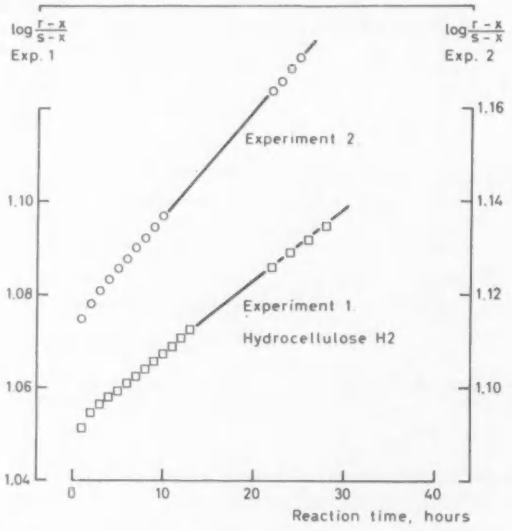

Fig. 11. The reaction rate plot at the oximation of hydrocellulose.

values of x found by reducing the original x values by an amount corresponding to the share of the third reaction at each instant. It should be borne in mind that at any time the effective concentration of R also is reduced by this same amount. Accordingly, when the new curve is plotted, the quantity $(r - x)$ has the same value as in the original plot, but s_{abc} is replaced by s_{ab}, and x is replaced by the corrected x value. If the third reaction is much slower than the preceding reactions the x correction may be so small that it can be neglected. However, if more than three components are present, each single component being separated from the others by the procedure described above, small corrections in x must also be taken into account, as the corrections throughout the different stages of the computation exert a cumulative influence.

In a general case of n components in the mixture,

$$l_n = (r - \sum_{i=1}^{n-1} a_i)/(s_n - \sum_{i=1}^{n-1} a_i) \tag{16}$$

and

$$\sum_{i=1}^{n-1} a_i = (l_n s_n - r)/(l_n - 1) \tag{17}$$

where log l_n represents the intersection of the last straight line with the y axis, a_i represents carbonyl groups of different kinds, s_n is the sum of all carbonyl groups, and r is the initial concentration of hydroxylamine hydrochloride.

After calculation of eq. (17), the computation is carried out in reverse as described, and the components separated step by step from each other. In the general case, $n - 1$ graphs must accordingly be drawn, each plot giving the remaining sum $\sum_{i=1}^{n-1} a_i$, or the slowest reacting component

$$a_n = s_n - \sum_{i=1}^{n-1} a_i \tag{18}$$

EXPERIMENTAL

Reagents

Reagents used were: hydroxylamine hydrochloride, $NH_2OH \cdot HCl$, analytical grade; sodium hydroxide solution, 0.020 ± 0.00002N; hydrochloric acid solution, approximately 0.1N; sodium chloride solution, 25 g./l. (the pH is lowered to 3.5 by the addition of hydrochloric acid).

Apparatus

Apparatus used consisted of a water thermostat, temperature 20 ± 0.1°C.; Radiometer TTT 1a automatic titrator, equipped with two magnetic valves connected to a switch contact; a voltage stabilizer, by which the titrator is connected to 220 v. alternating current; two glass/calomel electrodes, type radiometer GK 2021C; two microburets of 10 ml. capacity connected to the magnetic valves; two adjustable stirrers with spiral stems; two cylindrical reaction vessels of 800 ml. capacity, inner diameter 8 cm.

Procedure

Cellulose (3–5 g.; dry weight determined from a separate sample) is weighed accurately (±0.001 g.) into a beaker containing 500 ml. of the acid sodium chloride solution, and allowed to stand overnight. The pH of the suspension is determined the next morning.

An accurately weighed quantity (150–250 mg.) of hydroxylamine hydrochloride is dissolved in 990 ml. of distilled water at 20 ± 0.1°C. and 0.1N hydrochloric acid is added until the pH of the solution is equal to the

TABLE I. Reaction of Periodate Oxycellulose (RJ 271, Experiment 1) with Hydroxylamine Hydrochloride, Temperature 20°C.[a]

Time, min.	NaOH consumption x, mequiv.	$r - x$, mequiv.	$s_n - x$, mequiv.	log $r - x/s_n - x$	Correction Δx_n	x_{n-1}, mequiv.	$s_{n-1} - x_{n-1}$, mequiv.	log $r - x/s_{n-1} - x_{n-1}$
1	0.0050	1.1765	0.3109	0.5780	≈ 0	0.0050	0.1530	0.8859
2	0.0095	1.1720	0.3064	0.5826		0.0095	0.1485	0.8972
3	0.0131	1.1684	0.3028	0.5865		0.0131	0.1449	0.9065
4	0.0167	1.1648	0.2992	0.5903		0.0167	0.1413	0.9161
5	0.0200	1.1615	0.2959	0.5938	0.0001	0.0199	0.1381	0.9252
6	0.0234	1.1581	0.2925	0.5976		0.0233	0.1347	0.9347
7	0.0256	1.1559	0.2903	0.6001		0.0255	0.1325	0.9407
8	0.0278	1.1537	0.2881	0.6026		0.0277	0.1303	0.9471
10	0.0331	1.1484	0.2828	0.6086	0.0002	0.0329	0.1251	0.9628
12	0.0375	1.1440	0.2784	0.6137		0.0373	0.1207	0.9767
14	0.0414	1.1401	0.2745	0.6184	0.0003	0.0412	0.1168	0.9895
16	0.0450	1.1365	0.2709	0.6226		0.0447	0.1133	1.0013
18	0.0484	1.1331	0.2675	0.6270	0.0004	0.0481	0.1099	1.0133
20	0.0514	1.1301	0.2645	0.6307		0.0510	0.1070	1.0237
22	0.0545	1.1270	0.2614	0.6346	0.0005	0.0540	0.1040	1.0350
24	0.0570	1.1245	0.2589	0.6378	0.0006	0.0564	0.1016	1.0442
26	0.0592	1.1223	0.2567	0.6407	0.0007	0.0585	0.0985	1.0565
28	0.0614	1.1201	0.2545	0.6436		0.0607	0.0973	1.0611
30	0.0639	1.1176	0.2520	0.6469	0.0008	0.0631	0.0949	1.0712
33	0.0667	1.1148	0.2492	0.6507	0.0009	0.0658	0.0922	1.0824
36	0.0698	1.1117	0.2461	0.6549	0.0010	0.0688	0.0892	1.0955
39	0.0726	1.1089	0.2433	0.6588	0.0011	0.0715	0.0865	1.1079
42	0.0753	1.1062	0.2406	0.6626	0.0012	0.0741	0.0839	1.1199
45	0.0778	1.1037	0.2381	0.6661	0.0013	0.0765	0.0815	1.1316
50	0.0820	1.0995	0.2339	0.6722	0.0014	0.0806	0.0774	1.1526
55	0.0856	1.0959	0.2303	0.6775	0.0016	0.0840	0.0740	1.1706
60	0.0884	1.0931	0.2275	0.6817	0.0017	0.0867	0.0713	1.1855

65	0.0912	1.0903	0.2247	0.6859	0.0019	0.0893	0.0687	1.2006
70	0.0940	1.0875	0.2219	0.6903	0.0021	0.0919	0.0661	1.2162
75	0.0965	1.0850	0.2194	0.6942	0.0022	0.0943	0.0637	1.2312
80	0.0990	1.0825	0.2169	0.6982	0.0023	0.0967	0.0613	1.2470
85	0.1012	1.0803	0.2147	0.7017	0.0025	0.0987	0.0593	1.2606
90	0.1029	1.0786	0.2130	0.7045	0.0027	0.1002	0.0578	1.2709
95	0.1045	1.0770	0.2114	0.7071	0.0029	0.1016	0.0564	1.2810
100	0.1059	1.0756	0.2100	0.7094	0.0030	0.1029	0.0551	1.2905
105	0.1073	1.0742	0.2086	0.7118	0.0032	0.1041	0.0539	1.2995
110	0.1084	1.0731	0.2075	0.7137	0.0033	0.1051	0.0529	1.3073
120	0.1106	1.0709	0.2053	0.7173	0.0037	0.1069	0.0511	1.3214
130	0.1126	1.0689	0.2033	0.7208	0.0040	0.1086	0.0494	1.3353
140	0.1145	1.0670	0.2014	0.7241	0.0043	0.1102	0.0478	1.3487
150	0.1162	1.0653	0.1997	0.7271	0.0046	0.1116	0.0464	1.3610
160	0.1179	1.0636	0.1980	0.7301	0.0050	0.1129	0.0451	1.3725
170	0.1195	1.0620	0.1964	0.7330	0.0053	0.1142	0.0438	1.3847
180	0.1212	1.0603	0.1947	0.7361	0.0056	0.1156	0.0424	1.3981
190	0.1226	1.0589	0.1933	0.7386	0.0060	0.1166	0.0414	1.4079
200	0.1243	1.0572	0.1916	0.7418	0.0063	0.1180	0.0400	1.4221
220	0.1270	1.0545	0.1889	0.7468	0.0069	0.1201	0.0379	1.4444
240	0.1295	1.0520	0.1864	0.7516	0.0075	0.1220	0.0360	1.4657
260	0.1315	1.0500	0.1844	0.7554	0.0081	0.1234	0.0346	1.4822
280	0.1334	1.0481	0.1825	0.7591	0.0088	0.1246	0.0334	1.4967
300	0.1351	1.0464	0.1808	0.7625	0.0094	0.1257	0.0323	1.5106
330	0.1373	1.0442	0.1786	0.7669	0.0104	0.1269	0.0311	1.5261
360	0.1387	1.0428	0.1772	0.7698				
390	0.1401	1.0414	0.1758	0.7726				
420	0.1412	1.0403	0.1747	0.7749				
450	0.1423	1.0392	0.1736	0.7771				
500	0.1443	1.0372	0.1716	0.7813				
550	0.1462	1.0353	0.1697	0.7854				
600	0.1479	1.0336	0.1680	0.7809				
700	0.1510	1.0314	0.1658	0.7939				

[a] v = 500 ml., r = 1.1815 mequiv., s_n = 0.3159 mequiv., pH 3.55.

value measured in the pulp suspension. The solution is diluted to an accurate volume of 1 liter, and then divided into two equal 500-ml. portions which are poured into the reaction vessels. The vessels are placed in the thermostat and equipped with the appropriate stirrers and electrodes. An accurate regulation of the pH to the desired value is then made with the aid of the titrator.

The pulp suspension is filtered by suction, and the cellulose recovered quantitatively. The moist cellulose is quickly transferred, under vigorous stirring, to one of the reaction vessels. At the same instant, the titrator is connected and a stop-watch started. At suitable intervals, there are recorded the sodium hydroxide consumptions in both vessels. Each electrode should be connected for at least 30 sec. before a buret reading is taken. To effect a good separation of the reactive components, the earlier stages of the reaction should be followed at short intervals. Care should be taken to avoid the disturbing influence of acidic or basic vapors in the surrounding atmosphere. If these cannot be avoided, flushing with nitrogen in a closed reaction system is necessary. The sodium hydroxide consumption of the blank should be less than 0.10 ml./hr., and in no case should it exceed 50% of the consumption in the reaction vessel.

The sodium hydroxide consumption during the oximation reaction is the difference between the buret readings of the reaction suspension and the blank. The base consumption x is plotted against t, and slight irregularities may be corrected on the drawing of the curve. However, major irregularities cannot be allowed, and if they appear, a new experiment must be carried out. After the reaction has been stopped, it is recommended that the degree of oximation be checked by determining the nitrogen content of the reaction product according to the Kjeldahl method, especially if the sodium hydroxide consumption of the blank is appreciably high. The total carbonyl content of the cellulose is determined from a separate sample by means of a total oximation test.[10]

A reaction-rate curve is constructed on the basis of the sodium hydroxide consumption, the total carbonyl content, and the hydroxylamine hydrochloride concentration, as is shown in the following examples.

RESULTS AND DISCUSSION

This paper reports on results obtained with periodate oxycellulose (sample RJ 271) and hydrocellulose (sample H2). The sodium hydroxide consumption as a function of time is given in Tables I–III and is also shown graphically in Figures 3 and 4. The necessary analytical data (total carbonyl content s_n as determined by a total oximation test, and hydroxylamine hydrochloride concentration) are also given in Tables I–III. Table I further includes a detailed calculation of the two slowest stages of the reaction between periodate oxycellulose and hydroxylamine hydrochloride.

The extrapolation to zero time of the straight line portion of the reaction rate curve may seem uncertain. However, in a sense the method is

self-controlling; even a small error at the extrapolation makes the last portion of the next plot either raise steeply or descend gradually. This

TABLE II

Reaction of Periodate Oxycellulose (RJ 271) with Hydroxylamine Hydrochloride, Temperature 20°C., Experiment 2.[a]

Time, min.	NaOH consumption x, mequiv.	Time, min.	NaOH consumption x, mequiv.
1	0.0033	55	0.0834
2	0.0078	60	0.0862
3	0.0122	65	0.0884
4	0.0161	70	0.0904
5	0.0195	75	0.0923
6	0.0228	80	0.0940
7	0.0261	85	0.0956
8	0.0292	90	0.0970
9	0.0320	100	0.0998
10	0.0345	110	0.1023
11	0.0367	120	0.1045
12	0.0389	130	0.1068
13	0.0409	140	0.1087
14	0.0428	150	0.1106
15	0.0445	160	0.1126
16	0.0461	180	0.1151
18	0.0495	200	0.1173
20	0.0523	220	0.1193
22	0.0545	240	0.1209
24	0.0570	270	0.1234
26	0.0592	300	0.1262
28	0.0614	330	0.1287
30	0.0637	360	0.1312
32	0.0656	390	0.1334
35	0.0687	420	0.1351
38	0.0714	450	0.1365
41	0.0739	480	0.1379
44	0.0762	510	0.1390
47	0.0784	550	0.1407
50	0.0803	600	0.1423

[a] $v = 500$ ml., $r = 1.2604$ mequiv., $s_n = 0.3130$ mequiv. pH 3.6.

can be obviated by employing a correct extrapolated value at the calculation. Probably because of this self-controlling property of the method, even components with relatively small differences in their reaction rates can be separated.

Experiments with Periodate Oxycellulose

The reaction between periodate oxycellulose and hydroxylamine hydrochloride can be differentiated into six stages by the method described

(Figs. 5–10). From the intersections with the y axis, the amounts of carbonyl groups reacting at different rates are calculated according to eqs. (17) and (18). The results are summarized in Table IV. Table IV also

TABLE III
Reaction of Hydrocellulose (H2) with Hydroxylamine Hydrochloride, Temperature 20°C.

Time, hr.	NaOH consumption x, mequiv.	
	Experiment 1[a]	Experiment 2[b]
1	0.00083	0.00085
2	0.00153	0.00154
3	0.00200	0.00214
4	0.00231	0.00265
5	0.00267	0.00313
6	0.00300	0.00359
7	0.00334	0.00402
8	0.00367	0.00441
9	0.00403	0.00486
10	0.00439	0.00530
11	0.00473	
12	0.00509	
13	0.00545	
22	0.00826	0.01055
23		0.01100
24	0.00890	0.01146
25		0.01188
26	0.00945	
28	0.01001	

[a] v = 500 ml., r = 1.0000 mequiv., s = 0.0897 mequiv. pH 3.5.
[b] v = 300 ml., r = 1.1070 mequiv., s = 0.0858 mequiv. pH 3.5.

shows the specific reaction rate constants, calculated in accordance with eq. (4), from the slopes of the corresponding straight line portions of the graphs, using the appropriate values of r and a.

As can be seen from the results given in Table IV, the separation into the different components is equally good in both experiments, although in the fifth stage the values of the rate constants do not agree very well. It should be pointed out that the determination of the carbonyl group content of cellulose by conventional methods cannot usually be performed to an accuracy better than ±0.1 mequiv./100 g. In view of this, the reproducibility of the present method may be regarded as very satisfactory.

Experiments with Hydrocellulose

Figure 11 shows that the reaction between hydrocellulose and hydroxylamine hydrochloride cannot be differentiated into separate stages. Hydrocellulose is believed to contain reducing endgroups (intramolecular hemiacetal linkages) only, and thus the result is in accordance with this hypothesis. From the slopes of the graphs, $k = 3.2 \times 10^{-5}$ and $2.6 \times$

TABLE IV

Reaction of Periodate Oxycellulose (RJ 271) and of Hydrocellulose (H2) with Hydroxylamine Hydrochloride. Amounts and Reaction Rates of the Different Components

		Experiment 1			Experiment 2		
Sample	Reaction	Amount of component, mequiv./100 g.	Percentage of total	Second order rate constant, 10^4k,	Amount of component mequiv./100 g.	Percentage of total	Second order rate constant, 10^4k,
Periodate oxycellulose RJ 271	1	0.71	8.5	397.0	0.55	6.6	465.0
	2	1.23	14.8	145.0	1.16	13.9	181.0
	3	0.32	3.8	72.3	0.48	5.8	60.4
	4	0.70	8.4	30.9	0.77	9.3	28.9
	5	1.20	14.5	8.4	1.41	16.9	4.2
	6	4.16	50.0	1.5	3.95	47.5	1.4
Hydrocellulose H2		2.10	100	0.32	2.10	100	0.26

10^{-5} (mequiv./l.)$^{-1}$min.$^{-1}$ are obtained for experiments 1 and 2, respectively; a fair reproducibility is thus to be found in this instance also.

The rate constant at the oximation of hydrocellulose is seen to be approximately one-fifth of the smallest k value at the oximation of periodate oxycellulose. According to viscometric determinations, the endgroup content of the periodate oxycellulose is 0.51 mequiv./100 g. This endgroup content seems to be masked by the comparatively large amount of the slowest reacting component of the periodate oxycellulose, and is thus included in this amount.

The sum of the two fastest reacting components of periodate oxycellulose is seen to constitute approximately 21% of the total carbonyl content. Recent results obtained at the Finnish Pulp and Paper Research Institute[8] show that only 19–22% of the carbonyl groups of periodate oxycellulose condense with Girard's reagent (acethydrazide-pyridium chloride) at pH 8. Furthermore, according to Nevell,[15] only 24% of the carbonyl groups of periodate oxycellulose are involved in the formation of a cyclic hemiacetal with methanol. A definite proportion of the reactive groups of periodate oxycellulose thus seems to take part in different reactions.

As yet, no definite assignments can be given for the different reactivities. Periodate oxycellulose is believed to contain potential aldehyde groups which are bound as hydrates, intra- or intermolecular hemiacetals, and as hemialdals. Presumably, these different types of bound aldehyde groups possess different reactivities. According to Spedding,[16] approximately 75% of the aldehyde groups in dry samples are bound as hemialdals, the remaining 25% being composed of free aldehyde groups and hemiacetal groups. The large, slowly reacting portion could then tentatively be attributed to the hemialdal groups present. Also, free or hydrate-bound aldehyde groups may be expected to possess greater reactivity than do hemiacetal or hemialdal groups.

The low reactivity of hydrocellulose at oximation at least gives an indication of the condensation affinity of intramolecular hemiacetal endgroup linkages. It may be remarked, that the reactivity of these endgroups at borohydride reduction, and at chlorite oxidation also, is less than the reactivity of aldehyde groups in other positions.

References

1. Stübchen-Kirchner, H., *Österr. Chem.-Ztg.*, **61**, 132 (1960).
2. Cyrot, J., *Chim. Anal.*, **39**, 449 (1957).
3. Rochas, P., L. Gavet, and P. Bussière, *Bull. Inst. Textile France*, **87**, 19 (1960).
4. Albertsson, U., and O. Samuelson, *Anal. Chim. Acta*, **27**, 434 (1962).
5. Christofferson, K., and O. Samuelson, *Svensk Papperstidn.*, **64**, 195 (1961).
6. Wennerblom, A., *Svensk Papperstidn.*, **64**, 519 (1961).
7. Sihtola, H., *Faserforsch. Textiltech.*, **13**, 304 (1962).
8. Sihtola, H., "Cellulosans funktionella grupper och deras bestämning," paper presented at 11th Scandinavian Chemists' Congress, Symposium on Cellulose Chemistry, Turku (Finland), August 23, 1962.
9. Laamanen, L., H. Sihtola, and L. Blomberg, "Om bestämning av cellulosans karbonylgrupper med användande av Girards reagens," paper presented at 11th

Scandinavian Chemists' Congress, Section of Analytical Chemistry, Turku (Finland), August 22, 1962.

10. Neimo, L., and H. Sihtola, "Om bestämning av cellulosans karbonylgrupper i närvaro av karboxylgrupper genom kondensation med hydroxylamin," paper presented at 11th Scandinavian Chemists' Congress, Section of Analytical Chemistry, Turku (Finland), August 22, 1962; *Paperi ja Puu*, **45** (1963), in press.
11. Lee, T. S., and I. M. Kolthoff, *Ann. N.Y. Acad. Sci.*, **53**, 1093 (1951).
12. Fowler, L., *Anal. Chem.*, **27**, 1686 (1955).
13. Fowler, L., H. R. Kline, and R. S. Mitchell, *Anal. Chem.*, **27**, 1688 (1955).
14. Siggia, S., and J. G. Hanna, *Anal. Chem.*, **33**, 896 (1961).
15. Nevell, T. P., *Chem. Ind. (London)*, **1958**, 389.
16. Spedding, H., *J. Chem. Soc.*, **1960**, 3147.

Synopsis

A method has been developed for the classification and quantitative determination of carbonyl groups with different reactivity in cellulose; it is based on different reaction rates at oximation, and the proportions and reaction rate constants of the different components are obtained from a reaction rate plot of a second order reaction. The reproducibility seems to be good. The results obtained show that in hydrocellulose there is only one type of carbonyl group, a finding which is in agreement with the prevalent view. The carbonyl groups in periodate oxycellulose could be classified in six types, the reaction rate constant of the fastest reacting carbonyls being about 300 times higher than that of the slowest-reacting ones, which again react 5 times more quickly than the aldehyde groups in hydrocellulose.

Résumé

On a développé une méthode pour la classification et la détermination quantitative des groupements carbonyles de réactivité différents dans la cellulose; elle est basée sur la différence de vitesse de réaction d'oximation; les proportions et constantes de vitesse de formation des différentes substances ont été obtenues à partir d'une graphique de vitesse d'une réaction de deuxième ordre. La reproductibilité semble être suffisante. Ces résultants obtenus montrent que dans l'hydrocellulose il n'y a qu'un type de groupement carbonyle, ce qui est en accord avec le point de vue prévalent. On peut classifier les groupements carbonyliques dans l'oxycellulose périodée en dix groupes; la constante de vitesse de la réaction la plus rapide est environ 300 fois plus grande que celle des réactions les plus lentes, lesquelles réagissent 5 fois plus rapidment que le groupement aldéhyde dans l'hydrocellulose.

Zusammenfassung

Eine Methode zur Klassifizierung und quantitativen Bestimmung von Karbonylgruppen mit verschiedener Reaktivität in Cellulose wurde entwickelt; sie beruht auf Unterschieden in der Oximierungsgeschwindigkeit, wobei die Verhältnisse und die Reaktionsgeschwindigkeitskonstanten der verschiedenen Komponenten aus dem Formalismus für eine Reaktion zweiter Ordnung erhalten werden. Die Reproduzierbarkeit scheint gut zu sein. Die Ergebnisse zeigen, dass in Hydrocellulose nur ein einziger Karbonylgruppentypus vorhanden ist, was mit der herrschenden Meinung übereinstimmt. Die Karbonylgruppen in Perjodat-Oxycellulose konnten in sechs Gruppen eingeteilt werden; die Reaktionsgeschwindigkeitskonstante des am schnellsten reagierenden Karbonyls ist etwa 300 mal höher als die des am langsamsten reagiereden, welches immer noch 5 mal rascher reagiert also die Aldehydgruppe in der Hydrocellulose.

JOURNAL OF POLYMER SCIENCE: PART C NO. 2, PP. 311–320 (1963)

Verification of Trace Amounts of Acids in Cellulose

OLLI ANT-WUORINEN and ASKO VISAPÄÄ, *Chemico-Technical Laboratory, The State Institute for Technical Research, Helsinki, Finland*

Recently, there have been published a number of research papers which discuss the removal of the last traces of acid from cellulose which has been immersed in acid solution for long or short periods. Many of these reports[1,2,3] maintain that after acid treatment cellulose material can be washed free of acid without any difficulty by the use of only a few portions of washing water. On the other hand, the present authors have reported on experimental results which show that the removal by washing of the last traces of acid from cellulose is a very tedious undertaking.[4] Those who have reached the conclusion that cellulose can easily be freed from acid by means of simple washing with sufficiently pure water, with no precautions being taken, and with the cellulose in free contact with the CO_2 of the atmosphere, have in part used titration methods, and in part radioactive tracer technique with labelled HCl. We obtained our results—which contradict the findings of others—partly by a very sensitive titration technique, and partly by spectrophotometric methods, with the strict exclusion of atmospheric impurities.

It seemed desirable to undertake the study of this controversial problem, which is of fundamental importance from both the scientific and practical points of view, by the application of experimental techniques not previously used in studies of this difficult question.

The type of cellulose used for this investigation was bleached sulfite pulp. Before the different washing treatments, parallel samples of this cellulose were soaked either in 0.1*N* HCl or in 0.1*N* HBr; the latter was used because Br—as opposed to Cl—can be detected by the commercially available x-ray emission spectrography outfit, even in the ppm range, and thus it is possible to ascertain directly whether traces of acid are retained by fiber which has undergone different washing treatments.

The washing procedure was carried out either in a vertical tube into which the test specimen had been loosely packed to form a column as suggested by Sjöström,[1] or after soaking in acid, the samples were washed by shaking them for short or long periods in successive portions of washing water in an Erlenmeyer flask through which pure nitrogen could be led. Consequently, the washing process could be effected with a shield against atmospheric impurities.

After washing, the samples were dried overnight at 105°C. It is well

TABLE I
Washing Experiments in a Vertical Tube According to Sjöström[a]

Acid	Duration of the acid treatment	Water used for the washings	$[\eta]$ after washing steps							
			1	2	3	4	5	6	7	8
0.1*N* HCl	18 hr.	In equilibrium with air	2.14	2.23	2.18	2.20	2.22	2.12	2.12	2.19
"	"	"	2.32	2.70	3.04	3.01	2.93	2.80	2.82	2.88
"	"	Free from CO_2	2.25	2.69	2.69	2.75	2.80	2.84	2.88	2.97
"	7 days	In equilibrium with air	2.18	2.54	2.84	2.95	2.74	3.38	3.03	2.77
"	"	"	2.46	2.89	3.02	2.76	2.95	2.87	2.95	3.07
0.1*N* HBr	18 hr.	In equilibrium with air	2.23	2.24	2.75	2.73	2.77	2.89	2.78	2.91
"	"	Free from CO_2	2.22	2.60	2.69	2.69	2.65	3.17	3.13	3.21
"	7 days	In equilibrium with air	2.28	2.53	2.42	2.58	2.48	2.75	2.51	2.55
"	"	Free from CO_2	2.36	2.54	2.54	2.56	2.55	2.46	2.63	2.68
Untreated	—	In equilibrium with air	6.64	6.65	6.72	6.75				

[a] Bleached sulfite pulp, air-dry weight of the samples 1.00 g. each. All samples dried after washing overnight at 105°C.

known that if cellulose is dried at this temperature a slow depolymerizing effect is exerted on it. The presence of even very minute traces of acid in the fiber is bound to enhance this effect, which can be detected by viscometric determinations. The purpose of this investigation was thus that of verifying the presence of acid traces in fiber after immersion in acid followed by washing and drying procedures, either by a direct x-ray emission spectrographic method to show the presence of Br and thus also of HBr, or by their depolymerizing effect during the drying period.

Table I gives the results of washing experiments in a vertical tube. The samples denoted by 1 were washed once with 25 ml. of distilled water: samples 2 twice; samples 3, three successive times, and so on. After washing, each sample was dried overnight at 105°C. It is clear from this table that even up to eight washing cycles the $[\eta]$ values of the dried samples differ comparatively little from the value obtained after only one washing step, and that drying at 105°C. has a very marked lowering effect upon the $[\eta]$ for all the acid-treated, washed samples when compared against the same values of samples which have not been immersed in acid, but which have been washed only 1–4 times with distilled water and subsequently dried overnight at 105°C. The two acids used, HCl and HBr, are in this respect quite similar in their effects. It is thus obvious that washing in a vertical tube was unable to remove the last traces of the two acids from the cellulose material. The results also show that when the washing is carried out in a vertical tube, the expulsion of CO_2 from the washing water has no positive effect.

One consequence of these findings should be that the successive washing water portions, after contact with the fiber, contain minute amounts of titrable acid. This can also be confirmed by titrating suitable aliquots of the successive washing water portions with 0.01*N* acid, as described in the

TABLE II

Titrimetric Determinations of the HCl Content of the Successive Washing Water Lots from the Vertical Tube Washing Experiments[a]

Washing no.	Aliquot taken for the titration, ml.	Consumption of 0.01*N* NaOH, ml.	Total amount of HCl in the washing water, aliquot, μequiv.
1	1	4.52	11300
2	10	0.81	20.3
3	10	0.04	1.0
4	10	0.02	0.5
5[b]	10	0.05	1.3
6	10	0.02	0.5

[a] Bleached sulfite pulp, air-dry weight of the sample 1.00 g. washing started in the vertical washing tube after the sample had been immersed for 7 days in 0.1*N* HCl; each washing water portion consisted of 25 ml. of distilled water in equilibrium with the atmosphere.

[b] After the fifth washing water portion had been added to the tube, its contents were stirred (see text).

experimental section. Table II gives the results of these titrations, and from this table it can be seen that the washing water portions are by no means acid-free after three or four washing steps, as stated by Sjöström.[1] A certain channelling effect of washing water in a material such as cellulose in a vertical washing tube could be expected, and the experimental series of Table II gives evidence that channelling does, in fact, occur, as when the contents of the tube had been stirred with a glass rod after addition of the fifth washing water portion, after removal from the tube this portion clearly had a higher acid content than the two previous ones, which had not been stirred. It is clear from this that no reliable results can be expected from washing operations with the aid of a vertical tube.

The washing process was accordingly modified in such a way that cellulose samples which had previously been immersed in acid were washed by shaking them for 10 min. each under nitrogen cover in successive washing water portions. Following the washing all the samples were dried overnight at 105°C., and their [η] determined. The results shown in Table III for these experimental series clearly demonstrate that in this case the last traces of acid were continuously removed, although very slowly and even somewhat capriciously.

The washing procedure was now rearranged so that each washing step under nitrogen cover was lengthened to 24 hr. The results of this modification of the washing procedure are presented in Table IV. From this table, it can be seen that eight prolonged washing steps, with 100 ml. distilled water each time for a period of 24 hr. under nitrogen cover, are capable of freeing cellulose from the last traces of acid—both HCl and HBr. After the eight washing steps, the [η] of the dried samples were found to be practically identical with the values obtained when bleached sulfite pulp not treated with acid was dried overnight at 105°C. after washing steps with distilled water in equilibrium with air. The last-mentioned values are contained in Table I.

TABLE III

Washing Experiments with Cellulose Samples Which Had Been Immersed in Acid, by Shaking Them under Nitrogen in Successive Portions of Washing Water for 10 min. Each[a]

Acid	Duration of acid treatment	[η] of dried samples							
		1	2	3	4	5	6	7	8
0.1*N* HCl	1 hr.	3.10	3.05	3.49	3.47	3.88	3.47	3.97	4.45
"	"	2.71	2.83	2.90	2.91	2.73	3.72	3.52	3.81
"	18 hr.	2.36	2.83	2.94	2.97	3.28	4.24	3.82	4.56
0.1*N* HBr	1 hr.	2.28	2.76	2.82	3.08	3.46	3.91	3.51	4.43
"	18 hr.	2.38	2.71	2.81	3.09	3.33	5.25	4.95	5.15
"	7 days	2.18	2.75	3.06	3.93	4.02	5.18	4.76	5.12

[a] Bleached sulfite pulp, air-dry weight of samples 1.00 g. each. All samples dried overnight at 105°C.

TABLE IV

Washing Experiments with Cellulose Samples Which Had Been Immersed in Acid by Shaking Them under Nitrogen in Successive Portions Washing Water for 24 hr. Each[a]

Acid	Duration of the acid treatment, hr.	[η]							
		1	2	3	4	5	6	7	8
0.1*N* HCl	1	3.58	3.40	3.52	3.90	4.08	4.37	5.61	6.67
"	18	3.28	3.16	3.96	3.62	4.99	4.43	6.93	6.83
0.1*N* HBr	1	3.34	3.37	3.58	4.55	4.97	5.26	6.68	6.61
"	18	3.45	4.59	4.53	5.79	5.61	5.51	5.67	6.55

[a] Bleached sulfite pulp, air-dry weight of samples 1.00 g. each. All samples dried overnight at 105°C.

TABLE V

Relative Bromine Content Determinations of the HBr-Treated and Washed Samples by X-Ray Emission Spectrography

Acid	Duration of acid treatment	Washing method	Net intensity after washing steps, counts/sec.							
			1	2	3	4	5	6	7	8
0.1*N* HBr	18 hr.	Vertical tube	2657	92	58	69	51	49	65	58
"	7 days	Shake washing under nitrogen	63	59	57	40	26	28	7	2

The results obtained by viscosity determinations after the different washing steps followed by overnight drying at 105°C. could be further corroborated by the employment of the direct x-ray emission spectrographic method.

For this purpose, two different test series were run. In the first of these, eight parallel samples of cellulose were immersed for 18 hr. in 0.1*N* HBr, and following this the samples were washed in the vertical tube, according to Sjöström. Sample 1 was washed with only one portion of 25 ml. distilled water, sample 2 twice with the same amount of washing water, sample 3 three times, and so on, and after these treatments the samples were again dried overnight. Eight parallel samples were included also in the second test series, in which before washing the samples were immersed for 7 days in 0.1*N* HBr. Sample 1 was washed for one day and night, being shaken with 100 ml. distilled water under nitrogen; sample 2 was washed for two days in a similar manner the washing water being changed in between, sample 3 was washed for three successive days, with the washing water changed between the days, and so on. After these different washing treatments, all the samples were again dried overnight at 105°C., and their Br, and consequently also the HBr content assayed by determination of the number of net counts per second resulting from this element in the x-ray emission spectrography as described in the experimental part. The values of net counts per second serve as comparative units for the remaining trace amounts of HBr in the samples.

The results of these experiments compiled in Table V clearly show that with vertical-tube washing according to Sjöström there occurs no continuous expulsion of HBr traces, whereas the shake-washing under nitrogen is capable of bringing down the Br content and thus also the HBr content almost to zero in eight successive washing steps.

The results obtained by means of these two experimental techniques, viscometric determination, and x-ray spectrographic determination should remove any surviving doubts about the very real difficulties involved in eliminating the last traces of acid with which cellulose fiber has been in contact. They also emphasize the importance of penetration and accessibility phenomena when dealing with the heterogeneous system of electrolyte solution surrounding cellulose fiber. Furthermore, they lend no support to the idea of Donnan equilibrium maintaining the electrolyte concentration inside the cellulose fiber at a lower level than that of the surrounding electrolyte solution.

EXPERIMENTAL

1. Washing Experiments in a Vertical Tube According to Sjöström

The samples (bleached sulfite pulp, air-dry weight 1.00 g.) were suspended in 100 ml. of 0.1*N* HCl or HBr at room temperature for various periods. After this, each suspension was in turn poured into a vertical glass tube, the bottom of which was covered with a plug of glass wool. After the excess acid had passed through, the sample was gently pressed against the bottom of the tube with a flattened glass rod, and the first portion of washing water (25 ml.) was poured into the tube and left in contact with cellulose for 10 min. before being allowed to run off. The sample was removed from the tube with clean forceps, pressed free of excess liquid, put on a cover glass, and dried overnight at 105°C. in a drying oven.

The second sample acid suspension was treated in exactly the same way as the first, but was washed twice with two successive lots of distilled water (25 ml. each); the third parallel sample was washed three times, and so on up to eight washing steps.

2. Washing Treatments Under Nitrogen

The samples (bleached sulfite pulp, air-dry weight 1.00 g.) were suspended in 100 ml. of 0.1*N* HCl or HBr at room temperature for various periods, following which the sample was filtered by means of a glass tube with a coarse sintered-glass bottom (G 1). The sample was then pressed dry against the bottom of the filtering tube, and transferred quantitatively into a 300-ml. Erlenmeyer flask with a ground-glass stopper fitted with gas inlet and outlet tubes. A 100-ml. portion of distilled water was measured into the flask, the flask was closed and placed in a shaking machine. Pure cylinder nitrogen was led through the suspension during the course of the shaking, which lasted either 10 min. or 24 hr. After the shaking, the sam-

ple was filtered as above, pressed dry, put on a cover glass, and dried overnight at 105°C.

The second sample was washed in the same manner as the first by shaking under nitrogen, was filtered as described above, and re-washed by shaking under nitrogen, filtered, pressed dry, and dried. The third sample was treated similarly, but was washed three times with intermediate filterings, and so on up to the eighth sample.

3. Determination of $[\eta]$

Samples dried overnight at 105°C. were disintegrated with clean forceps, and allowed to stand for two days in the laboratory air and protected from dust in order to attain equilibrium with the air moisture. The $[\eta]$ values of the samples were then determined in FeTNa (an alkaline solution of the iron tartaric acid complex) according to Valtasaari.[5] The moisture content of the samples was determined on separate parallel samples from the corresponding lots.

4. Titrimetric Determinations of the HCl Content of the Washings

The sample of bleached sulfite pulp (air-dry weight 1.00 g.) was allowed to stand in 100 ml. of 0.1*N* HCl for one week, after which it was washed with 25-ml. portions of distilled water in the vertical washing-tube as described above. The washings were collected separately in beakers, weighed, and suitable aliquots of them added to 200 ml. of 0.01*M* KCl solution and titrated under nitrogen cover up to pH 7.00 with 0.01*N* NaOH according to Ant-Wuorinen and Visapää.[6] After the fifth washing water portion had been added to the tube, its contents were stirred for 1 min. with a glass rod before filtering. The sixth washing treatment was again normal, i.e., the sample was not stirred.

5. Determination by X-Ray Emission Spectrography of the Relative Residual Bromine Content of the HBr-Treated and Washed Samples

To ascertain whether the residual bromine of the HBr-treated samples could be detected by means of x-ray emission spectrography, the samples (air-dry weight 1.00 g.), after treatment with 0.1*N* HBr and the respective washing treatments either by washing in vertical tube or by shake-washing, with each washing step lasting 24 hr., were dried at 40°C. and pressed into Philips' pressed-sample holders using a pressure of 2000 kg./cm.^{2} for 1 min.

In view of the rather complex x-ray instrumentation, the apparatus used and the operating conditions are listed below in detail, to facilitate duplication of these tests elsewhere. The following apparatus by Philips was used: constant potential x-ray generator PW 1010, universal vacuum x-ray spectrograph attachment PW 1540, wide range goniometer PW 1050, electronic measuring panel PW 1051 equipped with a recorder type PR 2262/00, high-intensity x-ray tube PW 25714 (W-anode), scintillation counter PW 1964/10 with preamplifier, power supply PW 4029/01, linear

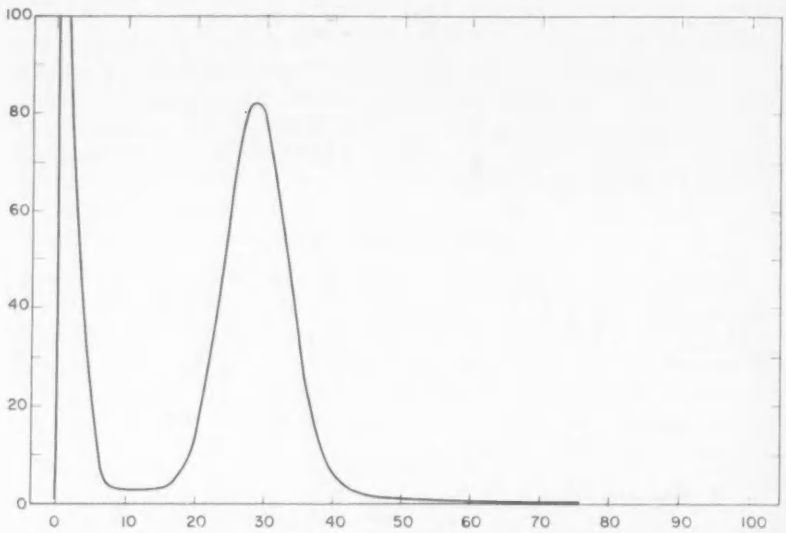

Fig. 1. Pulse height distribution curve of BrKαI line from chemically pure potassium bromide; goniometer setting 29.97° = 2θ.

amplifier/distribution unit PW 1053, discriminator PW 4082 automatic scanner PW 4083/01.

Lithium fluoride crystal ($2d$ = 4.0267 A.) was used as an analyzer. The samples were rotated (30 rpm) in their own plane during the analysis.

To ensure a better signal-to-background ratio, a pulse height distribution analysis for the BrK α I line was made, using chemically pure potassium bromide by Merck. The pulse height distribution curve (Fig. 1) of this BrK α I line, the goniometer setting of which is 29.97° = 2θ,[7] was recorded under the following conditions: tube (W-anode): 20 k.v., 6 ma. (at higher intensities the discriminator begins to choke since it is unable to handle all the incoming pulses); scintillation counter: 920 v.; analyzing crystal: LiF; scanning time (100—0 v.): 14 min.; discriminator window: 1 v.; discriminator attenuation: 2×; discriminator differential time constant: ∞ μsec.; discriminator integral time constant: 0.2 μsec.; rate meter time constant: 2 sec. rate meter scale factor: adjusted as to keep the peak between 50 and 100 chart divisions; chart speed: 1600 mm./hr.

Pulse height discrimination settings obtained from the curve (amplitude 30.0 v., window 28 v., attenuation 2×) were used in the relative bromine content determinations of the pressed samples. The other instrument settings during the actual analytical runs were: tube (W-anode): 50 k.v., 20 ma.; goniometer settings: 29.97° 2θ for the BrK α I line and 29.10° 2θ for the background; scintillation counter: 920 v.; analyzing crystal: LiF; sample rotation: on; vacuum was not used.

The time required for 64,000 counts to accumulate both for the BrK

α I line and for the background was determined. The net intensities in counts per second due to the residual Br contents were obtained by subtracting the background intensity values from the line intensity values of the samples.

This investigation forms a part of a research project under U. S. PL 480 83rd Congress, and the authors wish to express their gratitude for the support thus obtained.

References

1. Sjöström, E., and P. Haglund, *Svensk Papperstidn.*, **64**, 438 (1961).
2. Andersson, R., and O. Samuelson, *Svensk Papperstidn.*, **61**, 1001 (1958).
3. Franzon, O., O. Samuelson, B. Bodforss, and E. Ehn, *Svensk Papperstidn.*, **60**, 706 (1957).
4. Ant-Wuorinen, O., and A. Visapää, *Svensk Papperstidn.*, **61**, 27 (1958); The State Institute for Technical Research, Finland, Report Series IV, Chemistry 15 (1958).
Ant-Wuorinen, O., and A. Visapää, *Suomen Kemistilehti*, **B31**, 90 (1958); The State Institute for Technical Research, Finland, Report Series IV, Chemistry 16 (1958).
Ant-Wuorinen, O., and A. Visapää, *Makromol. Chem.*, **30**, 1 (1959); The State Institute for Technical Research, Finland, Report Series IV, Chemistry 21 (1959).
Ant-Wuorinen, O., and A. Visapää, *Paper Timber* (*Helsinki*), **42**, 33 (1960); The State Institute for Technical Research, Finland, Report Series IV, Chemistry 24 (1960).
5. Valtasaari, L., *Paper Timber* (*Helsinki*), **39**, 243 (1957); The State Institute for Technical Research, Finland, Report Series IV, Chemistry 9 (1957).
6. Ant-Wuorinen, O., and A. Visapää, *Paper Timber* (*Helsinki*), **43**, 699 (1961); The State Institute for Technical Research, Finland, Report Series IV, Chemistry 38 (1962).
7. Pickett, H. W., "X-ray Wavelengths for Spectrometer," General Electric Cat. No. 4961 DA (1959).

Synopsis

A study has been made of the unsolved problem of how cellulose fiber which has been in contact with an acid can be freed from the last traces of this acid. Two new experimental techniques were used for verification of the presence of minute amounts of acid which remain attached to this fiber. The first of these techniques is based on the fact that the presence of residual acid in fiber enhances the depolymerization of the cellulose when dried at 105°C. This depolymerization effect, determined viscometrically, can be used to ascertain the presence of even the most minute amounts of acid remaining in the fiber after washing. The second newly developed experimental technique uses x-ray emission spectrography to determine the Br content of cellulose which has, before washing, been in contact with aqueous HBr. Both of these methods gave results which confirm beyond a doubt that the removal by washing of the last traces of acid from cellulose is a very difficult and lengthy process which has to be carried out with a shield against the CO_2 of the atmosphere.

Résumé

Une étude a été entreprise au sujet d'un problème non-résolu à savoir comment une fibre de cellulose qui a été en contact avec un acide peut être débarassée des dernières traces de cet acide. Deux nouvelles techniques expérimentales ont été utilisées pour vérifier la présence de faibles quantités d'acide restant attaché à cette fibre. La primière de ces techniques est basée sur le fait que la présence d'acide résiduel sur la fibre augmente la dépolymérisation de la cellulose quand on la sèche à 105°C. Cet effet de dépolymérisation, déterminé viscosimétriquement, peut servir pour s'assurer de la présence même des plus faibles quantités d'acide restant sur la fibre après lavage. La seconde technique expérimentale nouvellement développée fait intetvenir la spectro-

graphie d'émission des rayons-X pour déterminer la contenance en Br de la cellulose qui, avant le lavage, a été en contact avec HBr aqueux. Chacune de ces méthodes donne des résultants qui confirment sans aucun doute possible le fait que l'enlèvement par lavage des dernières traces d'acide de la cellulose est un processus vraiment difficile et d'assez longue durée qui doit être effectué en l'absence de CO_2 atmosphérique.

Zusammenfassung

Das ungelöste Problem der Entfernung der letzten Säurespuren aus einer mit dieser Säure in Berührung gebrachten Cellulosefaser wurde untersucht. Zwei neue Verfahren wurden zum Nachweis der winzigen Säuremengen, die an der Faser gebunden bleiben, angewendet. Die erste Methode beruht auf der Tatsache, dass die Gegenwart von Säureresten in der Faser die Depolymerisation der Cellulose beim Trocknen bei 105°C begünstigt. Dieser viskosimetrisch bestimmte Depolymerisationseffekt kann zur Erkennung auch der geringsten, nach dem Auswaschen in der Faser verbleibenden Säurespuren herangezogen werden. Die zweite, neu entwickelte Methode verwendet die Röntgen-Emissionsspektrographie zur Bestimmung des Br-Gehaltes von Cellulose, die vor dem Auswaschen in Berührung mit wässrigem HBr gestanden war. Die Ergebnisse beider Methoden zeigen zweifelsfrei, dass die Entfernung der letzten Säurespuren aus Cellulose durch Auswaschen ein sehr schwieriger und langwieriger Prozess ist, der unter Abschirmung gegen das atmosphärische CO_2 durchgeführt werden muss.

JOURNAL OF POLYMER SCIENCE: PART C NO. 2, PP. 321–330 (1963)

Viscosity Measurements on Chemically Modified Cellulose

Ø. ELLEFSEN, *The Norwegian Pulp and Paper Research Institute, Oslo, Norway*

1. INTRODUCTION

Viscosity measurements on cellulose in alkaline solutions as cuprammonium and cupriethylenediamine are commonly used in the pulp and paper industry as a tool for the evaluation of new pulp qualities and the control of pulp production. Such measurements have been subjected to standardization.

Another technique which is also widely used, especially in connection with dissolving pulp qualities, is viscosity measurements of cellulose trinitrates in an appropriate solvent, such as acetone, butyl acetate, or ethyl lactate.

In certain cases discrepancies between the two different techniques are observed,[1–9] and it is the reasons for these discrepancies which are going to be dealt with in the present paper.

2. EXPERIMENTAL

Cuam Viscosity Determination

The viscosity values in cuprammonium (cuam) solution were determined according to Swedish standard method CCA-16.[10] The cuam solution contains 15 g. Cu and 200 g. NH_3 per liter and the viscosity of this solution is 1.30 cpoise. The viscosities of the cellulose samples were determined in 1% concentration. The measured viscosities were converted to limiting viscosity numbers by means of Martin's equation[11] using $k = 0.13$. The degree of polymerization was calculated from $DP = 1/K_m [\eta]$, where the value of K_m was 5×10^{-4} as suggested by Staudinger et al.,[12–14] i.e., $1/K_m = 2$ when the limiting viscosity numbers were expressed in Staudinger units (cc./g.).

Nitration

Each sample was nitrated according to the method of Davidson[15] with a nitration mixture of nitric acid–phosphoric acid–phosphorus pentoxide (48:50:2). The nitrates were filtered, washed with 50% acetic acid, and then with distilled water till free from acid. They were then extracted with methanol and finally washed with water and dried.

Viscosities of Nitrates and DP Determinations

The viscosities of the cellulose nitrates in acetone solution were determined in an Ostwald viscometer with a sphere volume of 1.9 cm.^{3} and an efflux time of 120 sec. for pure acetone. The limiting viscosity numbers $[\eta]$ were determined according to Martin's equation[11] using $k = 0.20$,[16] following a principle previously described.[17]

The degrees of polymerization were determined from DP $= 1/K_m\ [\eta]$. The empirical constant $1/K_m$, which is dependent on the nitrogen content of the nitrates, and the applied correction factor are based on the results of Jullander,[18] as previously described.[7]

Preparation of Alkali Cellulose

Each sample was steeped, in the form of sheets, in 18% sodium hydroxide for 1 hr. at 20°C. (Cellulose: lye ratio 1:14 w/v). After pressing, the pulps were neutralized with 10% acetic acid and then washed with distilled water till free from acid. The products were air-dried.

Reduction with Sodium Borohydride

Each sample (5 g.) was suspended in 0.01M aqueous sodium borohydride (250 ml.) and set aside at room temperature for 24 hr. The reaction product was filtered off, resuspended in cold 1N acetic acid, filtered, and washed with water till free from acid. The reduction products were all air-dried.

3. RESULTS AND DISCUSSION

In Table I the data on limiting viscosity numbers demonstrate how the results from the two different techniques deviate from each other. The results in section A, covering the comparison of the nontreated original rayon pulp samples, are in very good agreement with the results published by other authors,[3,5] i.e., that the ratio $[\eta]_{\text{nitrate}}/[\eta]_{\text{cuam}}$ of 2.6 is usually found for original pulp samples.

In section B of Table I, where the data for mercerized samples are given, it is seen that the ratio is changed to 2.3. This difference between original pulp samples and samples measured after a mercerization and regeneration treatment is also found when the DP values are determined.

Assuming that the error is to be ascribed to the ratio found for mercerized samples, there are two alternatives: (*1*) the nitrate viscosities are too low owing to some special degradation effect appearing after the pulp has been treated with 18% NaOH; or (*2*) the cuam viscosities are too high because of a polymerization effect.

As neither of these alternatives seems very probable, the error must lie in the ratio found for the original pulp samples.

If this is taken as a basis for the further discussion, there are again two alternative possibilities, viz.: (*1*) the cuam values for the original non-

TABLE I
$[\eta]_{nitrate}/[\eta]_{cuam}$ and $DP_{nitrate}/DP_{cuam}$ Ratios for Original and Mercerized Rayon Pulps

Sample	$[\eta]_{cuam}$, cm.³/g.	$[\eta]_{nitrate}$, cm.³/g.	$\frac{[\eta]_{nitrate}}{[\eta]_{cuam}}$	DP_{cuam}	$DP_{nitrate}$	$\frac{DP_{nitrate}}{DP_{cuam}}$
A. Original samples						
1	432	1100	2.55	864	1165	1.35
2	422	1040	2.47	844	1342	1.59
3	397	950	2.40	794	930	1.17
4	382	950	2.49	764	1062	1.39
5	378	1175	3.10	756	1155	1.53
6	377	980	2.60	754	1022	1.36
7	375	1070	2.85	750	1138	1.52
		Mean value	2.64		Mean value	1.42
B. Mercerized samples						
1	408	1020	2.51	816	918	1.13
2	376	820	2.18	752	872	1.16
3	372	865	2.33	744	812	1.09
4	357	770	2.16	714	780	1.09
5	346	790	2.28	692	750	1.08
6	340	750	2.21	680	700	1.03
7	335	750	2.24	670	700	1.04
		Mean value	2.27		Mean value	1.09

treated samples are too low owing to degradation effects, or (*2*) the $DP_{nitrate}$ values are too high owing to some crosslinking effect in the cellulose nitrates, and obviously also both of these effects may be present simultaneously.

With this working theory as a basis, it was quite obvious that some chemical modification of the original pulp samples had to be undertaken in order to throw light on this problem. As it seemed logical that the cuam viscosities of the original pulp samples were too low, owing to some degradation effect during the viscosity measurements in alkaline solutions, treatment with reducing agent was tried before the measurement in cuam solution.

In Table II the results from the cuam viscosity measurements before and after the reducing treatment with sodium borohyride have been recorded, as well as the corresponding DP values. The table comprises both a series of paper pulp as well as a series of rayon pulp samples.

In the last column the increase in degree of polymerization as a function of the reducing pretreatment has been given in percentage of the original DP values. As will be seen the Δ DP values vary from 3 to 11% for the paper pulps, whereas they range from 0 to 5% in the case of rayon pulps.

The reducing effect of the borohydride treatment on the pulps was followed by copper number measurements before and after the borohydride treatment.

TABLE II

Cuam Viscosities and the Corresponding Degrees of Polymerization (DP) of a Series of Pulps Before and after Reduction with Sodium Borohydride

Sample	Cuam viscosity, (cpoise)		DP		
	Original	After reduction	Original	After reduction	Δ DP, %
A. Paper pulps					
P 1	95.6	130.6	1490	1640	10.1
P 2	72.6	97.7	1364	1502	10.1
P 3	83.1	116.6	1424	1584	11.2
P 4	75.2	103.0	1380	1524	10.4
P 5	70.7	91.0	1352	1464	8.3
P 6	47.9	63.0	1176	1302	10.7
P 7	47.1	54.3	1168	1232	5.5
P 8	38.4	41.7	1080	1114	3.2
P 9	28.9	38.1	962	1076	11.9
P 10	29.9	37.5	974	1070	9.9
P 11	33.5	40.5	1020	1102	8.0
P 12	44.6	55.7	1144	1244	8.7
B. Rayon pulps					
R 1	26.2	26.2	920	920	0
R 2	23.0	23.0	868	868	0
R 3	18.0	20.0	772	812	5.2
R 4	17.8	19.7	764	804	5.2
R 5	16.9	17.4	744	756	1.6
R 6	15.5	16.1	716	728	1.7

A statistical analysis[19] of the correspondence of the observed decrease in copper numbers and the increase in DP values revealed the following facts.

When the decrease in copper numbers was below 0.2, a very good statistical correlation between the decrease in copper numbers and the increase in degree of polymerization was found, whereas in the range where the copper number values had decreased more than 0.2 no significant correlation was found at all.

If we now return to the original pulp and reason in terms of introduced alkali labile carbonyl groups, the following interpretation seems probable.

Starting with a theoretical pulp having no alkali labile groups the introduction of a relatively small amount of such groupings, i.e., a difference in copper numbers of less than 0.2, is followed by a proportional degrading effect when the pulp is subjected to viscosity measurements in cuprammonium solutions. A further increase in the number of alkali labile groups does not have a similarly strong effect within the copper number limits comprised in this investigation.

By these experiments it has thus been demonstrated that in part, the "too high" ratio found for original pulp samples with respect to $[\eta]_{\text{nitrate}}/[\eta]_{\text{cuam}}$ may be accounted for by the alkali labile groups which cause a "too low" value in the cuam viscosity measurements.

TABLE III
Viscosities and Degrees of Polymerization (DP) Obtained by the Cuene Method before and after Reduction with Sodium Borohydride[a]

Sample	Cuene viscosity, cpoise		DP		Δ DP, %
	Original	After reduction	Original	After reduction	
P 5	67.9	93.9	1356	1504	10.9
P 8	34.5	36.8	1060	1086	2.5
P 9	26.6	34.5	948	1060	11.7

[a] Cuene viscosity determined according to the Swedish standard method CCA-28:57.

In order to demonstrate that the effect of the borohydride treatment is also the same when a cupriethylenediamine is used instead of the cuprammonium solution, the data in Table III are presented.

A comparison with the data in Table II shows that the effects are also quantitatively equal to those found in the cuprammonium experiments.

Turning now to the other side of the problem, viz., the question whether the nitrate viscosities for original pulp samples are higher than they ought to, a possible reason for too high values in this dissolving system could be some kind of crosslinking between neighboring chains of cellulose nitrates.

In order to investigate whether the carbonyl groups present in the original pulp samples could also be involved in the crosslinking effect, a borohydride treatment was applied to the original pulp prior to nitration and viscosity measurement in acetone solution.

TABLE IV
Results of DP Determinations by the Nitration Method of a Series of Paper and Rayon Pulps before and after Reduction with Sodium Borohydride

Sample	Before reduction			After reduction			Δ DP, %
	N, %	[η]	DP	N, %	[η]	DP	
P 1	13.8	1920	1852	13.9	1886	1742	−5.9
P 2	13.6	1884	1922	13.7	1797	1761	−8.4
P 3	13.7	1881	1843	14.0	1877	1671	−9.3
P 4	13.7	1860	1823	13.9	1842	1695	−7.0
P 5	13.7	1773	1737	13.7	1624	1592	−8.3
P 6	13.7	1605	1573	13.8	1555	1474	−6.3
P 7	13.7	1567	1536	13.7	1445	1416	−7.8
P 8	13.7	1451	1422	13.7	1363	1336	−6.0
P 9	13.7	1396	1368	13.7	1298	1272	−7.0
P 10	13.8	1513	1438	13.7	1265	1240	−13.8
P 11	13.7	1506	1476	13.9	1344	1238	−16.1
R 2	13.9	1114	1033	14.0	1090	970	−6.1
R 3	13.8	1026	975	13.9	1018	935	−4.1
R 4	13.7	1034	995	14.0	904	904	−9.1
R 5	13.8	958	910	13.9	830	830	−8.8
R 6	13.8	942	895	14.0	917	821	−8.3

The results are presented in Table IV. Here the nitrogen contents of the nitrates, the limiting viscosity numbers, and the corresponding degree of polymerization are given for a series of samples of paper pulps as well as rayon pulps before the reducing treatment with borohydride and after the same treatment. In the last column are also given the Δ DP values, i.e., the decrease in degree of polymerization obtained as a percentage of the original DP values. In all cases the degree of polymerization decreases.

It will further be observed that the effects as given in Δ DP values are even more pronounced than was found in connection with the borohydride treatment and subsequent viscosity measurements in alkaline solution. It may further be mentioned that in this case also copper number measurements were undertaken and correlated with the Δ DP values. A statistically significant correlation was, however, not obtained. In spite of this lack of correlation, there is no doubt that the borohydride treatment which reduces the carbonyl groups to alcohol groups, has a significant influence upon the crosslinking effect. It appears that the groups mainly responsible for the crosslinking are the carbonyl groups introduced in the pulp.[19–21]

The proposed mechanism is that the crosslinking is caused by hydrogen bonding between a keto group in one chain and a carbonyl group in its enol form in the neighboring chain. The mechanism is demonstrated by eqs. (1)–(4).

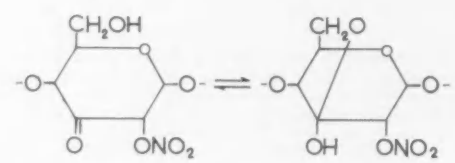

(1)

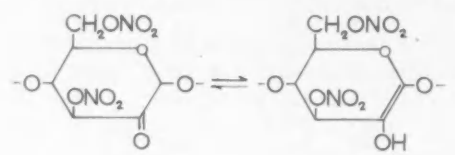

(2)

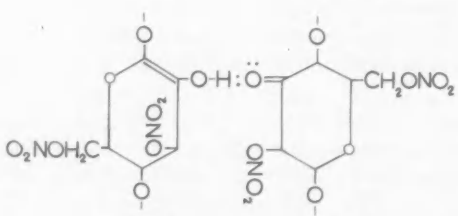

(3)

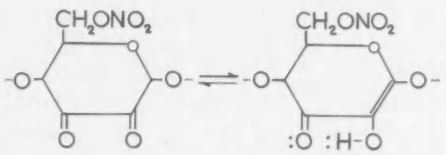

(4)

The first possibility [eq. (1)] where acetal formation is involved, cannot be disregarded in all cases, but it is only possible in nitrates containing less than the theoretical maximum of nitrogen, because of the fact that one of the hydroxyl groups will participate in the enol formation.

On the other hand, if enol formation as illustrated in this formula, actually exists during nitration, one might expect that the enol form would undergo nitration, thus bringing the equilibrium over to the right, and prevent the hydrogen bonding. Furthermore, one will also expect the nitrogen content to approach the theoretical value for cellulose, i.e., 14.1%. However, from the results of Rogovin et al,[20] it appears that the nitrogen content decreases as the number of carbonyl groups increases.

The next alternative for equilibrium between the keto and the enol form in the nitrated cellulose containing carbonyl groups is presented in eq. (2).

Bearing in mind that, for instance, the pure keto form of ethyl acetoacetate is isolated from a nonaqueous medium containing hydrogen chloride, it might seem plausible that the nonaqueous nitration liquor might bring the equilibrium 100% to the left, and that the actual crosslinking takes place in the later stages of the process of nitration, i.e., during the washing with water, acetic acid, and methanol.

An actual crosslinking between glucose units in neighboring cellulose nitrate chains may, according to eq. (2), be presented by the system given in eq. (3). It was mentioned above that statistical relationship between the number of carbonyl groups and the degree of crosslinking was not directly found. Following the previous argument, this can be explained as follows.

If two carbonyl groups formed during processing of the pulp are present in one and the same anhydroglucose unit, situated in positions 2 and 3, then it will be expected that these two groups would combine through hydrogen bonding, so that the net result would be intramolecular hydrogen bonds, which again would prevent such carbonyl groups taking part in intermolecular crosslinking. This is illustrated by eq. (4).

It is obvious that no quantitative relationship between the number of carbonyl groups in the pulp and the calculated Δ DP is to be expected in such a case. One might in fact expect that the higher the Δ copper number value is for the pulp, the greater is the possibility of having two adjacent carbonyl groups, and therefore the greater the possibility for intramolecular hydrogen bondings.

Leaving now this theoretical interpretation of the crosslinking effect, and returning to the problem of viscosity measurements, it appears that sodium borohydride reduction of bleached sulfite pulps prior to nitration and

viscosity measurements decreases the viscosities and thus the calculated DP values. Similarly, it was demonstrated that sodium borohydride reduction increased the DP values calculated on basis of the cuprammonium viscosities. Accordingly it follows that the ratio $DP_{nitrate}/DP_{cuam}$ after sodium borohydride reduction of the pulp will be lowered. This is illustrated by the data in Table V.

It is seen that the $DP_{nitrate}/DP_{cuam}$ ratio is now in the range 1.1 both for paper pulps and for rayon pulps. In Table I it was demonstrated that the original pulp samples had a $DP_{nitrate}/DP_{cuam}$ ratio of approximately 1.4,

TABLE V

DP Values of a Series of Bleached Sulfite Paper and Rayon Pulps Obtained by the Cuam and the Nitrate Methods after Reduction of the Pulps with Sodium Borohydride

Sample	DP_{cuam}	$DP_{nitrate}$	$\frac{DP_{nitrate}}{DP_{cuam}}$
P 1	1640	1742	1.06
P 2	1502	1761	1.17
P 3	1584	1671	1.05
P 4	1524	1695	1.11
P 5	1464	1592	1.09
P 6	1302	1474	1.13
P 7	1232	1416	1.15
P 8	1114	1336	1.20
P 9	1076	1272	1.18
P 10	1070	1240	1.16
P 11	1102	1238	1.12
		Mean value	1.13
R 2	868	970	1.12
R 3	812	935	1.15
R 4	804	904	1.12
R 5	756	830	1.10
R 6	728	821	1.13
		Mean value	1.12

whereas pulps which had undergone an alkali treatment with 18% sodium hydroxide came out with a ratio of approximately 1.1, i.e., the same as found for the pulps after treatment with borohydride.

Considering these results it seems that the DP values calculated on basis of the nitrate viscosity method on original commercial pulps are too high due to crosslinking, which again is due to the presence of carbonyl groups. Similarly, the DP values based on the viscosities in cuam solution are too low, due to the degradation of the pulps in alkaline solutions. This degradation is also due to the carbonyl groups present in the pulps.

Both these effects should be eliminated if a pulp did not contain any carbonyl groups at all. One way of achieving this has been demonstrated to be the reduction of the carbonyl groups with sodium borohydride.

On the other hand, it should be equally well possible to remove the carbonyl groups from the pulps by steeping the latter in alkali. This would undoubtedly lead to degradation of the pulp, but the final product should neither degrade in cuam solution nor crosslink when nitrated, and furthermore, it should be possible to show this by the fact that sodium borohydride reduction of the regenerated alkali cellulose should not effect the DP determinations neither by the cuam nor by the nitrate method.

Two paper pulps having rather high contents of carbonyl groups, were selected for a demonstration of this effect, and the pulps were treated with 18% sodium hydroxide, and after regeneration the DP values of the samples were determined both by the cuam and the nitrate methods, and both before and after reduction with sodium borohydride. The results are presented in Table VI.

TABLE VI

DP Determinations of Regenerated Alkali Celluloses by the Cuam and the Nitrate Methods before and after Reduction with Sodium Borohydride

Sample	N, %		Nitrate method		Cuam method		$\frac{DP_{nitrate}}{DP_{cuam}}$
	By weight	By Kjeldahl	$[\eta]$	DP	$[\eta]$	DP	
Sample 1	13.7	13.7	1015	995	418	836	1.19
Sample 1 after reduction	13.8	13.8	1038	986	414	828	1.19
Sample 2	13.7	13.8	1268	1205	510	1020	1.18
Sample 2 after reduction	13.8	13.7	1231	1206	508	1016	1.19

It will be seen from the results that the sodium borohydride treatment of these regenerated alkali celluloses does not alter the DP values as calculated from the cuam viscosities or from the trinitrate viscosities in acetone. The calculated ratio also agrees well with those calculated for the original paper pulp series after reduction with sodium borohydride, and this agrees with the predictions made above.

Finally, it should be emphasized that the ratio $DP_{nitrate}/DP_{cuam}$ is yet not equal to 1, even after the reduction. Whether this is significant or not is impossible to say at this stage. It might well be that the difference which is still present is due to errors in connection with the K_m constant or the nitrogen correction factor employed in the calculations in connection with the DP values.

This will, however, need further investigation before any definite conclusion can be drawn. It seems, however, that by employing the technique described in this paper it is possible to eliminate the main discrepancy between the cuam and the nitrate methods for determining a pulp's DP value, irrespective of whether the pulp is in its original or alkalized form.

References

1. Staudinger, H., and A. W. Sohn, *Ber.*, **72**, 1709 (1939).
2. Coppick, S., *Tech. Assoc. Papers*, **27**, 219 (1944).
3. Husemann, E., and M. Goecke, *Makromol. Chem.*, **2**, 298 (1948); *ibid.*, **4**, 194 (1949).
4. Tribot, A., and A. Marsaudon, *Mém. Serv. Chim. Etat (Paris)*, **38**, 67 (1953).
5. Schulz, G. V., and M. Marx, *Makromol. Chem.*, **14**, 52 (1954).
6. Ellefsen, Ø., *Norsk Skogind.*, **9**, 399 (1955).
7. Ellefsen, Ø., and F. A. Abadie-Maumert, *Norsk Skogind.*, **10**, 238 (1956).
8. Ellefsen, Ø., *Schriften Ver. Zellcheming.*, **27**, 155 (1958).
9. Ellefsen, Ø., and S. V. Vardheim, *Norsk Skogind.*, **13**, 42 (1959).
10. Svenska Pappers- och Cellulosaingeniörsföreningens Tekn. Med. CCA-16 (1944).
11. Ott, E., *Cellulose and Cellulose Derivatives*, Interscience, New York, 1943, p. 966.
12. Staudinger, H., and R. Mohr, *Ber.*, **70**, 2296 (1937).
13. Staudinger, H., and G. Damviller, *Ber.*, **70**, 2508 (1937).
14. Staudinger, H., *Papier Fabr.*, **36**, 381 (1938).
15. Davidson, G. F., *J. Textile Inst.*, **29**, 195T (1938).
16. Doyle, G. J., et al., *J. Phys. Colloid. Chem.*, **51**, 569 (1947).
17. Abadie-Maumert, F. A., and Ø. Ellefsen, *Norsk Skogind*, **11**, 540 (1957).
18. Jullander, I., *Arkiv Kemi Mineral. Geol.*, **21A**, No. 8 (1945).
19. Ellefsen, Ø., and S. V. Vardheim, *Norsk Skogind*, **12**, 438 (1958).
20. Rogovin, Z. A., et al., *Zh. Prik. Khim.*, **22**, 857 (1949).
21. Anthoni, B., Ph.D. thesis, University of Helsinki (1958).

Synopsis

When viscosity measurements are performed on cellulose in alkaline solution (e.g., cuam solution), and the results are compared with the data obtained on the corresponding cellulose nitrates measured in acetone solution, certain discrepancies are observed. The cause of these discrepancies is very probably to be found in deviations in the chemical structure of the cellulose samples. In this paper it has been demonstrated how pretreatments with a reducing agent, e.g., sodium borohydride, eliminate the main part of the discrepancies, and thus also seem to offer a plausible reason for the effects met with in such measurements.

Résumé

Lorsqu'on fait des mesures de viscosité de la cellulose dans des solutions alcalines, p.e., des solutions cupriammoniacales, et lorsqu'on compare les résultats obtenus avec ceux mesurés dans des solutions d'acétone, on constate quelques écarts. La cause de cet écart entre les résultats est probablement due aux différences de structure chimique des échantillons de cellulose. Dans cet article on démontre comment on peut éliminer la plupart des écarts en traitant d'abord la solution avec un agent réducteur, p.e., le borohydrure de sodium, ce qui semble donner une raison plausible aux effets rencontrés dans ces mesures.

Zusammenfassung

Beim Vergleich der Ergebnisse von Viskositätsmessungen an Cellulose in alkalischer Lösung (z.B. Cuam-Lösung) mit Daten, die an den entsprechenden Cellulosenitraten in Acetonlösung erhalten wurden, ergeben sich gewisse Widersprüche. Die Ursache dafür liegt höchstwahrscheinlich in Unterschieden in der chemischen Struktur der Celluloseproben. In der vorliegenden Mitteilung wurde gezeigt, dass eine Vorbehandlung der Unstimmigkeiten eliminiert und daher eine plausible Erklärung für die bei solchen Messungen gefundenen Effekte zu bieten scheint.

JOURNAL OF POLYMER SCIENCE: PART C NO. 2, PP. 331-340 (1963)

Study of the Pyrolytic Decomposition of Cellulose by Gas Chromatography

ROBERT F. SCHWENKER, JR., and LOUIS R. BECK, JR., *Textile Research Institute, Princeton, New Jersey*

Introduction

Knowledge of the products from the thermal degradation of a polymer is essential for the elucidation of the mechanism or mechanisms involved. However, at the elevated temperatures characteristic of decomposition the processes become extremely complex due to intramolecular rearrangements and the occurrence of second order interactions between the degradation products.[1] Therefore, although the pyrolytic degradation of polymeric materials has been the subject of extensive study, in many instances knowledge as to the exact nature, number and distribution of pyrolytic degradation products remains incomplete as in the case of cellulose. The technique of gas chromatography appears to be admirably and uniquely suited to this most difficult task.

The thermal behavior of cellulose has commanded much attention due to the importance of this highly flammable natural polymer as the most widely used textile and building material known. Its pyrolytic decomposition gives rise to highly volatile, fixed gases, a spate of volatile products usually obtained as an aqueous distillate laced with intractable tars, and a carbonaceous residue.[2-4] The fixed gases, largely CO and CO_2, have been well characterized by mass spectrometry,[4] and by gas–solid chromatography.[7,8] The carbonaceous residues can be readily analyzed by elemental, infrared, and x-ray analytical techniques. However, the largest and most important group of products, the volatile products, covering a wide range of boiling points and condensable from about 100°C. to −78°C. comprise upwards of 70% of the products of pyrolytic degradation and have as yet not been completely analyzed.

Pictet and Sarasin[9] found 1,6-anhydro-β-D-glucopyranose (levoglucosan) to be the major volatile product from the pyrolysis of cotton cellulose under reduced pressure. Schwenker and Pacsu[5] studied the slow pyrolysis of cotton cellulose in air at temperatures to 375°C. and by classical organic techniques and paper chromatography identified eight products to include levoglucosan, water, aldehydes, ketones and organic acids with evidence for seven more which were not identified. Madorsky et al.[4,10] studied the slow pyrolysis of cellulose in vacuum and under nitrogen and analyzed the

products by mass spectrometry and infrared spectroscopy. Preliminary work on cellulose pyrolysis by isothermal gas chromatography has recently been reported by Martin and Ramstad,[7] Greenwood et al.,[11] and Berkowitz-Mattuck and Noguchi.[8]

Experimental

The apparatus used was an F & M Model 500 linear-programmed high temperature gas chromatograph with a hot wire filament detector. This unit can be operated isothermally as well as by temperature programming at various heating rates at column temperatures to 500°C. Three different columns, made from $^1/_4$ in. O.D. aluminum tubing with 30–60 mesh Haloport F (perfluorocarbon polymer) as the solid support, were employed and are further described in Table I.

TABLE I
Gas Chromatographic Columns

Column no.	Liquid phase		Maximum operating temp., °C.	Length, ft.
	Compound	Polarity		
9	Octoil-S (di[2-ethyl hexyl] sebacate)	Polar	175	18
13	Silicone oil-550	Nonpolar	225	12
14	Carbowax-20M (polyethylene glycol)	Polar	225	12

All columns had 10% by weight of the liquid phase on the solid support. Helium, at a tank pressure of 30 psi, was used as the carrier gas. The gas flow rate was 30 cc./min. for column 13 and 60 cc./min. for columns 9 and 14. The detector block temperature was 275°C., and the injection port temperature was 225°C. Since there was a wide range of boiling points of the pyrolysis products the linear-programmed gas chromatography technique was used. Runs were usually initiated at a column temperature of 60°C. and programmed at 4.0°C./min., for the Octoil-S and silicone oil columns and 7.9°C./min. in the case of the Carbowax column, to the maximum safe operating temperature for each column and then continued isothermally until the run was completed.

Purified cotton fabric was pyrolyzed in a conventional pyrolysis apparatus by preheating the samples (ca. 10 g.) at 110°C. to drive off sorbed moisture followed by heating at ca. 15°C./min. to 370°C. in an atmosphere of air or purified nitrogen. The products were trapped at 75°C. and −78°C. to yield tarry pyrolyzates, 10 μl. aliquots of which were injected into the gas chromatograph. Samples of cotton yarn (10 mg.) were also pyrolyzed for 10–12 sec. within the injection port of the gas chromatograph on a hot Nichrome wire loop to afford a more direct examination of the de-

gradation products as suggested by the work of Lehrle and Robb and others.[12–14]

The primary method of component identification was by comparison of the retention volumes for unknown peaks with those of known compounds. In addition, the effluents for various unknown peaks, trapped and collected as they emerged from the column, were tested with various qualitative organic reagents for the presence of aldehydes, ketones, alcohols, and acids.[15] The retention volumes for unknowns and knowns were determined on three different columns to provide a cross-check. Another identification aid involved the inclusion of suspected knowns in the unknown mixtures in the case of liquid pyrolyzates.

Results and Discussion

Typical chromatograms obtained from the analysis of cellulose pyrolysis products on the Carbowax-20 (polyethylene glycol) column are shown in Figure 1. Chromatogram *A* was obtained by direct analysis of the degradation products, without prior condensation, by means of hot wire pyrolysis at ca. 450° C. for ten seconds in the carrier gas stream. Chromatograms *B* and *C* were obtained on liquid pyrolyzates prepared by condensing the products of slow cellulose pyrolysis (15 min. at 370°C.) in nitrogen atmosphere at 75°C. and at −78°C. Corresponding peaks in the three chromatograms are indicated by the same number and the products that have been identified are listed by peak number in Table II. In all cases the starting column temperature was 60°C., and temperature was increased at a rate of 7.9°C./min. until 225°C. after which isothermal conditions were maintained.

A minimum of 37 different volatile products is indicated (although only 34 numbered peaks are shown in chromatogram A, peak 1 contains the three or four unresolved fixed gases and levoglucosan did not come off the column), whereas earlier studies using other analytical methods have indicated 8–18 products[4,5,10] and the recent studies on cellulose pyrolysis by isothermal gas chromatography[7,8,11] have indicated no more than 18 decomposition products. These results indicate the same products irrespective of the pyrolysis conditions, but significant differences in product distribution are shown. The pyrolyzate condensed at 75°C. from cellulose pyrolysis in nitrogen shows the more volatile components as minor constituents with the intermediate and high boiling compounds as the most significant, whereas in the case of products condensed at −78°C. the converse is indicated. These variations reflect the expected effect of condensation temperature as well as the difficulty in quantitatively trapping all products from conventional pyrolysis for subsequent analysis. Direct analysis of products from hot wire pyrolysis shows an intermediate distribution which could be expected to approximate the true distribution of products.

Intuitively, controlled pyrolysis in the carrier gas stream as described by Lehrle and Robb[12] and others[13–15] would seem to constitute the most rea-

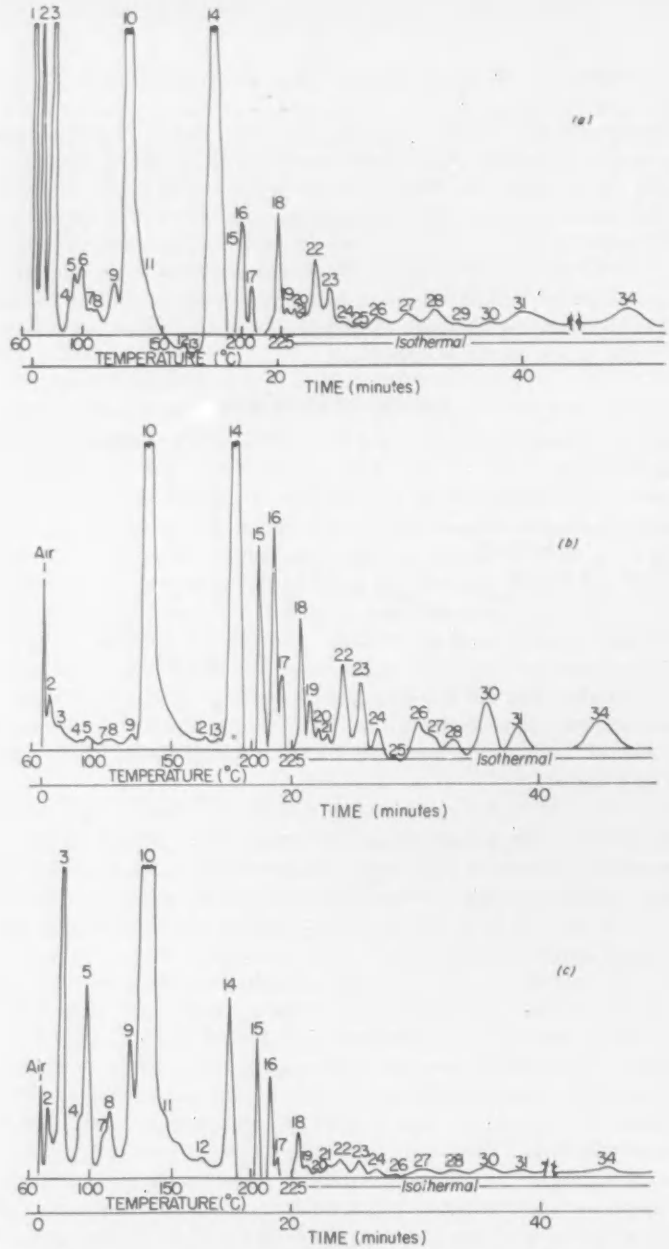

Fig. 1. Gas chromatograms of cellulose pyrolysis products on column 14 (Carbowax-20M): (*a*) products of hot wire pyrolysis in the carrier gas stream; (*b*) products condensed at 75°C. from pyrolysis of cellulose in nitrogen; (*c*) products condensed at −78°C. from pyrolysis of cellulose in nitrogen.

TABLE II
Identification of Cellulose Pyrolysis Products

Column 9 (Octoil-S)		Column 13 (Silicone oil-550)		Column 14 (Carbowax-20M)	
Peak no.	Compound	Peak no.	Compound	Peak no.	Compound
1	Fixed gases	1	Fixed gases	1	Fixed gases
2	Formaldehyde	2	Water/Formaldehyde	2	Formaldehyde
3	Acetaldehyde	3	Acetaldehyde	3	Acetaldehyde
4	Water	4	Propionaldehyde/ Acrolein/Acetone	4	Propionaldehyde
5	Propionaldehyde/ Acrolein/Acetone	6	Acetic acid	5	Acetone
6	Carbonyl containing	7	Methyl Ethyl Ketone/*n*-Butyraldehyde	6	Acrolein
7	Methyl Ethyl Ketone/*n*-Butyraldehyde	8	Glyoxal	7	*n*-Butyraldehyde/ Methanol
9	Glyoxal	10	Unidentified carbonyl compound	8	Methyl Ethyl Ketone
10	Formic acid	17	Furfural	10	Water
11	Acetic acid	31	5-Hydroxymethyl Furfural	14	Glyoxal
13	Carbonyl containing			15	Acetic acid
15	Furfural			16	Formic acid/ Furfural
23	Lactic acid			18	Carbonyl containing
				30	Lactic acid
				34	5-Hydroxymethyl Furfural

listic conditions for polymer degradation studies. Under ideal conditions a thin layer of polymer can be rapidly decomposed so that the effects of thermal gradients in the sample and of the diffusion of products are minimized. The carrier gas stream flowing past the sample removes the products from the hot reaction zone as they are formed thus reducing the opportunity for interactions between products. Further, no appreciable loss of products is possible and the analysis is not complicated by the presence of solvents frequently required to handle the condensed products obtained in conventional pyrolysis procedures.

The results of analysis with other columns are indicated by the chromatograms in Figures 2 and 3. Figure 2 is a typical chromatogram of hot wire pyrolysis products analyzed on the Silicone oil-550 column (column 13) with component identifications given in Table II. Cotton cellulose samples were pyrolyzed in air as well as in nitrogen with temperature programming to 370°C. and the decomposition products, condensed in two fractions as previously described, were analyzed on the Octoil-S column (column 9)

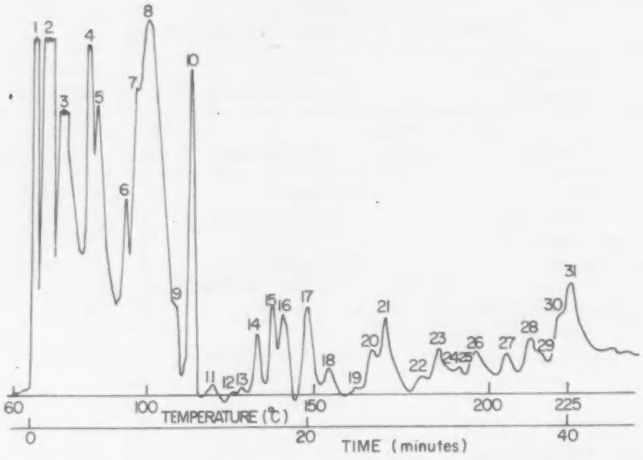

Fig. 2. Gas chromatogram of cellulose pyrolysis products on column (13 silicone oil-550) from hot wire pyrolysis in the carrier gas stream.

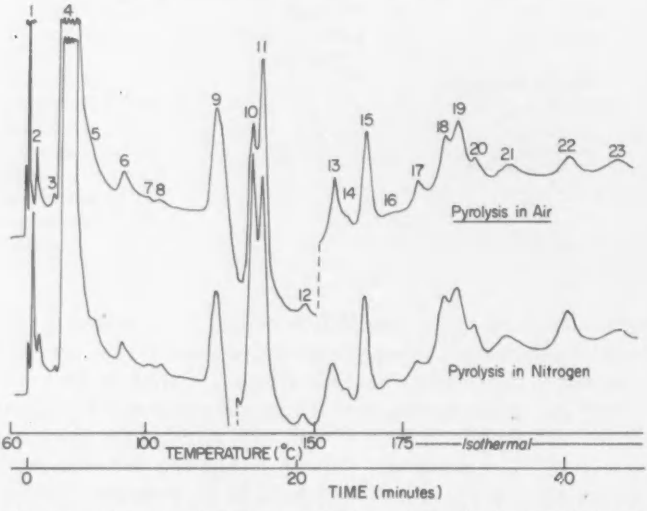

Fig. 3. Gas chromatograms of cellulose pyrolysis products of column 9 (Octoil-S) from pyrolysis in air and in nitrogen.

with temperature programming at 4°C./min. to 175°C. The chromatograms (Fig. 3) were found to be essentially identical with respect to the number, shape and occurrence of peaks. This result indicates that the same products are formed irrespective of whether the pyrolytic degradation of cellulose is carried out in an oxidizing or a nonoxidizing atmosphere. Consequently, the degradation mechanism must be nonoxidative in character. Peak identifications for these chromatograms are also given in Table II.

TABLE III

Comparison of Retention Volume (V_R) Data of Known Compounds and Unknown Components[a]

Compound	Column 9			Column 13			Column 14		
	Known V_R	Unknown V_R	Peak no.	Known V_R	Unknown V_R	Peak no.	Known V_R	Unknown V_R	Peak no.
CO, CO_2	12	12	1	6	6	1	12	12	1
Formaldehyde	48	48	2	21	24	2	42	42	2
Acetaldehyde	132	132	3	51	57	3	96	84	3
Propionaldehyde	294	282	5	120	114	4	192	174	4
Acetone	294	282	5	120	114	4	222	198	5
Acrolein	294	282	5	120	114	4	240	252	6
Methyl ethyl ketone	546	540	7	222	225	7	342	312	8
n-Butyraldehyde	546	540	7	222	225	7	306	286	7
Water	168	198	4	78	75	2	463	462	10
Glyoxal	856	840	9	282	261	8	912	858	14
Formic acid	990	1008	10	—	—	—	1056	1050	16
Acetic acid	1032	1062	11	204	207	6	978	978	15
Lactic acid	2652	2628	23	—	—	—	—	—	—
Furfural	1512	1512	15	597	609	17	1056	1050	16
5-Hydroxymethyl furfural				1230	1194	31	3360	3360	34

[a] Corrected volumes in cc.

It has been indicated that the identification of the components of a heterofunctional mixture separated by gas chromatography by retention data from a single column is open to question.[15] Therefore, data have been obtained on three columns differing in liquid phase and in phase polarity. The retention volume data obtained on unknown components are compared in Table III with similar data on suspected, known compounds. According to Walsh and Merritt,[15] data on qualitative functional group analysis of gas chromatographic effluents when combined with retention volume data can provide positive identification of the components in a mixture. Accordingly, the effluent gases for certain of the unknown peaks were condensed as they came off the columns and the condensates analyzed for functional groups by qualitative reagents. Thus, for example, formaldehyde, acetaldehyde, and glyoxal were confirmed by their 2,4-dinitrophenyl hydrazine and dimedone derivatives.

Levoglucosan, a major volatile product from cellulose pyrolysis, was not found in any of the chromatograms obtained on the columns described earlier. The melting point of levoglucosan is 180°C.,[16] which indicates a boiling point well above the maximum operating temperature (225°C.) of any of the columns involved. Apparently levoglucosan was not eluted from the column due to relatively low volatility. However, preliminary results on a column containing 3 wt.-% of polyethylene glycol (Carbowax-20M) as the liquid phase instead of the usual 10% have indicated a product that has been tentatively identified as levoglucosan. Chromatograms on the pyrolysis products of cellulose and starch obtained on this column with temperature programming to 245°C. showed a large, well defined peak well

TABLE IV
Pyrolytic Degradation Products of Cellulose Indicated by Gas-Liquid Chromatography

Compound	Columns indicating[a]	Identification[b]
Volatile gases: CO, CO_2	9, 13, 14	P
Formaldehyde	9, 13, 14	P
Acetaldehyde	9, 13, 14	P
Acrolein	9, 13, 14	P
Propionaldehyde	9, 13, 14	P
n-Butyraldehyde	9, 13, 14	T
Glyoxal	9, 13, 14	P
Furfural	9, 13, 14	P
5-Hydroxymethyl furfural	13, 14	P
Acetone	9, 13, 14	P
Methyl ethyl ketone	9, 13, 14	P
Methanol	9, 14	T
Formic acid	9, 14	T
Acetic acid	9, 13, 14	P
Lactic acid	13, 14	T
Water	9, 13, 14	P
Levoglucosan	3% Carbowax-20M	T

[a] 9 = Octoil S, 13 = Silicone oil-550, 14 = Carbowax-20M.
[b] P = positive identification, T = tentative identification.

beyond the last peak normally observed. The effluent gases from this peak gave a negative test for carbonyl groups and gave a syrupy condensate from which a white crystalline solid was obtained. The crystalline product was readily soluble in water, relatively insoluble in acetone and had a melting point of 179°C. and further characterization is in progress. It is, of course, possible to etherify levoglucosan[17] to form a more volatile derivative that could be analyzed by gas-liquid chromatography at lower column temperatures.

In Table IV the results on component identification are summarized. There is some evidence to indicate that isobutyraldehyde, valeraldehyde, ethylene glycol, methyl propyl ketone, and glycolic acid may be among the products but more data are required to establish any of these as pyrolytic degradation products of cellulose.

Summary and Conclusions

The remarkable identity of the gas chromatograms of the volatile products arising from the pyrolytic decomposition of cellulose in different atmospheres and at different rates suggest a common degradation mechanism that is nonoxidative and essentially thermal in nature. This finding is entirely consonant with, and offers strong support to, the mechanism for the pyrolytic decomposition of cellulose as previously discussed in papers from these laboratories and elsewhere.[4,5,18,19] According to this mechanism, cellulose depolymerizes at elevated temperatures by scission of the 1,4 glycosidic linkages followed by intramolecular rearrangement of the monomer units to levoglucosan. Levoglucosan subsequently undergoes (*1*) fragmentation to form volatile, low molecular weight products and (*2*) polymerization and aromatization to form char.[5,17]

Gas chromatography indicates a greater number of products from the thermal decomposition of cellulose than has previously been reported. At least 37 different compounds, consisting largely of levoglucosan and water plus a variety of low molecular weight aldehydes, ketones, and organic acids, were found. Many of these products appear to be present only in trace amounts and have not yet been identified.

The application of the linear-programmed temperature technique for gas chromatography greatly facilitated the separation of the products, many of which would not have been found with the isothermal technique alone. Columns with 3–10% of a polar liquid phase, polyethylene glycol (Carbowax-20M), on a perfluorcarbon solid support appeared to be the most useful for the separation of cellulose decomposition products.

The authors gratefully acknowledge many valuable discussions with Professor Eugene Pacsu.

References

1. Saad, I. A., and F. R. Eirich, *Ann. N. Y. Acad. Sci.*, **82**, 782 (1959).
2. Venn, H. J. P., *J. Textile Inst.*, **15**, T414 (1924).
3. Coppick, S., in *Flameproofing Textile Fabrics*, R. W. Little, Ed., ACS Monograph 104, Reinhold, New York, 1947.

4. Madorsky, S. L., V. E. Hart, and S. Straus, *J. Res. Natl. Bur. Std.*, **56**, 343 (1956).
5. Schwenker, R. F., Jr. and E. Pascu, *Chem. Eng. Data*, **2**, 83 (1957).
6. Holmes, F. H., and C. J. G. Shaw, *J. Appl. Chem. (London)*, **11**, 210 (1961).
7. Martin, S. B., and Ramstad, R. W., *Anal. Chem.*, **33**, 982 (1961).
8. Berkowitz-Mattuck, J. B., and T. Noguchi, paper presented to Division of Cellulose, Wood and Fiber Chemistry, 140th Meeting, American Chemical Society, Chicago, Ill., September 1961.
9. Pictet, A., and J. Sarasin, *Helv. Chim. Acta*, **1**, 87 (1918).
10. Madorsky, S. L., V. E. Hart, and S. Straus, *J. Res. Natl. Bur. Std.*, **60**, 343 (1958).
11. Greenwood, C. T., J. H. Knox, and E. Milne, *Chem. Ind. (London)*, **1961**, 1878.
12. Lehrle, R. S., and J. C. Robb, *Nature*, **183**, 1671 (1959).
13. Strassburger, J., G. M. Brauer, M. Tryon, and A. F. Forziati, *Anal. Chem.*, **32**, 454 (1960).
14. Barlow, A., R. S. Lehrle, and J. C. Robb, *Polymer*, **2**, 27 (1961).
15. Walsh, J. T., and C. Merritt, *Anal. Chem.*, **32**, 1378 (1960).
16. Montgomery, E. M., N. K. Richtmeyer, and C. S. Hudson, *J. Am. Chem. Soc.*, **65**, 3 (1943).
17. Jones, H. G., and M. B. Perry, *Can. J. Chem.*, **40**, 1339 (1962).
18. Parks, W. G., R. M. Esteve, Jr., M. H. Gollis, R. Guercia, and A. Petrarca, paper presented to Division of Cellulose Chemistry, 127th Meeting, American Chemical Society, Cincinnati, Ohio, April 1955.
19. Ivanov, V. I., O. P. Golova, and A. N. Pakomov, *Izv. Akad. Nauk S.S.S.R., Otd. Khim. Nauk*, **1956**, 1266.

Synopsis

The pyrolytic decomposition of cellulose was examined by gas–liquid chromatography by use of the linear-programmed temperature technique. Purified cotton cellulose was pyrolyzed in oxidizing and nonoxidizing atmospheres and the degradation products analyzed on three different chromatographic columns. At least 37 different compounds were indicated as cellulose pyrolysis products and about half of these were identified by retention volume data and functional group analysis. Essentially the same products resulted irrespective of pyrolysis conditions, indicating the dominant mechanism of decomposition to be of a nonoxidative character.

Résumé

La décomposition pyrolytique de la cellulose a été étudiée par chromatographie "gaz-liquide" en utilisant la technique de programmation linéaire de la température. La cellulose de coton purifiée a été pyrolysée en atmosphère oxydante et non-oxydante et les produits de dégradation ont été analysés sur 3 colonnes chromatographiques différentes. 37 produits différents au moins ont été identifiés comme produits de pyrolyse de la cellulose et environ la moitié de ceux-ci ont été identifiés par des données de rétention de volume et par analyses de groupes fonctionnels. Indépendamment des conditions de pyrolyse, il en résulte essentiellement les mêmes produits. Ceci indique que le mécanisme principal de la décomposition est de nature non-oxydante.

Zusammenfassung

Die pyrolytische Zersetzung von Cellulose wurde mit Hilfe der Gas-Flüssig-Chromatographie mit linear-programmiertem Temperaturverlauf untersucht. Gereinigte Baumwollcellulose wurde in oxydierender und nicht-oxydierender Atmosphäre pyrolysiert und die Abbauprodukte an drei verschiedenen Chromatographiesäulen analysiert. Mindestens 37 verschiedene Verbindungen wurden als Pyrolyseprodukte der Cellulose festgestellt und etwa die Hälfte davon durch Retentionsvolumsangaben und Analyse auf funktionelle Gruppen identifiziert. Unabhängig von den Pyrolysebedingungen entstanden im wesentlichen die gleichen Produkte, was für einen nicht-oxydativen Charakter des beherrschenden Zersetzungsmechanismus spricht.

JOURNAL OF POLYMER SCIENCE: PART C NO. 2, PP. 341–355 (1963)

Sodium Dithiocarbonate as a By-Product in Xanthating Reactions. A Contribution to the Chemistry of Viscose

S. G. HOVENKAMP, *Central Research Institute, A. K. U. (Algemene Kunstzijde Unie N. V.) and affiliated Companies, Arnhem, Netherlands*

1. INTRODUCTION

The formation and decomposition of cellulose xanthate and the so-called ripening reaction of viscose have been the subject of many investigations. Much work has also been devoted to the reactions of model compounds (simple alcohols and polyalcohols) with NaOH and CS_2, and to the inevitable side reactions between carbon disulfide and alkali.

In explaining their results, many authors[1–10] mention as unstable intermediate compound a compound which has never been proved to exist, namely dithiocarbonate, written as $CS_2O^=$, CS_2OH^-, Na_2CS_2O, or $NaHCS_2O$.

The hypothetical dithiocarbonate is believed to be the first reaction product when carbon disulfide reacts with alkaline solutions. This in accordance with the observation that the rate-determining reaction is of first order with respect to both carbon disulfide and hydroxyl:[7b,8]

$$CS_2 + OH^- \rightarrow CS_2OH^- \rightleftharpoons CS_2O^= + H^+ \qquad (1)$$

Dithiocarbonate is supposed to disproportionate in one or more rapid steps into carbonate and sulfide, according to the gross equation:

$$CS_2O^= + 2OH^- \rightarrow CO_3^= + 2SH^- \qquad (2)$$

There are differing opinions as to the importance of the dithiocarbonate for the formation of xanthates. Grotjahn[2] is of the opinion that the formation of cellulose xanthate takes place exclusively via dithiocarbonate. Philipp, however, while assuming that dithiocarbonate is capable of forming xanthates, regards a direct reaction between carbon disulfide and alkali cellulose as the main reaction.[7d]

The decomposition of xanthates in alkaline solutions has been amply discussed in the literature. This reaction is of considerable technical importance, as it is the main reaction taking place in ripening viscose. Dithiocarbonate has more than once been supposed to be the first decomposition product. Philipp[7e] is of the opinion that the decomposition of ethyl xanthate in dilute alkaline solution should be formulated as

$$C_2H_5OCS_2^- + OH^- \rightarrow C_2H_5OH + CS_2O^= \qquad (3)$$

Previous attempts by Weeldenburg[9] and Philipp[7b] to prove the existence of measurable amounts of dithiocarbonate have not been successful. In all publications dithiocarbonate is supposed to be very unstable.

However, by virtue of its importance as a possible intermediate compound in the xanthating reaction as well as in ripening viscose, a closer consideration is fully justified.

Recently we succeeded in proving the existence of an unstable intermediate compound in the reaction between carbon disulfide and sodium hydroxide, which we believe to be the hypothetical dithiocarbonate. Although we are well aware of the fact that we have no definite proof that the compound in question actually is dithiocarbonate, we have based the interpretation of our experimental material on the hypothesis that we are right in our belief. For the sake of brevity we have indicated the intermediate compound in the following sections by DTC, which may alternatively be read as dithiocarbonate or as directly formed temporary compound.

DTC is characterized by an ultraviolet spectrum with a strong absorption peak at 272 mμ. Its high molar absorptivity, combined with an unexpected stability, especially in strong alkaline solutions, made it possible for us to investigate some of its properties. In all our experiments homogeneous solutions were used.

2. EXPERIMENTAL

Materials

Carbon disulfide, sodium hydroxide and alcohols were of p.a. grade. Sodium sulfide solutions were made from freshly recrystallized sodium sulfide. They were standardized in two independent ways: (a) by iodine consumption; (b) by precipitation with copper acetate and determination of the excess copper.

In all the experiments a small amount of KCN was present (1 g./l.) to reduce traces of polysulfides such as $S_x^=$ and $CS_4^=$.

Ultraviolet Measurements

Complete spectra between 400 and 230 mμ were taken with a recording instrument (Beckman DR) at temperatures varying between 20 and 30°C. The instrument is equipped for measuring three solutions simultaneously against the same blank.

Decomposition constants of DTC were determined with a Beckman DU spectrophotometer, provided with a thermostated cuvet housing (25°C.) and a thermostatted bath (25.0°C.).

Molar absorptivities of sodium sulfide and DTC were determined with a Unicam SP 500 spectrophotometer. Quartz cells with an optical path of 1 cm. and provided with a lid were used throughout.

Spectra of Stable Compounds

Sodium Sulfide. Sulfide was the main component in our systems. As an influence from the alkali content on the spectrum could be expected ($SH^- + OH^- \leftrightharpoons S^= + H_2O$), spectra were determined at different hydroxide concentrations of the solvent. The results for 0.1*N* NaOH and 5*N* NaOH are shown in Figure 1. The shift of the spectrum was found to be proportional to the hydroxide concentration and amounted to 0.6 mμ/mole NaOH/l., between 260 and 235 mμ, towards the blue side.

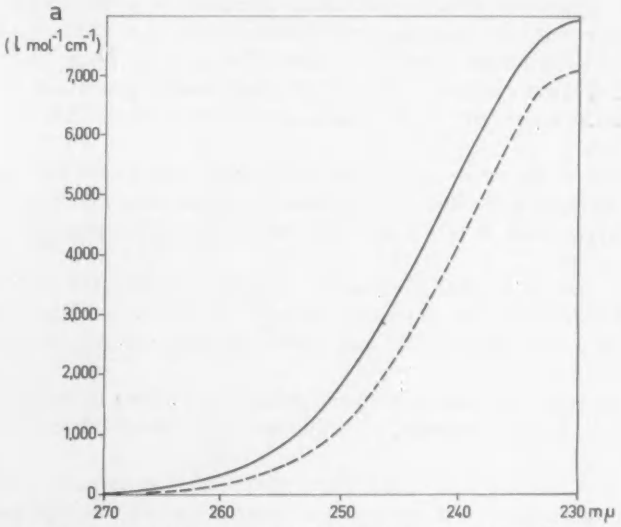

Fig. 1. Spectrum of Na_2S; (——) in 0.1*N* NaOH; (- - - -) in 5*N* NaOH.

Xanthate. Potassium ethyl xanthate solutions were prepared from carbon disulfide and alcoholic potassium hydroxide solutions. A rounded-off value of 17,500 l./mole cm. for the molar absorptivity at 301 mμ in alkaline solutions was taken from the work of Maurice and Mulder.[11]

Trithiocarbonate, $CS_3^=$. Sodium trithiocarbonate was prepared by shaking 0.2*N* NaOH with excess carbon disulfide. The molar absorptivity (17,000 l./mole cm.) at 336 mμ was taken from unpublished results of work conducted in our laboratories. The shape and the molar absorptivity were found to be identical with those published by Dux and Phifer.[12]

Tetrathiopercarbonate, $CS_4^=$. Sodium tetrathiopercarbonate was prepared from sodium trithiocarbonate by shaking with sulfur. Molar absorptivities were taken from unpublished data on work carried out in our laboratories.

Trithiopercarbonate, $CS_3O^=$. A dilute solution of trithiocarbonate was kept in contact with air for 5 days. A new compound was formed with absorption maxima at 308 and 378 mμ, while trithiocarbonate disappeared

completely. The new spectrum has been described for the first time by Ingram and Toms.[4] According to these authors, the spectrum is to be ascribed to trithiopercarbonate, $CS_3O^=$. The molar absorptivity is unknown.

3. DTC, FORMATION AND PROPERTIES

Ultraviolet Spectrum of DTC

When a small amount of carbon disulfide was added to a concentrated sodium hydroxide solution, the rapid formation of a compound (DTC) with an ultraviolet spectrum quite different from that of the compounds hitherto known was observed. Solutions containing about 10^{-4} mole/l. DTC in 5*N* sodium hydroxide were obtained by adding solutions of carbon disulfide in water (10^{-3} mole/l.) to a ninefold amount of 5.5*N* sodium hydroxide.

DTC is rather stable in 5*N* sodium hydroxide, and for the first hours the solutions obtained in this way are almost free from sulfide (sulfide is formed by decomposition of DTC) and trithiocarbonate. The spectrum is shown in Figure 2*A*.

Some spectra of other compounds which may be expected in the system NaOH–CS_2–alcohol are shown in Figure 2. It will be seen that DTC absorbs at a wave length (272 mμ) where the other compounds hardly interfere.

When larger amounts of carbon disulfide were added to the sodium hydroxide, a marked formation of trithiocarbonate was observed (absorbance at 336 mμ).

As DTC is so stable under these conditions that formation of sulfide hardly takes place, a direct reaction between carbon disulfide and DTC must be assumed, possibly according to the equation:[10]

$$CS_2 + CS_2O^= \rightarrow CS_3^= + COS \qquad (4)$$

(COS reacts rapidly further to give carbonate and sulfide). For this reason it is not possible to make DTC solutions of higher concentration in this way without incurring considerable amounts of trithiocarbonate as a contaminant.

Molar Absorptivity of DTC

When a freshly prepared solution of DTC in 5*N* sodium hydroxide is diluted 25-fold with water, its spectrum rapidly changes. After about half an hour no difference can be seen between the new spectrum and a spectrum of sodium sulfide at the same alkali concentration.

The change of the spectrum of a freshly prepared DTC-solution was followed after dilution with water. The spectra thus obtained were compared with spectra of solutions with known amounts of sodium sulfide (and the same alkali concentration), and with the spectrum of the same DTC-solution diluted with 5*N* sodium hydroxide.

On the assumption that DTC quantitatively decomposes into sulfide, the molar absorptivity of DTC at 272 mμ could be calculated. We found a value of 10,500 l./mole cm. in 0.2*N* sodium hydroxide. In 5*N* NaOH the value is about 7% lower, viz., 9,800 l./mole cm. At 250 mμ the molar

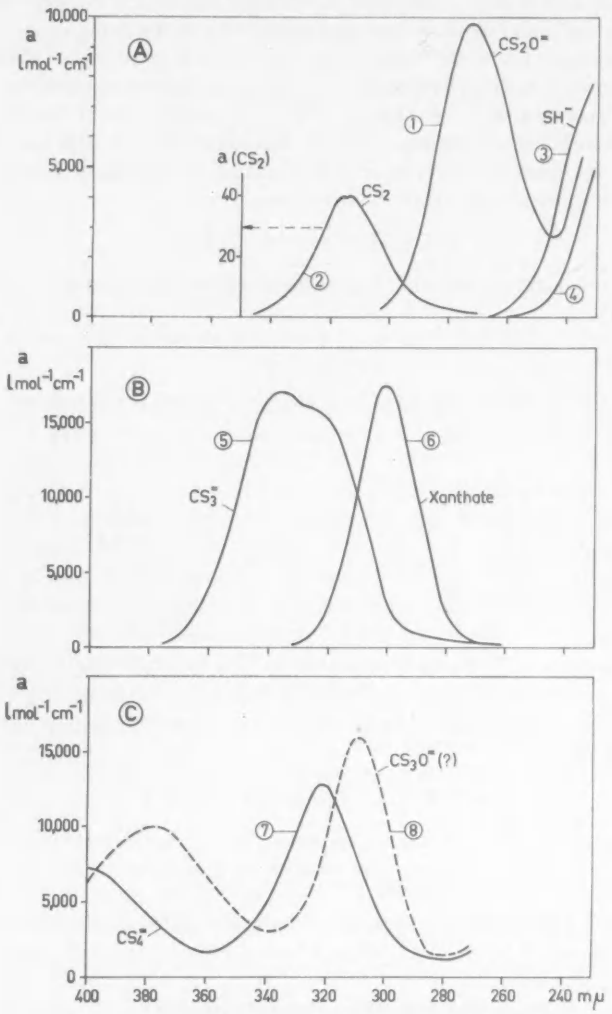

Fig. 2. Spectra of sulfur-containing compounds in the system CS_2–NaOH–alcohol: (*1*) DTC in 5*N* NaOH; (*2*) Carbon disulfide (molar absorbance to be read from a special scale); (*3*) Na_2S in 0.1*N* NaOH; (*4*) Bender's salt (C_2H_5OCOSK) (data from Treiber[13]); (*5*) trithiocarbonate ($CS_3^=$); (*6*) K ethyl-xanthate; (*7*) tetrathiopercarbonate ($CS_4^=$); (*8*) trithiopercarbonate ($CS_3O^=$) (?) (no molar absorptivity known, relative values are given).

absorptivity was found to be 3,250 l./mole cm. at both alkali concentrations.

Stability of DTC

DTC is not stable. Solutions containing about 1.5×10^{-4} mole/l. and different amounts of sodium hydroxide were made from a freshly prepared solution (1.5×10^{-3} mole/l. in 5.5*N* NaOH) by dilution with ninefold amounts of sodium hydroxide solutions of various concentrations.

The decomposition velocity at 25°C. was derived from the decrease of the absorbance at 272 mμ. Within the range studied (0.6–5.6 mole/l. NaOH), the decomposition at each fixed alkali concentration could be described as a pseudo-monomolecular reaction:

$$d[\mathrm{DTC}]/dt = -k'\,[\mathrm{DTC}]$$

The decomposition constant k' depends strongly on the alkali concentration (Table I).

TABLE I
Decomposition Constant of DTC at Different Alkali Concentrations

[NaOH], mole/l.	k', hr.$^{-1}$ (25°C.)
0.6	2.0
1.3	0.6
2.3	0.2
2.9	0.09
3.9	0.04
5.6	0.02

The results from Table I are plotted in a log–log diagram (Fig. 3). The slope of the regression line through the points is about −2. Consequently the decomposition may roughly be described (within the range studied) by

$$d[\mathrm{DTC}]/dt = -k[\mathrm{DTC}]/[\mathrm{OH}^-]^2$$

As the amount of free dithiocarbonic acid is proportional to $[\mathrm{DTC}]/[\mathrm{OH}^-]^2$,

$$[\mathrm{H_2CS_2O}] \sim [\mathrm{CS_2O^=}]/[\mathrm{OH}^-]^2$$

it may be concluded that decomposition takes place via the unstable free acid.

Decomposition Products from DTC

As DTC decomposes in alkaline medium via free dithiocarbonic acid, two possible paths of decomposition are conceivable:

$$\mathrm{H_2CS_2O} \rightarrow \mathrm{H_2O} + \mathrm{CS_2} \qquad (5a)$$

$$\mathrm{H_2CS_2O} \rightarrow \mathrm{H_2S} + \mathrm{COS} \qquad (5b)$$

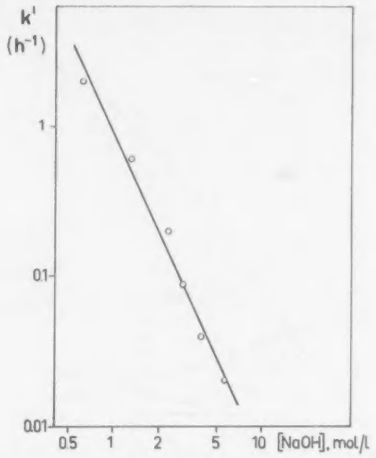

Fig. 3. Apparent monomolecular decomposition constant k' of DTC at different concentrations of NaOH.

Carbonyl sulfide is unstable; in alkaline medium it reacts rapidly to form SH^- and $CO_3^=$. Carbon disulfide formation [reaction (5a)] was proved to be negligible in the following way.

A 10-ml. portion of a freshly prepared DTC solution (~0.002 mole/l.) in sodium hydroxide (6 mole/l.) was diluted with 80 ml. water and 10 ml ethyl alcohol. After 5 hr. the spectrum showed sulfide (350 μmole/l., calculated from the absorbance at 250 mμ), but not even a trace of xanthate. DTC had vanished completely. The absence of xanthate formation proves the absence of carbon disulfide during the decomposition.

In a simultaneous experiment the addition of alcohol was postponed until DTC had decomposed. The spectrum again showed only sulfide, but this time in a concentration of 420 μmole/l. The differences in sulfide concentrations may perhaps be explained from reaction (5b), followed by a reaction of part of the carbonyl sulfide with alcoholate, giving Bender's salt:

$$COS + C_2H_5OH + OH^- \rightarrow C_2H_5OCOS^- + H_2O \qquad (6)$$

This compound has no absorption peak between 400 and 250 mμ, and its absorbance at 250 mμ is small as compared with the absorbance of an equivalent amount of sulfide (cf. Fig. 2*A*). We have no definite proof, however, that carbonyl sulfide is indeed an intermediate compound in the decomposition reactions of DTC.

DTC as an Intermediate Compound in the Reaction between Carbon Disulfide and Sodium Hydroxide

The composition of homogeneous reacting mixtures of carbon disulfide and sodium hydroxide as a function of the reaction period was studied at two hydroxide concentrations, viz., 0.167*N* and 0.67*N*.

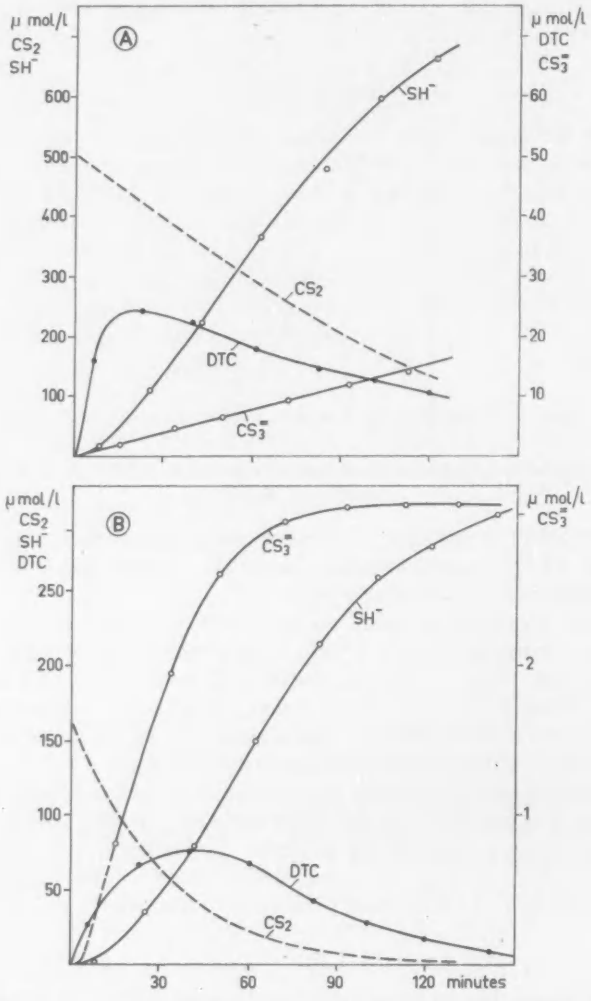

Fig. 4. Reaction of CS_2 with NaOH: (*A*) [NaOH] 0.167 mole/l., [CS_2] 500 μmole/l. (initial); (*B*) [NaOH] 0.67 mole/l., [CS_2] 165 μmole/l. (initial).

Solutions of carbon disulfide in water were mixed with sodium hydroxide solutions. The mixtures were immediately transferred to quartz cuvets which were completely filled and provided with a lid. Complete spectra (400–240 mμ) were taken about every 20 min. The reaction took place in the cuvet housing which was not thermostatted, so that probably there was some warming up. However, as the reactions in the two experiments proceeded simultaneously, the results are comparable.

TABLE II
Molar Absorptivities of Some Components

	Molar absorptivity, l./mole cm.			
	336 mμ	301 mμ	272 mμ	250 mμ
DTC	[a]	600	10,500	3,250
Trithiocarbonate	17,000	3,600	[a]	[a]
Xanthate	[a]	17,500	[a]	[a]
Sulfide (0.17 mole/l. NaOH)	[a]	[a]	22	1,780
Sulfide (0.67 mole/l. NaOH)	[a]	[a]	20	1,710
Sulfide (0.77 mole/l. NaOH)	[a]	[a]	19	1,690

[a] Absorptivity is negligible in our systems.

The absorbance at 336 mμ was used to calculate the trithiocarbonate concentration. The absorbances at 272 and 250 mμ were used to determine DTC and sulfide. Use was made of the molar absorptivities given in Table II. The concentration of carbon disulfide was calculated by means of a sulfur balance.

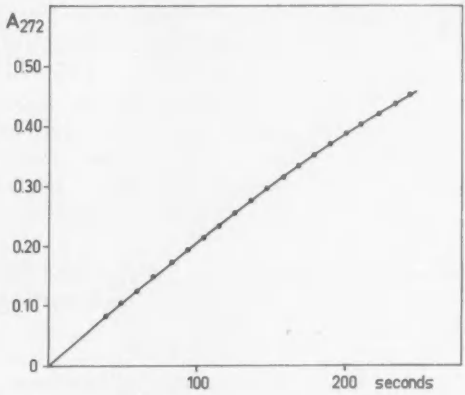

Fig. 5. Formation of DTC (absorbance at 272 mμ); [NaOH] 0.18 mole/l.

The results are shown in Figures 4*A* and 4*B*. The intermediate character of DTC is clearly demonstrated. A marked induction period for the formation of sulfide and trithiocarbonate indicates that these compounds are formed by secondary reactions.

A separate experiment was run in which the formation of DTC was studied by measuring the absorbance at 272 mμ only, at shorter time intervals. The result is shown in Figure 5. There is no indication of an induction period (Hence the name directly formed temporary compound).

The results are in agreement with eqs. (7–11).

$$CS_2 + OH^- \rightarrow CS_2OH^- \leftrightharpoons CS_2O^- + H^+ \qquad (7)$$

$$CS_2O^{=} + 2H^{+} \leftrightharpoons H_2CS_2O \rightarrow COS + H_2S \quad (8)$$

$$COS + 3OH^{-} \xrightarrow{\text{Rapid}} SH^{-} + CO_3^{=} + H_2O \quad (9)$$

$$CS_2 + SH^{-} \rightarrow HCS_3^{-} \leftrightharpoons CS_3^{=} + H^{+} \quad (10)$$

$$CS_2 + CS_2O^{=} \xrightarrow{\text{Rapid}} CS_3^{=} + COS \quad (11)$$

It may safely be assumed that in alkaline medium DTC is present in the form of $CS_2O^{=}$, not as HCS_2O^{-}. Its spectrum is almost independent of the alkali content of the solution. Moreover, both carbonate and trithiocarbonate are present in the double ionized form at the same alkali concentrations, so that the same may be assumed to hold for dithiocarbonate.

The reaction of COS with alkali has been studied by Philipp.[7b] As it reacts at least 100 times faster than carbon disulfide, its concentration may be neglected in our experiments. Monothiocarbonate might be expected in the reaction between COS and alkali, as an intermediate compound. Probably it is far less stable than DTC; in an orienting experiment it was found that carbonyl sulfide reacted quantitatively with 0.7*N* sodium hydroxide within 5 min., to sulfide. No DTC was formed in the meantime.

Treiber[13] has reported the spectrum of a reaction product from COS and alkali cellulose. This spectrum is remarkably consistent with our spectrum of DTC, obtained from only CS_2 and NaOH. In view of the above it seems probably that Treiber's carbonyl sulfide was contaminated with some carbon disulfide and that actually the spectrum was that of DTC.

Philipp[7a] has demonstrated that from reaction mixtures of carbon disulfide and alkali, carbonyl sulfide is liberated in small amounts after acidifying. He ascribes the carbonyl sulfide to small amounts of monothiocarbonate.

In view of the reactions stated above it is highly improbable that monothiocarbonate would give carbonyl sulfide. Dithiocarbonate will, however, probably give some carbonyl sulfide.

Formation and Decomposition of Xanthates

The formation of the xanthates of ethanol, 2-propanol, and 1,2,3-propanetriol (glycerol) was followed to clarify the role of DTC. Solutions of carbon disulfide were added to solutions of sodium hydroxide containing small amounts of alcohol. Spectra were taken about every 15 min. (400–250 mμ).

The amounts of xanthate, DTC, trithiocarbonate, and sulfide were calculated with the help of Table II from the absorbances at 301, 272, 336, and 250 mμ. Corrections were applied for simultaneous absorbances.

The results from these experiments are shown in Figures 6 and 7. Along with the experiments with 2-propanol and with glycerol, which were made simultaneously, a third experiment was carried out without alcohol addition. The results from the latter are not given, because, except for the

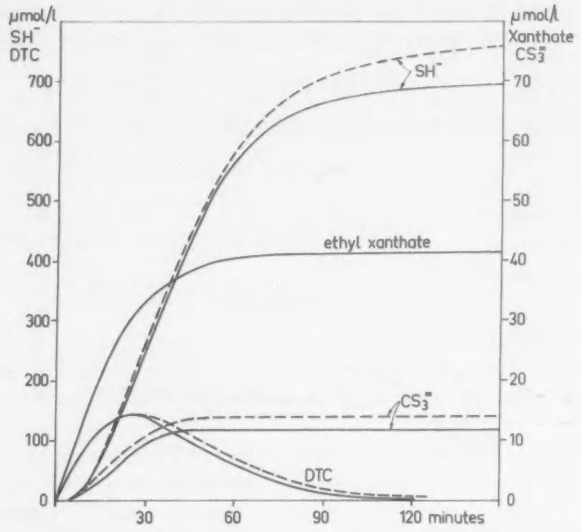

Fig. 6. Reaction of CS_2 with NaOH and ethanol at [NaOH] 0.67 mole/l., [CS_2] 400 µmole/l. (initial): (- - - -) no ethanol; (——) ethanol 0.034 mole/l.

formation of xanthate, they were nearly identical with the results of the test with 2-propanol.

It may be seen that the formation of xanthate is independent of the concentration of DTC. In all the experiments the xanthate formation has come to an end long before DTC has vanished from the solutions. (The same conclusion might have been drawn from the observation, stated earlier, that no xanthate is formed when DTC decomposes in the presence of ethanol.) Hence the conclusion may be drawn that DTC has no xanthating properties, at least not in the presence of these three alcohols. This makes it all the more probable that the xanthate formation is a direct reaction between carbon disulfide and alcoholates.

Glycerol xanthate proves to be very unstable. As an increased rate of sulfide formation is observed, while the maximum DTC concentration is appreciably lower when glycerol is present, the decomposition of glycerol xanthate is not attended with a splitting off of carbon disulfide or DTC. Probably a decomposition via glycerol monothiocarbonate, as suggested by Philipp,[7e] takes place:

$$ROCS_2^- + OH^- \rightarrow ROCOS^- + SH^- \qquad (12)$$

followed by a decomposition of the glycerol monothiocarbonate. It is clear that the well-known impossibility of preparing xanthates of polyalcohols with vicinal–OH groups has to be ascribed to instability of the xanthates rather than to a very slow formation of the xanthates. Matthes[14] has come to the same conclusion. From our data it may be calcu-

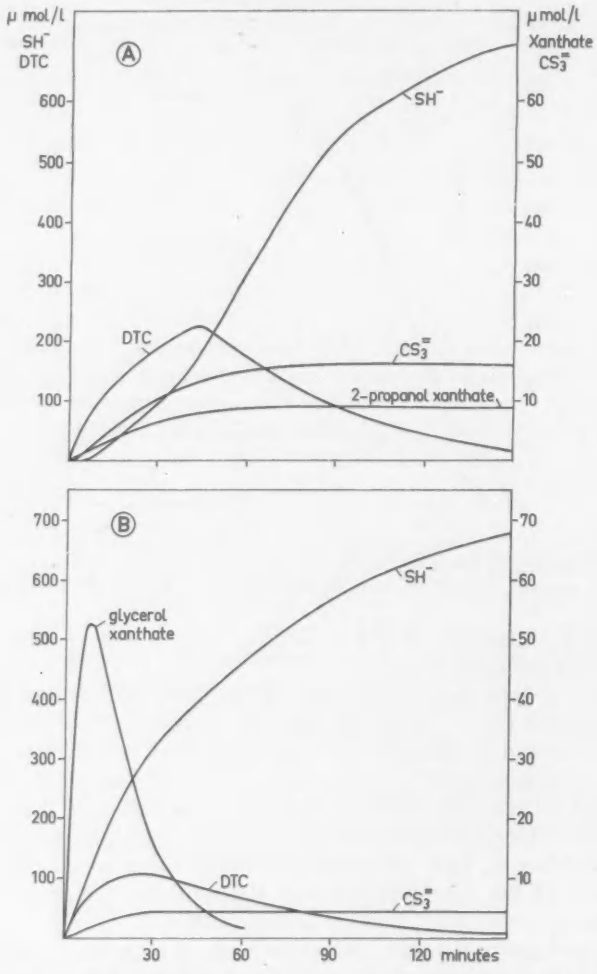

Fig. 7. Reaction of CS_2 with NaOH and (*A*) 2-propanol, 0.13 mole/l., and (*B*) 1,2,3-propanetriol (glycerol), 0.04 mole/l.; [NaOH] 0.77 mole/l., [CS_2] 400 μmole/l. (initial).

lated that ethanol is xanthated about 20 times as fast as isopropyl alcohol. Glycerol shows a still faster rate of xanthation.

As to the decomposition of ethyl xanthate, in our opinion a reaction in which carbon disulfide is liberated has to be considered to be the main reaction:

$$C_2H_5OCS_2^- + H^+ \rightarrow C_2H_5OH + CS_2 \qquad (13)$$

This reaction can explain satisfactorily the observations of Vermaas[8]

and Philipp[7c] that ethyl xanthate in alkaline solutions may be stabilized by ethanol addition, by taking into account the reverse reaction:

$$C_2H_5O^- + CS_2 \rightarrow C_2H_5OCS_2^- \qquad (14)$$

The stabilization is explained by Philipp[7c] by assuming the equilibrium:

$$C_2H_5OCS_2^- + OH^- \leftrightharpoons C_2H_5OH + CS_2O^- \qquad (15)$$

The reverse reaction does not occur, however, as shown by our experiments. Hence this mechanism has to be rejected.

4. DTC AND THE VISCOSE PROCESS

A few words may now be devoted to the significance of DTC for the viscose process. These considerations bear a rather speculative character, because we did not perform measurements on viscose or other cellulose-containing systems.

The concentration of DTC in yellow crumbs (xanthated alkali cellulose) will be low and limited by the reaction between DTC and CS_2 which results in the formation of trithiocarbonate.

In viscose, carbon disulfide will be formed by the decomposition of the xanthate. Part of the carbon disulfide forms xanthate again; the other part will be the source of continuous formation of DTC in viscose. As the decomposition constant of the "parent" (cellulose xanthate) is small as compared with the decomposition constant of the "daughter" (DTC), enrichment of the latter cannot take place. Its concentration will be very low.

However, the continuous formation and decomposition of DTC will probably be accompanied with the continuous formation of carbonyl sulfide, and hence by the formation of "pseudo-xanthates" of the type ROCOS$^-$. The same holds for the xanthating period. The occurrence of "pseudo-xanthates" in yellow crumbs and fresh viscose has been established by Philipp.[7a] Whether enrichment of this type of compounds can occur during the viscose ripening process depends on the relative values of the decomposition constants of the real and the "pseudo" xanthates.

These values are not constant during the ripening process (in consequence of the three different alcoholic groups in cellulose), and no prediction can be made at the moment.

The author wishes to thank Dr. D. Vermaas for the lively interest he took in this work and for many valuable suggestions.

References

1. Geiger, E., *Helv. Chim. Acta*, **13**, 281 (1930).
2. Grotjahn, H., *Z. Elektrochem.*, **57**, 305 (1953).
3. Herrent, P., and G. Jnoff, *J. Polymer Sci.*, **3**, 487, 834 (1948); *ibid.*, **5**, 727 (1950).
4. Ingram, G., and B. A. Toms, *J. Chem. Soc.*, **1957**, 4328.
5. Kagawa, I., and H. Kobayashi, *J. Polymer Sci.*, **7**, 421 (1951).
6. Klauditz, W., *Papier-Fabr.*, **37**, 251 (1939).

7. (a) Philipp, B., *Faserforsch. Textiltech.*, **6**, 13 (1955); (b) *ibid.*, **6**, 433 (1955); (c) *ibid.*, **6**, 509 (1955); (d) *ibid.*, **8**, 45 (1957); (e) B. Philipp and C. Fichte, *ibid.*, **11**, 118 (1960); (f) *ibid.*, **11**, 172 (1960); (g) B. Philipp and H. Dautzenberg, *ibid.*, **11**, 374 (1960).

8. Vermaas, D., *Chem. Weekblad*, **54**, 33 (1958).

9. Weeldenburg, J. G., Dissertation, Delft, 1927; *Rec. Trav. Chim.*, **47**, 496 (1928).

10. Wronsky, M., *Faserforsch. Textiltech.*, **8**, 32 (1957).

11. Maurice, M. J., and J. L. Mulder, *Mikrochim. Acta*, **5**, 661 (1957).

12. Dux, J. P., and L. H. Phifer, *Anal. Chem.*, **29**, 1842 (1957).

13. Treiber, E., G. Porod, and W. Lang, *Österr. Chemiker-Z.*, **53**, 162 (1952); E. Treiber, *Kolloid-Z.*, **130**, 57 (1953).

14. Matthes, A., *Faserforsch. Textiltech.*, **3**, 127 (1952).

Synopsis

Dithiocarbonate, $CS_2O^=$, is often mentioned as a hypothetical intermediate compound in reactions concerning the formation and decomposition of xanthates, as well as in the reaction between carbon disulfide and alkali. In this work an intermediate compound in the reaction between carbon disulfide and sodium hydroxide has been proved to exist. It is believed that this compound (DTC) is identical with dithiocarbonate. The following properties of DTC have been determined by ultraviolet measurements on homogeneous solutions or reacting mixtures. The ultraviolet spectrum shows an absorption peak at 272 mμ. The molar absorptivity a_{272} is 10,500 l./mole cm. (measured in dilute alkali). DTC is unstable. In about 0.6*N* NaOH its average life is about 0.5 hr., whereas in 5.6*N* NaOH it is about 50 hr. The stability is about proportional to the square of the alkali content. Decomposition of DTC in alkaline medium yields sulfide, probably via a reaction route which includes formation of carbonyl sulfide. No carbon disulfide is formed during the decomposition. When traces of carbon disulfide react with sodium hydroxide, DTC is formed without an induction period. Sulfide and trithiocarbonate formation show induction periods. DTC is incapable of reacting with ethanol, 2-propanol, or glycerol in alkali to give xanthates. DTC reacts probably at a fast rate with carbon disulfide, yielding trithiocarbonate and perhaps carbonyl sulfide. The investigations have yielded the following additional information. In homogeneous solutions containing about 0.8 mole/l. sodium hydroxide and small amounts of alcohols, ethanol is xanthated by carbon disulfide about 20 times as fast as 2-propanol. The formation of glycerol xanthate occurs at a still higher rate; the xanthate is very unstable, however (lifetime less than 10 min. at room temperature). In all probability the relatively stable ethyl xanthate decomposes via formation of carbondisulfide, not via splitting off of DTC. The xanthate of glycerol decomposes via a different mechanism, but not via formation of DTC. The ultraviolet spectrum of sodium sulfide was determined at various alkali contents of the solvent.

Résumé

On mentionne souvent le dithiocarbonate $CS_2O^=$ comme un intermédiaire hypothétique dans les réactions concernant la formation et la décomposition de xanthate, et dans la réaction entre le disulfure de carbone et une base. Dans ce travail on a mis en évidence un intermédiaire dans la réaction entre le CS_2 et l'hydroxyde de sodium. On croit que cette substance (DTC) est identique au dithiocarbonate. On a déterminé les propriétés suivantes du DTC par des mesures U.V. de solutions homogènes en des mélanges réactionnels: (a) dans le spectre U.V. il y a une bande d'absorption à 272 mμ. L'absorption molaire a_{272} est de 10.500 l mol^{-1} cm^{-1} (mesurée dans une solution diluée d'hydroxyde). (b) DTC n'est pas stable. La durée de vie est environ de 0.5 heure dans une solution de 0.6 *N* NaOH, et de 50 heures dans 5.6 *N* NaOH. La stabilité est environ proportionnelle au carré de la quantité de base. (c) La décomposition du DTC en milieu alcalin produit du sulfure, probablement à la suite d'une réaction qui suppose la formation de sulfure de

carbonyle. Il ne se forme pas de CS_2 durant la décomposition. (d) quand on fait réagir du CS_2 avec NaOH, le DTC se forme sans période d'induction, tandis que la formation de sulfure et de trithiocarbonate montre des périodes d'induction. (e) le DTC ne réagit pas avec l'éthanol, le 2-propanol ou la glycérine en solution alcaline pour donner des xanthates. (f) DTC réagit probablement très vite avec CS_2 formant le trithiocarbonate et peut être le sulfure de carbonyle. Les expériences ont fourni en plus l'information suivante: Dans des solutions contenant environ 0.8 mole/l de NaOH et des traces d'alcool, l'éthanol et CS_2 donnent des xanthates environ 20 fois plus vite que le 2-propanol. Le xanthate de glycérine se forme encore plus rapidement, il est cependant très instable (durée de vie moins de 10 minutes à la température ambiante). Très probablement le xanthate d'éthyle qui est relativement stable, se décompose, par la formation du CS_2, et non pas par perte de DTC. Le xanthate de glycérine se décompose selon un mécanisme différent, mais pas via la formation de DTC. On a déterminé le spectre U.V. du sulfure de sodium à des concentrations différentes d'alcali du solvant.

Zusammenfassung

Dithiokarbonat, CS_2O^{2-}, wird oft als hypothetisches Zwischenprodukt bei Bildungs- und Zersetzungsreaktionen von Xanthogenaten und bei der Reaktion zwischen Schwefelkohlenstoff und Alkali angenommen. In der vorliegenden Arbeit wird ein Zwischenprodukt bei der Reaktion zwischen Schwefelkohlenstoff und Natriumhydroxyd nachgewiesen. Es wird angenommen, dass diese Verbindung (DTC) mit Dithiokarbonat identisch ist. Folgende Eigenschaften von DTC wurden durch UV-Messungen an homogenen Lösungen oder Reaktionsmischungen bestimmt: (a) Das UV-Spektrum zeigt ein Absorptionsmaximum bei 272 mμ. Der molare Extinktionskoeffizient a_{272} ist 10500 l mol^{-1} cm^{-1} (in verdünntem Alkali gemessen). (b) DTC ist instabil. In etwa 0,6*N* NaOH beträgt seine mittlere Lebensdauer etwa 0,5 Stunden, dagegen in 5,6*N* NaOH etwa 50 Stunden. Die Stabilität ist etwa dem Quadrat des Alkaligehaltes proportional. (c) Zersetzung von DTC in alkalischem Medium liefert Sulfid, wahrscheinlich über einen Reaktionsweg mit Bildung von Karbonylsulfid. Während der Zersetzung bildet sich kein Schwefelkohlenstoff. (d) Bei der Reaktion von Spuren von Schwefelkohlenstoff mit Natriumhydroxyd entsteht DTC ohne Induktionsperiode. Die Sulfidund Trithiokarbonatbildung zeigt eine Induktionsperiode. (e) DTC ist unfähig durch Reaktion mit Äthanol, 2-Propanol oder Glycerin in Alkali Xanthogenate zu liefern. (f) DTC reagiert wahrscheinlich mit grosser Geschwindigkeit mit Schwefelkohlenstoff unter Bildung von Trithiokarbonat und vielleicht auch Karbonylsulfid. Folgende zusätzliche Ergebnisse wurden erhalten: In homogener Lösung mit 0,8 mol/l Natriumhydroxyd und kleinen Alkoholmengen wird Äthanol durch Schwefelkohlenstoff etwa 20 mal so rasch xanthogeniert als 2-Propanol. Die Bildung des Glycerinxanthogenats verläuft mit noch höherer Geschwindigkeit; das Xanthogenat ist jedoch sehr instabil (Lebensdauer bei Raumtemperatur kleiner als 10 Minuten). Das verhältnismässig stabile Äthylxanthogenat zersetzt sich mit aller Wahrscheinlichkeit unter Schwefelkohlenstoffbildung und nicht unter Abspaltung von DTC. Das Glycerinxanthogenat zersetzt sich nach einem anderen Mechanismus, aber nicht unter DTC-Bildung. Das UV-Spektrum von Natriumsulfid wurde bei verschiedenem Alkaligehalt des Lösungsmittels bestimmt.

JOURNAL OF POLYMER SCIENCE: PART C NO. 2, PP. 357–376 (1963)

New Contributions to the State of Solution of Viscose. Gel Particle Counting and Optical Rotatory Dispersion Studies on Viscose*

ERICH TREIBER and HENRYK C. NADZIAKIEWICZ,† *The Central Laboratory of the Swedish Cellulose Industry, Stockholm, Sweden*

INTRODUCTION

While we have a relatively reliable model for the state of solution of macromolecules in a good solvent and at very low concentrations, there is some controversy about the state of solution of polymers at relatively high concentration.[1,2] We have many indications that solution state influences both the spinning process and the quality of final products.[3] Therefore it is easily understood that the question of solution state of such solutions has a technical interest. The different opinions about this are in general based on indirect conclusions going back to various observations, and they lie—if we restrict ourselves to viscose—between two extreme suppositions. According to one, cellulose substance is mainly in the form of large aggregates, as micelles, micelle aggregates with a pronounced biostructure, etc.; according to the other, one can in the main part regard cellulose as a quasimolecular dispersion. Hence with a dilution of, for instance, 8% cellulose xanthate solution, a continuous change resulting in a practically molecularly dispersed solution occurs, while the micellar solution should to an appreciable extent keep the more persistent crystallites. Such questions involve the main part of the cellulose substance. A very small part of the cellulose substance is coarsely dispersed, which means it is in the form of particles of microscopic dimensions.

THE PARTICLE SPECTRUM

Our working hypothesis to describe the viscose solution state has been to look at the solution as a continuum of particles of all possible dimensions, or in other words to describe the solution with the help of a continuous particle spectrum,[2,4] going from the unreacted wood fiber down to the isolated cellulose molecule (Fig. 1). Furthermore we have assumed that the cellulose substance distributes itself in this spectrum according to a

* After a paper presented at the meeting 11, Nordiska Kemistmötet, Åbo, Finland, August 20–28, 1962.

† Present address: Research Institute of Artificial and Synthetic Fibers, Lódź, Poland.

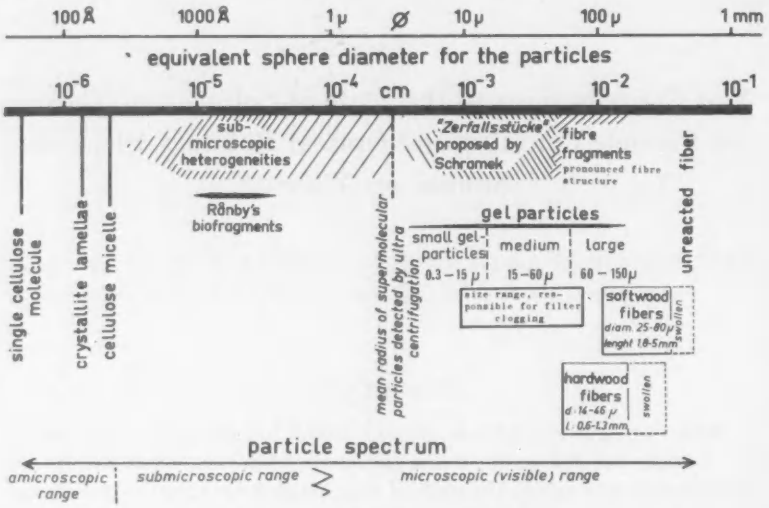

Fig. 1. Particle spectrum.

Gaussian distribution with a maximum in the molecular region. Up till now observations made show that points in certain available spectral regions satisfy the supposed distribution curve (Fig. 2).

It should be pointed out that all observations indicate that the spectrum is continuous, and it seems therefore reasonable that no pronounced maxima-minima in the distribution curve are anticipated.

Recently, Durso, Sperling, and Parks[7] have shown by a special particle fractionation procedure that there exists—in their own terminology—"small gels" of an order of magnitude of about 0.3 μ. The number of these particles, related to the number of particles in the expected size distribution curve, is higher by approximately a factory of 100, indicating a peak in the size-distribution curve describing the whole particle spectrum, would exist. But one might ask whether this result is not caused by the sedimentation distribution, which means that all particles larger than a given size, depending on the experimental conditions, are separated quantitatively. However the separation of smaller particles occurs to a lesser extent the smaller they are. In this case, we would find a much smaller number of particles $\ll 0.3\ \mu$ in spite of the fact that the real number might be very high. A loss of these particles can cause a peak in the curve. The above interesting result and the interpretation given by the authors must, of course, be carefully studied, but besides this we have no indication to suppose that pronounced maxima or minima occurs in the distribution spectrum.

In spite of this it is practical to split up the region into two or more particle size regions; the division is not, of course, a sharp one and must be to a

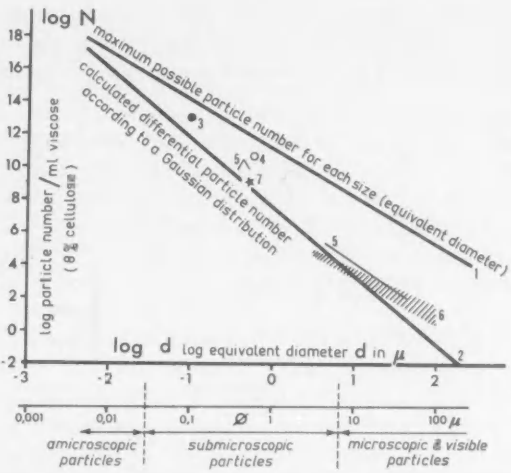
log N
maximum possible particle number for each size (equivalent diameter)
calculated differential particle number according to a Gaussian distribution
log particle number / ml viscose (8 % cellulose)
log d Log equivalent diameter d in μ
amicroscopic particles
submicroscopic particles
microscopic & visible particles

Fig. 2. Calculated particle numbers vs. equivalent sphere diameter (log-log plot) and observed values resulting from different measurements and authors: (*1*) calculated maximum possible particle number for each size; (*2*) calculated differential particle number according to a Gaussian distribution; (*3*) observed by Sperling[7] and Rånby;[1] (*4*) observed by Manley;[5] (*5*) observed by Durso;[7] (*6*) results for a large number of laboratory prepared viscoses, obtained by Kolos;[6] (*7*) observed by Gray.[3]

certain extent subjective. The first part should demarcate and specially treat the region for microscopically visible particles. Within that region we have the so-called gel particles, which represent the low substituted, highly swollen cellulose particles which more or less are without a pronounced fiber structure. Such particles with an equivalent diameter of about 10–80 μ are especially responsible for filter clogging. All undissolved particles down to a certain diameter—its value is lower the finer the holes in the spinneret and the higher tenacity aimed at in the thread—which remain in the filtered spin solution disturb the spinning process and influence the thread's textile mechanical quality.[3]

GEL PARTICLE COUNTING

During the past 20 years many automatic counting apparatuses have been developed for the determination of both number and size of undissolved microscopic particles in viscose, the so-called gel particle counters.[6,8,9] During the last years a method has without a doubt been firmly established, namely particle counting by the conductometric method (Fig. 3).

Examinations by F. Kolos in our laboratory resulted in the development of a suitable technique, assuming faultless particle counting, which also led to an absolute calibration.[9,10] Our work has furthermore contributed to further developments of the apparatus itself.

The new particle counter (Celloscope 202) counts particles in a viscose solution at two independent and optional size levels at the same time, in two counting channels, with a threshold sensitivity of approximately 4 μ

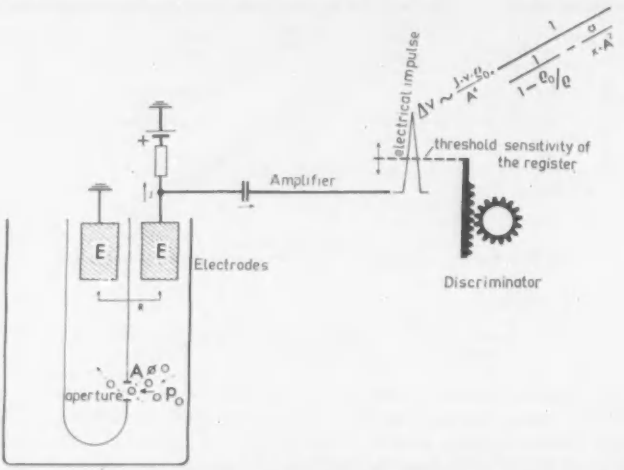

Fig. 3. The principle for counting undissolved particles (p) in a solution by the Coulter method (conductometric measurement method): R = electric resistance; ΔV = pulse voltage; J = current intensity; v = particle volume; A = aperture diameter; ρ = specific resistance of the particles; ρ_l = specific resistance of the solution; a = normal particle area; x = steric factor (for isodimensional particles = 1).

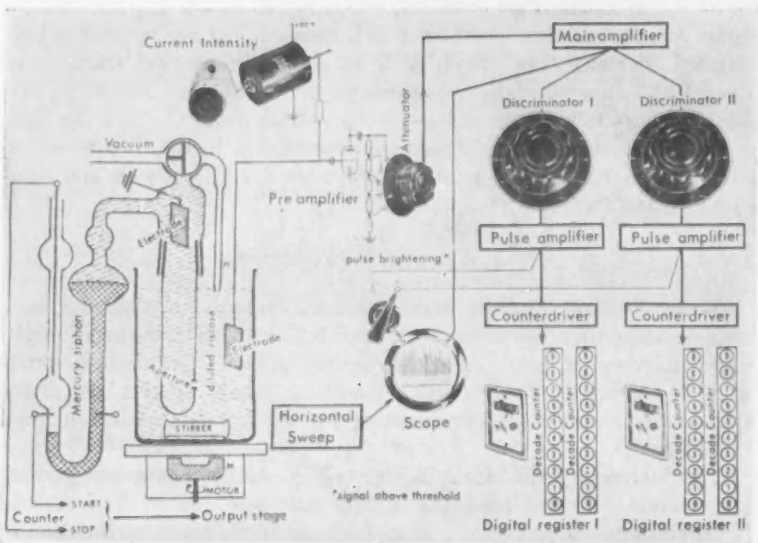

Fig. 4. Block diagram of the Celloscope 202 for counting particles in viscose.

for an aperture diameter of 100 μ. The principle is shown in Figure 4. For constant conditions and at suitable dilution of viscose to the same cellulose and free NaOH content, we can make with different aperture diameters an absolute calibration of the discriminator, so that the particle number–size distribution curve comprised of the greatest part of the so-called microscopical region in the particle spectrum can be drawn.

The calibration was made in two ways (as earlier described).[9,10] One method was to calibrate the Celloscope against a calibrated optical counter (Scienta Counter[4]), the other was a calibration with pollen grain, spherical glass, and plastic beads of well known size distribution, dispersed in a KCl solution of suitable conductivity.[9,11] The calibration with pollen grain involves certain assumptions about the relationship between the conductivities of the solvents and the solids.[9] Even if absolute numerical values are not needed, one can feel that this is a weak link for this type of calibration. For this reason we have now carried out a calibration with glass and plastic pellets dispersed in the above mentioned KCl-solution.[12] In all cases, we found a reasonable agreement between the calibration values.

The possible uses for such a counter in technology, plant supervision,

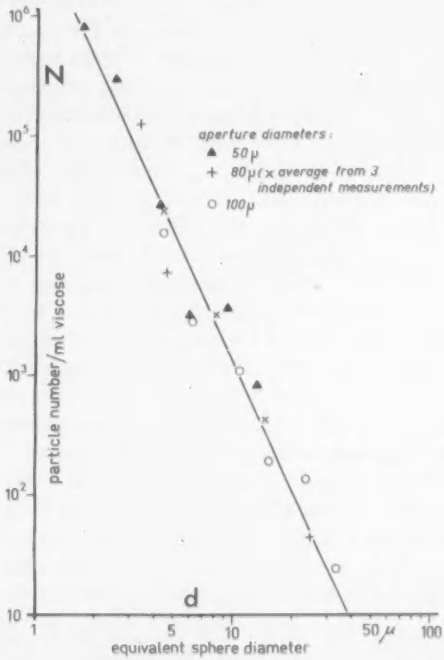

Fig. 5. Particle number versus equivalent sphere diameter for an unfiltered cord viscose measured with a Celloscope 202: (▲) values with a 50 μ aperture after a slight prefiltration of the viscose; (+) 80 μ; (○) 100 μ.

and research are quite large and several important questions connected with viscose filtration are being studied at present.[10,11,13]

In this communication only one examination involving the use of the new counter will be presented. Vosters[14] has already shown that there exists a linear relationship between the logarithm of the cumulative particle number and the logarithm of the particles equivalent diameter. We have verified these statements and shown that this relationship, which can be derived from the model conception about a successive breaking up of cellulose substance in the fiber wall, is relatively satisfactorily fulfilled.[2] Also there are now equivalent observations from other sources. However, all measurements have as a matter of fact ended at a diameter of about 5 μ. With the help of the new apparatus we have followed the distribution curve for a cord viscose made from a prehydrolyzed Southern pine pulp, down to about 1.5 μ (Fig. 5). It still verifies the straight-line relationship, and no suggestion of a faster increase in the particle proportion (maximum) or the opposite (minimum) can be found.

ROTATORY DISPERSION STUDIES

The gel particle count has increased our knowledge about the inhomogeneities in spinning solutions, as these lie in the microscopic region of the particle spectrum. In the following section we want to show some results, obtained by using a completely different method, which gives insight into the amicroscopic region, i.e., the molecular and micellar size region.

Djerassi and co-workers[15] have with success used rotatory dispersion measurements, especially the study of the so-called complex dispersion for the solving of stereochemical, structural, and analytical questions. Furthermore, it can be shown that the method is also useful for the investigation of the supermolecular structure of polypeptides. Protein solutions in which chain molecules are in the random coiled state show the type of normal dispersion of optical rotation, while with an increased degree of order, for example, in the case of the ordered helical conformation, a complex dispersion pattern appears. The anomaly is easily shown if one plots that part of the dispersion curve lying outside the Cotton effect in a modified Lowry diagram. While with a plain normal dispersion a straight line is obtained, a bend appears with an anomalous dispersion (Figs. 6*a* and 6*b*).

A complex rotatory dispersion can be considered fairly simplified as a result of superposition of partial rotations originating from different asymmetric elements in the system. An asymmetric supermolecular architecture as in the α-helical conformation of polypeptides has the peculiarity that even the whole system acts as an independent excited system, causing additional optical activity. Biot showed that by mixing substances of opposite sign and different dispersions (different values of K and λ_c) it was possible to get a mixture which did not obey Biot or Drude's law. In a generalization of these findings we may expect that other types of specific supermolecular arrangements of other kinds of optically active polymers

of sufficient chain length also show a corresponding anomalous optical rotatory dispersion. Such effects which largely change the specific rotation with solvent or temperature are hydrogen bond formation, inter- or intramolecular hydrogen bonding or other bondings, ring formation, and specific conformational changes. Polysaccharides, even if they cannot form a

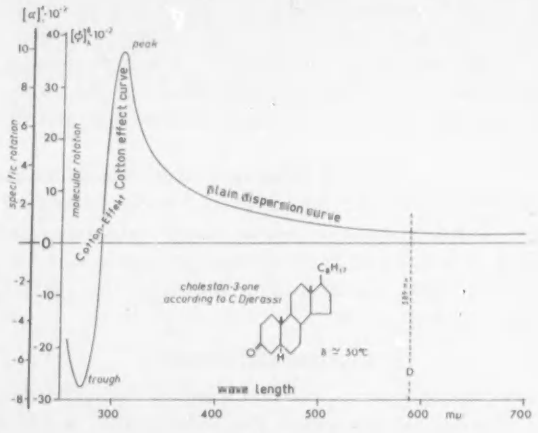

(*a*)

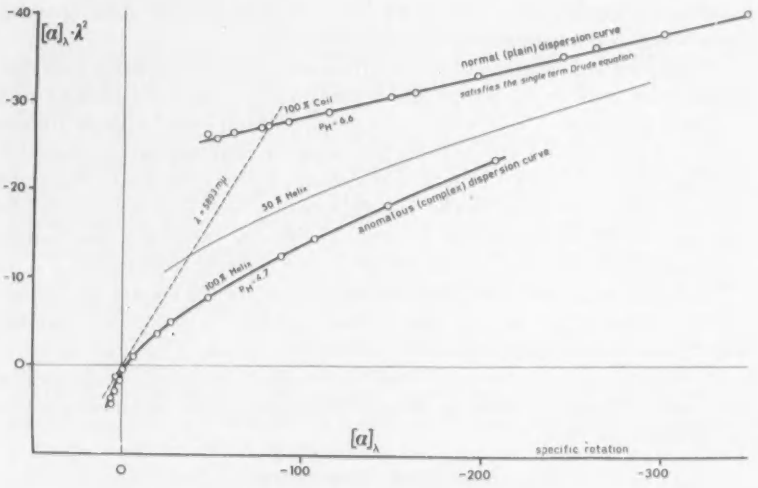

(*b*)

Fig. 6. (*a*) Rotatory dispersion curve of cholestan-3-one as an example for a Cotton effect curve according to Djerassi;[14] (*b*) modified Drude plots (Lowry plot) of dispersion data for poly-L-glutamic acid in the helical and randomly coiled forms and a 1:1 mixture of the two forms. The curve for 100% helical conformation showing the anomalous or complex dispersion effect (after Yang and Doty[28]).

helix, can aggregate to crystalline grids and microcrystals, possibly with a folded chain structure.* Maybe even the small ordered nonpersistent regions in a concentrated solution, as expected in a Hermans gel solution, already cause such an effect. We know, for example, that the optical anisotropy of free macromolecules is not identical to the anisotropy in the condensed state. Crystallization under certain circumstances, even in a far-reaching one-dimensional order, gives rise to optical anisotropy, as we see in the spherulites and pseudospherulites. Polyelectrolytes in solution show special formations of the macroions.[17] A special state of order in a polymer solution or in the dispersed solid phase can therefore change the character of the dispersion curve, so that the values do not fit the simple Drude equation.

Neely[18] applied this method for the first time on a cellulose derivative, namely methylcellulose, and Nadziakiewicz,[19] in our laboratory started to look at some polysaccharides as simple model substances and to study some questions of a more technical measuring nature and finally investigated filtered resin-free viscose after removal of the partially strongly colored inorganic anions.

Experimental Details

For our main measurements we used a self-recording Rudolph spectrophotometer (Rudolph Instruments Engineering Co., Little Falls, New Jersey). Some measurements were made with a Perkin-Elmer precision polarimeter, model 141, a mercury lamp in combination with spectral filters being used as a monochromatic light source.

All samples were purified to remove dust and undissolved larger particles by filtration and/or by centrifugal separation so that the turbidity was kept to a minimum. In the case of viscose, all samples were made from a high-α, prehydrolyzed sulfate pulp practically free from resin by the sheet steeping process under optimal conditions. By a somewhat prolonged aging of the alkali cellulose the viscose viscosity was kept a little on the low side, which facilitated the treatment with the extremely basic anion exchanger (IRA-400) and the above mentioned cleaning technique.

The blank values and their fluctuations caused by the apparatus, including the recording system, the cell window, and the solvent, were recorded directly as well as being calculated indirectly by measuring aqueous solutions of dextrose and fructose of well known concentration and dispersion behavior. Errors in rotatory measurements have been discussed further by Downie et al.[20]

Some Model Experiments

It is well known that solutions of macromolecules show an appreciable turbidity and light-scattering effect. In the scattered light beams a certain

* Kargin[16] considers that packets of folded or unfolded chains form ribbons and lamellar structures, which are a precursor of the crystals. Many of the polymers can change the type of conformation depending on external conditions. Helicoidal structures can consequently be observed, e.g., in polyethylene.

depolarization occurs.[21] The degree of polarization depends both on the turbidity (concentration and particle size) and the size of the incident beam.[22] Furthermore, the reduction in light transmission of a colloidal solution due to scattering, which reduces the intensity of the transmitted light, influences the signal output on the photo tube and, if certain values are exceeded, also influences the comparator system, which results in incorrect values. In the presence of optically inactive, colored by-products, deviations in the specific rotation of an active substance in the spectral range for the light absorption of these colored substances can sometimes be observed.

TABLE I

	$-[\alpha]$ for fructose solutions				
			$0.05M$ Na_2SO_4 solution		
Wavelength λ, mμ	Water	Water + Ludox	Without $BaSO_4$	With $BaSO_4$	With $BaSO_4$ and methyl orange
578	99.1	99.1	99.1	98.5	98.6
546	111.9	111.8	111.9	111.6	111.5
436	183.4	183.5	183.4	183.5	183.5
365	276.40	—[a]	276.4	277.1	277.5
313	403.0	—[a]	403.0	404.7	405.0

[a] Not measurable.

Readings on an aqueous suspension of vitreous silica (Ludox, du Pont de Nemours & Co.) showed no effect on the blank value or background reading. An addition of Ludox to a solution of fructose had no visible effect on the rotatory values, as Table I indicates, providing the current of the photomultiplier is kept in the acceptable range. We had the same findings with the addition of barium chloride to fructose dissolved in $0.05M$ sodium sulfate solution (see Table I). However, in our attempt to record the optical rotatory power of a cellulose xanthate in the region of the Cotton effect we obtained, due to the strong light absorption of the xanthate chromophore, nonreproducible results.

Also the question of whether or not fairly large particles which can sediment show a rotatory effect was not yet answered. Aqueous suspensions of starch, milled cellulose, flocculated regenerated cellulose, hydrocellulose powder, and free alginic acid were therefore studied. Generally we observed a rotatory effect, which decreased with increasing time as a settlement proceeded and became zero if the whole substance sedimented. Redispersion gave the initial values. One of our most instructive examples was alginic acid, which is reported below.

In this preliminary investigation different polysaccharides were studied, such as cellulose dissolved in cadoxen, partially methylated cellulose, ethyl hydroxyethyl cellulose, amylose, dextran, and sodium alginate. Many of these polysaccharides were selected for special reasons, e.g., the rein-

vestigation of methylated cellulose because of the data available as a result of the study of Neely,[18] ethyl hydroxyethyl cellulose (Modocoll) because of the content of aggregated material arising from biological structure element,[23] dextran by reason of the high crystallization tendency, and alginate by reason of the change in molecular conformation and dimension influenced by the degree of ionization. Among these substances,

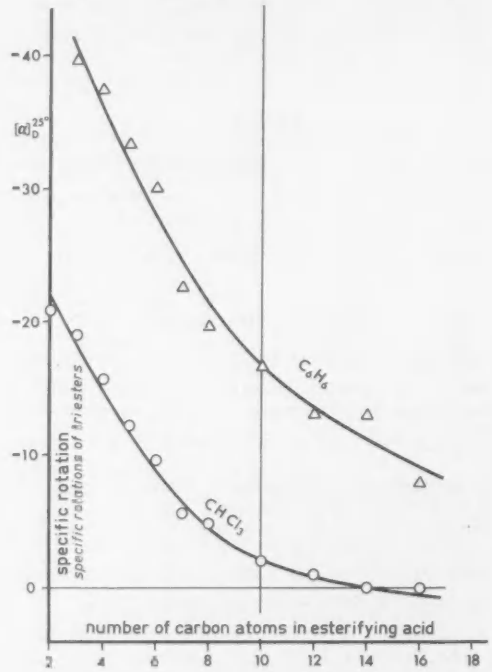

Fig. 7. Specific rotations of triesters according to Malm,[24] illustrating the influence of the solvent and the chain length of the esterifying acid on the optical rotation of cellulose.

dextran and sodium alginate have given clear and interesting results, which has stimulated a somewhat thorough treatment and justify a mention here.

With regard to the influence of the substituent groups and solvents on the rotatory power of the cellulose skeleton, we refer to an investigation by Malm et al.,[24] from which work the instructive Figure 7 is reproduced.

Dextran Solutions

The specific rotation of aqueous dextran solutions was investigated at concentrations of 0.05, 0.5, 1.0, and 2.5 g./100 ml. in the range of 300–700

mμ. All rotatory dispersion curves can be described by a single-term Drude equation:

$$[\alpha]_\lambda = K/(\lambda^2 - \lambda_c^2) \tag{1}$$

The dispersion constant λ_c, which indicates the position of an optically active absorption band, has been calculated as $0.162 \pm 0.007\ \mu$, which agrees with the fact that unsubstituted polysaccharides are practically optically inactive in the quartz-ultraviolet.[25]

Just as many substances show, K is dependent on the concentration of the solid. $[\alpha]\lambda$ can be described by a hyperbolic equation of the form:

$$[\alpha]_\lambda = A + [Bc/(D + c)] \tag{2}$$

where c is concentration in grams/100 ml.
By extrapolation to infinite dilution we obtained:

$$[\alpha]_D\big|_{c \to 0} = 140.6° \tag{3}$$

It is known that dextran in aqueous solutions, especially fractions of relatively low molecular weight, show a pronounced crystallization tendency, with the result that after a long period of standing dextran separates in the form of a crystalline powder. The separation can be accelerated by the addition of ethanol. We added an alcohol–water mixture to a dextran stock solution in this way, so that the dextran concentration of the system was constant and equal to 1 g./100 ml. The alcohol concentrations were 0, 40, 42, and 48% (Fig. 8). An increase in the alcohol concentration results in a strong increase in turbidity, however, the addition was stopped before any dextran was flocculated during a relatively short time.

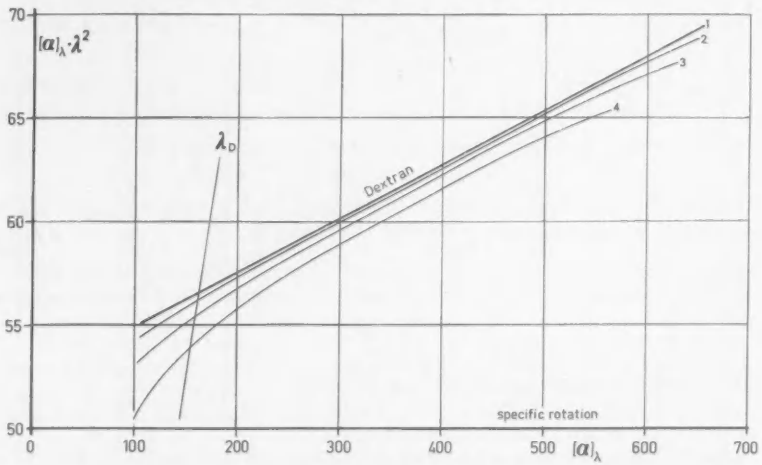

Fig. 8. Modified Drude plots (Lowry plot) of aqueous dextran solutions after an addition of increasing amounts of alcohol (*1*) = 0, (*2*) = 40%, (*3*) = 42%, (*4*) = 48%.

$[\alpha]_\lambda\lambda^2$ plotted against $[\alpha]_\lambda$ shows with increased alcohol addition a more and more pronounced anomalous or complex dispersion, obviously indicating an ordered supermolecular conformation (Fig. 8).

Alginic Acid

A purified sample of the sodium salt of alginic acid at concentrations of 0.05, 0.1, and 0.5 g./100 ml. water was used. By adding sodium hydroxide or sulfuric acid the pH of the solution was varied in the range between 1.8 and 10.7; this was accompanied by a pronounced change in turbidity and viscosity. Below a pH of about 2 the free alginic acid was fairly quickly flocculated. In all these experiments the concentration of the polysaccharide was kept constant.

Solutions of sodium alginate, with or without an addition of NaOH show a plain normal dispersion curve, which satisfies the single-term Drude equation with a λ_c of 0.142 μ.

With decreasing pH the rotatory dispersion undergoes characteristic changes. The value for the specific rotation decreases and the dispersion becomes complex in character (Fig. 9). This behavior is similar to the changes which occur in polypeptide and protein solutions on varying the pH. A pronounced anomaly—although smaller than is seen in proteins—is shown by the flocculated alginic acid providing the particles are kept in suspension during the measurements.

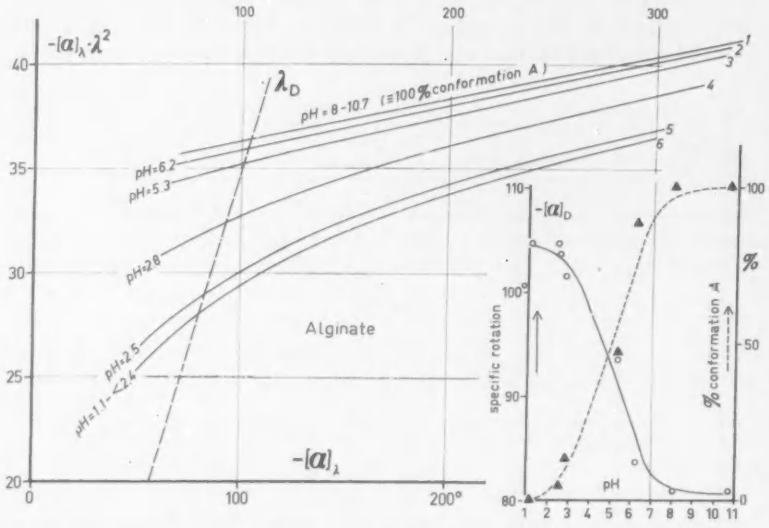

Fig. 9. Modified Drude plots (Lowry plot) of alginate solutions at different pH. (The ordinate values in the right-hand side diagram for specific rotation are inverted and misplaced vertically. For the solid curve the specific rotation $-[\alpha]_D$ for pH <2.4 is 80.8°, for pH 5.3 = 101.4°, and pH >8 = 104.5°.)

If we assume that in the alkaline region only a nonordered conformation (called A) is present and at the lowest pH an ordered conformation B exists, then we can calculate the percentage of A and B present in the solution at different pH. On the right-hand side in Figure 9 we see the percentage of A as well as the values of the specific rotation plotted against the pH of the solution.

ROTATORY MEASUREMENTS ON VISCOSE

Viscose and dilutions of it show, like other cellulose derivatives (see Fig. 7), an optical rotation (negative) of approximately the expected magnitude.

It might be mentioned here that a dispersion of hydrocellulose residues, made from ramie fiber, a so-called "micelle sol," shows a $(\alpha)_D \approx -201°$; however, it must once again be pointed out that we have to distinguish between the activity in the crystalline state and the activity of the molecule itself.*

As is well known, there are for example some substances, which show optical activity only in the crystalline state.

The specific rotation of viscose is dependent upon the concentration (in our experiments expressed as p, the number of grams of cellulose per 100 g. solution), upon the degree of substitution (DS), and the sodium hydroxide concentration (% NaOH) of the solvent. The influence of these factors has been investigated.

Keeping the degree of substitution (DS value about 45) and the lye concentration nearly constant, we observe an increase in the specific rotation with increasing cellulose content p, as many substances show. Also in the case of viscose we can express the concentration dependence by a hyperbolic equation.

$$[\alpha]_D = A + [Bp/(C + p)] \tag{4}$$

in which A represents the specific rotation at infinite dilution ($[\alpha]_{D_{p\to 0}}$) (Fig. 10). The numerical values in this particular case were: $A = -5.755°$, $B = -14.425$, $C = 5.862$.

For an investigation of the influence of the NaOH content in the dissolving lye, we dissolved a xanthate (39% CS_2 on the basis of cellulose)

* The optical rotation of such a sol, made from mercerized ramie, shows a specific rotation expressed in degrees per millimeter layer of the material in a supposed dry state $(\alpha) = \alpha/L \simeq -862°$. Cellulose in a hypothetical water solution has a calculated specific rotation $[\alpha]$ of only about $-2.1°$,[26] and in the case of a dispersion of a freshly prepared precipitate or a solution of this in lye nearly no rotation could be observed and even the sign, plus or minus, is not defined at present (cellulose dissolved in 51% H_2SO_4 shows a $[\alpha]$ of $+2°$, in phosphoric acid $+6°$, and in trimethylbenzylammonium hydroxide $-80°$). Therefore the strong rotation must be ascribed to the crystalline state. It should be mentioned here that unexpected high values are observed in liquid crystals if we have ordered layers of optically active molecules in a helical conformation, the so-called "cholesterinische Phasen."[27]

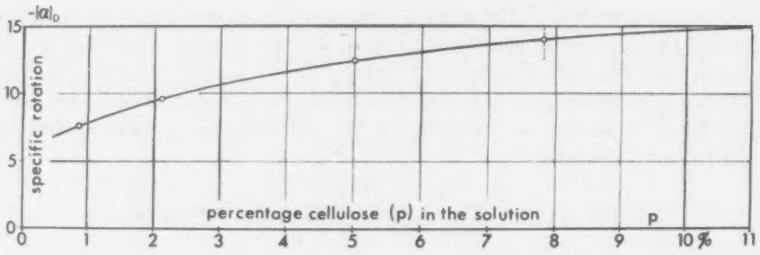

Fig. 10. Specific rotation $-[\alpha]_D$ of a viscose of normal composition (7.8% cellulose, 5.9% NaOH, 40% CS_2, measured after dissolving the xanthate to viscose) at different dilutions.

at a very low temperature in water to a viscose with approximately 8.7% cellulose and 5.5% total alkali (free NaOH = 3.5%). From this stock solution, after treatment with the anion exchanger, a series of viscoses with $p = 2.16\%$ cellulose and increasing NaOH content were prepared by dilution with cooled lye of different strengths. The lye dependence of the specific rotation $[\alpha]_{578\,m\mu}$ is given as the change in specific rotation per 1% NaOH in eq. (5):

$$\Delta[\alpha]/\Delta\%\ \text{NaOH} = -1.96° \tag{5}$$

For the evaluation of the influence of the degree of substitution we prepared a xanthate with 50% CS_2, expressed on the basis of cellulose in the alkali cellulose, and dissolved it at a low temperature to a viscose with 7.6% cellulose and about 9% total NaOH. Portions of viscose were at different stages in the ripening process purified with the anion exchanger, diluted to a cellulose concentration of $p = 2.4\%$, and measured immediately. During the measurement a determination of the DS value on the ion-exchanged yet undiluted viscose was performed. The results of the influence of DS in the xanthate as change in specific rotation per 0.01 degree of substitution are given by eq. (6):

$$\Delta[\alpha]/\Delta(\text{DS}/100) = +0.054° \tag{6}$$

An unexpected phenomenon occurs after the syneresis of the xanthate. An investigation of the solid gel gave an indication that a positive rotation exists. Experimental difficulties and an insufficient number of observations make it impossible to discuss this phenomenon at present.

The above mentioned investigations have shown that the value for the specific rotation increases with increasing cellulose concentration and degree of substitution and decreases with the NaOH content in the viscose. Therefore no absolute value for the specific rotation of viscose can be reported. The specific rotation one observes on a viscose is largely dependent on its composition and degree of aging.

Rotatory Dispersion Behavior of Viscose

Optical rotatory dispersion of viscose solutions shows a plain curve in the visible spectral range, like many simple alcohol xanthogenates, as reported in the literature.[15] In passing from the violet end of the spectrum to the ultraviolet we enter the region of the Cotton effect, in which the xanthate chromophore absorbs the light. The first strong absorption band

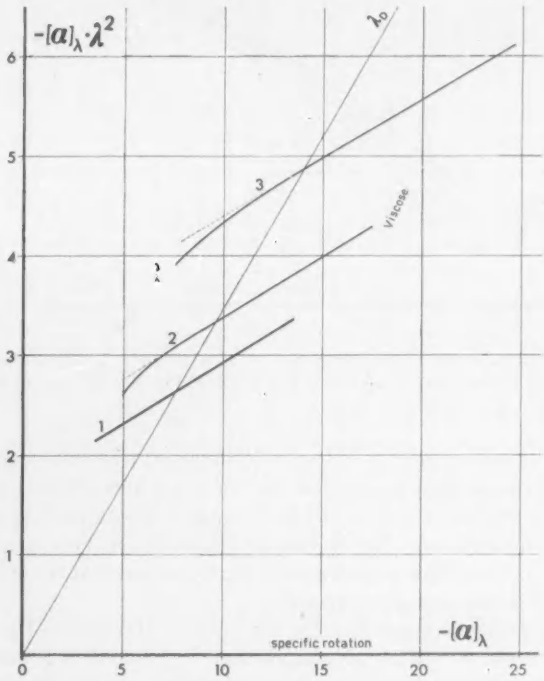

Fig. 11. Modified Drude plots (Lowry plot) of a viscose at different dilutions. The cellulose contents p are: (*1*) 0.86%; (*2*) 2.12%; (*3*) 7.8%. For the measured values, taken from the records of the Rudolph spectropolarimeter see Table II.

appears at 302 mμ;[25,29] a weak absorption band exists at 370 mμ. At sufficiently low concentrations, that means below about 1%, we observe no anomaly in the region for the plain curve, there obviously exists a random conformation and the single term Drude equation is valid. We obtain from this a value of 0.348μ for λ_c (curve *1* in Fig. 11).

With increasing cellulose concentration an anomalous dispersion occurs, as Figure 11 shows. (A phenomenologically equivalent concentration effect was observed on poly-γ-benzyl-L-glutamate, which goes over at higher concentrations into the helical form.[20]) The deviation is due to an anomalous decrease of the specific rotation with increasing wave-

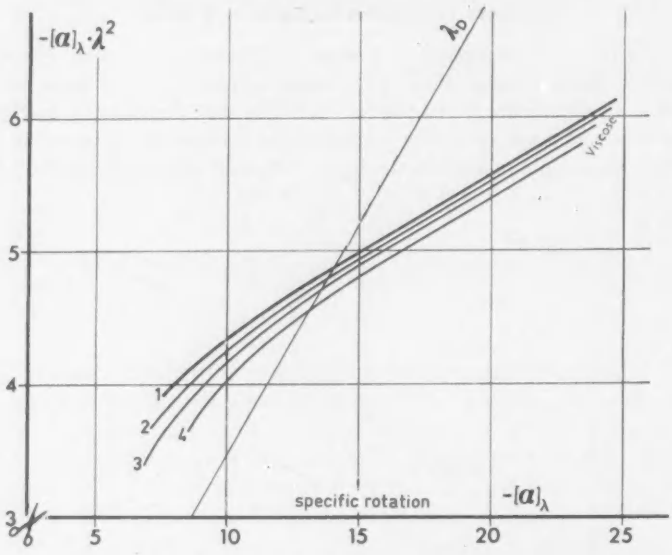

Fig. 12. Modified Drude plots (Lowry plot) of a viscose (p = 7.8%) at different ripening stages: (*1*) DS ± 0.49 (= curve *3* in Fig. 11); (*2*) DS ± 0.46; (*3*) *DS* ± 0.40; and (*4*) DS ± 0.33.

length, but it seems that the values of λ_c obtained from the square root of the slope of the straight line part of the curve are almost unchanged. We assume that this effect is caused by a change in conformation due to the change in concentration. In the case of a dilution any type of supermolecular order in the solution must be easily destroyed, so that the state of solution becomes more random in character.

This assumption is supported by the fact that the observed effect, studied on a viscose of industrial composition, i.e., about 8% cellulose, increases with the ripening of the viscose (Fig. 12). Other known observations such as birefringence, structural viscosity, and x-ray measurements also indicate increasing association phenomena.[30] It is believed that, for instance, the number of crystallite laminas as well as their degree of perfection is higher at the end of the ripening period.

The obtained values for plotting the curves in Figures 11 and 12 are tabulated in Table II.

DISCUSSION

We supposed that up till now the result may be interpreted in the following manner. In a spinning solution of a normal concentration there exists an intermolecular interaction, partly due to some kind of short-range order, and partly due to different kinds of supermolecular structure. The molecular architecture of a viscose, in accordance with other observations, in-

TABLE II

	Figure 11						Figure 12					
	Curve 1		Curve 2		Curve 3[a]		Curve 2		Curve 3		Curve 4	
λ mμ	$-[\alpha]$	$-[\alpha]\lambda^2$	$-[\alpha]$	$-[\alpha]\lambda^2$	$-[\alpha]$	$-[\alpha]\lambda^2$	$-[\alpha]$	$-[\alpha]\lambda^2$	$-[\alpha]$	$-[\alpha]\lambda^2$	$-[\alpha]$	$-[\alpha]\lambda^2$
720	4.33	2.243	5.13	2.660								
710	4.49	2.263	5.40	2.722	7.90	3.982	7.34	3.700				
700	4.66	2.284	5.68	2.783	8.24	4.036	7.83	3.835	6.94	3.401		
690	4.84	2.306	5.97	2.842	8.60	4.096	8.23	3.920	7.54	3.589		
680	5.04	2.329	6.25	2.890	9.02	4.170	8.65	4.000	8.11	3.750		
670	5.24	2.354	6.55	2.940	9.47	4.250	9.13	4.100	8.65	3.881		
660	5.47	2.381	6.84	2.980	9.93	4.325	9.62	4.190	9.19	4.002		
650	5.70	2.410	7.16	3.025	10.41	4.400	10.13	4.280	9.78	4.130	8.76	3.700
640	5.96	2.440	7.50	3.072	10.91	4.470	10.64	4.360	10.28	4.211	9.65	3.952
630	6.23	2.474	7.82	3.116	11.45	4.545	11.21	4.450	10.83	4.300	10.31	4.091
620	6.53	2.509	8.22	3.160	12.02	4.622	11.79	4.532	11.46	4.405	10.98	4.221
610	6.85	2.548	8.63	3.211	12.62	4.695	12.39	4.610	12.07	4.490	11.64	4.330
600	7.20	2.590	9.07	3.264	13.27	4.776	13.06	4.700	12.75	4.590	12.35	4.445
590	7.57	2.636	9.54	3.322	13.95	4.855	13.76	4.791	13.46	4.685	13.07	4.550
580	7.98	2.685	10.06	3.384	14.69	4.942	14.51	4.880	14.22	4.785	13.82	4.648
570	8.43	2.740	10.63	3.453	15.52	5.042	15.33	4.980	15.11	4.910	14.62	4.749
560	8.93	2.800	11.25	3.528	16.39	5.140	16.21	5.085	15.94	5.000	15.50	4.861
550	9.47	2.866	11.94	3.612	17.40	5.265	17.19	5.200	16.91	5.115	16.43	4.970
540	10.08	2.939	12.70	3.704	18.48	5.390	18.26	5.324	17.95	5.235	17.46	5.090
530	10.75	3.021	13.55	3.807	19.76	5.550	19.55	5.491	19.22	5.400	18.66	5.241
520	11.51	3.112	14.50	3.922	21.09	5.702	20.84	5.636	20.50	5.542	19.93	5.390
510	12.36	3.215	15.58	4.052	22.57	5.870	22.31	5.804	21.97	5.715	21.33	5.549
500	13.33	3.333	16.80	4.200	24.25	6.062	24.00	6.000	23.60	5.901	22.92	5.730
589.3	7.60		9.58		14.00		13.85		13.55		13.18	
p, %	0.8595		2.115		7.82		7.82		7.82		7.82	
λ_c, μ	0.348											
K	1.72											

[a] Equals curve 1 in Figure 12.

creases with increasing desolvation and the splitting off of substituted groups, that is to say with increasing degree of ripening. The dilution series finally shows that the short range order and obviously a part of the existing supermolecular structure is not persistent, a fact which speaks strongly against the hypothesis of a predominantly micellar solution state caused by solution resistant crystallites. Therefore we have no reason to revise our model conception about the particle spectrum.

The authors wish to express their gratitude to the Research Director of the Institute Professor L. Stockman, for his interest, support, and encouragement. Special thanks are due to Professor Tiselius and Professor Lindberg for their kind permission to use the instruments. During this study, one of us (H. C. N.) was the recipient of a fellowship established by the Department of Economic and Social Affairs of the United Nations Secretariat for Technical Assistance and by the Swedish Cellulose Association (Cellulosaindustriens Stiftelse för Teknisk och Skoglig Forskning samt Utbildning), which is acknowledged with deep gratitude. The authors are also indebted to Mr. A. Topham for revising the English text.

References

1. Treiber, E., *Das Papier*, **15**, 728 (1961); E. Treiber, and H. Meier, *Holzforsch.*, **12**, 1 (1958); J. Schurz, *Papper och Trä*, **42**, 401 (1960); B. G. Rånby, H. W. Giertz, and E. Treiber, *Svensk Papperstidn.*, **59**, 117, 205 (1956).

2. Treiber, E., *J. Polymer Sci.*, **51**, 297 (1961).

3. Gray, K. L., and R. W. Yorke, *J. Polymer Sci.*, **61**, S5 (1962); see also the following reviews: F. Kolos, *Lenzinger Ber.*, **12**, 18 (1962); E. Treiber, *Lenzinger Ber.*, **12**, 5 (1962).

4. Treiber, E., O. F. Fex, J. Rehnström, and M. Piova, *Svensk Papperstidn.*, **58**, 287 (1955).

5. Manley, R. J., and A. Bengtsson, *Svensk Papperstidn.*, **61**, 471 (1958).

6. Kolos, F., *Lösungszustand und Gelteilchen*, Technical Information from Viscose Department, Central Laboratory of the Swedish Cellulose Industry, December 1961.

7. Durso, D., and L. R. Parks, *Svensk Papperstidn.*, **64**, 853 (1961); L. H. Sperling, and M. Easterwood, *J. Appl. Polym. Sci.*, **4**, 25 (1960).

8. Treiber, E., *Svensk Papperstidn.*, **61**, 794 (1958); M. Teichgräber, *Faserforsch. Textiltechn.*, **12**, 489 (1961).

9. Kolos, F., *Svensk Papperstidn.*, **64**, 533 (1961).

10. Kolos, F., and E. Treiber, *Svensk Papperstidn.*, **64**, 577 (1961).

11. Hinweise zur Kontrolle, Kalibrierung, Handhabung und Wartung des Celloscope 202. Instruction manual of the L. Ljungberg Comp., Stockholm, Sweden.

12. Kolos, F., and E. Treiber, unpublished data.

13. Kolos, F., *Svensk Papperstidn.*, **65**, 107 (1962); F. Kolos and E. Treiber, *Svensk Papperstidn.*, in press.

14. Vosters, H. L., *Svensk Papperstidn.*, **54**, 122 (1950).

15. Djerassi, C., *Optical Rotatory Dispersion. Applications to Organic Chemistry*, McGraw-Hill, New York, 1960; P. Urnes and P. Doty, *Adv. Protein Chem.*, 16, 681 (1962); C. Cohen, *Nature*, **175**, 129 (1955); P. Doty and J. T. Yang, *J. Am. Chem. Soc.*, **78**, 498, 4810 (1956); M. K. Hargreaves, *Nature*, **195**, 560 (1962); K. Linderstrøm-Lang and J. A. Schellman, *Biochim. Biophysica. Acta*, **15**, 156 (1954).

16. Kargin, V. A., *Pure Appl. Chem.*, **4**, 201 (1962).

17. Rice, St. A., M. Nagasawa, and H. Morawetz, *Polyelectrolytic Solutions*, Academic Press, New York, 1961.

18. Neely, W. B., *J. Am. Chem. Soc.*, **82**, 4354 (1960).

19. Nadziakiewicz, H. C., *Studien über die Dispersion der optischen Drehung von Poly-*

saccharider, I, II, Technical Information from the Viscose Department, Central Laboratory of the Swedish Cellulose Industry, August 1962.

20. Downie, A. R., A. Elliot, W. E. Hanby, and B. R. Malcolm, *Proc. Roy. Soc. (London)*, **A242**, 325 (1957).

21. Stuart, H. A., *Die Physik der Hochpolymeren*, Vol. I, Springer, Berlin, 1952–53, pp. 393, 410ff.; *ibid.*, Vol. II, p. 512; A. Boutaric and M. Chapeaux, *J. Chim. Phys.*, **39**, 73 (1942).

22. Oster, G., *Anal. Chem.*, **25**, 1165 (1953).

23. Manley, R. St. J., *Arkiv Kemi*, **9**, 519 (1956).

24. Malm, C. J., J. W. Mench, D. L. Kendall, and G. D. Hiatt, *Ind. Eng. Chem.*, **43**, 688 (1951).

25. Treiber, E., *Kolloid-Z.*, **130**, 39 (1953); E. Treiber and W. Felbinger, *Das Papier*, **7**, 13 (1953); E. Treiber, W. Berndt, and H. Toplak, *Angew. Chem.*, **67**, 69 (1955).

26. Purves, C. B., in *Cellulose and Cellulose Derivatives*, E. Ott, Ed., Interscience, New York, 1943, p. 71.

27. Stumpf, F., *Ann. Physik.*, **37**, 351 (1912).

28. Tsi Yang, J., and P. Doty, *J. Am. Chem. Soc.*, **79**, 761 (1957).

29. Treiber, E., *Monatsh. Chem.*, **82**, 53 (1951).

30. Meyer, W., thesis, Bern, 1943; R. Signer and W. Meyer, *Helv. Chim. Acta*, **28**, 325 (1945); *Papper och Trä*, **42**, 401 (1960); J. Schurz and R. Bartunek, *Das Papier*, **10**, 97 (1956); J. Schurz, *Das Papier*, **12**, 210 (1958); E. Treiber, H. Koren, W. Felbinger, and W. Lang, *Monatsh. Chem.*, **83**, 259 (1954); W. Koblitz, *Das Papier*, **9**, 262 (1955); W. Koblitz, H. Kiessig, and K. Hess, *Z. Elektrochem.*, **58**, 872 (1954).

Synopsis

The state of solution of a technical viscose can, according to the authors conception, simply be described with the help of a particle spectrum for the cellulose substance, which stretches continuously from the nonreacted wood fiber down to the single molecule dimension. Both from a practicle and didactic point of view it is, however, expedient to split up the spectrum into a microscopic region and a sub- and amicroscopic region. The comparatively large inhomogeneities in the solution (gel particles etc.) in the so-called microscopic part of the particle spectrum can be quantitatively described with the help of a conductometric counting method. A completely new apparatus is briefly described, and practical use possibilities and results are mentioned. For the study of the other part of the spectrum we tried to apply a spectropolarimetric method. Rotatory dispersion measurements were made on several polysaccharides as model substances and finally on viscose solutions after anion-exchange. With higher cellulose concentrations in the viscose solutions a complex dispersion curve occurs, which probably indicates the appearance of a state of order in the solution. The nonpersistent state of order increases with increasing degree of ripening.

Résumé

L'état de la solution d'une viscose technique peut, suivant la conception des auteurs, être simplement décrit à l'aide d'un spectre de diffusion de la substance cellulosique, qui s'étend de façon continue depuis la fibre de bois qui n'a pas réagi jusqu'à une dimension de l'ordre d'une molécule isolée. Pourtant de points de vue pratique et didactiqué il est pratique de subdiviser le spectre des particules en un domaine microscopique et un domaine subet amicroscopique. Les hétérogénités relativement grandes dans la solution (particules de gel etc.) dans le domaine microscopique du spectre de particules peuvent être déterminées quantitativement à l'aide d'une méthode conductométrique de détermination des particules. Un appareil entièrement neuf basé sur ce principe est décrit brièvement et des possibilités d'applications pratiques ainsi que des résultats sont donnés. Pour l'étude de l'autre partie du spectre de particules, il a été tenté de fare appel à une méthode de recherche spectropolarimétrique. Des mesures de dispersion rotatoire ont

été effectuées sur plusieurs polysaccharides comme substances de référence et finalement sur des solutions de viscose après échange anionique. En présence de concentrations plus grandes en cellulose dans les solutions de viscose une courbe de dispersion complexe se présente, ce qui indique probablement un état ordonné dans la solution. La non-persistance de l'état ordonné augmente avec l'accroissement du degré de murissement.

Zusammenfassung

Der Lösungszustand einer technischen Viskose kann nach Auffassung der Autoren am einfachsten mit Hilfe eines Zerteilungsspektrums für die Cellulosesubstanz beschrieben werden, welches sich kontinuierlich von der nichtreagierten Holzfaserzelle bis zu der Dimension der Einzelmoleküle erstreckt. Jedoch ist es aus praktischen und methodischen Gesichtspunkten angezeigt das Teilchenspektrum in einen mikroskopischen und einen sub- und amikroskopischen Bereich zu unterteilen. Die relativ grossen Lösungsinhomogenitäten (Gelteilchen udgl.) in diesem mikroskopischen Bereich des Teilchenspektrums können quantitativ mit Hilfe der konduktometrischen Partikelrechenmethode ermittelt werden. Ein vollständig neues Gerät nach diesem Prinzip wird kurz beschrieben und praktische Anwendungsmöglichkeiten sowie Resultate werden erwähnt. Für das Studium des anderen Teiles des Teilchenspektrums wurde versuchsweise eine spektropolarimetrische Untersuchungsmethode herangezogen. Rotationsdispersionsmessungen wurden an mehreren Polysacchariden als Modellsubstanzen durchgeführt und schliesslich wurde Viskose nach einem Anionenaustausch untersucht. Bei höheren Cellulosekonzentrationen in den Viskoselösungen erhält man eine komplexe Dispersionskurve, die offenbar die Ausbildung eines Ordnungszustandes in der Lösung anzeigt. Diese nichtpersistente Strukturierung in der Lösung nimmt mit steigender Nachreife der Viskose zu.

JOURNAL OF POLYMER SCIENCE: PART C NO. 2, PP. 377–386 (1963)

Polymerization within Cellulose Matrices. Nature of the Strength Reinforcement

EVELYN S. PUTNAM, *Rock Island Arsenal Laboratory, Rock Island Arsenal, Rock Island, Illinois*

INTRODUCTION

In the last few years several articles have been published reporting various graft copolymers obtained when monomers are polymerized in the presence of cellulose or cellulose derivatives. Several techniques have been employed in an attempt to generate free radicals on the cellulose molecule for initiation of polymerization: oxidation by ceric ions,[1–4] use of the large chain transfer constant of SH groups in mercaptoethyl side chains,[5,6] formation of polyperoxides on cellulose by ozonization,[7] use of anthraquinoid dye sensitizers and ultraviolet radiation,[8] use of diazonium derivatives of cellulose,[9] the "anchored catalyst" technique of Lipson and Speakman[10] using ferrous ammonium sulfate and hydrogen peroxide,[4,11–13,14] and gamma radiation.[7,15–17]

Each of the referenced authors with the exception of Landells and Whewell[11,12] and Boardman and Lipson[14] present evidence to indicate that a graft polymer has been formed. Basically the proof presented rests upon the fact that the polymer cannot be extracted quantitatively or that curves on fractional precipitation of the product from a mutual solvent differ from similar curves obtained with physical mixtures. On the contrary, Landells and Whewell consider the polymer to be simply deposited within the fiber wall and use staining techniques to locate its position.

Although several of the above methods have been attempted at the Rock Island Arsenal Laboratory, work has been concentrated on polymerization of acrylonitrile initiated by gamma radiation in the presence of cellulose in nonaqueous, nonswelling media for two reasons: (*1*) it is a rapid method and technically the simplest; (*2*) wet and dry strength reinforcement of the cellulose matrix is equal to, if not greater than that resulting from any of the above methods.

The work covered by this report consists of physical property measurements made on filter paper which had been treated by suspending the paper in 50% solutions of acrylonitrile in ethanol, acetone, and benzene, respectively, and exposing to 10^6 rads gamma radiation.

PROCEDURE

Reagents

Reagent grade chemicals were used in all cases without further purification. The inhibitor was not removed from acrylonitrile before use.

Experimental Design

Whatman No. 2 filter paper was used as the cellulose matrix. Approximately 1000 strips were cut, 4 in. long and 1.5 cm. wide. The 1.5 cm. width was obtained using a JDC Model 15 precision sample cutter. The specimens were randomized prior to use.

Ten specimens were used for each treatment and each control experiment. Two of the specimens were used to obtain the load–elongation curve to rupture before extraction and two to obtain the deformation parameters before extraction. Four specimens were extracted. Two of the extracted specimens were used to obtain the load–elongation to rupture curves and two to obtain the deformation parameters. The two remaining specimens were reserved for use in the event of damage to the other specimens.

Treatment and Controls

A test tube was filled with a 50 wt.-% solution of acrylonitrile in the appropriate solvent. Ten paper specimens were numbered and weighed individually and placed in the solution. A second test tube was filled with the solvent used in the treatment and ten weighed paper specimens were placed in it. After rubber stoppers were affixed, the two test tubes were placed in a canister for exposure to radiation.

All treated and control samples were exposed to ionizing radiation from a 240 curie, Brookhaven design, cylindrical Co^{60} source having a dose rate of 6.8×10^4 rads/hr. A total dose of 1×10^6 rads was used in each exposure.

After exposure, control specimens were removed from the solvent, placed on absorbent toweling and allowed to air dry in the conditioning room. Treated specimens were removed from the homopolymer by breaking the test tube. The group of specimens was immediately placed in a beaker of the solvent. Each specimen was removed individually from the beaker and loose homopolymer removed with a blunt straightedge. Treated specimens were then placed on absorbent toweling in the conditioning room to dry and condition.

Extraction Procedure

Four treated specimens were chosen for extraction at random. Each was weighed and then placed in 200 ml. boiling *N,N'*-dimethylformamide in a 1500 ml. beaker. A watch glass was placed on the beaker to prevent evaporation of the solvent. The specimens remained in the gently boiling solvent for three hours. Upon removal from the solvent they were placed on absorbent toweling in the conditioning room to dry and condition.

Physical Properties

All weights and physical properties were determined in the conditioning room which is maintained at 73 ± 2°F. and 50 ± 4% R. H.

Load, elongation, and cyclic deformation curves were obtained on a Model TT-C Instron tensile testing machine with integrator assessory. Tests were performed with the use of a 2-in. jaw width, 0.1 in./min. crosshead speed (rate of sample extension), and 10 in./min. chart speed.

Reversible and irreversible deformation values were approximated by the method suggested by Higgins[18] as shown in Figure 1.

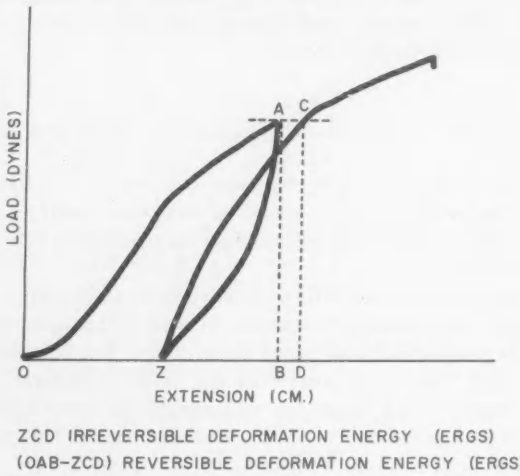

Fig. 1. Definition of the irreversible and reversible deformation quantities.

The load equivalent to the line AC was chosen in such a way that it represented 80% of the rupture load. Loading and unloading was performed at the same rate, i.e., 0.1 in./min.

Infrared spectra were obtained on a Baird Associates, Inc. double-beam recording infrared spectrophotometer. Samples of the extract were prepared by evaporation onto sodium chloride windows. Reference spectra were obtained by dissolving in DMF the homopolymer obtained during polymerization in various solvents. The solution was boiled for 3 hr. to duplicate the conditions of the extraction procedure and samples prepared by evaporation onto sodium chloride windows.

RESULTS AND DISCUSSION

Examination of Table II reveals that the strength reinforcement resulting from the treatments is lost with the extractable polymer. Since the polymer is extractable, normally the rupture of primary valence bonds

would not be suspected. However, in view of the rather severe extraction conditions, infrared spectra were obtained on the extract and compared to the spectra of polyacrylonitrile homopolymer prepared in a like manner from solution. As Figure 2 shows, the spectra are the same in both cases. Spectra were obtained on extracts of the other two treatments and were identical. Therefore, the major portion of the polymer add-on was not grafted to the cellulosic backbone.

Since the polymer did cause a large increase of strength not due to a primary valence bond, to what forces can this added strength be attributed? It might be that the growing polymer molecules intertwine through the structure and reinforce it mechanically through frictional forces. Contrarywise, the added strength might also be due to secondary valence forces, possible hydrogen bonds of the structure

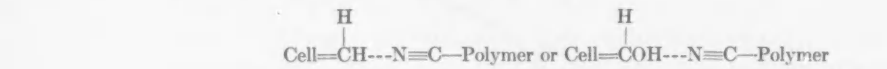

To explore this question it is necessary to consider the rheological behavior of untreated paper to determine what effects would be predicted if frictional forces as opposed to secondary bonding forces were responsible for the reinforcement.

Two predominant structural theories have been advanced to explain the nonlinear elasticity exhibited by paper in load elongation curves. Nissan[19,20] constructs a model of paper fibers linked together by extensible hydrogen bonds. He reasons that since the variation of force with stretch of hydrogen bonds is not linear, the load elongation curve also will not be linear. Elastic deformation is thus considered to be the result of the stretching, breaking, and reforming of hydrogen bonds.

Rance,[21] on the other hand, considers the nonlinear nature of the elasticity curves to be due to progressive stress concentration within a disintegrating material rather than to nonlinear elasticity of the bonds. Elongation of paper is visualized as the straightening up of bent and curved fibers, firmly fixed at junction points to other fibers by hydrogen bonds. Toward the end of the straightening process some tensile elongation of the fiber may begin, but this is quickly terminated by rupture of the hydrogen bond linking the fiber to its neighbor.

Simple deposition of polymer within the model fiber network proposed by Nissan would introduce a linear, inelastic contribution to the strength. Similar deposition in the network proposed by Rance might cause a small

TABLE I

Swelling liquid	Sorptive capacity, mg./g.
Acetone	2.4
Benzene	3.9
Ethanol	5.7
(Water)	(45.2)

TABLE II

Properties of Paper Exposed to 10^6 Rads Gamma Radiation while Suspended in 50% Solutions of Acrylonitrile in Various Solvents

Solvent	% Polymer after treatment	% Polymer after extraction	Breaking load, lb.	Elongation, %	Young's modulus, dynes/cm.^{2} $\times 10^{10}$	Rupture energy, ergs $\times 10^{-5}$	Rupture energy, ergs/cm.^{2} $\times 10^{-6}$	Reversible deformation, ergs	Irreversible deformation, ergs	Ratio of irreversible to reversible deformation
Acetone										
Treated	51		20.5	3.1	3.0	9.67	7.44	215,830	55,370	0.26
Extracted		4.3	6.5	3.0	1.0	3.06	2.35	65,992	49,720	0.75
Control			9.4	2.3	1.8	3.40	2.62	69,608	26,216	0.38
Extracted			5.8	2.8	1.1	2.54	1.95	46,556	38,420	0.83
Benzene										
Treated	39		19.3	2.8	2.6	8.43	6.48	181,900	33,900	0.19
Extracted		4.9	7.5	2.7	1.1	3.01	2.32	47,000	20,792	0.44
Control			9.2	2.0	1.9	2.83	2.18	65,500	20,340	0.31
Extracted			5.3	2.7	1.0	2.36	1.82	33,900	23,504	0.69
Ethanol										
Treated	54		19.3	2.4	2.8	7.28	5.60	185,320	38,420	0.21
Extracted		8.5	8.2	2.5	1.4	3.00	2.31	62,376	27,120	0.43
Control			8.6	2.4	1.7	3.39	2.61	51,980	19,436	0.37
Extracted			5.1	2.6	.9	2.10	1.62	23,052	12,656	0.55
Untreated	—	—	9.2	2.3	1.77	3.39	2.61	42,488	9,944	0.23

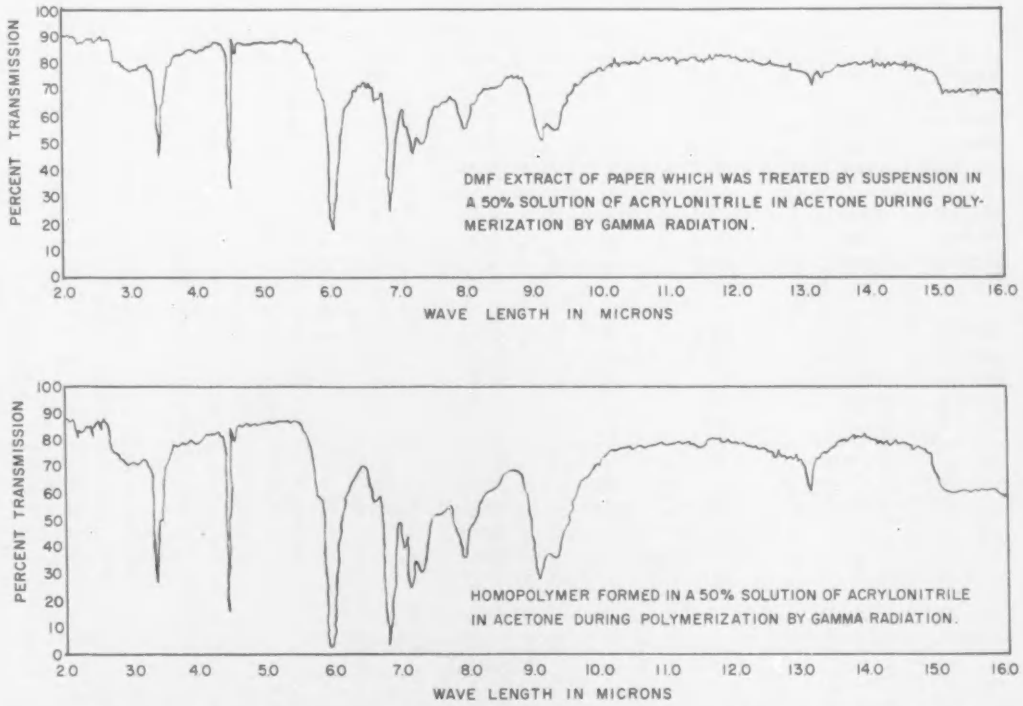

Fig. 2. Comparison of the spectra of polyacrylonitrile homopolymers and the DMF extract of the treated paper.

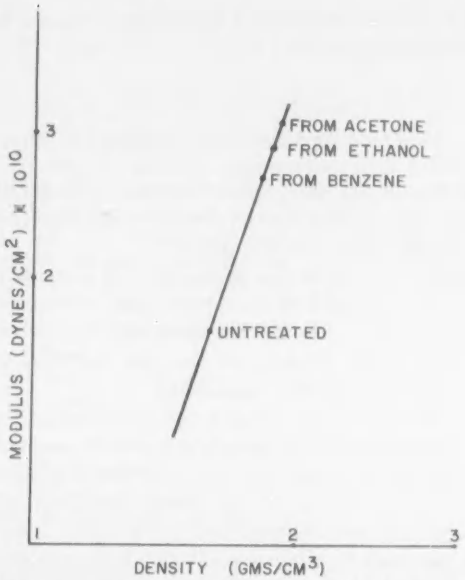

Fig. 3. Relationship between density and Young's modulus for treated and untreated paper.

elastic contribution due to bending of the polymer molecules at low loads, but since "frictional" forces must be less than hydrogen bonding energy, the major contribution would be due to slippage and, hence, inelastic.

As shown in Table I, although the amount of reversible and irreversible deformation is increased as a result of the treatment, the ratio of irreversible to reversible deformation is nearly the same in the treated materials as in the untreated paper. Hence, the strength contribution could not be due to slipping of entangled polymer molecules in tension unless the unlikely assumption is made that the polymer molecules can "slip back" to their former position during unloading.

With reference to possible hydrogen bonding, it is interesting to consider the work of Onogi and Sasaguri[22] with respect to the correlation between the density and modulus of elasticity of various untreated papers. The structural fibrous network upon which their mathematical model is based is the same as the Rance model. The derived mathematical model predicts that the logarithm of the density plotted versus the logarithm of the dynamic modulus should yield a straight-line relationship. This relationship is borne out by their experimental evidence obtained on a wide variety of papers. A similar treatment of the data in Table I for treated papers compared to the untreated matrix is shown in Figure 3. Although not exact, a linear relationship is indicated with slope equal to about 3.0. The slopes of similar plots on various sheets tested by Onogi and Sasaguri ranged between 2 and 3.

Therefore, it would appear likely that secondary valence forces, possibly hydrogen bonds of the structure

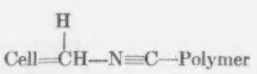

are responsible for the strength reinforcement. Polymer is deposited on the surface of the fiber, increasing the density of the paper and the number of fiber-fiber hydrogen bond junction points.

If polymerization of acrylonitrile in nonswelling solvents in the presence of cellulose results in a secondary bond formation between polymer and the exterior of the fiber, it is difficult to understand why polymerization in a different position (in the interior) of the fiber network would result in primary bond or graft copolymer formation.

The effect of the solvent used for acrylonitrile upon the retention of polymer in these treatments may be revealing in this connection. In a paper concerning the sorption of polymer on cellulose, Luce and Robertson[23] discuss the effect of the nature of the solvent and the swelling of the sorbent on the amount of polymer adsorbed on cellulose. The extent of sorption of polyvinyl acetate from benzene solution is found to depend markedly upon the degree to which the pulp has been swollen in pretreatments with various solvents. The sorptive capacity of cellulose for polyvinyl acetate from benzene for preswollen pulps for solvents used in the above investigation[23] is given in Table I.

Luce and Robertson[23] conclude that the extent of sorption measures the degree of swelling and is correlated with the properties of the swelling liquid.

The values above correspond roughly to the amount of polymer remaining in the paper treated with acrylonitrile in solutions of the solvents after extraction (see Table I). That the degree of swelling of the cellulose is related to the amount of unextractable polymer remaining in cellulose after similar treatments with gamma radiation has been more extensively studied by Usmanov et al.,[7] who state that graft polymer formation takes place in those cases where the cellulose is well wetted by the solvent for the acrylonitrile, and where the solvent is sorbed by the cellulose; this would thus further the penetration of the acrylonitrile into the intermolecular space of the cellulose.

The difficulty in quantitatively extracting polymers sorbed by cellulose from aqueous solutions has been examined by Bhargava et al.[24] If the paper is dried before extraction, in the case of the beater addition of polyvinyl acetate to pulp, Soxhlet extraction for 48 hr. with acetone removes only 66% of the sorbed polymer. Thus, it is observed that certain polymers when sorbed from water are "trapped" in the pulp matrix by subsequent drying. This example may well be analogous to the polymerization of monomers from swelling solvents.

The intention of the foregoing remarks is not to repudiate claims that graft copolymers may be formed with cellulose. Rather, it is to offer

a possible alternate explanation, most applicable to the internal polymerization of monomers from swelling liquids initiated by gamma radiation.

References

1. Mino, G., and S. Kaizerman, *J. Polymer Sci.*, **31**, 242 (1958).
2. Schwab, E., V. Stannett, and J. J. Hermans, *Tappi*, **44**, 251 (1961).
3. Daniel, J. H., Jr., S. T. Moore, and N. R. Segro, *Tappi*, **45**, 53 (1962).
4. Richards, G. N., *J. Appl. Polymer Sci.*, **5**, 539 (1961).
5. Chaudhuri, D. K., Ray, and J. J. Hermans, *J. Polymer Sci.*, **48**, 159 (1960).
6. Chadhuri, D. K. Ray, and J. J. Hermans, *J. Polymer Sci.*, **51**, 373 (1961).
7. Usmanov, Kh. U., B. I. Aĭkhodzhaev, and U. Azizov, *J. Polymer Sci.*, **53**, 87 (1961).
8. Geacintov, N., V. Stannett, E. W. Abrahamson, and J. J. Hermans, *J. Appl. Polymer Sci.*, **3**, 54 (1960).
9. Richards, G. N., *J. Appl. Polymer Sci.*, **5**, 558 (1961).
10. Lipson, M., and Speakman, *Nature*, **157**, 590, 736 (1946).
11. Landells, G., and C. S. Whewell, *J. Soc. Dyers Colourists*, **67**, 338 (1951).
12. Landells, G., and C. S. Whewell, *J. Soc. Dyers Colourists*, **71**, 171 (1955).
13. Lohani, B. K., L. Valentine, and C. S. Whewell, *J. Textile Inst.*, **49**, T265 (1958).
14. Boardman, N. K., and M. Lipson, *J. Soc. Dyers Colourists*, **69**, 335 (1953).
15. Kobayashi, Y., *J. Polymer Sci.*, **51**, 359 (1961).
16. Arthur, J. C., Jr., and R. J. Demint, *Textile Res. J.*, **30**, 505 (1960).
17. Demint, R. J., J. C. Arthur, Jr., and W. F. McSherry, *Textile Res J.*, **31**, 821 (1961).
18. Higgins, H. G., *APPITA*, **12**, 1 (July 1958).
19. Nissan, A. H., *Tappi*, **39**, 93 (1956).
20. Nissan, A. H., and H. G. Higgins, *Nature*, **184**, 1477 (1959).
21. Rance, H. F., *Tappi*, **39**, 104 (1956).
22. Onogi, S., and K. Sasaguri, *Tappi*, **44**, 874 (1961).
23. Luce, J. E., and A. A. Robertson, *J. Polymer Sci.*, **51**, 317 (1961).
24. Bhargava, R., H. A. Hoffman, and V. Stannett, *Tappi*, **38**, 383 (1955).

Synopsis

The strength reinforcement resulting from the radiation polymerization of acrylonitrile from nonswelling solvents in the presence of a cellulose matrix is lost with the extractable polymer. Study of the rheological behavior of the treated and extracted material indicates that the strength reinforcement is due to additional hydrogen bonds formed between the polymer and the cellulose fiber matrix. The amount of unextractable polyacrylonitrile remaining after polymerization from various solvents is compared with the ability of the solvent to swell cellulose. The data indicate that in the treatments described, polymer molecules may be physically trapped within the microfibril lumen, resisting extraction, rather than being grafted to the cellulose molecule.

Résumé

Le renforcement de la tension qui résulte de la polymérisation de l'acrylonitrile initiée par radiation à partir des solvants non-gonflants en présence d'une matrice de cellulose se perd par exraction des polymères. L'étude du comportement rhéologique du matériel traité et extrait indique que le renforcement de la tension est dû aux liaisons hydrogènes additionelles formées entre le polymère et la matrice de fibres de cellulose. On a comparé la quantité d'acrylonitrile qu'on ne peut pas extraire et qui reste après la polymérisation dans de différents solvants avec la capacité de faire gonfler le cellulose. Les données indiquent que, dans les traitements décrits, des molécules de polymère peuvent être

captées d'une manière physique dans le lumen microfibrillaire résistant à l'extraction plutôt que d'être greffées sur la molécule de cellulose.

Zusammenfassung

Die Festigkeitsverstärkung die durch Strahlungspolymerisation von Acrylnitril aus nicht-quellenden Lösungsmitteln in Gegenwart einer Cellulosematrix erzielt wird, geht mit der Extraktion des Polymeren wieder verloren. Eine Untersuchung des rheologischen Verhaltens des behandelten und extrahierten Materials zeigt, dass die Festigkeitsverstärkung auf einer Ausbildung zusätzlicher Wasserstoffbindungen zwischen dem Polymeren und der Cellulosefasermatrix beruht. Die Menge des nach der Polymerisation aus verschiedenen Lösungsmitteln zurückbleibenden nichtextrahierbaren Polyacrylnitrils wird mit der Quellfähigkeit des Lösungsmittels für Cellulose verglichen. Die Daten sprechen dafür, dass bei der beschriebenen Behandlung Polymermoleküle wahrscheinlich im Mikrofibrillenlumen physikalisch festgehalten werden und der Extraktion widerstehen und keine Aufpfropfung auf das Cellulosemolekül stattfindet.

JOURNAL OF POLYMER SCIENCE: PART C NO. 2, PP. 387–402 (1963)

Preparation and Characterization of Some Cellulose Graft Copolymers. Part I

H. YASUDA,* J. A. WRAY, and V. STANNETT,* *State University College of Forestry Syracuse, New York*

In recent years a voluminous literature concerning graft polymerization has appeared, and a recent review of this work has been presented by Smets.[1] In most cases however, the solubility differences between the graft copolymers and the two homopolymers are not large enough to allow adequate separation, and the actual composition of most of these materials is therefore not known. This is a serious gap in our knowledge, since many graft polymers are produced by heterogeneous reactions and by reactions such as chain transfer where considerable homopolymer formation may be anticipated. This is particularly true with radiation methods, where the degree of grafting is normally obtained as the increase in weight of a substrate after washing in a suitable solvent. In particular, the proportion of the original polymeric substrate which has grafted side chains attached is normally not known at all. Furthermore, the difficulty of removing occluded homopolymer by any simple means leads at best to only a maximum figure for the amount of grafting onto the substrate.

This lack of knowledge has prevented the establishment of any accurate picture of the mechanism and kinetics of grafting in most cases. Perhaps a more serious consequence is that no meaningful study of the properties of graft copolymers is possible until well defined grafts free from the two homopolymers become available. These should also have known structures from the point of view of the molecular weight and molecular weight distribution of the backbone and grafted side chains.

Recently, many of the methods of graft polymerization originally developed with synthetic polymers have been successfully applied to cellulose and its derivatives, and a number of interesting special methods have been described.[2] Apart from their intrinsic interest, cellulose graft polymers have the following two advantages from the point of view of composition studies: (*1*) the solubility difference between the cellulosic backbone and the grafted side chain polymer is usually sufficiently great to enable adequate separations to be made; (*2*) the cellulosic backbone can be hydrolyzed away, thus enabling the molecular weight and molecular weight distribution of the grafted side chains to be measured. A number of interesting preliminary results of such studies have recently been presented

* Present address: Camille Dreyfus Laboratory, Box 490, Durham, N. C.

by Huang, Immergut, and Rapson,[3] Kobayashi,[4] Goodman and Horowitz,[5] Richards,[6] and others.[2]

This present paper describes the results of a more detailed study of a number of cellulosic graft copolymers and, in the case of cellulose acetate–styrene copolymers, the isolation of the grafted products and a preliminary study of some of their properties.

PREPARATION OF THE GRAFT COPOLYMERS

Two types of films were used for the preparations: (*a*) unmodified cellophane, 0.02 mm. thick, specially prepared by the American Viscose Company; (*b*) cellulose acetate film 0.03–0.04 mm. thick, solvent-cast from cellulose acetate powder of degree of substition of 1.75 obtained from the Eastman Kodak Company.

The monomers and solvents used were all freshly distilled before use.

Cellulose–Acrylamide Grafts Prepared by the Ceric Ion Method

The grafting reaction was carried out in a 35-mm. diameter glass tube which was sealed onto a fritted glass filtering funnel which contained an extension on the narrow end of the funnel to allow nitrogen to pass through the monomer solution.

The procedure consisted of placing a piece of film and 100 ml. of 5% aqueous acrylamide solution in the vessel. Nitrogen was passed through this mixture for about a half hour to remove any oxygen and then 2.5 ml. of 0.1*N* ceric ammonium nitrate catalyst solution in 0.1*N* nitric acid was added to initiate polymerization. The reaction was allowed to proceed for a predetermined time, after which the film was removed from the solution, washed in boiling water, and placed in a vacuum oven at 60°C. to dry.

Cellulose–Acrylamide, Cellulose Acetate–Styrene, and Cellulose Acetate–Methyl Methacrylate Grafts

(a) **Ultraviolet Method.**[2,7] The cellulose–acrylamide samples were prepared in a regular Pyrex test tube, diameter 25 mm., of appropriate length which was equipped with a rubber stopper containing two glass tubes to allow purging of the monomer solution with nitrogen in order to remove the oxygen present.

The general procedure was to place a piece of cellophane of known weight into the tube; sufficient aqueous solution of 15% acrylamide containing 0.5% sodium 2,7-anthraquinonedisulfonate was then added to cover the film. The rubber stopper, fitted with the degassing tubes, was placed on the cell, and the cell was purged for about 1 hr. with oxygen-free nitrogen. After the purging was complete, the cell was placed in front of a G. E. H-400, E-1, 400-w. mercury lamp to initiate polymerization. The mercury lamp was connected to a G. E. ballast and the voltage was stabilized by a 500 Kv. G. E. transformer which regulated voltage at about 115 v. The reaction was carried out in a constant temperature bath at 30°C.

The cellulose acetate–styrene samples were prepared in a 25-mm. test tube which was modified with ground glass joints and a ground glass stopcock to permit removal of oxygen by degassing in a high vacuum system (10^{-5} mm.) by alternate freezing and thawing cycles.

The general procedure was to place the film in the bottom of the tube so that the entire area of one side of film clings to the wall of the tube. A solution of 10% dimethylformamide and 90% distilled styrene monomer (by volume) containing 2-methylanthraquinone (50 mg. dye for every 10 ml. solution) was added to cover the film. The mixture was then exposed to three cycles of freezing, degassing, and thawing to remove all oxygen. It should be mentioned that this degassing procedure was tried with the aqueous cellulose–acrylamide system, but had to be discontinued because the cellulose film fractured into many pieces during the treatment. After the cellulose acetate–styrene sample was degassed and sealed, the reaction tube was attached to the revolving portion of an electric stirring motor and placed in front of the 400-w. mercury vapor lamp. The sample was then rotated in an attempt to produce an even radiation dose within the film.

The cellulose acetate–methyl methacrylate samples were prepared essentially the same as for the cellulose acetate–styrene system, except the monomer was distilled into the tube. A piece of film was placed in the bottom of the reaction tube with a given amount of dye and degassed at room temperature for about 2 hr. The bottom of the tube was then immersed in liquid air, and methyl methacrylate was distilled under vacuum directly into the reaction tube. It was found that this monomer swelled the cellulose acetate film sufficiently and produced high yields in about 4 hr.

(b) Gamma-Ray Radiation Method. Grafts were prepared by both the mutual and preirradiation techniques with radiation from a Co^{60} radiation source.

The mutual method consisted of placing a weighed piece of film in the bottom of the reaction tube, adding a solution of 90% distilled styrene monomer and 10% distilled dimethylformamide, degassing three times by the freeze-thaw method, and finally sealing off the tube while under vacuum. The cell and its contents were then irradiated for a predetermined time and dose rate. The preirradiated polymers were prepared by irradiating the degassed film at room or dry ice temperature and then admitting the degassed monomer solution through a break seal on a high vacuum line at 0°C. The polymerization was then allowed to proceed at room temperature for two days.

ANALYSIS OF GRAFTED PRODUCTS

The method of analysis depended on the components of the grafting system. The initial aim was to establish how much actual grafting had occurred. Later the graft was isolated from the parent homopolymers and characterized with respect to the degree of polymerization of the side chains and a number of properties examined. The only materials examined in

detail were the cellulose acetate–styrene graft copolymers, and this system will be discussed first. In all cases the samples were washed free from accessible homopolymer with a suitable solvent to constant weight.

Cellulose Acetate–Styrene Grafts

These were analyzed by three different methods: (*1*) fractional extraction after the cellulose acetate was saponified to cellulose; (*2*) fractional precipitation; and (*3*) selective alternate extraction with solvents for the two homopolymers.

The first method was used to show whether grafting had indeed occurred. The method of Malm et al.[8] utilizing pyridine to ensure a homogeneous saponification system was used. After saponification the precipitate was washed with methanol and then extracted three times with benzene. The benzene extracts were combined and the extracted polymer isolated by evaporation, weighed, and the infrared spectra measured. The same procedure was repeated on physical mixtures of cellulose acetate and polystyrene. The infrared spectrum indicated that complete separation of the mechanical mixture had been achieved by the extraction method. The benzene-soluble portion of the grafted product showed the characteristic cellulose peaks, indicating a small amount of solubilization of the cellulose presumably by the grafting polystyrene side chains. Similarly, the benzene-insoluble portion showed clearly the characteristic polystyrene peaks. The cellulose peaks disappeared after hydrolysis with trifluoracetic acid.

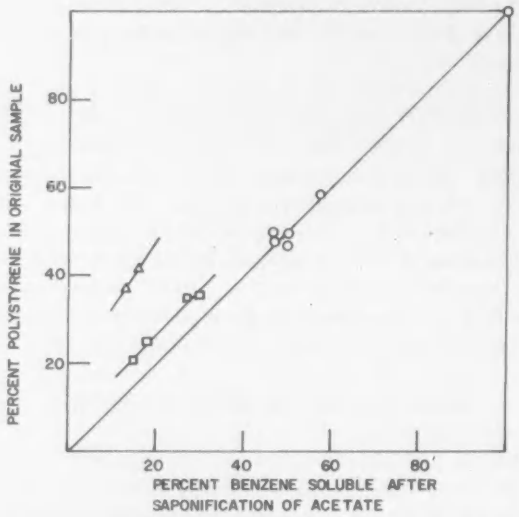

Fig. 1. Proof of grafting for styrene–cellulose acetate system: (O) physical mixture; (□) ultraviolet grafting (△) gamma preirradiation grafting.

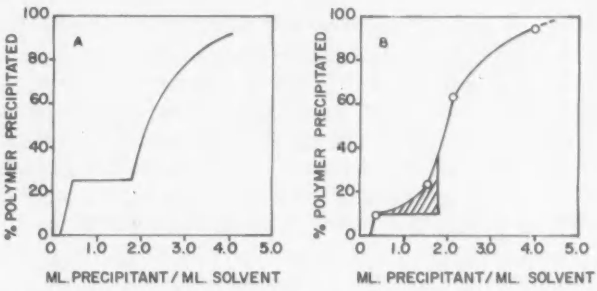

Fig. 2. Fractional precipitation curve for styrene–cellulose acetate (25–75 ratio) system: (*A*) physical mixture; (*B*) ultraviolet grafting. The shaded area is probably the region of graft copolymer precipitation.

The weights of both fractions were determined for a number of gamma-ray and ultraviolet-initiated grafted products, and the results are plotted in Figure 1. It can be clearly seen that a considerable quantity of the polystyrene is insoluble in benzene. Since the polymers were precipitated from solution in a fine, flocculent form, it seems reasonable to assume the insolubilization is caused by the grafted cellulose backbone. It is also interesting to note that the gamma-ray preirradiation product showed much more grafting than the ultraviolet products. This low yield of true graft with the ultraviolet method had been shown also by use of C^{14}-tagged alcohols and will be discussed in a later publication.[9] This method of separation indicates that grafting has occurred and gives a measure of the amount of polystyrene which is grafted but gives no indication of the amount of the original cellulose acetate which had grafted chains attached. It should be pointed out that the saponification process would also remove any grafted polystyrene attached to the ester groups. The reported percentages grafted polystyrene are probably therefore lower than reality.

The method of fractional precipitation from solution was used to throw more light on the composition of the grafted copolymer, and consisted of the following steps. About 0.3 g. of grafted sample (or physical mixture of polystyrene and cellulose acetate) was dissolved in 30 ml. of pyridine in a 100-ml. centrifuge tube. A slightly acid solution was prepared by adding 0.5 ml. of concentrated HCl to 100 ml. of distilled water. The aqueous HCl solution was added dropwise to the pyridine–polymer solution, slowly, while stirring with a magnetic stirrer. At an appropriate point in the fractionation procedure (when some apparent precipitation occurs) addition of the aqueous solution was stopped and the sample centrifuged. The supernatant liquid was decanted into another clean centrifuge tube, and the addition of the non-solvent was continued. The precipitate was redissolved in pyridine, poured into a tared aluminum weighing cup, dried under vacuum at room temperature until most of the solvent was evaporated, and then finally dried under vacuum at about 60°C. until constant weight. The weight of the polymer which was still soluble after about

TABLE I
Yields and Efficiency of Grafting Styrene Onto Cellulose Acetate Film

Technique	Irradiation time, hr.	Dose rate, r./hr.	Pick-up, %	Temperature during irradiation	Polystyrene in graft copolymer, %	Cellulose acetate in graft copolymer, %	Efficiency polystyrene grafting, %	Efficiency cellulose acetate grafting, %
U.V.	24		27.6	Room temp.	51.3	48.7	48.2	12.7
U.V.	24		29.4	Room temp.	71.4	28.6	32.3	3.8
U.V.	24		23.8	Room temp.	70.4	29.6	27.5	2.7
U.V.	24		21.9	Room temp.	70.1	29.9	25.8	2.4
U.V.	24		23.0	Room temp.	82.1	17.9	38.4	1.9
U.V.	24		19.5	Room temp.	78.2	21.8	50.0	3.2
U.V.	24		23.5	Room temp.	70.3	29.7	31.2	3.1
Mutual	45	21,200	148	Room temp.	73	27	30.5	16.8
Mutual	45	21,200	146	Room temp.	73	27	30.5	16.5
Mutual	22	21,200	107	Room temp.	77	23	36.8	11.7
Mutual	58	7,650	183	Room temp.	87	13	51.8	13.6
Mutual[a]	197	7,650	58	Room temp.	87	13	70.8	6.1
Preirr.	58	21,200	90	−78°C.	94	6	93.2	5.2
Preirr.[a]	204	21,200	34	−78°C.	96	4	98.8	1.5
Preirr.	22	21,200	31	Room temp.	85	15	92.0	5.3
Preirr.	23	21,200	45	Room temp.	83	17	94.5	8.8
Preirr.	23	21,200	42	Room temp.	80	20	93.5	9.7

[a] 2/3 of the monomer was replaced by toluene in this experiment.

25 ml. of water had been added was determined by placing the remaining solution in acetone, evaporating an aliquot to dryness and weighing the residue.

From data obtained in this way the precipitation curves shown in Figure 2 were obtained. It can be seen that a clean separation of polystyrene can be achieved by this method in the case of physical mixtures, but the grafted products show continuous precipitation. The infrared examination of the various fractions showed the gradual change from pure polystyrene to pure cellulose acetate. Although this method is useful for proving the presence of graft copolymer and for isolating small amounts it is not readily adapted to the separation of large amounts of graft.

The method of selective extraction was chosen to prepare larger quantities. It was found from examination of the homopolymers and the precipitated grafts that benzene was highly specific toward polystyrene and that a mixture of 70% acetone, 20% 2-ethoxyethanol, and 10% water was highly specific towards the grade of cellulose acetate used. Alternate extractions of the grafted films by these two solvents were continued until no further precipitate was obtained on pouring the extracts into methanol and benzene for the benzene and mixed acetone solvent extracts, respectively. The infrared spectra of the extracts showed no contamination of one polymer with the other.

Apart from enabling the preparation of larger quantities of graft copolymer, the selective extraction method made it possible to give maximum figures for the efficiency of the grafting process in terms of the percentage of each polymer actually combined in grafted form. These data are summarized in Table I for a number of preparations made in various ways. It is clear that with the preirradiation method nearly all the polymerized styrene is attached to the cellulose acetate, whereas the mutual radiation and the ultraviolet methods lead to large proportions of occluded homopolystyrene. These remarks apply to samples already washed free from accessible homopolystyrene, as noted in the experimental section. The situation with respect to the degree of grafting onto the cellulosic backbone itself is surprisingly different, even with the preirradiation method only a small percentage of the cellulose acetate has attached polystyrene side chains. In other words, even where most of the polymerization arises by a grafting mechanism, only a small fraction of the cellulosic substrate participates in the grafting process.

This is probably due to the lack of accessibility of the cellulose acetate to monomer under the heterogeneous conditions used. Many "graft" copolymers probably have similar compositions, but the lack of means for effecting the necessary separations has prevented this being known. The disappointing performance of many graft copolymers in their physical characteristics is undoubtedly due to this gross heterogeneity and to the great length of the grafted side chains as will be shown later.

A number of other observations can be made from the data collected in Table I and from other grafting experiments. The ultraviolet method gave

the greatest lack of reproducibility both in composition and in yield. The mutual method gave greater yields per total dose at lower dose rates, indicating the importance of diffusion of monomer in the grafting process. The preirradiation method gave increased yields when the irradiation was carried out at −78.5°C., presumably due to the prevention of migration and mutual termination of the radicals.

Cellulose–Acrylamide Grafts

These were analyzed by the technique described previously.[2,7] The grafts were completely dissolved in cuprammonium hydroxide solution and then acidified by the gradual addition with stirring of dilute hydrochloric acid. The solution was kept cold by immersing in an ice bath; this was

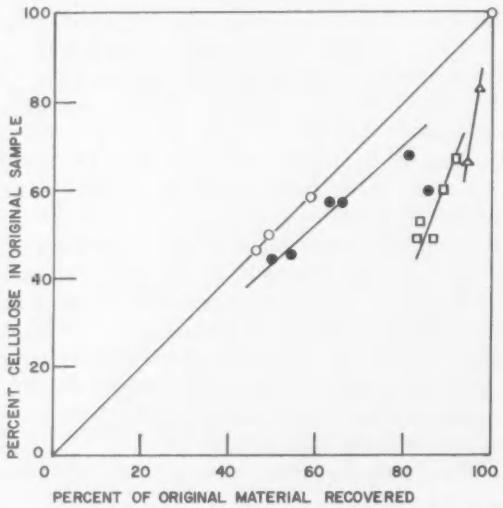

Fig. 3. Proof of grafting for acrylamide–cellulose system: (○) physical mixture; (●) ceric ion grafting; (□) ultraviolet grafting; (△) gamma preirradiation grafting.

found to be important, since acidification at higher temperatures resulted in removal, by hydrolysis, of the grafted side chains. After acidification the mixture was centrifuged, the precipitate washed with acid, distilled water, and finally methanol, dried at 60°C. under vacuum, and weighed. The method used with physical mixtures of polyacrylamide and cellulose showed complete separation by this method (see Fig. 3) it was assumed that any increase in weight over the original cellulose content was therefore due to grafted acrylamide. The results for a number of grafts prepared in different ways are shown in Figure 3. In all cases it is clear that grafting has indeed occurred. However the efficiency of the grafting is very different for the various methods, again the preirradiation technique is shown to give the greatest efficiency. The ceric ion method appears to

give a large amount of occluded homopolyacrylamide and this was confirmed by direct extraction with hot water. It should be emphasized that this method of analysis gives little idea of the efficiency of the grafting process as far as the cellulose is concerned, nor does it allow an estimate of the amount of cellulose solubilized by the grafted acrylamide.

Cellulose Acetate–Methyl Methacrylate Grafts

A number of these graft copolymers were analyzed by the fractional precipitation method. A mixture of 95% pyridine and 5% acetone was found to be a useful solvent with water as the precipitant. The data obtained

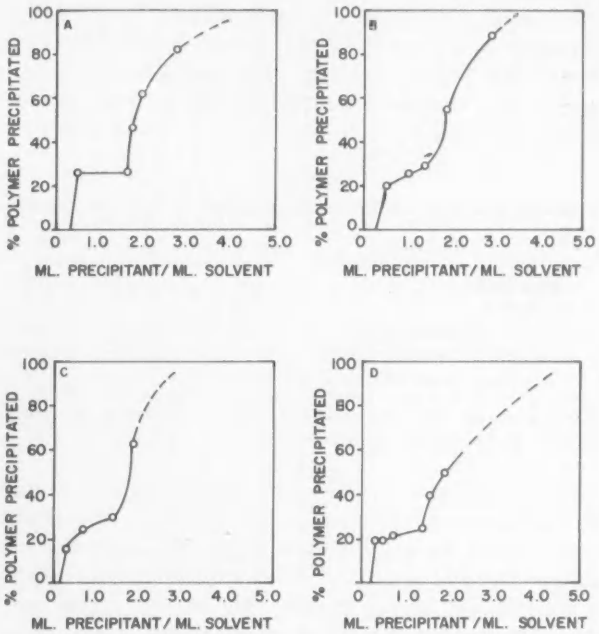

Fig. 4. Fractional precipitation curves for methyl methacrylate–cellulose acetate (25–75 ratio) system: (*A*) physical mixture; (*B*) gamma radiation mutual grafting; (*C*) gamma preirradiation grafting; (*D*) ultraviolet grafting.

are plotted in the usual way in Figure 4. In all three examples clear evidence of grafting was obtained; again, preirradiation was the most efficient, followed by the mutual method and the ultraviolet process. No other experiments were conducted on these graft copolymers.

COMPOSITION OF THE SEPARATED CELLULOSE ACETATE–STYRENE GRAFT COPOLYMERS

The composition of the graft copolymers was estimated from the selective extraction data and determined directly by hydrolysis of the weighed sam-

ple with trifluoracetic acid and reweighing. Excellent agreement was always found between the estimated and measured compositions.

The intrinsic viscosity of the original cellulose acetate was determined in dimethylformamide at 25°C. This solvent was chosen as it was found to dissolve also the polystyrene, the graft, and physical mixtures of the two homopolymers. No viscosity–molecular weight relationships are available for this grade of acetate or for this solvent. However an approximation could be made by using the relationship found for secondary acetate in acetone at 25°C.; this leads to a viscosity-average molecular weight of about 53,000. In order to check whether degradation occurs during the radiation, grafting experiments were conducted with α-methylstyrene replacing the styrene. This monomer has a similar affinity for radicals, but cannot propagate, and it was felt that this was a better control than radiation without a free radical acceptor. The results are recorded in Table II. It can be seen that no substantial change in intrinsic viscosity resulted for the doses used.

TABLE II
Effect of Radiation on Intrinsic Viscosity of the Cellulose Acetate

Treatment	$[\eta]$ in DMF at 25°C.
Unirradiated	1.02
Irradiated[a]	
U.V. irradiated, 24 hr.	0.99
γ-Rays (mutual), 1 Mrad	1.05
γ-Rays (preirradiation), 1 Mrad	0.96

[a] The irradiations were carried out under the same conditions as the grafting experiments but with α-methyl-styrene replacing styrene.

The viscosity-average molecular weight was determined for the polystyrene sides chains obtained by hydrolysis of a number of grafted samples. The results obtained are summarized in Table III, where the composition of the grafts is expressed in terms of the approximate number of polystyrene branches for cellulose acetate chains. The correct values can only be obtained from the number-average molecular weights, and consequently the results are in error by the ratio of the factors of the viscosity-average to number-average molecular weights for both polymers.

In spite of these limitations it is clear that the grafts consist of very few immensely long branches attached to each comparatively short cellulose acetate backbone. This is undoubtedly due to the growing radical chains being isolated in the cellulosic gel leading to delayed termination.[3,4] Diluting the monomer led, as expected, to shorter chains and to more side chains per cellulose acetate molecule.

In the case of one mutual radiation graft sample, the intrinsic viscosity was measured of the graft and of physical mixtures of the cellulose acetate and polystyrene obtained by hydrolysis of the same sample. The results are plotted in Figure 5. It can be seen that the physical mixtures give a

TABLE III
Characterization Data of some Polystyrene–Cellulose Acetate Graft Copolymers

Technique used	Irradiation time, hr.	Dose rate, r./hr.	Pick-up, %	Polystyrene in graft copolymer, %	(η) Polystyrene branches toluene, 25°C.	Calc. mol. wt. polystyrene branches[a]	Number polystyrene chains per cellulose acetate chain
Mutual	58	7,650	183	87	6.65	1.2×10^6	0.41
Mutual	197	7,650	58[b]	87	2.95	5.0×10^5	0.86
Preirr.	36	21,200	98	95	5.80	1.05×10^6	1.15
Preirr.	58	21,200	90	94	4.35	8.0×10^5	1.26
Preirr.	204	21,200	34[b]	96	2.60	4.37×10^5	3.44

[a] Calculated by use of the formula[12] $(\eta) = 1.89 \times 10^{-5} M^{0.91}$.
[b] Normal monomer system was changed to 30% styrene, 60% toluene, and 10% DMF.

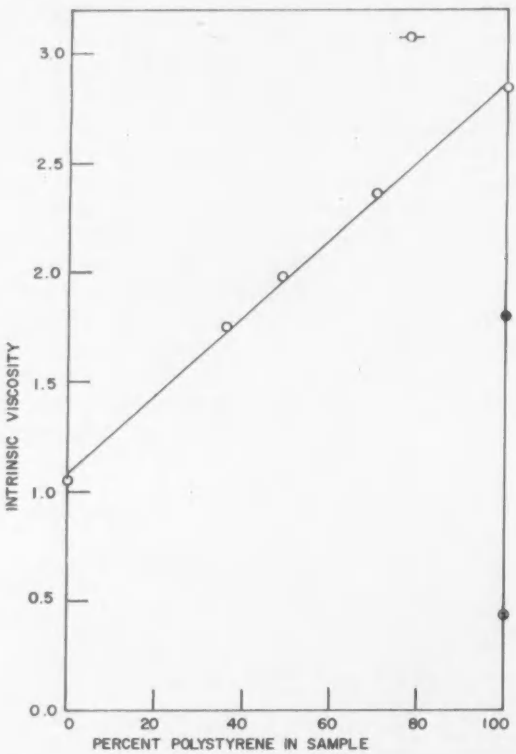

Fig. 5. Intrinsic viscosity in DMF at 25°C. of polystyrene–cellulose acetate systems: (O) physical mixtures; (–O–) graft copolymer; (●) extractable homopolystyrene from grafted film; (⊗) polystyrene produced in solution during grafting.

simple linear additive relationship, but the graft has a viscosity much higher than that of the corresponding physical mixture. Similar results have been reported by Chaudhuri and Hermans[10] and were presented as further proof of actual grafting. The intrinsic viscosities of the polystyrene produced in the free solution during the irradiation and of the homopolymer produced *in situ* are also shown in Figure 5. The results again demonstrate the importance of the gel effect in the grafting process; similar measurements made with the ultraviolet-initiated graft showed again the high molecular weight of the grafted and occluded polystyrene compared with the polymer produced in the free solution.

To check whether the very high molecular weights of the separated polystyrene could be due to association of, e.g., glucose units at the chain ends, the viscosity determinations were repeated in 1% butanol–99% benzene solutions. Similar intrinsic viscosities were obtained to those found in pure benzene, showing that no appreciable association had taken place.

PHASE EQUILIBRIA

Among the many interesting properties of graft copolymers are their solution properties and their apparent ability to render compatible physical mixtures of dissimilar polymers. The results of Anderson et al.[11] in measuring the tensile strength of blends of polystyrene and polyethylene compared with the graft copolymers and mixed graft and blends shows this effect clearly. It is also suggested by the extreme clarity, for example, of cellulose films to which large proportions of polystyrene have been grafted. Such products are known to contain large amounts of ungrafted polystyrene and cellulose.

It was thought of interest to study these phenomena with the separated grafted products we had available. Initially, a solution system was chosen since it is easier to reach equilibrium conditions; it is planned later to extend this work to the solid state.

The studies were conducted in the following way. Separate 5% solutions of cellulose acetate and polystyrene in dimethylformamide were prepared, from which given amounts of solution were measured into test tubes to give 5 cc. of mixture of the two polymers. At 5% all mixtures gave turbid solutions, and phase separation occurred after keeping overnight at constant temperature. If phase separation was observed, the solutions

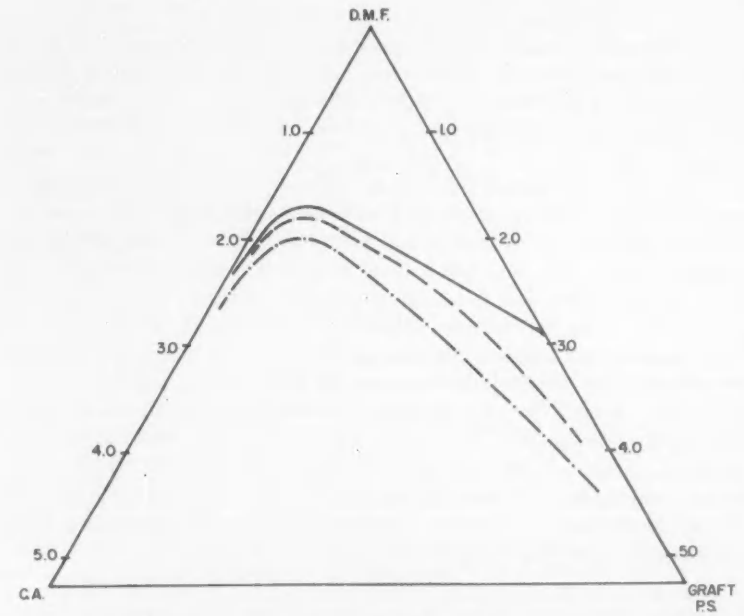

Fig. 6. Phase equilibria: (——) 85/15 styrene–cellulose acetate graft; (- -) polystyrene (obtained by hydrolysis of graft; (·—) polystyrene, m.w. = 50,000.

were shaken well and 0.5 cc. of solvent was added from an automatic buret with drying tubes. The test tubes were kept overnight again to examine the phase separation, and the same procedures were repeated until no phase separation was observed and the solution became completely clear. The weight per cent of polymer solution was calculated from the amount of solvent added. These critical concentrations were plotted in a ternary phase diagram and are shown in Figure 6. To make the comparisons valid, the polystyrene used was obtained by hydrolysis of a similar sample of the graft copolymer used. The effect of molecular weight of the polystyrene on the phase equilibria is shown in the same diagram. The phase diagrams for cellulose acetate and the graft copolymer are similar, except that the latter intercepts the copolymer base line. It can be seen that the graft is somewhat less compatible with the cellulose acetate than the polystyrene itself. This effect is probably due qualitatively to the solvated and expanded cellulose acetate backbone increasing the size of the polymer coil leading to interactions at lower concentrations. Since dimethylformamide is a poor solvent for polystyrene (the intrinsic viscosity is about one half that found in toluene for the same sample) and a good solvent for the grade of cellulose acetate used, this effect should be quite pronounced.

The observation was made that solutions of the pure graft copolymer became very thick and turbid at high concentrations, almost gellike in consistency, but no macroscopic phase separation occurred. Below about 3% the solutions became completely clear, as noted in Figure 6.

The graft polymer isolated and used is not too suitable for detailed study, since it consists mainly of polystyrene chains of extremely high molecular weight attached to a low molecular weight backbone. These phase equilibria studies are being continued, therefore, with more equally distributed graft structures.

During the separation of the graft copolymers, an interesting phenomena was observed. The cellulose acetate films used for grafting were cast from the solution of acetone–cellosolve–water mixed solvent. After the grafting process, the films are a little more brittle than the original cellulose acetate films but are still transparent. Upon immersing these grafted films into the acetone–cellosolve–water solvent, the films are no longer soluble and become opaque; at first the films swell up, and after extraction of the homocellulose acetate the films become smaller and very soft in the solvent. As soon as these films leave the solvent, they become stiff but are still opaque. On drying these films, white opaque films were obtained. However, on immersion of these white films in benzene, they become transparent and the size of the films become much smaller. On drying the films from benzene, transparent films are obtained. These processes are quite reversible.

We would like to thank the U.S. Army Research Office (Durham) for their generous sponsorship of this work; also Dr. H. Sumitomo and Mr. P. N. Grover for their help with the molecular weight determinations and radiation experiments.

References

1. Smets, G., and R. Hart, *Fortschr. Hochpolymer Forsch.*, **2**, 173 (1960).
2. Schwab, E., V. Stannett, and J. J. Hermans, *Tappi*, **44**, 251 (1961).
3. Huang, R. Y. M., E. H. Immergut, B. Immergut, and W. N. Rapson, *J. Polymer Sci.*, **A1**, 1257 (1963); *J. Polymer Sci.*, **51**, 368 (1961).
4. Kobayashi, Y., *J. Polymer Sci.*, **51**, 359 (1961).
5. Goodman, M., and C. Horowitz, I.U.P.A.C. Symposium on Macromolecular Chemistry, Montreal, August 1961.
6. Richards, G. N., *J. Appl. Polymer Sci.*, **5**, 539, 553, 558 (1961).
7. Geacintov, N., V. Stannett, and E. W. Abrahamson, *Makromol. Chem.*, **36**, 52 (1959); N. Geacintov, V. Stannett, E. W. Abramhamson, and J. J. Hermans, *J. Appl. Polymer Sci.*, **3**, 54 (1960).
8. Malm, C. J., L. B. Genung, R. F. Williams, and M. A. Pile, *Ind. Eng. Chem., Anal. Ed.*, **16**, 501 (1944).
9. Geacintov, N., Ph.D. Thesis, Syracuse, N.Y., 1961.
10. Chaudhuri, D. K. R., and J. J. Hermans, *J. Polymer Sci.*, **48**, 159 (1960).
11. Anderson, L. C., D. A. Roper, and J. K. Rieke, *J. Polymer Sci.*, **43**, 423 (1960).
12. Hengstenberg, J., and G. V. Schulz, *Makromol. Chem.*, **2**, 5 (1948).

Synopsis

The following graft copolymers were prepared by use of the ceric ion, ultraviolet light, mutual radiation, and preirradiation methods: (*1*) cellulose–acrylamide, (*2*) cellulose acetate–styrene, and (*3*) cellulose acetate–methyl methacrylate. Fractional precipitation and extraction methods were developed to show proof of grafting and to estimate the efficiency of the grafting process. It was shown that only a small proportion of the cellulosic chains participated in the grafting reaction under heterogeneous conditions. On the other hand, the vinyl polymer was present from 30% to nearly 100% in grafted form. The cellulose acetate–styrene graft copolymer was isolated from the homopolymers by a fractional extraction technique and the molecular weight of the side chain determined after hydrolysis of the cellulose backbone. In general, grafts consisted of very long polystyrene side chains attached to comparitively short cellulose acetate backbone chains. The solubility behavior of such grafts was shown to be quite different from that of the corresponding physical mixtures. The graft polymers were less soluble than either of the homopolymers alone. The graft polymer was found to tolerate less cellulose acetate in a mutual solvent than the polystyrene itself.

Résumé

En faisant usage d'ions cériques, de lumière U.V., de méthodes d'irradiation simultanée et de préirradiation, on a préparé les copolymères greffés suivants (*1*) cellulose-acrylamide, (*2*) acétate de cellulose–styrène, (*3*) acétate de cellulose–méthacrylate de méthyle. On expose les méthodes de précipitation fractionnée et d'extraction qui servent à mettre le greffage en évidence et à estimer l'efficacité du processus de greffage. On a montré qu'il n'y avait qu'une faible proportion des chaînes cellulosiques qui participait à la réaction de greffage dans des conditions hétérogènes. D'autre part le polymère vinylique était présent sous forme de greffon à raison de 30 à près de 100%. On a isolé le copolymère greffé acétate de cellulose–styrène des homopolymères par une technique d'extraction fractionnée et on a déterminé le poids moléculaire de la chaîne latérale après hydrolyse de la chaîne cellulosique principale. En général, les greffés sont constitués de très longues chaînes latérales attachées à des chaînes principales d'acétate de cellulose relativement courtes. On montre que la solubilité de tels polymères greffés est tout à fait différente de celles du mélange physique correspondant. Les polymères

greffés sont moins solubles que chacun des homopolymères seuls. Le polystyrène greffé tolère moins d'acétate de cellulose dans un solvant mutuel que le polystyrène seul.

Zusammenfassung

Folgende Pfropfcopolymeren wurden mit Cer-4-ionen, UV-Licht, gegenseitiger Verzögerung und Vorbestrahlung erhalten: (*1*) Cellulose–Acrylamid, (*2*) Celluloseacetat–Styrol und (*3*) Celluloseacetat–Methyl–methacrylat. Zum Nachweis der Aufpfropfung und zur Bestimmung der Aufpfropfungsausbeute wurde fraktionierte Fällung und Extraktion verwendet. Es wurde gezeigt, dass nur ein kleiner Teil der Celluloseketten an der Pfropfungsreaktion unter heterogenen Bedingungen teilnimmt. Andererseits wurde das Vinylpolymere zu 30% bis nahezu 100% aufgepfropft. Das Pfropfcopolymere aus Celluloseacetat–Styrol wurde von den Homopolymeren durch fraktionierte Extraktion getrennt und das Molekulargewicht der Seitenketten nach Hydrolyse der Cellulosehauptkette bestimmt. Im allgemeinen bestanden die Pfropfcopolymeren aus sehr langen Polystyrolseitenketten, die an, im Verhältnis dazu, kurze Celluloseacetathauptketten gebunden waren. Das Löslichkeitsverhalten dieser Substanzen war von dem der entsprechenden physikalischen Mischungen recht verschieden. Die Pfropfpolymeren waren weniger löslich als jedes der beiden Homopolymeren allein. Das Pfropfpolymere zeigte in einem gemeinsamen Lösungsmittel eine geringere Verträglichkeit mit Celluloseacetat als Polystyrol selbst.

JOURNAL OF POLYMER SCIENCE: PART C NO. 2, PP. 403–414 (1963)

Ceric Ion-Initiated Polymerization of Acrylonitrile in the Presence of Alcohols

A. A. KATAI, V. K. KULSHRESTHA, and R. H. MARCHESSAULT,
Cellulose Research Institute, State University College of Forestry, Syracuse, New York

I. Introduction

Several detailed studies have appeared on the mechanism and kinetics of polymerization involving ceric ions and alcohol systems.[1–4] The proposed mechanistic and kinetic schemes have been based on an important simplifying feature of the systems studied, viz. that the rate of initiation is equal to one-half the rate of disappearance of ceric ion. When pinacol was the organic reducing agent, the evidence overwhelmingly supported this simplification.[4] Thus, it was found that in the presence of a radical scavenger, the reaction sequence:

$$\mathrm{Ce(IV) + CH_3{-}\overset{\displaystyle CH_3}{\overset{|}{C}}{-}\overset{\displaystyle CH_3}{\overset{|}{C}}{-}CH_3 \xrightarrow{k_1} Ce(III) + H^+ + (CH_3)_2C{=}O + (CH_3)_2C{-}OH}$$

$$\mathrm{(CH_3)_2\dot{C}{-}OH + Ce(IV) \xrightarrow{k_2} (CH_3)_2C{=}O + Ce(III) + H^+}$$

wherein the number of moles of Ce(IV) reduced just equals the moles of acetone formed, was changed so that the ratio of acetone to Ce(IV) reduced became 1:2. This indicates that the intermediate is indeed a radical species which was terminated by reaction with ceric ion.

There is evidence, however, that other glycol reducing agents do not allow a similar simplification in their kinetic treatment. Preliminary studies on ethylene glycol,[5] for example, showed that the reaction scheme:

$$\mathrm{\begin{matrix}CH_2{-}OH\\|\\CH_2{-}OH\end{matrix} + Ce(IV) \rightarrow \dot{C}H_2OH + HCHO + H^+ + Ce(III)}$$

where the ratio of Ce(III) to formaldehyde is 1:1, was not obeyed. The observed ratio was nearly 2:1, suggesting that the formaldehyde had been further oxidized by ceric to formic acid.[6,7] Unpublished studies on the oxidation of the methyl glycoside of xylose showed a ceric ion consumption far greater than might be accountable by the obvious, simple reactions of

the vicinal alcohol groups.[8] Finally, it has been shown that the rate of attack by ceric ions on the glycol moieties of polyvinyl alcohol is considerably faster than on the normal head-to-tail structures.[3]

These facts suggest that the radical generating step in ceric–alcohol redox reactions is not generally as straightforward as for the pinacol system. In view of the above as well as of the possible application of the ceric–alcohol redox systems to synthesize graft copolymers of polysaccharide materials, a generalized study of the kinetics was undertaken. The system under study involved water, ethylene glycol, ceric sulfate and acrylonitrile. The choice of the latter being based on the fact that acrylonitrile is sufficiently water soluble to allow an initially homogeneous reaction system. On the other hand, the polymer is quite hydrophobic thereby complementing the hydrophilic properties of cellulose when the above system is used for bringing about polymerization inside the fiber matrix.

II. Theoretical Considerations

The generalized reactions to be expected in a system containing aqueous solution of ethylene glycol, ceric sulfate, sulfuric acid, and acrylonitrile are the following:

$$\mathrm{Ce(IV)} + \mathrm{A} \overset{K}{\rightleftarrows} \mathrm{B} \overset{k_d}{\rightarrow} \mathrm{A}\cdot + \mathrm{HCHO} + \mathrm{Ce(III)} + \mathrm{H}^+ \tag{1}$$

$$\mathrm{A}\cdot + \mathrm{M} \overset{k_i}{\rightarrow} \mathrm{M}\cdot \tag{2}$$

$$\mathrm{Ce(IV)} + \mathrm{M} \overset{k_i'}{\rightarrow} \mathrm{M}\cdot + \mathrm{Ce(III)} + \mathrm{H}^+ \tag{3}$$

$$\mathrm{M_n}\cdot + \mathrm{M} \overset{k_p}{\rightarrow} \mathrm{M_{n+1}}\cdot \tag{4}$$

$$\mathrm{M_n}\cdot + \mathrm{Ce(IV)} \overset{k_t}{\rightarrow} \mathrm{M_n} + \mathrm{Ce(III)} + \mathrm{H}^+ \tag{5}$$

$$\mathrm{A}\cdot + \mathrm{Ce(IV)} \overset{k_0}{\rightarrow} \text{oxidation products} + \mathrm{Ce(III)} + \mathrm{H}^+ \tag{6}$$

where Ce(IV) is ceric ion or any inorganic complex thereof, M is monomer (acrylonitrile), A is alcohol (ethylene glycol), k's are rate constants for the reactions, K is an equilibrium constant, and B is ceric–alcohol complex. Reaction (1) is similar to the one proposed by Duke and co-workers[9,10] and used by Mino and Kaizerman.[1] It is in accordance with the findings of Offner,[11] whereby ceric forms 1:1 complexes with alcohols. Reaction (3) accounts for the fact that ceric ion is capable of initiating homopolymerization even in the absence of sensitizers.[12–14]

Preliminary experiments in this laboratory indicated that the amount of polyacrylonitrile formed in the absence of alcohol is by no means negligible and that the ratio of the rates of propagation (rates of polymerization, R_p) of comparable systems in the presence and absence of alcohol is about 3 (see Table I). Convincing evidence has been provided[4] that the termina-

tion reaction, eq. (5), involves ceric ion. Similar experiments in this laboratory with the ethylene glycol system led to the same conclusion.[5]

TABLE I
Rate of Polymerization of Acrylonitrile in the Presence and Absence of Ethylene Glycol at [Ce (IV)] = 0.025 mole/l. at 35°C.

	[A] = 0.5 mole/l.		[A] = 0		
[M], mole/l.	R_p, g./l. hr.	$R_p/[M]^2$	R_p', g./l. hr.	$R_p'/[M]^2$	R_p/R_p'
0.10	0.12	12	0.060	6.0	2.0
0.25	1.04	17	0.364	5.8	2.9
0.50	6.40	26	1.88	7.5	3.4

In view of the foregoing it is proposed that the kinetics of ceric ion initiated polymerization of acrylonitrile can best be represented by reactions (1), (2), and (3) as initiation steps, reaction (4) as propagation, and reaction (5) as termination. This leads to the expressions:

$$d[M\cdot]_{Ce}/dt = k_i'[M][Ce(IV)] \tag{7}$$

$$d[M\cdot]_{A\cdot}/dt = k_i[M][A\cdot] \tag{8}$$

$$-d[M]/dt = R_p = k_p[M][M\cdot] \tag{9}$$

$$-d[M\cdot]/dt = k_t[M\cdot][Ce(IV)] \tag{10}$$

Applying the steady-state assumption to both [M·] and [A·] separately and assuming that the equilibrium between ceric ion and alcohol to form complex is established rapidly compared to the rate at which the complex is decomposed, one obtains the following expression for the rate of polymerization:

$$R_p = \frac{k_p}{k_t}[M]^2\left\{k_i' + \frac{k_dK[A]}{[M] + (k_0/k_t)[Ce(IV)]}\right\} \tag{11}$$

Equation (11) shows a square dependence on the monomer concentration in the absence of alcohol. However, when alcohol is present the extent of deviation from the square dependence is determined by the magnitude of [M] versus $(k_0/k_t)[Ce(IV)]$. The initial rate of polymerization is directly proportional to the concentration of alcohol, therefore, an initial R_p versus [A] plot at a particular monomer concentration should yield a straight line. It is noteworthy that the rate of polymerization is inversely related to the ceric ion concentration. This leads to the interesting situation where the rate of polymerization at low ceric concentration may actually be greater than at high ceric concentration.

Kinetic equations involving the disappearance of ceric ion due to reaction with alcohol, alcohol radical, monomer, and polymer radical, lead to the following expression:

$$\left(\frac{-1}{[\mathrm{Ce(IV)}]}\right)\frac{d[\mathrm{Ce(IV)}]}{dt} = 2\left\{k_d K[\mathrm{A}] + k_i'[\mathrm{M}]\right\} \tag{12}$$

Equation (12) represents the relationship that governs the ceric ion disappearance in a relatively easily verifiable form. However, this equation does not give an entirely accurate description of the processes involved, since Ce(IV) was conveniently defined as the sum of all inorganic species involving tetravalent cerium. This is evidently an oversimplification, from which eq. (12) implies that all these species form identical complexes with the same dissociation constants, and that all these complexes react at the same rate with alcohol. To correct for this oversimplification, a more comprehensive relationship has been derived taking into account the constants governing the various equilibria involving ceric and sulfate ions. This equation can be written as follows:

$$-d[\mathrm{Ce(IV)}]/dt = 2[\mathrm{A}][\mathrm{Ce}_0]f[\mathrm{SO_4^-}] \tag{13}$$

where Ce_0 refers to the concentration of uncomplexed ceric ion and $f[\mathrm{SO_4^-}]$ is a cubic function of the sulfate concentration. The latter dependence, for which there is good experimental justification, underlines the importance of controlling ionic concentrations in these ceric ion systems. In the present study all measurements were made at constant ionic strength.

III. Experimental

Ceric solution was standardized with sodium oxalate by a method described in the literature,[15] and also with standard ferrous sulfate, the titer of which was determined against potassium permanganate. It was found that ceric solutions in the presence of acid are stable and no concentration changes were noted upon storage in well stoppered bottles even after many months.

The apparatus used to study the rate of polymerization of acrylonitrile is shown in Figure 1.

For reactions in the presence of ethylene glycol, two solutions were made up totaling 400 ml. Solution I contained ceric sulfate, sulfuric acid and water. It was found that the volume change on mixing is negligible (<0.1%). The two solutions were thermostatted at 35.0 ± 0.1°C. and were flushed with nitrogen using an ice condenser to retain the water taken up by the dry gas. After 25 min. of flushing, the solutions were mixed.

In the absence of glycol all reagents were measured into the reaction vessel with the exception of acrylonitrile which was added at the start of the reaction.

After all the reactants were measured in, totaling 400 ml. less the acrylonitrile (2–8 ml.), nitrogen was bubbled into the system (see Fig. 1). The nitrogen was passed through a calcium chloride drying tube (A) and was passed by a safety outlet (L) which consisted of a test tube filled with mercury to let the nitrogen out if the pressure should increase in the line. The nitrogen entered the flask through the three-way stopcocks (B) and (D) and tube (G). It left the flask through the ice condenser (I) and stopcock (J). After 25 min. the condenser (I) was lifted off, and the proper amount of acrylonitrile was added while nitrogen was still bubbling in order to keep the oxygen out. A mercury-seal stirrer (H) was used to keep the mixture homogeneous even after the precipitation of polymer.

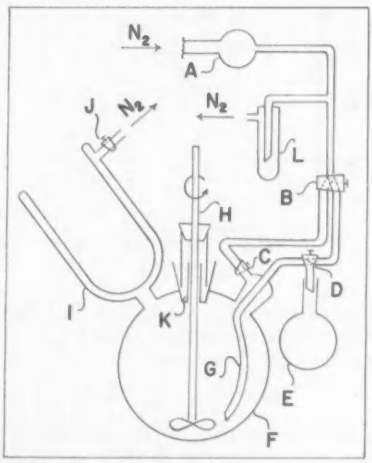

Fig. 1. Apparatus for kinetic study.

Samples were taken by letting nitrogen through stopcocks (B) and (C) with stopcock (J) closed. The liquid thereby rose in tube (G) and through stopcock (D) it filled the 50 ml. volumetric flask (E). The mercury seal (K) acted as a safety valve against pressure increase in the reaction vessel, by letting the excess nitrogen escape through the mercury. The sample withdrawn was washed into a solution of ferrous sulfate to stop the reaction. The excess was back titrated to determine the ceric concentration of the reaction mixture. The precipitated polymer was filtered out of the mother liquor with a fine pore fritted disc crucible. The crucible and precipitate was washed thoroughly with dilute sulfuric acid, followed by distilled water, and was dried at 70°C. under vacuum until no decrease in weight was observed. Knowing the original dry weight of the crucible the weight of the polymer was determined by difference.

IV. Results

To test the dependence of R_p on the concentration of monomer, a series of experiments were performed at constant ceric and alcohol concentration with varying [M]. The results of these experiments are shown in Figure 2.

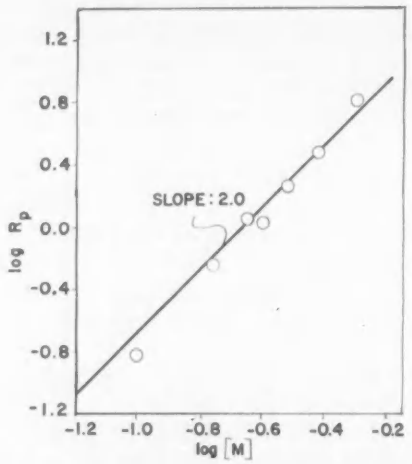

Fig. 2. The rate of polymerization of acrylonitrile as a function of monomer concentration. Composition of reaction mixture: [Ce(IV)] = 0.025 mole/l., [A] = 0.5 mole/l., [H_2SO_4] = 0.2 mole/l., [$SO_4^=$] = 0.1 mole/l.

By plotting log R_p against log [M], a straight line is obtained with slope very nearly 2 as required by eq. (11) if [M], in the denominator, is small compared to (k_0/k_t)[Ce(IV)]. By setting [A] = 0, eq. (11) becomes:

$$R_p = (k_p/k_t)k_i'[M]^2 \tag{14}$$

The measurement of R_p as a function of [M] in the absence of alcohol was complicated by an unexpected adhesion of the newly formed polymer to the wall of the reaction vessel. As a result of this, the experimental error was considerably higher than when alcohol was present. However, the near constancy of the quantity $R_p'/[M]^2$ (cf. Table I) points to the validity of the postulated square dependence. Although the ratio $(R_p/R_p'$ in Table I) of the equivalent rates, with and without alcohol, does not vary in the expected direction, its magnitude indicates clearly that homopolymerization is a significant factor in these circumstances.

The general dependence of the rate of polymerization on alcohol concentration is shown in Figure 3, where the rate of polymerization for experiments at [A] = 0.25, 0.50 and 0.75 mole/l. with initial [M] = 0.09 mole/l.

are plotted against alcohol concentration. Extrapolation of the data to [A] = 0 shows reasonable agreement with data obtained in the absence of alcohol, bearing in mind the greater experimental error of the latter measurements.

The corresponding plot for ceric ion disappearance as a function of alcohol concentration is shown in Figure 4 which indicates clearly that the major consumption of this species is due to reaction of Ce(IV) with glycol. The added drain on the ceric ion concentration due to initiation and termination of the polymerization is negligibly small at [A] = 0. The effect of monomer concentration on ceric ion reduction is illustrated by the data of Table II.

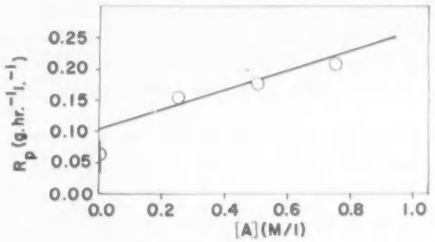

Fig. 3. Rate of polymerization as a function of alcohol concentration for initial [M] = 0.09 mole/l.

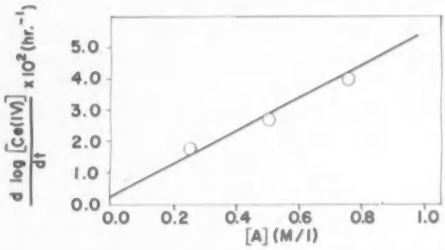

Fig. 4. Rate of ceric ion consumption as a function of alcohol concentration for initial [M] = 0.09 mole/l.

Quite obviously, consumption due to monomer is relatively small compared to that due to glycol. In fact, in a series of first-order plots of log [Ce(IV)] versus t at fixed [A], monomer concentrations ranging from 0 to 0.375 mole/l., the change in rate of ceric disappearance was less than the experimental error. Since the rate of polymerization is appreciable even in the absence of alcohol, it follows that of the free radicals A· produced by reaction (1), only a small percentage initiate polymer chains, while the remaining either recombine or react further with Ce(IV) in accordance with reaction (6). Even at relatively high monomer concentration, the ceric ion reduction due to acrylonitrile is less than 9% of the total reduction.

TABLE II
Decrease of Ceric Ion Concentration for Comparable Systems. Reaction Time: 10 hr.

[M], mole/l.	[Ce(IV)] reduced, mole/l.		Sum of reductions due to [M] only + 0.0141
	[A] = 0	[A] = 0.5 mole/l.	
0.00	0.0000	0.0141	0.0141
0.10	0.0003	0.0142	0.0144
0.25	0.0010	0.0147	0.0151
0.50	0.0013	0.0152	0.0154

The dependence of ceric ion reduction on acrylonitrile can be evaluated in the absence of alcohol. From eq. (12) a straight-line dependence was expected, whereas the data of Figure 5 shows an initial linear portion with subsequent curving off. The latter effect is probably due to the increasing heterogeneity of the propagation and termination reactions at higher

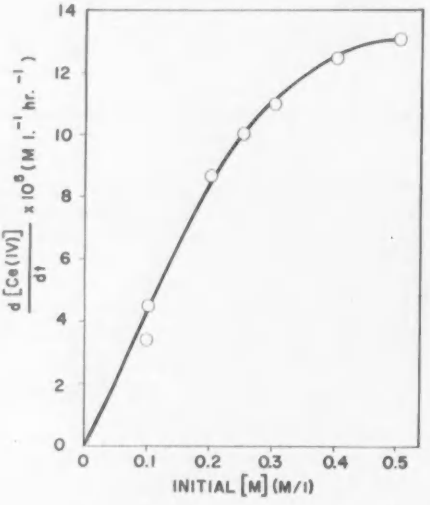

Fig. 5. Dependence of the rate of ceric ion reduction on the concentration of monomer in the absence of alcohol.

monomer concentration equivalent to a decrease in k_p and k_t with increasing monomer concentration. This could develop if the effective monomer concentration were less than the real one due to heterogeneity of the propagation reaction or complexing of the monomer with ceric.[4] It should be remembered that polyacrylonitrile is insoluble in the reaction medium, hence, growing polymer radical may become increasingly inaccessible to ceric ions with respect to termination.

V. Discussion

From the foregoing data several of the basic rate constants for the kinetic scheme outlined above can be evaluated. Thus, from the initial slopes of Figures 4 and 5, the constants k_t and k_dK can be evaluated, while the intercept of Figure 3 is equivalent to $R_p = k_t(k_p/k_t)[\mathrm{M}]^2$, from which the important ratio k_p/k_t can be evaluated. Finally, an average value of k_0/k_t can be derived from the ratios R_p/R_p' of Table I by using eq. (18). The constants and ratios are: $k_t' = 9 \times 10^{-3}$ l./mole hr., $k_0/k_t = 50$; $k_dK = 6.1 \times 10^{-2}$ l./mole hr., $k_p/k_t = 30$. Since k_0 and k_t are the rate constants for the consumption of A · by Ce(IV) and by M, respectively, the magnitude of the k_0/k_t ratio clearly indicates that only a small percentage of the total alcohol radicals initiate polymerization while the remainder are consumed by reaction with ceric ion. (At high alcohol concentrations disproportionation and combination reactions between alcohol radicals must be considered.)

By comparison with most free radical polymerizations the ratio k_p/k_t cited above is remarkably large. This can only be understood if termination and propagation in this system are similar reactions, i.e., the former cannot be due to a free radical combination. This assumption was made in deriving the kinetic scheme presented above. Mino et al.[2] arrived at the same conclusion on the basis of other considerations.

With values for these constants in hand, it is instructive to return to eq. (11) in order to appreciate their significance. Thus, the value of k_0/k_t being considerably greater than unity ensures that the term $(k_0/k_t)[\mathrm{Ce(IV)}]$ is always greater than [M], assuring the square dependence of R_p on monomer as observed. With a water-soluble monomer such as acrylamide, much higher monomer concentrations would be attainable; hence, the $[\mathrm{M}]^2$ dependence is not expected to hold at high monomer concentrations or at extremely low ceric ion concentrations. However, the present system may be said to be typical of what might be used if it is desired to graft a water insoluble polymer onto cellulose. The square dependence of R_p on monomer concentration is therefore a desirable feature from a practical point of view, but it tends to favor the formation of a relatively high molecular weight polymer.

Under polymerization conditions where termination is only by combination of growing polymer chains, the relatively large value for k_p/k_t would ensure that the polymer has a large molecular weight. The present kinetic system predicts a number-average degree of polymerization:

$$\bar{P}_n = k_p[\mathrm{M}]/k_t[\mathrm{Ce(IV)}] \qquad (15)$$

Since the ceric ion concentration was 0.025 mole/l., a molecular weight of about 4,000 to 10,000 is expected under the conditions used in the present experiments. Although molecular weights were not measured, it is almost certain that the gel-like polymer which formed in the absence of alcohol

was in this low molecular weight range. With alcohol present, there is of course a much more efficient initiation system, but there is also a wastage of ceric ions due to reaction (10). If ceric ion is always the principal terminating species, then increased molecular weights are to be expected in the presence of alcohol. However, there is always the probability of termination by other species than Ce(IV) particularly alcohol radicals. This probability increases with the ratio of [A]/[Ce(IV)].

Recent experiments[16] in this laboratory with the use of radioactive ethanol (0.02 mole/l.), ceric ammonium nitrate (0.005 mole/l.), and acrylonitrile (0.75 mole/l.) have shown that under these conditions at least 45% of all polymer molecules have been both initiated and terminated by alcoholic radicals. This means that in the above reaction scheme, a second termination process involving biradical combination, should be considered under certain conditions.

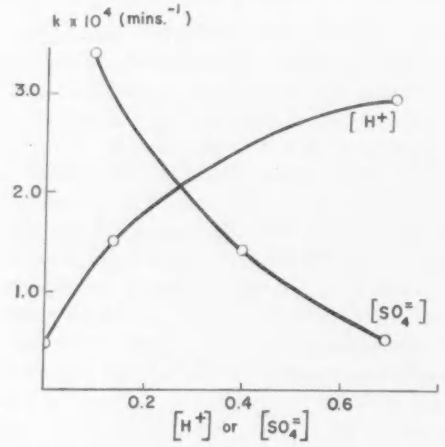

Fig. 6. Effect of hydrogen ion and sulfate ion concentration on rate of ceric ion reduction. For both curves: [A] = 0.5 mole/l., [Ce(IV)] = 0.025 mole/l. For varying sulfate ion: $[H_2SO_4] = 0.2$ mole/l.; for varying hydrogen ion $[SO_4^{=}] + [HSO_4^{-}] = 0.9$ mole/l.

The ceric system and other similar redox processes involving alcohols, present a complexity which is often not appreciated on first inspection. The complexity derives mainly from the numerous molecular complexes which are possible in these systems. The complexes are known to involve inorganic anions, alcohols, and possibly some monomers.[4] The various complexes have different reactivities toward alcohols, hence, any change in conditions which affects the relative concentration of the complexes will change the absolute and relative values of k_d, k_t, k_0. Such changes are bound to affect the rate of polymerization. In the ceric ion–sulfuric acid–sulfate system, for example, the concentrations of the various species are

interrelated by a series of equilibria. Although the exact nature of the complexes is not known, it seems that sulfate ions are involved. Thus, in a set of experiments wherein at constant initial glycol and ceric concentration the disappearance of the latter was followed at various [$SO_4^=$] levels, a sixfold change in the rate was observed. The results are shown in Figure 6. The effect of hydrogen ion is the reverse, i.e., the rate increases with increasing [H^+]. For these reasons, values of the rate constants derived from this study are valid only for the particular conditions of ceric, hydrogen and sulfate ions used. The effect of varying the sulfate ion concentration has been studied in detail and will be discussed elsewhere.

Since ceric ion polymerization systems have been extensively used to modify cellulosic fibers, one may ask what major advantage is there for this technique as a means of modifying cellulosic fibers. Unquestionably it is the potential for easy, direct attachment of the synthetic chain to the cellulose substrate, bearing in mind that not all conditions will favor this reaction. For certain desired results, direct attachment may not be important. On the other hand it is likely to be all important when substantial modification of the physical properties is the aim. It may safely be stated that complete control of the ceric system with respect to size and distribution of the added chains has not yet been achieved.

The financial support of the American Cyanamid Co. is gratefully acknowledged as well as guidance and advice from Dr. J. J. Hermans.

References

1. Mino, G., and S. Kaizerman, *J. Polymer Sci.*, **31**, 243 (1958).
2. Mino, G., S. Kaizerman, and E. Rasmussen, *J. Polymer Sci.*, **38**, 393 (1959).
3. Mino, G., S. Kaizerman, and E. Rasmussen, *J. Polymer Sci.*, **39**, 523 (1959).
4. Mino, G., S. Kaizerman, and E. Rasmussen, *J. Am. Chem. Soc.*, **81**, 1494 (1959).
5. Brase, P., unpublished results, quoted in Master's Thesis by A. A. Katai, State University College of Forestry, Syracuse, N. Y. (1963).
6. Hargreaves, G., and L. H. Sutcliff, *Trans. Faraday Soc.*, **51**, 1105 (1955).
7. Smith, G. F., and F. R. Duke, *Ind. Eng. Chem., Anal. Ed.*, **15**, 120 (1943).
8. Glaudemans, C. P. J., American Viscose Corporation, Marcus Hook, Pa., private communication.
9. Duke, F. R., and R. F. Bremer, *J. Am. Chem. Soc.*, **73**, 5179 (1951).
10. Duke, F. R., and A. A. Forist, *J. Am. Chem. Soc.*, **71**, 2790 (1949).
11. Offner, H. G., Doctoral Thesis, Stanford University, Palo Alto, California (1957).
12. Park, H. F., U. S. Pat. 2,485,535, October 18, 1949.
13. Richards, G. N., *J. Appl. Polymer Sci.*, **5**, 539 (1961).
14. Saldick, J., *J. Polymer Sci.*, **19**, 73 (1956).
15. Willard, H. H., H. Furman, and C. E. Bricker, *Elements of Quantitative Analysis*, 4th Ed., Van Nostrand, Princeton, N. J., 1956, p. 240.
16. Sankalia, S. M., Master's Thesis, State University College of Forestry, Syracuse, N. Y. (1963).

Synopsis

The polymerization of acrylonitrile in the presence of an aqueous ceric sulfate-ethylene glycol solution was investigated as a model system for cellulose graft copolymerization. The rate of polymerization R_p was directly proportional to the square of the monomer

concentration, linear with alcohol concentration, and inversely related to the concentration of ceric ion. The rate of ceric ion reduction was proportional to the initial ceric concentration and linear with the initial concentration of monomer and alcohol. A reaction scheme, involving initial complexing between ceric ion and alcohol, was proposed to account for the data. Evaluation of the ratio k_p/k_t (where k_p is rate constant for propagation and k_t is the termination constant) showed that these two constants were of similar magnitude, contrary to the usual results for free radical systems, wherein k_t is several orders of magnitude greater than k_p. It was concluded that propagation and termination are similar processes.

Résumé

On a étudié la polymérisation de l'acrylonitrile en présence d'une solution aqueuse de sulfate cérique-éthylène glycol en tant que système modèle pour la copolymérisation greffée sur la cellulose. La vitesse de polymérisation (R_p) est directement proportionnelle au carré de la concentration en monomère, linéaire avec la concentration en alcool, et inversément reliée à la concentration en ions cériques. La vitesse de réduction des ions cériques est proportionnelle à la concentration cérique initiale et linéaire avec la concentration initiale en monomère et alcool. Pour expliquer les résultats on propose un schéma de réaction impliquant une complexation initiale entre l'ion cérique et l'alcool. L'évaluation du rapport k_p/k_t (où k_p est la constante de vitesse de propagation et k_t la constante de terminaison) montre que ces deux constantes sont du même ordre de grandeur, contrairement aux résultats habituels pour des systèmes radicalaires, où k_t est supérieur de plusieurs ordres de grandeur à k_p. On conclut que la propagation et la terminaison sont des processur similaires.

Zusammenfassung

Die Polymerisation von Acrylnitril in Gegenwart einer wässrigen Cersulfat-Äthylenglykollösung wurde als Modellsystem für die Cellulose-Pfropfcopolymerisation untersucht. Die Polymerisationsgeschwindigkeit (R_p) war dem Quadrat der Monomerkonzentration direkt proportional, besass eine lineare Abhängigkeit von der Alkoholkonzentration und stand in inverser Beziehung zur Cerionenkonzentration. Die Geschwindigkeit der Reduktion der Cerionen war der Ausgangskonzentration des Cers proportional und verlief linear mit der Ausgangskonzentration an Monomerem und Alkohol. Zur Darstellung der Versuchsergebnisse wurde ein Reaktionsschema mit anfänglicher Komplexbildung zwischen Cerionen und Alkohol aufgestellt. Die Ermittlung des Quotienten k_p/k_t (wo k_p die Geschwindigkeitskonstante des Wachstums und k_t die des Abbruchs ist) zeigte, dass im Gegensatz zu den üblichen Ergebnissen für radikalische Systeme, bei welchem k_t um mehrere Grössenordnungen grösser als k_p ist, diese beiden Konstanten ähnliche Grösse besitzen. Daraus wurde geschlossen, dass es sich bei Wachstum und Abbruch um ähnliche Prozesse handelt.

JOURNAL OF POLYMER SCIENCE: PART C NO. 2, PP. 415–422 (1963)

Grafting of Styrene on Cellulose Acetate Films

H. SOBUE, K. MATSUZAKI, H. KOMAGATA, and A. ISHIDA,
Faculty of Engineering, The University of Tokyo, Bunkyo-ku, Tokyo, Japan

INTRODUCTION

In order to elucidate the mechanism of graft polymerization or to investigate properties of graft polymers, it is necessary to have information on the structure of the graft polymers obtained. For this purpose, the grafted side chains have been isolated from the backbone of some graft polymers, e.g., rubber[1] and cellulose,[2] and the molecular weight of the grafted side chains have been determined. Cellulose acetate is also suitable for this purpose, and the graft polymerization[3] of styrene on this polymer by means of γ-rays have been investigated. In this study, styrene in methanol was grafted on cellulose triacetate films which had been preirradiated by γ-rays in air, and the grafted polymer was isolated from the trunk polymer. The relation of grafting conditions to the molecular weight of the grafted polymer, the degree of grafting and graft efficiency and also the effect of dilution with methanol were investigated.

EXPERIMENTAL

Materials

Cellulose triacetate films (DP = 380, thickness = 0.1 or 0.2 mm., acetic acid content = 60.8%) were used as trunk polymer. The films were prepared from a solution of cellulose triacetate (a product of Dainippon Celluloid Co. Ltd.) in methylene chloride, soaked in benzene for 4 hr., dried *in vacuo* at room temperature, and stored in a desiccator before use. Styrene monomer was washed successively with aqueous sodium hydroxide, aqueous sodium bisulfite, and water to remove the inhibitor, dried over calcium chloride, distilled under reduced pressure, and stored at 0°C. Methanol was dried over anhydrous calcium sulfate and distilled under atmospheric pressure.

Grafting by Preirradiation Techniques

About 0.35 g. of the cellulose triacetate film was placed in a glass ampule and irradiated by γ-rays from a Co^{60} source at 2.3×10^5 r/hr. for 24 hr. at 0°C. in air. After irradiation, styrene monomer and methanol were

charged; the total volume of the monomer solution was kept at 6 ml. The ampule was sealed at a pressure of ca. 10^{-4} mm. Hg after repeated freezing and thawing and heated to various temperatures.

After various times of standing, the ampule was opened. The films were separated from the solution and washed with cold benzene several times. The solution was poured into methanol. The precipitate formed, i.e., homopolystyrene produced outside the films (in the polymerized solution), was filtered, dried, and weighed. The films were dissolved in methylene chloride and the solution was poured in methanol. The precipitate was cut into small pieces and subjected to Soxhlet extraction with benzene to remove the homopolystyrene produced inside the films. The degree of grafting (DG) and the graft efficiency (E_g) were calculated from eqs. (1) and (2):

$$\text{DG} = \frac{\text{Wt. grafted polystyrene}}{\text{Wt. trunk cellulose triacetate}} \tag{1}$$

$$E_g = \frac{\text{Wt. grafted polystyrene}}{\text{Wt. grafted polystyrene} + \text{wt. homopolystyrene}} \tag{2}$$

Isolation of the Grafted Polystyrene

The polystyrene grafted to the acetyl groups was isolated by alkali saponification. The residue after the extraction of homopolystyrene was dissolved in methylene chloride. Ethanolic potassium hydroxide solution was added to the solution to contain 0.6 g. of potassium hydroxide per gram of the trunk cellulose triacetate. After storage for 24 hr., the mixture was precipitated into methanol and subjected to extraction with benzene for removal of polystyrene grafted to acetyl groups. The residue, that is cellulose and polystyrene grafted onto cellulose, was subjected to acid hydrolysis to isolate the grafted polystyrene. The graft copolymer was treated with $5N$ hydrochloric acid for 1 hr. at 100°C. The residue after the treatment was soluble in benzene and consisted of polystyrene grafted at places other than acetyl groups.

The homopolystyrene produced outside and inside the films, the polystyrene grafted to acetyl groups and elsewhere and the residue obtained by the alkali saponification treatment were identified by means of infrared spectroscopy. Viscosities of the grafted polystyrene and homopolystyrene in benzene solution were measured at 30 ± 0.05°C. and the values of $[\eta]$ (in 100 ml./g.) were obtained. The number-average degree of polymerization was calculated from eq. (3):[4]

$$\overline{\text{DP}}_n = 1770\ [\eta]^{1.40} \tag{3}$$

RESULTS AND DISCUSSION

Isolation of the Grafted Polystyrene

On comparing the infrared spectrum of graft copolymer (Fig. 1) with that of the residue obtained by alkali saponification (Fig. 2), it is obvious that acetyl groups were saponified into hydroxyl groups by the alkaline treatment described above.

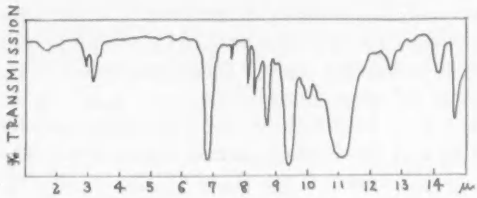

Fig. 1. Infrared spectrum of graft copolymer.

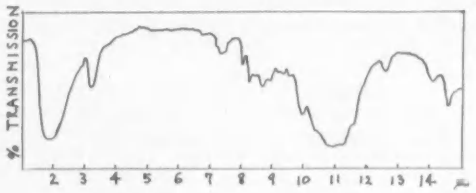

Fig. 2. Infrared spectrum of the residue obtained by alkali saponification.

Results of the isolation of grafted polystyrene by alkali saponification and acid hydrolysis and values of $[\eta]$ of the isolated material are shown in Table I. Table I suggests that 40–50% of the branched polystyrene was grafted onto acetyl groups.

TABLE I
Isolation of the Grafted Polystyrene[a]

Degree of grafting	Polystyrene isolated by alkali saponification		Polystyrene isolated by acid hydrolysis	
	Fraction	$[\eta]$	Fraction	$[\eta]$
0.27	0.50	3.50	0.50	3.50
0.34	0.46	5.04	0.54	5.10
0.59	0.48	5.57	0.52	5.56
0.80	0.36	7.00	0.64	—
0.98	0.40	6.74	0.60	6.90

[a] Grafting condition: same as in the experiments in Table II.

Effect of Dilution with Methanol

Studies on the polymerization of styrene in methanol which causes precipitation of the polymer have been carried out by Mark et al.,[5] who investigated benzoyl peroxide-catalyzed polymerization, and by Chapiro,[6] who used γ-ray irradiation to initiate reaction. In such a heterogeneous solution polymerization, below a certain monomer concentration, the polymer separates as a gelatinous precipitate, and increased rates and molecular weights are observed.

On the other hand, Sakurada et al.[7] reported that in the case of grafting styrene onto cellulose good results were obtained when styrene monomer was diluted with methanol; these authors suggested that methanol accelerates monomer diffusion into cellulose.

Table II and Figure 3 show the effect of monomer concentration on the degree of grafting and the number-average degree of polymerization ($\overline{DP}_n$) of the grafted polystyrene. Table II gives the number of grafted poly-

TABLE II
Effect of Monomer Concentration on the Degree of Grafting and the Number-Average Degree of Polymerization ($\overline{DP}_n$) of the Grafted Polystyrene[a]

Styrene content, vol.-%	Degree of grafting	$\overline{DP}_n$ of the grafted polystyrene	Number of the grafted polystyrene chains $\times \frac{1.04}{N_A} \times 10^7$
100	0.98	25,600	3.8
75	0.34	16,200	2.2
60	0.59	19,600	3.0
50	0.80	27,100	3.0
25	1.25	39,000	3.2
12.5	0.01	—	—

[a] Grafting conditions: temperature, 50° C.; time, 24 hr.; film thickness, 0.2 mm.

styrene chains per gram of trunk cellulose triacetate as calculated from the $\overline{DP}_n$ of the branched polystyrene and the degree of grafting (DG) by eq. (4):

Number of grafted polystyrene chains/gram substrate

$$= \frac{(DG) \times N_A}{(\overline{DP}_n) \times 104} = \frac{(DG)}{(\overline{DP}_n) \times 10^{-5}} \times \frac{N_A}{1.04} \times 10^{-7} \qquad (4)$$

where N_A is Avogadro's number, and 104 is the molecular weight of the polymerizing unit of polystyrene. Table II and Figure 3 show that the degree of polymerization of the grafted polystyrene and the degree of grafting decreased with diminishing monomer concentration down to 75

vol.-% styrene, then rose and reached a maximum at about 25% styrene. At this concentration, the $\overline{DP}_n$ of the grafted polystyrene was higher than that of the grafted polystyrene at 100% styrene. In the range from 100 to 75% styrene, the polystyrene produced outside the films was soluble in the reaction solution. Below 60% styrene, the polystyrene separated as a precipitate and the films turned opaque as the reaction proceeded. Thus, the increased $\overline{DP}_n$ of the grafted polystyrene and the precipitated homopolystyrene produced outside the films were in the same range. This might suggest that the increased $\overline{DP}_n$ of the grafted polystyrene was due to a reduction of the rate of termination arising from a decrease of mobility of the propagating polymer radicals in the films. The number of grafted polystyrene chains changed little below 60% styrene. Then, the increase of $\overline{DP}_n$ of the grafted polystyrene may account for the increase of degree of grafting with dilution.

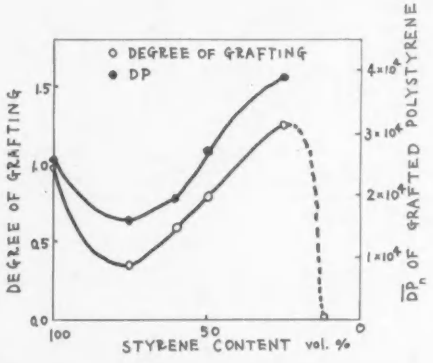

Fig. 3. Effect of monomer concentration on the degree of grafting and the number-average degree of polymerization ($\overline{DP}_n$) of the grafted polystyrene. Grafting temperature, 50°C.; grafting time, 24 hr.

The effect of film thickness on the degree of grafting and the $\overline{DP}_n$ of the grafted polystyrene is shown in Table III. In grafting for 3 hr. at 50°C. the degree of grafting onto 0.1 mm. films, was about twice as much as that onto 0.2 mm. films, but in grafting for 7 and 24 hr., the degree of grafting and the number of grafted polystyrene chains were not much affected by film thickness.

The degree of grafting at 50, 80, and 100°C. in grafting for 6 hr. is shown in Table IV. At 80 and 100°C., a larger degree of grafting was observed when styrene was diluted with methanol.

Figure 4 shows the effect of monomer concentration on the weight of the homopolystyrene produced inside and outside the films per gram of trunk cellulose triacetate along with the graft efficiency. In the range of 50–

TABLE III
Effect of Film Thickness on the Degree of Grafting and the $\overline{DP}_n$ of the Grafted Polystyrene[a]

Film thickness, mm.	Styrene content, vol.-%	Grafting time, hr.	Degree of grafting	Grafted polystyrene	
				$\overline{DP}_n$	Number of chains $\times$ $(1.04/N_A)$ $\times 10^7$
0.1	50	3	0.05	—	—
0.1	50	7	0.71	24,600	2.9
0.1	50	24	0.99	29,900	3.3
0.1	100	3	0.09	—	—
0.1	100	7	0.62	18,600	3.3
0.1	100	24	1.33	36,300	3.7
0.2	50	3	0.03	—	—
0.2	50	7	0.62	21,400	3.0
0.2	50	24	0.80	27,100	3.0
0.2	100	3	0.05	—	—
0.2	100	7	0.78	23,700	3.3
0.2	100	24	0.98	25,600	3.8

[a] Grafting condition: temperature, 50° C.

TABLE IV
Degree of Grafting at Various Temperatures[a]

Styrene content, vol.-%	Grafting temp., °C.	Degree of grafting
25	50	0.31
25	80	0.24
25	100	0.23
100	50	0.22
100	80	0.07
100	100	0.02

[a] Grafting conditions: time, 6 hr.; film thickness, 0.2 mm.

25% styrene, good graft efficiency was obtained, which may be due to the reduction of the weight of the homopolystyrene produced outside the films with dilution.

Relation Between the Grafted Polystyrene and the Homopolystyrene Produced Inside the Films

Although the homopolystyrene produced inside the films was much less than the grafted polystyrene except at 100% styrene, both of these quantities showed the same variation with dilution (Fig. 4). The number-average degrees of polymerization of the homopolystyrene produced inside the films and of the grafted polystyrene were almost the same, as shown in

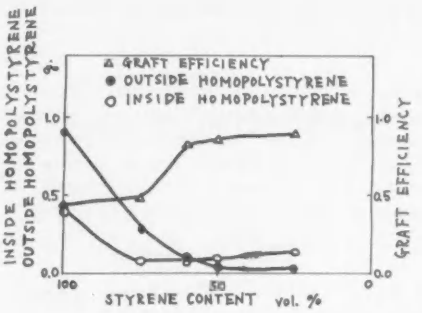

Fig. 4. Effect of monomer concentration on graft efficiency. Grafting temperature, 50°C.; grafting time, 24 hr.; film thickness, 0.2 mm.

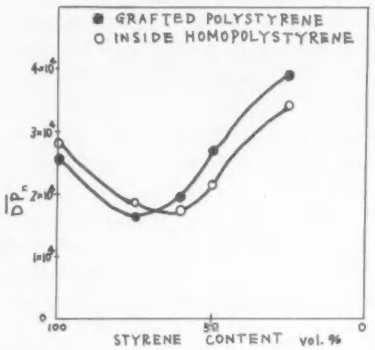

Fig. 5. DP_n of the grafted polystyrene and the homopolystyrene produced inside the films. Grafting temperature, 50°C.; grafting time, 24 hr.; film thickness, 0.2 mm.

Figure 5. It seems that the homopolystyrene produced inside the films and the grafted polystyrene polymerize by the same mechanism.

References

1. Cooper, W., G. Vaughn, and P. W. Madden, *J. Appl. Polymer Sci.*, **1**, 329 (1959).
2. Huang, R. Y.-M., *J. Polymer Sci.*, **51**, 368 (1961) (in discussion).
3. Matsuda, T., K. Hayakawa, and K. Kawase, *Kobunshi Kagaku*, **19**, 318 (1962).
4. Tobolsky, A. V., *J. Am. Chem. Soc.*, **74**, 938 (1952).
5. Abere, J., G. Goldfinger, G. Naidus, and H. F. Mark, *J. Phys. Chem.*, **49**, 211 (1945).
6. Chapiro, A., *J. Chim. Phys.*, **47**, 747 (1950).
7. Sakurada, I., T. Okada, and F. Kimura, *Sen-i Gakkaishi*, **18**, 687 (1962).

Synopsis

Styrene in methanol was grafted on cellulose triacetate films which had been pre-irradiated by γ-rays in air, and the grafted polymer was isolated from the trunk polymer. The relation of grafting conditions to the molecular weight of the grafted polymer, the

degree of grafting and graft efficiency and also the effect of dilution with methanol were investigated.

Résumé

On a greffé du styrène, en solution dans le méthanol, sur des films de triacétate de cellulose, préalablement irradiés avec des rayons-γ dans l'air. Le polymère greffé a été séparé du polymère de départ. On a étudié la relation entre les conditions de travail pendant le greffage et le poids moléculaire du polymère greffé, le degré de greffage et l'efficacité de greffage, ainsi que de la dilution dans le méthanol.

Zusammenfassung

Styrol in Methanol wurde auf Cellulosetriacetatfilme aufgepfropft, die mit γ-Strahlen in Luft vorbestrahlt worden waren; dass aufgepfropfte Polymere wurde vom Rumpfpolymeren abgetrennt. Die Abhängigkeit des Molekulargewichts des aufgepfropften Polymeren, des Aufpfropfungsgrades und der Pfropfungsausbeute von den Reaktionsbedingungen sowie auch der Einfluss der Verdünnung mit Methanol wurde untersucht.

JOURNAL OF POLYMER SCIENCE: PART C NO. 2, PP. 423-427 (1963)

Confirmation d'une Hypothese de P. H. Hermans: Chaîne de la Cellulose II

T. PETITPAS, M. OBERLIN, et J. MERING *Institut National de Recherche Chimique Appliquée, Paris, France*

P. H. Hermans a développé dans plusieurs travaux[1,2] l'aspect stéréochimique de la configuration moléculaire de la cellulose en rapprochant des données connues en chimie, comme les distances interatomiques et les angles de valence, du résultat obtenu au moyen de l'étude par les rayons X donnant pour la longueur de 2 groupes glucose (ou 1 groupe cellobiose) 10,3 Å. De ces considérations il résulte que la succession des groupes glucose est plus ou moins en "zig-zag" et que deux alternatives sont possibles: une forme appelée par P. H. Hermans zig-zag purement vertical et une autre obtenue en combinant un zig-zag vertical et horizontal. Dans cette deuxième alternative on a une chaîne plus plate qui permet des liaisons hydrogène le long de la chaîne elle-même (en plus des liaisons entre chaînes). On remarque aussi que l'on peut passer d'une forme à l'autre par une rotation autour des liaisons glucosidiques. (La Figure 1 donne un schéma très idéalisé de ces deux formes en projection sur le plan moyen de la chaîne.)

Il semble que par la suite cet aspect de la question de la structure de la cellulose ait été un peu abandonné et que l'on ait implicitement admis un seul modèle de chaîne. Ce modèle résulte du travail quantitatif fait par Meyer et Misch[3] sur la cellulose native à partir des données des intensités des diagrammes de rayons X. Si l'on construit une chaîne avec les coordonnées des atomes données par Meyer et Misch on voit qu'elle correspond à la forme zig-zag purement vertical, un peu distordue. Un peu plus tard d'autres auteurs, par exemple Pierce,[4] avaient suggéré quelques modifications à cette chaîne.

D'autre part il avait été admis jusqu'à maintenant que le passage de la cellulose I (native) à la cellulose II (mercerisée) n'affecte que l'arrangement des chaînes dans la maille, la chaîne individuelle étant supposée identique dans les deux formes de cellulose. Mais il n'existait pas pour la cellulose II de travail d'analyse de structure comparable à celui de Meyer et Misch pour la cellulose I.

Si l'on aborde par une méthode quantitative l'étude de la structure de la cellulose II (méthode plus "directe" que celle de Meyer et Misch), on trouve que non seulement la maille a changé mais que le modèle de chaîne valable pour la cellulose I n'est plus valuable pour la cellulose II.

La méthode dite "directe" a été décrite en détails dans plusieurs travaux.[5,6] Cette méthode consiste à calculer à partir d'une photométrie précise des diagrammes de rayons X, c'est-à-dire à partir de données expérimentales et sans faire d'hypothèse, une probabilité de répartition $P(\rho)$ des distances interatomiques ρ définies en longueur et en direction. Dans une fibre orientée la distribution $P(\rho)$ est à symétrie cylindrique. Elle couvre toutes les distances aussi bien entre les atomes d'une chaîne qu'entre les atomes appartenant à des chaînes différentes, mais si l'on

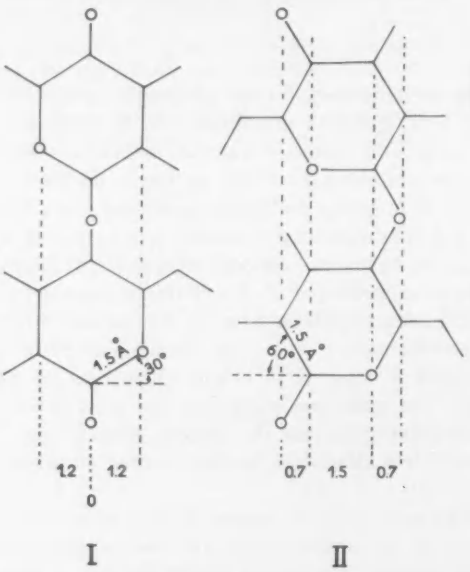

Fig. 1. Deux modèles de l'unité cellobiose considérés par P. H. Hermans: (*I*) zig-zag purement vertical (modèle de Meyer et Misch); (*II*) zig-zag vertial et horizontal.

considère seulement la partie centrale de $P(\rho)$ qui de ce fait correspond à de petites distances, on est renseigné sur la structure de la chaîne d'une manière indépendante de l'organisation des chaînes. C'est de cette façon que nous avons pu voir que la chaîne de la cellulose II diffère de celle de la cellulose I.

Pratiquement, pour des raisons techniques développées précédemment,[5] la distribution $P(\rho)$ a été remplacée par ses projections: horizontale, $P(r)$, r est la projection horizontale de ρ et verticale, $P(y)$, y est la projection de ρ sur l'axe de fibre.

Sur la Figure 1 on reconnaît à gauche le modèle de Meyer et Misch (modèle I) et à droite le modèle suggéré par P. H. Hermans (modèle II), plus plat. On peut prévoir ce que doit être pour chaque modèle la forme de la distribution $P(r)$.

a. Modèle I. Le modèle I comporte des liaisons "presque verticales" il doit en résulter un maximum de distribution à l'origine de $P(r)$. Les directions des autres liaisons se répartissent autour d'une moyenne d'environ 30° avec l'horizontale. La longueur approximative des liaisons C—C et C—O se situant autour de 1,5 Å on doit s'attendre à un maximum de $P(r)$ au voisinage de $r = 1{,}5 \cos 30° \cong 1{,}3$ Å.

b. Modèle II. Le modèle II comporte des liaisons "presque horizontales" ce qui doit donner lieu à un maximum situé un peu au-dessous de $r = 1{,}5$ Å. Les directions des autres liaisons se répartissent autour d'une moyenne d'environ 60° avec l'horizontale, le maximum de $P(r)$ doit se situer au voisinage de $r = 1{,}5 \cos 60° \cong 0{,}75$ Å.

La Figure 2 reproduit les portions centrales de $P(r)$ tracées expérimentalement pour la cellulose I (ramie) et pour la cellulose II (fortisan). On voit que les maximums observés se placent assez bien aux positions prévues d'aprés les modèles. Ainsi la courbe relative à la cellulose I confirme pour

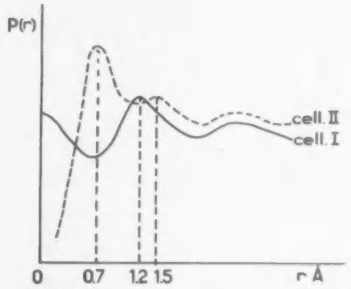

Fig. 2. Portion centrale de la projection horizontale, $P(r)$, de la probabilité de répartition des distances interatomiques; courbes expérimentales pour la cellulose I (ramie) et la cellulose II (fortisan).

celle-ci la configuration de Meyer et Misch, la courbe relative à la cellulose II est en meilleur accord avec la configuration en "zig-zag" à la fois vertical et horizontal.

Ces résultats relatifs à $P(r)$ sont confirmés par la distribution verticale $P(y)$. On voit sur la Figure 3, courbe du milieu, la distribution $P(y)$ obtenue expérimentalement pour la cellulose II. La distribution $P(y)$ est plus confuse, présente plus de pics que la distribution $P(r)$, aussi on ne peut pas prévoir sa forme d'après les schémas comme on l'a fait pour $P(r)$. Il a été nécessaire de construire une courbe "synthétique" complète correspondant à chaque modèle et de confronter chacune avec la courbe expérimentale. C'est ainsi que sur la Figure 3 on a représenté en haut la courbe synthétique correspondand au modèle I et dans la partie inférieure la courbe synthétique correspondant au modèle II. Les maximums observés de la courbe du milieu coincident en nombre et en position avec la courbe synthétique infèrieure relative au modèle II.

En conclusion on peut dire que le modèle de chaîne de Meyer et Misch valable pour la cellulose I ne se conserve pas dans la cellulose II. La configuration de la chaîne de la cellulose II, peut être représentée par le modèle en "zig-zag" à fois horizontal et vertical proposé par P. H. Hermans en partant de considérations stéréochimiques.

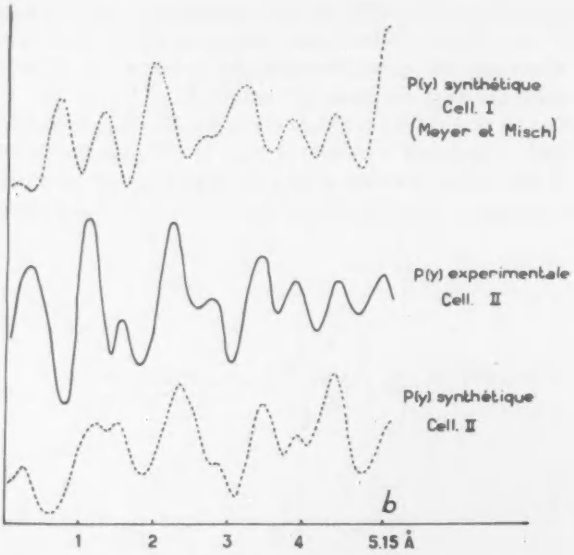

Fig. 3. Projection verticale, $P(y)$, de la probabilité de répartition des distances interatomiques: (- -) courbes synthetique pour les modèles I et II de la Figure 1; (——) courbe experimentale pour la cellulose II.

On peut ajouter que toute une série d'études de la cellulose par l'infrarouge[7] arrive aussi à la conclusion que les formes I et II de la cellulose n'ont pas tout à fait la même chaîne, indépendamment de la position respective des chaînes dans la maille.

References

1. Hermans, P. H., J. de Booys, et C. Maan, *Kolloid Z.*, **102,** 169 (1943).
2. Hermans, P. H., *Physics and Chemistry of Cellulose Fibres,* Elsevier, Amsterdam, 1949.
3. Meyer, K. H., et L. Misch, *Helv. chim. Acta,* **20,** 232 (1937).
4. Pierce, F. T., *Trans. Faraday Soc.*, **42,** 360 (1956).
5. Oberlin, M., Thèse, Paris, 1960.
6. Petitpas, T., M. Oberlin, et J. Mering, *Compt. Rend.*, **244,** 346 (1957).
7. Voir par ex.: R. H. Marchessault et C. Y. Liang, *J. Polymer Sci.*, **43,** 71 (1960); J. Mann et H. T. Marrinan, *J. Polymer Sci.*, **32,** 357 (1958).

Résumé

La photométrie précise des diagrammes de diffraction des Rayons X montre que la transformation de la celluloes I en cellulose II ne se limite pas à un réarrangement des chaînes, mais que la structure des chaînes individuelles est également transformée.

Synopsis

Precision photometry on x-ray diagrams of cellulose I and cellulose II have shown that the lattice transformation involves more than a simple change in chain packing, the cellulose chains themselves undergoing a conformational rearrangement.

Zusammenfassung

Die Präzisionsphotometrie der Röntgendiagramme von Cellulose I und Cellulose II zeigte, dass die Gitterumwandlung nicht nur in einer einfachen Veränderung der Kettenpackung besteht, sondern, dass die Celluloseketten selbst eine Konformationsumlagerung erleiden.

JOURNAL OF POLYMER SCIENCE: PART C NO. 2, PP. 429–448 (1963)

Comparative X-Ray Orientation Measurements on Hermans Model Filaments

W. KAST, *Wissenschaftliches Laboratorium des Werkes Dormagen der Farbenfabriken Bayer A. G. Germany*

I. INTRODUCTION

Kratky et al.[1] have observed "ribbonlike" orientation in cellulose fibers by the "Halbreiten method" (halfwidth method) of x-ray examination. Attempts were made[2] to measure the quantity and quality of orientation by this method. During these experiments it was observed that as the planar orientation (quality) in cellulose fibers increased, the extensibility and flexibility decreased even though axial orientation (quantity) was of the same order of magnitude. To evaluate this "quality of orientation" a new parameter was introduced. Two other methods[3,4] to measure the orientation, including the quantitative determination of the ribbon effect, were also developed.

It was felt that the comparison of the results on the same filament material obtained by these three methods, which are complicated as far as the measurement techniques are concerned, could lead to a fair judgment about the accuracy of the methods and/or their interrelation.

It is thanks to P. H. Hermans and O. Kratky, that the cooperation between the laboratories of Utrecht, Graz, and Dormagen the results herein could be obtained.

II. EXPERIMENTAL MATERIALS

As uniform experimental material, Hermans chose some model filaments from his institute in Utrecht. This material was available in the form of filaments initially prepared for x-ray measurements and was investigated in the three laboratories according to each of the three different methods. The filaments had been spun from viscoses of different DP and cellulose concentration. One series of filaments had been stretched to different degrees in the primary xanthate state (filaments X), another series after regeneration in the freshly swollen cellulose state (F). The degree of elongation presented in Table I is the so-called affine degree of elongation v_a which accounts for the change in degree of swelling during stretching. In Table I the samples have been coded 5XA to 4FB.

The experimental material was completed by model filaments from the Institute in Graz, henceforth called Treiber filaments. For a number of

TABLE I
Experimental Material–Hermans Filaments

Viscose no.	Cellulose concn., %	DP	Degree of elongation V_a for various samples				
			XA	XB	XC	FA	FB
5	1.9	660	1.36	1.68	2.28	1.25	1.35
1	4.1	380	1.32	1.82	2.56	1.53	2.04
6	6.1	400	1.28	1.84	2.53	1.62	2.13
4	10.5	170	1.37	1.93	2.38	1.27	1.75

filaments Treiber changed the production method of the model filaments, omitting the usual "stabilization" step practiced in Utrecht. In Graz two viscoses with different cellulose concentrations were used. The filaments were stretched to different degrees in the freshly swollen state (F), or after drying in the reswollen state (R) (Table II). The samples have been coded IF to IIRs.

TABLE II
Experimental Material–Treiber Filaments

Viscose no.	Cellulose concn., %	Degree of elongation v_a for various samples			
		F	F_s	R	R_s
I	1.9	1.66[a]	1.53	1.76[a]	1.67
II	6.0	1.50[a]	1.66	1.80[a]	1.74

[a] Stabilization step omitted.

III. METHODS

In the methods considered here the measurement of x-ray orientation is based on the estimation of the azimuthal blackening curves of either the equatorial reflections A_0 (ribbon plane 101) and A_3 (side plane), or of the meridian reflection II_0 (basic plane 020). To separate the background blackening, the photometer traces were made in the radial directions. The two methods differ as to the procedure of estimating the blackening curves $F(\alpha_0)$ and $F(\alpha_3)$ or $F(\beta)$. Figure 1 serves as a typical example; here one of the experimental azimuthal blackening curves $F(\alpha_0)$ is plotted amidst the family of theoretical curves calculated by Porod[4] according to the theories of Kratky[2] for rodlike and ribbonlike micelles for a number of stretch ratios.

a. Method of Orientation Angle Halfwidth

The first and "classical" method is the method of Kratky[5] called the halfwidth method, which uses the azimuthal blackening curves of the equatorial reflections A_0 and A_3. With his theory of affine deformation it is possible to establish a relation between the width of these curves and the orientation distribution of the micelle axes. According to this theory the

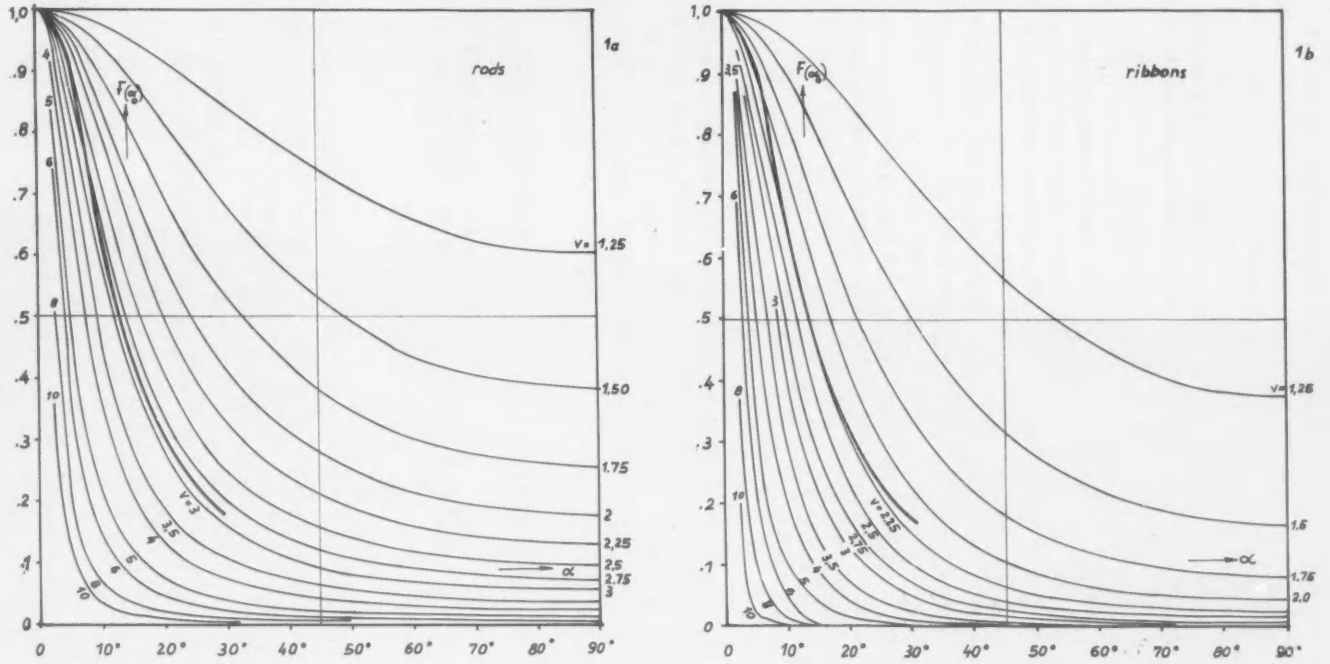

Fig. 1. Experimental azimuthal blackening curve $F(\alpha_0)$ (heavy curve) plotted amidst the family of the so-called Porod curves for: (*a*) rodlike micelles; (*b*) ribbonlike micelles.

axes of the rodlike micelles follow the deformation of the material in which they lie embedded, without preferential orientation of side planes taking place. As it was found with the halfwidth method that the two principal equatorial reflections behaved differently on stretching, it was necessary to introduce the ribbon micelle as a refinement of the theory. The normals of the ribbon planes (101) whose orientation runs ahead are assumed to follow the affine deformation in the same way as the axes of the micelles. Consequently, there is a difference between axial orientation and ribbon orientation, but a fixed correlation exists between two mechanisms. In his experiments with the generally well-oriented cupro fibers, the author[2] had the advantage to be able to evaluate the meridian reflection II_0, the blackening curve $F(\beta)$ of which is directly related to the orientation distribution of the micelle axes. At relatively low degrees of orientation this method presents serious difficulties due to the azimuthal overlapping of this reflection and of the second layer line reflection II_1 (021) or even the equatorial reflection A_3 (101), both of them having Bragg angles approximately equal to that of II_0. In this way the axial orientation could be measured directly by determining $1/\beta_h$ and related to the ribbon orientation measured by $1/\alpha_{0h}$, α_{0h} being the halfwidth of A_0. This orientation ratio

$$\alpha_{0h}/\beta_h = O_v$$

varies over a wide range and parallels the breaking elongation of the fibers. For this reason it was introduced as a measure of the quality of the orientation. Multiplication by the quantity of the orientation $1/\beta_h$ leads to a classification factor of orientation which appears to be proportional to the textile factor obtained by multiplying breaking strength by breaking elongation.

b. Method of Average Squared Sines of Orientation Angle

P. H. Hermans and J. J. Hermans[6] made an attempt to come to a simple mathematical expression for the axial orientation. They introduced the orientation factor

$$f_x = 1 - {}^3/_2 \, \overline{\sin^2} \, \beta$$

as a measure of axial orientation. Here $\overline{\sin^2} \, \beta$ is the average squared sine of the angle β between the micelle axis and fiber axis. In order to avoid the use of the $F(\beta)$ curve which is often difficult to determine, in most cases they resorted to measuring $F(\alpha_0)$ and $F(\alpha_3)$, from which the mean squares $\overline{\sin^2} \, \alpha_0$ and $\overline{\sin^2} \, \alpha_3$ can be derived. Since the paratropic planes 101 and $10\bar{1}$ are perpendicular to each other, it is possible to use the relations

$$\overline{\sin^2} \, \beta = \overline{\sin^2} \, \alpha_0 + \overline{\sin^2} \, \alpha_3$$

and

$$\overline{\sin^2} \, \alpha = \frac{\int_0^{\pi/2} F(\alpha) \sin^2 \alpha \cos \alpha \, d\alpha}{\int_0^{\pi/2} f(\alpha) \cos \alpha \, d\alpha}$$

At lower orientations, a complication arises, because then the equatorial reflection $10\bar{1}$ is overlapped by the layer line reflection 021. In this case the total mean squared sine, $\overline{\sin^2 t}$, of the two overlapping reflections is determined experimentally. By introducing the angle, γ, which is the complement of the angle between the normal to the 021 planes and the fiber axis, $\overline{\sin^2 t}$ can be expressed by

$$\overline{\sin^2 t} = K\,\overline{\sin^2 \alpha_3} + (1 - K)\,\overline{\sin^2 \gamma}$$

(K being a constant which can be determined experimentally.) Besides, $\overline{\sin^2 \gamma}$ is related to $\overline{\sin^2 \alpha_0}$ and $\overline{\sin^2 \alpha_3}$ by the direction cosines. For this reason it is possible to eliminate $\overline{\sin^2 \gamma}$ from the two correlations and to calculate $\overline{\sin^2 \alpha_3}$ and f_x directly from $\overline{\sin^2 \alpha_0}$ and $\overline{\sin^2 t}$.

In the final formulas there are small differences in the coefficients in the publications of P. H. Hermans and J. J. Hermans. These differences must be of a secondary nature because the direction cosines are always correspondingly given and have been calculated again in Graz, with the same results. For the convenience of the reader, the formulas are given below.

$$\overline{\sin^2 t} = K\,\overline{\sin^2 \alpha_3} + (1 - K)\,\overline{\sin^2 \gamma}$$

$$\overline{\sin^2 \gamma} = p^2 + (q^2 - p^2)\,\overline{\sin^2 \alpha_0} + (r^2 - p^2)\,\overline{\sin^2 \alpha_3}$$

where

$$p^2 = 0.7106$$

$$q^2 = 0.0586$$

$$r^2 = 0.2480$$

The revision leads to final equations with coefficients that deviate somewhat from the up till now used figures. With these new figures all the calculations were made.

$$\overline{\sin^2 \alpha_3} = 0.1475\,\overline{\sin^2 \alpha_0} + 1.331\,\overline{\sin^2 t} - 0.1608$$

$$f_x = 1.241 - 1.721 \cdot \overline{\sin^2 \alpha_0} - 1.997 \cdot \overline{\sin^2 t}$$

Using this method Hermans and Kast[3] got a more suitable characterization of the quality of orientation than the halfwidth ratio discussed above: as a quantitative measure of the ribbon effect the paratropic ratio

$$P_r = \overline{\sin^2 \alpha_0} / \overline{\sin^2 \alpha_3}$$

can be used, which reaches the value 1 in the case of rods and decreases with increasing ribbon effect.

c. Method of Curve Simulation

Kratky, Porod, and Treiber[4] have developed a new method by which it is possible to characterize the position of the real deformation behavior between the extreme cases of ribbonlike and rodlike deformation by using a

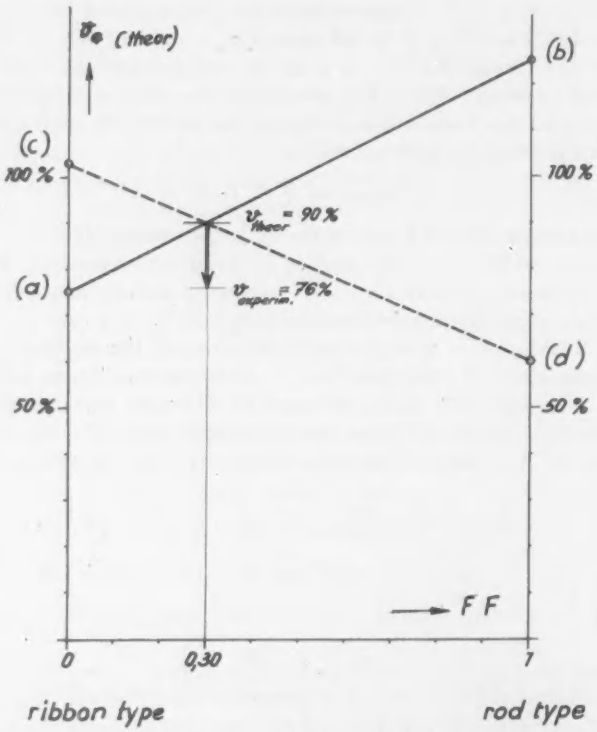

Fig. 2. The evaluation process in the method of curve simulation.

characteristic number with values between zero and one. In this method, they compare the experimental trends of the azimuthal blackening curves for reflections A_0 and A_3 (if necessary $A_3 + 021$) with the theoretical curves calculated by Porod for the deformation behavior of rods and of ribbons (see above Fig. 1). In this way they find two theoretical ratios of elongation V_a (theor.) for each planes (a and c for the ribbon plane A_0 and b and d for the side plane A_3) according to the two theories of ribbons and of rods respectively, all deviating from the experimental ratio V_a (expt.). Setting them upon two ordinates, the left one for the ribbon type and the right one for the rod type, as it is shown in Figure 2, and connecting them by two straight lines (a-b and c-d) each point of these straight lines represents a defined deformation behavior lying between the theoretical behavior of ribbons and of rods. The real deformation behavior therefore is determined by the horizontal coordinate of the intersection point of the crossing lines between the two coordinates for ribbon type, arbitrarily called "zero," and for rod type, called "one." In this way is termed the shape factor (FF), which naturally has values between zero (ribbon type) and one (rod type). The vertical coordinate of this point, as it lies below or above the experi-

mental elongation ratio, indicates whether the experiment had required a lower or higher stretch ratio than the theory requires. When the point of intersection lies below the experimental stretch ratio, the orientation proceeds more rapidly; in the reverse case more slowly than predicted by the theory. It is possible to define, in this way, a velocity factor:

$$VF = (v_a(\text{theor.}) - 1)/(v_a(\text{expt.}) - 1)$$

IV. RESULTS

a. Reproducibility of the Measurements

Since this is the first time that three authors present results of measurements (admittedly a small number) by the same methods on the same fiber samples, an effort will be made to give a picture of the reproducibility of measurements from different sources. From the deviations from the mean of the values found in the three laboratories, the absolute average error

$$m = \pm([vv]/2)^{1/2}$$

was calculated, $[vv]$ being the sum of the squares of the deviations. Owing to the difficulties arising from the above mentioned overlapping, the measurement of the angles (halfwidths) β_h of the meridional reflex 020 was possible only in the laboratory of Krefeld, but not in all cases, though this method had been developed for routine measurements.

For the Hermans filaments, the equatorial ribbon reflection A_0 was measured in all three laboratories; for the Treiber filaments it was measured in Graz and Krefeld only. In both series a quadratic increase of the absolute mean error with the measured values was found, according to the equation:

$$m = \pm 0.005\alpha_h^2$$

or

$$r = m/\alpha_h = \pm 0.005\alpha_h$$

r being the relative mean error which increases linearly (Table III). This strong increase of the error with α_h is due to the increasing uncertainty in drawing the background curve.

In the case of azimuthal blackening curves with large halfwidth an additional uncertainty is caused by overlapping of the left and right hand sickles. It is then necessary to subtract a correction which increases with α_h. This correction was calculated for three theoretical profiles, viz., for Kratky's affine cases of rods and ribbons and for the Gauss curve. Table III shows that this correction is of the order of magnitudes of the measuring errors.

In the method of mean squared sines the average absolute errors are proportional to the measured values:

TABLE III
Average Errors m and r in Measurements of α_h and Overlap Correction $\Delta\alpha$

Halfwidth α_h, °	Average error		Correction for overlapping, $\Delta\alpha$, °		
	$\pm m$, °	$\pm r$, %	Theory for ribbons	Theory for rods	For Gauss curve
10	0.5	5	0.05	0.3	0.0
20	2	10	0.15	0.8	0.0
30	4.5	15	0.35	1.4	0.0
40	8	20	0.65	2.1	0.0
50	12.5	25	1.00	3.0	0.9
60	18	30	1.35	4.0	6.5
90	40.5	45	2.8	7.3	25.0

For $\overline{\sin^2}\,\alpha_0$:

$$m = \pm 0.12\ \overline{\sin^2}\,\alpha_0$$

and for $\overline{\sin^2}\,t$:

$$m = \pm 0.04\ \overline{\sin^2}\,t$$

The relative absolute errors are independent of the measured value and amount to 12 and 4%, respectively. This difference also reflects the uncertainty of the background, which at the large angle of the reflection A_3, is less than at the small angle of the interior reflection A_0. The resulting errors in f_x and P_v are presented in Table IV.

TABLE IV
Final Errors in Orientation factor f_x and Paratropic Ratio P_v

Measured value	f_x		P_v	
	$\pm m$, °	$\pm r$, %	$\pm m$, °	$\pm r$, %
0.1	0.084	84.0	0.038	28
0.2	0.073	37.0	0.050	25
0.3	0.062	21.0	0.065	22
0.4	0.052	13.0	0.080	20
0.5	0.043	8.6	0.095	19
0.6	0.035	5.8	0.113	19
0.7	0.028	4.0	0.130	19
0.8	0.022	2.8	1.150	19
0.9	0.017	1.9	0.170	19
1.0	0.013	1.3	0.195	19

For comparison, the values of α_{0h} and $\overline{\sin^2}\,\alpha_0$ measured on the Hermans filaments by all three authors, are represented in Figure 3. Between the values there is a linear relationship. In the curve the sines square value zero corresponds with the halfwidth of 6°. Obviously, this is the natural halfwidth of the reflection A_0 at complete orientation. At large values of

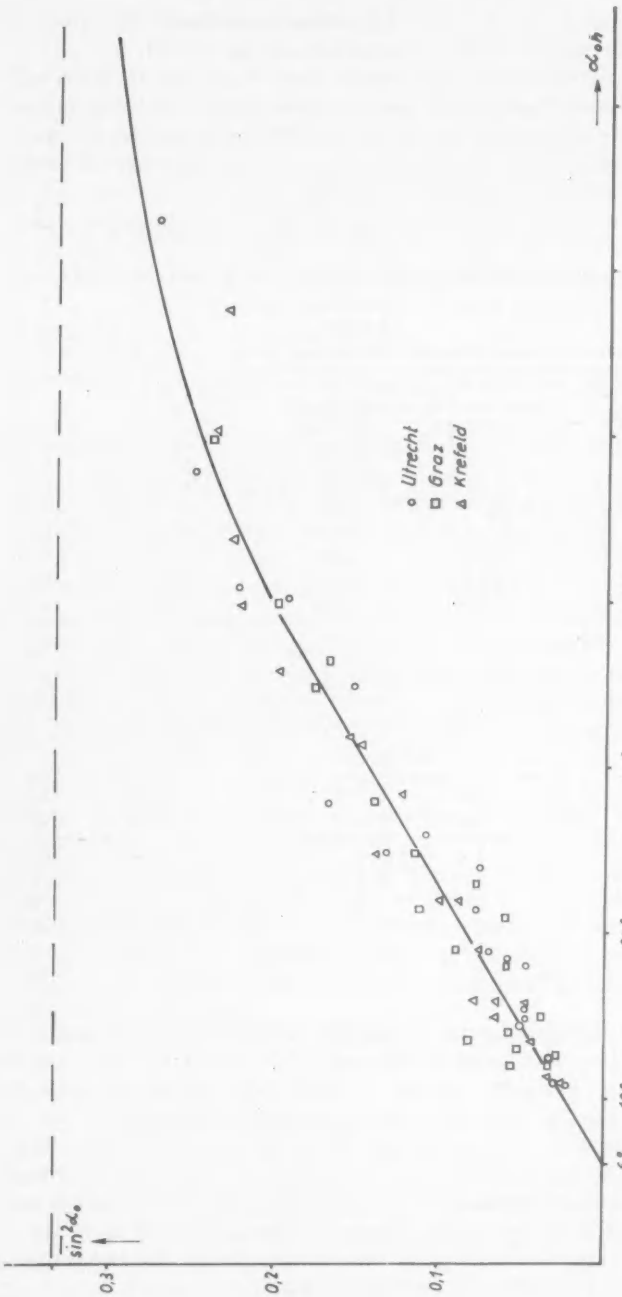

Fig. 3. Relation between α_{oh} and $\overline{\sin^2}\,\alpha_0$ for Hermans filaments.

$\overline{\sin^2}\ \alpha_0$, the curve flattens out. The halfwidth method is not applicable to the case of complete random orientation ($\overline{\sin^2}\ \alpha_0 = 0.33$).

Further results of the comparison of the two methods are given in Table V. The diatropic sine square $\overline{\sin^2}\ \beta$ and the orientation factor f_x has been calculated: (a) from the sum of the paratropic sines squares $\overline{\sin^2}\ \alpha_2 + \overline{\sin^2}\ \alpha_3$ and (b) directly by integration of the experimental azimuthal blackening curve of the meridian reflection according to:

$$\overline{\sin^2}\ \beta = \int_0^{\pi/2} F(\beta) \sin^3 \beta d\ \beta / \int_0^{\pi/2} F(\beta) \sin \beta d\ \beta$$

The agreement between the values obtained in both ways in satisfactory.

TABLE V

Comparison of the Paratropic and Diatropic Determinations of $\overline{\sin^2}\ \beta$ and f_x

	$\overline{\sin^2}\ \beta$		f_x	
Sample	Paratropic	Diatropic	Paratropic	Diatropic
1XB	0.24	0.22	0.64	0.67
1XC	0.13	0.13	0.80	0.81
6XB	0.22	0.20	0.71	0.70
6XC	0.11	0.12	0.84	0.82
4XA	0.30	0.29	0.55	0.56
4XB	0.15	0.16	0.78	0.77
4XC	0.097	0.092	0.86	0.88

TABLE VI

Per Cent Error in the Method of Curve Simulation

	Relative deviation from the mean value, %					
	V_a (theor.) from				Velocity	Shape
Sample	A_0 ribbons	A_0 rods	A_t ribbons	A_t rods	factor VF	factor SF
6XA	4.6	4.0	(13.8)	(12.0)	9.4	(50.0)
6XB	1.9	3.0	0.4	2.4	0.4	(17.0)
6XC	0.8	2.0	4.2	1.4	1.2	4.5
6FA	0.3	2.4	0.1	4.2	0.8	8.1
6FB	7.2	2.0	1.5	0.2	0.8	8.1
4XC	3.0	3.2	7.7	3.9	2.9	13.5

As to the method of curve simulation, comparative measurements on at least six Hermans filaments were available from Graz (area simulation method and halfwidth method), Krefeld [area simulation method with $F(\alpha)$ and $F(\alpha) \cos \alpha$ curves] and Utrecht (halfwidth method). The agreement is good in most cases, but there are a few exceptions. For this reason it was not possible to formulate an error law. Accordingly in Table VI, the percentile deviation from the mean values is given as such. Columns 2–5 represent the values of v_a(theor.) derived from the curve simulation (points a, b and c, d of the schematic Fig. 2), the last two columns give the velocity factor VF and shape factor SF.

In spite of the satisfactory agreement between the stretch degrees v_a(theor.) estimated in the different laboratories [only in four out of 24 cases does the error exceed 5%, (in two cases 10%)], there are larger errors especially in the horizontal coordinate of the point of intersection (shape factor). For small values of the theoretical stretch ratios on the ribbon axis (ac) and/or the rod axis (b, d) the vertical coordinate of the point of intersection is satisfactorily defined in spite of the relatively great uncertainty, whereas the horizontal coordinate is less defined because of the small magnitude of the crossing angle. There is an additional reason for the relative uncertainty, because the scale of the shape factor runs from zero to one. Consequently the same absolute error gives a larger relative error on the left side of the diagram than on the right.

b. Comparison and Discussion of the Results Obtained by the Different Methods

1. Ribbon Effect. In his paper, Kratky[4] was able to explain the decrease of the quality of the orientation with increased ribbon effect with the help of a new model. This model is characterized by rigid "linear hinges" between the ribbonlike micelles of the regenerated cellulose, so that on ribbon orientation the hinges are strained by torsion. For this reason it has become of interest to consider the real deformation behavior as being intermediate between rodlike and ribbonlike behavior. At the same time a new way of interpolating is provided by the new method of curve simulation. Today there exist three different parameters for the quantitative description of the ribbon effect, viz. (*1*) the orientation ratio $O_v = \alpha_h/\beta_h$ with values >1 for rods and $\leqslant 1$ for ribbons; (*2*) the paratropic ratio $P_v = \overline{\sin^2 \alpha_0}/\overline{\sin^2 \alpha_3}$ with values of 1 for rods and 0 for ribbons; (*3*) the shape factor FF (defined above), with the values of 1 for rods and 0 for ribbons. The P_v–f_z diagram published earlier by Hermans and Kast[3] was again confirmed by all three laboratories in the new measurements on the Hermans filaments. In Figure 4*a* the mean values from all three laboratories are represented in the same form. At small orientations the measured points lie at equal distances from the descending theoretical curve for ribbons. Above $f_z = 0.7$ there is tendency of the measured points to approach the theoretical value for rods, $P_v = 1$. The dotted line refers to earlier measurements on filaments which had a higher orientation.

For the Treiber filaments there is a better correspondence between the theoretical P_v curve for ribbons and the measured values (Fig. 4*b*). This implies a behavior that is in complete accordance with the theoretical ribbon effect, it remains unchanged on stabilizing the samples (1→2, 3→4, 5→6, 7→8). The more complete ribbon effect of the Treiber filaments can be understood from the fact that these filaments had been stretched in the freshly swollen regenerated state or in the reswollen state after drying, whereas the majority of the filaments in diagram 4*a* had been stretched in the xanthate state. In Figure 5 a diagram is given in which instead of the paratropic ratio, the shape factor of the Hermans filaments

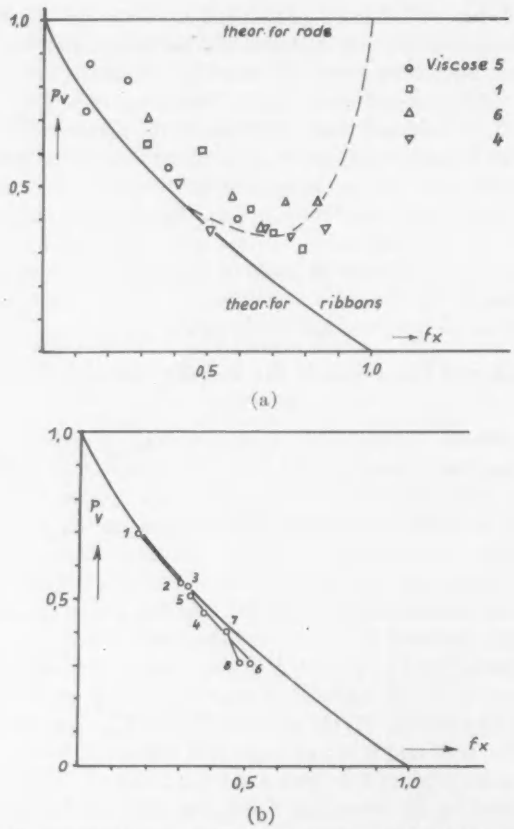

Fig. 4. P_v–f_x diagram for Hermans filaments (above); and Treiber filaments (below).

is represented. For comparison with Figure 4*a*, it should be noted that in Figure 5 the theoretical course of the shape factor for ribbons coincides with the abscissa. This diagram is in agreement with Figure 4*a*, but shows more clearly that with increasing orientation the shape factor grows at an increasing rate indicating the behavior of the system gradually changing from ribbon-like to rodlike. Similarly the course of the shape factor on stabilization of the Treiber filaments confirms the behavior representation of the P_v–f_x diagram (see Fig. 4*b*). Indeed the measurements in all three laboratories [using the methods of area simulation and halfwidth in Graz, and only the first method for both the $F(\alpha)$ and $F(\alpha)\cdot\cos\alpha$ curves in Dormagen] show an increase of the shape factor or a decrease of the ribbon effect on stabilization in all the samples. However, this increase lies within the range of error of the single values got by different methods or by the same methods if operated by different authors (Table VII).

Also, the measurements of the orientation ratio point to the preservation

TABLE VII
Influence of the Stabilization on the Shape Factor of the Treiber Filaments

	F Filaments		R Filaments	
	I	II	I	II
ΔSF	$+0.35 \pm 0.22$	$+0.23 \pm 0.24$	$+0.09 \pm 0.27$	$+0.17 \pm 0.29$

of the ribbon effect on stabilization. The halfwidth of the ribbon reflection A_0 decreases on an average by 30% for the F filaments and by 4% for the R filaments, but also the axial orientation is improved. It was not possible to measure it directly because β_h was not available. However, we know the increase of $f_x = 1 - 3/2\ \overline{\sin^2 \beta}$. Its increase of 80% and 8% for F filaments and R filaments, respectively, corresponds to a decrease of the fluctuation square and also of the halfwidth β_h amounting to 30% and 5% for F and R fibers, respectively. This is the same decrease as that of α_{0h}; the orientation is, therefore, not affected by the stabilization.

In the series of Hermans filaments the dependence of the ribbon effect on the cellulose concentration can also be checked. Kratky et al.[4] have shown that their model with the linear hinges leads to the expectation of a stronger ribbon effect at higher concentrations or lower swelling degrees under otherwise equal conditions. Only at low concentration or high swelling degrees is an influence of the linear hinges possible. In systems of higher density this is suppressed in favor of the affine movements of the individual ribbon planes.

The dependence of the paratropic ratio on the concentration confirms the previous predictions only to some extent. Figure 6, taken from an earlier paper by Hermans and Kast,[3] shows that only at small stretch ratios is there a steeper decrease of the paratropic ratio with increasing concentration pointing to an increasing ribbon effect. Above the stretch

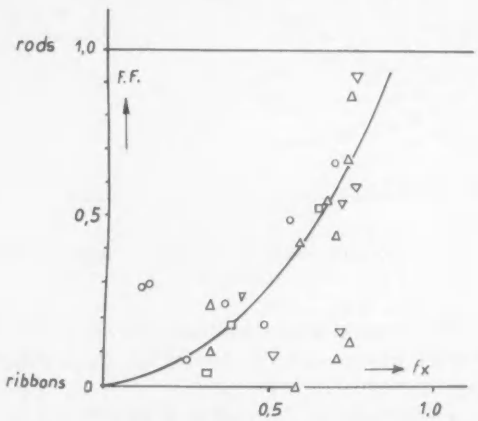

Fig. 5. FF–f_x diagram for Hermans filaments.

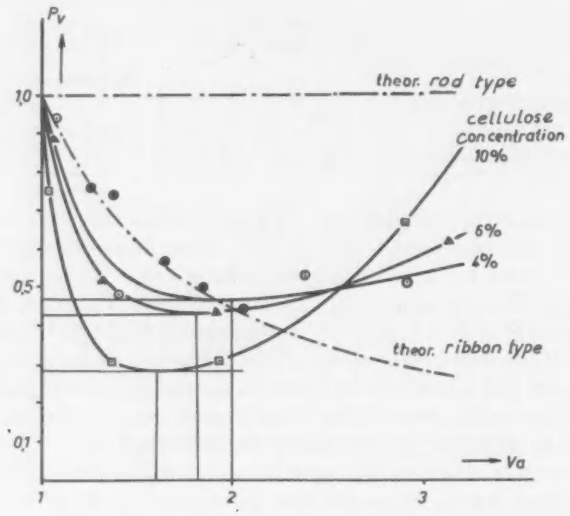

Fig. 6. Variation of the paratropic ratio with the stretch ratio at different cellulose concentrations (data of Hermans and Kast[3]).

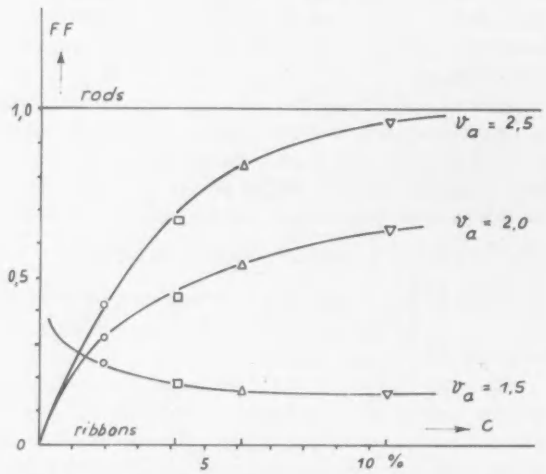

Fig. 7. Variation of the shape factor with the cellulose concentration at different stretch ratios.

ratio 2.6, at higher concentrations rodlike behavior prevails. We shall return to this effect which is also visible in the P_v–f_x diagram (Fig. 4*a*) in the discussion of the orientation velocity.

This unexpected increase of the rodlike behavior can be more clearly seen in the diagram which shows the shape factor *SF* as a function of the

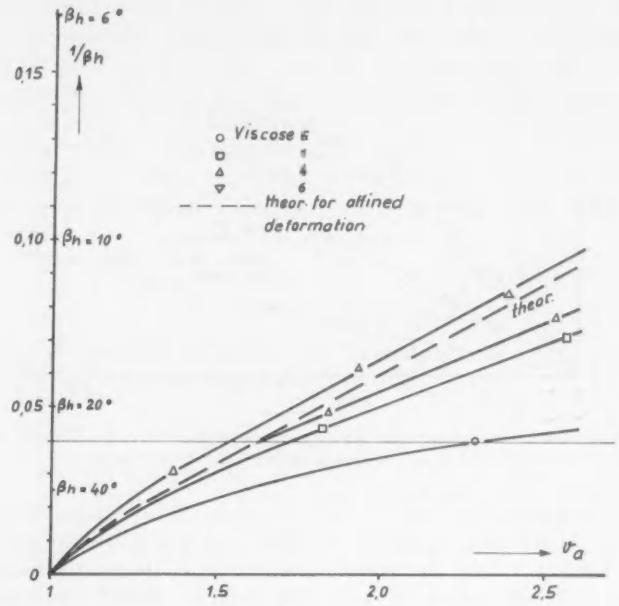

(*a*)

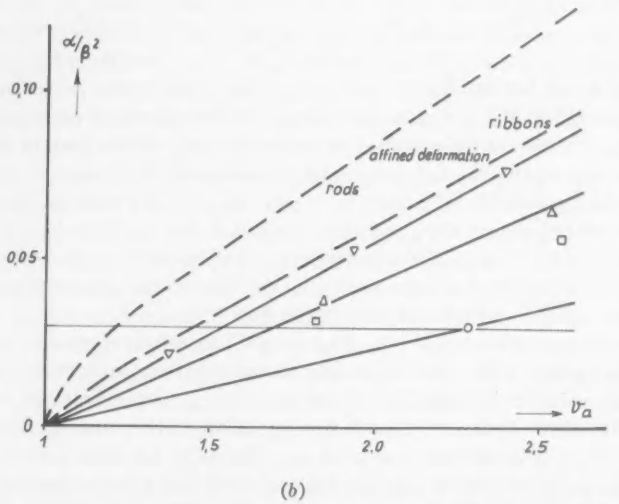

(*b*)

Fig. 8. Plots of (*a*) axial orientation $1/\beta_h$ (above) and (*b*) classification of orientation α_h/β^2_h (below) as a function of the stretch ratio ν_a at different cellulose concentrations.

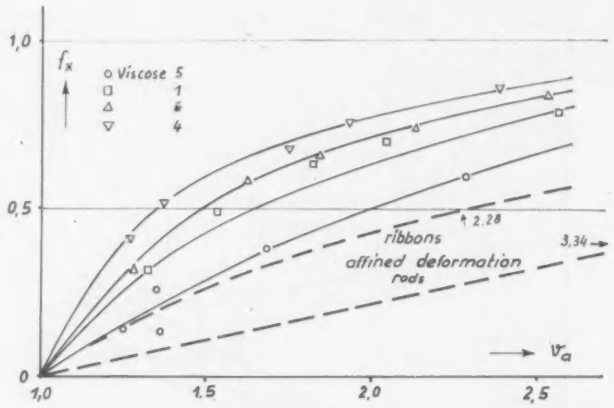

Fig. 9. Variation of the orientation factor f_x vs. stretch ratio v_a at different cellulose concentrations.

cellulose concentration (Fig. 7). Only at a stretch ratio 1.5 a decrease of the shape factor with increasing cellulose concentration is found. At a stretch ratio of 2.5 and a cellulose concentration of 10.5%, the behavior is almost purely rodlike with $FF = 0.96$ (ideal value: 1.00). Obviously in a system of high density at sufficiently high orientation, the micelle chains can follow the deformation without the linear hinges being strained by torsion.

2. Orientation Velocity. Finally, the experiments also allow a comparison of practice and theory with respect to orientation velocity. Up till now it was only possible to compare the experimental relation between stretch ratio and orientation with the theoretical relation for rodlike behavior on the one hand and for ribbonlike behavior on the other. The new method of Graz now allows this comparison with the theoretical stretch ratio v_a(theor.), valid for the actual deformation behavior which is somewhere in between rodlike and ribbonlike behavior. Determinations of the former type are shown in Figures 8*a*, 8*b*, and 9, in which the axial orientation, the classification of the orientation, and the orientation factor of the Hermans filaments have been plotted versus the experimental stretch ratio, in order to compare them with the theoretical values of these parameters calculated for both the rodlike and the ribbonlike behavior.

For the axial orientation $1/\beta_h$ (Fig. 8*a*) the theoretical curves for rods and ribbons are identical. The experimental curves become steeper, and the orientation velocity is higher at increasing cellulose concentrations, whereas the affine theories do not provide for any effect of the concentration. On the contrary, the network theory of J. J. Hermans[7] predicts a much slower orientation according as the network is looser or more statistical chain elements are present between two network joints. On the basis of the statement by P. H. Hermans, J. J. Hermans, et al.[8] that the regenerated

cellulose forms a denser network as the cellulose concentration is higher, Kratky[4] could explain the increase of the orientation velocity with increasing cellulose concentration. Indeed, the experimental curves for the axial orientation approach the theoretical curve for the affine deformation more closely, when the cellulose concentration is higher. At the highest concentration (10.5%) they even exceed it somewhat.

It is possible to calculate a velocity factor VF, defined as the quotient of the percentage theoretical and experimental stretch degree required for obtaining the same orientation ($1/\beta_h = 0.04$ or $\beta_h = 25°$):

$$VF = \left(\frac{v_a(\text{theor.}) - 1}{v_a(\text{expt.}) - 1} \right)_{\text{orientation} = \text{const.}}$$

Numerical values obtained in this way for a number of cellulose concentrations are represented in Table VIII.

TABLE VIII
Course of Velocity Factors Versus Cellulose Concentration

	Velocity factors at various cellulose concentrations			
	1.9%	4.1%	6.1%	10.5%
Axial orientation ($1/\beta_h$ = 0.04) for ribbons and rods)	0.49	0.85	1.00	1.17
Classification of orientation ($\alpha_h/\beta_h^2 = 0.03$)				
For ribbons	0.35	0.56	0.65	0.86
For rods	0.17	0.27	0.32	0.41
Orientation factor ($f_z = 0.5$)				
For ribbons	1.28	1.97	2.56	3.66
For rods	2.34	3.60	4.88	6.68

In the case of classification of orientation (Fig. 8*b*) two theoretical curves are obtained, of which the curve calculated for rods is markedly higher than that for ribbons. The calculation can be found in the paper by Hermans and Kast.[3] Again, the experimental curves are lower, only at the highest concentration they nearly reach the theoretical curves calculated for ribbons. The numerical values of the corresponding velocity factor, for the classification of orientation 0.03 can also be found in Table VIII. Finally the same process was used for the orientation factor f_x (Fig. 9). Similar curves had already been found by P. H. Hermans et al.[8] These authors stated for the first time that the velocity of orientation increases with concentration, and that it surpasses the theoretical values at low concentrations. In their paper as well as in the present one, at all concentrations the curves lie above the theoretical curve for ribbons and even above that for rods. It is interesting to note that the order of the theoretical curves is also reversed as compared with that in Figure 8*b* (classification of orientation). The results from the curves for f_z, calculated for $f_x = 0.5$, are also to be found in Table VIII.

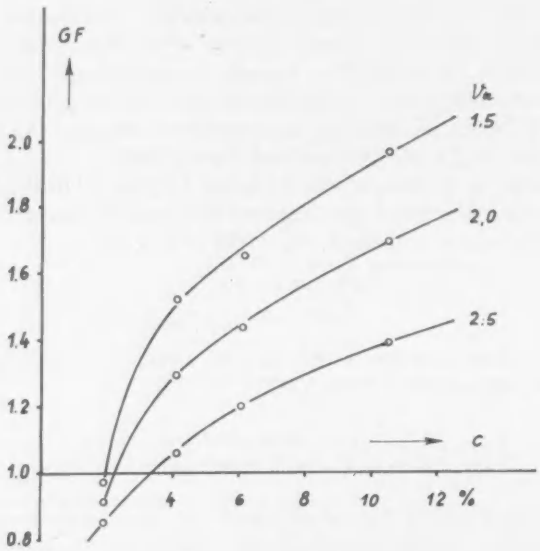

Fig. 10. Velocity factor vs. cellulose concentration at different stretch ratios.

Finally, we shall discuss the estimation of the velocity factor according to the method of curve simulation by Kratky et al.[4] In this method we know the theoretical elongation ratios v_a(theor.) which corresponds with the actual intermediate state of deformation behavior between ribbonlike and rodlike behavior, for they are determined by the vertical coordinate of the points of intersection according to Figure 2. Plotting them against the experimental stretch ratios it was possible to assess by interpolation the values v_a(theor.) at the stretch ratios 1.5, 2.0, and 2.5. With these values the velocity factors VF at these stretch ratios were calculated. The results are shown in Figure 10. Almost without exception, the velocity factors are greater than unity, also with respect to the observed ribbon effect. Only at the lowest cellulose concentration they are somewhat below this value. At the same time, its increase with concentration at first steep and then flatter, could be confirmed, and its dependence on the stretch factor could be established. Summarizing, the velocity factors are greater at higher cellulose concentrations and lower stretch ratios. This decrease of the orientation velocity with increasing stretch ratio should be consistent with the fact that the ribbon effect does not increase in the expected way, but decreases with increasing cellulose concentration at higher stretch ratios. Accordingly it was found that in general, the shape factor and the velocity factor follow an opposite course increasing elongation. This can be seen for the Hermans X-filaments in Table IX.

A lower velocity of orientation always corresponds with a higher shape factor or a lower ribbon effect.

TABLE IX
Variation in Shape Factor *SF* and Velocity Factor *VF* of Hermans Filaments By Stretching in the Xanthate State

Viscose no.	Cellulose concn., %	Sample	Elongation ratio	Shape factor *SF*	Velocity factor *VF*
1	4.1	XA	1,32	0,04	1,56
		XB	1,82	0,36	1,46
		XC	2,56	0,66	1.18
6	6.1	XA	1,28	0,07	1.72
		XB	1,84	0,45	1,50
		XC	2,53	0,86	1,32
4	10.5	XA	1,37	0,19	2,00
		XB	1,93	0,54	1,75
		XC	2.38	0,93	1,45

In Table X the results are given for the measurements of the velocity factor on the Treiber filaments. In these filaments, stretched in the regenerated state, it was found that already at low stretch ratios the velocity factors are greater according as the cellulose concentration is

TABLE X
Velocity Factors of the Treiber Filaments Before and After Stabilization

Sample	Viscose no.	Cellulose concn., %	Velocity factor	Effect of stabilization
F	I	1.9	0.59	+0.44 ± 0.09
Fs	I	1.9	1.03	
R	I	1.9	0.57	+0.27 ± 0.12
Rs	I	1.9	0.84	
F	II	6.0	0.85	+0.36 ± 0.08
Fs	II	6.0	1.81	
R	II	6.0	0.82	+0.13 ± 0.07
Rs	II	6.0	0.95	

higher. In consequence of the stabilization the velocity factor is further increased, the increase for the F filaments being around twice that for the R filaments. As the shape factor may increase on stabilization, but will certainly not decrease, as shown above, the stabilization has the effect that the filaments seem to be stretched at a higher rate without suffering from a higher ribbon effect. In this respect the quality of orientation would be improved by stabilization.

The author would like to express his gratitude to his colleagues, P. H. Hermans and O. Kratky and their co-workers, the late Mr. Weidinger and A. Krausz, and also his own co-workers, A. Prietzschk and H. Andree, for the continuing interest and the untiring cooperation during the whole course of this work.

References

1. Baule, B., O. Kratky and R. Treer, *Z. Physik. Chem. (Leipzig)*, **B50**, 255 (1951).
2. Kast, W., and A. Prietzschk, *Kolloid-Z.*, **114**, 23 (1949); W. Kast, *Kolloid-Z.*, **120**, 40 (1951).
3. Hermans, P. H., and W. Kast, *Kolloid-Z.*, **121**, 21 (1951); W. Kast, *Kolloid-Z.*, **125**, 45 (1952).
4. Kratky, O., G. Porod, and E. Treiber, *Z. Elektrochem.*, **55**, 481 (1951).
5. Kratky, O., *Kolloid-Z.*, **64**, 213 (1933); *ibid.*, **96**, 301 (1941).
6. Hermans, J. J., P. H. Hermans, D. Vermaas, and A. Weidinger, *Rec. Trav. Chim.*, **65**, 427 (1946).
7. Hermans, J. J., *J. Colloid Sci.*, **1**, 235 (1956); *Trans. Faraday Soc.*, **42B**, 160 (1946); *ibid.*, **43**, 591 (1947).
8. Hermans, P. H., J. J. Hermans, D. Vermaas, and A. Weidinger, *J. Polymer Sci.*, **1**, 393 (1946); *ibid.*, **2**, 632 (1947); *ibid.*, **3**, 1 (1948).

Synopsis

This paper deals with comparative measurements of orientation on the same Hermans model filaments using three methods developed in Dormagen, Utrecht, and Graz. All these methods permit determining not only the quantity, but also the quality of orientation by measuring the ribbon effect and the velocity of orientation. In all three laboratories, the three methods were used. The comparison of the results makes it possible to check the reproducibility and to state error laws for these methods. The results obtained by the three methods were compared with respect to: (*1*) the value of the ribbon effect and its course with the stretch ratio, the velocity of orientation, and the cellulose concentration; (*2*) the value of the velocity of orientation and its course with the stretch ratio and the cellulose concentration; (*3*) the influence of stabilization on the stretch ratio, the ribbon effect, and the velocity of orientation.

Résumé

Cet article traite des mesures comparatives effectuées sur les mêmes filaments répondant au modèle d'Hermans en utilisant trois méthodes développées (par order de temps) à Dormagen, Utrecht et Graz. Toutes ces méthodes permettent non seulement de déterminer la quantité mais aussi la qualité de l'orientation en mesurant l'effet de ruban, et la vitesse d'orientation. Dans les trois laboratoires, les trois méthodes sont utilisées. La comparaison des résultats permet de vérifier la reproductibilité et d'établir une loi des écarts pour ces trois méthodes. Les résultats obtenus par les trois méthodes sont composés en égard à: (*1*) La valeur de l'effet de ruban et son évolution avec le rapport d'étirement, la vitesse d'orientation et la concentration en cellulose; (*2*) la valeur de la vitesse d'orientation et son évolution avec le rapport d'étirement et la concentration en cellulose; (*3*) l'influence de la stabilisation sur le rapport d'étirement, l'effet de ruban et la vitesse d'orientation.

Zusammenfassung

Die vorliegende Arbeit bringt vergleichende Orientierungsmessungen an den gleichen Hermans-Modellfäden nach drei verschiedenen (in zeitlicher Reihenfolge) in Dormagen, Utrecht und Graz entwickelten Methoden. Alle Methoden erlauben durch Messung des Bändcheneffeks und der Orientierungsgeschwindigkeit nicht nur eine Bestimmung des Betrages sondern auch der Güte der Orientierung. In allen drei Laboratorien wurden die drei Methoden angewendet. Der Vergleich der Ergebnisse erlaubt eine Überprüfung der Reproduzierbarkeit und die Aufstellung von Fehlergesetzen für diese Methoden. Die mit den drei Methoden erhaltenen Ergebnisse wurden verglichen in bezug auf: (*1*) den Wert des Bändcheneffektes und seine Abhängigkeit von Streckungsverhältnis, Orientierungsgeschwindigkeit und Cellulosekonzentration; (*2*) den Wert der Orientierungsgeschwindigkeit und ihre Abhängigkeit von Streckungsverhältnis und Cellulosekonzentration; (*3*) den Einfluss der Stabilisierung auf Streckungsverhältnis, Bändcheneffekt und Orientierungsgeschwindigkeit.

JOURNAL OF POLYMER SCIENCE: PART C NO. 2, PP. 449–476 (1963)

Small-Angle X-Ray Investigations with Absolute Intensity Measurements on Regenerated, Air-Swollen Cellulose

O. KRATKY and G. MIHOLIC, *Institut für Physikalische Chemie der Universität Graz, Graz, Austria*

I. INTRODUCTION

About three decades ago the small-angle x-ray scattering of various materials[1,2] was discovered and correctly interpreted as being connected with their colloidal structure. One of these substances was cellulose.[1] Several years later, the attempts to develop a quantitative interpretation of small-angle scattering started. Shortly after Guinier[3] had tried to explain in his famous investigation, the phenomenon by the independent scattering of colloid particles ("particle scattering"), one of us[4,5] put forward the conception that one must distinguish between two types of objects, whose small-angle scattering must be treated differently: diluted systems, for which the particle scattering holds, and densely packed systems, in which interparticle interference effects are dominant. The most important system of those studied to demonstrate this idea was again cellulose. Here the colloid particles are represented by bundles of chain molecules, mostly called micelles.[6] Hosemann[7] has denied the importance of interparticle interferences for dense cellulose. We shall not enter into the previous discussion of this question,[8,9] but make an experimental contribution concerning the small-angle scattering of regenerated cellulose, which continues our earlier paper.[8]

A very dense system will yield a small-angle scattering, which, in the sense of the law of reciprocity of optics, can be interpreted as the scattering of the more or less randomly distributed voids. Since, however, we are not attempting a pore analysis, but an evaluation of particle size, the cellulose must be loosened up in such a way that an extensive separation of the micelles is accomplished, just as it is necessary in the preparation of samples for electron microscopic investigations. Suitable materials are the so-called air swollen (regenerated and porously dried) celluloses, whose preparation was pioneered by P. H. Hermans and co-workers.[10] In our former investigations[8] we demonstrated that the two limiting cases of the diluted and the dense system can very well be realized by this method.

II. EXPERIMENTAL

1. Preparation of the Samples

Isotropic xanthate fibers were spun from viscose according to the method of P. H. Hermans and de Leeuw.[10] By decomposition of the xanthate, they were transformed into highly swollen, "fresh" fibers of hydrate cellulose (F-fibers). If the water is replaced by an organic liquid and this again is evaporated, a porous gel is obtained which has retained the voids of the water swollen state, although with a certain reduction. The parallel alignment of neighboring micelles, however, which is noticeably present in water even at a very high degree of swelling, has given place to an extensive randomness. An F-fiber prepared from 8% technical viscose with $q \approx 5$ yields an air-swollen (porous) fiber, whose degree of swelling with regard to volume, q, lies not very much above 2. In order to obtain a higher degree of swelling, a 1.9% viscose made from cotton linters was used as starting material. From this an F-fiber with $q \approx 10$ was prepared, which again yielded a porous cellulose fiber with $q \approx 6$.

For the conversion to the air-swollen state the F-fibers were placed in turn into ethanol, absolute ethanol, xylene, and petroleum ether, being kept one day in each solvent. The petroleum ether was removed completely by evacuation for several hours. We obtained porous, white, very hydroscopic samples, which were sealed into the narrowest possible glass capillaries immediately after taking them out of the drying pistol. In this form the thickness of the samples could be measured, and the x-ray investigations were carried out. We designate these fibers as porous, fresh fibers (PF-fibers).

For the preparation of dense samples, the porous fibers are first placed in ethanol, then swollen in water, then dried in air, and finally evacuated over P_2O_5 at slightly above 100°C. for at least 18 hr. in the drying pistol. The fibers obtained in this way possess, by definition, a degree of swelling $q = 1$. They are called dense fibers (D-fibers).

In order to obtain also porous samples with low degrees of swelling, the dense fibers were reswollen in 96% ethanol for a short time, then treated according to the procedure described for the highly swollen fibers, and dried. Depending on the time of reswelling in 96% ethanol (several hours to several days), degrees of swelling of $q = 1.05$ to $q = 1.16$ were obtained. We designate these samples as porous, reswollen fibers (PR-fibers).* In Table I important characteristics of the samples investigated are compiled.

2. Experimental Method

An x-ray tube with Cu target was run with a commercial, highly stabilized x-ray unit. The small-angle camera used was practically free of slit

* P. H. Hermans[11] introduced the designations: fresh (F) fibers, reswollen (R) fibers, dense (D) fibers. We also use these symbols and add for F- and R-fibers which have been transformed to the porous state the prefix P.

scattering and is described fully elsewhere.[12] After several improvements it allowed measurements down to a scattering angle of 0.45 arc minutes (1.3×10^{-4} radians), corresponding to a Bragg value of 12,000 A.[13] With a distance a between sample and plane of registration of about 20 cm., the exposure begins then at an m value of 0.026 mm. (where m is the distance between counting tube slit and the center of the primary beam, $m/a \approx 2 \sin \theta$). The measurement of the scattered intensity is carried out by means of a Geiger counter placed at the end of an evacuated tube, which is inserted behind the sample in order to avoid air scattering. By means of a precision spindle, whose movement measures the m value, this tube together with the counter tube and the counter tube slit is rotated around an axis lying in plane of the sample.

The selection of the CuKα line from the radiation is done by means of the filter difference method according to Ross.[14]

Great care must be devoted to the elimination of the collimation error. The elimination of the length collimation error for an infinitely long primary beam was accomplished by the method of Guinier and Fournet;[15] that for primary beams of finite length according to Kratky, Porod, and Kahovec.[16] The breadth collimation error was eliminated by the method of Kratky, Porod, and Skala;[17] the latter procedure was necessary for the innermost part of certain scattering curves extending to very small angles corresponding to Bragg values of more than 1000 A. Concerning all questions pertinent to the elimination of the collimation error, which cannot be discussed here in detail, we refer to our summarizing treatment.[17] For the numerical collimation corrections we made use of the computer method developed at this institute by Heine and Roppert.[18]

Two types of primary beams were used for the exposures: short and relatively broad ones, and elongated, very thin ones.

All curves reproduced in the following sections and used in the calculations are collimation-corrected.

We shall designate the intensity of scattering curves uncorrected for length collimation errors by $\tilde{I}$, and the intensity of corrected scattering curves or of curves not affected by collimation errors by I.

Although the scattered intensity decreases very steeply from its very high values at the smallest angles, as the scattering angle increases, we still can, especially with the highly swollen samples, measure scattering up to $\sin 2\theta \approx 1/5$ (Bragg value $D \approx 8$ A.). Thus the range of angles measured comprises three orders of magnitude; the decrease of intensity between smallest and largest angles is up to five orders of magnitude. Therefore it was necessary to change the broadness of the entrance slit into the collimation system several times during the measurement. The smallest slit width used was 0.006 mm., the largest 0.3 mm. Of course the broadness of the counting tube slit had to be changed simultaneously. It lay between 0.006 and 0.8 mm. Care was always taken that the partial curves obtained overlapped in a sufficiently broad range, so that they could be adjusted and compared to one another. In general, we reproduce only the already com-

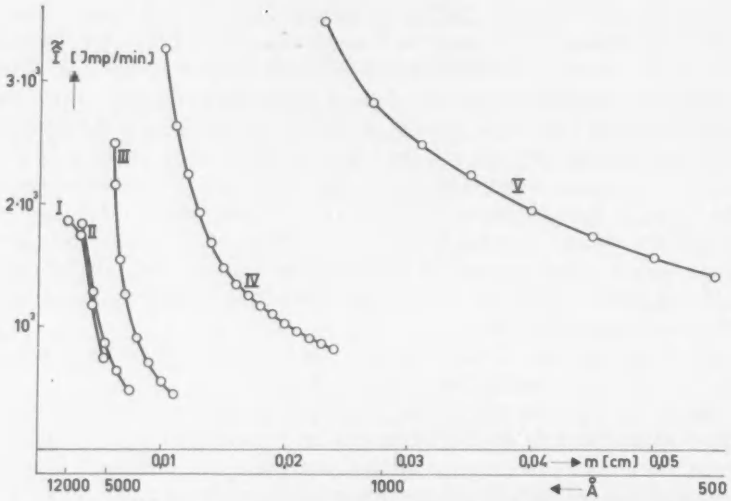

Fig. 1. Five partial curves of series 1. Scattered intensity $\tilde{I}$ (uncorrected for both length and breadth collimation error) of the sample PF with $q = 5.98$; entrance slit varied from 0.006 mm. to 0.06 mm., width of counting tube slit from 0.006 mm. to 0.1 mm.; range 12,000–500 A. ($a = 18.2$ cm.).

bined total curves. An example of the partial curves used for the construction of a scattering curve is found in Figures 1 and 2.

A very important experimental aim was the measurement of the absolute intensity, that is, the ratio between the scattered intensity and the primary energy; therefore it is necessary to measure the latter. The experimental difficulty is the great number of pulses per second in the primary beam. With average exposure conditions, about 10^7 to 10^8 pulses/sec. arrive at the counter while, due to the dead time of the measuring device, at most 10^4 counts/sec. can be registered directly. Therefore a reduction by a factor 10^3 to 10^4 is necessary. We have already reported a method we have developed, which brings about the reduction of the primary beam energy by means of a rotating disk with very small holes,[19] placed in front of the counter slit.

In the following, where we talk about the scattered intensity on the absolute scale, we always mean the quotient between scattered intensity and primary intensity. The scattered intensity is the directly measured number of pulses, divided by the counting tube slit area, or the intensity obtained from this figure by the correction for the collimation error. The primary intensity P_0 is, for primary beams without correction for collimation error, the number of pulses per second in the whole primary beam. In the case of correction for the length-collimation error it is the number of pulses corresponding to a portion 1 cm. long, everthing being referred to the plane of registration. (Nothing is changed in the quotient I/P_0 in case of cor-

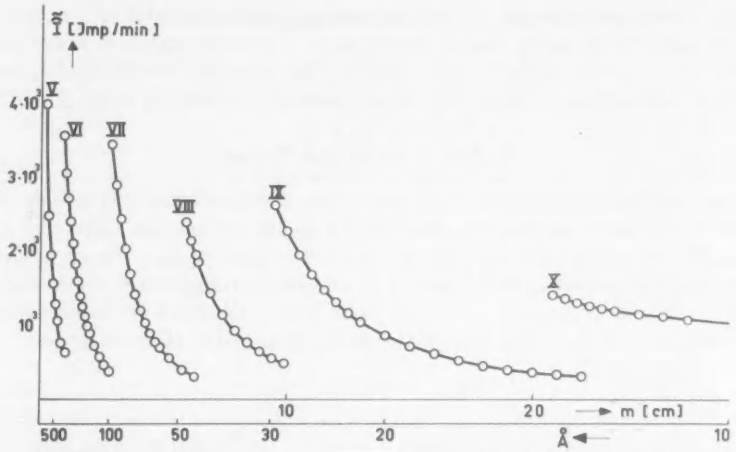

Fig. 2. Six partial exposures of series 1. Scattered intensity $\tilde{I}$ (uncorrected for both length and breadth collimation error) of the sample PF with $q = 5.98$; entrance slit varied from 0.06 mm. to 0.3 mm.; width of counting tube slit from 0.1 mm. to 0.8 mm.; range 500–10 A. ($a = 18.2$ cm.).

rection for the length collimation error if both the scattered and the primary energy are referred to the length of the counting tube slit, as we have done.)

III. REMARKS ON THE THEORETICAL ANALYSIS

Although certain basic features of the theory, e.g., the determination of the cluster fraction, arose only during the attempts at interpretation, it appears reasonable to present them prior to the evaluation procedure itself, together with a short summary of the relationships already known for the determination of shape, mass, inner surface, etc.

1. Applicability of the Principles of Particle Scattering

First, some doubt may arise whether these samples, even the most swollen ones with $q = 5.98$, may be regarded as "diluted," and subject to the principles of particle scattering. However, we may grant that the interparticle interference effects become the less important, the more anisotropic the particles are,[20] provided the arrangement of the particles is random, that is, not parallel. Now many investigations have proved the elongated, ribbonlike shape of the micelles; e.g., the study of the mechanism of deformation,[21] or the anisotropy of small-angle scattering by stretched and rolled (pressed) samples on irradiation in the stretching direction.[4] Polydispersity, of course, acts in the same way; but nothing is known about its extent initially.

We want to stress, however, that such a consideration based on the particle scattering finds its limit as the packing density increases, because very

anisotropic particles must show increasing parallel orientation on steric grounds as the packing density is enhanced. The comparative study of the scattering curves actually demonstrates the necessity to distinguish between both diluted systems and densely packed, interfering systems.

2. The Cross-Section Factor

Considering the typically elongated shape of the particle the cross-section factor,[22,23] $I\theta$ or Im suggests itself for use in the evaluation. The plot of ln (Im) versus m^2 (in analogy to the Guinier plot of ln I versus m^2 for corpuscular particles) then leads to a decreasing straight line, whose slope tan α in the inner portion (as far as it is not disturbed by interference effects) allows the calculation of the radius of gyration of the cross section R_q according to:

$$R_q = \frac{a\lambda}{2\pi}\sqrt{2 \times 2.3 \tan \alpha} \tag{1}$$

The plot of log Im versus log m leads to the shape of the cross section by comparison with theoretical scattering curves. It should be kept in mind that a lowering of the intensity compared to that of the theoretical curves is to be expected in the innermost portion, due to the influence of interferences (Fig. 8).

From the abscissa difference (log μ − log m) between both theoretical and experimental cross section factors R_q can be calculated according to:

$$R_q = \mu^* \lambda a/m^* 2\pi \tag{2}$$

where

$$\mu = R_q 4\pi \sin \theta/\lambda$$

In eq. (2) μ^* and m^* represent a corresponding pair of values.

3. The Mass per Unit Length of the Particles Determined from Absolute Intensity

We refer to our earlier investigations,[24] which show, that for elongated particles the mass per unit length $M/1$ A. can be calculated from the absolute intensity of the cross-section factor extrapolated to zero angle $(Im)_0$. Generally the extrapolation will be done by plotting ln Im against m^2. Then the relation will hold:

$$M/1 \text{ A.} = \mathrm{K}(Im)_0 a/P_0 dcz_1^2 \tag{3}$$

$$\mathrm{K} = 2/i_e N_L \lambda = 27.3$$

Here, z_1 = the number of mole electrons in 1 g. cellulose = 0.53; i_e = Thomson's constant = $7.9 + 10^{-26}$; λ = wavelength of the CuKα line = 1.54 A.; N_L = Loschmidt's number; d = thickess of sample (in centimeters).

4. Use of the Invariant in Relative and Absolute Scale

a. Absolute Value. As demonstrated in the theories of Debye and Bueche[25] and Porod,[26] the "invariant," defined according to

$$Q = \int_0^\infty Im^2 dm \tag{4}$$

does not depend on the geometrical structure (and therefore not on the degree of dispersion of the system), but only on the average square fluctuation of the electron density $\overline{(\Delta\rho)^2}$, which we call the scattering power of the system. Then,

$$Q = kP_0 da\overline{(\Delta\rho)^2} \tag{5}$$

$$k = (i_e/4\pi)\lambda^3 N_L{}^2 = 8.34 \times 10^{-3}$$

Here P_0 is the primary energy, as defined above.

For the special case of the two-phase system cellulose–air, which is of interest here, we have:

$$\overline{(\Delta\rho)^2} = w_1 w_2 (\rho_1 - \rho_2)^2 = w_1 w_2 \rho_1{}^2 \tag{6}$$

where ρ_1 = electron density of cellulose; ρ_2 = electron density of air = 0; w_1 = volume fraction of cellulose = $1/q$; w_2 = volume fraction of air = $1 - (1/q)$. Then, we obtain from relation (5):

$$Q = kP_0 da\rho_1{}^2 (w_1 w_2)_Q \tag{7}$$

As the left-hand side of the equation is given by eq. (4), the product of the volume fractions of both disperse phase and dispersing agent $(w_1w_2)_Q$ can be calulated if the primary energy P_0 is known. (The subscript Q is to indicate that the determination has been done by means of the invariant.) On the other hand, the product of the volume fractions is given by the macroscopic degree of swelling q:

$$(w_1 w_2)_q = (1/q)\ [1 - (1/q)] \tag{8}$$

These two values $(w_1w_2)_Q$ and $(w_1w_2)_q$ must agree if it is possible to calculate the invariant completely according to eq. (4). This, however, requires measurement of the scattering from the smallest angles to the complete decay of the scattering curve. Since this is ordinarily not completely possible, the quotient $(w_1w_2)_Q/(w_1w_2)_q$ will lie more or less below 1, and its magnitude is a measure for the degree to which the scattering power, theoretically expected for a two-phase system, shows up experimentally. We may call the quotient the experimentally accessible scattering power fraction.

The possible reasons for this difference shall be discussed in detail.

The separation of the background from the tail of the scattering curve, which is very low in intensity, is connected with uncertainties. An important help is here provided by the fact, derived from the theory of Porod,[26] that the tail behaves as $1/\theta^4$ (or $1/m^4$) in the scattering curve not afflicted with or else corrected for collimation errors. If there is a constant back-

ground additionally present due to density fluctuations in molecular and atomic regions (this is often so for curves not corrected for collimation error, while the correction procedure due to its differentiation eliminates an eventual constant part), we have:

$$I = (k/m^4) + \mathrm{K} \tag{9}$$

or

$$Im^4 = k + Km^4 \tag{10}$$

If we plot Im^4 versus m^4, we accordingly obtain a straight line whose intercept represents the factor of proportionality k. The partial invariant, beginning at a certain m^* and extending to infinity is then:

$$\int_{m^*}^{\infty} (k/m^4)\, m^2 dm = k/m^* \tag{11}$$

It can therefore be determined rather reliably, as soon as k is established.

Between the smallest angle for which the scattered intensity can still be measured and the angle zero lies a portion of the invariant which cannot be obtained experimentally. Therefore, the newly developed possibility of measuring down to angles considerably smaller than have so far been attained represents a significant improvement.

b. Relative Value. Since the invariant does not depend on the degree of dispersion, but the intensity extrapolated to zero angle does increase with the average volume of the particles, the quotient of these quantities represents a measure for the volume of the particle. By analogy we find, for very elongated particles, that the quotient of the cross-section factor extrapolated to zero intensity and the invariant represents a measure for the area of the cross section:[24]

$$F = \frac{(Im)_0 (a\lambda)^2}{Q\, 2\pi} \tag{12}$$

For a rectangular cross section, the axes A and B can be calculated from the area F and the radius of gyration R_q:

$$F = AB \tag{13}$$

$$R_q^2 = (1/12)\,(A^2 + B^2)$$

5. The Cluster Fraction

If we may assume, that the tail portion of the scattering curve has been measured with sufficient completeness, but the experimentally accessible scattering power fraction still remains significantly below 1, we shall postulate, that a portion f of the substance is present in the form of very large dense particles, so-called "clusters," whose scattering cannot be measured as it occurs at extremely small angles.

The fraction of the total scattering power, corresponding to the invariant Q' of the disperse fraction $(1 - f)$ only, we shall call r:

$$r = Q'/Q \tag{14}$$

Q meaning the total invariant. Also, formally we may take $(w_1w_2)_Q$, calculated from eq. (7), as a measure for the invariant. If we determine this product from Q' belonging to the disperse fraction, we must consequently denote it by $(w_1w_2)_{Q'}$:

$$(w_1w_2)_{Q'} = Q'/kP_0da\rho_1^2 \tag{15}$$

Then we may write r as follows:

$$r = (w_1w_2)_{Q'}/(w_1w_2)_q \tag{16}$$

That is, the product of the volume fractions derived from the external swelling according to eq. (8) corresponds to the total invariant.

Since the clusters are not swollen in themselves, the nonclustered portion $(1 - f)$ must possess a degree of swelling q', which is larger than the macroscopic degree of swelling q and, as we see immediately from what has been said above,

$$q' = q/r \tag{17}$$

The further formulation of this concept starts from the following relations between q, f, and q':

$$f + (1 - f)q' = q \tag{18}$$

$$q' = (q - f)/(1 - f)$$

From this

$$f = (q - q')/(1 - q')$$

and by inserting eq. (17):

$$f = q(1 - r)/(q - r) \tag{19}$$

For the further analysis, beside the total thickness d of the sample, that thickness is required which corresponds to the disperse fraction alone. As we readily see,

$$d' = d(1 - f)q'/q$$

From this we obtain, with eqs. (17) and (19):

$$d' = d(q - 1)/(q - r) \tag{20}$$

Briefly summarized: if that fraction of the scattering power r is known which we may assume to correspond to the nonclustered portion, then the internal degree of swelling q' of the disperse fraction is determined by eq. (17), the cluster fraction f by eq. (19), and the thickness d' of the nonclustered portion of the sample by eq. (20).

6. The Inner Surface

As has been mentioned above, the tail portion follows, apart from a constant term, the function $I = k/m^4$ for curves not affected by or cor-

rected for the collimation error. Now, according to Porod,[26] the quotient of k and the invariant Q is, for a two-phase system, proportional to the inner surface. The exact relation for the specific inner surface, that is the phase boundary area per unit volume of the disperse phase, is given by:

$$O_s = (2\pi^2/a\lambda)w_2(k/Q) \tag{21}$$

Assuming that the inner surface of the clusters can be neglected, we obtain for the disperse fraction:

$$O_s' = (2\pi^2/a\lambda)w_2'(k/Q') \tag{22}$$

Here w_2', the volume fraction of the voids in the nonclustered portion, is given by:

$$w_2' = 1 - 1/q' \tag{23}$$

For infinitely long ribbons the relation between O_s', and the axes B and A is given evidently by:

$$O_s' = 2(A + B)/AB \text{ A.}^{-1} \tag{24}$$

$$B = 2A/(AO_s' - 2)$$

IV. MEASUREMENTS AND THEIR INTERPRETATION

The experimental data and the figures derived from them in the course of the evaluation, are compiled in Table I.

1. Scattering Power of the Most Highly Swollen PF Sample with $q = 5.98$

Ten partial exposures of the series 1 (Fig. 1 and 2) yielded the experimental invariant, as shown in Figure 3. Figure 4 shows the innermost part with greatly enlarged abscissa scale. We should like to point out particularly, that this measurement extends down to an angle corresponding to a Bragg value of 12,000 A. By the correction for the breadth-collimation error, the innermost part of the curve is lost, therefore the corrected curve extends to about 9000 A. We obtained:

$$Q = 9.96$$

and from this with eq. (7):

$$(w_1w_2)_Q = 0.149$$

On the other hand, with eq. (8) we obtain from the macroscopic degree of swelling:

$$(w_1w_2)_q = 0.141$$

therefore

$$\frac{(w_1w_2)_Q}{(w_1w_2)_q} = 1.056$$

TABLE I

	Measurement series					
	1	2	3	4	5	6
Type of sample	PF	PF	PF	PR	PR	D
q	5.98	2.2	2.2	1.16	1.05	1.00
d, cm.	0.108	0.095	0.095	0.081	0.1003	0.0845
Primary beam	Infinitely long	Infinitely long	Finite	Infinitely long	Infinitely long	Infinitely long
a, cm.	18.2	24.0	25.8	24.0	24.0	24.0
P_0	5.54×10^3	2.01×10^7	5.5×10^6	10.02×10^7	6.84×10^7	
Q' (exptl.)	8.72	3.58×10^4	1.015×10^4	3.38×10^4	5.39×10^3	
$(w_1w_2)_q$ from eq. (8)	0.141	0.248	0.248	0.12	0.0453	
r from eq. (16)	0.875	0.514	0.496	0.23	0.119	
q' from eq. (17)	6.84	4.29	4.4	5.45	8.84	
f from eq. (19)	0.147	0.635	0.65	0.964	0.993	
w_2' from eq. (23)	0.854	0.767	0.774	0.816	0.887	
d' from eq. (20), cm.	0.106	0.055	0.055	0.0182	0.0054	
F from eq. (12)	9360	9000	9240	9260	—	
B from eq. (13)	61	60.0	60.5	60.9	—	
A from eq. (13)	152.5	150	151	152.3		
$(Im)_0$	6.52×10^2	1.48×10^6	3.74×10^5	1.44×10^6	—	
M/A. from eq. (3)	8480	8310	8480	8300	—	

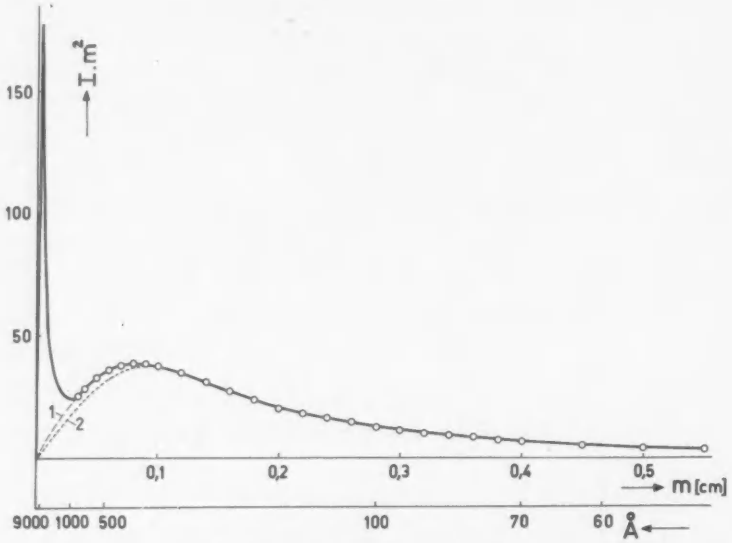

Fig. 3. Im^2 curve for the sample PF with $q = 5.98$. The dashed line *1* continues the right hand portion of the curve while the dashed line *2* separates the scattering of the disperse fraction from that of the cluster fraction ($a = 18.2$ cm.).

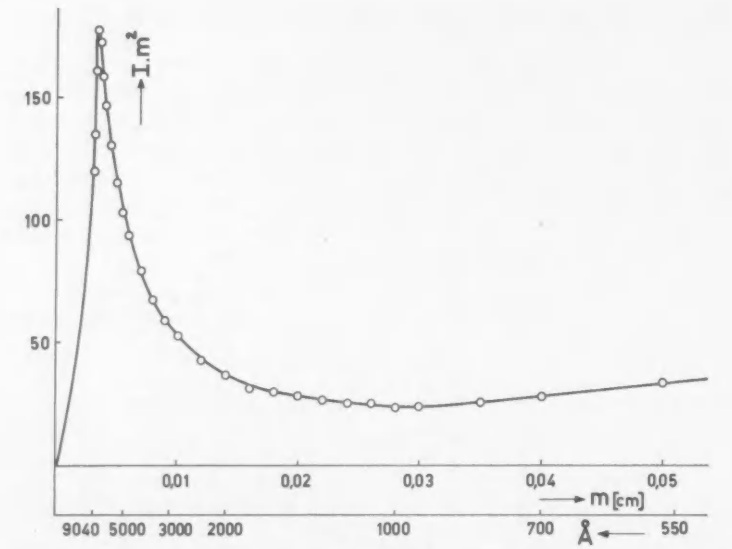

Fig. 4. Inner portion of Fig. 3 with abscissa scale enlarged 10-fold ($a = 18.2$ cm.).

Since this quotient cannot exceed unity on theoretical grounds, the deviation of 5.6% upwards must be regarded as experimental error. It certainly lies in a range which is understandable considering the particular difficulties of this measurement and the cumulation of many sources of error. These include errors in the absolute measurement of the primary energy, combination of measurements with ten different primary beams, errors in slit dimensions of the counting tube slit (particularly in the width), macroscopic determination of the degree of swelling, uncertainties in the density of the compact cellulose, and others.

Thus we can state, that the total scattering power to be expected from the composition, has indeed been found within the experimental accuracy.

If the measurement had extended only to an angle corresponding to a Bragg value of 1000 A., a limit which in x-ray small-angle measurements has been exceeded only rarely, the experimental curve in Figure 3 would have had to be extrapolated following the broken line *1*. There is no doubt that the second rise at small angles is caused by a cluster portion. This is the first time that such a rise of the invariant beginning at small angles could be followed beyond its maximum (at about 9000 A.) down to its final decrease.

Although Figure 3 could lead us to the idea of a structure composed of single particles and clusters, which will hold as a first approximation, the evaluation of the cross-section curve, (Figs. 7 and 8) as carried through later on, shows that the transition takes place continuously to a certain extent; that is, besides single particles there are still present further small aggregates. This structure of this sample is obviously caused by the method of preparation, which was directed at obtaining pronounced loosening up. It has turned out that the samples of medium degree of swelling are more rewarding in this regard, because they display essentially only single particles beside a larger cluster fraction. Obviously, for these samples everything that could not exist as single particles has already joined one of the larger clusters. Therefore, we shall first turn to the evaluation of the samples of medium degree of swelling, and then return to those showing the highest degree of swelling.

2. Behavior of the PF Sample with $q = 2.2$

a. Invariant and Cluster Fraction. In the following, we make use of the results of the two measuring series 2 and 3 (Table I) carried out independently, one with an infinitely long primary beam, the other with a short, relatively broad one. The first measurement has a higher resolution, the second has the advantage of being practically free from collimation error beginning at $m = 0.4$ cm.

In Figure 5, the intensity $\bar{I}$ together with I, as obtained after the collimation correction, is given for series 2 as a log–log plot. In accordance with the postulate of the theory, the tail portion of the uncorrected curve decreases with $\tan \alpha = -3$, the tail portion of the corrected curve with $\tan \alpha = -4$.

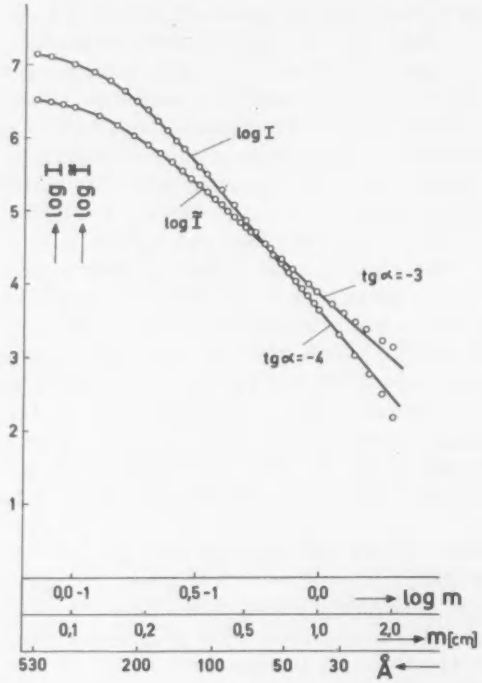

Fig. 5. Sample PF with $q = 2.2$, log–log plot of $\tilde{I}$ and I ($a = 18.2$ cm.).

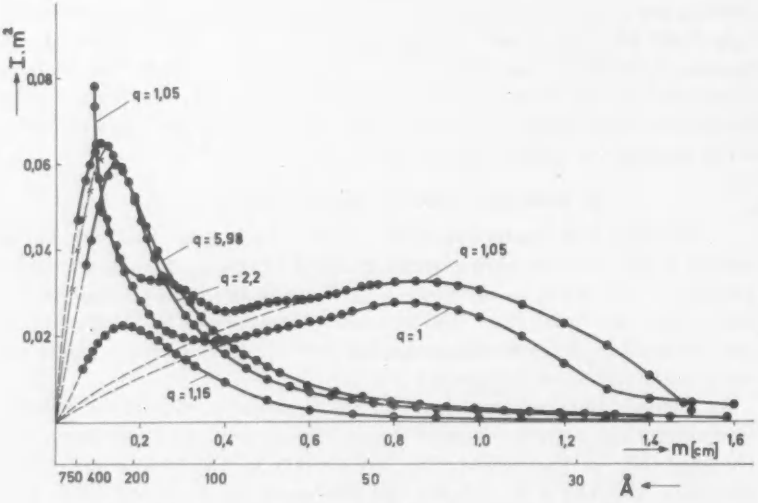

Fig. 6. Im^2 vs. m curves for all samples (recalculated to $a = 24$ cm.).

In Figure 6 the Im^2 curves for all samples are compiled. Their extrapolation to zero angle has been carried out long the broken lines. The evaluation according to the way discussed above, yielded for the measurements of series 2 the figures listed in Table I. From

$$r = 0.514$$

we learn, that only half of the scattering power to be expected from the material structure had been found. If we assume that it corresponds to the disperse fraction, we find with eq. (19):

$$f = 0.635$$

and with eqs. (17) and (23)

$$q' = 4.29$$

and

$$w_2' = 0.767$$

Therefore, the loosened-up fraction of the sample is considerably less dense than we had expected from the small total degree of swelling $q = 2.2$.

Measurements of series 3 yielded the same values, within the limit of error, for r, f, q', and w_2'.

b. Radius of Gyration and Axial Ratio of the Cross Section. Figure 7 shows, for the samples with $q = 5.98$, 2.2, and 1.16 the cross-section factors in the plot ln Im versus m^2. The decrease with $q = 2.2$ in the innermost part can be caused by either interparticle interference effects or the finite length of the particles. It may be disregarded in the determination of the cross section. The adjacent part of the curve is a nearly straight line over a sufficiently large range, so the slope, understood as the limiting slope for $m = 0$, can be determined without much ambiguity. We calculate therefrom:

$$R_q = 47 \text{ A.}$$

The shape of the cross-section factor curve justifies the assumption made for the calculation of the cluster fraction, that the observed scattering power could be assigned to the disperse fraction. Of course this statement can be regarded only as an approximation, since in spite of the decrease at small angles, there might be clusters present whose effect is overcompensated by interference effects. In any event, the assignment of the measured invariant to the disperse fraction should represent a reasonable approximation. This will be substantiated by further results in the following.

We have also plotted the cross-section curves in a log–log plot for the determination of the cross-section shape by means of a comparison with theoretical curves. Figure 8 shows, that the experimental curve for $q = 2.2$ fits an axial ratio of 0.4 well. The decreasing innermost part, which deviates from the theoretical curve corresponds to the innermost points of

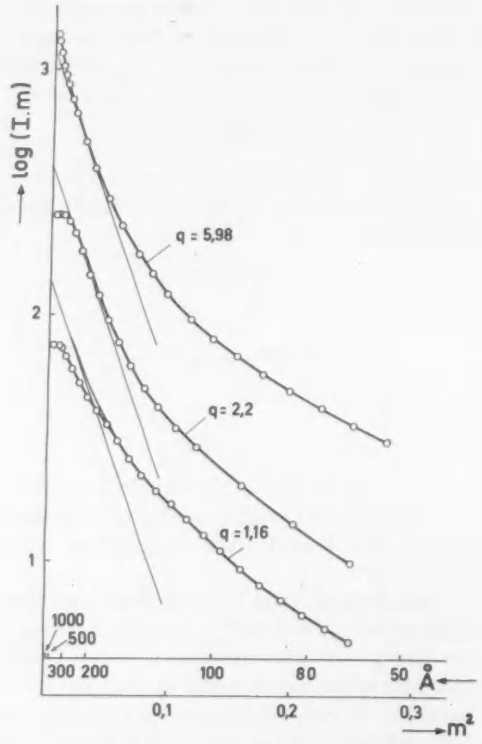

Fig. 7. Guinier plot of the cross-section factors (log Im vs. m^2 plot) for the samples with $q = 5.98$, 2.2, and 1.16 (recalculated to $a = 24$ cm.).

the Im curve of Figure 7. If we transfer from this Figure 7 the innermost part of the Guinier straight line extrapolated to $m^2 = 0$, into Figure 8, then we obtain the points (denoted by an open circle) which fit the theoretical curve perfectly.

From the abscissa difference of both theoretical and experimental curve $(\log \mu^* - \log m^*) = 0.9$ we calculate according to eq. (2)

$$R_q = 46.6 \text{ A.}$$

That is the same value as was obtained from the Guinier straight line in Figure 7.

With the axis ratio $B/A = 0.4$, and with $R_q = 46.6$ A., we find, using eq. (13)

$$A = 150 \text{ A.}$$

and

$$B = 60 \text{ A.}$$

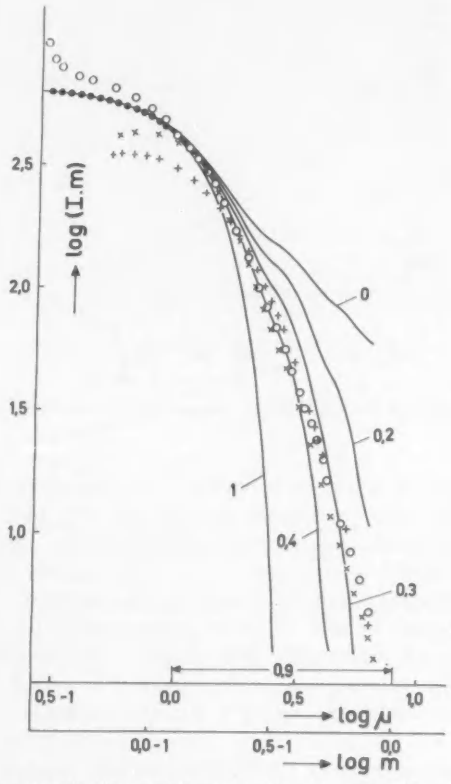

Fig. 8. Log–log plot of the theoretical cross-section curves for the axial ratio B and A of 0.2, 0.3, 0.4, and 1 with experimental values for the samples with (O) $q = 5.98$; (×) $q = 2.2$; and (+) $q = 1.16$ (recalculated to $a = 24$ cm.); (●) curve corresponding to the tangents of the Guinier plot in Fig. 7.

Measurements of series 3, with a short primary beam (Table I) lead to practically identical results with regard to the shape of the cross section.

The only serious objection which could be raised against the described determination of the shape of the cross section is the assumption of polydispersity. Actually, even for an isotropic cross section and a variety of diameters, a cross-section curve of any convex shape can result. Strictly speaking, we must therefore regard the calculated shape as equivalent in scattering, and understand the anisotropy found as that highest possible one which corresponds to the limiting case of uniform cross-sectional dimensions. Now, not only qualitative reasons are in favor of a ribbon shape.[21] From the anisotropy of the small angle scattering of stretched and pressed (rolled) samples on irradiation in the stretching direction, on the one hand, a ratio of the lateral dimensions of about 0.3 is obtained;[5] on the other hand, observations with the electron microscope[27] suggest more

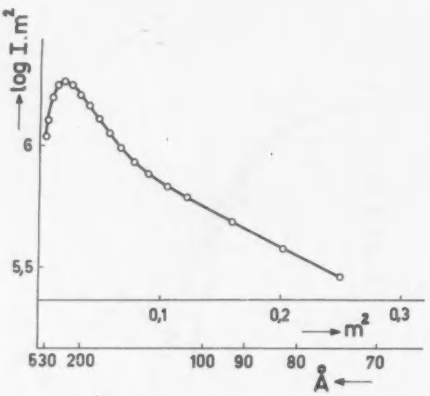

Fig. 9. Guinier plot of the thickness factor, (log Im^2 vs. m^2) for the sample PF with q = 2.20.

and more a nearly monodisperse behavior. Also, the well known investigations by P. H. Hermans[28] and co-workers, as well as by Heyn,[29] concerning the occurrence of equatorial interferences with swollen, regenerated cellulose fibers, can hardly be interpreted otherwise than by assuming rather uniform lateral dimensions of the supermolecular particles. Finally, in the next section we shall be able to derive a direct proof for rather uniform dimensions. So we may regard the calculated dimensions of the cross section, equivalent in scattering, as the true ones to a good approximation.

In Figure 9 for the sample with q = 2.2, the thickness factor log Im^2 is plotted against m^2. Its transition to a flat curve with decreasing scattering angle could make us conclude the existence of infinitely extended lamellae whose thickness can be determined from the slope of the innermost portion. But, while the cross-section factor can exhibit very different shapes depending on the anisotropy of the cross section, extending from a shape slightly concave relative to the abscissa to a very convex one (as in this case), the thickness factor has, strictly speaking, no possibility for variation at all. Its shape deviates very little from a straight line, unless there is a strong polydispersity. Since various reasons could formerly be raised against such an assumption, we arrive at the conclusion, that we are not allowed to infer the existence of typically lamellar particles from the flatness of the log Im^2 versus m^2 curve at decreasing angles.

c. Cross-Sectional Area. For the cross-sectional area, we find for series 2 from $(Im)_0$ and the invariant by means of eq. (12):

$$F = AB = 9000 \text{ A.}^2$$

From this relation and R_q = 47 A. we calculate according to eq. (13):

$$A = 150 \text{ A.}$$

and

$$B = 60 \text{ A.}$$

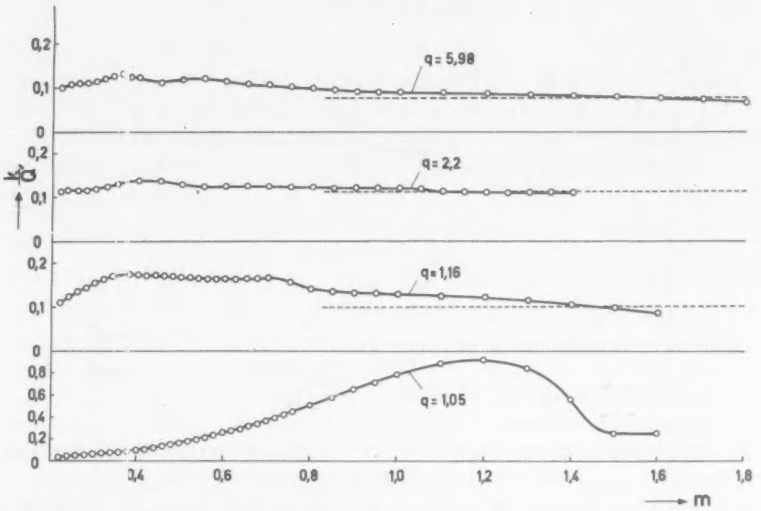

Fig. 10. k/Q' vs. m plot for the samples with $q = 5.98$, 2.2, 1.16, and 1.05. The dashed lines represent those values derived from dimensions of the cross section.

These are the same dimensions that had been obtained from the shape analysis of the cross-section curve.

d. Inner Surface. From the given model of ribbonlike particles, the inner specific surface to be expected according to eq. (24) can easily be calculated as:

$$O_s' = 0.0465/\text{A}.$$

According to the theory, this value should also result from the tail portion of the curves with the help of eq. (22). As Figure 10 shows, the $Im^4/Q' \equiv k/Q'$—ratios actually attain a constant value as a good approximation in the range of $m = 1$ cm. for the samples with $q = 5.98$, 2.2, and 1.16. In this range of angles, however, the intensity has fallen to such a small value, that the accuracy of the measurement is relatively poor. Since, therefore, doubt may arise at what point the final value can be regarded as attained, we have chosen the opposite way. That is, we have calculated the k/Q' to be expected according to eq. (22) by means of the above O_s'-value and the experimental numbers Q' and w_2', and we have indicated it on the experimental curves (dashed lines). We note that for $q = 2.2$ and $q = 5.98$ the fit is very satisfactory. Furthermore, the behavior seems to agree with the theoretical prediction by Kirste and Porod,[30] that the final value of Im^4 will be reached from above.

As Figure 11 shows, in measuring series 3 the tail portion in the Im^4 versus m^4 plot exhibits a slight linear rise, obviously because no correction for the collimation error had been applied and therefore the linear term K of eq. (9) has not been eliminated automatically. The quantity k is ob-

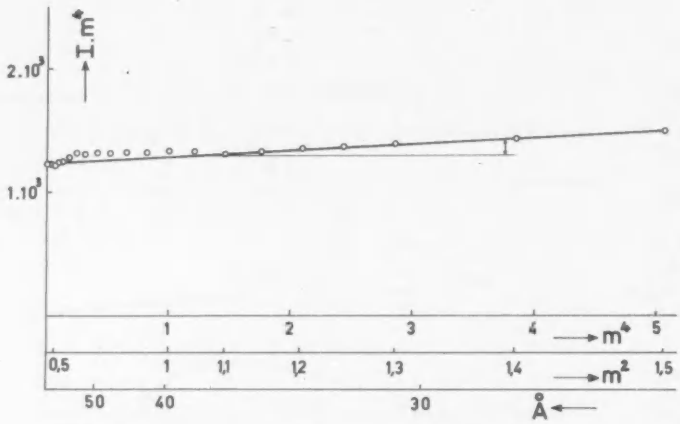

Fig. 11. Im^4 vs. m^4 plot for sample PF with $q = 2.2$, taken from series 3; short primary beam without correction for the collimation error.

tained, according to eq. (10), from the intercept of the straight line drawn in Figure 11. With eq. (22) we obtain:

$$O_s' = 0.0466/\text{A}.$$

a value, which fits the other results very well.

e. Mass per Unit Length from the Absolute Intensity of the Cross-Section Factor. The values listed in Table I yield, according to eq. (3), for the measurements of series 2:

$$M/1 \text{ A.} = 8310 \text{ molecular weight units}$$

and for series 3:

$$M/1 \text{ A.} = 8480 \text{ molecular weight units}$$

Now we shall compare this figure with that to be expected from the shape determination. From the cross-sectional area, already determined to be 9000 A.^{2}, we calculate with $d_{\text{cell}} = 1.615$:

$$M/1 \text{ A.} = 8640 \text{ molecular weight units}$$

The agreement within a few per cent can be regarded as very satisfactory.

We now return to our former remark, that our small-angle investigation also yields a direct argument for an extensive monodispersity with regard to the cross section of the ribbonlike particles. The inner surface depends on the number average of the lengths of the axes of the cross sections; the absolute intensity of the scattering, on the other hand, depends on the weight average of the cross-sectional areas. If we were dealing with a significantly polydisperse sample, therefore, the results obtained could not agree so well.

3. Reswollen PR Sample with $q = 1.16$

With some reservation we proceeded to the application of the evaluation procedures described to such a dense sample also. It is obvious, that the dense packing of the particles must modify the scattering behavior.

If here too we regard the portion of the scattering power found according to Figure 6 as an expression for the disperse, not clustered fraction, we find according to eq. (16):

$$(w_1w_2)_Q'/(w_1w_2)_q = 0.23 = r$$

Therefrom we can calculate the other values listed in Table I for the measurements of series 4. We wish to draw attention to the large cluster fraction of $f = 0.96$; therefore only 4% of the substance is present in a loosened form, which has a degree of swelling $q' = 5.45$.

Assuming that here too the same particles are present as with sample PF with $q = 2.2$, the specific inner surface in the disperse fraction must again be $O_s' = 0.0466$ A. The value of k/Q' calculated under this assumption is indicated in Figure 10. The agreement with the tail portions of the experimental curve can be regarded as satisfactory. This justifies the choice of the Guinier straight line in Figure 7, with a somewhat arbitrary accounting for the interparticle interference effect in such a way that a radius of gyration

$$R_q = 47 \text{ A.}$$

is obtained. With this the zero value of the cross-section factor $(Im)_0$ is fixed, and according to eq. (12) we can calculate the cross-sectional area as

$$F = 9260 \text{ A.}^2$$

From this value, together with the radius of gyration of the cross section, we obtain according to eq. (13) the axes of the cross section:

$$A = 152.3 \text{ A.}$$

and

$$B = 60.9 \text{ A.}$$

These data are supported rather convincingly by the comparison with the theoretical cross-section curve for an axial ratio 0.4 in the log–log plot (Fig. 8), and the abscissa difference obtained in this comparison, which, according to eq. (2), yields also

$$R_q = 46.6 \text{ A.}$$

The fact that the evaluation with a degree of swelling of $q = 1.16$ has led to practically the same results with regard to the cross section of the particles, suggests that in all samples the same cellulose particles are present regardless of the previous history.

4. Further Evaluation of the Scattering of the Most Highly Swollen PF Sample with $q = 5.98$

The chosen model could satisfactorily explain the behavior of samples as different as PF with $q = 2.2$ and PR with $q = 1.16$. Therefore it appeared meaningful, to check the scattering curves of the most diluted system with $q = 5.98$ with regard to the idea of ribbonlike particles also. As in the preceding results, the Guinier tangent was drawn for the cross-section curve in such a way that it led, according to eq. (1), to a radius of gyration (Fig. 7)

$$R_q = 47 \text{ A.}$$

The measurement of the scattering curve down to extremely small angles made it possible to separate the invariant immediately for both clustered and nonclustered fractions for this sample. The graphical separation in Figure 3 has been done in such a way that the right hand part together with the adjacent broken line 2 corresponds to the tail portion and the extrapolated Guinier straight line of Figure 7. Thus it represents the scattering of the individual particles. Its area yields:

$$Q' = 8.72$$

The determination of the cluster fraction can now be performed directly with Figure 3. According to eq. (14) we derive from it the area ratio

$$Q'/Q = 8.72/9.96 = 0.875 = r$$

The further values calculated therefrom are compiled in Table I. We want to point out particularly, that the internal degree of swelling $q' = 6.8$ is only slightly higher than the macroscopic one due to the small cluster fraction of $f = 0.147$.

The above determination of r and the values derived from it, is based, in a strict sense, on the assumption that the disperse fraction exhibits no significant interparticle interference effect, i.e., that its course is actually given by the Guinier straight line in Figure 7. Still present interference effects, which will keep within moderate limits, would change the values of r, f, and q' a little.

With the above value $Q' = 8.72$ and $(Im)_0$ taken from Figure 7, the cross-sectional area can be calculated according to eq. (12). We find

$$F = 9360 \text{ A.}^2$$

and with the radius of gyration we calculate according to eq. (13) the axes of the cross sections as:

$$A = 152.5 \text{ A.}$$

and

$$B = 61 \text{ A.}$$

An extensive match of the curves of both experimental and theoretical cross-section functions for the axial ratio 0.4 (Fig. 8) and the perfect agreement among the radii of gyration from both the abscissa difference and the extrapolated Guinier straight line are in any event a further proof for the hypothesis of the structural uniformity of the micellar particles of all samples.

The absolute determination of the molecular weight/A. yields, according to eq. (3), the satisfactory value

$$M/1 \text{ A.} = 8480 \text{ molecular weight units}$$

which deviates only slightly from the value $M/1$ A. = 8640 molecular weight units.

In conclusion we would like to emphasize with reference to Figure 7 that the choice of the same tangent for all three cross-section functions does not follow uniquely from the shape of the curves; one might draw a somewhat steeper tangent in such a manner as indicated by the innermost points of the curve corresponding to the sample with $q = 5.98$

Aside from the fact that only the square root of the tangent enters the radius of gyration and that therefore the calculated value of R_q is less sensitive to changes in the tangent, the best correspondence between the molecular weight per unit length, the cross-sectional area, the radius of gyration, the axial ratio of the cross section, and the specific surface are obtained only with the chosen tangent. Since the correlation of these five parameters for a single sample and the sufficient agreement of the corresponding parameters for the three samples depends essentially on the choice of a single characteristic parameter, namely, the tangent, that latter is practically determined.

Besides, the position of the tangent is plausible for all cases if one keeps the above in mind.

5. Densely Packed Systems

The comparative presentation of all Im^2 curves in Figure 6 shows how much the dense packing influences the scattered intensity and the shape of the scattering curve. The intensities are given in absolute scale, by division of Im^2 with P_0 and they are referred to the same amount of mass of irradiated compact cellulose, including clusters and swollen regions by division with d. The ordinates for both dense samples $q = 1.05$ and $q = 1$ are enlarged by a factor of 50.

a. Behavior of the PR Sample with $q = 1.05$. The last two measured points in the Im^4/Q' versus m plot (Fig. 10) correspond to $k = 1.41 \times 10^3$. With the help of this limiting value the graphically determined invariant could be extended to $m = \infty$ according to eq. (11). For the partial invariant from $m^* = 1.6$ on, we obtained:

$$\int_{m^*}^{\infty} Im^2 dm = 0.882 \times 10^3$$

In order to obtain the total value of the invariant belonging to the disperse fraction, an assumption concerning the course of the Im^2 curve versus zero angle is required. This had been made according to the broken line indicated in Figure 6. We obtain:

$$Q' = 5.39 \times 10^3$$

A comparison of the expression (w_1w_2) determined from Q' according to eq. (7)

$$(w_1w_2)_{Q'} = 5.35 \times 10^{-3}$$

and according to eq. (8)

$$(w_1w_2)_q = 0.0453$$

yielded the fraction of the scattering power belonging to the disperse portion according to eq. (16)

$$r = 0.119$$

and the cluster portion according to eq. (19)

$$f = 0.993$$

and the inner degree of swelling according to eq. (17):

$$q' = 8.84$$

It is very probable that the high value of the inner degree of swelling is caused mainly by large voids, which, beside very narrow voids, have the character of air clusters.

The specific inner surface of the unclustered portion is calculated, with the use of the value (eq. 23)

$$w_2' = 0.887$$

according to eq. (22) as

$$O_s' = 0.124/\text{A}.$$

The inner surface of the disperse fraction in the dense sample, therefore, is larger by a factor of 3 than that of the medium and highly swollen ones. It can be explained in terms of a system of very thin lamellae produced by splitting apart of the micelles. Assuming a model of ribbons with a breadth of $A = 150$ A., we calculate their average thickness according to eq. (24) to be $B = 18.1$ A.

Within the scope of the conception of the "fringed micelle," the opinion was laid down long ago[31] that the ribbon-shaped micelles are split apart above all in a laminar way. Of course this effect can enhance the inner surface considerably.

The fact that we have had no indication of such a strong splitting apart with the highly swollen samples may be interpreted as follows. In the preparation of the dense sample with $q = 1.05$, essentially all intact micelles

will be contained in compact clusters. Only where a strong splitting apart is present—and according to our calculation this is only the case for $(1 - f) = 0.7\%$ of the mass—will no dense packing result. Thus only the micelles which are split apart remain. It is understandable that this small amount in the highly swollen samples has no influence on the average behavior. Also, the few per cent of residual voids present in the dense sample, which produce an astonishingly high inner degree of swelling, do not play any essential role with the more highly swollen samples.

The very shape of the scattering curves for the dense samples in the Im^2 plot of Figure 6, provides a clear indication of a laminar system of narrow fissures whose scattering goes over a larger range approximately with $1/m^2$; to that degree they are therefore equivalent in scattering to very thin lamellae.

The maximum of the Im^2 curve at medium angle is in best agreement with the interpretation given. The lamellae will certainly be parallel to each other insofar as they belong to the same micelle, and neighboring micelles, too, will be approximately parallel due to the dense packing. Therefore an interference maximum must occur. The fact, that it is found at about 40 A., that is, at a considerably higher value than we have just calculated from the inner surface for the average thickness of the lamellae, can also be explained in a plausible way. The inner surface corresponds to the number average of the lamellae thickness, but the scattered intensity depends on the weight average of the cross-sectional areas. The large difference between the two values, therefore, indicates a strong polydispersity, as could readily be expected from the picture of a strong laminar splitting apart. A considerable portion of the mass will be present in an unsplit state (then the thickness is about 60 A.), another portion, on the other hand, will be split apart down to monomolecular layers of cellulose chains.

b. Behavior of Sample D with $q \approx 1$. The shape of the scattering curve is very similar to that of the sample just discussed. This suggests an essentially similar structure. An evaluation, to be carried out analogously, does not appear reasonable to us, since the external degree of swelling, which is decisive in all the relations must be regarded as unknown. While all other degrees of swelling are referred to the dense sample, which is assigned the degree of swelling $q = 1$, the correctness of this value cannot be checked due to the absence of accurate density data. That is, the true degree of swelling of the "dense" sample could be larger than unity by 1–2%. A swelling of this order of magnitude would explain the behavior satisfactorily, while a corresponding correction of the degrees of swelling of the other samples would not introduce a significant error into the evaluation of the measurements, as the calculation has shown.

Our thanks are due to the U. S. government for generously supporting this work. Director Harms has made possible the preparation of especially diluted viscose for making the highly swollen fibers in the laboratories of the Chemiefaser Lenzing. For this help and his advice we want to express our sincere thanks.

References

1. Mark, H., *Physik und Chemie der Zellulose*, Springer, Berlin, 1932, p. 139.
2. Krishnamurti, P., *Indian J. Phys.*, **5**, 473 (1930); S. B. Hendricks, *Z. Kristallog Mineral.*, **83**, 503 (1932); B. E. Warren, *J. Chem. Phys.*, **2**, 551 (1934).
3. Guinier, A., *Compt. Rend.*, **204**, 1115 (1937).
4. Kratky, O., *Naturwiss.*, **26**, 94 (1938); *ibid.*, **30**, 542 (1942).
5. Kratky, O., A. Sekora, and R. Treer, *Z. Elektrochem.*, **48**, 587 (1942).
6. Meyer, K. H., and H. Mark, *Ber. dtsch. chem. Ges.*, **61**, 611 (1928).
7. Hosemann, R., *Z. Physik*, **113**, 751 (1939); *ibid.*, **114**, 133 (1939); *Kolloid-Z.*, **117**, 13 (1950); *ibid.*, **119**, 129 (1950).
8. Janeschitz-Kriegl, H., O. Kratky, and G. Porod, *Z. Elektrochem.*, **50**, 146 (1952).
9. Kratky, O., and G. Porod, *Z. Elektrochem.*, **58**, 918 (1954); *ibid.*, **60**, 188 (1956); R. Hosemann, *Z. Elektrochem.*, **58**, 271 (1954); *ibid.*, **58**, 923 (1950); *ibid.*, **60**, 189 (1956).
10. Hermans, P. H., and P. Platzek, *Z. Physik. Chem.*, A **185**, 260 (1939); P. H. Hermans and A. J. de Leeuw, *Kolloid-Z.*, **83**, 58 (1938).
11. Hermans, P. H., *Physics and Chemistry of Cellulose Fibres*, *Elsevier*, New York–Amsterdam–London, 1949, p. 453 ff.
12. Kratky, O., *Z. Elektrochem.*, **58**, 49 (1954); *ibid.*, **62**, 66 (1958); *Kolloid-Z.*, **144**, 110 (1955); O. Kratky and A. Sekora, *Monatsh. Chem.*, **85**, 660 (1954); O. Kratky and Z. Skala, *Z. Elektrochem.*, **62**, 73 (1958).
13. Kratky, O., P. J. Schmitz, and K. Schier, *Monatsh. Chem.*, **93**, 321 (1962).
14. Ross, P. A. J., *J. Opt. Soc. Am.*, **16**, 433 (1928); K. Hoffmann, *Physik.-Z.*, **39**, 695 (1938); *Angew. Chem.*, **66**, 771 (1954).
15. Guinier, A., and G. Fournet, *J. Phys. Radium*, **8**, 345 (1947); J. M. W. du Mond, *Phys. Rev.*, **72**, 83 (1947).
16. Kratky, O., G. Porod, and L. Kahovec, *Z. Elektrochem.*, **55**, 53 (1951).
17. Kratky, O., G. Porod, and Z. Skala, *Acta Phys. Austriaca*, **13**, 76 (1960).
18. Heine, S., and J. Roppert, *Acta Phys. Austriaca*, **15**, 148 (1962); S. Heine, *Acta Phys. Austriaca*, in press.
19. Kratky, O., *Makromol. Chem.*, **35A**, 12 (1960); *Kolloid-Z.*, **182**, 7 (1962).
20. Kratky, O., and G. Porod, *Z. Physik. Chem.* (*Frankfurt*), **7**, 236 (1956).
21. Burgeni, A., and O. Kratky, *Z. Physik. Chem.* (*Leipzig*), **B4**, 401 (1929); B. Baule, O. Kratky, and R. Treer, *ibid.*, **50**, 255 (1941).
22. Kratky, O., and G. Porod, *Acta Phys. Austriaca*, **2**, 133 (1948).
23. Porod, G., *Acta Phys. Austriaca*, **2**, 255 (1948).
24. Kratky, O., and G. Porod, in *Die Physik der Hochpolymeren*, H. A. Stuart, Ed., Vol. II, Springer, Berlin–Göttingen–Heidelberg, 1953, p. 515 ff; O. Kratky, *Z. Elektrochem.*, **60**, 245 (1956).
25. Debye, P., and A. M. Bueche, *J. Appl. Phys.*, **20**, 518 (1949).
26. Porod, G., *Kolloid-Z.*, **124**, 83 (1951); *ibid.*, **125**, 51 (1951).
27. Mukherjee, S. M., S. Sikorski, and H. J. Woods, *J. Textile Inst.* **43**, 196 (1952).
28. Heikens, D., P. H. Hermans, and A. Weidinger, *Nature*, **170**, 369 (1952); D. Heikens, P. H. Hermans, P. F. van Velden, and A. Weidinger, *J. Polymer Sci.*, **11**, 433 (1953).
29. Heyn, A. N. J., *Nature*, **172**, 1000 (1953).
30. Kirste, R., and G. Porod, *Kolloid-Z.*, **184**, 1 (1962).
31. Hermans, P. H., *Physics and Chemistry of Cellulose Fibres*, Elsevier, Amsterdam, 1949; W. Kast and A. Prietzschk, *Kolloid-Z.*, **114**, 23 (1949); W. Kast, L. Flaschner, and E. Winkler, *Kolloid-Z.*, **111**, 1 (1949); K. H. Meyer and A. J. A. van der Wyk, *Z. Elektrochem.*, **47**, 353 (1941); W. O. Baker, C. S. Fuller, and N. R. Pape, *J. Am. Chem. Soc.*, **54**, 776 (1942); W. O. Baker, *Ind. Eng. Chem.*, **37**, 246 (1945); O. Kratky, *Kolloid-Z.*, **120**, 24 (1951); O. Kratky, G. Porod, and E. Treiber, *Kolloid-Z.*, **121**, 1 (1951); O. Kratky, G. Porod, and E. Treiber, *Z. Elektrochem.*, **55**, 481 (1951).

Synopsis

Subject of the investigation are isotropic, regenerated cellulose fibers, dried according to a procedure of P. H. Hermans to a porous state. Volume degrees of swelling in air up to 6 could be obtained. By this preparation, the micellar strands are brought out of contact and an extensive mutual randomness results. This is a prerequisite for the evaluation of the measurements on the basis of particle scattering. For an explanation of the fact that the scattering power in absolute scale is in general lower than expected on the basis of the material composition, it is assumed that a portion of the substance is present in the form of compact clusters scattering at extremely small angles. On this basis the cluster fraction can be calculated. It varies between 15% (for the most highly swollen sample) and 99.3% (for the least swollen one). In the case of the highest swollen sample the existence of these clusters could be directly proofed by an extension of the measurements to extremely small angles, corresponding to about 1.3×10^{-4} radians, resp. a Bragg value of 12,000 A., resp. 0.45 arc minutes. From the shape of the scattering curve, especially the cross-section factor, the existence of elongated ribbons having cross-sectional dimensions of 60×150 A. is inferred. The intensity is measured on an absolute scale; that is, the ratio to the primary intensity is determined. From the absolute zero-angle intensity of the cross-section factor the mass per unit length of the ribbons can be calculated if the cluster fraction is known. It is found to agree with the results of the shape determination. This is an argument for low polydispersity. A completely different type is represented by the scattering of the samples with $q = 1.05$ and $q \approx 1$. It cannot be treated according to the principles of particle scattering. Quantitatively it can be interpreted as the scattering of an interfering system of plane fissures.

Résumé

Le sujet de travail a été l'étude de fibres de cellulose régénérées et isotropiques séchées à l'état poreux en accord avec le procédé de P. H. Hermans. Un degré de gonflement en volume dans l'air même égal à 6 a été obtenu. Par cette préparation les couches micellaires sont séparées et une répartition statistique et extensive en résulte. Ceci permet l'évaluation des mesures sur la base de la dispersion des particules. Pour expliquer le fait que le pouvoir dispersant en échelle absolue est en général plus bas que celui auquel on s'attendrait sur la base de la composition matérielle, il est supposé qu'une partie de la substance est présente sous forme d'amas compacts qui diffusent sous angle très petit. Sur cette base, la fraction en amas peut être calculée. Elle varie entre 15% (pour l'échantillon le plus gonflé) et 99.3% (pour le moins gonflé). Dans le cas des échantillons les plus gonfles l'existence de ces amas peut être directement établie par des mesures a des ongles très petits, de l'ordere de $1,3 \times 10^{-4}$ radians, c.a.d. une valure de Bragg de 12,000 A.; c.a.d. 0.445 arc minutes. De la forme de la courbe de diffusion, spécialement du facteur de section transversale, on déduit l'existence de rubans allongés ayant une section transversale de 60×150 A. L'intensité est mesurée sur une échelle absolue, c.a.d. que le rapport à l'intensité primaire est déterminé au préalable. À partir de l'intesité du facteur de section transversale, on peut calculer la masse par unité de longueur de rubans, si la fraction en amas est connue. Ceci est en accord avec les résultats de la déterminatio-de la forme. C'est un argument en faveur d'une basse polydispersité. Un type complète. ment différent est représenté par la diffusion des échantillons avec $q = 0$ 1.5 et $q \approx 1$. Il ne peut pas être traité en accord avec les principes de particules diffusantes. Quantitativement il peut être interprêté comme la diffusion d'un système a interférences à glissements planes.

Zusammenfassung

Gegenstand der Untersuchung sind isotrope, regenerierte Cellulosefäden, die nach einem von P. H. Hermans angegebenen Verfahren porös getrocknet wurden, wobei sich Volumsquellungsgrade in Luft bis 6 erzielen liessen. Durch diese Präparation werden

die Micellarstränge ausser Kontakt gebracht und es kommt eine weitgehend gegenseitige Unordnung zustande, Voraussetzungen für die Auswertung der Messungen auf Basis der Partikelstreuung. Zur Erklärung der Tatsache, dass die Streukraft im absoluten Mass im allgemeinen kleiner ist als nach der materiellen Zusammensetzung zu erwarten wäre, wird angenommen, dass ein Teil der Substanz in Form von kompakten Clustern vorliegt, die zu extrem kleinen Winkeln streuen. Auf dieser Grundlage kann der Clusteranteil berechnet werden, der sich zwischen 15% (beim höchstgequollenen Präparat) und 99.3% (beim niedrigstgequollenen) bewigt. Im Falle des höchstgequollenen Präparates konnte die Existenz dieser Cluster direkt bewiesen werden und zwar durch eine Ausdehnung der Messungen bis zu extre kleinen Winkeln (etwa 1.3×10^{-4} radians bzw einem Bragg'schen Wert von 12,000 A. bzw eine Streuwinkel von 0.45 Bogenminuten). Aus der Form der Streukurve, insbesonders des Querschnittsfaktors wird erschlossen, dass langgestreckte Bändchen imt dem Querschnitt 60×150 A. vorliegen. Die Intensität wird im absoluten Mass gemessen, d.h. das Verhältnis zur Primärintensität bestimmt. Aus der absoluten Nullintensität des Querschnittsfaktors kann bei Kenntnis des Clusteranteils die Masse pro Längeneinheit der Bändchen berechnet werden, die in Übereinstimmung mit den Ergebnissen der Formbestimmung steht. Dies spricht für geringe Polydispersität. Einen völlig anderen Typus stellt die Streuung der Präparate mit $q = 1.05$ und $q \approx 1$ dar, die nicht nach den Prinzipien der Partikelstreuung behandelt werden kann. Qualitativ ist sie als die eines interferierenden System von flächigen Spalten deutbar.

JOURNAL OF POLYMER SCIENCE: PART C NO. 2, PP. 477–486 (1963)

Penetration of Polymetaphosphate Solution into Regenerated Cellulose

LARS AGGEBRANDT and OLOF SAMUELSON, *Department of Engineering Chemistry, Chalmers Tekniska Högskola, Göteborg, Sweden*

INTRODUCTION

With certain ion-exchanging materials such as ion exchange resins a reliable measure of the water taken up in the solid phase can be obtained by determining the nonsolvent water (δ) with a common electrolyte as reference substance and extrapolating the data to zero concentration.[1] With cellulose and other materials which contain only a small amount of charged groups this method gives results which are rather inaccurate.[2] When polymetaphosphate is used as reference substance, its concentration has a small and often negligible effect upon the δ values when both cation exchange resins[3] and rayon fibers[2] are studied. The explanation is that, in contradistinction to common electrolytes, the polyelectrolyte is unable to penetrate into the solid phase. With such materials the δ value obtained at one comparatively low concentration, e.g., $0.01N$, can be used as a reliable measure of the true swelling. In extremely dilute solutions ($0.0001N$) a slight decrease in the δ value has been observed with some rayon samples. This is due to an adsorption which has, however, a negligible effect upon the determination of nonsolvent water at higher polymetaphosphate concentrations.[4]

With some native cellulose materials, such as highly swollen wood pulps, the δ values in polymetaphosphate solution decrease with an increase in polymetaphosphate concentration.[5] The different behavior of various cellulose materials makes it necessary to elucidate more fully the penetration of polymetaphosphate into cellulose materials. The experiments described in the present work are restricted to regenerated cellulose.

EXPERIMENTAL

Cellulose Materials

Polynosic fiber and supercord which have been used in the experiments were commercial samples. Rayon III was a laboratory sample with poor tensile strength and extremely high swelling. The membranes used were all commercial sausage casings made from viscose. Membranes A and D

were 0.3 mm. thick, B and C were 0.5 mm. in the water-swollen state. The samples were purified as described earlier.[2]

Sodium Polymetaphosphate

Two samples of radioactive polymetaphosphate were prepared as described in an earlier paper.[5] One of the samples was prepared from monosodium orthophosphate. The degree of polymerization DP_n was 85 determined according to the endgroup method.[6] The other sample was prepared from potassium hydroxide and orthophosphoric acid with the ratio K:P = 1.005. The degree of polymerization could not be determined with any accuracy for this high molecular weight phosphate. For the sake of simplicity this will be denoted as $DP_n = 1000$.

Procedure

The determinations of δ were carried out as described in earlier papers.[2,5] In the experiments with rayon the centrifuge was run at a speed corresponding to a relative centrifugal force of 100 G. No centrifugation was performed in the experiments with cellulose films.

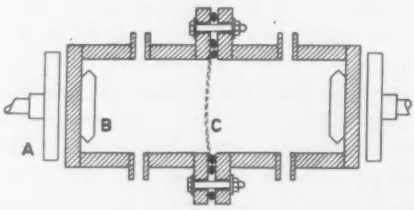

Fig. 1. Dialysis cell: (A) motor-driven magnet: (B) slave magnet; (C) cellulose membrane.

The dialysis experiments were carried out in a Plexiglas cell (Fig. 1). The membrane was clamped between the half cells with rubber gaskets. The half cells had a volume of approximately 70 ml. each, and the solution was stirred magnetically. The effective membrane area was 12.6 sq. cm. One half cell was filled with radioactive polymetaphosphate solution and the other half cell with water. In some experiments sodium chloride was added to the polymetaphosphate solution, and in these experiments the dialysis was made against sodium chloride solution of the same concentration. After a steady state had been reached (30 min.) the diffusate was replaced with pure solvent.

The influence of time upon the rate of dialysis is demonstrated by the results given in Figure 2. It is seen that over a wide time interval the amount of polymetaphosphate which passed through the membrane is a linear function of time, i.e., that within this interval the rate of dialysis is constant.

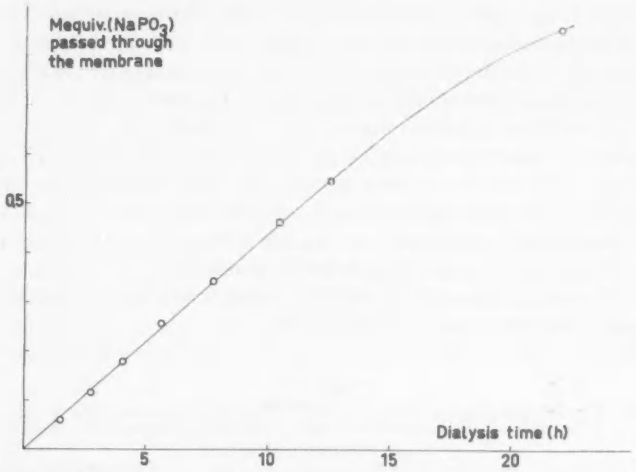

Fig. 2. Dialysis of sodium polymetaphosphate of $DP_n = 85$ against water.

The results from most dialysis experiments have been reported as overall dialysis coefficients U_0, defined as the rate of dialysis divided by the product of membrane area and the difference in concentration in the two half-cells. The rate of dialysis is expressed in milliequivalents per hour, the membrane area in square centimeters, and the concentration in milliequivalents per cubic centimeter. The dialysis time was so chosen that the amount of polymetaphosphate which diffused through the membrane was sufficient for a reliable radiometric determination (20–60 min.). Under these conditions the difference in concentration can be put equal to the concentration of the added polymetaphosphate solution. The dialysis coefficients reported in this paper are average values obtained from two or three determinations.

The results given in Figure 2 indicate that the polymolecularity of the polymetaphosphate has no influence upon the dialysis coefficients determined as described above. In a separate experiment the time of dialysis was further prolonged (48 hr.) so that 18% of the polymetaphosphate had passed through the membrane. Determinations of U_0 for the dialyzed solution at concentrations of 0.06 and 0.04 equiv./l. gave the values 2.14×10^{-2} and 1.18×10^{-2} cm./hr., respectively. The corresponding values obtained with the original solution were 2.18×10^{-2} and 1.22×10^{-2} cm./hr., respectively. From these results it can be concluded that the polymolecularity has a negligible influence when the time of dialysis is short.

RESULTS AND DISCUSSION

In experiments on the influence of the polymetaphosphate concentration upon the δ values for rayon reported earlier[2] the determinations have been

restricted to the concentration interval 0.005–0.1N solutions. It was found that the value increased only slightly for a decreased concentration and that the value determined with 0.01N solution agreed well with the value obtained at the lowest concentration. The results given in Table I show that with the polynosic fiber the concentration dependency is slight even over a much larger range in concentration. The supercord sample investigated exhibits no change in δ within the concentration interval 0.001–0.1N, whereas at the lowest concentration a decrease in δ is observed. This is, as already mentioned, due to adsorption of polymetaphosphate, which affects the δ value at this low concentration. With both these samples a determination of δ in 0.01N or 0.001N polymetaphosphate solution gives a reliable measure of the swelling.

TABLE I
Influence of the Concentration of the Polymetaphosphate Solution upon δ; DP_n = 85

	Polymetaphosphate concn., equiv./l.	δ, g. H_2O/g. cellulose
Polynosic fiber	0.0001	0.559
	0.001	0.552
	0.01	0.548
	0.1	0.543
Supercord	0.0001	0.541
	0.001	0.599
	0.01	0.599
	0.1	0.602
Rayon III	0.0001	1.160
	0.001	1.114
	0.01	0.955
	0.1	0.662
Cellulose film C	0.0001	3.60
	0.001	3.64
	0.01	3.46
	0.1	1.98

Rayon III, which was a laboratory sample exhibiting a high milkiness with pores visible under a microscope, exhibited a behavior different to that of the commercial samples investigated. A marked decrease in δ occurred with an increase in concentration. The value observed in 0.01N polymetaphosphate was much lower than the value obtained by extrapolation to zero concentration, but it is likely that the δ value obtained at the lowest concentration can give a fairly good measure of the swelling. The results with cellulose films reported below lend support to this assumption.

Similarly, the polymetaphosphate concentration has a great influence upon the δ value in experiments with cellulose films; but here the influence is very strong within the interval 0.01–0.1N solution, whereas within the lower concentration range this influence is small.

Dialysis experiments with cellulose films as membranes have been carried out in order to elucidate the penetration of polymetaphosphate into the film. The results given in Table II show that the overall dialysis coefficient approaches zero at low polymetaphosphate concentrations but increases rapidly with an increase in concentration. These results demonstrate that at high concentration polymetaphosphate has the ability to penetrate into and through cellulose films, whereas at low concentration the penetration is negligible. These observations are qualitatively in agreement with those obtained in the determinations of δ at various concentrations of polymetaphosphate. The δ values obtained at the lowest concentration can, therefore, be used as a measure of the true swelling of the film. From the values observed at the higher concentrations an average equilibrium concentration of polymetaphosphate inside the cellulose film can be calculated.

TABLE II
Correlation between Overall Dialysis Coefficient and δ; Membrane A; Polymetaphosphate of $DP_n = 85$

Polymetaphosphate concn., equiv./l.	$U_0 \times 10^2$, cm./hr.	δ, g. H_2O/g. cellulose
0.001	0.018	1.604
0.002	0.023	1.603
0.004	0.036	1.600
0.01	0.053	1.598
0.02	0.20	1.583
0.03	0.50	1.535
0.05	0.96	1.437
0.1	1.84	1.288

In the dialysis experiments the solutions in both chambers were stirred and, therefore, it can be assumed that the diffusion inside the membrane is the rate-determining step. The rate of dialysis should, therefore, be proportional to the concentration gradient inside the membrane which in turn can be expected to be approximately proportional to the average equilibrium concentration inside the film determined as described above. The results presented in Figure 3 confirm that the rate of diffusion through a given membrane is directly proportional to the inside concentration of polymetaphosphate determined in equilibrium distribution experiments.

With highly swollen wood pulps it has been observed that a marked decrease in δ (determined with polymetaphosphate as reference substance) occurs in solutions containing a common electrolyte, e.g., sodium chloride.[5] The results indicate that the presence of sodium chloride increases the penetration of polymetaphosphate. With rayon this effect is negligible at high polymetaphosphate concentrations ($0.01N$), whereas the effect is very great at low polymetaphosphate concentrations. With $0.0001N$ solutions, even negative δ values have been observed with some rayon samples. Evidently a strong adsorption can occur with certain cellulose materials. Results obtained with cellulose film are reproduced in Table III. It is

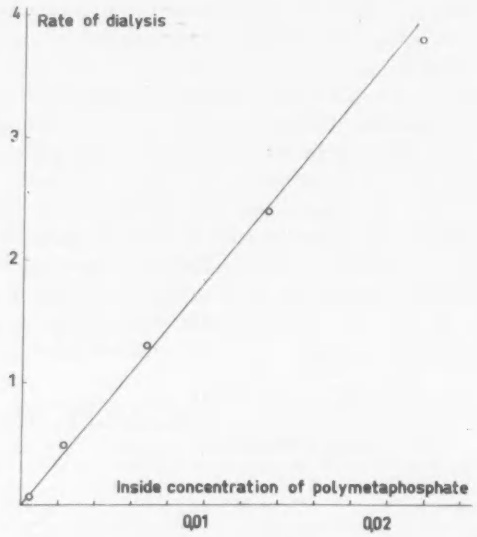

Fig. 3. Rate of dialysis expressed in microequivalents of polymetaphosphate (DP_n = 85) per square centimeter per hour as a function of the polymetaphosphate concentration inside the cellulose film. The inside concentration is determined in equilibrium experiments and is expressed as weight normality (equivalents per 1000 g. water). Membrane D.

seen that the δ values in 0.5N sodium chloride are, over the whole range of polymetaphosphate concentration, lower than those obtained in water (cf. Table II). Within a wide interval the δ values are almost independent of the polymetaphosphate concentration and it can be observed that within this interval the dialysis coefficient in 0.5N sodium chloride is subjected to only small changes. The results show that addition of sodium chloride increases the penetration of polymetaphosphate into and through cellulose films.

Dialysis experiments have also been carried out with polymetaphosphate solutions containing increasing amounts of sodium chloride. The results

TABLE III

Nonsolvent Water (δ) with Polymetaphosphate as Reference Substance and Dialysis Coefficient in 0.5N Sodium Chloride Solution; Dialysis against 0.5N Sodium Chloride; Membrane A; DP_n = 85

Polymetaphosphate concn., equiv./l.	$U_0 \times 10^2$, cm./hr.	δ, g. H_2O/g. cellulose
0.001	1.04	1.27
0.005	1.16	1.21
0.01	1.17	1.15
0.05	1.17	1.09

TABLE IV

Dialysis of 0.004*N* and 0.04*N* Sodium Polymetaphosphate in Sodium Chloride Solutions; $DP_n = 85$; Dialysis against Sodium Chloride Solutions of the Same Concentration; Membrane B

Sodium chloride concn., equiv./l.	$U_0 \times 10^2$, cm./hr.	
	0.004 equiv./l. polymetaphosphate	0.04 equiv./l. polymetaphosphate
0	0.049	2.22
0.01	0.79	2.30
0.05	1.99	2.62
0.1	2.70	2.83
0.5	3.49	3.19

given in Table IV show that over the whole range of concentration the dialysis coefficient increases for an increased sodium chloride concentration.

It might be expected that an increased molecular weight of the polymetaphosphate would lead to a decreased penetration, i.e., to decreased dialysis coefficients and increased δ values under otherwise identical conditions. The experimental results given in Table V confirm this assumption. The high molecular weight polymetaphosphate ($DP_n = 1000$) is hindered from entering the cellulose phase even at high concentrations. Dialysis experiments carried out in sodium chloride solution show that in sodium chloride medium even this high molecular weight polymetaphosphate can diffuse through the membrane.

Two cooperating factors can explain the increased penetration of polyelectrolyte into the cellulose phase which occurs at higher polyelectrolyte concentration and upon addition of sodium chloride. One of these factors is the increased coiling of the polymer, which would facilitate the invasion of the polyelectrolyte into the narrow structure in the cellulose phase. The lower rate of dialysis observed at a higher molecular weight of the polymetaphosphate can also be ascribed to a "molecular sieve effect."

The second factor is the effect of the charged carboxyl groups present in the cellulose. This factor has in earlier papers been shown to have an influence upon the nonsolvent water of rayon fibers determined with low molecular weight electrolytes.[7] Similarly, it affects the δ values observed

TABLE V

Correlation between Overall Dialysis Coefficient and δ; Membrane D; Polymetaphosphate of $DP_n = 85$ and 1000

Polymetaphosphate concn., equiv./l.	$DP_n = 85$		$DP_n = 1000$	
	$U_0 \times 10^2$, cm./hr.	δ, g. H_2O/g. cellulose	$U_0 \times 10^2$, cm./hr.	δ, g. H_2O/g. cellulose
0.001	0.021	3.20	0.008	3.23
0.01	0.12	3.19	0.011	3.24
0.04	1.20	3.04	0.013	3.24

for beaten wood pulps when polymetaphosphate is used as reference substance.[5] The effect of the carboxyl groups can be eliminated by working in sufficiently acid medium where these groups are essentially nondissociated.

The results given in Table VI show that polymetaphosphoric acid prepared from the sodium salt by ion exchange penetrates much more rapidly through the cellulose membrane than does the sodium salt. After the experiment the free acid was reconverted into the sodium salt. This sodium salt gave dialysis coefficients which were only slightly higher than those observed with the original sodium polymetaphosphate. This indicates that only a slight degradation had occurred during the experiment. A comparison between the viscosity of the original polymetaphosphate solution with that of the sodium salt obtained from the polymetaphosphoric acid used in these experiments confirmed that the degradation was slight.

TABLE VI

Comparison between the Overall Dialysis Coefficients Determined with Sodium Polymetaphosphate and Polymetaphosphoric Acid; Membrane D; Original $DP_n = 85$

Polymetaphosphate concn., equiv./l.	Overall dialysis coefficient $U_0 \times 10^2$, cm./hr.		
	$(HPO_3)_n$	$(NaPO_3)_n$	
0.001	0.074	0.021	(0.025)[a]
0.018	4.14	0.30	(0.32)[a]
0.057	11.8	2.01	(2.21)[a]

[a] Values given within parenthesis refer to control experiments carried out with the sodium salt obtained from the free acid used in the dialysis experiments.

The differences in viscosity between solutions containing the sodium salt and the free acid were comparatively small, which indicates that the size of the polymer coil differs rather little. The results given in Table VI can, therefore, not be explained by differences in size of the polyelectrolyte coil (molecular sieve effect).

The different behavior of the free acid in comparison to the sodium salt is explained by the fact that the cellulose film behaves as an ion exchange membrane. In salt solution the membrane acts as an electrical barrier which, however, is eliminated in acid medium. The decreased penetration observed with the sodium salt compared to the free acid is explained by the increased number of charged groups in the cellulose film.

According to the Donnan theory, the retarding effect of the charged groups in the cellulose upon the penetration of polymetaphosphate should decrease for an increased concentration of the polyelectrolyte and of added sodium chloride. Qualitatively, even the influence of the increased molecular weight (increased charge) of the polyelectrolyte can be explained as an effect of the charged groups in the membrane. In fact, the resulting rate of diffusion through the membrane and the equilibrium distribution between the cellulose phase and the outer solution is, in neutral medium, determined both by the charged carboxyl groups and by the size of the

polymer coil. The latter factor can, under certain conditions, be predominating, which is demonstrated by experiments carried out with polymetaphosphoric acid prepared from the high molecular weight polymetaphosphate with $DP_n = 1000$. It has not been possible to prevent degradation completely, but despite this fact the dialysis coefficients were about 100 times lower than those determined for the acid prepared from a polymetaphosphate of $DP_n = 85$.

The financial support of the Swedish Technical Research Council is gratefully acknowledged.

References

1. Samuelson, O., *Studier rorande jonbytande fasta amnen*, Esselte, Stockholm, 1944.
2. Andersson, B., and O. Samuelson, *Svensk Papperstidn.*, **61**, 1001 (1958).
3. Samuelson, O., paper presented at the 120th Meeting of the American Chemical Society, September 1951; K. W. Pepper, D. Reichenberg, and D. K. Hale, *J. Chem. Soc.*, **1952**, 3129.
4. Aggebrandt, L., R. Grundelius, and O. Samuelson, *Svensk Papperstidn.*, in press.
5. Grundelius, R., and O. Samuelson, *Svensk Papperstidn.*, **65**, 273 (1962).
6. Samuelson, O., *Svensk Kem. Tidskr.*, **56**, 343 (1944).
7. Andersson, B., and O. Samuelson, *Svensk Papperstidn.*, **62**, 775 (1959).

Synopsis

Determinations of nonsolvent water (δ) and dialysis experiments with cellulose films confirm that the δ values determined with sodium polymetaphosphate as a reference substance can be used as a measure of the true swelling of regenerated cellulose. With certain types of regenerated cellulose, e.g., cellulose films, δ is dependent upon the polyelectrolyte concentration and the determinations have to be carried out at low concentration. A relationship exists between δ and the rate of dialysis with cellulose membranes which confirms that the variation in δ with concentration is due to a penetration of the polyelectrolyte into the cellulose. The exclusion of the polyelectrolyte is not only due to a molecular sieve effect but also to the presence of charged carboxyl groups in the cellulose. This latter effect is eliminated in acid medium.

Résumé

Les déterminations des valeurs (δ) de l'eau-non solvant et les expériences de dialyse avec des films de cellulose confirment que les valeurs δ déterminés avec le polymétaphosphate de sodium comme substance de référence peuvent être utilisées comme mesure du gonflement véritable de la cellulose régénérée. Dans certains types de cellulose régénérée, par example les films de cellulose, les valeurs δ dépendent de la concentration du polyélectrolyte et les déterminations doivent être effectuées à basse concentration. Il y a une relation entre les valeurs δ et la vitesse de dialyse avec les membranes de cellulose ce qui confirme que la variation des valeurs δ avec la concentration est due à la pénétration du polyélectrolyte dans la cellulose. L'exclusion du polyélectrolyte n'est pas eulement due à un effet moléculaire de tamisage, mais également à la présence de groupes carboxyliques, chargés dans la cellulose. Ce dernier effet est éliminé en milieu acide.

Zusammenfassung

Bestimmung des nicht als Lösungsmittel aufgenommenen Wassers (δ) und Dialyseversuche mit Cellulosefilmen bestätigen, dass die mit Natriumpolymetaphosphat als Bezugssubstanz bestimmten δ-Werte als Mass für die wahre Quellung der regenerierten Cellulose verwendet werden können. Bei gewissen Typen von regenerierter Cellulose, z.B. von

Cellulosefilmen, hängt δ von der Polyelektrolytkonzentration ab und die Bestimmung muss daher bei niedriger Konzentration durchgeführt werden. Es besteht eine Beziehung zwischen δ und der Dialysegeschwindigkeit mit Cellulosemembranen, was eine Bestätigung dafür bildet, dass die Konzentrationsabhängigkeit von δ durch ein Eindrigen des Polyelektrolyten in die Cellulose verursacht wird. Die Exklusion des Polyelektrolyten ist nicht nur die Folge eines Molekularsiebeffekts sondern auch durch das Vorhandensein von geladenen Karboxylgruppen in der Cellulose bedingt. Letzterér Effekt wird in saurem Medium ausgeschaltet.

JOURNAL OF POLYMER SCIENCE: PART C NO. 2, PP. 487–497 (1963)

Fractional Extraction of Regenerated Cellulose Fibers with Iron–Sodium Tartrate Solutions

P. PAULUSMA and D. VERMAAS, *Central Research Institute of A.K.U. (Algemene Kunstzijde Unie N. V.) and Affiliated Companies, Arnhem, Netherlands*

INTRODUCTION

Although fractional extraction appears to be a possible means for determining lateral order (L.O.) distribution in cellulose fibers, this method has seldom been used for the purpose. In 1957 Marchessault and Howsmon[1] published a critical review of the existing literature on the determination of L.O. distribution. These authors mention only two papers in which stepwise dissolution of the fibers was the method employed. However, in the investigations published by Maeda[2] and by Yurugi,[3] the fibers were pretreated by mild acid hydrolysis followed by drying. Such a pretreatment may induce partial crystallization[4] and, therefore, bring about changes in the original L.O. distribution of the fiber.

In the course of an investigation into the structure of regenerated cellulose fibers we found that fractional extraction with certain solvents is a very effective means to discriminate between fibers of differing L.O.

Solvents which are very well suited to our purpose can be made by using the iron–sodium tartrate complexes described by Jayme et al.[5–7] It is possible to prepare a series of mixtures in which the behavior of the fibers ranges from complete dissolution to complete insolubility by dilution of one and the same well-chosen standard solution of the iron–sodium tartrate complex with water.

Studies of the solubility of cellulose fibers—in most cases native and modified native fibers—in this type of solvent have been published by Malm et al.[8] and others.[9–11] However, to our knowledge, systematic studies on the fractional extraction of regenerated cellulose with iron–sodium tartrate solutions have not been published so far.

Regenerated cellulose fibers of widely divergent L.O. distribution are now commercially available, but for a fundamental study of the extraction phenomenon we wished to have fiber samples of exactly known production conditions at our disposal. Moreover, the necessity was felt that these fibers should be as uniform as possible throughout the cross section; they should, therefore, display no skin-core effect.

The solubility behavior of cellulose fibers is governed by the factors L.O. distribution and D.P. distribution. Hence, four fiber samples were pre-

pared, representing the possible combinations of two given D.P. distributions and two L.O. distributions. This was accomplished by preparing two viscoses of exactly the same composition, but differing in ageing time of the alkali cellulose used. Both viscoses were spun under two different sets of conditions, respectively, leading to skinless core-cellulose fibers of high average L.O. and all-skin fibers of the super tire yarn type, which are characterized by low average L.O.

In the present report the results of extraction experiments made with these samples will be presented, together with an attempt to reach a quantitative interpretation on the base of a simple model of fiber structure.

EXPERIMENTAL

Preparation of the Fiber Samples

Two viscoses containing 7.3% cellulose and 5.5% total NaOH were prepared from the same alkali cellulose. The alkali cellulose used for one of the viscoses had been aged for 24 hr. at 21°C.; the alkali cellulose of the other viscose had been aged for 120 hr. at 21°C. Both viscoses contained the same amount of a commercially used modifier. Each viscose was spun (a) in a slightly acidified bath containing 8% $(NH_4)_2SO_4$ and 18% Na_2SO_4, and (b) in a H_2SO_4–Na_2SO_4–$ZnSO_4$ bath under conditions leading to an all-skin type of yarn.

A spin stretch of 50% was applied in all cases. After spinning, the samples were washed free of acid and dried.

Preparation of Solvents

As the preparation of solutions according to Jayme is complicated by the necessity of isolating an intermediate tartratoferric acid, we chose the more convenient type of reagents introduced by Valtasaari,[12] which has also been used by other authors.[8,9,11]

For a detailed description of the preparation of the iron–sodium tartrate standard solution used throughout the investigation we refer to the paper by Malm et al.[8] The concentrations used by us deviated somewhat from those mentioned by Malm. The NaOH solution contained 106 g. NaOH in 250 ml. distilled water. The sodium tartrate solution had a concentration of 256 g. in 400 ml. water. A ferric nitrate solution of 149 g. in 160 ml. water was used. The final mixture was stabilized by the addition of 90 g. sodium tartrate. From the standard solution series of dilutions with distilled water were made. The concentration c is expressed in volume fractions of the standard solution.

Extraction Experiments

The fiber sample was cut into pieces about 1 mm. in length and dried at 105°C. for 16 hr. About 400 mg. of the cut and dried sample was weighed and brought into contact with 200 ml. of a solvent of the selected composi-

tion. The mixture was kept at 18°C. for 16 hr., while under constant vigorous agitation with a vibrating stirrer.

After 16 hr. stirring the solution was centrifuged, decanted, and filtered as described by Malm et al.[8] We also used the techniques of deswelling with glycerol and washing described by these authors.

A G2 glass filter was used. Drying was done at 105°C. for 2 hr. Then the dried fibrous mass was weighed. The results are always given as the fraction r of undissolved cellulose based on the original weight of dry cellulose. In separate experiments it was found that, in general, after 1 hr. stirring the extraction process had been completed. In most cases there is no significant increase in percentage of extracted material on further extraction.

Viscosity Determinations

The limiting viscosity number $[\eta]$ of the fiber samples was measured in the iron–sodium tartrate solvent of the composition used by Edelmann and Horn[11] for the purpose; $[\eta]$ was derived by linear extrapolation of the η_{sp}/c–η_{sp} plot to $\eta_{sp} = 0$. With the aid of the calibration curve published by the same authors the weight-average degree of polymerization ($\bar{P}_w$) of the samples was computed.

The results are given in Table I.

TABLE I

	$[\eta]$	$\bar{P}_w$
Fibers from high viscosity viscose	4.78	655
Fibers from low viscosity viscose	3.04	375

For an estimation of the average degree of polymerization of the extracted fraction the relation between $[\eta]$ and $\bar{P}\eta$ was needed in a solvent consisting of 40% of standard solution and 60% of water. Assuming that in this solvent $\bar{P}\eta$ is not too much different from $\bar{P}_w$ and that the relation $[\eta] = K\bar{P}\eta^{\alpha}$ is valid, viscosity determinations on our fiber samples dissolved in this mixture yielded $K = 11 \times 10^{-3}$ and $\alpha = 0.93$, when the cellulose concentration is expressed in grams/100 ml.

RESULTS AND DISCUSSION

The results of the extraction experiments have been summarized in Figure 1, which gives the fractions of undissolved material as a function of the solvent concentration c for the four fiber samples investigated.

Figure 1 may serve as a key to the interpretation of the extraction phenomena. Obviously it is possible to spin two regenerated cellulose fibers of exactly the same molecular weight distribution, one of which dissolves spontaneously and completely in a solvent of a given composition, whereas of the other fiber only little material goes into solution. In the whole range

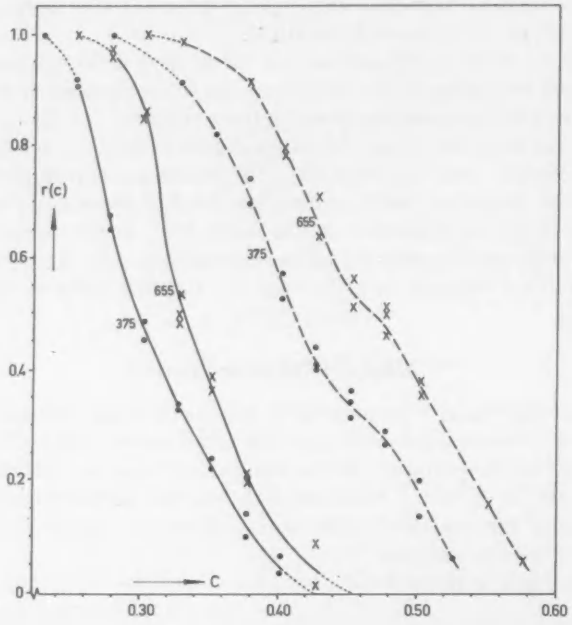

Fig. 1. Weight fraction $r(c)$ of undissolved material vs. solvent concentration c: (——) skin cellulose; (- -) core cellulose. Figures refer to $\bar{P}_w$ values of samples.

of solvent compositions used the cellulose solutions are stable; once the fiber has been dissolved in the most active solvent, the composition of the latter may be changed by dilution with water to that of the lowest dissolving power, without any precipitation of the cellulose.

Whatever may be the reason for the solubility of cellulose in iron–sodium tartrate solutions, there is little doubt that the results of the extraction experiments have to be described in terms of the accessibility of cellulose gels of varying L.O. to the iron–sodium tartrate complex. The extraction equilibria are, therefore, not true equilibria in the thermodynamic sense; ultimately they should be treated physically in terms of the energy of activation involved in the dissolution process which changes with varying L.O. The reason why we use the term fractional extraction throughout this article is that we want to stress the fundamental difference between the phenomena we are concerned with here and the fractional dissolution of amorphous polymers which is thermodynamically equivalent to fractional precipitation of the polymer from its solution, the latter phenomena being governed by the thermodynamic potential of the system.

There are two factors which govern the possibility that a given cellulose molecule will be extracted from the fiber by the solvent, viz., the accessibility of all parts of the chain to the dissolving reagents, and the freeness

of the molecule, once unfastened from its neighbors, to diffuse from the swollen fiber into the solution. Our observations lead us to believe that the latter factor does not play a significant part in most of the experiments. Already in solvent compositions in which only 20% of the material is extracted, the fiber is in a state of extremely high swelling. The smallness of the fiber diameter and the observed time dependence of the percentage of material extracted strongly suggest that the diffusion process as such has come to an end after about 1 hr. Further, the high degree of axial orientation in the fiber material and the relative shortness and stiffness of the cellulose molecules make any considerable occurrence of molecular entanglements in the swollen fiber improbable. As a first approximation we will, therefore, consider accessibility as the only factor involved. For a quantitative treatment of fractional extraction we start from the generally accepted network model of a water-swollen regenerated cellulose fiber.[13] For convenience we shall denote the parts of the chains that are accessible to the water molecules as amorphous, whereas the junction points of the network will be named ordered regions. The ordered regions diverge from one single hydrogen bond of sufficient strength to withstand the influence of the water present to relatively large and well-ordered crystallites.

Our mathematical model will now be based upon the assumption of a random distribution of ordered regions over the system of chain molecules. The ordered regions will be classified according to the minimum concentration c of the solvent to which they are accessible. Thus c will be used as the L.O. parameter; a higher value of c means increased order in the region under consideration. Further it will be assumed that the size of an ordered region will be a function of its L.O., and therefore of c.

Now the probability f that an arbitrary chain molecule of degree of polymerization P is involved in one or more ordered regions of a given class of L.O. will be assumed to be proportional (1) to the number of ordered regions of that class per unit weight of cellulose, (2) to the size of these regions, and (3) to P. Combinations of the assumptions (1) and (2) yields proportionality between f and the total number of hydrogen bonds in the system which just resist a solvent concentration c.

Considering a mass W of fibrous material, we define $Q(c)dc$ as the number of intermolecular hydrogen bonds which are broken when the concentration of the complex agent in the solvent is increased from c to $(c + dc)$. The total number of hydrogen bonds which are resistant to a solvent concentration c will then be

$$\int_c^1 Q(c)dc$$

The probability F that a chain molecule of length P is involved in ordered regions which are not dissolved at a concentration c will then be given by

$$F = aP \int_c^1 Q(c)dc$$

in which a is a proportionality constant.

If $N(P)dP$ is the number of molecules of length between P and $P + dP$ in the sample, and b is the weight of the monomeric unit, the weight of material of degree of polymerization between P and $P + dP$ in the sample which remains bound to the network at concentration c becomes

$$abP^2N(P)dP \int_c^1 Q(c)dc \tag{1a}$$

and the total weight $R(c)$ which remains undissolved at c

$$R(c) = ab \int_1^\infty P^2N(P)dP \int_c^1 Q(c)dc \tag{1}$$

Now the expression $b \int_1^\infty P^2 N(P)dP$ can be replaced by $\bar{P}_wW$, in which $\bar{P}_w$ is the weight-average degree of polymerization of the sample. It follows that the weight fraction $r(c)$ of fiber material that does not dissolve at a concentration c is given by

$$r(c) = R(c)/W = a\bar{P}_w \int_c^1 Q(c)dc \tag{2}$$

From eq. (1a) the weight-average degree of polymerization ${}^c\bar{P}_w$ of the fraction which dissolves at a solvent concentration c can be calculated. On substituting $I(c)$ for the integral $\int_c^1 Q(c)dc$, the expression for ${}^c\bar{P}_w$ becomes:

$${}^c\bar{P}_w = b \int_1^\infty P^2N(P)[1 - aPI(c)]dP/b \int_1^\infty PN(P)[1 - aPI(c)]dP$$

Dividing by the equality $\bar{P}_wW = b \int_1^\infty P^2N(P)dP$ and remembering that $W = b \int_1^\infty PN(P)dP$, we obtain:

$${}^c\bar{P}_w/\bar{P}_wW = [1 - aI(c) \int_1^\infty P^3N(P)dP/\int_1^\infty P^2N(P)dP]/$$
$$W(1 - aI(c) \int_1^\infty P^2N(P)dP/\int_1^\infty PN(P)dP)$$

or

$${}^c\bar{P}_w/\bar{P}_w = [1 - aI(c)\bar{P}_z]/[1 - aI(c)\bar{P}_w] \tag{3}$$

Finally, on combining eqs. (2) and (3) one finds:

$$\bar{P}_z = \{\bar{P}_w - [1 - r(c)]{}^c\bar{P}_w\}/r(c) \tag{4}$$

In principle the validity of eq. (2) can be checked by experiment. When two fibers have been spun under the same spinning conditions from viscoses which are only different with respect to their $\bar{P}_w$ value, the weight ratio ρ of the undissolved fractions should be given by:

$$\rho = r_1(c)/r_2(c) = (\bar{P}_w)_1/(\bar{P}_w)_2$$

irrespective of the solvent concentration used and independent of the spinning conditions.

In Table II values of ρ have been computed as derived from the curves of Figure 1 for a number of solvent concentrations in which the fraction of dissolved material varied between about 15 and 90%.

The following conclusions seem justified. (*a*) The ratio ρ is fairly independent of the solvent concentration. A large part of the scattering of

TABLE II

Weight Fractions r of Undissolved Material and Their Ratio ρ for Varied Solvent Concentrations[a]

Concn. solvent, c, vol. fractions of standard solution	Skin cellulose			Core cellulose		
	$r_1(c)$	$r_2(c)$	$r_1(c)/r_2(c) = \rho$	$r_1(c)$	$r_2(c)$	$r_1(c)/r_2(c) = \rho$
0.30	0.47	0.86	0.5_5			
0.32_5	0.34	0.53	0.6_4			
0.35	0.23	0.37	0.6_2			
0.37_5	0.12	0.21	0.5_7			
0.40				0.56	0.79	0.7_0
0.42_5				0.42	0.68	0.6_2
0.45				0.34	0.54	0.6_3
0.47_5				0.28	0.48	0.5_8
0.50				0.19	0.37	0.5_1
		Average ρ	0.6_0		Average ρ	0.6_1

[a] Subscript 1 refers to fibers of $\bar{P}_w = 375$, subscript 2 to fibers of $\bar{P}_w = 655$; ratio $(\bar{P}_w)_1:(\bar{P}_w)_2 = 0.57$.

the individual ρ values can be ascribed to experimental errors which may result in deviations of the order of magnitude of 5–10% in ρ. In the case of core cellulose there is a trend of decreasing ρ with increasing solvent concentration.

(*b*) Although the solubility behavior of the two types of fibers (skin and core cellulose) is very different, the respective average ρ values are practically identical.

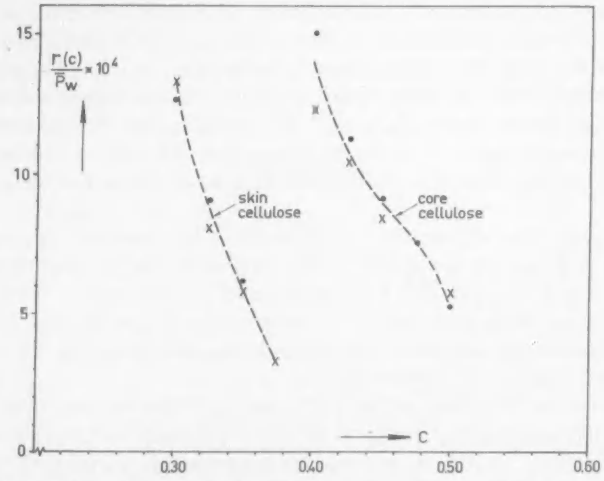

Fig. 2. Reduced weight fraction of undissolved material vs. solvent concentration: (●) $\bar{P}_w = 375$; (×) $\bar{P}_w = 655$.

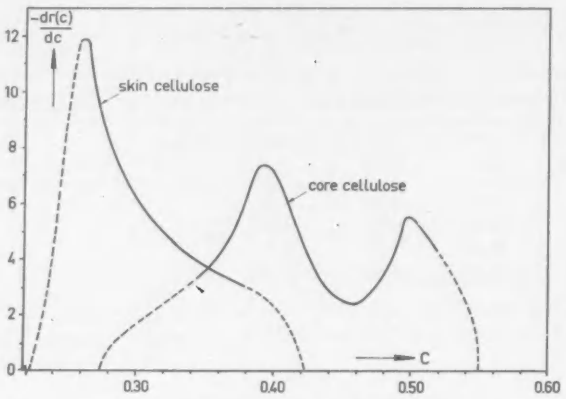

Fig. 3. Differential L.O. distribution for skin and core cellulose of $\bar{P}_w = 375$.

(c) The average value of ρ tallies reasonably with the ratio $(\bar{P}_w)_1$: $(\bar{P}_w)_2$.

These results may also be graphically presented by plotting the "reduced" value $r(c)/\bar{P}_w$ as a function of c. On doing this the four curves should reduce to two, representing the integral L.O. distribution curves for core and skin cellulose, respectively. In Figure 2 it is seen that the skin cellulose shows the predicted behavior, whereas in the core fibers there is a systematic deviation which becomes larger at decreasing c values. By graphical differentiation of the original integral curves (Fig. 1) differential L.O. distribution curves are obtained which, but for a factor $a\bar{P}_w$, represent the respective $Q(c)$ functions. Unfortunately, the extraction technique is not suitable to determine the parts of the distribution curve which correspond to c values where either the swelling is low or the percentage of solubility exceeds about 90%. In these cases deviations from the theoretical behavior occur which can be easily explained. At very high solubilities the accuracy of the experimental $r(c)$ values becomes poor, whereas in the region of very low swelling there is an increased hindrance of diffusion of the cellulose chains.

In Figure 3 the differential L.O. curves for the core and skin cellulose samples of $\bar{P}_w = 375$ are shown. The parts of the curves relating to solubilities between 15 and 90% have been drawn as solid curves; the less reliable extreme parts are dashed. The two-topped distribution curve for core cellulose appears to be characteristic for this structure, as could be confirmed in separate experiments.

It is not easy to define the physical meaning of the constant a, and there may be discussion as to whether it has the same value for all types of cellulose networks. Further it is tempting to identify $\int_0^1 Q(c)dc$ with the total number of water-resistant intermolecular hydrogen bonds in the system estimated from other types of experiments.

In principle, additional checking of the theory is possible, using eqs. (3) and (4). From eq. (3) it is readily seen that the weight-average degree of polymerization of the extracted material should always be smaller than the total average, because $\bar{P}_z > \bar{P}_w$. This is what is actually found. A few examples are given in Table III.

TABLE III

$\bar{P}_w$ of fiber	Cellulose type	$r(c)$	$[\eta]$ of extract[a]	[c]$\bar{P}_w$	$\bar{P}_z$ of fiber[b]
375	Core	0.49	2.50	331	420
375	Skin	0.53	2.52	334	411
655	Core	0.33	4.48	617	733
655	Skin	0.40	4.56	627	700

[a] Determined in solvent of 40% by volume at 18°C.
[b] By eq. (4).

From these data $\bar{P}_z$ was calculated with the aid of eq. (4); the results are also shown in Table III. No attempt was made to determine $\bar{P}_z$ in an independent way, but we regard the fair constancy of the $\bar{P}_z$ values found for either of the two pairs of fibers as a further indication of the fundamental correctness of the trend of thought developed above.

It can be concluded that, considering the simplicity of the mathematical model and the possible disturbing factors which may play a role in the experiments, there is a fair amount of agreement between theoretical prediction and experimental results, sufficient to have some confidence in the correctness of the approach. A practical result of this work may then be that on the basis of our treatment it has become possible to derive comparable L.O. distribution curves of regenerated cellulose fibers of differing $\bar{P}_w$ value by making use of eq. (2).

We wish to thank Prof. Dr. W. Prins (Technical University of Delft, Holland) for discussions on the subject and Miss D. N. van Neerbos for carrying out the extraction and viscometrical experiments.

References

1. Marchessault, R. H., and J. A. Howsmon, *Textile Res. J.*, **27**, 30 (1957).
2. Maeda, H., *Sen-i Gakkaishi*, **12**, 6 (1956).
3. Yurugi, T., *Kogyo Kagaku Zasshi*, **58**, 27 (1955).
4. Hermans, P. H., and A. Weidinger, *J. Polymer Sci.*, **4**, 317 (1949).
5. Jayme, G., and W. Bergmann, *Das Papier*, **11**, 280 (1957).
6. Jayme, G., and W. Bergmann, *Rayon, Zellwolle u. Chemiefasern*, **34**, 27 (1956).
7. Jayme, G., and W. Verburg, *Rayon, Zellwolle u. Chemiefasern*, **32**, 193, 275 (1954).
8. Malm, C. J., R. E. Clegg, and M. Luce, *Tappi*, **44**, 102 (1961).
9. Centola, G., and D. Borruso, *Ind. Carta (Milan)*, **16**, 37 (1962).
10. Jayme, G., and P. Kleppe, *Das Papier*, **15**, 492 (1961).
11. Edelmann, K., and E. Horn, *Faserforsch. Textiltech.*, **9**, 493 (1958).
12. Valtasaari, L., *Papier Puu*, **39**, 243 (1957).
13. Hermans, P. H., *Physics and Chemistry of Cellulose Fibres*, Elsevier, Amsterdam, 1949, p. 373 ff.

Synopsis

Fractional extraction experiments of regenerated cellulose fibers with iron–sodium tartrate solvents are described. Four fiber samples were investigated, representing the possible combinations of two D.P. distributions and two lateral order (L.O.) distributions. The L.O. distributions were characteristic for those present in the core and the skin of commercial rayons. A simple mathematical model was developed which reasonably well accounts for the quantitative results obtained. The model is that of a water-swollen network of chains, the junction points of which are ordered regions of varying degree of L.O. and size. The concentration of the active agent in the solvent which just suffices to dissolve a particular ordered region is used as an L.O.-parameter, and it is assumed that also the size of the ordered region is functionally related to this concentration. Further underlying fundamental hypotheses are: (*1*) the ordered regions are randomly distributed over the system of chain molecules; (*2*) the probability that a chain molecule takes part in ordered regions of a given class of L.O. is proportional to its degree of polymerization, and to the number and size of the ordered regions under consideration. The model leads to the result that the fraction of undissolved material at a given solvent concentration is proportional to the weight-average degree of polymerization of the sample and, naturally, further depends on its L.O. distribution. But for a proportionality constant, this L.O. distribution can be derived from the experiments with certain limitations with regard to the extreme parts of the distribution curve. In principle the model allows for a determination of the *z*-average degree of polymerization of the sample by means of fractional extraction.

Résumé

On décrit des expériences d'extraction fractionnée de fibres de cellulose régénérée à l'aide de solvants contenant du tartrate de fer et de sodium. Quatre échantillons de fibres furent étudiés, représentant les combinaisons possibles de deux distributions de D.P. et de deux distributions d'ordre latéral (O.L.). Les distributions d'O.L. sont caractéristiques pour celles présentes à l'intérieur et à la surface de rayonnes commerciales. Un modèle mathématique simple fut développé qui correspond suffisamment bien aux résultats quantitatifs obtenus. Le modèle est celui d'un réseau de chaînes gonflées à l'eau, dont les points de jonction sont des régions ordonnées d'un degré variable d'O.L. et de grandeur. La concentration en agent actif dans le solvant suffisant juste à dissoudre une région particulière est employée comme paramètre O.L., et on considère que les dimensions de la région ordonnée sont proportionnelles à la concentration. Les autres hypothèses fondamentales sont (*1*) les régions ordonnées sont distribuées aux contours du système de chaînes moléculaires; (*2*) La probabilité qu'une chaîne moléculaire se trouve dans une région ordonnée d'une classe donnée d'O.L. est proportionnelle à son degré polymérisation et au nombre et dimensions des régions des régions ordonnées considérées. De ce modèle, il résulte que la fraction de matériel non-dissous à une concentration donnée de solvant est proportionnelle au D.P. moyen en nombre de l'échantillon et naturellement elle dépend aussi de sa distribution en O.L. Mais pour une constante de proportionnalité, cette distribution d'O.L. peut être dérivée des expériences, sous certaines réserves en ce qui concerne les extrémités de la courbe de distribution. En principe le modèle se prête à une détermination par extraction fractionnée du D.P. moyen-*z* de l'échantillon.

Zusammenfassung

Versuche zur fraktionierten Extraktion regenerierter Cellulosefasern mit Eisen-Natriumtartratlösung werden beschrieben. Vier Faserproben, welche die möglichen Kombinationen zweier D.P.-Verteilungen und zweier Seitenordnungs-(L.O.)-verteilungen vorstellen, wurden untersucht. Die L.O.-Verteilungen waren charakteristisch für die

im Kern und in der Haut von handelsüblichen Rayons vorhandenen. Ein einfaches mathematisches Modell wurde entwickelt, das eine befriedigende Übereinstimmung mit den quantitativen Ergebnissen liefert. Dieses Modell besteht aus einem in Wasser gequollenen Netzwerk, bei dem die Vernetzungsstellen der Ketten durch geordnete Bereiche mit verschiedenem L.O.-Grad und verschiedener Grösse gebildet werden. Die Konzentration des Reaktionsmittels im Lösungsmittel, die gerade zur Auflösung eines bestimmten geordneten Bereiches ausreicht, dient als L.O.-Parameter und es wird angenommen, dass auch die Grösse des geordneten Bereiches in funktioneller Abhängigkeit von dieser Konzentration steht. Weitere zugrundeliegende Annahmen sind: (*1*) die geordneten Bereiche sind über das System der Kettenmoleküle statistisch verteilt; (*2*) die Wahrscheinlichkeit, dass ein Kettenmolekül sich an geordneten Bereichen einer bestimmten L.O.-Klasse beteiligt, ist seinem Polymerisationsgrad, sowie der Anzahl und Grösse der betrachteten, geordneten Bereiche proportional. Das Modell führt zu dem Ergebnis, dass der Bruchteil an ungelöstem Material bei gegebener Lösungsmittelkonzentration dem Gewichtsmittelwert von D.P. der Probe proportional ist und, wie zu erwarten, von ihrer L.O.-Verteilung abhängt. Abgesehen von einem Proportionalitätsfaktor kann diese L.O.-Verteilung aus den Experimenten abgeleitet werden, wobei allerdings gewisse Beschränkungen in bezug auf die äussersten Teile der Verteilungskurve bestehen. Im Prinzip gestattet das Modell eine Bestimmung des Z-Mittels von D.P. per Probe durch fraktionierte Extraktion.

JOURNAL OF POLYMER SCIENCE: PART C NO. 2, PP. 499–513 (1963)

Structural Study of Cellulosic Fibers

J. K. SMITH, *Research Department, Courtaulds North America Inc., Mobile, Alabama,* and W. J. KITCHEN and D. B. MUTTON, *Industrial Cellulose Research Ltd., Hawkesbury, Ontario, Canada*

Introduction

The attributes of high wet modulus fibers, it is believed, are determined by a variety of properties within the fiber, such as crystallinity, orientation of crystalline units or fibrils, and size of structural units. It is well known that these properties vary drastically with the origin of the cellulose and its molecular weight, the conditions of regeneration, and any subsequent after-treatments.[1] By a study of several of these parameters, one might be able to relate the fine structure of a fiber to its physical properties. Several methods are currently used and others have been proposed for such an investigation. Among these is the determination of crystallinity by infrared spectrophotometric methods. This technique has been confined to cellulosic films because of the experimental difficulties involved. In this paper, a method will be described whereby the crystallinity and an order of the orientation of the crystalline region of individual fibers may be determined by an extension of this technique to fibers.

Theory

There are several theories concerning the structure of cellulosic fibers; the most generally accepted one is that in cellulose the chains of anhydroglucose units are in many different relative arrangements, ranging from highly ordered, or crystalline, to complete disorder, or amorphous.[2–4] A theory which has been recently revitalized is that cellulose is completely crystalline and that imperfections in the crystal lattice network can account for those properties normally associated with an amorphous region.[5] Regardless of which theory one may prefer, the conclusions obtained from accessibility measurements are essentially the same. All of the theories predict regions of high order, and these measurements are intended to give an order of magnitude to them. It is ambiguous to consider such regions as mutually exclusive, but, for convenience, the present paper will regard cellulose as consisting of three distinct phases: crystalline, noncrystalline ordered material, and noncrystalline unordered (amorphous) material. The crystalline phase is considered to be that which gives a sharp x-ray diffraction pattern. The noncrystalline ordered phase is inaccessible for exchange with D_2O, but is not sufficiently ordered to produce a well defined

x-ray diffraction pattern. The amorphous phase is the material not contained in the other regions and is an area of disorder. In this paper, the term, highly ordered region, is understood to consist of both the crystalline and noncrystalline ordered phases.

Many methods have been proposed for determining the relative order in a fiber, and all give slightly different results. Two of the more prominent are x-ray diffraction and accessibility measurements. Comparison of these two types of data allows the determination of the noncrystalline highly ordered material. From the accessibility data a measure of the highly ordered region can be obtained. This value, of course, is not normally the same as that obtained by x-ray analysis. The differences that arise can be attributed to the inability of x-rays to detect very small crystallites, imperfections in the crystal structure, the accessibility of OH groups that lie on the surface of crystallites, and hydrogen bonding that may occur outside the crystalline unit. These differences may be related to some of the fiber's physical properties.

Mann and Marrinan[6] have shown that the isotopic exchange reaction between the OH groups of cellulose and gaseous D_2O gives a measure of accessibility and an estimate of the percentage of the highly ordered region. Only a relative measure of this region may be obtained by means of infrared spectroscopy unless the extinction coefficients for the OH and OD absorption bands are known. Mann and Marrinan used a ratio of 1.11 for the extinction coefficient of these two bands, using the peak optical density of OD bands at 2530 cm.$^{-1}$ and that of the OH band at 3360 cm.$^{-1}$. However, it was found in the present experiments that because of scattering of radiation by the sample, it was preferable to use the ratio of integrated absorbances instead of the peak optical density. This method reduced the

TABLE I
Crystallinity Determined by Different Authors

	Crystallinity, %			
	Mann and Marrinan[6]	Tyler and Wooding[2]	Pennings[14]	Present work
Fibro	—	45.2	—	42.5
Viscose film	26	—	27.5	28.0

error introduced in peak intensities and positions due to scattering.[7] By using integrated absorbances, the extinction coefficients may not be the same as those at a particular peak, and, indeed, it was found that a ratio of 1.00 between the extinction coefficients of the integrated absorbance gave a better correlation with previously reported data than the value reported in the literature. A comparison of the determined values with those of other authors is shown for Fibro and viscose film in Table I.

On using the ratio of 1.00 between the extinction coefficients, and assum-

ing Beer's law holds, the integrated absorbance[8] for a particular band is related to the concentration of absorbing material by the equation:

$$B = 2.303(1/cl) \int \log (I_0/I)$$

Where $\log I_0/I$ represents the absorbance of the fiber bundle, c the concentration of material absorbing expressed in moles/liter, l the path length of the radiation through the bundle, and B the integrated molar extinction coefficient. Therefore, a ratio of the integrated absorbance of the two bands is given by:

$$\frac{\log (I_0/I)_{OD}}{\log (I_0/I)_{OH}} = \frac{B_{OD}c_{OD}}{B_{OH}c_{OH}}$$

where $c_{OD} + c_{OH} = 1$ and $l_{OD} = l_{OH}$. If $B_{OD} = B_{OH}$, then this equation will reduce to:

$$\frac{[\int \log (I_0/I)]_{OD}}{[\int \log (I_0/I)]_{OH}} c_{OH} + c_{OH} = 1$$

This relationship was used to calculate the percentage of highly ordered material given later in this paper.

The infrared absorption bands that arise are due to transitions between different vibrational levels in the cellulose molecule, normally from the lowest level to some higher energy state. The atoms in the cellulose molecule may vibrate in a number of ways. Each particular mode of vibration has a characteristic frequency which is common to all the atoms vibrating, though the phases and amplitudes of the motion of various atoms may not coincide.

These vibrations are directional, and maximum absorption occurs when the direction of the electric vector is the same as the direction in which the average dipole moment changes during the vibration. Hence, if polarized radiation is used to examine a specimen in which the molecules are oriented with respect to the fiber axis, it is often possible to infer the direction of some of the bonds in the structure; conversely, it is possible to characterize the

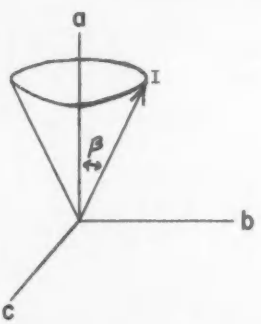

Figure 1.

orientation of the molecule with respect to the fiber axis by the same techniques.

All molecules in a cellulosic fiber would be affected by polarized radiation, but only those which exist in ordered or crystalline regions would contribute to changes in the measured absorption with a change in the direction of the incident electric vector. The amorphous region would not contribute to these variations since, by definition, this region is completely random. A summation of all of the electric vectors of a segment of the cellulose molecules in the amorphous region would yield the same results regardless of direction in which the electric vector strikes the sample. The experimental difficulties of obtaining useful data can partially be resolved if the absorption frequencies of the amorphous and ordered regions can be separated. By the use of the isotopic exchange reaction, the OH groups of the amorphous region are replaced by OD groups, which absorb at a lower frequency than the OH groups of the ordered region. By this method, one can study the orientation of the highly ordered region in a fiber without experimental interference from the amorphous region.

If the basic unit of cellulose is considered as cellobiose, the individual OH vectors around the 1,4-axis of the molecule could be summed to give a resultant OH vector. Assume that the resultant OH vector, I, of a cellobiose unit makes an angle with the 1,4-axis of the molecule of β. For each crystallite, therefore, the OH vectors will lie in the surface of a cone with the same axis as the crystallite axis and angle β (Fig. 1).

These vectors can be resolved into component vectors along three mutually perpendicular axes, one of which coincides with the crystallite axis. Let these axes be a, b, and c. Let the angle of rotation around the circular section of the cone be φ. The vector components must be averaged through values of from 0 to 360°. For reasons of symmetry, however, only one quadrant of the cone need be considered.

$$I_a = \frac{\int_0^{\pi/2} I \cos\beta \, d\varphi}{\int_0^{\pi/2} d\varphi}$$

$$= I \cos\beta$$

$$I_b = \frac{\int_0^{\pi/2} I \sin\beta \cos\varphi \, d\varphi}{\int_0^{\pi/2} d\varphi}$$

$$= I \sin\beta \left[\frac{\sin\varphi}{\varphi}\right]_0^{\pi/2}$$

$$= 2/\pi \, I \sin\beta$$

$$I_c = \frac{\int_0^{\pi/2} I \sin\beta \sin\varphi \, d\varphi}{\int_0^{\pi/2} d\varphi}$$

$$= I \sin\beta \left[\frac{-\cos\varphi}{\varphi}\right]_0^{\pi/2}$$

$$= 2/\pi \, I \sin\beta$$

Let the angle by which a crystallite axis deviates from the fiber axis be α. The crystallites will thus lie in the surface of a cone with the same axis as the fiber axis and with angle α. One of the component OH vectors of the crystallite will lie in the surface of the cone and the other two will be perpendicular to it. These other two vectors can be chosen so that one will always lie in the X–Y plane and one will make an angle α with the X–Y plane.

To determine the contributions made to absorption of parallel and perpendicularly polarized infrared radiation, we must resolve each of the component vectors for the crystallites into its components along the Z and X axes. As before, these must be averaged over angles of rotation about the Z axis from $\varphi = 0$ to $\varphi = 360°$.

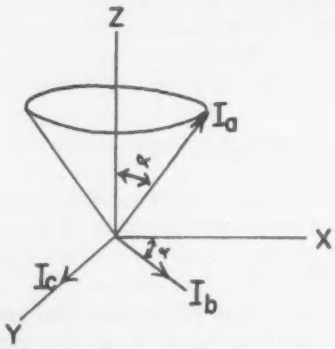

$I_a = I \cos \beta$

$I_b = 2/\pi \quad I \sin \beta$

$I_c = 2/\pi \quad I \sin \beta$

$I_Z = I_{aZ} + I_{bZ} + I_{cZ}$

Figure 2.

In the following, I_Z refers to the average OH vector in the Z axis, I_{aZ} refers to the Z axis component of the I_a vector, etc. (Fig. 2).

$$I_{aZ} = \frac{\int Ia \cos \alpha \, d\varphi}{\int d\varphi} = I_a \cos \alpha = I \cos \beta \cos \alpha$$

$$I_{bZ} = \frac{\int Ib \sin \alpha \, d\varphi}{\int d\varphi} = I_b \sin \alpha = 2/\pi \, I \sin \beta \sin \alpha$$

$$I_{cZ} = 0$$

$$\therefore \qquad I_Z = I \, (\cos \beta \cos \alpha + 2/\pi \sin \beta \sin \alpha)$$

Following the same procedure for I_X yields:

$$I_X = (2/\pi) \, I \, (\cos \beta \sin \alpha + 2/\pi \sin \beta \cos \alpha + 2/\pi \sin \beta)$$

$$\frac{I_X}{I_Z} = (2/\pi) \, \frac{(\cos \beta \sin \alpha + 2/\pi \sin \beta \cos \alpha + 2/\pi \sin \beta)}{(\cos \beta \cos \alpha + 2/\pi \sin \beta \sin \alpha)}$$

From the preceding equation, one should be able to calculate the orientation of the highly ordered region if β is known and the parallel and perpendicular vectors can be determined.

For cellulosic fibers the value of β will be a constant, and since the integrated molar extinction coefficients are proportional to the electric vectors, the relationship between I_X, I_Z, and the experimental data is given by:

$$\frac{I_X}{I_Z} \cong \frac{c_{\mathbf{E}_\perp}}{c_{\mathbf{E}_\parallel}} = k \frac{[\int \log (I_0/I)]_{\mathbf{E}_\perp}}{[\int \log (I_0/I)]_{\mathbf{E}_\parallel}}$$

where $c_{\mathbf{E}_\parallel}$ is the apparent magnitude of the parallel vector, $c_{\mathbf{E}_\perp}$ is the apparent magnitude of the perpendicular vector, and k is the ratio of B parallel and B perpendicular. Since k is unlikely to be 1.0, due to differences in the dichroism of the OH vibrations, it is necessary to determine the value of this constant for an absolute determination of the orientation.

At the present time, insufficient data have been obtained to fully evaluate k or B. However, the ratio

$$[\int \log (I_0/I)]_{\mathbf{E}_\parallel} / [\int \log (I_0/I)]_{\mathbf{E}_\perp}$$

gives an order to the orientation of the highly ordered region and will be used as an infrared orientation factor in this report.

Experimental

All of the samples for the experiment were prepared by the means of single end spinning with varying degrees of imposed stretch, except for Fortisan, which was supplied by Celanese Fibers Corporation, and a standard cotton sample furnished through the courtesy of U.S.D.A., Southern Regional Research Laboratories at New Orleans, Louisiana. All these fibers, except the cotton sample, had finishes of some nature applied. However, it was found that these finishes did not interfere in any manner with the test employed.

There are several major requirements for the fiber sample to be suitable for measurements by infrared methods: (*a*) it must be sufficiently thin to give an absorbance less than 2.0, preferably less than 1; (*b*) it should possess the orientation of an individual fiber; (*c*) the fibers should be damaged as little as possible in the sample preparation; (*d*) scattering by the sample should be minimized; and (*e*) the sample should still be available for exchange with D_2O.

We have found that suitably oriented samples may be obtained by utilizing the following technique. Approximately a 12-ft. section is cut from the continuous filament yarn. Individual fibers of this length are pulled from this section, and 30 to 40 of these are tied end-to-end. These are then wound onto a wire fork being turned by a constant speed motor. The fiber is advanced along the fork by a guide needle, which is capable of advancing one fiber diameter per revolution of the fork. At the conclusion of winding,

each side of the fork is glued to the fiber. An insert fork is then placed inside the large fork, and one side of the winding is glued to it. After the glue is dry, the side of the winding glued to the insert is cut with a razor blade and removed. The ribbon of fiber contained between the forks is then pressed at a load of 50,000 lb./in.^{2} for 1 min. The pressure is then released and one side of the sample is covered with powdered silver chloride (the amount of silver chloride used is not critical as long as the sample is covered) and repressed at 50,000 lb./in.^{2}. It has recently been shown that pressure of this magnitude might distort the fiber, but produces no significant structural changes.[9,10] The purpose of pressing and backing the fiber is to reduce light scatter and to provide a cohesive sample of convenient size that can be manipulated easily and mounted for examination.

This method of winding the fibers yielded parallel bundles of fiber which were acceptable for orientation studies. It was found that for samples which were not continuous filament yarns (e.g., cotton) acceptable spectra could be obtained by combing the fiber bundle until the fibers were parallel and uniform. These could then be pressed, and the same procedure followed as previously described.

The pressed sample is then mounted on a small ring insert that fits into a specially built deuteration cell. To obtain maximum intensity of radiation incident upon the fiber bundle, the deuteration cell was designed to place the sample at the focal point of the beam. A diagram of this cell is shown in Figure 3. The cell was constructed to allow the passage of gas over the sample while mounted and in the spectrophotometer.

A Perkin-Elmer Model 21 double-beam spectrophotometer was used for all observations. To obtain reasonable instrument response, it was necessary to use maximum slit widths and radiant energy output. Under these operating conditions, it was possible to obtain good reproducibility, and a resolution of the order of 30 cm.$^{-1}$. Radiation was plane-polarized by passing it through a Perkin-Elmer infrared polarizer, Model 127-1164. It is constructed of six silver chloride sheets arranged at the polarizing angle and placed immediately in front of the entrance slit of the spectrophotom-

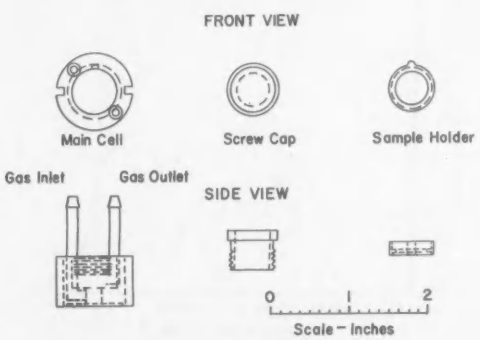

Fig. 3. Deuteration cell for the Perkin-Elmer Model 21.

eter. The plane of polarization of the radiation was altered by rotating the polarizing unit, the polarizing cell being so constructed that no displacement of the image occurred. To determine if any error was introduced due to polarization of the radiant beam, a check was made with only the silver chloride plane polarizer mounted in the sample beam. The spectrum was scanned from 2 to 15 μ, with polarization of 0 and 90°. It was found that less than 5% difference in per cent transmittance occurred due to polarization.

After mounting the sample, the cell was placed in the spectrophotometer, from which it was not moved until completion of the test on that sample. The sample was completely dried by passing a stream of dry nitrogen over it for twelve hours while in the radiant beam. This led to some heating of the sample which aided in drying. The nitrogen was dried by bubbling it through concentrated sulfuric acid, then over phosphorous pentoxide and through an air trap prior to passing over the sample. Upon completion of drying, the spectrum was obtained, after which the dried nitrogen was diverted through a D_2O bubbler, and the sample was deuterated for 4 hr.[6] After deuteration, the sample was again dried for 12 hr. and the spectrum obtained.

Results and Discussion

Errors inherent in experiments such as these arise from: (*a*) changes in the extinction coefficients of the various OH bands with a change in polarization angle; (*b*) the imperfections that occur in obtaining parallel bundles; and (*c*) the necessity of extrapolating in the determination of the integrated absorbances because of an overlapping of OH and CH_2 bands (Fig. 4).

Even though such an extrapolation was required, it was found that because of scattering of radiation by the sample it was preferable to use the ratio of integrated absorbances instead of the peak optical density. This method reduces the error introduced in peak intensities and positions due to scattering.[7]

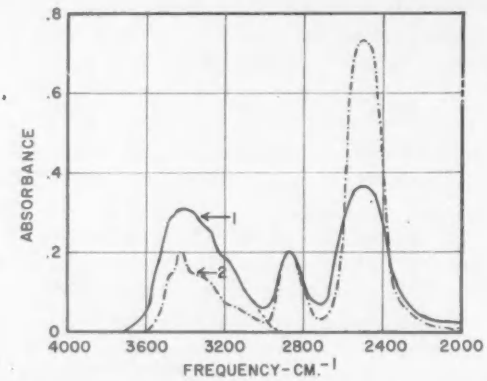

Fig. 4. Unpolarized deuterated infrared spectra of: (*1*) Fibro; (*2*) viscose film.

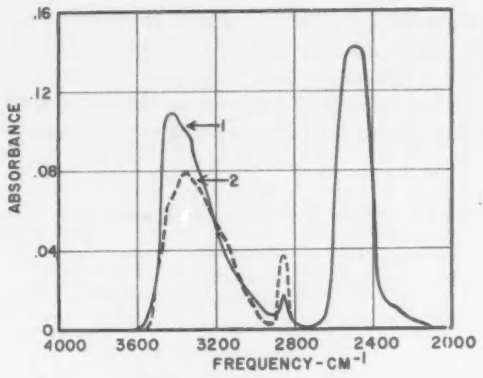

Fig. 5. Plane-polarized deuterated infrared spectrum of sample 1: (*1*) vector parallel to chain direction; (*2*) vector perpendicular to chain direction.

It is estimated that all of these conditions lead to a maximum deviation of ±2% in accessibility and orientation. In no case should this error change the relative order of values within a sample series.

All spectra were converted from per cent transmittance to absorbance and replotted versus frequency. Typical spectra are depicted in Figures 4 and 5. From the type of plots shown in Figure 4, the integrated absorbance of the OH and OD bands was obtained and the per cent highly ordered material calculated. Similarly, from plots such as Figure 5, the integrated absorbance of the OH bands at 0 and 90° polarization was determined and

TABLE II
Composition of the Fiber Structure

Sample	Highly ordered material (by infrared), %	Crystallinity (by x-ray), %
1	58	30
1 (repeat)	60	—
2	50	32
3	53	—
4	47	27
5	44	33
6	52	—
7	39	30
7 (repeat)	41	—
8	54	31
Fibro	43	30
Fibro (repeat)	42	—
Fortisan	57	39
Fortisan (repeat)	58	—
Commercial avril	28	—
Cotton	59	—
Viscose film	28	30

the order of orientation with the fiber axis of the ordered region in a given fiber calculated. These data are depicted in Tables II and III.

The same techniques have been employed in calculating an overall orientation of cellulose within the fiber using the CH and CH_2 vibrations. These data are presented in Table IV as a matter of academic interest.

TABLE III
Orientation of the Ordered Material with Respect to the Fiber Axis

Type	Order of orientation (from infrared)[a]	f_r (from x-ray)
1	1.23	0.84
2	0.64	—
3	0.89	0.80
4	0.48	0.64
5	1.07	0.85
6	1.09	0.78
7	0.88	0.78
8	0.98	0.75
Fibro	0.64	0.67
Fortisan	1.35	0.90
Cotton	0.53	—

[a] This arrangement is based on data obtained from the OH vibrations.

TABLE IV
Orientation of Cellulose with Respect to the Fiber Axis

Type	Order of orientation (from infrared)[a]
1	0.39
2	—
3	0.49
4	0.83
5	0.61
6	0.72
7	0.25
8	0.27
Fibro	0.53
Fortisan	—
Cotton	0.62

[a] This arrangement is based on data obtained from the CH and CH_2 vibrations.

An orientation parameter for the crystalline material was calculated from x-ray data according to the method proposed by Hermans et al.[11] Azimuthal intensity distributions of the required diffraction maxima were obtained by slowly rotating a bundle of parallel fibers in the x-ray beam with the counter set at the required 2θ angle. These curves were corrected for the amorphous background by using intensities obtained from radial scans of the fiber pattern as described in the above mentioned paper. The

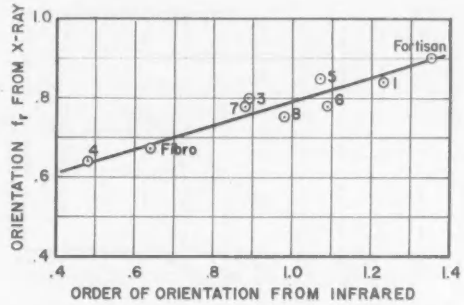

Fig. 6. Correlation of infrared and x-ray data. Numbers correspond to samples listed in the tables.

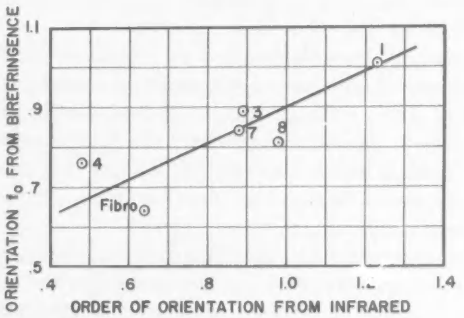

Fig. 7. Correlation of infrared and birefringence data. Numbers correspond to samples listed in the tables and can be correlated with Ref. 12 as follows: *1* = MX − 1, *3* = MX − 2, *4* = MX − 3, *7* = MZ − 1, *8* = MZ − 2, Fibro = Textile.

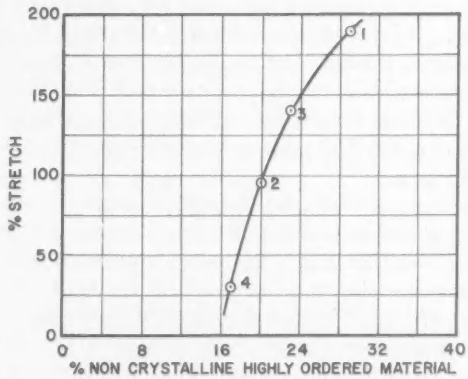

Fig. 8. The effect of stretch upon percentage of noncrystalline highly ordered material. Numbers correspond to samples listed in the tables.

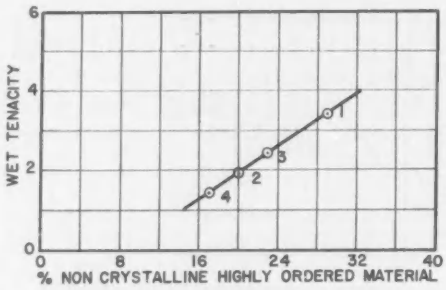

Fig. 9. The relation of noncrystalline highly ordered material and wet tenacity. Numbers correspond to samples listed in the tables.

correlation between the values obtained by this technique and the infrared data are presented in Figure 6.

Klein and Bosarge[12] have determined an overall orientation from birefringence measurements for part of the group of samples studied. If the same definition of fiber regions as used herein is applied to their study, then the calculated orientation should agree with the data from infrared studies. However, the absolute value may not agree since this value depends, in their calculations, on an "ideal" fiber birefringence. The correlation that is obtained is reasonable and is shown in Figure 7.

A crystallinity parameter was also determined by using x-ray diffraction data. This method involves dividing the area under the diffraction curve obtained from a sample of randomized fibers into portions attributed to crystalline and amorphous scattering. This separation was carried out as shown in a paper presented by Hermans and co-workers.[13] The values presented in Table II represent the percentage of crystalline area in the total area under the diffraction curve.

The values from x-ray analysis agree well with those previously reported for viscose fibers. A large spread in crystallinity might be expected due to the varying spinning stretch obtained in the sample preparation. Since only small differences are noted, one may conclude that the physical methods, such as stretch, that are used for imposing order have little or no effect on the crystallinity, but that this value is determined from the sample's prior chemical history.

If a comparison is made between the crystallinities and the percentage of highly ordered material as in Table II, a marked difference is noted. The percentage of the fiber that makes up the highly ordered region is larger than the corresponding crystallinity value and evidently varies with the methods of preparation. If this difference does depend on the method of preparation, such as stretch, then the values of crystallinity and highly ordered material for a viscose film where there is no imposed orientation should agree. Such agreement is obtained with approximately 30% of the fiber's structure being found in a crystalline state by both experimental methods.

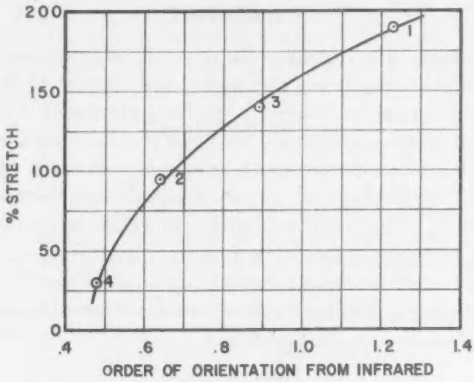

Fig. 10. The effect of stretch on orientation. Numbers correspond to sample numbers listed in the tables.

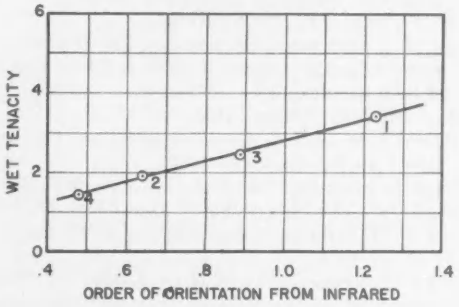

Fig. 11. The relation of orientation and wet tenacity. Numbers correspond to samples listed in the tables.

The difference in crystallinity and percentage of highly ordered material for a particular stretch series is plotted versus stretch in Figure 8.

Since this group of fibers vary drastically in their physical properties, some relation may exist between the above difference and these physical attributes. A plot of one of these physical properties, wet tenacity, versus the noncrystalline ordered material is shown in Figure 9. There is marked dependence of this property on the difference between the percentage crystallinity and total amount of highly ordered material. The same dependency of physical properties on the orientation of the highly ordered material exists and is shown in Figures 10 and 11. It is to be remembered, however, that other factors such as crystallite size and distribution also affect a fiber's physical properties, but it is assumed that these do not vary within a stretch series. Therefore, for a particular series, the amount and orientation of highly ordered material is related to the fiber's physical properties.

Conclusion

The technique of obtaining the percentage of highly ordered material and characterizing the orientation of this region with respect to the fiber axis by infrared spectrophotometric methods has been examined. Although these techniques need further refinement to yield the maximum in information and precision, the methods employed have removed many obstacles which have confronted infrared spectroscopists in obtaining information about the structure of fibers. These two structural properties, when used in conjunction with x-ray data, are shown to be directly related to the physical properties of a fiber series where order is imposed upon the fibers by stretch. This method of exploring a fiber series should yield information valuable in the development of improved cellulosic fibers.

References

1. Marrinan, H. J., *Recent Advances in the Chemistry of Cellulose and Starch*, J. Honeymann, Ed., Interscience, New York–London, 1959.
2. Tyler, D. N., and N. S. Wooding, *J. Soc. Dyers Colourists*, **74**, 283 (1958).
3. Jones, D. W., *J. Polymer Sci.*, **32**, 371 (1958).
4. Mann, J., and H. J. Marrinan, *J. Polymer Sci.*, **32**, 375 (1958).
5. Recent discussion at Second Congress Man-Made Fibers, London (1962).
6. Mann, J., and H. J. Marrinan, *Trans. Faraday Soc.*, **52**, Part 3, 481 (1956).
7. Willis, H. A., Chem. Ind. (*London*), **1957**, 201.
8. Jones, N. R., and C. Sandorfy, *Chemical Applications of Spectroscopy*, W. West, Ed., Interscience, New York–London, 1956, p. 276.
9. Burgess, S., and H. Spedding, *Chem. Ind.* (*London*), **1961**, 1166.
10. Cumberbirch, R. J. E., and H. Spedding, *J. Appl. Chem.*, **12**, 83 (1962).
11. Hermans, J. J., P. H. Hermans, D. Vermaas, and A. Weidinger, *Rec. Trav. Chim.*, **65**, 427 (1956).
12. Klein, E., and J. K. Bosarge, presented at the Atlantic City Meeting of American Chemical Society, Division of Polymer Science, September 1962; also *J. Polymer Sci., Part C*, No. **2**, 515 (1963).
13. Hermans, P. H., and A. Weidinger, *J. Polymer Sci.*, **4**, 135 (1949).
14. Pennings, A. J., W. Prins, R. D. Hale, and B. G. Ranby, *J. Appl. Polymer Sci.*, **5**, 676 (1961).

Synopsis

A series of cellulosic fibers has been studied by x-ray and infrared techniques. The methods employed in obtaining and interpreting the experimental data are described. The infrared determination of accessibility and order of orientation of cellulosic fibers involves a new approach in the measuring of the plane polarized and unpolarized infrared spectra of deuterated fibers. The correlation of x-ray and infrared data is discussed, and the relationship of data to fiber structure is examined. It is shown that the data obtained can be related, in special cases, to fiber properties.

Résumé

On a étudié une série de fibres cellulosiques par les techniques aux rayons-X et à l'infrarouge. On décrit les méthodes employées pour obtenir et interprèter les résultats expérinentaux. La détermination infra-rouge de l'accessibilité et du degré d'orientation des fibres cellulosiques implique une nouvelle méthode d'approche à savoir la mesure des spectres infra-rouges des fibres deutérées avec de la lumière polarisée et non-polarisée.

On discute la corrélation des résultats obtenus au moyen des rayons-X et à l'infra-rouge, et on examine la relation entre les résultats et la structure des fibres. On montre que les résultats obtenus peuvent être mis en relation, dans des cas particuliers, aux propriétés des fibres.

Zusammenfassung

Eine Reihe von Cellulosefasern wurden mit Röntgen- und Infrarotmethoden untersucht. Gewinnung und Auswertung der experimentellen Daten wird beschrieben. Die Infrarotbestimmung der Zugänglichkeit und des Orientierungsgrades der Cellulosefasern beruht auf einem neuartigen Verfahren zur Messung der Spektren deuterierter Fasern im linear polarisierten und unpolarisierten Infrarot. Die Korrelation zwischen Röntgen- und Infrarotdaten wird diskutiert und die Beziehung der Daten zur Faserstruktur untersucht. Die erhaltenen Daten lassen sich in speziellen Fällen zu Fasereigenschaften in Beziehung setzen.

JOURNAL OF POLYMER SCIENCE: PART C NO. 2, PP. 515–526 (1963)

Optical Dispersion and Birefringence of High Tenacity Cellulose Fibers

E. KLEIN and K. BOSARGE, *Research Department, Courtaulds North America, Inc., Mobile, Alabama*

INTRODUCTION

In the study of fiber structure, the determination of birefringence is one of the more useful techniques. When combined with x-ray orientation measurements, it yields one of the few indications of "amorphous" orientation.

The techniques often employed utilize some form of Becke refraction, or a method whereby the refractive index of the mounting medium is made to coincide with one of the fiber indices.[1] Two variations of the latter technique have been described. In one form the temperature of the mountant is varied by means of a microscope hot stage. Since the temperature coefficient of refractive index for liquids is usually much higher than for solids, one finds a temperature at which the refractive indices of the mountant and fiber coincide. Because this method utilizes a variation of the Becke line method, the errors of small sample, skin/core differentiation, etc., are not alleviated.

A more elegant method which depends on the difference in optical dispersion between the mountant and the fiber was described by Freeman and Preston.[2] This technique, we felt, was especially valuable for cellulosic fibers since it allows the use of bone-dry fibers, employs a relatively large sample, and yields the optical dispersion of the sample as well as its refractive index. This paper describes an adaptation of the dispersion method to a high resolution spectrophotometer, and some comments on the Hermans[3a] corrections for water content. While the experiments deal only with regenerated cellulosic fibers, the procedure is equally applicable to other synthetic fibers.

EXPERIMENTAL

A. Sample Preparation

The fibers used here were in both staple and continuous filament form. When staple was used, combed, parallelized bundles approximately two fibers thick were mounted with epoxy cement on a 0.9 × 5.0 cm. brass shimstock frame having a 0.7 × 1.7 cm. aperture cut near the center.

After curing the epoxy, the bottom of the tab was bent to provide a footing in the 1 cm. rectangular spectrophotometer cell. All samples were dried overnight at 80°C. under vacuum, and immediately dropped into the spectrophotometer cells containing the dispersion oil. The cells were degassed, until no bubbles were visible, in the flask of a low pressure hydrogenator connected through one valve to a vacuum pump. Dry helium was stored in the ballast tank of the hydrogenator at 60 psi, and this was used to force penetration of the fibers by the oil. The degassing step is of definite benefit, but the pressure cycle has dubious merit. In later experiments it was eliminated.

When continuous filaments were employed, a small stainless steel frame made from welding rod was used to wind the filaments. Care was taken not to form any doubled layers, since the winding process by necessity led to a minimum of two layers. Subsequent handling was identical to the staple procedure; however, no cementing was necessary.

B. Immersion Oils

Because of the strong desiccant properties of dry cellulose, and the concomitant changes caused in refractive index, the requirements for a suitable immersion oil are stringent. The vapor pressure requirements inherent in the degassing operation pose additional problems.

We were fortunate to obtain from Cargille Laboratories a series of suitable immersion oils consisting of a two component mixture of chlorinated aromatics. Near-infrared and infrared spectra showed the absence of any water traces, both before and after an experiment. Refractive index measurements after degassing showed no measurable change in the mixture due to the vacuum.

The end-members of the series (the two components) were calibrated by the National Bureau of Standards, as well as a mixture having a n_D^{25} value of 1.55610. The calibrations were carried out at wavelengths of 6563, 5893, 5461, 4861, 4358, and 4057 A. From a knowledge of the dispersion curve of the end-members and the n_D^{25} value of a mixture, it is possible to con-

TABLE I
N.B.S. Values of Refractive Index

Wavelength, A.	n_D^{25}			
	Component I	Component II	Mixture A	Mixture A (calc.)
6563	1.45523	1.61832	1.55110	1.55117
5893	1.45755	1.62508	1.55610	—
5461	1.45957	1.63117	1.56042	1.56051
4861	1.46331	1.64302	1.56896	1.56902
4358	1.46783	1.65836	1.57984	1.57991
4057	1.47159	(1.67196)[a]	1.58948	—

[a] Calculated from mixture A and component I data; measurement impossible on N.B.S. minimum deviation spectrometer.

struct the dispersion curve of the mixture. A test of these calculations was provided by the values obtained by the National Bureau of Standards on the $n_D^{25} = 1.55610$ mixture, and showed deviations not exceeding 0.00009. These data are shown in Table I.

C. Spectrophotometer Measurements

For all measurements a Cary Model 14 recording spectrophotometer equipped with polaroid filters in both reference and sample compartments was employed. The reference beam was attenuated with a 1 cm. cell containing the immersion oil, and when necessary, a neutral screen filter. Temperature control was achieved by thermostatting the cells prior to measurement at 25°C. and by circulating the same bath through the cell compartment during the measurement. Beam heating was minimized by taking only one scan per sample; prior to replication checks, the cells were replaced in the constant temperature bath to attain equilibrium.

The absorbance curve was traced from 7000 A. to approximately 3600 A. The lower spectrum end was determined by the slit opening due to the absorption of the oil. The upper useable end of the spectrum was dictated by the scatter of the sample. For highly scattering samples requiring a neutral screen in the reference beam, the point at which the slit opened to 0.3 mm. was taken as the longest wavelength useable. A strong attenuation of the reference beam by the neutral filters causes the slit to open and resolution is sharply reduced at longer wavelengths leading to erroneous minima in the absorbance spectra. Sample preparation techniques thereby influence the useable range of the spectrum.

RESULTS

The procedure for determining fiber refractive index is essentially as follows. One assumes that the three spatial axes of the fiber correspond to three optical axes. One further assumption is that due to the quasi-cylindrical fiber shape, the two refractive indices perpendicular to the fiber length direction are equal. To determine the fiber refractive index in the direction parallel to the fiber length, light polarized so that the electric vector is parallel to this direction is used. If this polarized beam is then attenuated by a 1 cm. length of the dispersion oil, a small but measurable absorbance is found. If in addition to the oil a transparent body differing in refractive index from the oil is interposed, a further increase in absorbance results due to refraction at each body–oil interface. This loss, or scattering, reaches a minimum when the refractive indices of the oil and the interposed fiber bundle coincide. By choosing a series of oils having refractive indices which coincide with the fiber refractive index at various wavelengths in the visible spectrum, a number of "matches" are obtained. Since they will coincide at differing wavelengths, an optical dispersion curve of one of the fiber's refractive indices is obtained. Figure 1 demonstrates the construction of the dispersion curve from data typified by Figure 2.

By repeating the procedure with polarized light oriented perpendicular to the fiber axis, the second refractive index is determined in a like manner. The technique fails if in addition to the fiber–oil interface a high scattering contribution results from a preponderance of fiber–air interfaces.

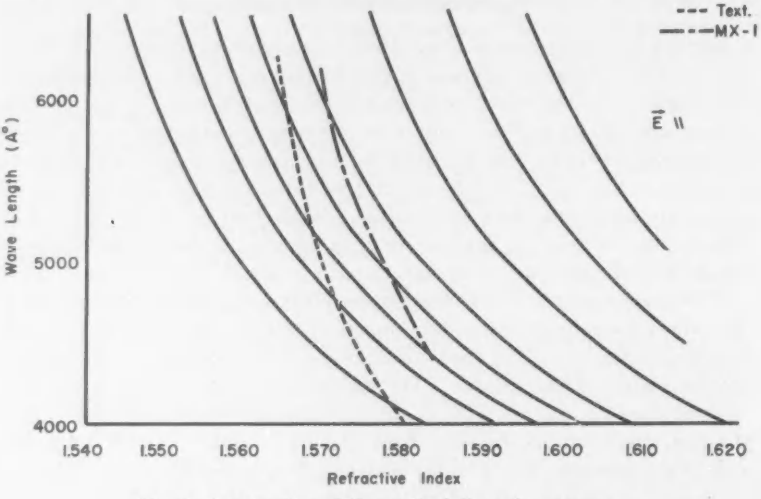

Fig. 1. Construction of fiber optical dispersion curves.

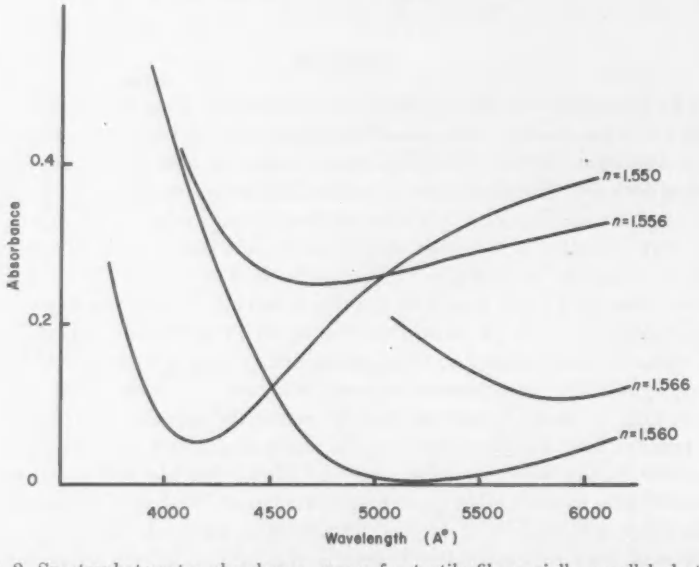

Fig. 2. Spectrophotometer absorbance curves for textile fiber axially parallel electric vector.

TABLE II
Refractive Index Values Taken From Constructed Dispersion Curves[a]

Sample[b]	589 mμ			550 mμ			500 mμ			450 mμ			589 mμ (Becke)		
	$n_{\|\|}^{\circ}$	$n_{\perp}^{\circ}$	n°	$n_{\|\|}^{\circ}$	$n_{\perp}^{\circ}$	n°	$n_{\|\|}^{\circ}$	$n_{\perp}^{\circ}$	n°	$n_{\|\|}^{\circ}$	$n_{\perp}^{\circ}$	n°	$n_{\|\|}$	$n_{\perp}$	n
MX-1 Exptl. HWM, maximum stretch	1.5704	1.5159	0.0545	1.5729	1.5187	0.0542	1.5770	1.5231	0.0539	1.5820	1.5286	0.0534	1.559	1.517	0.042
MX-2 Exptl. HWM, 50% stretch	1.5685	1.5199	0.0486	1.5707	1.5229	0.0478	1.5740	1.5272	0.0468	1.5783	1.5323	0.0460	1.556	1.517	0.039
MX-3 Exptl. HWM, 0% stretch	1.5591	1.5181	0.0410	1.5614	1.5213	0.0401	1.5649	1.5257	0.0392	1.5695	1.5309	0.0386	1.547	1.518	0.029
MZ-1 Exptl. HWM, low D.P.	1.5713	1.5255	0.0458	1.5725	1.5278	0.0447	1.5750	1.5309	0.0441	1.5796	1.5346	0.0450	1.556	1.5 7	0.039
MZ-2 Exptl. HWM, low D.P.	1.5726	1.5282	0.0444	1.5743	1.5299	0.0444	1.5769	1.5324	0.0445	1.5811	1.5356	0.0455	1.558	1.517	0.041
MC-1 Commercial HWM	1.5703	1.5308	0.0395	1.5729	1.5332	0.0397	1.5763	1.5350	0.0413	1.5796	1.5369	0.0427			
Textile staple	1.5649	1.5300	0.0349	1.5666	1.5323	0.0343	1.5693	1.5354	0.0339	1.5734	1.5388	0.0346	1.550	1.518	0.032

[a] The superscript zero (0) used here refers to completely dry fiber and is omitted where reference is to conditioned sample data.
[b] HWM = high wet modulus fiber.

This is observed in fibers such as Fortisan, where apparently the macrovoids, or vacuoles, are not contiguous with the surface. These can be demonstrated by observing Fortisan mounted in a medium where the Becke line method indicates a match has been achieved; the vacuoles are then still clearly visible.

To demonstrate this technique, a series of high wet modulus cellulosic fibers were examined. The sample descriptions and their n_λ^{25} values are listed in Table II, as well as the n_D^{25} values obtained from conditioned fibers via the Becke line method.

DISCUSSION

A. Dispersion

In Figures 3–5 are shown the dispersion curves of the samples, as well as the dispersion of their birefringence. Contrary to the conclusions of Free-

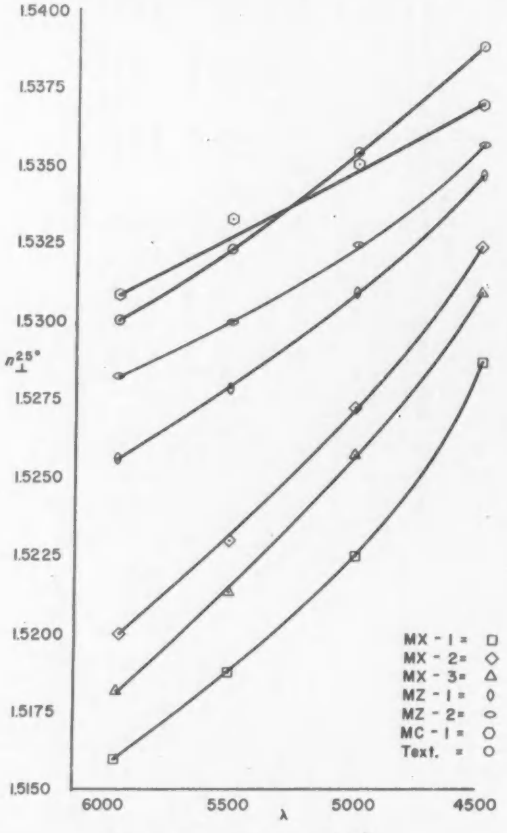

Fig. 3. Optical dispersion $\overrightarrow{E\perp}$.

man and Preston,[2] we do not find identical dispersion for all samples. All of the curves show characteristics associated with "normal" dispersion, but the curves are "irrational" in that they do not differ by a constant factor.[4]

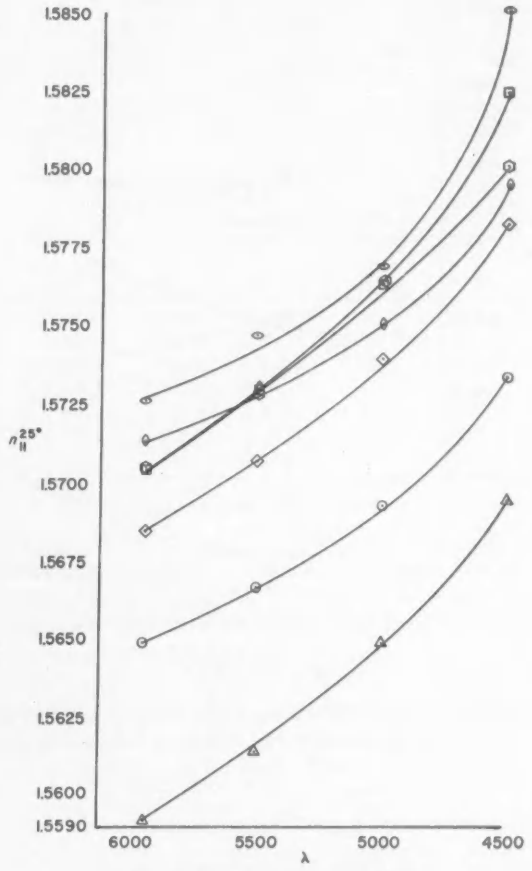

Fig. 4. Optical dispersion $\overrightarrow{E\parallel}$.

It is interesting to note that the birefringence dispersion does not follow a uniform pattern. The MX series shows a linear relationship described by $d(\Delta n)/d\lambda = -k_1$, whereas the other fibers pass through minima. The latter are all related by the fact that they were spun through zinc containing baths. The significance of these differences has not yet been established.

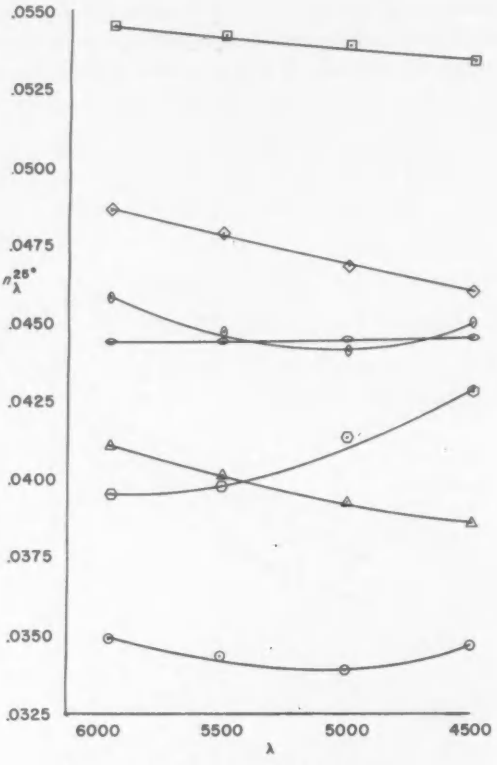

Fig. 5. Optical dispersion of birefringence.

B. Density

The applicability of the Gladstone-Dale relationship to cellulose fibers has been reviewed by Hermans.[3b] By using the relationships

$$(n_{\text{iso}}^{\circ} - 1)/d = [0.3572]_{\text{D}}^{25°} \tag{1}$$

$$n_{\text{iso}}^{\circ} = {}^{1}/_{3}(n_{||} + 2n_{\perp}) \tag{2}$$

the densities shown in Table III are found. Since the Gladstone-Dale relationship should be valid for the individual indices, i.e.,

$$(n_{||} - 1)/d = C_1$$

and

$$(n_{\perp} - 1)/d = C_2$$

where C_1 and C_2 are true constants if the same conditions of orientation prevail, the calculated densities can now be used to determine C_1 and C_2. It is obvious that the difference $(C_1 - C_2)$ is related to birefringence so that

TABLE III
Calculated Bone Dry Fiber Densities and Constants From Gladstone-Dale Equation

Sample	n°_{iso}	d_{25}	C_1	C_2
MX-1	1.5341	1.4952	0.3815	0.3450
MX-2	1.5361	1.5008	0.3788	0.3464
MX-3	1.5318	1.4888	0.3755	0.3480
MZ-1	1.5408	1.5140	0.3773	0.3471
MZ-2	1.5430	1.5202	0.3767	0.3475
MC-1	1.5440	1.5230	0.3745	0.3485
Textile	1.5416	1.5163	0.3726	0.3495

TABLE IV
Fiber Orientation Factors

Sample	Δn_D^{25}	d_{25}	$\Delta n_{corr.}$	f_0	$(C_1 - 0.3572)$	$(C_2 - 0.3572)$
MX-1	0.0545	1.4952	0.0554	1.01	0.0243	−0.0122
MX-2	0.0486	1.5008	0.0492	0.89	0.0216	−0.0108
MX-3	0.0410	1.4888	0.0419	0.76	0.00183	−0.0092
MZ-1	0.0458	1.5140	0.0460	0.84	0.0201	−0.00101
MZ-2	0.0444	1.5202	0.0444	0.81	0.0195	−0.0097
MC-1	0.0395	1.5230	0.0394	0.72	0.0173	−0.0087
Textile	0.0349	1.5163	0.0350	0.64	0.0154	−0.0077

the values of $C_1 - 0.3572$, and $C_2 - 0.3572$ are a measure of orientation effects on the individual indices. These calculated values as well as the orientation factor f_0 as defined by Hermans[3c] and based on the "ideal" fiber birefringence of 0.055 are shown in Table IV. The birefringence are reduced to a common density of 1.520 for calculating f_0.

That the differences $(C_2 - 0.3572)$ and $(C_1 - 0.3572)$ are related to f_0 is demonstrated in Figure 6. The entire calculation, of course, rests on the assumption that eq. (1) is valid, and that the constant 0.3572 found by Hermans to hold for the samples cited at 20°C. is not highly temperature-sensitive.

If one accepts the validity of the Hermans derivations, there arises the dilemma of rationalizing the very low densities calculated by eq. (1). Since these fiber types have not been reported on extensively in the literature, the relationships between density, crystallinity, and orientation established previously[5] for other fiber types may need re-examination.

One further point is of interest. Starting from the assumption that the molar refraction of a mixture is the sum of the component refractions weighted on a weight basis, i.e.,

$$(n - 1)/d_m = [(n_1 - 1)/d_1]w_1 + [(n_2 - 1)/d_2]w_2 \qquad (3)$$

where the subscripts m, 1, and 2 refer to the mixture, component 1, and

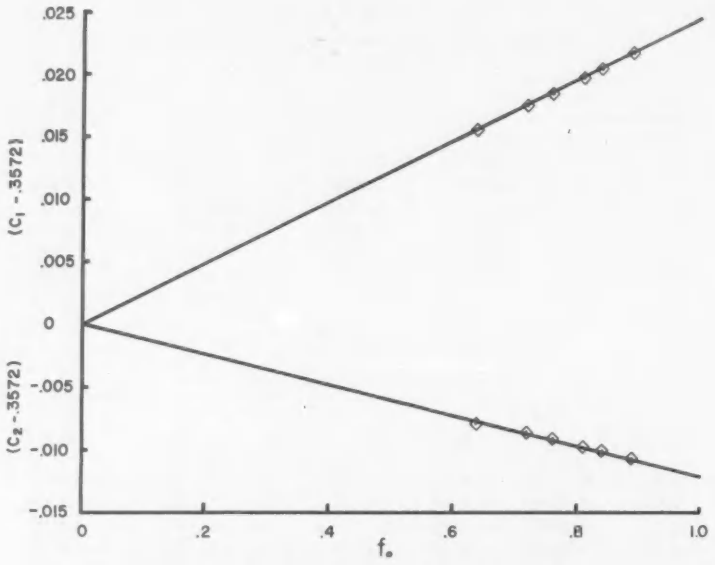

Fig. 6. Gladstone-Dale constant vs. orientation factor.

component 2, respectively, Hermans derived the relationships between refractive index of cellulosic fibers and their moisture content,

$$(n_a - 1)v_a = [(n_0 - 1)/d_0] + 0.333a \tag{4}$$

where

$$v_a = (1 + a)/d_a$$

a is the weight of H_2O per gram of cellulose, and d_a is the density of the conditioned fiber. The subscript zero indicates the values for bone dry fiber.

This derivation is based on the assumption that no change in structure occurs on drying, or from the chemical point of view that water forms an ideal solution in the fiber. It can be tested for self-consistency by calculating d_a for both the parallel and perpendicular refractive index data for

TABLE V
Calculated Conditioned Fiber Densities

Sample	d_0 (calc.)	a	$d_{a\parallel}$	$d_{a\perp}$	Δd_a
MX-1	1.4952	0.1103	1.481	1.500	−0.019
MX-2	1.5008	0.1132	1.491	1.498	−0.007
MX-3	1.4888	0.1334	1.476	1.496	−0.020
MZ-1	1.5140	0.1204	1.492	1.496	−0.004
MZ-2	1.5202	0.1184	1.499	1.494	+0.005
MC-1	1.5230	0.1388	1.494	1.489	+0.005
Textile	1.5163	0.1254	1.489	1.486	+0.003

the conditioned fibers as determined by the Becke line method and shown in Table II and the equilibrium moisture regain found in the usual manner. That the derived values cannot have a high order of precision is to be expected, since the errors in each technique may be additive. The calculated d_a values and the regains used are shown in Table V.

It appears again that the zinc-spun (MZ) fibers form a group consistent with earlier experiments, whereas the MX series do not. For example, the $d_a^{\perp}$ values do not decrease to the extent that would be predicted on the basis of eq. (4). The significance of these data are, of course, directly related to the questions raised previously about the relationships between density, crystallinity, and orientation.

References

1. Heyn, A. N. J., *Fiber Microscopy*, Interscience, New York, 1954.
2. Freeman, K., and J. M. Preston, *J. Textile Inst.*, **34**, 19 (1943).
3. Hermans, P. H., *Physics and Chemistry of Cellulose Fibres*, Elsevier, Amsterdam–New York, 1949, (a) p. 218; (b) *ibid.*, p. 202; (c) *ibid.*, p. 230.
4. Jenkins, F. A., and H. E. White, *Fundamentals of Optics*, McGraw-Hill, New York, 1950.
5. Tyler, D. N., and N. S. Wooding, *J. Soc. Dyers Colourists*, **74**, 283 (1958).

Synopsis

A method previously described by Freeman and Preston for measuring birefringence and optical dispersion of fibers has been adapted to a high resolution spectrophotometer, Utilizing the technique described, several high tenacity regenerated cellulose fibers have been examined; from the data obtained, densities, and orientation factors were derived. Contrary to the conclusions of Freeman and Preston, optical dispersion curves for the various samples were not identical. Birefringence dispersion did not follow a uniform pattern in that some samples showed a minimum. Bone dry densities calculated from the optical data by using the equation derived by Hermans are found to be considerably lower than those normally reported for regular rayon. Conditioned fiber densities calculated from the separate perpendicular and parallel refractive indices also show unexpected deviations. Data gathered indicate an apparent need for reexamination of the density, crystallinity, and orientation relationships which are in general use.

Résumé

Une méthode antérieurement décrite par Freeman et Preston mesurant la biréfringence et la dispersion optique de fibres a été adaptée à un spectrophotomètre à haute résolution. A l'aide de la technique décrite, plusieurs fibres de cellulose régénérée de haute résistance ont été examinées; à partir des données recueillies, les densités et les facteurs d'orientation ont été déduits. Contrairement aux conclusions de Freeman et Preston, les courbes de dispersion optique de différents échantillons ne sont pas identiques. La dispersion de la biréfringence ne suit pas un modèle uniforme à telle enseigne que certains échantillons ont montré un minimum. On a trouvé que les densités de fibres à l'état absolument sec calculées à partir des données optiques en utilisant l'équation dérivée par Hermans sont considérablement plus faibles que celles normalement obtenues pour la soie artificielle habituelle. Les densités de fibres conditionnées calculées séparément à partir des indices de réfraction perpendiculaire et parallèle sé montrent également des déviations inattendues. Les données réunies indiquent une obligation évidente de réexaminer les relations liant la densité, la cristallinité et l'orientation, qui sont généralement utilisées.

Zusammenfassung

Eine früher von Freeman und Preston zur Messung der Doppelbrechung und optischen Dispersion von Fasern angegebene Methode wurde für ein Spektralphotometer mit hoher Auflösung adaptiert. Einige hochfeste Fasern aus regenerierter Cellulose wurden untersucht; aus den Versuchsdaten wurden Dichte und Orientierungsfaktoren abgeleitet. Im Gegensatz zu den Befunden von Freeman und Preston waren die optischen Dispersionskurven für die verschiedenen Proben nicht identisch. Die Doppelbrechungsdispersion zeigte kein einheitliches Verhalten, da einige Proben ein Minimum aufwiesen. Die aus den optischen Daten mit der Gleichung von Hermans (3) berechnet Dichte im knochentrockenen Zustand erweist sich als beträchtlich niedriger als die für normales Rayon angegebenen Werte. Auch die aus den getrennt bestimmten senkrechten und parallelen Brechungsindices berechnete Dichte konditionierter Fasern zeigt unerwartete Abweichungen. Die gesammelten Daten lassen die offenbare Notwendigkeit einer Uberprüfung der allgemein benützten Dichte-, Kristallinitäts- und Orientierungsbeziehungen erkennen.

JOURNAL OF POLYMER SCIENCE: PART C NO. 2, PP. 527–546 (1963)

Elasticity of Polyvinyl Alcohol Model Filaments in Swelling Equilibrium with Water

H. ABE* and W. PRINS, *Laboratory of Physical Chemistry, Technische Hogeschool, Delft, The Netherlands*

INTRODUCTION

Many polymers exhibit long-range elasticity only after swelling in a diluent has sufficiently reduced the interchain forces. In the case of polyvinyl alcohol, water is a suitable diluent, provided the polyvinyl alcohol has been chemically crosslinked or otherwise treated so as to ensure a limited swelling only.

Quite generally, a study of crosslinked polymer networks under an imposed elastic strain, while maintaining swelling equilibrium with a diluent, proves to be interesting from various points of view. In the first place, measurements of elasticity and swelling as a function of temperature (thermoelasticity) can be analyzed thermodynamically to yield the energy as well as the entropy component of the free energy of deformation. These quantities are of interest in ascertaining the molecular mechanism of elastic deformation. If one relies on a statistical mechanical model of amorphous polymer networks, composed of Gaussian chains, conformational information regarding the polymer chain in the presence of the diluent may be obtained. In the second place, the measurements can be analyzed to yield the partial molar heat of dilution of the swollen polymer network. If, moreover, the above-mentioned theoretical model of a polymer network is applicable, one can determine the two components of the heat of dilution, viz. the partial molar heat of mixing and the partial molar heat of elastic deformation. By varying the crosslinking density, and therefore the extent of swelling, such data can be obtained over a considerable range of polymer concentrations.

It seemed of interest to compare the earlier work on the thermoelasticity of cellulose model filaments[1] with measurements on a similar polymer, but a polymer without the complications introduced by crystallites and capable of sustaining much larger reversible elastic deformations. In the present article we communicate the results obtained on model filaments of polyvinyl alcohol (PVA), prepared by spinning a concentrated PVA solution or gel, into a coagulating bath. By treating the coagulated filaments with formal-

* On leave from the Dainippon Celluloid Company. Present address: Dainippon Celluloid Company Ltd., Central Research Laboratory Oi-mura, Iruma-gun, Saitama-Ken, Japan.

dehyde or thiodiacetaldehyde, filaments are obtained which on subsequent immersion in water do no longer dissolve up to at least 100°C. These filaments are subjected in water to unidirectional elastic extension. Stress–strain as well as dimensional data are recorded over a temperature range of 20–90°C. The extent of formalization or thiodiacetalization is determined by chemical analysis.

THERMODYNAMICS

Thermoelasticity

If we consider a swollen cylindrical filament in contact with a reservoir of diluent as our (open) thermodynamic system, we can write for the differential of the Helmholtz free energy

$$dF = -SdT - pdV + fdL + \mu dN$$

where all symbols have the customary meaning and in addition f = retractive force, L = length of the filament, μ = thermodynamic potential of the diluent, and N = the number of diluent molecules in the filament.

Thus we can define

$$\begin{aligned} f &= (\partial F/\partial L)_{VTN} = (\partial E/\partial L)_{VTN} - T(\partial S/\partial L)_{VTN} \\ &= (\partial E/\partial L)_{VTN} + T(\partial f/\partial T)_{VLN} \\ &= f_e + f_s \end{aligned} \tag{1}$$

We have on purpose used the Helmholtz free energy F (sometimes called A), because this gives us the conditions of constant volume and constant diluent content N, which allow us to draw conclusions from f_e and f_s, not obscured by thermal expansion or changes in diluent content. In this case f_e and f_s will be exclusively related to the deformational process.

Experimentally one can obtain, of course, only f and $(\partial f/\partial T)_{pLe}$, where e denotes that swelling equilibrium is maintained with the reservoir. It has been stressed by Flory, Ciferri and Hoeve[2] that conversion of $(\partial f/\partial T)_{pLe}$ to the desired quantity $(\partial f/\partial T)_{VLN}$ cannot be rigorously achieved without recourse to a theoretical model of network deformation. Considering the network in the usual way as an assembly of Gaussian chains between crosslinks, they derived

$$(\partial f/\partial T)_{VLN} = (\partial f/\partial T)_{pLe} + f\gamma(\alpha^{*3} - 1)^{-1} \tag{2}$$

where

$$\gamma = (\partial \ln V/\partial T)_{pLe}$$

and

$$\alpha^* = \alpha(q_1/q)^{1/3}$$

with $\alpha = L/L_1$ = the elongation with respect to the initial, swollen state and q_1 and q the volume degrees of swelling before and after stretch,

respectively. According to eq. (2) the desired conversion can be achieved if the diameter of the cylindrical filament is measured as a function of temperature and elongation.

However, one cannot always be certain that the theoretical model used in the derivation of eq. (2), applies to the filament under study. This is most certainly the case with swollen, semicrystalline cellulose filaments[1] and very likely also with swollen PVA filaments at low temperatures (see below). In the absence of detailed molecular models for the elasticity of such filaments, one has to make use of an approximation in order to convert $(\partial f/\partial T)_{pLe}$ to the desired quantity $(\partial f/\partial T)_{VLN}$. The approximation often used is the one offered by Elliott and Lippmann and Gee:[3]

$$(\partial f/\partial T)_{VLN} \cong (\partial f/\partial T)_{pN\alpha} \tag{3}$$

where the quantity on the right-hand side can subsequently be converted rigorously to $(\partial f/\partial T)_{pLe}$. Flory, Ciferri, and Hoeve[2] have shown that for Gaussian chain networks the precise relation should be:

$$(\partial f/\partial T)_{VLN} = (\partial f/\partial T)_{pN\alpha} + \gamma_0 f/3$$

where

$$\gamma_0 = (\partial \ln V/\partial T)_{pN}$$

Since the experimentally obtainable accuracy for swollen filaments is usually not very high, omission of the term $\gamma_0 f/3$ is not serious. Moreover, on the basis of thermodynamic relations it is possible to show more generally that the error committed by using eq. (3) for swollen isotropic filaments (whether semicrystalline or not) will not exceed the experimental accuracy in an important way.[4]

Using eq. (3), then, as a basis for thermoelastic studies for swollen filaments of most any type, provided they are isotropic if unstretched, we can complete the desired conversion as shown earlier:[2]

$$(\partial f/\partial T)_{VLN} \cong (\partial f/\partial T)_{pN\alpha} = (\partial f/\partial T)_{pLe} - (\partial f/\partial N)_{pLT}$$
$$[(\partial N/\partial T)_{pLe} + L\lambda_0(\partial N/\partial L)_{pfT}] \tag{4}$$

where $\lambda_0 = \gamma_0/3$. In the present case it was found that under the loads employed, the change in swelling with elongation, $(\partial N/\partial L)_{pfT}$, is isotropic. Therefore eq. (4) reduces to

$$(\partial f/\partial T)_{pN\alpha} = (\partial f/\partial T)_{pLe} - (\partial f/\partial V)_{pLT}(\partial V/\partial T)_{pLe} \tag{5}$$

A comparison with eq. (2) shows that eq. (5) requires the determination of the additional quantity $(\partial f/\partial V)_{pLT}$. A suitable way of measuring this quantity is to induce changes in diluent content and retractive force by replacing the pure diluent by a polymer solution of lower solvent activity. If c is the concentration of this polymer which is assumed not to diffuse into the swollen filament, one has

$$(\partial f/\partial V)_{pLT} = (\partial f/\partial c)_{pLT}(\partial V/\partial c)^{-1}_{pLT} \tag{6}$$

Partial Molar Heat of Dilution

If we consider the reservoir plus the swollen filament as our (closed) thermodynamic system, we derive from the differential of the Gibbs free energy:

$$f = (\partial H_t/\partial L)_{pTe} + T(\partial f/\partial T)_{pLe} \tag{7}$$

where H_t is the total enthalpy of the system. Considering the swollen filament separately we can write

$$f = (\partial H/\partial L)_{pNT} + T(\partial f/\partial T)_{pNL} \tag{8}$$

Since H_t is additively composed of the enthalpy of the filament H and the enthalpy H' of the reservoir, we have

$$(\partial H_t/\partial L)_{pTe} = (\partial H/\partial L)_{pTe} + (\partial H'/\partial L)_{pTe}$$
$$= (\partial H\partial/L)_{pTe} + (\partial H'/\partial N')_{pTL}(\partial N'/\partial L)_{pTe}$$

The latter result follows from the fact that H' depends on L only through the number of diluent molecules in the reservoir, N', which changes when a force is applied to the filament, because the swelling of the filament changes (N). Since furthermore

$$(\partial H/\partial L)_{pTe} = (\partial H/\partial L)_{pTN} + (\partial H/\partial N)_{pTL}(\partial N/\partial L)_{pTe}$$

and

$$(\partial N/\partial L)_{pTe} = -(\partial N'/\partial L)_{pTe}$$

one finds by combining eqs. (7) and (8) with the above

$$f - T(\partial f/\partial T)_{pLe} = (\partial H/\partial L)_{pTN} + \overline{\Delta H}(\partial N/\partial L)_{pTe} \tag{9}$$

with

$$\overline{\Delta H} = (\partial H/\partial N)_{pTL} - (\partial H'/\partial N)_{pTL} = \bar{H} - \bar{H}^0$$

Equation (9) was derived in this way by Oth and Tompa,[5] and by Oplatka, Michaeli, and Katchalsky.[19] Oth proposed to determine $(\partial H/\partial L)_{pTN}$ and $\overline{\Delta H}$ by plotting the left-hand side of eq. (9) versus $(\partial N/\partial L)_{pTe}$ for different values of L. This procedure has, however, been criticized by Hoeve and Flory,[2] who showed that for a network of Gaussian chains $(\partial H/\partial L)_{pTN}$ will in general not be independent of L. This objection can be overcome by making use of the relation:

$$(\partial f/\partial T)_{pLe} = (\partial f/\partial T)_{pLN} + (\partial f/\partial N)_{pLT}(\partial N/\partial T)_{pLe} \tag{10}$$

In conjunction with eqs. (7), (8), and (9) we then obtain

$$\overline{\Delta H} = -T(\partial f/\partial N)_{pLT}(\partial N/\partial T)_{pLe}(\partial N/\partial L)^{-1}_{pTe} \tag{11}$$

where all quantities on the right-hand side of eq. (11) are experimentally accessible.

The quantity $\overline{\Delta H}$ represents the partial molar heat of dilution, under the restraint of constant length. As such, it contains a mixing ($\overline{\Delta H}_m$) as well as an elastic ($\overline{\Delta H}_{el}$) term. Oth[5] has suggested that in many cases the latter term will be minor and that therefore $\overline{\Delta H}$ can be equated to the heat of mixing only. By varying the crosslinking density, and therefore the extent of swelling, it would thus be feasible to determine the heat of mixing of polymer solutions over a considerable range of concentrations through elasticity measurements on gels rather than through cumbersome calorimetry on solutions. A check on Oth's assumption ($\overline{\Delta H} \cong \overline{\Delta H}_m$), however, cannot be obtained from thermodynamics but requires again recourse to the theoretical model of Gaussian chain networks (see below).

EXPERIMENTAL TECHNIQUES

Preparation of Filaments and Analysis

As indicated in Table I two types of polyvinyl alcohol, varying in the amount of residual acetyl, were used for the spinning of cylindrical model filaments. In the case of the PA-5 polymer (11–14% acetyl content), a 40% solution in water was spun through a capillary into a coagulating bath of cold methanol. The cold methanol was subsequently replaced by an acidic Na_2SO_4 solution containing formaldehyde. After 24 hr. at 25°C. the filament appeared uniform in cross section with a diameter of 0.603 mm. and remained insoluble in boiling water. The formaldehyde treatment does not actually crosslink the polyvinyl-alcohol but yields intrachain formals instead:[6]

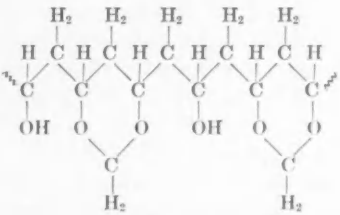

The formaldehyde content was determined with 5,5-dimethylcyclohexane-1,3-dione (Dimedone) according to Yoe and Reid.[7] The various data on the formalized filaments (F) are collected in Table I. The second type of filament was spun from a fully hydrolyzed polyvinyl alcohol sample. In this case cylindrical filaments were obtained by a gel spinning method. A gel of 20% PVA in water was made by heating the mixture at 160°C. for 9 hr. in a closed pressure tube. The clear gel was put in an electrically heated metal spinning tube with a nozzle of 0.6 mm. diameter. The temperature was initially raised to 90°C. and then lowered to 30–32°C. A piston was subsequently driven down at a speed corresponding to a rate of discharge of 0.5 cm.^{3}/min. A final filtration occurred just before the nozzle through a cotton cloth. The filaments were collected in a cold

TABLE I
Preparation of PVA Model Filaments and Analytical Data

	C-I	C-II	C-III	F
Starting PVA	Dupont, Elvanol 71/30	Dupont, Elvanol 71/30	Dupont, Elvanol 71/30	Dupont, PA-5
$\overline{DP}_v$	1830	1830	1830	1600
Ester residue, %	<1	<1	<1	11–14
Spinning condition	Gel spinning	Gel spinning	Gel spinning	Wet spinning
Concentration, wt.-%	20	20	20	40
Coagulation bath	Cold methanol	Cold methanol	Cold methanol	
Modification	Crosslinked by thiodiacetaldehyde $(CHOCH_2)_2S$			Formalized
Bath composition	Dialdehyde: H_2SO_4: Na_2SO_4: H_2O = 0.9:4:20:75.1			HCHO: H_2SO_4: Na_2SO_4: H_2O = 10:10:20:60
Temp., °C. (and time, hr.)	20 (1) + 60 (1)	20 (1) + 40 (1)	35 (1⅓)	25 (24)
Analysis				
S content, %	1.90	1.26	0.10	—
HCHO content, %	—	—	—	11.7
Degree of substitution, %	11.0	7.2	0.55	36
Diameter (90°C., mm.)	0.567	0.623	0.832	0.603
Degree of swelling (V/V_{dry}, 90°C.)	2.53	3.61	8.48	2.2

methanol bath of about 30 cm. depth. Crosslinking was achieved by means of thiodiacetaldehyde after replacing the methanol by an aqueous Na_2SO_4 coagulation bath. The thiodiacetaldehyde was prepared as an acetal (bis-2,2-diethoxyethylsulfide) which was hydrolyzed prior to use.

First bromoacetal was made by reacting vinylacetate with Br_2 in alcohol, according to McElvain and Kundiger.[8] Bromoacetal (140 g.) was subsequently refluxed in 1 liter ethanol with 300 g. sodium sulfide for a period of 24 hr. The solution was concentrated under vacuum as far as possible and separated from the unreacted crystalline sodium sulfide. The remaining solution was diluted with 1.5 liter water and extracted with ether. Bis-2,2-diethoxyethyl sulfide (40 g.) was obtained from the ether extract after evaporation of the ether and two distillations under v[illegible][9] b.p. 152–154°C./17 mm. Hg, $n_D^{23.5} = 1.4490$; analysis: C = 54.15% (54.11% theor), H = 9.74% (9.84% theor.).

With this agent crosslinks are formed as follows:[10]

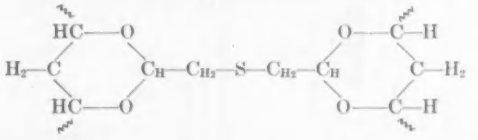

The sulfur atom provides a check on the number of crosslinks. One has to assume, however, that all reacted thiodiacetaldehyde molecules have indeed reacted at both ends and are not engaged in elastically ineffective, intrachain rings. The exact procedure was as follows: 8 ml. of the diacetal of thiodiacetaldehyde were mixed with 20 ml. ethanol; 2.4 ml. concentrated H_2SO_4 and 100 ml. H_2O were then added, and the whole heated at 65–70°C. for 5 min. After this period a clear solution was obtained, which was cooled down. Additional H_2SO_4, Na_2SO_4, and water was then added to adjust the bath composition as indicated in Table I. The filaments, swollen in 15% Na_2SO_4, were put in this bath (ratio dry PVA/bath = 1/300) and kept there at various times and temperatures (see Table I) in order to obtain filaments of various degrees of crosslinking. The data on the crosslinked filaments (C) are again collected in Table I.

Dynamometer

A diagram of the dynamometer set up is shown in Figure 1. The force is measured by means of a strain gauge (model G1-1.5-350, Statham Inst., Hato Rey, Puerto Rico), whose output can be amplified on a DC amplifier (model 150 A, Keithley Inst., Cleveland, Ohio) and plotted on one of the axes of an *XY* recorder (PR 2220 A/00, Philips, Eindhoven, Netherlands). The temperature is measured with a thermocouple and plotted on the other axis. By means of a microscope with micrometer eyepiece the changes in diameter of the filament can be observed in a double-walled container made of square glass tubing. The length of the filament is measured with a cathetometer to 0.05 mm. The elongation can be effected either

manually by means of a screw micrometer (to 0.01 mm.), or automatically by means of a reversible synchronous motor which drives the rod carrying the lower clamp at any of three selected speeds (1, 2.5, and 8 mm./min.). The motion of the elongation rod is coupled to a helically wound potentiometer. This feature makes it possible to record force–elongation data on the XY recorder. For the present work this was, however, not essential. The rods extending into the water bath, holding the filament, are made of Invar metal of very low thermal expansion, so as to keep the fila-

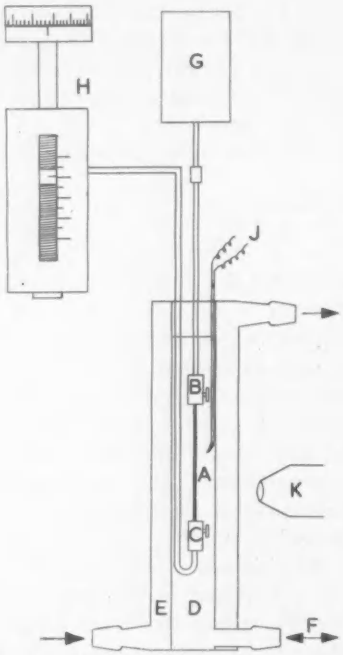

Fig. 1. Schematic drawing of experimental arrangement of filament dynamometer: (A) filament; (B) upper clamp; (C) lower clamp; (D) square glass cell; (E) water jacket; (F) level regulation; (G) strain gauge; (H) micrometer (0.01 mm./div.); (J) thermocouple; (K) microscope.

ment at an (almost) constant length during the force–temperature measurements. The level of the water in the double-walled vessel has to be maintained constant in order to prevent changes in buoyancy of the upper clamping rod. It is also of importance to note that the Statham strain gauge is quite sensitive to small temperature changes. A correction for this effect has to be applied sometimes. For the measurements of the deswelling effect [Eq. (6)] use is made of solutions of sodium carboxymethyl cellulose (NaCMC 70 L, by courtesy of Hercules Powder Company, Wilmington, Delaware).

RESULTS

All filaments were conditioned by repeated loading and unloading at 90°C. at a degree of stretch exceeding the one used during the final measurements. In this way irreversible flow could be eliminated even in the case of the noncrosslinked F filaments.

In Figure 2 the results of the stress–temperature measurements are given for a series at 10% elongation (8% for the F filaments). Figures 3 and 4 show the cross-sectional changes as a function of temperature and elongation. These data suffice for the calculation of f_e and f_s, if we make use of eq. (2). If we want to employ eq. (5) we need in addition the cross-sectional and force changes induced by deswelling the filament in polymer

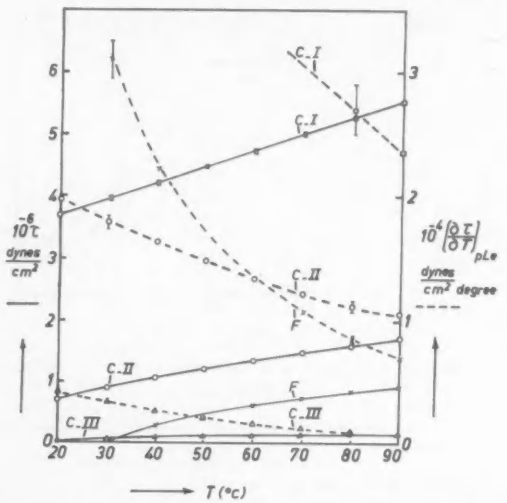

Fig. 2. Stress–temperature data for formalized (F) as well as crosslinked (C) polyvinyl alcohol model filaments. C filaments 10% stretch, F filament 8% stretch.

solutions [eq. (6)]. These data are given in Figure 5 for the C-II filament and in Table II for the other filaments. In Figure 5 are also given the length changes and cross-sectional changes at constant stress. We find $(1/\sigma)(\partial\sigma/\partial c)\tau = -1.72$ ml./g. and $(1/L)(\partial L/\partial c)\tau = -0.98$ ml./g., indicating that the filament is sufficiently isotropic to justify the use of eq. (5) instead of eq. (4). The same is assumed for the other filaments.

The desired energy and entropy components of the stress, as given in Figure 6, were calculated by using eq. (5). Interestingly, the same values are obtained from eq. (2) when and only when the data at temperatures above 70°C. are employed. This is in line with expectation, because only at high temperatures does the filament exhibit rubbery behavior (i.e., an entropy decrease on stretching) and eq. (2) is based on such behavior (see next section).

In Table III we have collected the thermodynamic information which can be obtained from the data at 90°C. The partial molar heat of dilution, $\overline{\Delta H}$, was calculated from the data by using eq. (11). The required $(\partial N/\partial T)_{pLe}$ values were obtained from $(1/\sigma)(\partial\sigma/\partial T)_{pLe}$ by subtracting

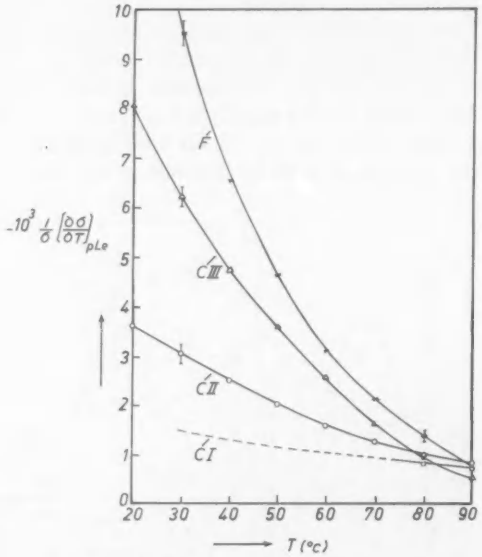

Fig. 3. Relative cross-sectional change with temperature as a function of temperature for all filaments.

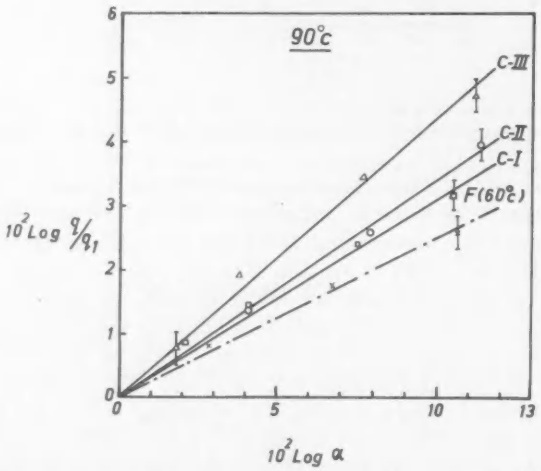

Fig. 4. Relative increase in degree of swelling as a result of the degree of elastic stretch α for all filaments.

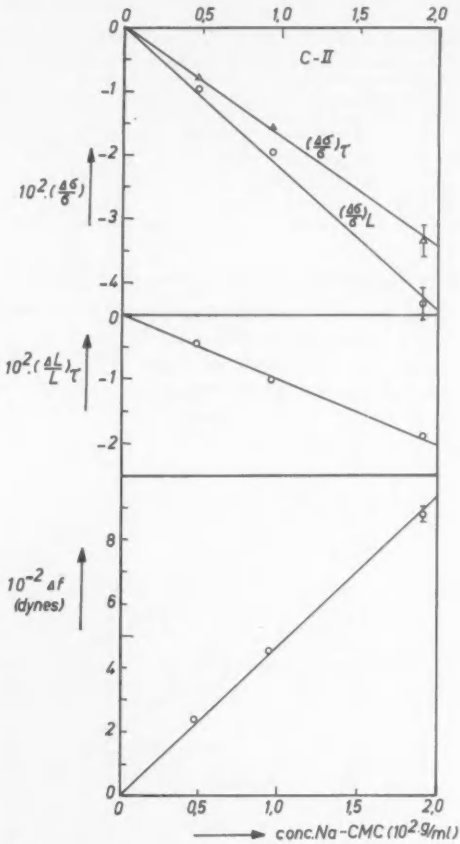

Fig. 5. Dimensional and force changes of the C-II filament as a result of replacing the water around the filament by sodium carboxymethyl cellulose solutions.

the thermal expansion of the PVA and water. For this purpose the value $(\partial \ln V/\partial T)_{pLN} = 2.7 \times 10^{-4}$/°C. for PVA was used.[11] For water the data were taken from the International Critical Tables.

TABLE II
Cross-Sectional and Force Changes Induced by Deswelling PVA Filaments in Na-CMC Solutions

Filament	$10^{-4}(\partial f/\partial c)_{pTL}$, dynes ml./g.	$(1/\sigma)(\partial\sigma/\partial c)_{pTL}$, ml./g.
PA-F	2.21	−1.31
FH-C-I	2.84	−0.73
FH-C-II	4.68	−2.23
FH-C-III	1.00	−5.00

TABLE III

Energy Contribution to the Retractive Force, f_e/f, and Partial Molar Heat of Dilution, $\overline{\Delta H}$, as Calculated from the Data for 10% Extension (8% for F Filaments) at 90°C.

Filament	$\phi_{PVA} = q_1^{-1}$	f_e/f	$\overline{\Delta H}$, cal./mole
PA-F	0.455	−1.3 (±0.2)	−2.2
FH-C-I	0.395	0.3 (±0.3)	−10.2
FH-C-II	0.277		−5.0
FH-C-III	0.118		−0.24

For the C-II filaments data were also obtained at 20 and 30%, as shown in Figures 7, 8, and 9. The corresponding deswelling data in NaCMC solutions do not differ from those at 10% stretch.

At low temperatures steady force readings during a cooling sequence could not always be obtained. This is the reason why in Figure 5 not all

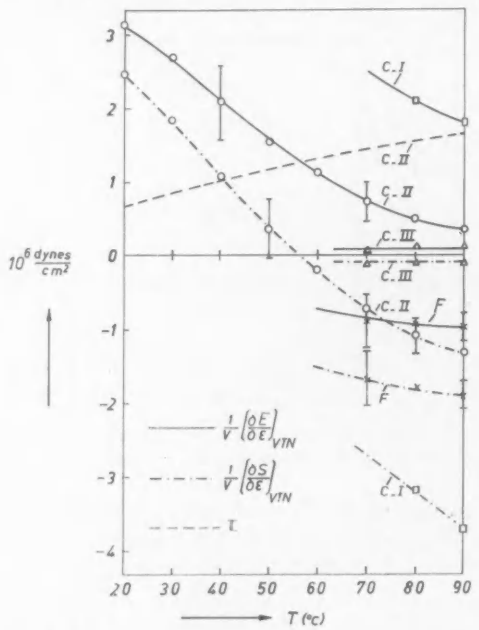

Fig. 6. Stress and its energy and entropy components for all filaments as a function of temperature, as calculated from the data and eq. (5) or eq. (2) (above 70°C. only) $\epsilon = (L - L_1)/L_1$.

lines are drawn down to room temperature. This time dependence of the force seems to be related to the tendency of the PVA network to form a somewhat ordered hydrogen-bonded structure at lower temperatures, which is a well known phenomenon in concentrated PVA solutions.[12] The pro-

found changes which f_e and f_s undergo at lower temperatures may be indicative of a different deformation mechanism due to this structuring effect (see below).

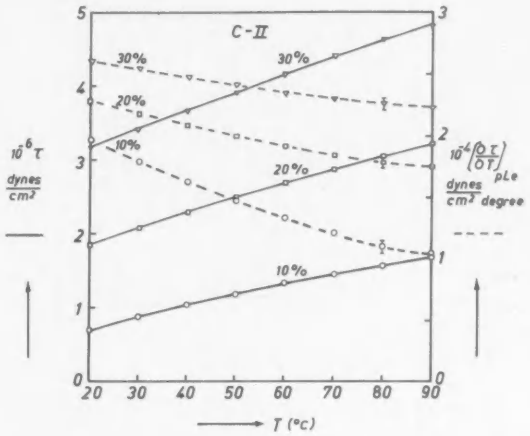

Fig. 7. Stress–temperature data for the C-II filament at various degrees of stretch: (——) $10^{-6}\,\tau$; (- -) $10^{-4}\,(\partial\tau/\partial T)_{pLe}$.

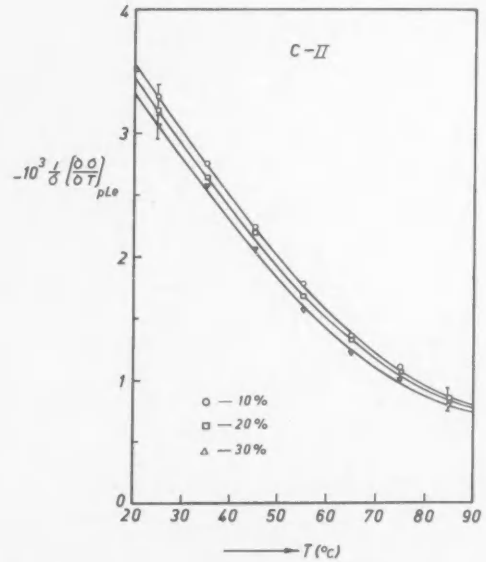

Fig. 8. Relative cross-sectional changes with temperature as a function of temperature for the C-II filament at various degrees of stretch.

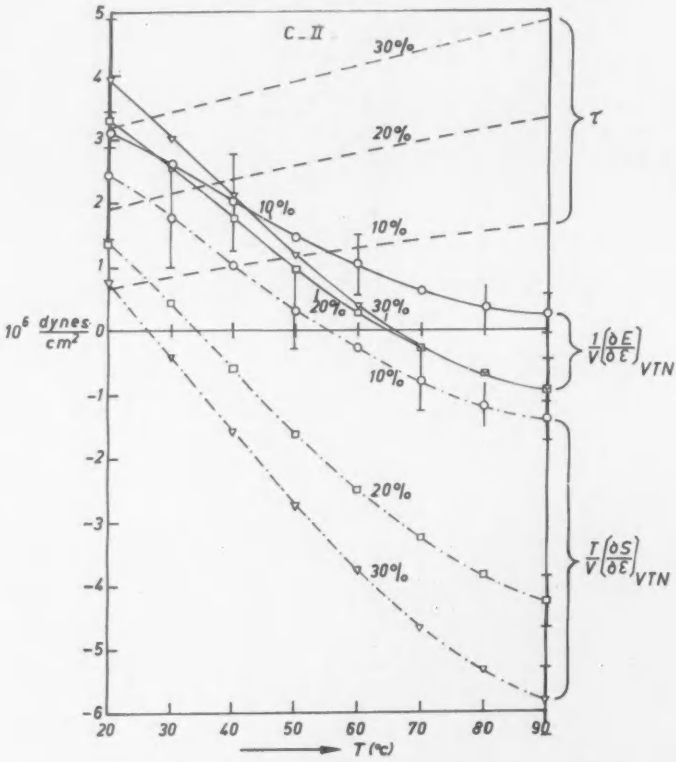

Fig. 9. Stress and its energy and entropy components for the C-II filament at various degrees of stretch; $\epsilon = (L - L_0)/L_0$.

DISCUSSION

At temperatures above 70°C., all filaments exhibit an entropy decrease on stretching (Figs. 6 and 9). Since at this temperature the filaments consist of fully amorphous, swollen networks of polymer chains, it seems reasonable to assume that any existing interchain forces are not strain-dependent. In that case the entropy decrease on stretching should be related to the uncoiling of polymer chains, i.e., the filaments are typically rubber elastic. The experimentally found, nonzero energy changes on stretching should then also be related to this uncoiling process. In the case of the formalized (F) filaments we find f_e to be large and negative, whereas f_e is small and probably positive for the crosslinked (C) filaments. A tentative explanation of these results may perhaps be found in the fact that the F chains carry bulky formal groups and some residual acetyl whereas the C chains do not. Stretching the F chains then would bring the chains in more extended conformations with less steric hindrance and therefore lower energy ($f_e < 0$).

For the C chains it is conceivable that isotactic sequences would give rise to an energy decrease on stretching because the more extended conformations would possibly lead to more intrachain hydrogen bonds. Syndiotactic sequences, on the other hand, would give an energy increase on stretching because the extended conformations would have less opportunities for hydrogen bonds. Since the PVA used in our experiments was atactic, with perhaps a slight preponderance of syndiotactic sequences, the resultant f_e would be small and positive. Experimentally we find f_e indeed to be small, but the accuracy is not good enough to state unequivocally that f_e is positive.

The above hypothesis is of course in need of further verification. Experimental work is therefore under way in our laboratory with filaments spun from PVA of varying tacticity. Theoretically, a connection between f_e and the conformational behavior of polymer chains is predicted from the well known force–elongation relation derived for polymer networks consisting of Gaussian chains between crosslinks:[13,14]

$$f = (kT\nu/L_1)\ (q_1/q_0)^{2/3}[\alpha - (q/q_1\alpha^2)] \tag{12}$$

In eq. (12) all symbols have been defined earlier except ν, which is the number of chains in the network, and q_0, which is the degree of swelling at which the chains are unstrained. In this state the chains have the same mean-square end-to-end distance $\langle r_0^2 \rangle$ as they would have if they were freely dispersed in a solvent at the same concentration. It then follows that

$$f_e/fT = -(\partial \ln f/T/\partial T)_{LVN} = {}^2/_3\ (\partial \ln q_0/\partial T)_{LVN}$$
$$= (\partial \ln \langle r_0^2 \rangle/\partial T)_{LVN} \tag{13}$$

For the F filaments we find $\partial \ln \langle r_0^2 \rangle/\partial T$ to be $-3.6\ (\pm 0.6) \times 10^{-3}$°K. and for the C filaments $+0.7\ (\pm 0.7) \times 10^{-3}$/°K. A model calculation showing these values to be plausible has not yet been undertaken.

From the C-II data in Figure 9 it would seem that f_e/f depends on the degree of elongation and possibly reverses sign at 30% stretch. We have restricted our analysis to the data at lower stretch, where the assumptions underlying the rubber elasticity theory would seem to be best fulfilled. Also, Roe and Krigbaum[15] have shown that the use of the approximation $(\partial f/\partial T)_{LVN} = (\partial f/\partial T)_{pNe}$ ought to be more reliable, the closer α is to unity.

Turning next to the $\Delta\bar{H}$ $(=\Delta\bar{H}_m + \Delta\bar{H}_{el})$ data collected in Table III, we note that evaluation of the mixing term, $\Delta\bar{H}_m$, can only be achieved if we have a theoretical expression for the elastic free energy, F_{el}, of the deformed swollen network or if it can be shown that $\Delta\bar{H}_{el}$ is negligible. From the previous discussion it follows that at elevated temperatures the PVA filaments behave rubber-elastically. We will therefore use the theoretical expression for F_{el} as derived on the basis of the Gaussian chain network model. The equilibrium swelling under unidirectional elongation will be given by the equality of the partial molar thermodynamic potential, μ, of the diluent inside (g) and outside (s) the gel, as follows:[16]

$$\mu^E = \mu^E$$

$$\mu^0 = \mu^0 + (\partial F_m/\partial N)_{VTL} + (\partial F_{el}/\partial N)_{VTL} = \mu^0 + \bar{F}_m + \bar{F}_{el}$$

$$0 = \bar{F}_m + (RT/p)[(q_1/q_0)^{2/3}/q_1\alpha - 1/q] \tag{14}$$

All symbols in eq. (14) have been defined earlier except p, which is equal to $V_d/v_1\nu$, where V_d = dry volume of polymer, v_1 = partial molar volume of diluent, ν = number of chains in the network.

Since for the system under consideration all enthalpy effects differ only negligibly from the energy effects, we can obtain $\overline{\Delta H}_{el} \cong \overline{\Delta E}_{el}$ from eq. (14):

$$\overline{\Delta H}_{el} = \overline{\Delta E}_{el} = -T^2(\partial \bar{F}_{el}/T/\partial T)_{VLN} = (2RT/3p\alpha)\,(q_1q_0^2)^{-1/3}$$

$$(\partial \ln q_0/\partial T)_{VLN}$$

Using eq. (13) we find:

$$\overline{\Delta E}_{el} = (RT/p)(q_1q_0^2)^{-1/3} f_e/f\alpha \tag{15}$$

In order to evaluate $\overline{\Delta E}_{el}$ we need the parameters q_0 and p. A reasonable estimate for q_0 will be $q_0 \cong 2$, because this corresponds to the degree of swelling just prior to crosslinking where presumably the chains have their unstrained end-to-end distance. From eq. (12) we then obtain p, which turns out to be in reasonable correspondence (Table IV) with the p_a value derived from the sulfur analysis data.

TABLE IV

Estimation of the Heat of Mixing of PVA and Water, $\overline{\Delta H}_m$, at various volume fractions ϕ_{PVA} ($= q_1^{-1}$) from the $\overline{\Delta H}$ of crosslinked PVA networks at 90°C. from Eqs. (12) and (15), $\alpha = 1.1$, $q_0 = 2$, $f_e/f = 0.2$

Filament	q_1 ($= \phi_{PVA}^{-1}$)	$\overline{\Delta H}$, cal./mole	p	p_a	$\overline{\Delta H}_{el}$, cal./mole	$\overline{\Delta H}_m$, cal./mole
FH-C-I	2.53	−10.2	41	33	1.5	−11.7
FH-C-II	3.61	−5.0	122	52	0.4	−5.5
FH-C-III	8.48	−0.24	580	730	0.06	−0.30

Inserting now the various experimental data in eq. (15) we obtain $\overline{\Delta E}_{le}$ as shown in Table IV. It is seen that in our case $\overline{\Delta E}_{el}(= \overline{\Delta H}_{el})$ is almost negligibly small, in line with Oth's speculation. The values found for $\overline{\Delta H}_m$ are negative, indicating that at 90°C. the dissolution of PVA in water is energetically favored. The decrease in absolute magnitude of $\overline{\Delta H}_m$ with decreasing polymer concentration (higher degree of swelling) is, of course, in line with expectation. If the well known Flory-Huggins theory of polymer solutions were to be applicable, we would have $\overline{\Delta H}_m = RT\phi^2\kappa$, where κ is an enthalpy constant related to the χ-parameter through $\kappa = d\chi/d\ln T$. Calculating κ from the data in Table IV we find the Flory-Huggins theory only very roughly obeyed for PVA solutions from $\phi \cong 0.1$ to $\phi \cong 0.4$. Since κ is negative, this means that χ increases with temper-

ature. It is of interest to note in this connection that Matsuo and Inagaki,[17] in their work on dilute PVA solutions, find the second virial coefficient A to be decreasing with increasing temperature, until at some temperature above 80°C. the Θ-point is reached. Since $dA/dT < 0$ implies $d\chi/dT > 0$, their result is in line with ours. At first glance the well-known fact that PVA solutions form gels at lower temperature might be felt as contradictory to the existence of a Θ-point at higher temperature. The gelation, however, is very likely a result of random interchain hydrogen bonding, which does not occur at high temperature and therefore does not play a role in the energy interaction between PVA and water at 90°C.

Returning now to the elasticity of the C filaments, we still have to consider the transition from rubbery behavior at high temperature to a quite different behavior at temperatures below 70°C., where f_s has a different sign and where f_e assumes large positive values. An apparently analogous behavior has been found previously at temperatures below 60°C. for cellulose model filaments.[1] In that case there were strong indications from the elasticity measurements as well as accessibility determinations[18] that a reversible, stress-induced recrystallization occurred. More specifically, it was suggested that the opening up of crystallites under stress at elevated temperatures and a subsequent binding of water at new hydrogen-bonding sites would explain the large differences in f_e and f_s value below and above the transition temperature. In other words, in the case of cellulose; the changes in f_e and f_s values did not necessarily reflect changes in deformation mechanism of the cellulose chains, but were thought to relate to the water component also present in the filament.

In the present case such an interpretation is not ruled out by the present data, but is not very likely. In the first place, at high temperatures the PVA behaves like an almost ideal rubber with $f_e/f = 0.3$, whereas for cellulose $f_e/f = -4.5$ at 90°C. In cellulose at 90°C. about 30% of the polymer is considered crystalline, whereas the PVA probably forms a fully amorphous swollen network at this temperature. The lower temperature very likely induces the formation of inter- and intrachain hydrogen bonds,[12] but a structural ordering of the extent found in swollen cellulose has never been found for PVA.

Therefore, instead of relating the f_e and f_s changes with temperature to stress-induced recrystallization and to the water component, the best conjecture at the present time seems to be that at lower temperatures the interaction between chains is no longer independent of strain due to hydrogen bonding. The elastic deformation then can lead to a large energy increase and some entropy increase (rather than decrease as above 70°C.), more or less similar to what has been found for certain proteins.

The PVA gel spinning facilities of the Central Laboratory TNO, Delft, Netherlands, were kindly put at our disposal by Mr. C. van Bochove. Mr. E. J. van der Kraats at the Organic Chemistry Department, Technische Hogeschool, Delft, Netherlands, has ably synthesized the bis-2,2-diethoxyethylsulfide, which was used by us as a crosslinking agent.

References

1. Gabrail, S., and W. Prins, *J. Polymer Sci.*, **51**, 279 (1961).

2. Flory, P. J., A. Ciferri, and C. A. J. Hoeve, *J. Polymer Sci.*, **45**, 235 (1960); C. A. J. Hoeve and P. J. Flory, *J. Polymer Sci.*, **60**, 155 (1962).

3. Elliott, D. R., and S. A. Lippmann, *J. Appl. Phys.*, **16**, 50 (1945); G. Gee, *Trans. Faraday Soc.*, **42**, 585 (1946).

4. Prins, W., *J. Polymer Sci.*, **60**, S65 (1962).

5. Oth, J., *J. Chim. Phys.*, **57**, 720 (1960); J. Oth, and H. Tompa, *J. Chim. Phys.*, **57**, 726 (1960).

6. Noma, N., T. Oh, and T. Tsumeda, *Kobunshi Kagaku*, **6**, 439 (1949); C. van Bochove, Central Lab. TNO, Delft, Netherlands, private communication.

7. Yoe, J. H., and L. S. Reid, *Ind. Eng. Chem. Anal. Ed.*, **13**, 238 (1941).

8. McElvain, S. M., and D. Kundiger, *Org. Synth. Coll.* Vol. III, 123.

9. Fischer, E., *Ber.*, **42**, 1070 (1909); R. D. Coghill, *J. Am. Chem. Soc.*, **59**, 801 (1937).

10. Sakurada, I., A. Yamamoto, Y. Yasutake, and W. Tsuji, *Proc. Inst. Chem. Fibers, Kyoto Univ., Japan*, No. **10–11**, 55 (1954); C. van Bochove, Central Lab. TNO, Delft, Netherlands, private communication.

11. Yano, Y., *J. Chem. Soc. Japan*, **73**, 708 (1952).

12. Kainer, F., *Polyvinylalkohole*, Enke Verlag, Stuttgart, 1949; F. Matsuo and H. Inagaki, *Makromol. Chem.*, **53**, 130 (1962).

13. Ciferri, A., *J. Polymer Sci.*, **54**, 149 (1961); A. Ciferri, C. A. J. Hoeve, and P. J. Flory, *J. Am. Chem. Soc.*, **83**, 1015 (1961).

14. See, e.g., J. J. Hermans, *Trans. Faraday Soc.*, **43**, 591 (1947); J. Polymer Sci., **59**, 204 (1962).

15. Roe, R. J., and W. R. Krigbaum, *J. Polymer Sci.*, **61**, 167 (1962).

16. Flory, P. J., *Principles of Polymer Chemistry*, Cornell Univ. Press, Ithaca, N. Y., 1953, p. 512 ff.

17. Matsuo, F., and H. Inagaki, *Makromol. Chem.*, **55**, 150 (1962).

18. Yamada, S., and W. Prins, *J. Polymer Sci.*, **56**, S13 (1962).

19. Oplatka, A., I. Michaeli, and A. Katchalsky, *J. Polymer Sci.*, **46**, 365 (1960).

Synopsis

Two types of cylindrical polyvinyl alcohol model filaments were prepared, and their elastic and swelling behavior measured as a function of temperature from 25 to 90°C. The first type (C) was prepared by extruding a 20% aqueous gel of fully hydrolyzed PVA into a methanol coagulating bath, and crosslinking the filaments with thiodiacetaldehyde to various extents (0.5–11% hydroxyl substitution) with equilibrium swelling ratios in water varying from 2.5 to 8.5 and wet diameters ranging from 0.56 to 0.83 mm. The second type (F) was prepared by spinning a 40% partially acetylated (11–14% acetyl) PVA solution into methanol and treating the filaments with formaldehyde. In this case only intramolecular rings are formed (36% hydroxyl substitution) but the filaments, as the previous ones, remained insoluble in boiling water, with an equilibrium swelling ratio of 2.2 and a wet diameter of 0.6 mm. A thermodynamic analysis of the stress–temperature data, taken in a dynamometer, combined with microscopic measurements of the changes in swelling, yields the energy and entropy components of the retractive force. It was found that at temperatures above 70°C. both types of filaments are rubbery, i.e., exhibit an entropy decrease on stretching. The crosslinked filaments of fully hydrolyzed PVA are, however, much more ideally rubber elastic (energy component very small, $f_e/f \cong 0.3$) than the formalized filaments of partially acetylated PVA (energy component large, $f_e/f = -1.3$). This last result is tentatively attributed to the bulky formal groups and residual acetyl groups. The data also allow the determination of the heats of dilution of the various swollen PVA networks. From these, the heats of mixing (ΔH_m) can be obtained if a correction is applied for the heat effect caused by the

straining of the network chains. For the C filaments, ranging in polymer concentration from 10 to 40%, negative ΔH_m values at 90°C. were found, in line with the negative ΔH_m in dilute solution (<1%) reported by Matsuo and Inagaki. At temperatures below 70°C., the elasticity of the crosslinked filaments changes drastically; energy as well as entropy now increase on stretching. A possible explanation might be found in the formation of inter- and/or intrachain hydrogen bonds. This might make the stress-induced uncoiling of the chains no longer strain-independent, as is assumed for the rubbery behavior at high temperatures.

Résumé

Deux sortes de filaments d'alcool polyvinylique de forme cylindrique ont été préparés et on a mesuré leur élasticité et leur comportement lors du gonflement en fonction de la température entre 25° et 90°. Le premier type (C) a été préparé en extrudent dans un bain coagulant de méthanol, un gel à 20% d'eau de PVA complètement hydrolysé et en pontant les filaments avec du thioacétaldéhyde de façon à obtenir différents pourcentages de substitution des hydroxyles (0.5 à 11%); les valeurs du gonflement dans l'eau à l'équilibre, varient alors de 2.5 à 8.5 et les diamètres à l'état humide se situent entre 0.56 et 0.83 mm. Le second type (F) a été préparé en filant dans le méthanol une solution à 40% de PVA partiellement acétylé (11–14% d'acétyle) et en traitant les filaments par le formaldéhyde. Dans ce cas, il se forme seulement des cycles intramoléculaires (36% de substitution des groupements hydroxyles) mais les filaments, de même que les précédents, demeurent insolubles dans l'eau bouillante; la valeur du gonflement à l'équilibre est de 2.2 et le diamètre à l'état humide de 0.6 mm. Une analyse thermodynamique des données étirement-température, obtenus avec un dynamomètre et combinées avec des mesures microscopiques des variations du gonflement fournissent les composantes énergétiques et entropiques de la force de rétraction. On a trouvé qu'aux températures supérieures à 70°C, les deux types de filaments sont caoutchouteux, c.à.d. présentent une diminution d'entropie avec l'étirement. Les filaments pontés de PVA complètement hydrolysés possèdent toutefois une élasticité plus proche de celle du caoutchouc (composante énergétique très faible $f_e/f \cong 0.3$) que les filaments de PVA partiellement acétylés et traités au formaldéhyde (composante énergétique élevée $f_e/f = -1.3$). On essaye d'attribuer ce dernier résultat aux groupes formals volumineux et aux groupes acétylés résiduels. Les données permettent aussi de déterminer les chaleurs de dilution des différents réseaux de PVA gonflés. Partant de là, on peut obtenir les chaleurs de mélange ΔH_m si on applique une correction pour l'effet calorifique causé par la tension des chaînes du réseau. Pour les filaments C dont la concentration en polymère varie entre 10 et 40%, on a trouvé des valeurs négatives de ΔH_m à 90°C en accord avec les ΔH_m négatifs rapportés par Matsuo et Inagaki pour des solutions diluées (<1%). À des températures inférieures à 70°C, l'élasticité des filaments pontés varie brusquement; l'énergie de même que l'entropie augmente alors avec l'étirement. On pourrait en trouver l'explication dans la formation de liens hydrogènes entre deux chaînes ou à l'intérieur d'une même chaîne. Le déroulement de la chaîne, induit par l'étirement, pourrait de ce fait cesser d'être indépendant de la tension comme c'est le cas pour le comportement du caoutchouc aux hautes températures.

Zusammenfassung

Zwei Typen zylindrischer Polyvinylalkohol-Modellfäden wurden dargestellt und ihr elastisches und Quellungsverhalten in Abhängigkeit von der Temperatur zwischen 25 und 90°C gemessen. Die erste Type (C) wurde durch Auspressen eines 20% wässrigen Gels von völlig hydrolysiertem PVA in ein Methanol-Koagulierungsbad und Vernetzung der Fäden mit Thiodiacetaldehyd in verschiedenem Ausmass (0.5 bis 11% Hydroxylsubstitution) mit einem Wert des Gleichgewichtsquellungsgrades in Wasser zwischen 2,5 und 8,5 und Nassdurchmessern zwischen 0,56 und 0,83 mm hergestellt. Die zweite Type (F) wurde durch Spinnen einer 40% partiell acetylierten (11–14% Acetyl) PVA-

Lösung in Methanol und Behandlung der Fäden mit Formaldehyd dargestellt. In diesem Fall wurden nur intramolekulare Ringe gebildet (36% Hydroxylsubstitution), die Fäden blieben jedoch, ebenso wie die früheren, in siedendem Wasser unlöslich, mit einem Gleichgewichtsquellungsgrad von 2,2 und einem Nassdurchmesser von 0,6 mm. Eine thermodynamische Analyse der mit einem Dynamometer aufgenommenen Daten über die Temperaturabhängigkeit der Spannung liefert in Kombination mit einer mikroskopischen Messung der Quellung die energetische und entropische Komponente der elastischen Kraft. Bei Temperaturen overhalb 70°C zeigen beide Fadentypen Kautschukverhalten, d.h. bei der Dehnung nimmt die Entropie ab. Die vernetzten Fäden aus völlig hydrolysiertem PVA zeigen jedoch eine viel stärkere Annäherung an das ideale Kautschukverhalten (energetische Komponente sehr klein, $f_e/f \cong 0{,}3$) als die formaldehyd-behandelten Fäden aus partiell acetyliertem PVA (energetische Komponente gross, $f_e/f = -1{,}3$). Dieses Ergebnis wird vorläufig auf den Einfluss der sperrigen Formalgruppen und der restlichen Acetylgruppen zurückgeführt. Die Ergebnisse ermöglichen die Bestimmung der Verdünnungswärme für die verschiedenen gequollenen PVA-Netzwerke. Aus diesen kann bei Anbringung einer Korrektur für den durch die Spannung der Netzketten bedingten Wärmeeffekt die Mischungswärme ($\overline{\Delta H}_m$) erhalten werden. Für die C-Fäden mit einer Polymerkonzentration zwischen 10 und 40% ergaben sich bei 90°C negative $\overline{\Delta H}_m$-Werte, was in der gleichen Linie, wie die von Matsuo und Inagaki in verdünnter Lösung (<1%) gefundenen negativen $\overline{\Delta H}_m$-Werte liegt. Bei Temperaturen unterhalb 70°C ändert sich die Elastizität der vernetzten Fäden tiefgreifend; es nimmt nun sowohl die Energie als auch die Entropie bei der Dehnung zu. Eine Erklärung lässt sich möglicherweise durch die Bildung von Wasserstoffbindungen in und zwischen den Ketten geben. Dadurch könnte eine Temperaturabhängigkeit der spannungsinduzierten Aufknäuelung der Ketten bedingt sein und damit eine Voraussetzung für das Kautschukverhalten bei hohen Temperaturen nicht mehr erfüllt sein.

AUTHOR INDEX

(Page numbers in *italics* refer to discussion participation.)

Abe, H.: 527
Aggebrandt, L.: 477
Ant-Wuorinen, O.: 311
Beck, L. R., Jr.: 331
Bosarge, K.: 515
Charles, F. R.: 273
Clark, I. T.: 203, *212*
Clermont, L. P.: 253
Côté, W. A., Jr.: 201, 231
Cowling, E. B.: *212*, 243
Craver, J. K.: *152*, *167*, *286*
Donofrio, C. P.: 279
Eastman, N. C.: *152*, *286*
Edelson, M. R.: 145
Ellefsen, Ø.: 321
Glaudemans, C. P. J.: 189, *196*, *197*, *286*
Goring, D. A. I.: 9, 29, *48*, *152*, *212*
Hale, J. D.: 253
Hearon, W. M.: 277
Hermans, J. J.: *115*, 117, *196*
Hermans, Jan, Jr.: 129, 145, *152*
Hodgins, J. W.: 153, *167*
Hossain, S.: *188*
Hovenkamp, S. S.: 341
Huang, R. Y.-M.: 169, *188*
Ishida, A.: 415
Jen, Y.: *152*
Jones, J. K. N.: 63, *94*
Kast, W.: 429
Katai, A. A.: *197*, 403
Kitchen, W. J.: 499
Klein, E.: 515
Klaehn, F. U.: 263
Komagata, H.: 415
Kratky, O.: 449
Kulshrestha, V. K.: 403
LeBel, R. G.: 9, 29
Liese, W.: 213
Lipson, M. A.: *78*
Marchessault, R. H.: *47*, 49, *71*, *95*, *116*, *152*, *188*, *286*, 403
Mark, H.: 1
Matsuzaki, K.: 415
Meller, A.: 97
Mering, J.: 423
Miholic, G.: 449
Mutton, D. B.: *152*, *286*, 499
Nadziakiewicz, H. C.: 357
Neimo, L.: 289
Oberlin, M.: 423
Panzer, H. P.: *95*
Passaglia, E.: 189
Paulusma, P.: 487
Petitpas, T.: 423
Pew, J. C.: 203
Prins, W.: 529
Putnam, E. S.: 377
Ramalingam, K. V.: 153
Rapson, W. H.: 169, *188*, *197*
Reid, P. E.: 63, *71*
Richards, G. N.: *48*, *152*, *196*, *285*
Sachs, I. B.: 203
Samuelson, O.: 477
Schmut, R.: *167*, *188*
Schuerch, C.: 79, *94*, *95*, *212*, *286*
Schwenker, R. F., Jr.: 331
Semple, R. E.: 73, *78*
Shirley, H. L.: 5
Sihtola, H.: 289
Smith, J. K.: 499
Sobue, H.: 415
Stamm, A. J.: 243
Stannett, V.: 387
Sumiala, R.: 289
Thiesmeyer, L. R.: *286*
Timell, T. E.: 9, 49, *71*, 109, *115*, *116*
Treiber, E.: 357
Vermaas, D.: 487
Visapää, A.: 311
Werezak, G. N.: 153
Wharton, J.: 283
Wray, J. A.: 387
Yasuda, H.: 387

SUBJECT INDEX

Acids, in cellulose, 311
Acrylonitrile, polymerization of, 403
Arabinogalactans, water-soluble, 63, 73
Birch xylan, solution properties of, 9, 29
Birefringence, of cellulose fibers, 515
Carbohydrate graft copolymers, 189
Carbonyl groups, in cellulose, 289
Cellulose, absolute intensity measurements on, 449
  acids in, 311
  birefringence of fibers of, 515
  carbonyl groups in, 289
  chains of, 423
  fractional extraction of, 487
  future research, 273
  glycosidic linkages in, 109
  graft copolymers of, 387
  grafting polymers onto, 169
  microcrystals of, 129, 145
  optical dispersion of fibers of, 515
  ozonization of, 79
  polymerization within matrices of, 377
  polymetaphosphate solution penetration into, 477
  pyrolytic decomposition of, 331
  as a raw material, 277
  sedimentation, 117
  structural studies of fibers of, 499
  as a textile, 283
  viscosity of, 117, 321
Cellulose acetate, grafting of styrene on, 415
Configuration, birch xylan, 29
Decomposition, pyrolytic, of cellulose, 331
Elasticity, of polyvinyl alcohol filaments, 527
Fractionation, birch xylan, 29
Gas chromatography, for study of pyrolytic decomposition of cellulose, 331
Gel particle counting, of viscose, 357
Gels, of cellulose microcrystals, 129, 145
Genetic material, chemical nature of, 263
Glycosidic linkages, in cellulose, 109
Graft copolymers, of cellulose, 387
Graft polymerization, of styrene in wood, 153
Initiators, ceric ions as, 403
Kinetics, acid hydrolysis of poly- and oligosaccharides, 97
Lignin, distribution in woods, 203
Molecular weight, birch xylan, 9
Morphology, of prosenchyma cell wall, 253
Nonwoven fabrics, 279
Oligosaccharides, kinetics of acid hydrolysis, 97
  from 4-*O*-methylglucuronoxylan, 49
Optical dispersion, of cellulose fibers, 515
Optical rotatory dispersion, of viscose, 357
Ozonization, of cellulose and wood, 79
Paper, 279
Permeability, of wood, 231
Polyoligosaccharides, kinetics of acid hydrolysis, 97
Polyvinyl alcohol, elasticity of filaments of, 527
Radiation, for grafting polymers onto cellulose, 169
  for graft polymerization of styrene in wood, 153
Reaction rates, of carbonyl groups, 289
Sedimentation, of cellulosic macromolecules, 117
Solid-solution structures, in wood, 243
Strength reinforcement, 377
  graft polymerization in wood, 153
Styrene, grafting on cellulose acetate, 415
  radiation grafting onto cellulose, 169
Viscose, chemistry of, 341
  gel particle counting, 357
  optical rotatory dispersion, 357
  state of solutions of, 357
Viscosity, of cellulosic macromolecules, 117
  in chemically modified cellulose, 321
Wood, graft polymerization of styrene in, 153
  influence of morphology on, 253
  lignin distribution in, 203
  ozonization, 79
  permeability of, 231
  solid-solution structures in, 243
  tertiary wall in, 213
  warty layer in, 213
Xanthating reactions, 341
X-ray orientation, measurement of, 429
X-rays, for measurements, 449

PULP AND PAPER

Chemistry and Chemical Technology

Second Edition, in Three Volumes

VOLUME 1: PULPING AND BLEACHING
VOLUME 2: PAPERMAKING
VOLUME 3: PAPER TESTING AND CONVERTING

By **James P. Casey,** Director of Starch Sales, Union Starch and Refining Company, Columbus, Indiana; formerly Director of Applications Research, A. E. Staley Manufacturing Company, Decatur, Illinois; formerly Associate Professor, College of Forestry, State University of New York

This revised and greatly expanded edition of *Pulp and Paper* is concerned primarily with the subjects relating to chemistry and thus follows the same approach as the original: a fundamental presentation of the subject and pulp manufacturing, papermaking, and converting operations from the standpoint of the colloid and physical chemist. Within this framework, the author is able to effect a logical transition between theory and practical application—in the belief that this middle ground is *the* fertile field of growth where new ideas develop and further progress in the industry takes place.

This edition is the result of a complete revision with special emphasis on the latest advances in science and technology, and with appropriate attention given to recent developments in manufacturing operations. All chapters have been rewritten to accomplish the task of bringing the book up to date in these terms, and several subjects have been enlarged in accordance with the increase in knowledge in the field.

The three volumes of the Second Edition of Pulp and Paper provide mill chemists, technical operating personnel, and research chemists in the paper and allied fields with a modern and comprehensive reference and will also serve as a text for advanced study. *Volume I: 1960. 694 pages. Volume II: 1960. 842 pages. Volume III: 1960. 1008 pages.*

INTERSCIENCE PUBLISHERS a division of JOHN WILEY & SONS New York • London